TR A7627- Unrestricted

Report

EERA DeepWind'2017 Conference
18 – 20 January 2017

Radisson Blu Royal Garden Hotel, Trondheim

Author(s)
John Olav Tande (editor)

SINTEF Energy Research
Power Conversion and Transmission
2017-02-17

SINTEF Energi AS
SINTEF Energy Research
Address:
Postboks 4761 Sluppen
NO-7465 Trondheim
NORWAY
Switchboard: +47 73597200
Telefax: +47 73598354
energy.research@sintef.no
www.sintef.no/energi
Enterprise /VAT No:
NO 939 350 675 MVA

KEYWORDS:
Keywords

Report

EERA DeepWind'2017 Conference 18 – 20 January 2017

Radisson Blu Royal Garden Hotel, Trondheim

VERSION
1.0

DATE
2017-02-17

AUTHOR(S)
John Olav Tande

CLIENT(S)

CLIENT'S REF.

PROJECT NO.
502000965-3

NUMBER OF PAGES/APPENDICES:
325

ABSTRACT

This report includes the presentations from the 14th Deep Sea Offshore Wind R&D Conference, EERA DeepWind'2016, 18 – 20 January 2017 in Trondheim, Norway.

Presentations include plenary sessions with broad appeal and parallel sessions on specific technical themes:
a) New turbine and generator technology
b) Grid connection and power system integration
c) Met-ocean conditions
d) Operations & maintenance
e) Installation & sub-structures
f) Wind farm optimization
g) Experimental Testing and Validation
x) Floating wind turbines

Plenary presentations include frontiers of science and technologies and strategic outlook. The presentations and further conference details are also available at the conference web page: https://www.sintef.no/projectweb/eera-deepwind2017

PREPARED BY
John Olav Tande

SIGNATURE

CHECKED BY
Hans Christian Bolstad

SIGNATURE

APPROVED BY
Knut Samdal

SIGNATURE

REPORT NO.	ISBN	CLASSIFICATION	CLASSIFICATION THIS PAGE
TR A7627	978-82-594-3682-5	Unrestricted	Restricted

Document history

VERSION	DATE	VERSION DESCRIPTION
1.0	2017-02-17	

Table of contents

Detailed programme... 7
List of participants 12
Scientific Committee and Conference Chairs.. 16

Opening session – Frontiers of Science and Technology
Welcoming note by Deputy Mayor Hilde Opoku 18
Progress in offshore wind research and innovation, John Olav Tande, director NOWITECH.............................. 21
European wind research cooperation - Peter Hauge Madsen, DTU... 24
NORCOWE – highlights and future challenges, Kristin Guldbrandsen Frøysa, director NORCOWE.................. 27
HyWind Scotland, Bjørn Johansen, Statoil 33

A1 New turbine and generator
Can a wind turbine learn to operate itself? M. Collu, Cranfield University... 37
Development of a 12MW Floating Offshore Wind Turbine, H. Shin, University of Ulsan.................................. 39
A comparison of two fully coupled codes for integrated dynamic analysis of floating vertical axis wind turbines, B.S. Koppenol, Ventolines BV 49
A2 New turbine and generator technology
The Multi Rotor Solution for Large Scale Offshore Wind Power, P. Jamieson, University of Strathclyde 52
The C-Tower Project – A Composite Tower for Offshore Wind Turbines, T. van der Zee, Knowledge Centre WMC.. 56
Support structure load mitigation of a large offshore wind turbine using a semi-active magnetorheological damper, R. Shirzadeh, ForWind – University of Oldenburg 60
B1 Grid connection and power system integration
HVDC-connection of Large Offshore Wind Farms Using a Low-Cost Hybrid Converter, I. Haukaas, NTNU 64
Generator Response Following as a Primary Frequency Response Control Strategy for VSC-HVDC Connected Offshore Windfarms, R. McGill, NTNU 67
Scale models of Modular Multilevel Converters, K. Ljøkelsøy, SINTEF Energi AS 73
Experimental validation of high definition modular multilevel converter, R. Torres-Olguin, SINTEF Energi AS. 76
B2 Grid connection and power system integration
Strategies towards an Efficient future North Sea Energy Infrastructure (SENSEI), F. Papathanasiou, ECN 80
A hybrid wind-diesel-battery system for fish farming applications, M. Holt, NTNU 84
Assessing the impact of sampling and clustering techniques on offshore grid expansion planning, P. Härtel, Fraunhofer IWES 88
Multistage grid investments incorporating uncertainty in offshore wind development – A North Sea case study, H. Svendsen, SINTEF Energi AS 92
C1 Met-ocean conditions
Coherent structures in wind measured at a large separation distance, H. Ágústsson, Kjeller Vindteknikk 98
Design basis for the feasibility evaluation of four different floater designs, L. Vita, DNV GL.............................. 102
Air-Sea Interaction at Wind Energy Site in FINO1 Using Measurements from OBLEX-F1 campaign, M.B. Paskyabi, University of Bergen 106
Towards Recommended Practices for Floating Lidar Systems, O. Bischoff, University of Stuttgart 110
C2 Met-ocean conditions
Spectral characteristics of offshore wind turbulence, E. Cheynet, University of Stavanger.................................... 115
Offshore Wind Turbine Wake characteristics using Scanning Doppler Lidar, J. Jakobsen, UiS 119
LiDAR capability to model robust rotor equivalent wind speed, J.R. Krokstad, NTNU... 122
D1) Operations & maintenance
A metaheuristic solution method for optimizing vessel fleet size and mix for maintenance operations at offshore wind farms under uncertainty, E.Halvorsen-Weare, SINTEF Ocean... 126
Optimizing Jack-up vessel strategies for offshore wind farms, M. Stålhane, NTNU... 138
Short-Term Decision Optimization for Offshore Wind Farm Maintenance, C. Stock-Williams, ECN 139
Improved short term decision making for offshore wind farm vessel routing, R. Dawid, Strathclyde University... 144

D2) Operations & maintenance
Experience from RCM and RDS-PP coding for offshore wind farms, R.Sundal, Maintech.................................... 147
Enhance decision support tools through an improved reliability model, S. Faulstich, Fraunhofer IWES............... 150
Technology for a real-time simulation-based system monitoring of wind turbines,
D. Zwick, Fedem Technology/SAP SE 154
E1) Installation and sub-structures
Results of a comparative risk assessment of different substructures for floating offshore wind turbines,
R. Proskovics, ORE Catapult... 157
Conceptual optimal design of jackets, K. Sandal, DTU.. 161
Fatigue behavior of grouted connections at different ambient conditions and loading scenarios,
A. Raba, ForWind – Leibniz University Hannover... 166
Analysis of experimental data: The average shape of extreme wave forces on monopile foundations,
S. Schløer, DTU Wind Energy 170
E2) Installation and sub-structures
Fatigue Crack Detection for Lifetime Extension of Monopile-based Offshore Wind Turbines,
L. Ziegler, Ramboll... 175
Fabrication and installation constraints for floating wind and implications on current
infrastructure and design, D. Matha, Ramboll 179
TELWIND- Integrated Telescopic tower combined with an evolved spar floating substructure
for low-cost deep water offshore wind and next generation of 10 MW+ wind turbines,
B. Counago, ESTEYCO SAP... 183
F) Wind farm optimization
Influence of turbulence intensity on wind turbine power curves, L.M. Bardal, NTNU 190
A test case of meandering wake simulation with the Extended-Disk Particle model at the offshore
test field Alpha Ventus, J. Trujillo, University of Oldenburg.. 193
A comprehensive multiscale numerical framework for wind energy modelling, A. Rasheed, SINTEF ICT............ 196
Application of a Reduced Order Wind Farm Model on a Scaled Wind Farm,
J. Schreiber, Technische Universität München 200
G1) Experimental Testing and Validation
Model testing of a floating wind turbine including control, F. Savenije, ECN... 205
The Tripple Spar campaign: Model tests of a 10MW floating wind turbine with waves, wind and pitch control,
H. Bredmose, DTU 210
Validation of a time-domain numerical approach for determining forces and moments in floaters by using measured
data of a semi-submersible wind turbine model test, C. Luan, NTNU.. 215
Nacelle Based Lidar Measurements for the Characterization of the Wake on an Offshore Wind Turbine under
Different Atmospheric Conditions, D. Trabucchi, University of Oldenburg 219
G2 Experimental Testing and Validation
Testing philosophies for floating wind turbines in coupled model tests, E.L. Walter, DNV GL............................. 223
On the impact of non-Gaussian wind statistics on wind turbines – an experimental approach, J. Schottler, ForWind –
University of Oldenburg 227
Wind Tunnel Wake Measurements of Floating Offshore Wind Turbines, I. Bayati, Politecnico di Milano............. 236
Lidars for Wind Tunnels – an IRPWind Joint Experiment Project, M. Sjöholm, DTU Wind Energy...................... 239
X) Floating wind turbines
Sensitivity Analysis of Limited Actuation for Real-time Hybrid Model Testing of 5MW Bottomfixed Offshore
Wind Turbine, M. Karimirad, SINTEF Ocean 246
OC5 Project Phase II: Validation of Global Loads of the DeepCwind Floating Semisubmersible,
A. N. Robertson, NREL 249
Joint industry project on coupled analysis of floating wind turbines, L. Vita, DNV GL.. 252
Using FAST for the design of a TLP substructure made out of steel reinforced concrete composite components,
P. Schünemann, University of Rostock 256

Closing session – Strategic Outlook
ETIP wind Strategic Research and Innovation Agenda, Aidan Cronin, Siemens Wind Power 261
Bringing trust to the Internet of Things – When valuable insights can be gained from data to support
critical decisions in industry, issues such as the quality and integrity of the data has to be included in the risk picture,
M.R. de Picciotto, S. George, DNV GL 265
A new approach for going offshore, Frank Richert, SkyWind 268

SINTEF

Posters 273

Session A

1. *Power quality studies of a Stand-Alone Wind Powered Water Injection System without Physical Inertia, A. Gaugstad, NTNU*
2. *Multibody Analysis of Floating Offshore Wind Turbine System, Y. Totsuka, Wind Energy Institute of Tokyo Inc.*
3. *Investigation of design driving load cases for floating VAWT with pitched blades, F. Savenije, ECN*
4. *SKARV – Preventing bird strikes through active control of wind turbines, K. Merz, SINTEF Energi AS*
5. *An elemental study of optimal wind power plant control, K. Merz, SINTEF Energi AS*

Session B

6. *Inertia Response from HVDC connected Full Converter Wind Turbines, J. Ødegård, Statnett*
7. *Investigation of power sharing solutions for offshore wind farms connected by diode rectifier for HVDC grid, I. Flåten, NTNU*
8. *Offshore Wind Power Plants with 66 kV Collection Grids – Study of Resonance Frequencies, A. Holdyk, SINTEF Energi*
9. *Grid Integration of offshore wind farms using a hybrid composed by an MMC with an LCC-based transmission system*, R. Torres-Olguin, SINTEF Energi
10. *Review of Investment Model Cost Parameters for VSC HVDC Transmission Infrastructure*, T.K. Vrana, SINTEF Energi

Session C

11. *Meteorological Phenomena Influences on Offshore Wind Energy, S. Ollier, Loughborough University*
12. *Availability of the OBLO infrastructure for wind energy research in Norway, M. Flügge, CMR*
13. *Demonstrating the improved performance of an Ocean-Met model using bi-directional coupling, A. Rasheed, SINTEF ICT*
14. *A comparison of short-term weather forecast with the measured conditions at the Hywind Demo site, L. Sætran, NTNU*

Session D

15. *Diagnostic monitoring of drivetrain in a 5-MW spar type floating wind turbine using frequency domain analysis, M. Ghane, NTNU*
16. *Risk-based planning of operation and maintenance for offshore wind farms, M. Florian, Aalborg University*
17. *Improving fatigue load estimation of wind turbines using a neural network trained with short-duration measurements, J. Seifert, University of Oldenburg*
18. *Recommended practices for wind farm data collection and reliability assessment for O&M optimization, T. Welte, SINTEF Energi*
19. *Integration of Degradation Processes in a Strategic Offshore Wind Farm O&M Simulation Model, T. Welte, SINTEF Energi*
20. *Experiences from Wind Turbine Pilot Test of a Remote Inspection System, Ø. Netland, NTNU*
21. *A Framework for Reliability-based Controller Scheduling in Offshore Wind Turbines, J-T H. Horn, NTNU*
22. *Key performance indicators for wind farm operation and maintenance, H. Seyr, NTNU*
23. *Optimization of data acquisition in wind turbines with data-driven conversion functions for sensor measurements, L. Colone, DTU Denmark*

Session E

24. *Design and Fatigue Analysis of Monopile Foundations to Support the DTU 10 MW Offshore Wind Turbine, J.M Velarde, NTNU*
25. *Design load basis of a 10MW floating wind turbine: substructure modelling effects, M. Borg, DTU Wind Energy*
26. *New Foundation Models for Integrated Analyses of Offshore Wind Turbines, A.M. Page, NTNU*
27. *Damage assessment of floating offshore wind turbines using latin hypercube sampling, K. Müller, University of Stuttgart*
28. *Development and validation of an engineering model for floating offshore wind turbines, A.Pegalajar-Jurado, DTU Wind Energy*
29. *Improved estimation of extreme wave loads on monopiles using First Order Reliability Method, A. Ghadirian, DTU*
30. *A 3D fem model for wind turbines support structures, C. Molins, Universitat Politecnica de Catalunya*
31. *Fully integrated load analysis included in the structural reliability assessment of a monopile supported offshore wind turbine, J. Peeringa, ECN*
32. *Parametric study of mesh for fatigue assessment of tubular joints using numerical methods, J. Mendoza, NTNU*
33. *Lifetime extension for large offshore wind farms: Is it enough to reassess fatigue for selected design positions? C. Bouty, NTNU*
34. *Optimization of offshore wind farm installations, S. Backe, University of Bergen*
35. *Modelling of Marine Operations in the Installation of Offshore Wind Farms, A. Dewan, ECN*
36. *Effect of irregular second-order waves on the fatigue lifetime of a monopile based offshore wind turbine in shallow waters, F. Pierella, IFE*
37. *A review of slamming load application to offshore wind turbines from an integrated perspective, Y. Tu, NTNU*

Session F

38. *Offshore Turbine Wake Power Losses: Is Turbine Separation Significant?, P. Argyle, CREST, Loughborough University*
39. *Experimental study on the optimal control of three in-line turbines, J. Bartl, NTNU*
40. *A step towards a reduced order modelling of flow characterized by wakes using Proper Orthogonal Decomposition, E. Fonn, SINTEF ICT*
41. *Explaining the Torque vs TSR curve of a 5MW NREL reference turbine, M.S. Siddiqui, SINTEF ICT*
42. *A 3D Vs 2.5D Vs 2D CFD analysis of 5MW NREL reference wind-turbine to study impact of bluff sections, M. Tabib, SINTEF ICT*

43. *Simulating Single turbine and associated wake development - comparison of computational methods (Actuator Line Vs Sliding Mesh Interface Vs Multiple Reference Frame) for an industrial scale wind turbine, M.S. Siddiqui, SINTEF ICT*
44. *2D VAR single Doppler LIDAR vector retrieval and its application in offshore wind energy, R. Calhoun, Arizona State University*

Session G

45. *IRPWIND ScanFlow project, C. Hasager, DTU Wind Energy*
46. *Comparison of Numerical Response Predictions for a Bottom Fixed Offshore Wind Turbine, S.H. Sørum, NTNU*
47. *Comparison of the effect of different inflow turbulences on the wake of a model wind turbine, I. Neunaber, University of Oldenburg*
48. *IRPWIND ScanFlow Public database, J.W. Wagenaar, ECN*
49. *Wind Tunnel Hybrid/HIL Tests on the OC5/PhaseII Floating System, I. Bayati, Politecnico di Milano*
50. *Calibration and Validation of a FAST model of the MARINTEK Hybrid Semisubmersible Experiment, G. Stewart, NTNU*
51. *The TripleSpar campaign: Implementation and test of a blade pitch controller on a scaled floating wind turbine model, W. Yu,, University of Stuttgart*
52. *A computational fluid dynamics investigation of performance of tip winglets for horizontal axis wind turbine blades, K. Sagmo, NTNU*
53. *Numerical study of irregular breaking wave forces on a vertical monopile for offshore wind turbines*, A. Aggarwal, NTNU
54. *Modelling of the Viscous Loads on a Semi-Submersible Floating Support Structure Using a Viscous-Flow Solver and Morison Formulation Combined with a Potential-Flow Solver, S. Burmester, MARIN*

Wednesday 18 January		
09.00	Registration & coffee	
	Opening session – Frontiers of Science and Technology Chairs: John Olav Tande, SINTEF/NOWITECH and Michael Muskulus, NTNU/NOWITECH	
09.30	Opening and welcome by chair	
09.40	Welcoming note by Deputy Mayor Hilde Opoku	
10.00	*Progress in offshore wind research and innovation,* John Olav Tande, director NOWITECH	
10.30	*European wind research cooperation* - Peter Hauge Madsen, DTU	
11.00	*NORCOWE – highlights and future challenges*, Kristin Guldbrandsen Frøysa, director NORCOWE	
11.30	*HyWind Scotland*, Bjørn Johansen, Statoil	
11.55	Closing by chair	
12.00	Lunch	
	Parallel sessions	
	A1) New turbine and generator technology Chairs: Karl Merz, SINTEF Gerard van Bussel, TU Delft	**C1) Met-ocean conditions** Chairs: Halfdan Agustsson, Kjeller Vindteknikk, Birgitte Rugaard Furevik, met.no
13.00	Introduction by Chair	Introduction by Chair
13.05	*Can a wind turbine learn to operate itself?* M. Collu, Cranfield University	*Coherent structures in wind measured at a large separation distance,* H. Ágústsson, Kjeller Vindteknikk
13.30	*A step approach to model floating wind turbines: application to a novel type of tension-leg concept*, P. Bozonnet, IFP Energies Nouvelles	*Design basis for the feasibility evaluation of four different floater designs*, L. Vita, DNV GL Renewables Certification
13.50	*Development of a 12MW Floating Offshore Wind Turbine*, H. Shin, University of Ulsan	*Air-Sea Interaction at Wind Energy Site in FINO1 Using Measurements from OBLEX-F1 campaign*, M.B. Paskyabi, University of Bergen
14.10	A comparison of two fully coupled codes for integrated dynamic analysis of floating vertical axis wind turbines, B.S. Koppenol, Ventolines BV	*Towards Recommended Practices for Floating Lidar Systems*, O. Bischoff, Stuttgart Wind Energy
14.30	Closing by Chair	Closing by Chair
14.35	Refreshments	
	A2) New turbine and generator technology (cont.)	**C2) Met-ocean conditions (cont.)**
15.05	Introduction by Chair	Introduction by Chair
15.10	*The Multi Rotor Solution for Large Scale Offshore Wind Power*, P. Jamieson, University of Strathclyde	*Spectral characteristics of offshore wind turbulence,* E. Cheynet, University of Stavanger
15.30	*The C-Tower Project – A Composite Tower For Offshore Wind Turbines*, T. van der Zee, Knowledge Centre WMC	*Offshore Wind Turbine Wake characteristics using Scanning Doppler Lidar*, J. Jakobsen, UiS
15.50	*Support structure load mitigation of a large offshore wind turbine using a semi-active magnetorheological damper*, R. Shirzadeh, ForWind – University of Oldenburg	*LiDAR capability to model robust rotor equivalent wind speed,* J.R. Krokstad, NTNU
16.10	Closing by Chair	Closing by Chair
18.00	Conference reception including - Welcoming note by Deputy Mayor Hilde Opoku - Organ recital at Nidarosdomen Cathedral - Light food and drinks reception at Two Towers	

Side event: EERA SP offshore wind meeting 16.30 – 17.45

Thursday 19 January		
	Parallel sessions	
	D1) Operations & maintenance Chairs: Thomas Welte, SINTEF Energi AS Stefan Faulstich, Fraunhofer IWES	**E1) Installation and sub-structures** Chairs: Hans Gerd Busmann, Fraunhofer IWES Michael Muskulus, NTNU
09.00	Introduction by Chair	Introduction by Chair
09.05	*A metaheuristic solution method for optimizing vessel fleet size and mix for maintenance operations at offshore wind farms under uncertainty*, E.Halvorsen-Weare, SINTEF Ocean	*Results of a comparative risk assessment of different substructures for floating offshore wind turbines*, R. Proskovics, ORE Catapult
09.30	*Optimizing Jack-up vessel strategies for offshore wind farms*, M. Stålhane, NTNU	*Conceptual optimal design of jackets, K. Sandal, DTU*
09.50	*Short-Term Decision Optimisation for Offshore Wind Farm Maintenance*, C. Stock-Williams, ECN	*Fatigue behaviour of grouted connections at different ambient conditions and loading scenarios*, A. Raba, ForWind – Leibniz University Hannover
10.10	*Improved short term decision making for offshore wind farm vessel routing*, R. Dawid, Strathclyde University	*Analysis of experimental data: The average shape of extreme wave forces on monopile foundations*, S. Schløer, DTU Wind Energy
10.30	Refreshments	
	D2) Operations & maintenance (cont.)	**E2) Installation and sub-structures (cont.)**
11.00	*Experience from RCM and RDS-PP coding for offshore wind farms*, R.Sundal, Maintech	*Fatigue Crack Detection for Lifetime Extension of Monopile-based Offshore Wind Turbines*, L. Ziegler, Ramboll
11.20	*Enhance decision support tools through an improved reliability model*, S. Faulstich, Fraunhofer IWES	*Fabrication and installation constraints for floating wind and implications on current infrastructure and design*, D. Matha, Ramboll
11.40	*Technology for a real-time simulation-based system monitoring of wind turbines*, D. Zwick, Fedem Technology/SAP SE	*TELWIND- Integrated Telescopic tower combined with an evolved spar floating substructure for low-cost deep water offshore wind and next generation of 10 MW+ wind turbines*, B. Counago, ESTEYCO SAP
12.00	Closing by Chair	Closing by Chair
12.05	Lunch	
	B1) Grid connection and power system integration Chairs: Prof Kjetil Uhlen, NTNU Prof Olimpo Anaya-Lara, Strathclyde University	**G1) Experimental Testing and Validation** Chairs: Tor Anders Nygaard, IFE Ole David Økland, MARINTEK, Amy Robertson, NREL
13.05	Introduction by Chair	Introduction by Chair
13.10	*HVDC-connection of Large Offshore Wind Farms Using a Low-Cost Hybrid Converter*, I. Haukaas, NTNU	Model testing of a floating wind turbine including control, F. Savenije, ECN
13.35	*Generator Response Following as a Primary Frequency Response Control Strategy for VSC-HVDC Connected Offshore Windfarms*, R. McGill, NTNU	*The Tripple Spar campaign: Model tests of a 10MW floating wind turbine with waves, wind and pitch control*, H. Bredmose, DTU
13.55	*Scale models of Modular Multilevel Converters*, K. Ljøkelsøy, SINTEF Energi	*Validation of a time-domain numerical approach for determining forces and moments in floaters by using measured data of a semi-submersible wind turbine model test*, C. Luan, NTNU
14.15	*Experimental validation of high definition modular multilevel converter*, R. Torres-Olguin, SINTEF Energi AS	*Nacelle Based Lidar Measurements for the Characterisation of the Wake on an Offshore Wind Turbine under Different Atmospheric Conditions*, D. Trabucchi, University of Oldenburg
14.35	Refreshments	
	B2) Grid connection and power system integration (cont.)	**G2) Experimental Testing and Validation (cont.)**
15.05	*Strategies towards an Efficient future North Sea Energy Infrastructure (SENSEI),* F. Papathanasiou, ECN	*Testing philosophies for floating wind turbines in coupled model tests,* E.L. Walter, DNV GL
15.25	*A hybrid wind-diesel-battery system for fish farming applications*, M. Holt, NTNU	*On the impact of non-Gaussian wind statistics on wind turbines – an experimental approach,* J. Schottler, ForWind – University of Oldenburg
15.45	*Assessing the impact of sampling and clustering techniques on offshore grid expansion planning*, P. Härtel, Fraunhofer IWES	*Wind Tunnel Wake Measurements of Floating Offshore Wind Turbines*, I. Bayati, Politecnico di Milano
16.05	*Multistage grid investments incorporating uncertainty in offshore wind development – A North Sea case study*, H. Svendsen, SINTEF	*Lidars for Wind Tunnels – an IRPWind Joint Experiment Project, M. Sjöholm*, DTU Wind Energy
16.25	Closing by Chair	Closing by Chair
16.30	Refreshments	
17.00	Poster session	
19.00	Conference dinner	

Thursday 19 January

17.00 **Poster Session with refreshments**

Session A

1. *Power quality studies of a Stand-Alone Wind Powered Water Injection System without Physical Inertia, A. Gaugstad, NTNU*
2. *Multibody Analysis of Floating Offshore Wind Turbine System, Y. Totsuka, Wind Energy Institute of Tokyo Inc.*
3. *Winglet Design for Wind Turbine Application, F. Mühle, NMBU*
4. *Investigation of design driving load cases for floating VAWT with pitched blades, F. Savenije, ECN*
5. *SKARV – Preventing bird strikes through active control of wind turbines, K. Merz, SINTEF Energi AS*
6. *An elemental study of optimal wind power plant control, K. Merz, SINTEF Energi AS*

Session B

7. *Inertia Response from HVDC connected Full Converter Wind Turbines, J. Ødegård, Statnett*
8. *Investigation of power sharing solutions for offshore wind farms connected by diode rectifier for HVDC grid, I. Flåten, NTNU*
9. *Offshore Wind Power Plants with 66 kV Collection Grids – Study of Resonance Frequencies, A. Holdyk, SINTEF Energi*
10. *Grid Integration of offshore wind farms using a hybrid composed by an MMC with an LCC-based transmission system*, R. Torres-Olguin, SINTEF Energi
11. *Review of Investment Model Cost Parameters for VSC HVDC Transmission Infrastructure*, T.K. Vrana, SINTEF Energi

Session C

12. *Meteorological Phenomena Influences on Offshore Wind Energy, S. Ollier, Loughborough University*
13. *Availability of the OBLO infrastructure for wind energy research in Norway, M. Flügge, CMR*
14. *Demonstrating the improved performance of an Ocean-Met model using bi-directional coupling, A. Rasheed, SINTEF ICT*
15. *A comparison of short-term weather forecast with the measured conditions at the Hywind Demo site, L. Sætran, NTNU*

Session D

16. *Diagnostic monitoring of drivetrain in a 5-MW spar type floating wind turbine using frequency domain analysis, M. Ghane, NTNU*
17. *Risk-based planning of operation and maintenance for offshore wind farms, M. Florian, Aalborg University*
18. *Improving fatigue load estimation of wind turbines using a neural network trained with short-duration measurements, J. Seifert, University of Oldenburg*
19. *Recommended practices for wind farm data collection and reliability assessment for O&M optimization, T. Welte, SINTEF Energi*
20. *Integration of Degradation Processes in a Strategic Offshore Wind Farm O&M Simulation Model, T. Welte, SINTEF Energi*
21. *Experiences from Wind Turbine Pilot Test of a Remote Inspection System, Ø. Netland, NTNU*
22. *A Framework for Reliability-based Controller Scheduling in Offshore Wind Turbines, J-T H. Horn, NTNU*
23. *End-of-Life Management and Life Extension Decision Making for Offshore Wind Turbines, M. Shafiee, Cranfield University*
24. *Key performance indicators for wind farm operation and maintenance, H. Seyr, NTNU*
25. *Optimization of data acquisition in wind turbines with data-driven conversion functions for sensor measurements, L. Colone, DTU Denmark*

Session E

26. *Design and Fatigue Analysis of Monopile Foundations to Support the DTU 10 MW Offshore Wind Turbine, J.M Velarde, NTNU*
27. *Conceptual optimal design of jackets, K. Sandal, DTU*
28. *Design load basis of a 10MW floating wind turbine: substructure modelling effects, M. Borg, DTU Wind Energy*
29. *New Foundation Models for Integrated Analyses of Offshore Wind Turbines, A.M. Page, NTNU*
30. *Damage assessment of floating offshore wind turbines using latin hypercube sampling, K. Müller, University of Stuttgart*
31. *Development and validation of an engineering model for floating offshore wind turbines, A.Pegalajar-Jurado, DTU Wind Energy*
32. *Improved estimation of extreme wave loads on monopiles using First Order Reliability Method, A. Ghadirian, DTU*
33. *A 3D fem model for wind turbines support structures, C. Molins, Universitat Politecnica de Catalunya*
34. *Fully integrated load analysis included in the structural reliability assessment of a monopile supported offshore wind turbine, J. Peeringa, ECN*
35. *Parametric study of mesh for fatigue assessment of tubular joints using numerical methods, J. Mendoza, NTNU*
36. *Lifetime extension for large offshore wind farms: Is it enough to reassess fatigue for selected design positions? C. Bouty, NTNU*
37. *Optimization of offshore wind farm installations, S. Backe, University of Bergen*
38. *Influence of met-ocean condition forecasting uncertainties and biases on weather window predictions for offshore operations, T.Gintautas, Aalborg University*
39. *Modelling of Marine Operations in the Installation of*
40. *Offshore Wind Farms, A. Dewan, ECN*
41. *Effect of irregular second-order waves on the fatigue lifetime of a monopile based offshore wind turbine in shallow waters, F. Pierella, IFE*
42. *A review of slamming load application to offshore wind turbines from an integrated perspective, Y. Tu, NTNU*

Session F

43. *Offshore Turbine Wake Power Losses: Is Turbine Separation Significant?, P. Argyle, CREST, Loughborough University*
44. *The effect of rotational direction on the wake of a wind turbine rotor – an experimental comparison study of aligned co- and counter rotating turbine arrays, F. Mühle, NMBU*
45. *Experimental study on the optimal control of three in-line turbines, J. Bartl, NTNU*
46. *A step towards a reduced order modelling of flow characterized by wakes using Proper Orthogonal Decomposition, E. Fonn, SINTEF ICT*

47. *Explaining the Torque vs TSR curve of a 5MW NREL reference turbine, M.S. Siddiqui, SINTEF ICT*
48. *A 3D Vs 2.5D Vs 2D CFD analysis of 5MW NREL reference wind-turbine to study impact of bluff sections, M. Tabib, SINTEF ICT*
49. *Simulating Single turbine and associated wake development - comparison of computational methods (Actuator Line Vs Sliding Mesh Interface Vs Multiple Reference Frame) for an industrial scale wind turbine, M.S. Siddiqui, SINTEF ICT*
50. *Development of a hybrid Vortex Particle-Mesh Method and its application to modelling flow around aerofoils and cylinders, F.G.Fuchs, SINTEF ICT*
51. *2D VAR single Doppler LIDAR vector retrieval and its application in offshore wind energy, R. Calhoun, Arizona State University*

Session G

52. *IRPWIND ScanFlow project, C. Hasager, DTU Wind Energy*
53. *Comparison of Numerical Response Predictions for a Bottom Fixed Offshore Wind Turbine, S.H. Sørum, NTNU*
54. *Comparison of the effect of different inflow turbulences on the wake of a model wind turbine, I. Neunaber, University of Oldenburg*
55. *IRPWIND ScanFlow Public database, J.W. Wagenaar, ECN*
56. *Wind Tunnel Hybrid/HIL Tests on the OC5/PhaseII Floating System, I. Bayati, Politecnico di Milano*
57. *Comparison of simulations on the NewMexico rotor operating in yawed conditions, L. Oggiano, IFE*
58. *Reproduction of steep long crested 2D irregular waves with CDF using the VOF method, L.Oggiano, IFE*
59. *Calibration and Validation of a FAST model of the MARINTEK Hybrid Semisubmersible Experiment, G. Stewart, NTNU*
60. *The TripleSpar campaign: Implementation and test of a blade pitch controller on a scaled floating wind turbine model, W. Yu,, University of Stuttgart*
61. *A computational fluid dynamics investigation of performance of tip winglets for horizontal axis wind turbine blades, K. Sagmo, NTNU*
62. *Numerical study of irregular breaking wave forces on a vertical monopile for offshore wind turbines*, A. Aggarwal, NTNU
63. *Modelling of the Viscous Loads on a Semi-Submersible Floating Support Structure Using a Viscous-Flow Solver and Morison Formulation Combined with a Potential-Flow Solver, S. Burmester, MARIN*

Friday 20 January		
	Parallel sessions	
	X) Floating wind turbines Chairs: Tor Anders Nygaard, IFE Ole David Økland, MARINTEK, Amy Robertson, NREL	**F) Wind farm optimization** Chairs: Yngve Heggelund, CMR Henrik Bredmose, DTU Wind Energy
09.00	Introduction by Chair	Introduction by Chair
09.05	*Sensitivity Analysis of Limited Actuation for Real-time Hybrid Model Testing of 5MW Bottom-fixed Offshore Wind Turbine*, M. Karimirad, MARINTEK	*Influence of turbulence intensity on wind turbine power curves*, L.M. Bardal, NTNU
09.25	*OC5 Project Phase II: Validation of Global Loads of the DeepCwind Floating Semisubmersible*, A. N. Robertson, NREL	*A test case of meandering wake simulation with the Extended-Disk Particle model at the offshore test field Alpha Ventus*, J. Trujillo, University of Oldenburg
09.45	*Joint industry project on coupled analysis of floating wind turbines,* L. Vita, DNV GL	*A comprehensive multiscale numerical framework for wind energy modelling,* A. Rasheed, SINTEF ICT
10.05	*Using FAST for the design of a TLP substructure made out of steel reinforced concrete composite components*, P. Schünemann, University of Rostock	*Application of a Reduced Order Wind Farm Model on a Scaled Wind Farm,* J. Schreiber, Technische Universität München
10.25	Closing by Chair	Closing by Chair
10.30	Refreshments	
	Closing session – Strategic Outlook Chairs: John Olav Tande, SINTEF/NOWITECH and Trond Kvamsdal, NTNU/NOWITECH	
11.00	Introduction by Chair	
11.05	*ETIP wind Strategic Research and Innovation Agenda*, Aidan Cronin, Siemens Wind Power	
11.35	*Bringing trust to the Internet of Things – When valuable insights can be gained from data to support critical decisions in industry, issues such as the quality and integrity of the data has to be included in the risk picture*, M.R. de Picciotto, S. George, DNV GL	
12.05	*A new approach for going offshore,* Frank Richert, SkyWind	
12.35	Poster awards and closing	
13.00	Lunch	

Side event: IEA OC5 meeting 10.45 – 17.30

EERA DeepWind'2017 Conference, 18 – 20 January 2017, Radisson Blu Royal Garden hotel, Trondheim

Last name	First name	Institution
Adaramola	Sam	Norwegian University of Life Sciences
Aggarwal	Ankit	NTNU
Ágústsson	Hálfdán	Kjeller Vindteknikk
Anaya-Lara	Olimpo	Strathclyde University
Andersen	Håkon	Dr.techn. Olav Olsen
Argyle	Peter	CREST, Loughborough University
Armando	Alexandre	DNV GL
Bachynski	Erin	NTNU
Backe	Stian	Universitetet i Bergen
Bakhoday Paskyabi	Mostafa	Geophysical Institute
Bardal	Lars Morten	NTNU
Bartl	Jan	NTNU
Bayati	Ilmas	Politecnico di Milano
Belloli	Marco	Politecnico di Milano
Berthelsen	Petter Andreas	SINTEF Ocean
Bischoff	Oliver	University of Stuttgart
Bjørdal	Thomas	Nasjonalt Vindenergisenter AS
Bolstad	Hans Christian	SINTEF Energi AS
Borg	Michael	DTU Wind Energy
Bouty	Corantin	Supméca - Institut Supérieur de Mécanique de Paris
Bozonnet	Pauline	IFPEN
Bredmose	Henrik	DTU Wind Energy
Burmester	Simon	MARIN (Maritime Research Institute Netherlands)
Busmann	Hans Gerd	Fraunhofer IWES
Busturia	Jesús M.	NAUTILUS Floating Solutions, S.L.
Cai	Jifeng	China General Certification
Calhoun	Ronald	Arizona State University
Chabaud	Valentin	NTNU
Cheng	Zhengshun	NTNU
Cheynet	Etienne	University of Stavanger
Collu	Maurizio	Cranfield University
Colone	Lorenzo	Technical University of Denmark
Cronin	Aidan	Siemens Wind Power
Dawid	Rafael	Strathclyde University
De Picciotto	Marte	DNV GL
Desmond	Cian	University College Cork - MaREI
Dewan	Ashish	ECN
Eecen	Peter	ECN
Eliassen	Lene	NTNU
Faulstich	Stefan	Fraunhofer IWES
Favre	Mathieu	IDEOL

Last name	First name	Institution
Ferriday	Thomas	NTNU
Feyling	Ingrid	Research Network for Sustainable Energy at UIS/IRIS
Florian	Mihai	Aalborg University
Flügge	Martin	Christian Michelsen Research AS
Flåten	Ida	NTNU
Fonn	Eivind	SINTEF
Frøysa	Kristin Guldbrandsen	NORCOWE
Fu	Pengcheng	China General Certification
Furevik	Birgitte Rugaard	met.no
Gao	Zhen	NTNU
Gaugstad	Alexander	NTNU
George	Scott	DNV GL
Ghadirian	Amin	DTU
Ghane	Mahdi	NTNU
Goeing	Jan	NTNU
Gueydon	Sebastien	MARIN
Halvorsen-Weare	Elin Espeland	SINTEF Ocean
Hasager	Charlotte	DTU Wind Energy
Haukaas	Inga	NTNU
Heggelund	Yngve	CMR
Holdyk	Andrzej	SINTEF Energi AS
Holt	Marius	NTNU
Horn	Jan-Tore	NTNU AMOS
Huijs	Fons	GustoMSC
Härtel	Philipp	Fraunhofer IWES
Høegh Sørum	Espen	NTNU
Jakobsen	Jasna Bogunovic	University of Stavanger
Jamieson	Peter	University of Strathclyde
Jensen	Bjarne	DHI
Johansen	Bjørn	Statoil
Jonkman	Jason	NREL
Karimirad	Madjid	SINTEF Ocean
Karl	Christian	ForWind - Leibniz Universität Hannover
Kelberlau	Felix	NTNU
Koppenol	Boy	Ventolines BV
Koreman	Debbie	NTNU
Krokstad	Jørgen	Fugro Norge AS/NTNU
Kvamsdal	Trond	NTNU
Lacas	Pierre Paul	STX France Solutions
Lindal	Ask Ibsen	NTNU
Ljøkelsøy	Kjell	SINTEF Energi AS
Lorenzo	Counago	Esteyco SAP
Luan	Chenyu	NTNU

Last name	First name	Institution
Madlener	Anna	NTNU
Madsen	Peter Hauge	DTU Wind Energy
Malmo	Oddbjørn	Kongsberg Maritime AS
Matha	Denis	Ramboll
McGill	Ryan	NTNU
Mendoza	Jorge	NTNU
Merz	Karl	SINTEF Energi AS
Metlid	Mathias	NTNU
Molins	Climent	Universitat Politècnica de Catalunya (UPC)
Mueller	Kolja	University of Stuttgart
Muskulus	Michael	NTNU
Mühle	Franz	University of Life Science (NMBU)
Nejad	Amir	NTNU
Netland	Øyvind	NTNU
Neunaber	Ingrid	University of Oldenburg, ForWind
Nielsen	Finn Gunnar	University of Bergen
Nygaard	Tor Anders	IFE
Oggiano	Luca	IFE
Ollier	Sarah	Loughborough University
Opoku	Hilde	Deputy Mayor
Ormberg	Harald	Sintef Ocean
Page	Ana	NTNU
Papathanasiou	Fotis	Energy research Centre of the Netherlands
Peeringa	Johan	Energy research Centre of the Netherlands
Pegalajar-Jurado	Antonio	DTU Wind Energy
Pierella	Fabio	IFE
Popko	Wojciech	Fraunhofer IWES
Preede Revheim	Pål	Nasjonalt Vindenergisenter AS
Proskovics	Roberts	The Offshore Renewable Energy Catapult
Qvist	Jacob	4subsea
Raba	Alexander	Leibniz Universität Hannover
Rasheed	Adil	SINTEF Digital
Richert	Frank	SkyWind
Robertson	Amy	NREL
Rodriguez	Raul	Fundacion Tecnalia
Ruud Hagen	Torbjørn	OWEC Tower AS
Sagmo	Kristian	NTNU
Sandal	Kasper	DTU Wind
Savenije	Feike	Energy research Center of the Netherlands
Schafhirt	Sebastian	NTNU
Schløer	Signe	Technical University of Denmark
Schottler	Jannik	ForWind - University of Oldenburg
Schreiber	Johannes	Technical University of Munich

Last name	First name	Institution
Schünemann	Paul	University of Rostock
Seifert	Janna	ForWind - Carl von Ossietzky University of Oldenburg
Seyr	Helene	NTNU
Shin	Hyunkyoung	University of Ulsan
Shirzadeh	Rasoul	ForWind-Center for Wind Energy Research
Siddiqui	Muhammad Salman	NTNU
Sjöholm	Mikael	DTU Wind Energy
Smilden	Emil	NTNU AMOS
SMITH	MATT	ZEPHIR LTD
Sørum	Stian	NTNU
Stenbro	Roy	IFE
Stewart	Gordon	NTNU
Stock-Williams	Clym	ECN
Stålhane	Magnus	NTNU
Sundal	Roger	Maintech
Svendsen	Harald	SINTEF Energi AS
Sætran	Lars	NTNU
Tabib	Mandar	SINTEF
Tande	John Olav	SINTEF Energi AS
Thomassen	Paul	Simis AS
Torres Olguin	Raymundo	SINTEF Energi AS
Totsuka	Yoshitaka	Wind Energy Institute of Tokyo Inc.
Trabucchi	Davide	University of Oldenburg
Trujillo	Juan José	ForWind - University of Oldenburg
Tu	Ying	NTNU
Tveiten	Bård Wathne	SINTEF Ocean
Uhlen	Kjetil	NTNU
Van Bussel	Gerard	Tu Delft
Van der Zee	Tjeerd	WMC
Velarde	Joey	COWI A/S - Denmark
Vita	Luca	DNV GL
Vittori	Felipe	Fundación CENER - CIEMAT
Vrana	Til Kristian	SINTEF Energi AS
Wagenaar	Jan Willem	ECN
Walter	Erik Løkken	DNV GL
Welte	Thomas	SINTEF Energi AS
Yu	Wei	University of Stuttgart
Zakariyya	Ksenia	NTNU
Ziegler	Lisa	Ramboll
Zwick	Daniel	Fedem Technology AS
Ødegård	Jon	Statnett SF
Økland	Ole David	SINTEF Ocean

SINTEF

3 Scientific Committee and Conference Chairs

An international Scientific Committee is established with participants from leading institutes and universities. These include:

Agustsson, Halfdan, MET
Anaya-Lara, Olimpo, Strathclyde
Busmann, Hans-Gerd, Fraunhofer IWES
Eecen, Peter, ECN
Faulstich, Stefan, Fraunhofer IWES
Furevik, Birgitte, R., MET
Jørgensen, Hans Ejsing, DTU
Kvamsdal, Trond, NTNU
Leithead, William, Strathclyde
Lekou, Denja, CRES
Madsen, Peter Hauge, DTU
Merz, Karl, SINTEF Energi AS
Moan, Torgeir, NTNU
Muskulus, Michael, NTNU
Nielsen, Finn Gunnar, Statoil/UiB
Nygaard, Tor Anders, IFE
Reuder, Joachim, UiB
Robertson, Amy, NREL
Rohrig, Kurt, Fraunhofer IWES
Sempreviva, Anna Maria, CNR
Tande, John Olav, SINTEF Energi AS / NOWITECH
Thomsen, Kenneth, DTU Wind Energy
Uhlen Kjetil, NTNU
Van Bussel, Gerard, TU Delft
Welte, Thomas, SINTEF Energi AS
Økland, Ole David, MARINTEK

The Scientific Committee will review submissions and prepare the programme. Selection criteria are relevance, quality and originality.

The conference chairs were:

- John Olav Giæver Tande, Director NOWITECH, Chief scientist, SINTEF Energi AS
- Trond Kvamsdal, Chair NOWITECH Scientific Committee, Professor NTNU
- Michael Muskulus, vice-chair NOWITECH Scientific Committee, Professor NTNU

Opening session – Frontiers of Science and Technology

Welcoming note by Deputy Mayor Hilde Opoku

Progress in offshore wind research and innovation, John Olav Tande, director NOWITECH

European wind research cooperation - Peter Hauge Madsen, DTU

NORCOWE – highlights and future challenges, Kristin Guldbrandsen Frøysa,
director NORCOWE

HyWind Scotland, Bjørn Johansen, Statoil

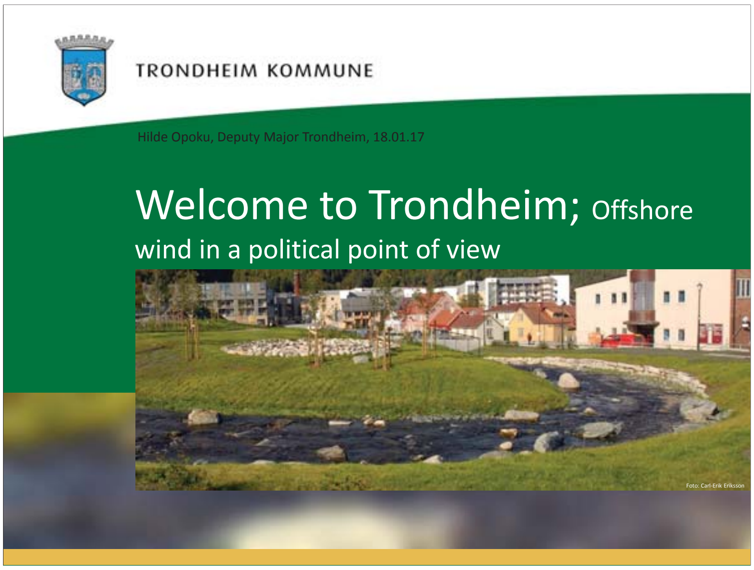
TRONDHEIM KOMMUNE
Hilde Opoku, Deputy Major Trondheim, 18.01.17
Welcome to Trondheim; Offshore wind in a political point of view

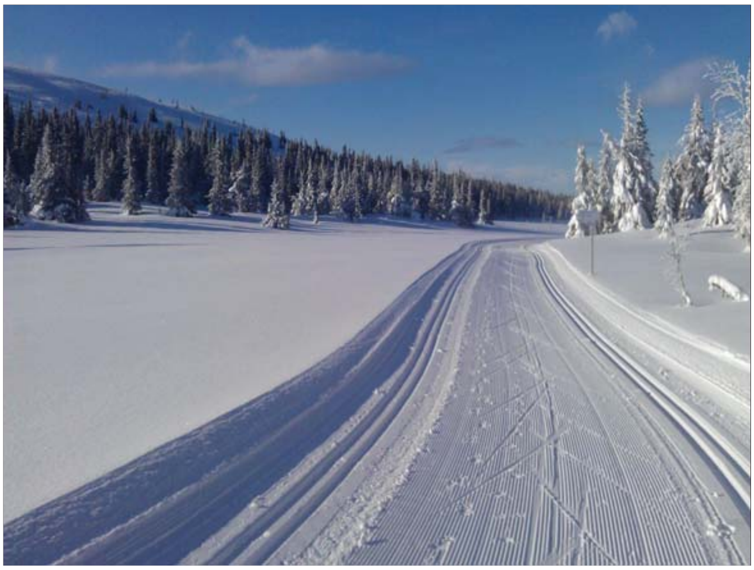


Technology capital


Wood city Trondheim

New buildings andrehabilitation

Åsveien skole
50% redusert CO_2 utslipp i et livssyklusperspektiv
Tre lagrer CO_2, Energieffektivt, Klimatilpasning

The emerging reality

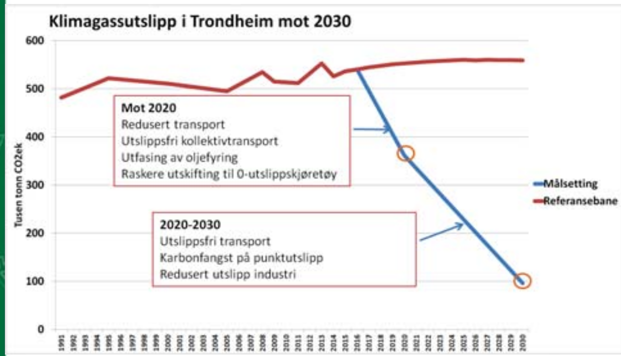

Eco-Schools

Trøndelag, the green battery of Europe?

Miljøpakken

Since 2010:

- 33 % more transportation on bike
- 8 % more transportation on walking
- 38 % more public transportation
- 11 % car transportation

Foto: Knut Oppeide

Planning for success in climate policy

- We are facing an energy revolution!
  - But we are lacking real political ambitions
  - **All** emissions must be eliminated
  - **All** use of fossil energy must stop
  - EU is still lagging behind

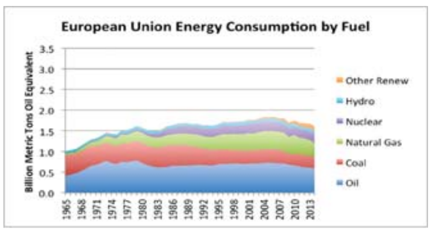

No time to waste, the carbon budget will be drained in less than 10 years.

No. of years worth of current emissions remaining in the carbon budget

	< 1.5C	< 2C	< 3C
66%	6.0	20.9	55.7
50%	9.8	28.4	65.6
33%	17.2	33.3	76.8

Calculations by Carbon Brief based on data contained in the IPCC AR5 Synthesis Report

- We need governments and businesses to start planning for success.

Foto: Vegard Eggen

Political measures

1. Demonstration plants for offshore wind to build the supply industry

2. Utilize Statkraft or establish other ways of government involvement

Norwegian opportunities in offshore wind: Two strategies

1.Build Norwegian supply industry
- Skills and competence from offshore petroleum sector
- Need active and supporting policies and political will

2. Floating wind power in Norwegian waters
- Could be realistic in the longer term

EERA DeepWind'2017

Progress in offshore wind research and innovation

John Olav Giæver Tande
Director NOWITECH
Chief Scientist / Research Manager
SINTEF Energy Research
John.tande@sintef.no

Exciting development of floating wind

Offshore wind is vital for reaching climate targets

- ✓ Currently small compared to onshore wind, but in strong growth
- ✓ Potential to supply 192 800 TWh/y, i.e. ~8 times the global el generation in 2014
- ✓ Can be deployed in proximity to big urban centres
- ✓ Provide long-term security of supply of clean energy
- ✓ Create new employment and industries
- ✓ Low negative environmental impact (WWF)

Stern Review (2006): ..strong, early action on climate change far outweigh the costs of not acting.

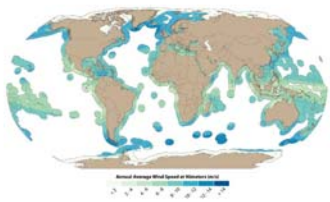

Arent, D. et al (2012) Improved Offshore Wind Resource Assessment in Global Climate Stabilization Scenarios. Technical Report. NREL/TP-6A20-55049

Moving towards an North-Sea offshore grid


Dolwin beta (ABB 2015)

A great science and engineering challenge!

Offshore wind is approaching grid parity

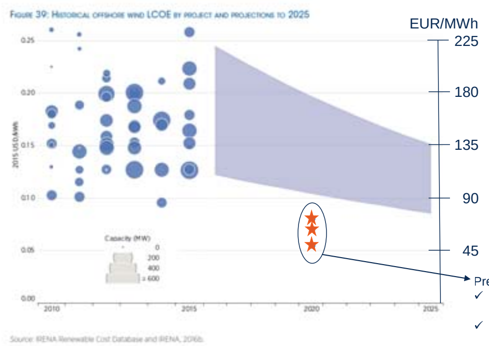

Press releases:
- ✓ 72.7 EUR/MWh; Borssele NL, 700 MW, Dong, 5 July 2016
- ✓ 63.8 EUR/MWh; Vesterhav DK, 350 MW, Vattenfall, 12 Sep 2016
- ✓ 49.9 EUR/MWh; Kriegers Flak DK, 600 MW, Vattenfall, 9 Nov 2016

http://www.irena.org/DocumentDownloads/Publications/IRENA_Power_to_Change_2016.pdf

NOWITECH in brief

- A joint pre-competitive research effort
- Focus on deep offshore wind technology (+30 m)
- Budget (2009-2017) EUR 40 millions
- Co-financed by the Research Council of Norway, industry and research partners
- 25 PhD/post doc grants
- Key target: innovations reducing cost of energy from offshore wind
- Vision:
  - large scale deployment
  - internationally leading

Research partners:
- SINTEF Energy (host)
- IFE
- NTNU
- MARINTEK
- SINTEF ICT
- SINTEF MC

Industry partners:
- CD-adapco
- DNV GL
- DONG Energy
- Fedem Technology
- Fugro OCEANOR
- Kongsberg Maritime
- Norsk Automatisering
- Statkraft
- Statoil

Associated research partners:
- DTU Wind Energy
- Michigan Tech Uni.
- MIT
- NREL
- Fraunhofer IWES
- Uni. Strathclyde
- TU Delft
- Nanyang TU

Associated industry partners:
- Devold AMT AS
- Energy Norway
- Enova
- Innovation Norway
- NCEI
- NORWEA
- NVE
- Wind Cluster Norway

40 innovations in progress

NOWITECH focus

Offshore wind LCOE

Offshore wind has cost reduction opportunities in multiple areas including scale effects

Turbines & plant | Substructures | Transmission | O&M

- Larger turbines and wind farms
- Increased reliability
- Scale effects and industrialisation

- Standardised and optimised offshore foundation design and design criteria
- Industrialised manufacturing

- eBoP optimisation of substation and transmission capex
- Innovative transmission solutions
- Improved grid access

- Low OPEX drivetrains
- Turbine and component quality
- Condition monitoring, diagnostics, preventive maintenance

Source: Siemens, MHI-Vestas, MAKE

Results are migrating to commercial use

- ✓ A total of 40 results are assigned a Technology Readiness Level (TRL)
- ✓ The results include new methods, software tools and hardware products
- ✓ The results are migrating to commercial use, licence agreements, and business developments providing value creation and cost reductions.

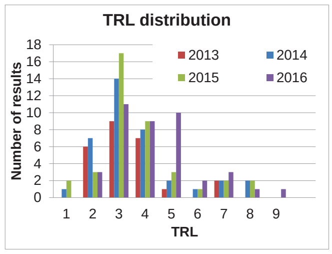

NOWITECH Innovation Award 2016: Thomas Sauder, Erin Bachynski, Maxime Thys, Valentin Chabaud and Lars Ove Sæther (not present), all NTNU/MARINTEK, for their work on real-time hybrid model testing of offshore wind turbines.

NOWITECH is producing excellent results


Successful innovations


Excellence in research


Strong educational program

An attractive partner on the international scene

- Active in EERA, ETIPwind, EAWE, IEA, IEC
- Heading offshore works within EERA JPwind
- Steering Committee member of ETIPwind
- Partner in EU projects, e.g.: Twenties (2009-), DeepWind (2010-), HiPRWind (2010-), EERA-DTOC (2012-), InnWind (2012-), WindScanner (2012-), LeanWind (2014-), EERA IRP wind (2014-), BestPaths (2014-) , Lifes50+ (2015-), AWESOME (2015-), + more in preparation!

LIFES50+ | Best Paths | EERA European Energy Research Alliance WIND ENERGY

Life after NOWITECH?

- ✓ Will be great ☺
- ✓ Excellent project portfolio
- ✓ Strong continued engagement
- ✓ Generating new knowledge, tools and innovations making offshore wind better
- ✓ Creating value for clients and society as a whole
- ✓ Contribute to reaching climate targets

13

NOWITECH Norwegian Research Centre for Offshore Wind Technology

NOWITECH Norwegian Research Centre for Offshore Wind Technology

OPWIND (2017-2020)

To develop knowledge and tools for optimized operation and control of wind power plants, reducing costs and increasing profitability.

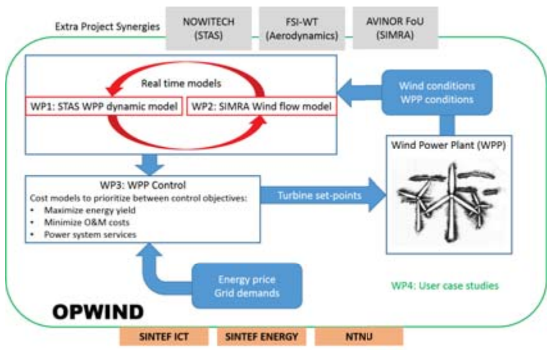

14

New knowledge building project granted by the Research Council of Norway

And now, a moment of zen ☺

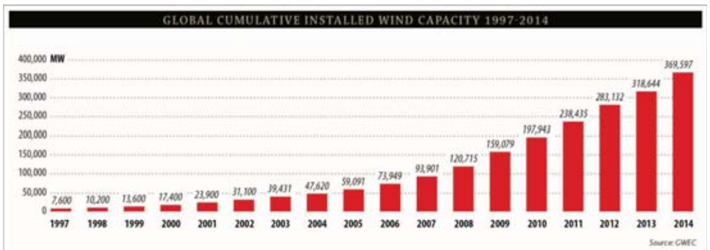

NOWITECH Norwegian Research Centre for Offshore Wind Technology

European Wind Research Cooperation

Peter Hauge Madsen
Head of DTU Wind Energy
Head of EERA JP WIND

EERA DeepWind 2017
Trondheim 18 Jan 2017

DTU Wind Energy
Department of Wind Energy

There is political support for offshore wind

- Energy Cooperation between the North Sea countries
- EU "winter package" including renewables directive
- SET-Plan priorities for Offshore Wind Energy

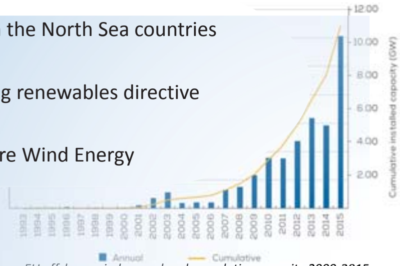

EU offshore wind annual and cumulative capacity 2000-2015, source: ETIPWIND SRIA 2016

"I want Europe's Energy Union to become the world number one in renewable energies."

Jean-Claude Juncker, President of the European Commission

The industry is breaking the records for prices of offshore KwH

World records...

..on time


New record for cheapest offshore wind farm

World's Cheapest Offshore Wind Farm Seen Online Early

Already beating the targets defined in the SET-Plan offshore strategy in January 2016:
- ✓ **less than 10 ct€/kWh by 2020** and to
- **less than 7ct€/kWh by 2030**;

Europe is the worlds No. 1 in offshore Wind energy

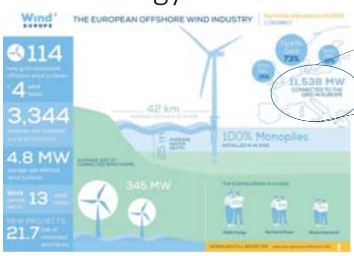

11,5MW Grid-connected by H1 2016

98GW by 2030

WindEurope target in scenario for 2030

So,

how do we as the European R&D community enable Europe to reach the targets for offshore wind energy deployment 2030?

What objectives do we pursue?

EERA

ETIPWind objectives

EERA JP WIND agrees

EERA

What are our challenges?

Increase collaboration
- Access to data

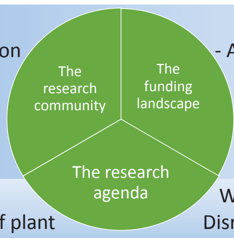

- A funding system creating a new valley of death
- Lack of commitment to long term R&D strategies

Floating
Balance of plant
Environmental impact
Wake and loads
Disruption
Social acceptance

EERA

We can reduce costs….

…facilitate system integration…

…and educate first-class human resources

EERA

EERA JP WIND a vehicle to collaborate

EERA JP WIND

- An organisation under the EU SET-Plan
- 49 member organisations
- Building trust & knowledge exchange
- Major EU projects setup through EERA JP WIND collaboration
- IRPWIND project supporting JP WIND coordination and research

EERA

But to make sure that this benefits Europe we need to reinforce European technological leadership

EERA

EERA JP WIND medium to long term strategy for offshore wind energy

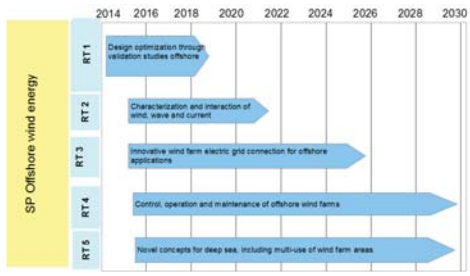

IRPWIND – a stronger engine in JP WIND

Total budget: 9,8 M EUR

- 6 M EUR for CP
  - Offshore
  - Structural Reliability
  - Integration
- 4 M EUR for CSA
  - Mobility
  - Research Infrastructure
  - Secretariat, management

+ new initiatives on open data and institutional collaboration

Nationally funded collaborative projects

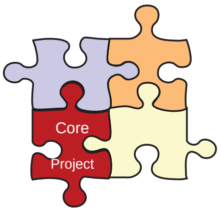

We have 1 year left of IRPWIND to develop a new and stronger EERA JP WIND

Let's collaborate

Thank you for your attention

NORCOWE –highlights and future challenges

Kristin Guldbrandsen Frøysa
Christian Michelsen Research(CMR) and UiB
Director NORCOWE
kristin@cmr.no

Improve production.
An effort across scales and disciplines.

Mesoscale	Park scale	Rotor scale	Blade scale
10000 -10 km Days -Hours	10 -1 km 20 min - 20 sec	200 - 50m 10 – 2 sec	5 - .5m 0.5 – 0.01 sec

Factor O(20*E06) on time and length scale

What is the our key challenge?

- Levelized cost of electricity (LCOE)!

$$LCOE = \frac{\sum_{t=1}^{n} \frac{I_t + M_t}{(1+r)^t}}{\sum_{t=1}^{n} \frac{E_t}{(1+r)^t}}$$

t : Year number
n : Lifetime of project (years)
I_t : Investments
M_t: O&M costs
E_t : Energy produced
r : Discount rate

- What are the most important terms?

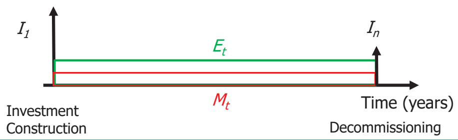

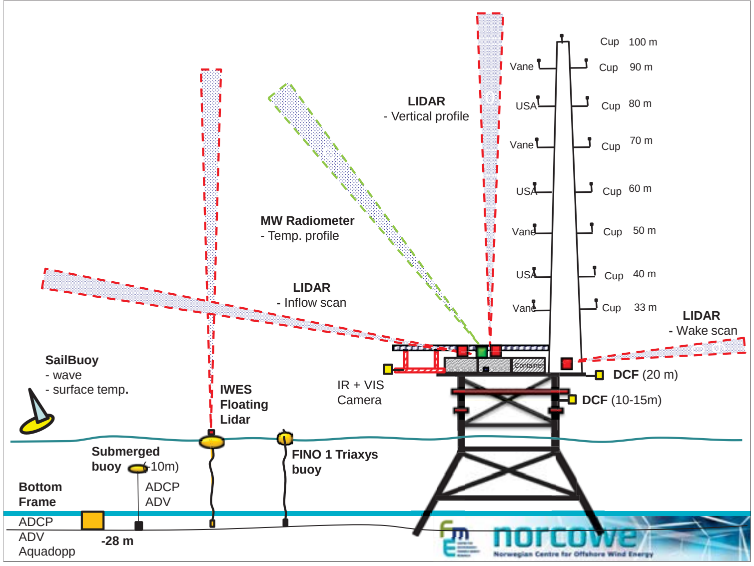

Why NORCOWE?

- Mobilize new Norwegian research groups to address offshore wind (CMR, UiA, UiB, UiS, Uni Research)
- Help to solve current and future challenges for the offshore wind industry
- Help the industry to identify issues that need attention
- Joint effort, cooperation towards common goals
- Add value to the partners: Coordination, network and marketing

---

LiDAR scan pattern at OBLEX-F1

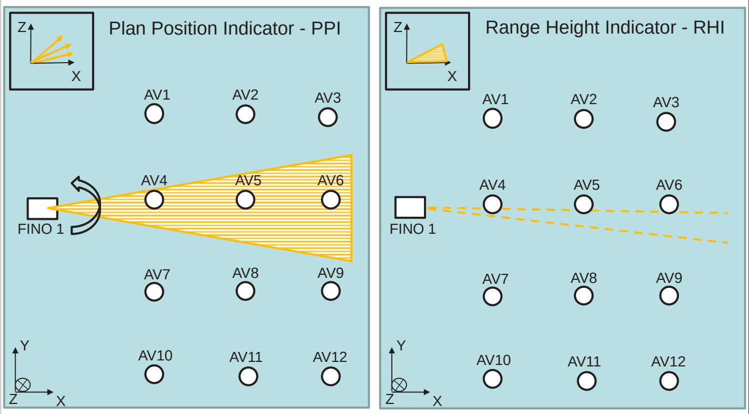

Scanning LiDAR - PPI

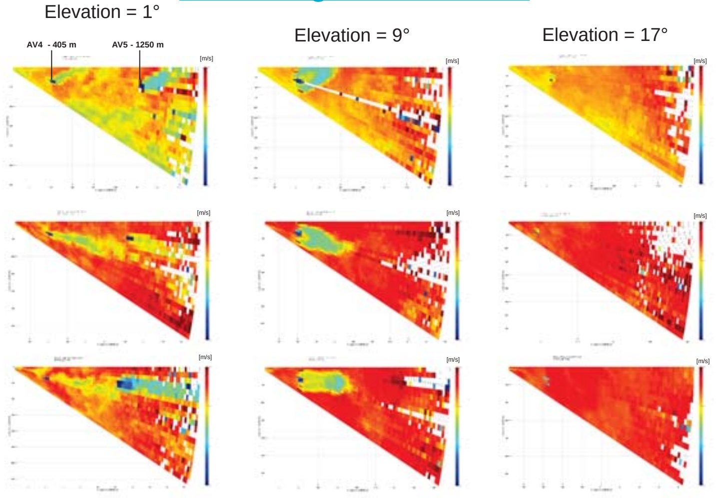

Optimized design and operation. Wind and waves key drivers

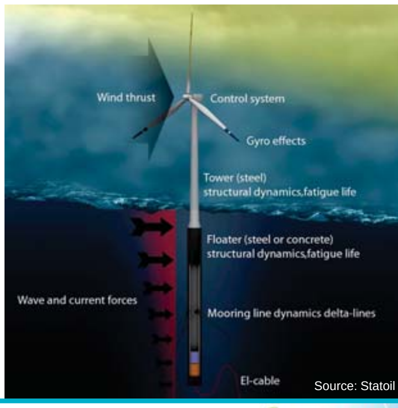

Scanning LiDAR - RHI

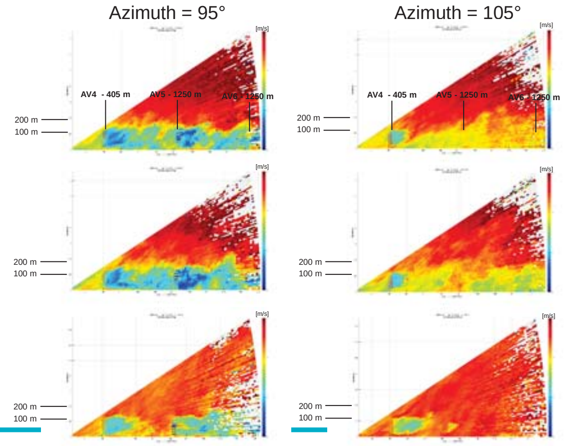

Towards the optimum O&M strategy

- Integrating load estimates, condition monitoring and failure estimates into reliability based O&M strategies.
- Reduce O&M costs
- Improve capacity factor
- Increase lifetime

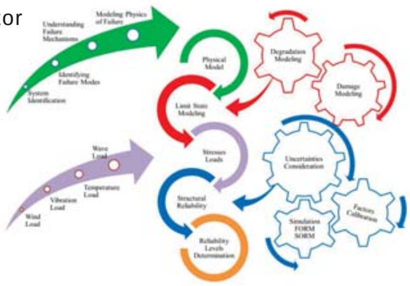

Courtesy: John Dalsgaard Sørensen, AAU

Web based data portal for OBLEX-F1

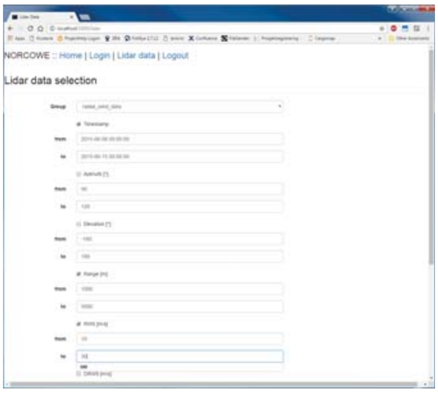

The reference wind farm – a platform for testing tools

- Optimum Wind farm design and operation
- Rules for farm design and operation
- Site wind and wave climatologies
- Levelised cost of energy
- https://rwf.computing.uni.no/

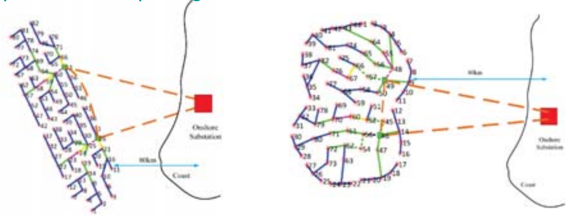

The Motion Lab at UiA – An integrating platform

- Instruments on moving platform
- Concepts for access
- Operation and maintenance

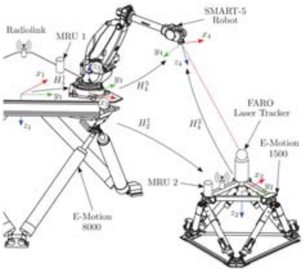

5 Static lidar wind profilers

3 Leosphere WindCube v1
1 Leosphere WindCube v2 866 (motion compensated)
1 Natural Power ZepIR 300

- Profiles of wind speed, wind direction and turbulence intensity between ca. 20 and 300 m above ground
- Vertical resolution 20 m
- Typical applications:
  - Inflow conditions
  - Site characterization
  - Average characteristics of single turbine wakes

Motion-Lab: Investments

- Funding through NORCOWE: ~ 4 MNOK (2010-2012)
- University of Agder (Building): ~ 10 MNOK (2012-2013)
- Research Council Infrastructure Funding: ~ 8 MNOK (2015)
- University of Agder (Full-time engineer): ~ 0.85 MNOK / year (2016-)

3 Scanning wind lidar systems

Leosphere WindCube 100 S

- Characterization of the wind and turbulence conditions up to a distance of 3.5 km from the instrument
- Spatial resolution 50 m
- Typical applications:
  - Inflow conditions
  - Advanced turbulence characterization (e.g. coherence)
  - 3-D structure and dynamics of wind turbine wakes
  - Investigation of wind farm wakes

OBLO infrastructure

OBLO (Offshore Boundary Layer Observatory) (http://oblo.uib.no/) advanced mobile instrumentation for field measurements of meteorological and oceanographic parameters related to offshore wind energy

2 passive microwave temperature/humidity profilers

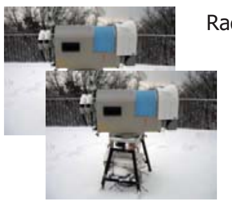

Radiometer Physics HATPRO RG4

- Temperature and humidity profiles up to ca. 5 km above ground
- Liquid water content of clouds
- Vertical resolution 50 m
- Typical applications:
  - Characterization of the stability of the atmosphere (key information for the interpretation of wind profile and wake measurements)

OBLO infrastructure - ocean

Wide range of oceanic instrumentation (sensors) and instrument platforms (bottom frames, surface and submerged buoys, drifters)

- Temperature and salinity profiles
- Current profiles
- Wave characteristics
  - Height
  - Direction
  - Frequency
- Oceanic turbulence
- Air-sea interaction

NORCOWE

The legacy of NORCOWE

- **Research Network for Sustainable Energy at UiS and IRIS**

RESEARCH AREA LEADERS

Energy efficientcy
Mohsen Assadi

Sustainable technology
Bjørn Hjertager

Green transition
Oluf Langhelle

Carbon capture, utilisation and storage (CCUS)
Ying Guo

Smart cities
Chunming Rong

- **Energy Lab at University of Bergen**
- The Energy Lab is a forum for exchange of information on research results and activities related to renewable energy and energy transition.
- The Energy Lab hosts weekly informal lunch-meetings and larger half-day seminars. These events are free of charge and open to all interested. Future events can be found in the calendar.

norcowe
Norwegian Centre for Offshore Wind Energy

The legacy of NORCOWE

NORCOWE –reducing LCOE through interdiciplinary research

norcowe
Norwegian Centre for Offshore Wind Energy

Norwegian offshore vessel providers go into offshore wind

Solstad Offshore has joined the list of offshore vessel providers in Norway that are turning to alternative markets to overcome the challenging circumstances in the offshore support vessel market.

Namely, the company informed on Friday it has entered into a contract with Dong Energy Wind Power for hire of the 2013-built construction support vessel (CSV) Rem Installer for a period of 23 months firm.

DONG Returns to Østensjø Rederi for Hornsea Project One SOV

Source: Astilleros Gondan

DONG Energy has exercised an option for a second Service Operation Vessel (SOV) at Østensjø Rederi, which once built will transfer turbine technicians to the 1.2GW Hornsea Project One wind farm.

The 81-metre long vessel will be delivered in the third quarter of 2018. She is a sister vessel to the SOV ordered by DONG Energy in October last year for the Race Bank wind farm.

The DP2 SOV has 60 single cabins which can accommodate up to 40 wind turbine technicians in addition to a marine crew of 20. The vessel will also have a motion compensated gangway system with an adjustable pedestal.

Special areas and functions of the vessel are made in accordance with the charterer's requirements. The vessel is expected to be equipped with a helideck.

The SOVs are designed by Rolls Royce in cooperation with Østensjø Rederi. Astilleros Gondan in Spain will again be the builder of the vessel.

"The new award is a further recognition of Østensjø efforts to expand our business into the renewable energy sector, following the strategy to diversify our operations. We are therefore very ... DONG Energy again has awarded us an exciting and important opportunity."
... Walland, CEO of Østensjø Rederi AS.

norcowe
Norwegian Centre for Offshore Wind Energy

The legacy of NORCOWE some examples

- LIMECS (at Stavanger Airport)
- WINTWEX-W (at Wieringermeer, ECN)
- OBLEX-F1 (FINO1)
- Shoreline
- Gwind
- Wind farm module in WRF
- OBLO
- Norwegian Motion Lab
- Science Meets Industry (Stavanger and Bergen)
- The NORCOWE network

norcowe
Norwegian Centre for Offshore Wind Energy

Hywind Scotland

Home » News » News (rightside) » Hywind Scotland

Search

Flere aspekter ved Hywind Scotland har nå i år vært presentert på NORCOWEs konferanser **Science Meets Industry** Stavanger og Bergen. Vi har samlet presentasjonene her:

Hywind Scotland - Assembly and logistics - *Hege Eskild, NorSea Group*
Mooring System for Hywind Scotland - *Jon Havik, MacGregor*
Hywind Scotland - Marine Operations - *Knut Harald Lien, Statoil*
The SCADA system for Hywind Scotland Pilot Park - *Jon Einar Skiele Handeland, Origo Solutions*
Statoil Hywind oil & gas concept including battery storage - *Rajnish Sharma, Statoil*
Hywind Scotland Pilot Park - Marine Operations - *Yngve Berstad, Technip*

News

16. 12. 2016
New laser tracker and cameras in place at the Motion Lab...
read more >>

28. 11. 2016
Hywind Scotland - samlede presentasjoner tilgjengelige...
read more >>

News archive >>

Calendar/ Upcoming Events

18. januar 2017
EERA DeepWind'2017...
read more >>

15. februar 2017
Klimafrokost...
read more >>

7. mars 2017
NORCOWE workshop on OBLEX-F1 data...
read more >>

Calendar Archive >>

NORCOWE | Phone: +47 55 57 40 40 | Fax: +47 55 57 40 41 | E-mail: post(at)norcowe.no

© NORCOWE 2010

norcowe
Norwegian Centre for Offshore Wind Energy

Offshore wind in Norway – why?

- Hywind - starting point in 2001: Power supply for oil and gas platforms
- Article from SINTEF/NTNU in 2007
- State budget 2017:

10) Stortinget ber regjeringen senest i forbindelse med statsbudsjettet for 2018 presentere en strategi for kommersiell utvikling av flytende vindmøller, som kan bidra til lønnsom elektrifisering av norsk sokkel

The possibilities
The 10 largest point emissions

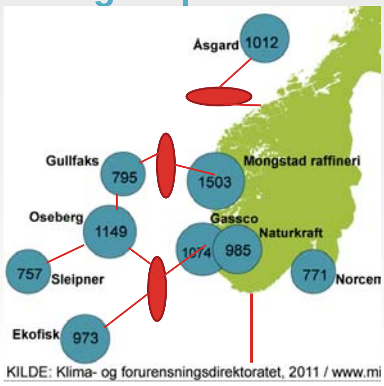

Courtesy: Finn Gunnar Nielsen, UiB

Next generation wind farms

8 MW turbins
100 turbines in a wind farm
Each farm produces 2.5-3.0 TWh

Placed close to large consumers (cities and industry)

Hydro power as balance

Job creation in a new maritime industry

Source: regjeringen.no

Courtesy: Finn Gunnar Nielsen, UiB

Wind power to private cars (W2PC)

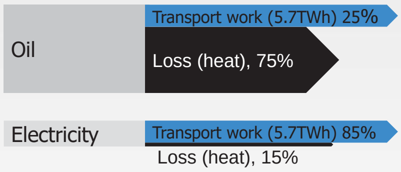

- Need 6.7 TWh/y to supply all private cars in Norway
- 2.2 GW wind power.
- Reduces emissions by 6.1 mill tons CO_2 /y. (-59%) relative to 2015, road transportation

Courtesy: Finn Gunnar Nielsen, UiB

UNIVERSITY OF BERGEN

CO_2 emissions in Norway (2015)

Source	Mill. Tons (2015)	Change since 1990 (%)
Total	**53.9**	**4.2**
Oil & gas	15.1	83.3
Industry	11.9	-39.3
Road transportation	10.3	32.6
Other	16.6	3.0

Source: SSB 13.12.16

Courtesy: Finn Gunnar Nielsen, UiB

What do we achieve?

- Achieve Norwegian emission goals (40% down from the 1990 level in 2030)
- Growth of a new wind / maritime industry
- Keep the swing producer role in Europe

Courtesy: Finn Gunnar Nielsen, UiB

Thank you for your attention!

www.norcowe.no

Statoil
Hywind Scotland
Trondheim, January 18th 2017
Classification: Internal
23 august 2015
© Statoil ASA

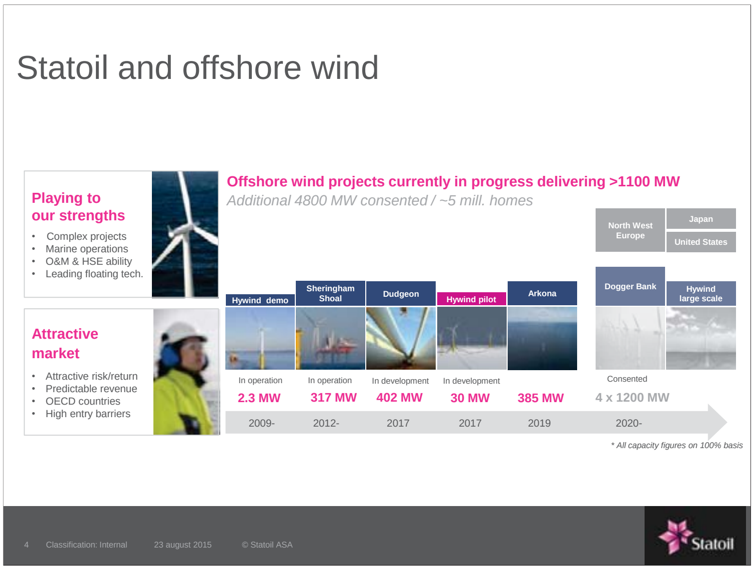

Statoil and offshore wind
Playing to our strengths
• Complex projects
• Marine operations
• O&M & HSE ability
• Leading floating tech.
Attractive market
• Attractive risk/return
• Predictable revenue
• OECD countries
• High entry barriers
Offshore wind projects currently in progress delivering >1100 MW
Additional 4800 MW consented / ~5 mill. homes
North West Europe
Japan
United States
Hywind demo
Sheringham Shoal
Dudgeon
Hywind pilot
Arkona
Dogger Bank
Hywind large scale
In operation
2.3 MW
2009-
In operation
317 MW
2012-
In development
402 MW
2017
In development
30 MW
2017
385 MW
2019
Consented
4 x 1200 MW
2020-
* All capacity figures on 100% basis
4
Classification: Internal
23 august 2015
© Statoil ASA
Statoil

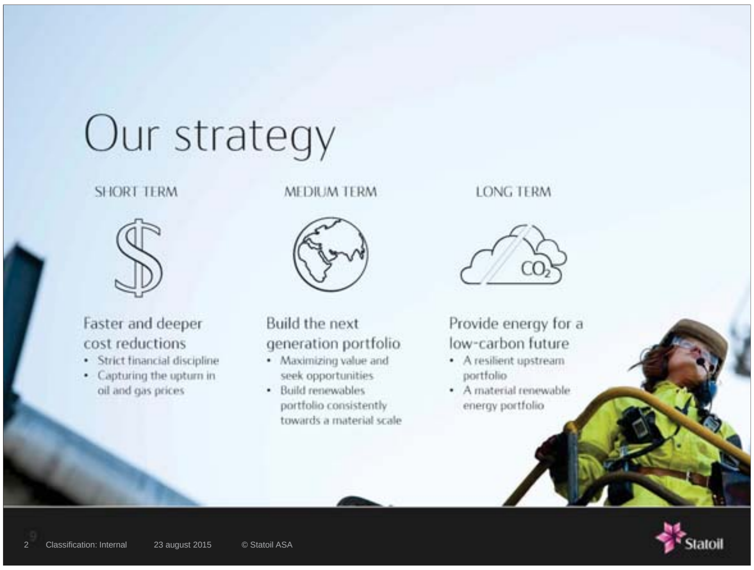

Our strategy
SHORT TERM
MEDIUM TERM
LONG TERM
Faster and deeper cost reductions
• Strict financial discipline
• Capturing the upturn in oil and gas prices
Build the next generation portfolio
• Maximizing value and seek opportunities
• Build renewables portfolio consistently towards a material scale
Provide energy for a low-carbon future
• A resilient upstream portfolio
• A material renewable energy portfolio
2
Classification: Internal
23 august 2015
© Statoil ASA
Statoil

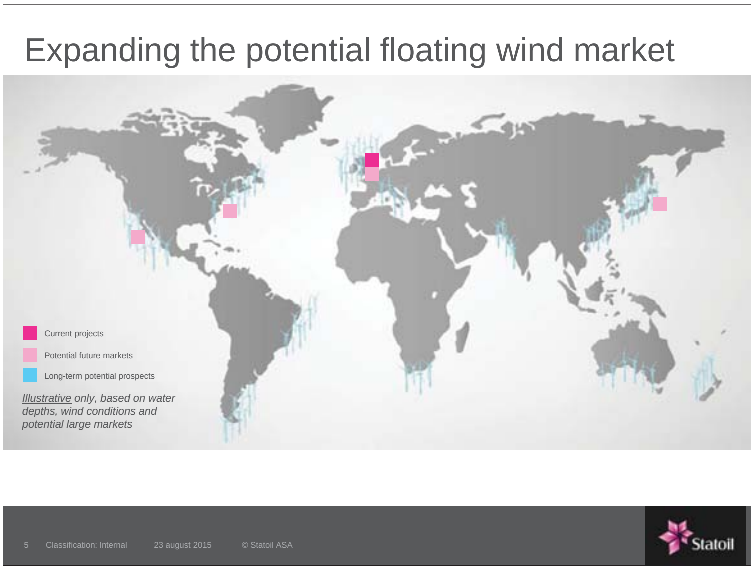

Expanding the potential floating wind market
Current projects
Potential future markets
Long-term potential prospects
Illustrative only, based on water depths, wind conditions and potential large markets
5
Classification: Internal
23 august 2015
© Statoil ASA
Statoil

NES Strategy
Build a profitable renewables business
OFFSHORE WIND
Fixed
Floating
SOLAR
ENERGY STORAGE
Develop new lower-carbon business opportunities for Statoil's core products
NCS – CO2 STORAGE
CO2 use /IOR
HYDROGEN
3
Classification: Internal
23 august 2015
© Statoil ASA
Statoil

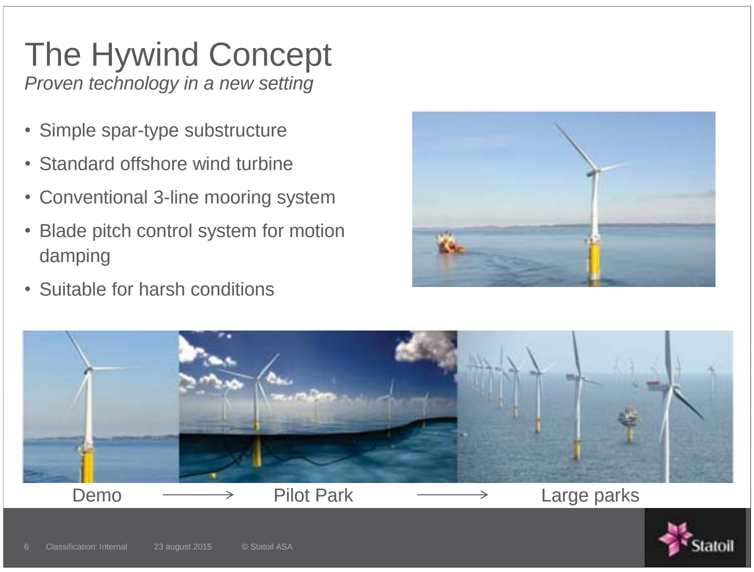

The Hywind Concept
Proven technology in a new setting
• Simple spar-type substructure
• Standard offshore wind turbine
• Conventional 3-line mooring system
• Blade pitch control system for motion damping
• Suitable for harsh conditions
Demo
Pilot Park
Large parks
6
Classification: Internal
23 august 2015
© Statoil ASA
Statoil

Hywind Demo Experience

- Excellent HSE record - No serious incidents
- Produced 55 GWh since start-up in 2009
- Production as good as or better than other 2.3 MW Siemens wind power turbines
- Experienced storms with wind speed over 44 m/s and maximum wave height of 19 m
- Verification of system integrity in operational mode

Hywind – Assembly methodology

Realising the Hywind Scotland pilot park

- **Investing around NOK 2 billion**
- **60-70% cost reduction** from the Hywind Demo project in Norway
- **Powering ~20,000 UK homes**
- **Installed capacity**: 30 MW
- **Water depth**: 95-120 m
- **Avg. wind speed**: 10.1 m/s
- **Area**: ~4 km^2
- **Average wave height**: 1.8 m
- **Export cable length**: ~30 km
- **Operational base**: Peterhead
- **Start power production**: 2017

Challenges – Technical

- Main challenges for Hywind installation
  - Water depth
  - Waves and swell during assembly
- Alternative installation methods under consideration

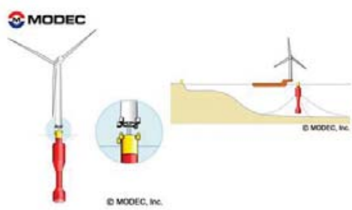

Hywind Scotland - Status

Challenges - Bringing down the cost

Cost reduction of 40-50% by 2030 a realistic target

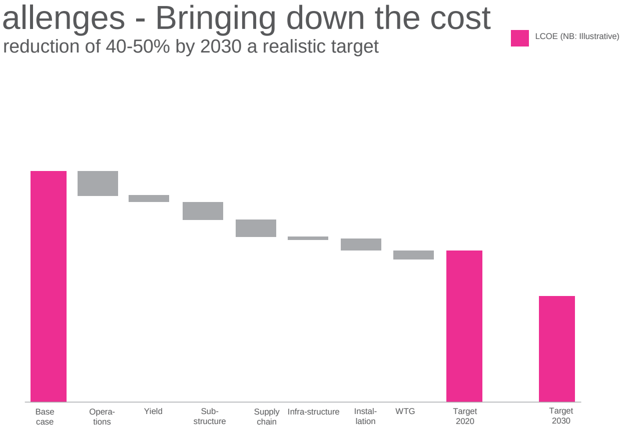

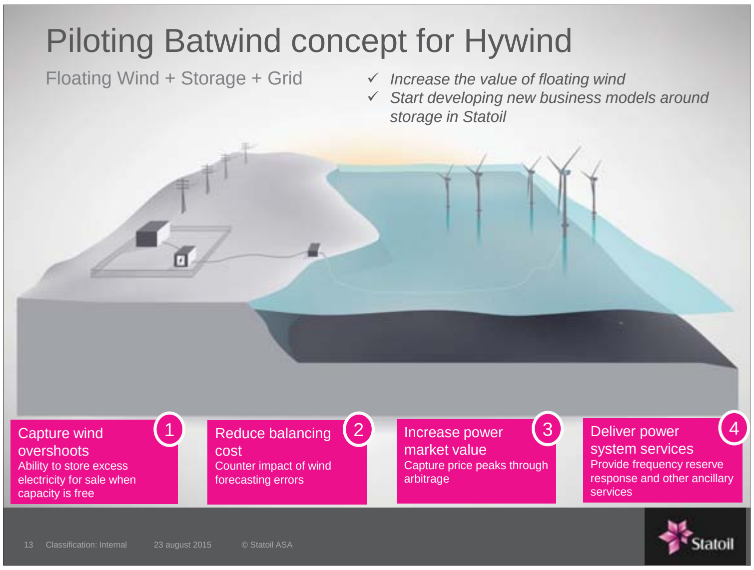
Piloting Batwind concept for Hywind
Floating Wind + Storage + Grid
✓ Increase the value of floating wind
✓ Start developing new business models around storage in Statoil
Capture wind overshoots 1
Ability to store excess electricity for sale when capacity is free
Reduce balancing cost 2
Counter impact of wind forecasting errors
Increase power market value 3
Capture price peaks through arbitrage
Deliver power system services 4
Provide frequency reserve response and other ancillary services
13 Classification: Internal 23 august 2015 © Statoil ASA
Statoil

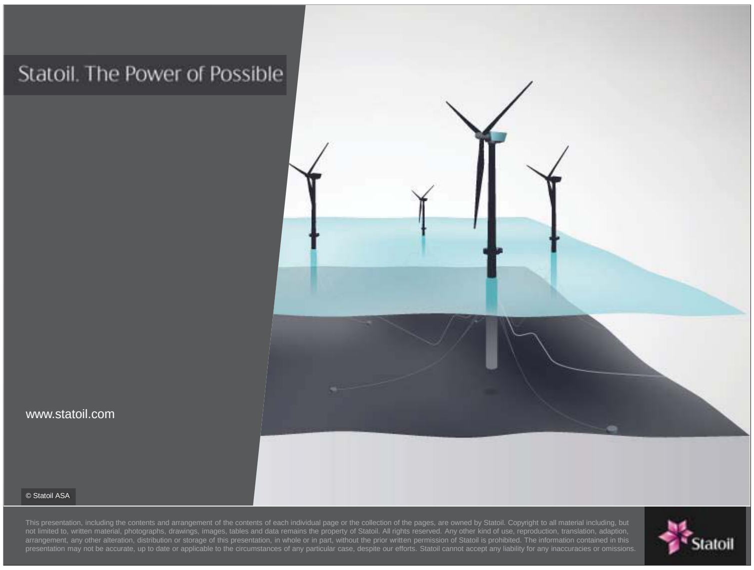
Statoil. The Power of Possible
www.statoil.com
© Statoil ASA
This presentation, including the contents and arrangement of the contents of each individual page or the collection of the pages, are owned by Statoil. Copyright to all material including, but not limited to, written material, photographs, drawings, images, tables and data remains the property of Statoil. All rights reserved. Any other kind of use, reproduction, translation, adaption, arrangement, any other alteration, distribution or storage of this presentation, in whole or in part, without the prior written permission of Statoil is prohibited. The information contained in this presentation may not be accurate, up to date or applicable to the circumstances of any particular case, despite our efforts. Statoil cannot accept any liability for any inaccuracies or omissions.
Statoil

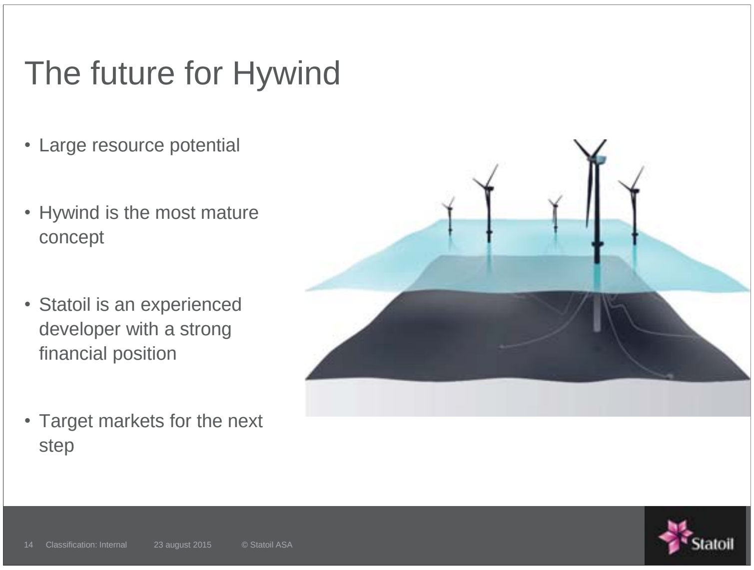
The future for Hywind
• Large resource potential
• Hywind is the most mature concept
• Statoil is an experienced developer with a strong financial position
• Target markets for the next step
14 Classification: Internal 23 august 2015 © Statoil ASA
Statoil


The future for Hywind
15 Classification: Internal 23 august 2015 © Statoil ASA
Statoil

A1) New turbine and generator technology

Can a wind turbine learn to operate itself? M. Collu, Cranfield University

Development of a 12MW Floating Offshore Wind Turbine, H. Shin, University of Ulsan

A comparison of two fully coupled codes for integrated dynamic analysis of floating vertical axis wind turbines, B.S. Koppenol, Ventolines BV

Can a Wind Turbine Learn to Operate Itself?

Evaluation of the potential of a heuristic, data-driven self-optimizing control system for a 5MW offshore wind turbine

Stefan G IORDANOV
Maurizio COLLU
Yi CAO

18 January 2017, EERA DeepWind '2017
Trondheim, Norway

www.cranfield.ac.uk

Context & problem statement

- Larger wind turbines, more complex loads
- Larger wind farms, more complex interactions
- Large amount of real-time data from monitoring system, largely used only for monitoring

MHI Vestas V164-8.0MW
[http://www.mhivestasoffshore.com/innovations/]

- Substantially benefit from more advanced control strategies
- BUT performance VS reliability

SIEMENS SWT-8.0-154
[http://www.siemens.com/global/en/home/markets/wind/turbines/swt-8-0-154.html]

2

Aim: can it learn from experience the optimum control strategy?

GIVEN:

Same as baseline controller

MANIPULATED VARIABLES (WHAT CAN BE CONTROLLED)

SENSORS (WHAT IS MEASURED)

WIND TURBINE

LEARN (FROM EXPERIENCE) HOW TO

FULFILL OBJECTIVE

Can be anything (ultimately, lowest LCOE!)

3

First step: check that it performs as well as baseline controller

GIVEN:

Same as baseline controller

MANIPULATED VARIABLES (WHAT CAN BE CONTROLLED)

SENSORS (WHAT IS MEASURED)

WIND TURBINE

LEARN (FROM EXPERIENCE) HOW TO

OBJECTIVE: MAXIMISE POWER (region 2)

Compare performance against baseline controller

4

Case study

SYSTEM

NREL 5MW offshore WT

LOAD CASES

Steady wind speed (no turbulence) (6 to 12 m/s)

Turbulent wind speed (6 to 12 m/s)

"VIRTUAL" EXPERIENCE (LEARNING FROM SYNTHETIC DATA)

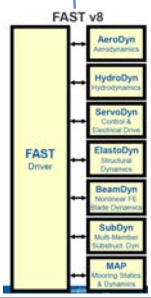

5

Methodology: global Self-Optimising Control (gSOC)

Brief review

- SOC: defining functions of process variables such that, when held constant, optimal operation is achieved (Skogestad 2000)
- Girei, Cao, et al. (2014): model-free approach (no linearisation) → global SOC
- Already proven at industrial level in the processing industry: oil reservoir waterflooding, 30% gain in Net Present Value

6

Methodology: gSOC

- Define objective function $J = \varphi(u, y, d)$
  u = manipulated
  y = sensors
  d = disturbances
- The deviation is approximated as (deviation → 0 near opt)
  $$J_{i+1} - J_i = \sum_{j=1}^{n_u} \frac{dJ}{du_j}(u_{i+1,j} - u_{i,j})$$
- Define controlled variables ($\theta = coefficients$)
  $$CV(y, \theta) = \frac{dJ}{du} = 0$$
- Obtain θ through regression
  $$min_\theta \sum_{i=1}^{N} \sum_{p=i_1}^{i_k} \left(J_p - J_i - \sum_{j=1}^{n_u} CV_j(y, \theta)(u_{p,j} - u_{i,j})\right)^2$$

Methodology: gSOC applied to Wind Turbine

- Define *u, y, d* $\quad u = [\Gamma, \beta], \quad y = [\Gamma, \beta, \omega_G, P], \quad d = [v]$
- Define objective function $\quad P = \Gamma \cdot \omega_G \cdot \eta$
- Then, deviation is
  $$P_{i+1} - P_i = \frac{dP}{d\Gamma}(\Gamma_{i+1} - \Gamma_i) + \frac{dP}{d\beta}(\beta_{i+1} - \beta_i)$$
- CVs
  $$\frac{dP}{d\Gamma} = CV_1 = \theta_0 + \theta_1 \cdot \omega_G + \theta_2 \cdot \Gamma$$
  $$\frac{dP}{d\beta} = CV_2 = \theta_3 + \theta_4 \cdot \omega_G + \theta_5 \cdot \beta$$
- For each disturbance value, build sample matrix [20 x 6] → "experience"
  - 6 pitch angles
  - 20 generator torques
- Then θ_i obtained through regression

8

Results (1): yes, it learns!

Maximise power →

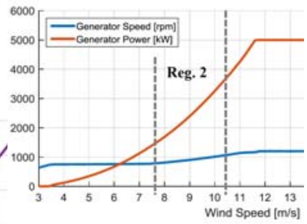

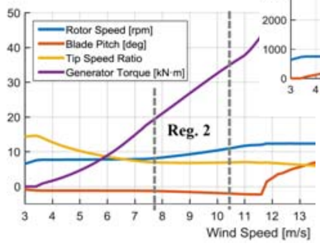

← How?
It learned to keep constant TSR (varying Γ) and β

9

Results (2): slightly better strategy

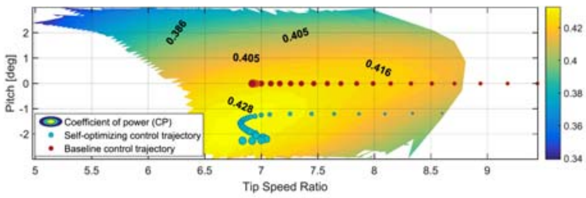

→ gSOC tracks maximum CP better than baseline control → learnt from experience

→ Not a substantial advantage, but proving that can perform well as approach
  → Can be used it to discover control approaches fulfilling more complex objectives

10

Conclusions

- The global self-optimising control strategy gSOC is able to deliver the same performance (in terms of energy extracted) as conventional control system
  - it "learned this from experience"
- Easy development and implementation, flexible, scalabledoes not compromise reliability / ease of use when scaled up to consider:
  - More sensor signals
  - More actuators

11

Next steps

- The "ideal" control strategy should (long-term vision):
  - minimise the Levelised Cost of Energy (LCoE) [cost/kWh]
  - taking into account all the data available
- Next steps: ***discover new optimum control strategies***
  - Numerical → Include in the objective function "J" additional criteria, e.g.:
    - 1 p and 3p loads on the blades – equivalent fatigue damage load
    - Loads at the tower base – equivalent fatigue damage load
    - Multiple wind turbines
    - …
  - Experimental → small scale wind turbine tested in wind tunnel
  - Feedback to simple, non data-driven control strategies

12

Development of a 12MW Floating Offshore Wind Turbine

Hyunkyoung SHIN

School of Naval Architecture & Ocean Engineering, University of Ulsan, Korea

EERA DeepWind'2017, JAN. 18, 2017, Trondheim, Norway

Ulsan , Korea

Wikipedia 2014

Light through Darkness

Outline

- Introduction
- UOU 12MW FOWT model
- Modified Control System
- Numerical Simulation
- Design Load Cases
- Novel Offshore Floater
- Conclusion

Growth in Size of Wind Turbine

➢ Turbines have grown larger and taller to maximize energy capture

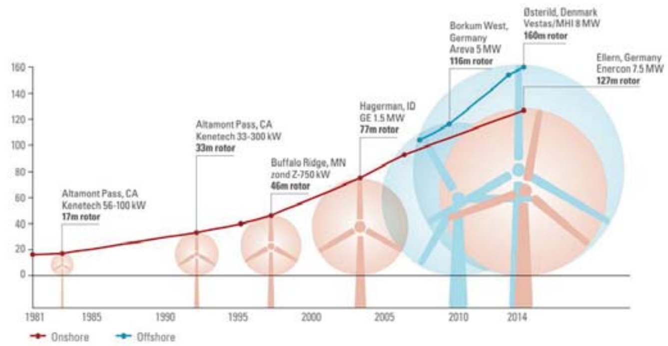

Source : http://www.sbcenergyinstitute.com/Publications/Wind

1. Introduction

Critical Needs for FOWTs
- Responsible and Sustainable Ocean Economy 2030 -

Industry	Compound annual growth rate for GVA between 2010 and 2030	Total change in GVA between 2010 and 2030	Total change in employment between 2010 and 2030
Industrial marine aquaculture	5.69%	303%	152%
Industrial capture fisheries	4.10%	223%	94%
Industrial fish processing	6.26%	337%	206%
Maritime and coastal tourism	3.51%	199%	122%
Offshore oil and gas	1.17%	126%	126%
Offshore wind	24.52%	8 037%	1 257%
Port activities	4.58%	245%	245%
Shipbuilding and repair	2.93%	178%	124%
Maritime equipment	2.93%	178%	124%
Shipping	1.80%	143%	130%
Average of total ocean-based industries	**3.45%**	**197%**	**130%**
Global economy between 2010 and 2030	**3.64%**	**204%**	**120%[1]**

1. Based on projections of the global workforce, extrapolated with the UN medium fertility rate.

Source: Authors' calculations based on OECD STAN, UNIDO INDSTAT, UNSD; Lloyd's Register Group (2014; 2013); World Bank (2013); IEA (2014); FAO (2015).

Why do we need FOWT ?

Objective (Motive)

- Why ?
  - ✓ Enlargement in size & capacity considering LCOE
  - ✓ Needs for innovative Floating Offshore Wind Turbines
  - ✓ Light through darkness
- How ?
  - ✓ Novel offshore floater without mooring lines
  - ✓ To reduce the Tophead mass
  - ✓ SCSG, Flexible Composite Shaft, Carbon Sparcap

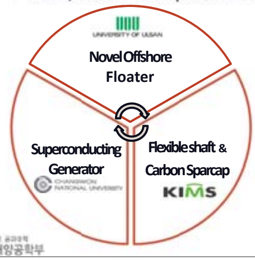

12MW FOWT

Target

Reason why we use a superconducting generator

The heavy top head causes the high mechanical stress and high cost of foundation and tower.

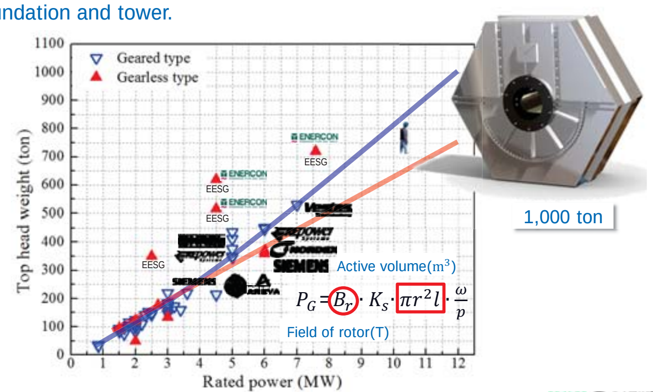

Source : Changwon National University, CAPTA

Suggestion of a new technology for the 12 MW

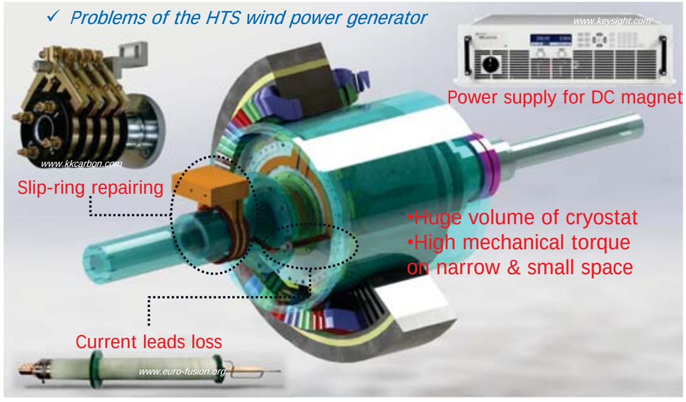

Source : Changwon National University, CAPTA

Modularized generator for the 12MW

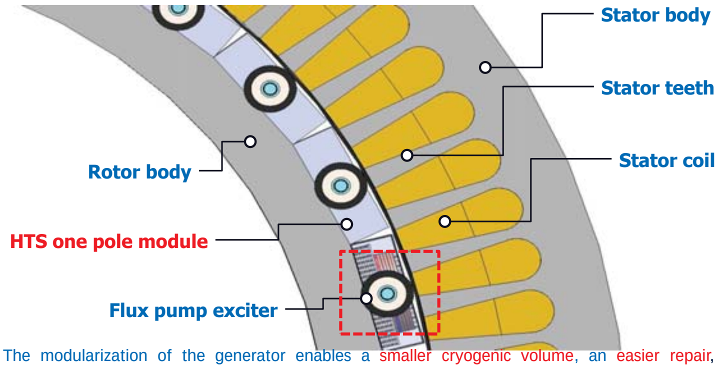

The modularization of the generator enables a smaller cryogenic volume, an easier repair, assembly, and maintenance of the HTS field coil. Modularization will be suitable for commercial mass production and will increase the operational availability of HTS generators in the wind turbine.

Source : Changwon National University, CAPTA

Detailed design for composite flexible shaft

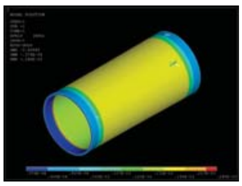
Glass composite shaft

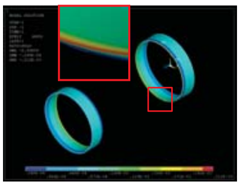
Carbon composite pad-up

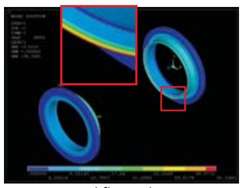
Metal flanged part


Global buckling

- Analysis for ultimate & fatigue strength
- Total Mass : 51.86 ton

	M.S.
Glass composite shaft	0.22 (First-ply failure)
Carbon composite pad-up	0.56 (First-ply failure)
Metal flanged part	0.88 (Von-mises stress)
Global buckling	46.2

Source : Korea Institute of Materials Science(KIMS)

Detailed design for new support structure

➢ Bending load case

Case	My (MNm)	Mz (MNm)
1	-37.69	4.68
2	66.55	5.13
3	-2.40	-44.09
4	-6.10	47.32

Source : Korea Institute of Materials Science(KIMS)

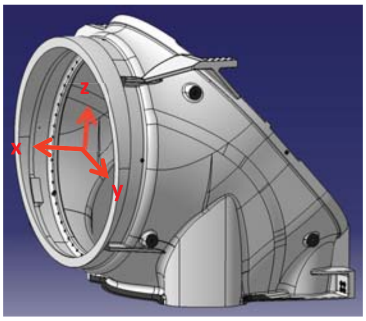

UOU 12MW Wind Turbine Model

Design Process

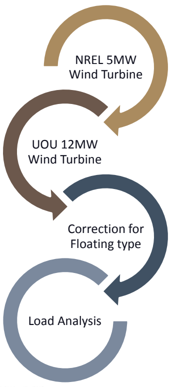

- Upscaling process SCSG/Flexible Shaft/Carbon Sparcap
- Blade (CFRP)
- Tower
- Control
- Platform
- Negative damping issue
- Tower 3P issue
- IEC61400-1
- IEC61400-3
- IEC61400-3-2

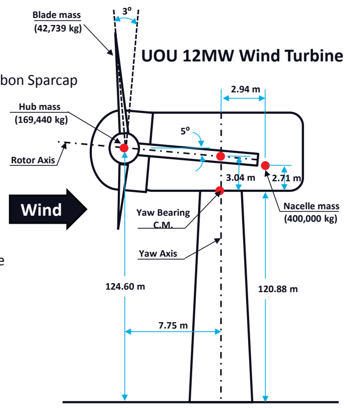

Design Summary

Rating	5 MW	12 MW
Rotor Orientation	Upwind, 3 Blades	Upwind, 3 Blades
Control	Variable Speed, Collective Pitch	Variable Speed, Collective Pitch
Drivetrain	High Speed, Multiple-Stage Gearbox	Low Speed, Direct Drive (SCSG)
Rotor, Hub Diameter	126 m, 3 m	195.2 m, 4.64 m
Hub Height	90 m	124.6 m
Cut-In, Rated, Cut-Out Wind Speed	3 m/s, 11.4 m/s, 25 m/s	3 m/s, 11.2 m/s, 25 m/s
Cut-In, Rated Rotor Speed	6.9 rpm, 12.1 rpm	3.03 rpm, 8.25 rpm
Overhang, Shaft Tilt, Pre-cone	5 m, 5°, 2.5°	7.78 m, 5°, 3°
Rotor Mass	110,000 kg	297,660 kg
Nacelle Mass	240,000 kg	400,000 kg (*Target*)
Tower Mass (for offshore)	249,718 kg	782,096 kg

2. UOU 12MW FOWT Model

Scaling Laws for 12MW power production

- $P = C_p * \frac{1}{2}\rho A V^3$
- $Scale\ ratio = \lambda = \sqrt{\frac{12MW}{5MW}} = 1.549$
- Blade length : NREL 5MW(61.5m) -> UOU 12MW(95.28 m)

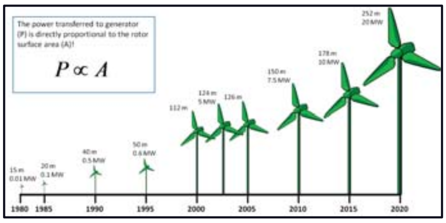

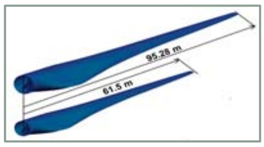

➢ Same geometry(Airfoil) with NREL 5MW blade

Source : EWEA, Wind energy—the facts: a guide to the technology, economics and future of wind power, 2009.

12MW Carbon blades

➢ 61.5 (m) 5MW glass blade : 17.7 ton
→ 95.28 (m) 12MW glass blade : 62.6 ton (Too heavy)
→ 95.28 (m) 12MW carbon (sparcap) blade : 42.7 ton

Sparcap
(43% of the total weight – 5MW class IIA)

	0° Stiffness [Gpa]	Density [kg/m³]	Blade Weight [ton]	Center of Gravity [m]
CFRP	130	1572	42.7 (Carbon Sparcap)	31.8
GFRP	41.5	1920	62.6	31.8

Source : Korea Institute of Materials Science(KIMS)

N.F. [Hz]	1st Flapwise	2nd Flapwise	1st Edgewise	2nd Edgewise
12MW Blade	0.5770	1.6254	0.8920	3.2676

- Scale-up blade properties(deflection)

$$\frac{EI_{12}}{EI_5} = \left(\frac{L_{12}}{L_5}\right)^4$$

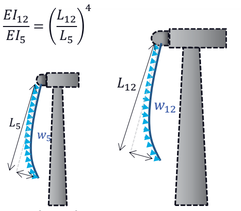

(5MW) (12MW)

How the blade compares to existing ones

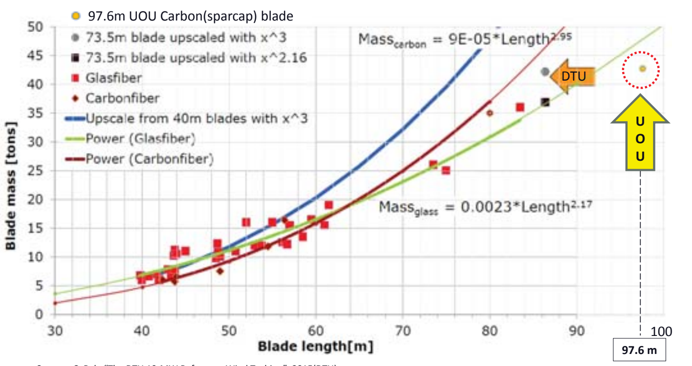

Source : C. Bak, "The DTU 10-MW Reference Wind Turbine", 2015(DTU)

Hub height

- Nacelle target mass: 400 ton, Hub mass: 169.4 ton (scale-up)
- Hub height :
  Rotor radius + Extreme wave height (half) with 50-year occurrence × S.F. of 1.8
  → 97.6 + 30.0 / 2 × 1.8 = 124.6 m

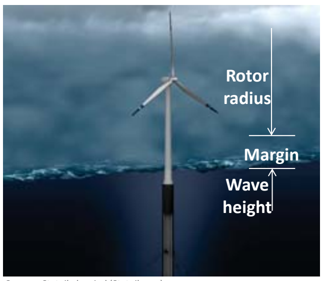

Source : Statoil –hywind (Statoil.com)

7MW offshore wind turbine(SHI)

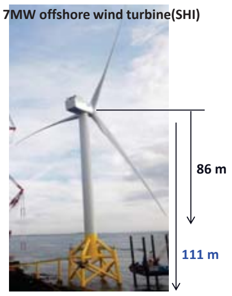

(cf. 86.0 + 30.0 / 2 × 1.8 = 113 m)

Source : http://www.ramboll.com/media/rgr/worlds-largest-turbine-installed

Scale-up tower properties

- Scale up using offshore tower from OC4 definition(5MW : Height : 78.2 m , Weight : 249.718 ton)
- 12MW "Material : steel, Height : 110.88 m, Weight : 782.096 ton (scale-up)"
  [cf. UPWIND report 2011 : 983 ton (10MW), 2,780 ton (20MW)]

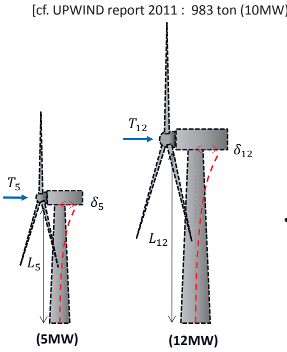

- Beam deflection

$$\delta = \frac{TL^3}{3EI} \qquad \frac{\delta_{12}}{\delta_5} = \frac{L_{12}}{L_5} \qquad \frac{T_{12}}{T_5} = \frac{12\ \mathrm{MW}}{5\ \mathrm{MW}}$$

$$\frac{EI_{12}}{EI_5} = \frac{12L_{12}^2}{5L_5^2} \qquad T = C_t * \frac{1}{2}\rho A V^2$$

- Scale-up tower properties

$$\boxed{\frac{EI_{12}}{EI_5} = \frac{12L_{12}^2}{5L_5^2}}$$

(Beam deflection)

Scale-up platform properties

- Ratio of W_{12}(1480ton) to W_5(600ton)
- OC4 semi-submersible "displaced volume" 13,917m³ (5MW) → 34,336m³ (12MW)

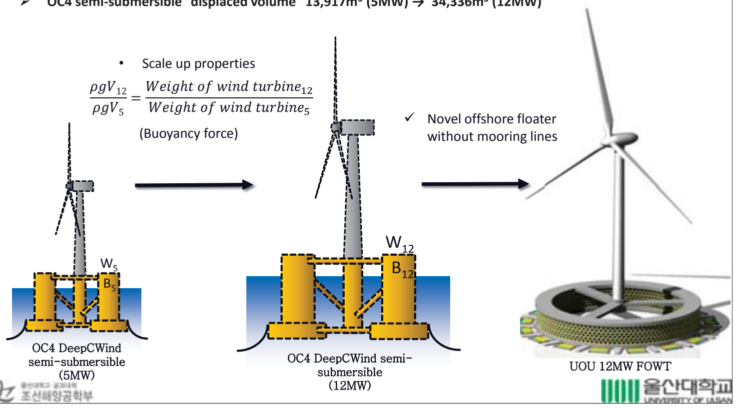

3. Modified Control System

Wind Turbine Power Curve

Region II

- Torque Control
- Variable speed,
- Constant pitch,
- Target : Cp = Cp_max
- Maximize the optimum power

Region III

- Pitch Control
- Constant speed,
- Variable pitch,
- Target : P = P_rated
- Maintain the rated power

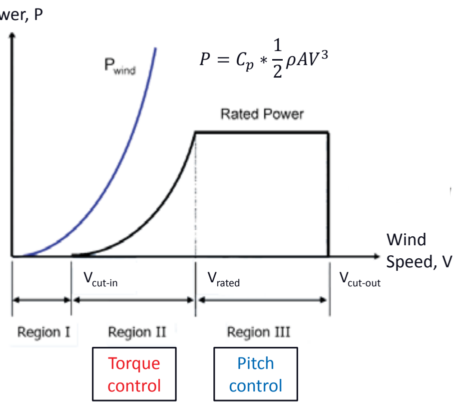

Source : https://www.e-education.psu.edu/aersp583/node/470

Maximum Cp and Optimal TSR(Tip Speed Ratio)

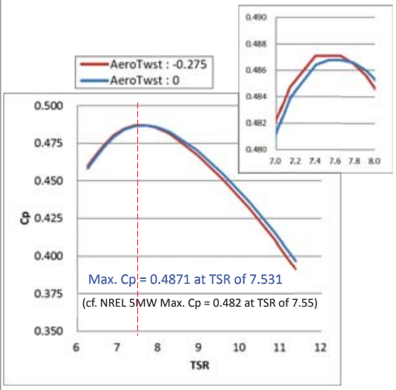

Cp – TSR curve

➢ Modification of the AeroTwst : - 0.275°

Node	Rnodes	AeroTwst	DRNodes	Chord	Airfoil Table
[-]	[m]	[°]	[m]	[m]	[-]
1	4.437	13.033	4.234	5.487	Cylinder1.dat
2	8.672	13.033	4.234	5.971	Cylinder1.dat
3	12.906	13.033	4.234	6.456	Cylinder2.dat
4	18.199	13.033	6.352	7.060	DU40_A17.dat
5	24.551	11.205	6.352	7.207	DU35_A17.dat
6	30.902	9.887	6.352	6.906	DU35_A17.dat
7	37.254	8.736	6.352	6.583	DU30_A17.dat
8	43.606	7.520	6.352	6.208	DU25_A17.dat
9	49.958	6.269	6.352	5.806	DU25_A17.dat
10	56.309	5.086	6.352	5.425	DU21_A17.dat
11	62.661	3.913	6.352	5.044	DU21_A17.dat
12	69.013	2.850	6.352	4.663	NC64_A17.dat
13	75.364	2.044	6.352	4.282	NC64_A17.dat
14	81.716	1.251	6.352	3.901	NC64_A17.dat
15	87.009	0.588	4.234	3.583	NC64_A17.dat
16	91.243	0.095	4.234	3.232	NC64_A17.dat
17	95.478	-0.169	4.234	2.198	NC64_A17.dat

Aerodynamic properties

Torque Scheduling for 12MW

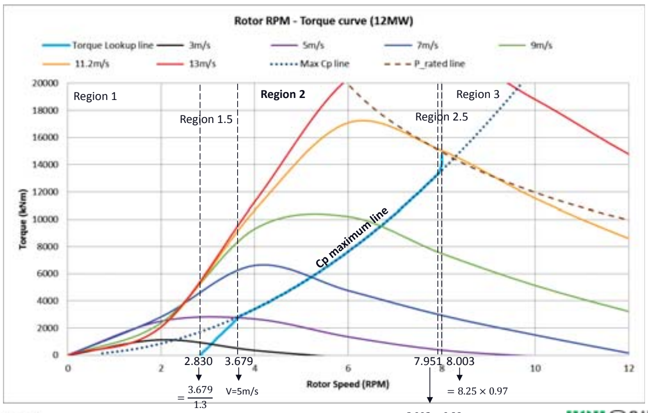

Simulation Study(Pitch gain-tuned)

- Steady wind(12m/s), Regular wave(H = 2m / T = 10s)

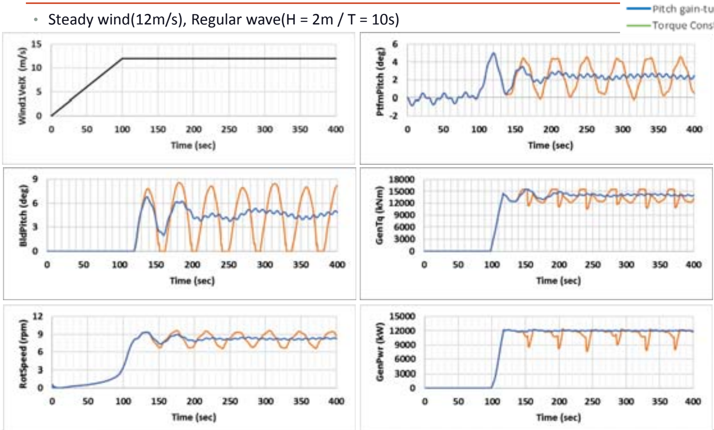

Simulation Study(Pitch gain-tuned Controller)

➢ NTM(23m/s), JONSWAP spectrum(Hs = 3.2m / Tp = 9.6s)

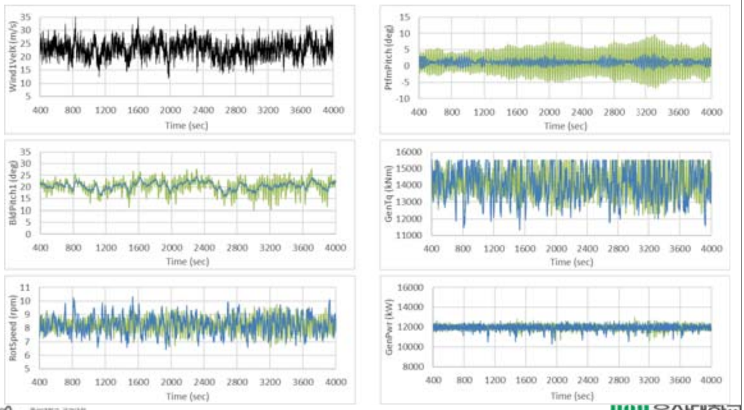

Steady state analysis

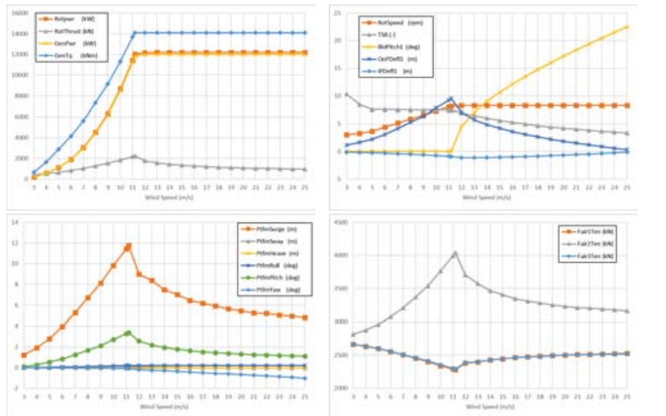

Campbell diagram (3P Issue)

Tower resonance
→ Need to redesign tower properties

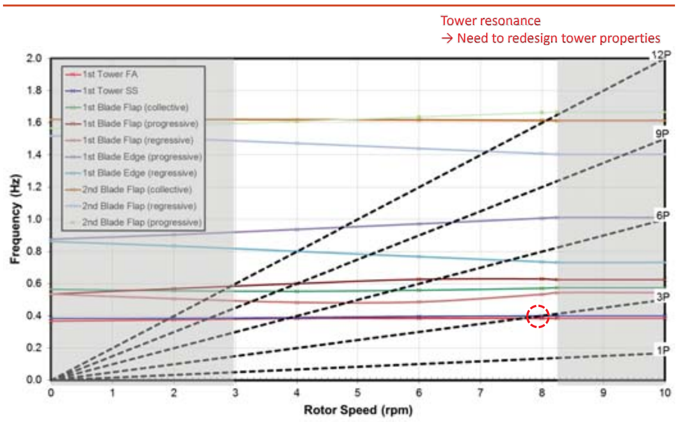

Natural frequency of the tower

Example 1: mass on cantilever

A machine of mass m is on light cantilevered bracket.

From 1.7.4, $k_{eff} = \frac{3EI}{l^3}$

$m\ddot{x} = -k_{eff}\,x$

$m\ddot{x} + k_{eff}\,x = 0$

$m\ddot{x} + \frac{3EI}{l^3}x = 0 \quad \Rightarrow \quad \omega_n = \sqrt{\frac{3EI}{m\,l^3}}$

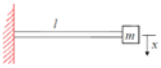

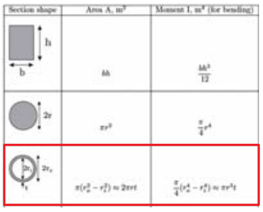

$$f_n = \frac{1}{2\pi}\sqrt{\frac{3E(\pi r^3 t)}{\left(\frac{33}{140} * \rho * 2\pi r t * l + M_{tophead}\right) l^3}} = C\sqrt{\frac{r^3}{l^3}} \propto \frac{D^{1.5}}{l^{1.5}}$$

- Rotor 3P-Excitation : 0.4125
- Tower 1st Side to Side Natural Frequency : 0.3982

Target	Tower Length
5% margin	104.84
2.5% margin	**106.53**
No margin	108.28

Campbell diagram(after)

Tower Length (to avoid 3P!!)
110.88 m → 106.53 m (-4.35m)

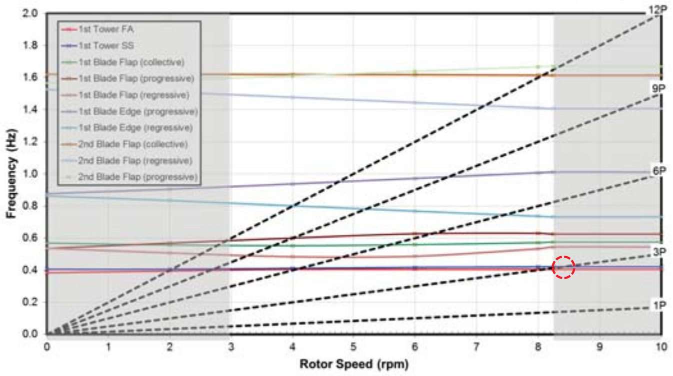

4. Numerical Simulation

Design process for a floating offshore wind turbine

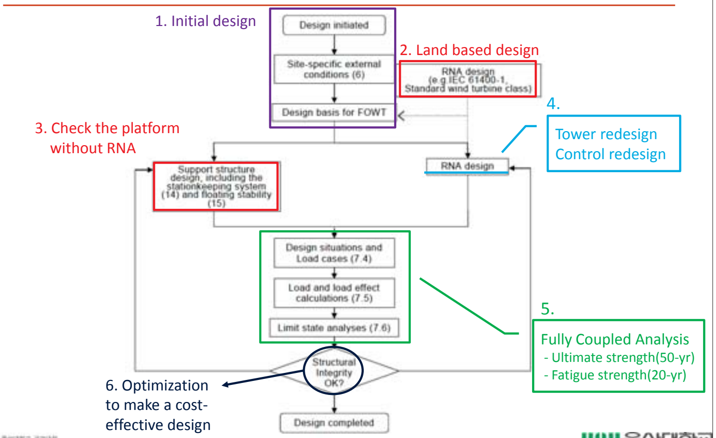

Source: IEC61400-3-2

Flow Diagram of UOU + FAST v8

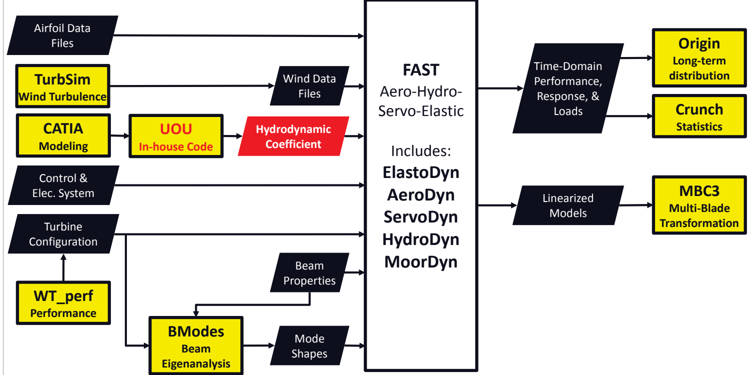

UOU in-house code

- **Hydrodynamic coefficients need for numerical simulation in hydro part**

Diffraction problem + Radiation problem = Motion equation

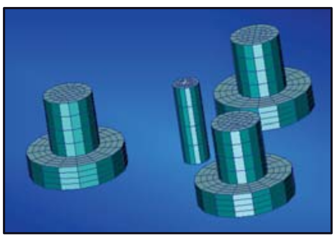

- **UOU in-house code**

3D panel method(BEM)
Element : 1024

Output
1. Added mass coefficients
2. Radiation Damping coefficients
3. Wave Excitation Forces/Moments

12MW Stability analysis

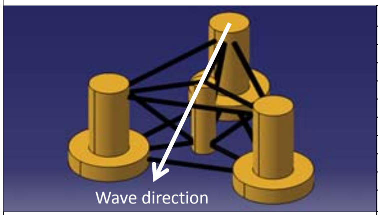

Floating Platform Geometry	5MW	12MW
Elevation of main column above SWL	10	10
Elevation of offset columns above SWL	12	16.215
Spacing between offset columns	50	67.562
Length of upper columns	26	35.132
Length of base columns	6	8.107
Depth to top of base columns below SWL	14	18.917
Diameter of main column	6.5	9.634
Diameter of offset (upper) columns	12	16.130
Diameter of base columns	24	32.260
Diameter of pontoons and cross braces	1.6	2.162

Transverse Stability (Roll)

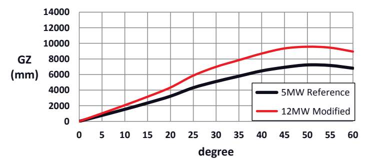

Longitudinal Stability (Pitch)

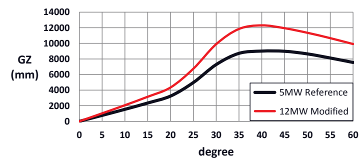

RAO results in regular wave

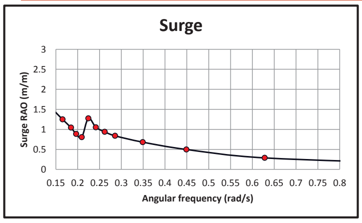

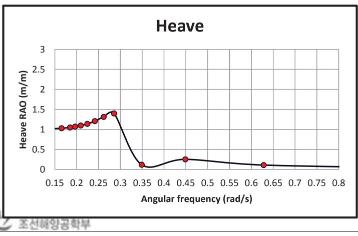

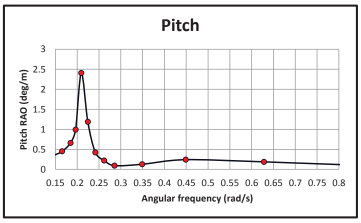

5. Design Load Cases(DLCs)

Design Load Cases

➢ IEC61400-3 : International Standards

DLC	Significant Wave height	Peak Period	Wind Model
DLC1.1 (NSS)	3.2 m	9.6 s	NTM
DLC1.3 (NSS)	3.2 m	9.6 s	ETM
DLC1.6 (SSS)	9.72 m	13.98 s	NTM
DLC6.1 (ESS)	11.32 m	15.1 s	EWM50

Preliminary study for ultimate strength analysis
- DLC1.1
- DLC1.3
- DLC1.6
- DLC6.1

DLC1.1(NSS/NTM)

Normal **S**ea **S**tate : H_s = 3.2m / T_p = 9.6s
Normal **T**urbulence **M**odel : I_{ref} = 0.14(B)

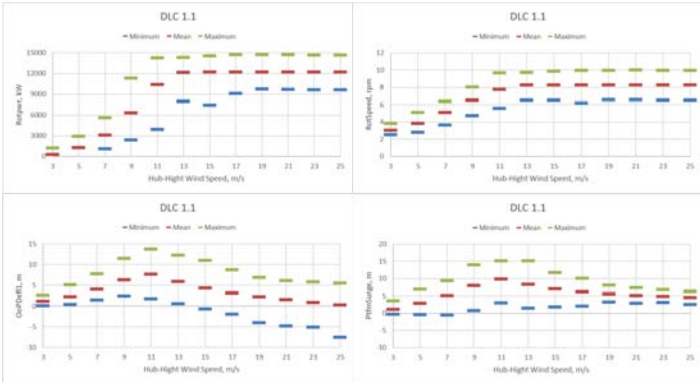

DLC1.3(NSS/ETM)

Normal **S**ea **S**tate : H_s = 3.2m / T_p = 9.6s
Extreme **T**urbulence **M**odel : I_{ref} = 0.14(B)

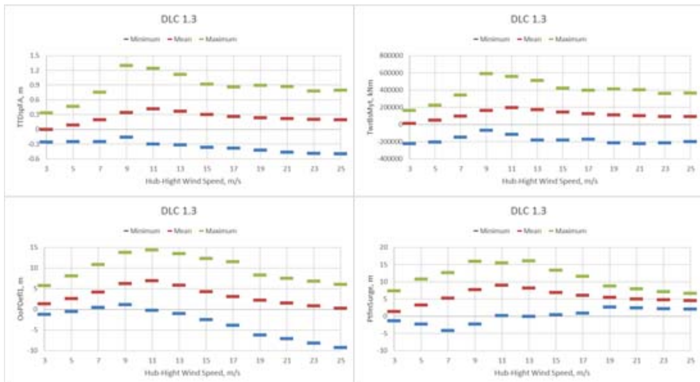

DLC1.6(SSS/NTM)

Severe **S**ea **S**tate : H_s = 9.72m / T_p = 13.98s
Normal **T**urbulence **M**odel : I_{ref} = 0.14(B)

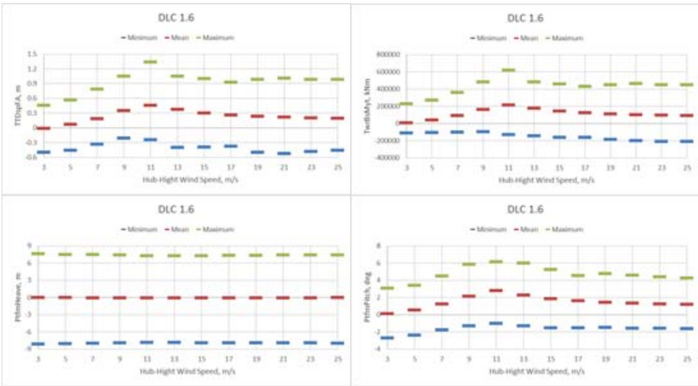

DLC6.1(ESS/EWM50)

Extreme **S**ea **S**tate : H_s = 11.32m / T_p = 15.1s
Extreme **W**ind Speed **M**odel : I_{ref} = 0.14(B)

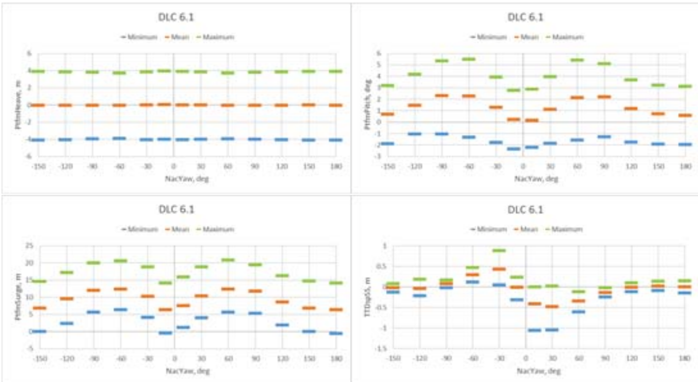

Summary

	Maximum	Units	DLC
Rotpwr	15,600.00	kW	DLC 1.6 (17 m/s)
GenPwr	15,370.00	kW	DLC 1.6 (17 m/s)
RotSpeed	10.56	rpm	DLC 1.6 (17 m/s)
OoPDefl1	14.33	m	DLC 1.3 (11 m/s)
TTDspFA	1.34	m	DLC 1.6 (11 m/s)
TTDspSS	0.88	m	DLC 6.1 (-30 deg)
TwrBsMyt	618,300.00	kNm	DLC 1.6 (11 m/s)
PtfmSurge	20.86	m	DLC 6.1 (+60 deg)
PtfmHeave	7.61	m	DLC 1.6 (3 m/s)
PtfmPitch	6.17	deg	DLC 1.6 (11.2 m/s)

Long-term distribution

- IEC61400-1 Annex F
  - Statistical extrapolation of loads for ultimate strength analysis

Extrapolation of out-of-plane tip deflection

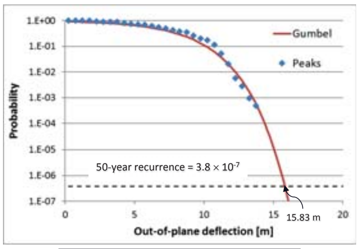

Out of plane tip Deflection
Extreme value 19.79 m
(safety factor 1.25)

Extrapolation of in-plane tip deflection

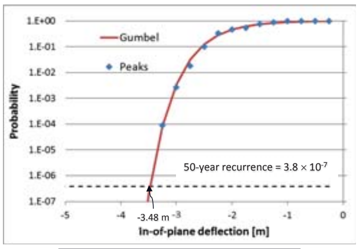

In plane tip Deflection
Extreme value -4.35 m
(safety factor 1.25)

5. Novel Offshore Floater

Wave Energy Propulsion

without foil

with foil

Wave Energy Propulsion

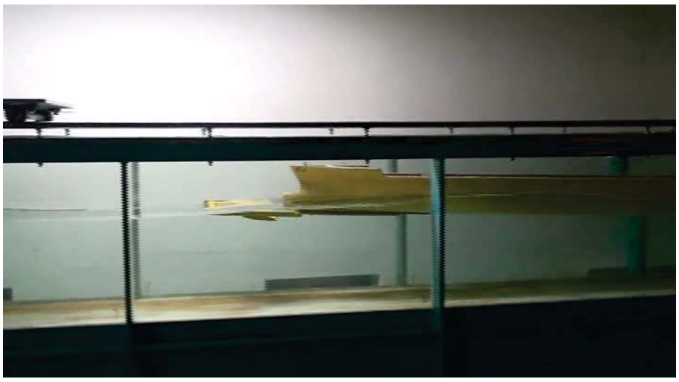

Wave Energy Propulsion

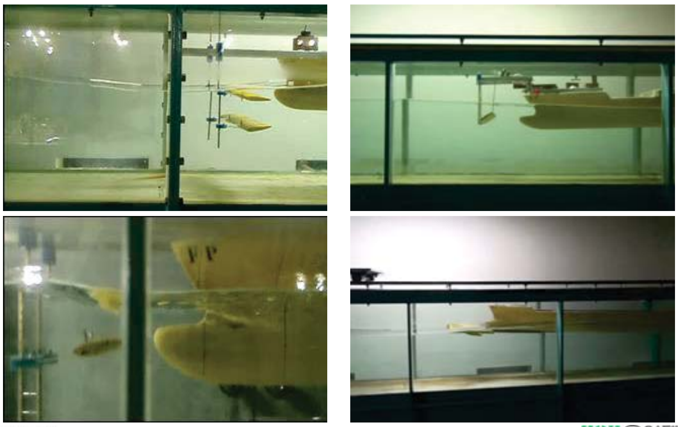

Passive/Active mode

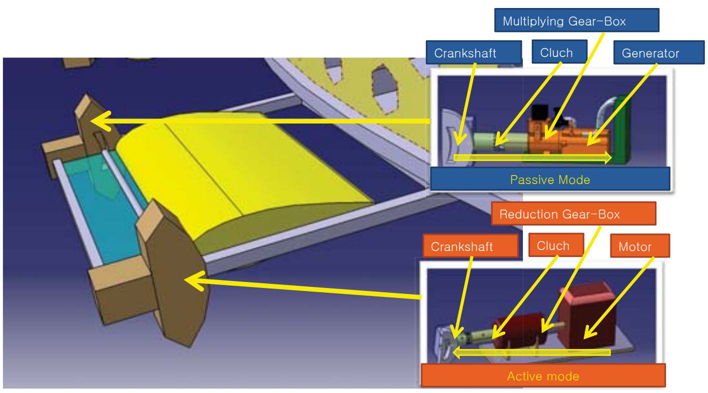

Novel Stationkeeping(passive mode)

Period : 2.43s, Wave Length : 9.18m, Wave Height : 0.075m, Frequency : 0.412Hz,

Wave propagating direction

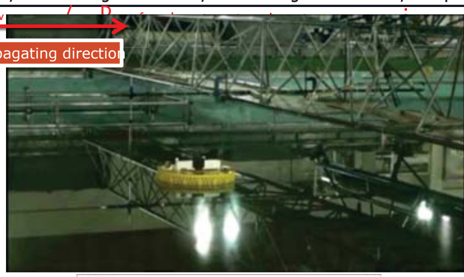

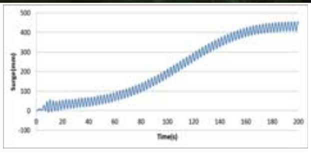

6. Conclusion

Conclusion

- Preliminary design of a UOU 12MW floating offshore wind turbine is made by being scaled up from NREL 5MW wind turbine and OC4 semi-submersible.
- An innovative floater without mooring systems for the UOU 12MW FOWT is suggested.
- In order to reduce the top head mass, SCSG, Flexible shaft and CFRP blades are adopted in UOU 12MW FOWT.
- To avoid the negative damping of FOWTs, controller was modified.
- Tower length was changed to avoid the 3P excitation.
- Long term analysis of the UOU 12MW FOWT was performed.
- Later, IEC61400-3-2 rule should be considered for the UOU 12MW FOWT.

THANK YOU!

ACKNOWLEDGMENTS

This work was supported by the Korea Institute of Energy Technology Evaluation and Planning(KETEP) and the Ministry of Trade, Industry & Energy(MOTIE) of the Republic of Korea (No. 20154030200970 and No. 20142020103560).

Floating vertical-axis wind turbines

Comparison of two numerical tools for integrated dynamic analysis

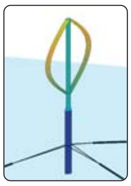

Boy Koppenol[1], Zhengshun Cheng[2], Zhen Gao[2], Carlos Simão Ferreira[3], Torgeir Moan[2]

[1] *Ventolines BV, The Netherlands*
[2] *Norwegian University of Science and Technology*
[3] *Technical University of Delft*

---

1 Introduction
2 Numerical tools
3 Methodology
4 Results
5 Summary

1. Introduction: **Floating VAWTs**

- **Floating wind turbines**
- **Vertical-axis wind turbines**
  - Simple design
  - Insensitive to wind direction
  - Low machinery position
- **VAWT characteristics**
  - Dynamic inflow conditions
  - Blade meets flow twice
  - Encounters own wake

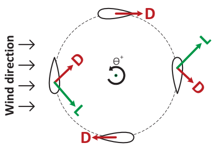

---

1 Introduction
2 Numerical tools
3 Methodology
4 Results
5 Summary

1. Introduction: **Aim / Scope**

- **VAWTs are different**
  - Aerodynamics
  - Load transfer to support structure
  - New simulation tools
- **Code-to-code comparison**
  - Modeling differences
  - Focus on implementation aerodynamics
  - Coupled analyses using a floating spar VAWT

---

1 Introduction
2 Numerical tools
3 Methodology
4 Results
5 Summary

2. Numerical tools: **Overview**

Current publicly available tools

1. FloVAWT — *Cranfield University*
2. CALHYPSO — *EDF R&D*
3. OWENS toolkit — *Sandia National Laboratories*
4. **HAWC2** — ***DTU Wind Energy***
5. SIMO-RIFLEX-DMS — *NTNU/Marintek*
6. **SIMO-RIFLEX-AC** — ***NTNU/Marintek***

SIMO-RIFLEX-AC:	**HAWC2:**
AC flow theory	AC flow theory
Potential flow	Morison's equation
Non-linear bar elements	Non-linear spring model

---

1 Introduction
2 Numerical tools
3 Methodology
4 Results
5 Summary

2. Numerical tools: **Aerodynamics**

- **Based on AC flow theory**
  1. Section rotor in ACs
  2. Loads from blade element theory
  3. Blade loads as body forces on the AC
  4. Solve pressure field for velocities
- **Additions in SIMO-RIFLEX-AC**
  - ✓ Local blade inclination
  - ✓ Tangential terms
  - ✓ Correction factor

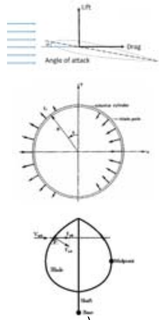

$$w_{x,j} = k_a \left(\sum_{i=1}^{i=N} Q_{n,i} R_{w_x,i,j} + \sum_{i=1}^{i=N} Q_{t,i} R_{w_y,i,j} - \left(Q_{n,N+1-j}\right)^* - \left(Q_{t,N+1-j} \frac{y_j}{\sqrt{1-y_j^2}}\right)^* \right)$$

---

1 Introduction
2 Numerical tools
3 Methodology
4 Results
5 Summary

3. Methodology: **Two cases**

1. **Aerodynamic modeling**
   - Rigid land-based VAWT
   - 5MW DeepWind rotor
   - Steady wind-only at 8, 14 and 20 m/s
2. **Fully coupled analyses**
   - Spar VAWT
   - Platform from OC3-Hywind
   - Turbulent wind and irregular waves

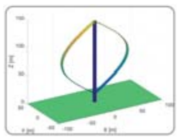

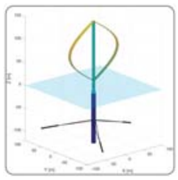

NTNU

4. Results: **Aerodynamic modeling**

- **Rotor-averaged thrust**
  - Similar at high wind speeds
  - C_T different at 8 m/s
- **Aerodynamic torque 8 m/s**
  - 2P effect, troughs and peaks
  - Tangential terms
  - Induced velocity

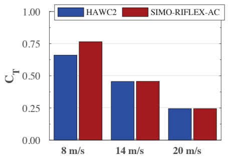

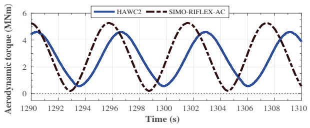

1 Introduction
2 Numerical tools
3 Methodology
4 Results
5 Summary

TUDelft

NTNU

4. Results: **Coupled analyses**

- **Platform response**
  - Larger offsets in HAWC2
  - Surge-heave coupling
  - Yaw in 1P and 2P

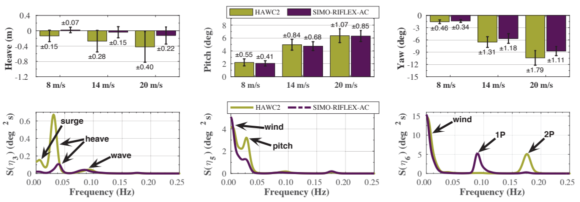

1 Introduction
2 Numerical tools
3 Methodology
4 Results
5 Summary

TUDelft

NTNU

4. Results: **Coupled analyses**

- **Mooring line tension**
  - 1P yaw in SIMO-RIFLEX-AC
  - Mooring line (hydro)dynamics

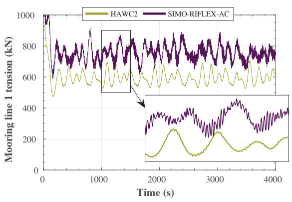

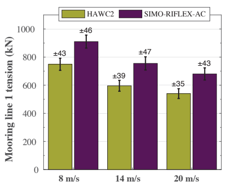

1 Introduction
2 Numerical tools
3 Methodology
4 Results
5 Summary

TUDelft

NTNU

4. Results: **Coupled analyses**

- **Tower base bending**
  - Dominated by 2P excitation
  - Pitch response
  - Wave contribution
  - Tower mode (0.35 Hz)

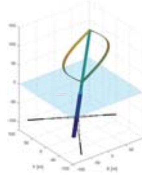

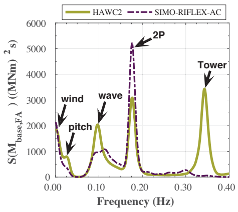

1 Introduction
2 Numerical tools
3 Methodology
4 Results
5 Summary

TUDelft

NTNU

5. Summary

- **Vertical axis wind turbines**
  - Benefits for floating applications
  - Complex aerodynamics
- **Aerodynamic modeling**
  - AC flow theory
  - Implementation important at low wind speeds
- **Fully coupled analyses**
  - Mooring line dynamics
  - Wave contribution
  - Tower mode

1 Introduction
2 Numerical tools
3 Methodology
4 Results
5 Summary

TUDelft

Boy Koppenol
Project engineer

E: boykoppenol@gmail.com
T: +31 649 828 765

Ventolines

Ventolines BV, The Netherlands
www.ventolines.nl

A2) New turbine and generator technology

The Multi Rotor Solution for Large Scale Offshore Wind Power,
P. Jamieson, University of Strathclyde

The C-Tower Project – A Composite Tower for Offshore Wind Turbines,
T. van der Zee, Knowledge Centre WMC

Support structure load mitigation of a large offshore wind turbine using a semi-active magnetorheological damper, R. Shirzadeh, ForWind – University of Oldenburg

Multi Rotor Solution for Large Scale Offshore Wind Power

Peter Jamieson

Deepwind, Trondheim 2017

History of Multi Rotor Systems

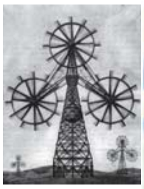
Honnef 1926


Heronemus 1976


Lagerwey 1995


Vestas 2016

2

MRS today


Vestas


Wind Lens Kyushu


Brose MRS

A variety of systems – different scales, different design objectives but common interests in R&D progress and growing concept credibility

3

Innwind.eu - Partners Roles

SU - Technical coordination, concept design, load calculation using:

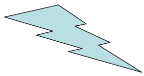

GLGH (Now DNV GL Energy) - Bladed for 45 rotors.

CRES – support structure and floater

NTUA – validation of aerodynamics: rotor interaction, structure blockage.

4

Multi Rotor System Concept

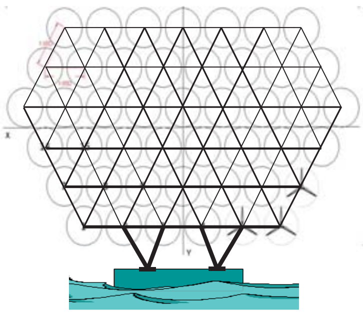

- 45 rotors each of 41 m diameter and of 444 kW rated output power comprising a net rated capacity of 20 MW
- Rotors on a triangular lattice arrangement with minimum spacing of 2.5% of diameter
- Variable speed, pitch regulated with direct drive PMG power conversion
- Jacket foundation for comparability with DTU 10 MW reference design although floating system could be advantageous

5

Why Multi-Rotors?

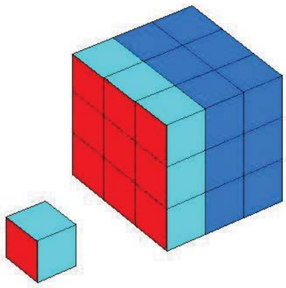


National Geographic 1976

6

Is cubic scaling really true? – Yes!

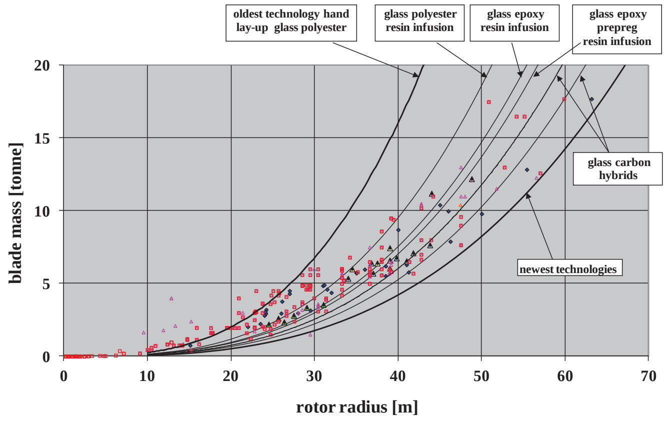

7

MRS Issues

a) Aerodynamic interaction of and array of closely spaced rotors

b) Mass and cost of support structure

c) Feasibility and cost of system yawing

d) Reliability with much greater total part count

8

Aerodynamic Evaluation (NTUA)

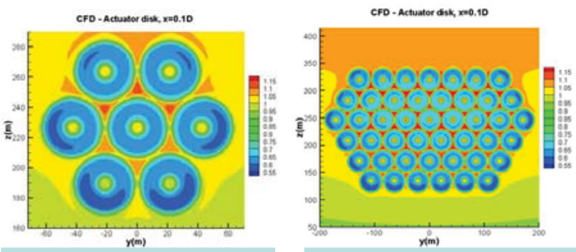

7 rotors, 2.6% power gain

45 rotors, 8.0% power gain

In the above the rotors are actuator discs. NTUA repeated the analysis using a vortex code (blades individually represented) with similar overall results.

In a separate study of the University of Strathclyde it was shown that the MRS would outperform a large rotor in turbulent wind conditions due to the small rotors having intrinsically faster dynamic response.

9

Comparison with 20 MW single rotor

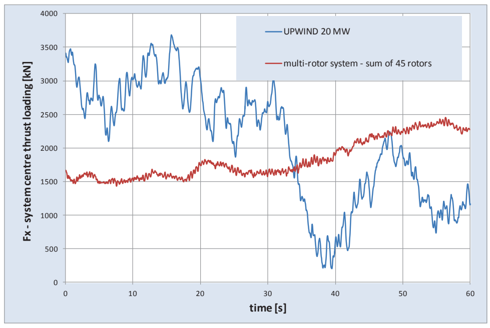

Loads were derived using a specially extended form of DNV GL Bladed software which could deal with independent operation of 45 rotors in a turbulent wind field. Time series of the 6 load components at each rotor centre were used as input for the support structure design.

10

Multi Rotor System –Structure Design (CRES)

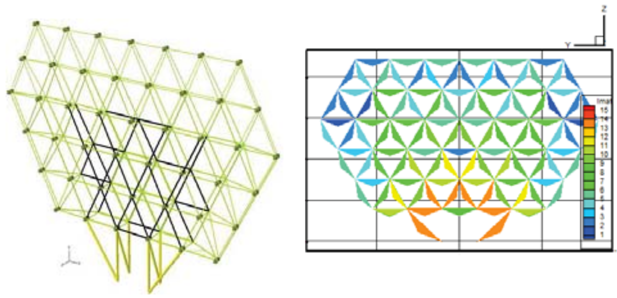

The structure design accommodates a severe robustness criterion – overall integrity is preserved according to demanded reliability criteria in event of failure of most highly stressed member

11

Yaw System Design

- Development of a yaw system specification
- Evaluation of bearing arrangements and loads
- Effects of structure aerodynamic drag on yaw stability
- Feasibility of yawing operation using differential control of rotor thrusts via blade pitch control (work in Innwind Task 1.4 ongoing in the PhD of Ewan McMahon of the University of Strathclyde)

12

Yaw System Design – twin bearings

Concept illustration at 5 MW scale

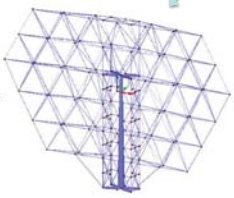

Design for 20 MW MRS developed by HAW Hamburg using RSTAB, a commercial analysis program for 3D beam structures. Prior to developing solutions with yawing capability, as a validation, they first evaluated the CRES design for DLC 1.3 with similar results for system mass.

	Semi-tower design	Reference design
	Mass [t]t	Mass [t]
Yaw Bearing connection top	390	-
Yaw Bearing connection bottom	17	-
Yaw bearings	78	
Tower	1520	-
Space Frame with rotor nacelle assemblies	1850	3760
Overall support structure	3855	3760

The semi-tower solution is a little more massive than the final CRES design but incorporates yawing capability. The overall structure weight and cost benefits from the frame being "hung" on the bearings with more members in tension compared to a base supported structure

13

MRS Feasibility and Cost?

a) Very large structure but not unusual. Similar to jacket above water. Lattice structure in this and many other applications is the most efficient in total weight of materials.

b) System yawing – somewhat new challenge, definitely feasible and looks to be quite affordable

c) Aerodynamic interactions – apparently not adverse maybe even beneficial

d) Reliability with much greater total part count? Offset by reduced impact of single rotor failures, improved unit reliability and overall maintenance strategy. Potential for advantage rather than penalty in O&M costs

16

O&M of the MRS

a) The MRS is significantly different from conventional technology in O&M aspects.

b) A detailed O&M model for cost optimisation of conventional wind farms (Dinwoodie, PhD thesis) was adapted to capture some of the most significant differences of the MRS

c) This was supported by work on availability and production (but excluding cost impacts) by DTU in Task 1.34 which highlighted availability penalties if all turbines required to be shut down during maintenance.

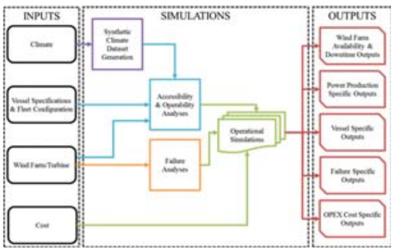

14

LCOE Evaluation and Sensitivity

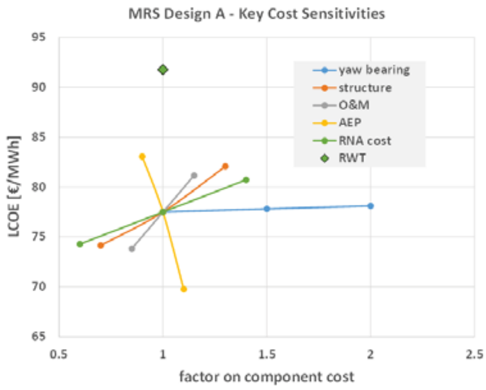

17

O&M Results

a) In respect of availability, the O&M modelling of Dinwoodie (Strathclyde) and of Gintautas (DTU, Task 13.4) was very similar for the MRS although Dinwoodie predicted lower availability of the DTU reference wind turbine (RWT) than the 97% assumed in Innwind

b) The Dinwoodie model predicted similar O&M costs as were attributed to the RWT in the Task 1.2 cost model and all results (O&M cost) of the UoS model were subsequently scaled by a factor so that agreement with the RWT was exact.

c) A 13% reduction in O&M cost was predicted for the MRS strongly related to the avoidance of using jack-up vessels for any level of rotor system failure.

15

PI Assessment of Innwind Innovations

LCOE Impact	%
MRS	-16.0
Low Induction Rotor	-6.0
Advanced Two Bladed Rotor	-7.6
Smart Rotor with Flaps	-0.5
Carbon Truss Blade Structure	-0.6
Bend-Twist Coupled Rotor	-0.8
Superconducting Generator	-0.4
PDD (Magnomatics) Generator	-3.2

This evaluation employing a common independent LCOE evaluation method for all innovations is without credit for predicted O&M benefit and suggested energy capture benefits of MRS

18

MRS Benefits?

a) Technology related LCOE reduction ~ 30% as in the present project (this is relative to current offshore LCOE)
b) Further substantial LCOE reduction from greatly reduced commercial risk related to turbine technology
c) Shortening of production and development cycles accelerating turbine cost reduction and reliability improvement
d) Potentially much larger unit capacities than conventional technology reducing the number of offshore sites per installed MW
e) Savings, perhaps ~ 80% reduction, in the use of non-recyclable glass-resin products per installed MW
f) Faster market implementation

Thank you for your attention!

MRS – the Vision for Large Scale

- ~ 50 % reduction in cost of energy from offshore wind
- roughly half (~25%) direct technology impacts as suggested in Innwind
- the rest from commercial and industrial benefits

MRS – The next steps?

- Enhanced and specially adapted modelling tools for aerodynamics, loads and O&M especially
- Detailed designs for fixed bed and floating offshore systems with specific attention to assembly, installation, maintenance and operational logistics
- Prototype design and testing

The C-Tower Project
A Composite Tower for Offshore Wind Turbines

18 January 2017, Deepwind

Trondheim, Norway

Tjeerd van der Zee (WMC)
Marten Jan de Ruiter (WMC)
Ivo Wieling (Jules Dock Composites)

Project introduction


Photo: Wikimedia Commons


Photo: Rob Faulkner

?

Contents

- Project introduction
- Deciding on a tower concept
- Flexible composite tower
- Manufacturing
- Conclusions and next phase

Project partners

- Wind2020: co-ordination
- Jules Dock Composites: production expertise
- WMC: composite and tower design knowledge, design and analysis tools, material and full-scale testing

WIND 2020 · JULES DOCK INNOVATION | DEVELOPMENT | COMPOSITES · Knowledge Centre WMC

Project introduction


Photo: By Cacophony - Own work, CC BY 3.0

Pros and cons of composite tower

- Weight reduction compared to steel
  - Lower installation costs
- Material may better dampen vibrations
- Opportunities for increasing lifetime
- But:
  - Complex production
  - Reduced stiffness (frequency issues)
  - End-of-life not clear
  - New technology – market is conservative

Project challenge

Design a composite offshore wind turbine tower which is:

- lighter
- more flexible but as strong
- more sustainable
- with better damping characteristics

compared to an equivalent steel tower.

Eigenfrequencies

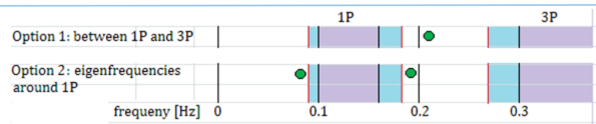

	Stiff	Flexible
Top thickness (D 5.5m)	200 mm	10 mm
Bottom thickness (D 80m)	450 mm	32 mm
Tower weight	1191 ton	92 ton
1st frequency	0.199 Hz	0.065 Hz
2nd frequency	Not relevant	0.217 Hz
Maximum stress	168.7 MPa	330.2 MPa
Buckling SF	47.4	<< 1

Project goals

- **Design a composite offshore wind turbine tower to carry a 10 MW turbine**
  - Uses a steel monopile
- **Show by software analysis that the concept is feasible (strength and fatigue life)**
- **Select production techniques for such a design**
- **Build a (roughly) 1:10-scale prototype and test it**

Optimization

- **Constraints:**
  - 1st side-to-side frequency: below 1P range
  - 2nd side-to-side frequency: over 3P range
  - Idem fore-aft frequencies
  - Buckling safety factor > 1
  - Stresses below critical value
- **Target: Minimization of tower mass**

Tower geometry

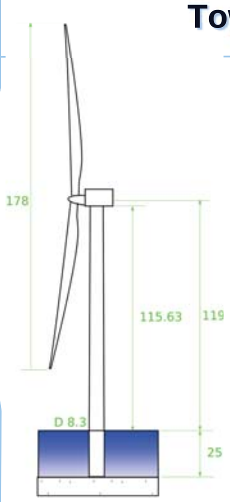

Reference model:

- DTU 10 MW reference turbine

Tower model using:

- Steel (baseline)
- composite

Two composite designs:

- **Stiff: design has similar eigenfrequencies to steel**
- **Flexible: design has similar strength to steel, but lower eigenfrequencies**

Environmental conditions

- **K13 North Sea location**
- **25 m water depth**
- **Load cases defined according to IEC 61400-3**

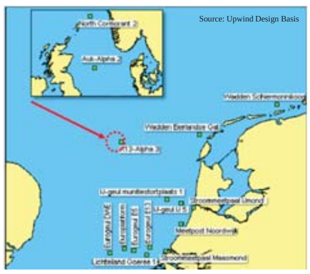

Ultimate strength analysis

- **Extreme load cases selected**
- **Parameters in optimization run**
  - Wall thickness distribution
  - Fibre orientation
  - Relative thickness of layers
- **Full FEM assessment at end of optimization loop**
- **Result: for a glass fibre reinforced epoxy stresses are below critical values**

Manufacturing

Filament winding:

- **Automation possible**
- **Consistent and highly controllable**
- **Angles close to 0 degrees**

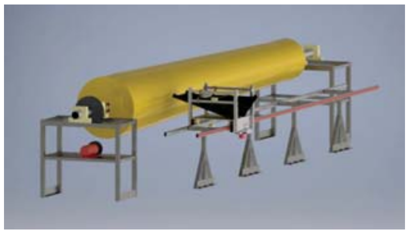

© Copyright WMC 2015

Fatigue analysis

- **Wind-wave directionality plays role in tower loading**
  - More aerodynamic damping by rotor for the tower motions when wave direction is aligned with wind
  - Results in large amount of load cases to consider
- **Slightly reduced set**
  - Maximum of 3 combinations of wave period and wave height per wind speed bin
  - 1824 load cases in total

© Copyright WMC 2015

Manufacturing

- **Machine for manufacturing scale model being built now**

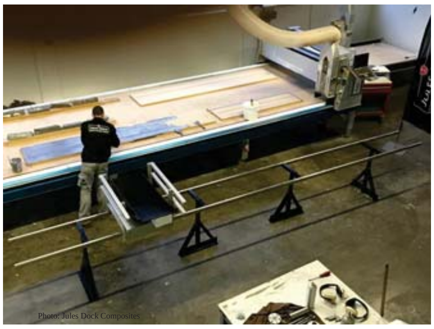

Photo: Jules Dock Composites

© Copyright WMC 2015

Fatigue analysis

- **Values for Ultimate Tensile Strength (UTS) and Ultimate Compressive Strength (UCS) assumed**
- **Fatigue Reserve Factors determined at locations at 4 m intervals throughout tower**
- **20 year fatigue lifetime possible with UTS = 132.7 MPa; UCS = 92.9 MPa**
- **All safety factors according to GL Guidelines taken into account**

© Copyright WMC 2015

Conclusions so far

- **Calculations show that flexible composite tower is feasible**
  - 34% mass reduction compared to steel baseline tower
  - Tower top deflection of less than 3 degrees
- **For a real competitive design, an integrated approach including substructure and control strategy is required**

© Copyright WMC 2015

Next phase

- Completion of filament winding machine
- Material testing on small test coupons

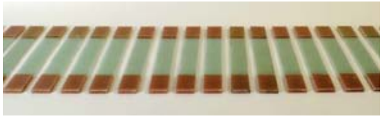

- Production of the scaled model
- Testing of the scaled model at WMC

Knowledge Centre WMC
Wind turbine Materials and Constructions

Thank you for your attention

Questions?

This research is financially supported by TKI Wind op Zee

WIND 2020

JULES DOCK
INNOVATION | DEVELOPMENT | COMPOSITES

Knowledge Centre WMC

Knowledge Centre WMC
Wind turbine Materials and Constructions

Support structure load mitigation of a large offshore wind turbine using a semi-active magnetorheological damper

Rasoul Shirzadeh, Martin Kühn
ForWind – Center for Wind Energy Research, Oldenburg, Germany

Content

- Introduction
- Campbell diagram
- Numerical simulations
- Load mitigation strategies
- Implementation of the MR damper
- Results
- Conclusions

Introduction

- The rotor diameter and the tower height sizes are pushing the engineering limits!
- Direct upscaling of support structure from 5 MW reference wind turbine → rotor-tower resonance problem

- Monopile foundations are limited up to 6-8 MW class
- Jacket structure is the most economic option for large wind turbines
- A strong and severe 3P resonance is expected for WTs with jacket foundation

Campbell diagram

INNWIND.EU 10MW Reference Wind Turbine

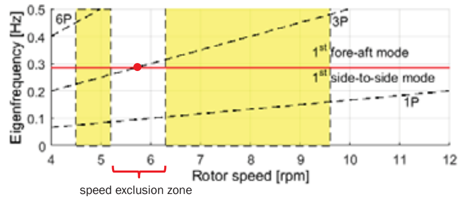

- Coincidence of the 3P mode and the first fundamental mode at 5.7 rpm → dynamic excitation
- Solution: mitigation via control strategy using an exclusion zone between 5.2 and 6.3 rpm

Numerical simulations

- OWT type: INNWIND.EU 10MW
- Aeroelastic simulations: DNV GL Bladed software
- Foundation: 4-leged jacket structure
- DLC 1.2 according to IEC61400-1 standard for operational condition
- Wind-wave misalignment: 0°
- 10 min simulations with 6 random seeds
- Post-processing: Fatigue Limit State (FLS)

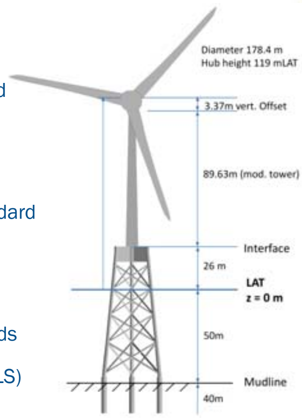

Load mitigation strategies

- Structural control and regulation

e.g.: active tower damping (collective pitch control, individual pitch control, generator torque, active idling)

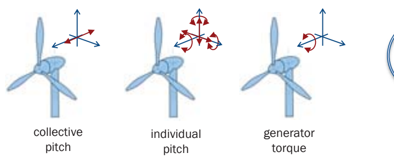

- Damping devices, e.g. passive or (semi)-active

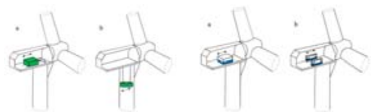

[O. Altay et al, RWTH Aachen, EURODYN 2014]

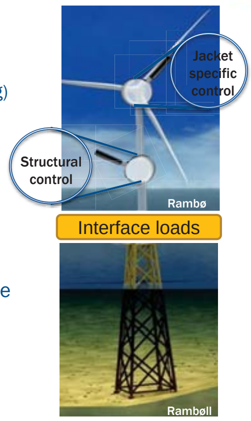

Semi-active Magneto-rheological (MR) damper

Main characteristics:
- requires low power sources, i.e. only several watts are needed to generate damper force as big as 3 kN.
- fast response time, i.e. less than a few milliseconds,
- can be easily controlled
- quite stable within a broad temperature

range between -40 to 150°C

20 t MR damper
- Inside diameter: 20.3 cm
- Stroke: 8 cm
- Length: 1 m
- Mass: 250 kg

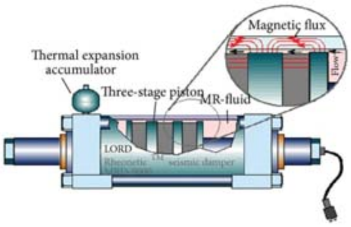

7

Semi-active MR damper modeling

Yang's model for MR dampers

$$f - f_0 = m\ddot{x} + c(\dot{x})\dot{x} + k\dot{x} + \alpha z$$

$$\dot{z} = -\gamma|\dot{x}|z|z|^{n-1} - \beta\dot{x}|z|^{n} + A\dot{x}$$

$$c(\dot{x}) = a_1\, e^{-(a_2\,|\dot{x}|)^{p}}$$

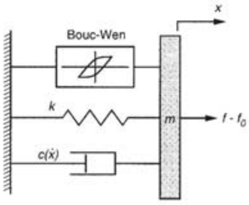

m: equivalent mass of the MR fluid which accounts inertia effects,
k: accumulator stiffness,
f_0: damper friction force resulted from seals and measurement bias,
$c(\dot{x})$: post-yield damping coefficient,
$\gamma.\beta.\alpha$ and A: parameters to adjust the shape of the hysteresis loop,
a_1, a_2 and *p* are positive constants.

8

Implementation of semi-active MR damper

Numerical modeling of the MR damper shows the mechanism to calculate the damper forces using the tower accelerations.

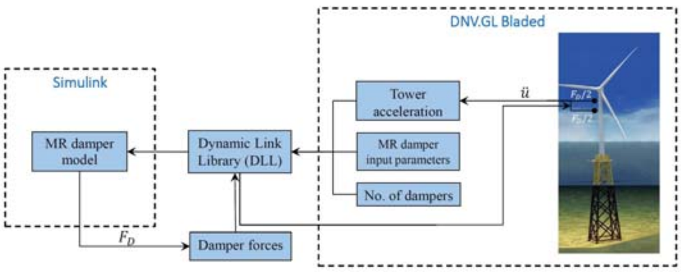

9

Results

Validation of MR damper model

Input:

Sinusoidal displacement excitation with A=1 in and f=0.5 Hz

Output:

Damper force

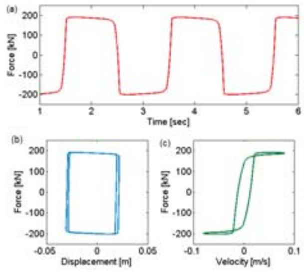

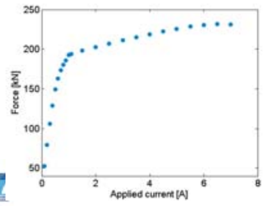

Damper force vs. applied current

For this study: *i*=2 A

10

Results

Nacelle displacement with and without MR damper at 22 m/s mean wind speed

fore-aft

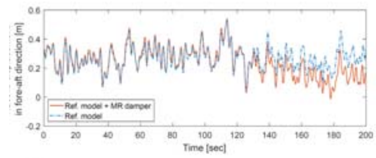

side-to-side

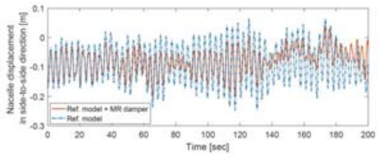

- Two MR dampers in 0º and 90º
- Tower top vibrations are dissipated mainly in the sideways direction

11

Results

Tower base moment with and without MR damper at 4 m/s mean wind speed

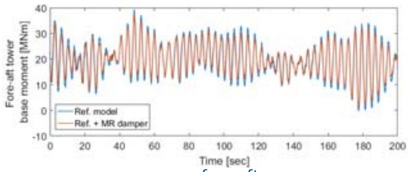

fore-aft

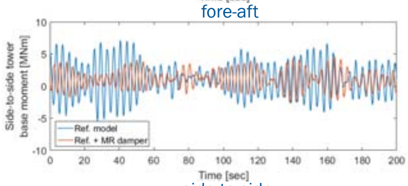

side-to-side

12

Conclusions

ForWind INNWIND.EU

- The numerical model of a semi-active MR damper is developed to mitigate the structural vibrations at the tower top location
- The preliminary results show that the semi-active damper can effectively alleviate the external loads within the whole operational range
- The integration of the semi-active dampers in the early stage phase of the jacket design could significantly alleviate the interface loads which would result in an optimized and economic jacket structure.

13

Acknowledgment

ForWind INNWIND.EU

The research leading to these results has received funding from the European Community's Seventh Framework Programme FP7-ENERGY-2012-1-2STAGE under grant agreement No.308974 (INNWIND.EU).

INNWIND.EU

ForWind INNWIND.EU

Thanks for your attention.

B1) Grid connection and power system integration

HVDC-connection of Large Offshore Wind Farms Using a Low-Cost Hybrid Converter, I. Haukaas, NTNU

Generator Response Following as a Primary Frequency Response Control Strategy for VSC-HVDC Connected Offshore Windfarms, R. McGill, NTNU

Scale models of Modular Multilevel Converters, K. Ljøkelsøy, SINTEF Energi AS

Experimental validation of high definition modular multilevel converter, R. Torres-Olguin, SINTEF Energi AS

NTNU
Norwegian University of Science and Technology

HVDC-connection of Large Offshore Wind Farms Using a Low-Cost Hybrid Converter

Inga Haukaas, Raymundo E. Torres-Olguin, Olimpo Anaya-Lara

DeepWind’2017, Trondheim

Outline

1. Introduction
2. New hybrid solution
3. System description
4. Control objectives
5. Control system
6. Simulation
7. Conclusion

Introduction

- Offshore wind capacity: 3% of global installed capacity.
- More than 90% installed in the north of Europe.

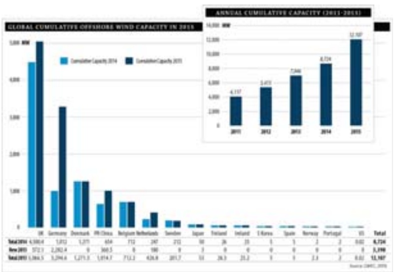

Introduction – Offshore wind farms

- Key benefits:
  - great wind resource
  - vast space
  - reduced visual noise and impact
- Challenge:
  - installation of big platforms
  - power transmission over long distances
- Ultimate goal: reduce cost.

Source: BorWin1, ABB

- Study by Ernst & Young (EY) in 2015:
  - promising results for long term development
  - One key priority: ensure cost-effective grid investments and connections
- HVDC most efficient for long sub-sea cables.
  - Need a converter station!

Introduction – Converter platform

- Challenge:
  - Reduce cost of converter platform.
- Solution:
  - Reduce size of platform and use less expensive and more robust power devices.
- A VSC station is smaller than a LCC station.
- Disadvantage of the VSC:
  - large switching losses and expensive power devices.
  - Reduce losses and cost by introducing a hybrid converter.

Cost of OWF:

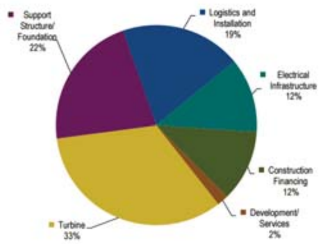

Navigant Consulting, 2013

New hybrid solution

- 12-pulse diode rectifier (DR) connected in series with a VSC.
- Anticipated results: (From ref: [1])
  - efficiency = 99.07% (VSC: 98.4%)
  - cost of power devices = 53.47% of VSC
  - same size as HVDC light station
- YYD - Transformer:
  - Eliminate 5th and 7th order harmonic current component.
- Takes advantage of both DR and VSC technology.
  - VSC: smaller filter banks
  - DR: higher efficiency
- More robust
  - less switching devices.

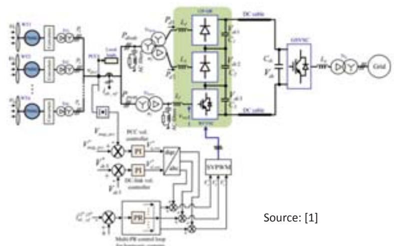

Source: [1]

System description

- BorWin1, reference project
- Simplified wind farm
- Control of the WFVSC is the focus of this paper

Power and Voltage	Parameters	Values
Base values	Power rating [MW]	400
	DC Voltage [kV]	±150
Filter values	C_{PCC} [μF]	6.0
	$C_{1,2,3}$ [μF]	300
	C_{dc} [μF]	70
	L_d [mH]	46
	L_c [mH]	35
	L_g [mH]	28
Transformers	T_{DR} [kV]	33/76/76; 0.1 p.u.
	T_{VSC} [kV]	33/67; 0.1 p.u.
	T_g [kV]	170/300; 0.1 p.u.

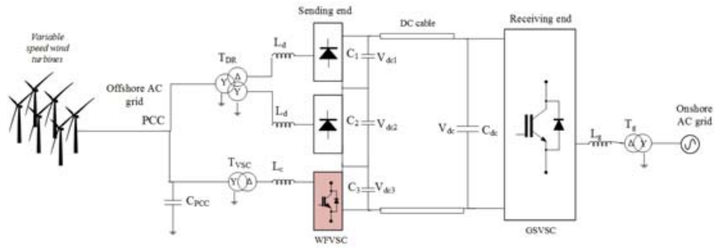

Control objective 3

Harmonic control $i_{WF} \longrightarrow i_{WF}^* = gV_{pcc}$

WFVSC works as an active filter by utilizing a proportional-resonant (PR) filter.

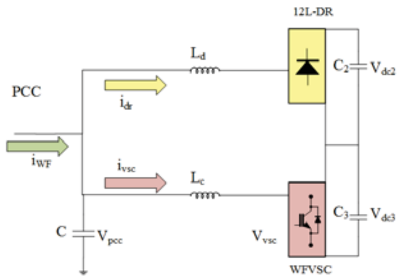

Transfer function for the integrator term of the PR controller:

$$G_{I_h}(s) = \sum_{h=11,13} K_{I_h} \frac{s}{s^2 + (\omega \cdot h)^2}$$

Control objective

1. Voltage tracking control $V_{pcc} \longrightarrow V_{pcc}^*$ (m,f)
2. Balancing control $V_{dc3} \longrightarrow V_{dc3}^*$
3. Harmonic control $i_{WF} \longrightarrow i_{WF}^* = gV_{pcc}$

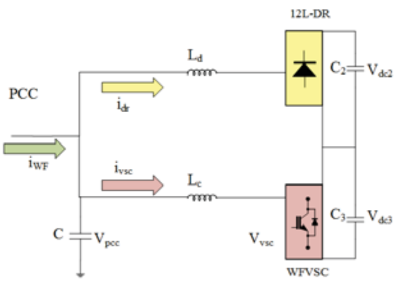

Control system

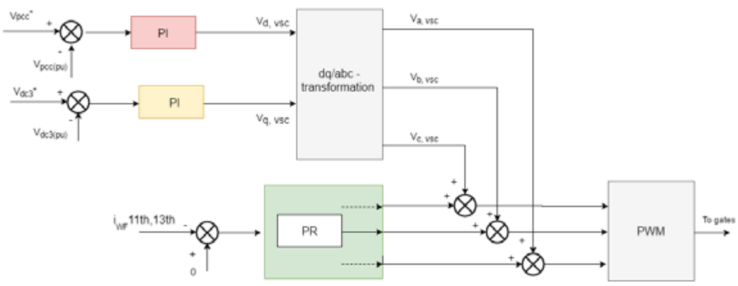

Control objective 1 & 2

1. Voltage tracking control $V_{pcc} \longrightarrow V_{pcc}^*$ (m,f)
2. Balancing control $V_{dc3} \longrightarrow V_{dc3}^*$

$$P = \frac{|V_{VSC}|\sin\delta}{\omega L_C} \cdot |V_{PCC}| \longrightarrow P = \frac{V_{q,VSC}}{\omega L_C} \cdot |V_{PCC}|$$

$$Q = \frac{|V_{VSC}|\cos\delta - |V_{PCC}|}{\omega L_C} \cdot |V_{PCC}| \longrightarrow Q = \frac{V_{d,VSC} - |V_{PCC}|}{\omega L_C} \cdot |V_{PCC}|$$

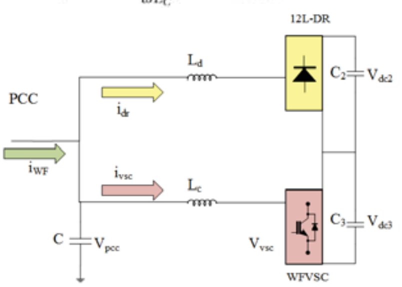

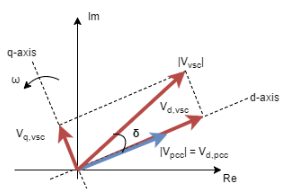

Simulation

- Control objective 1: Voltage tracking control

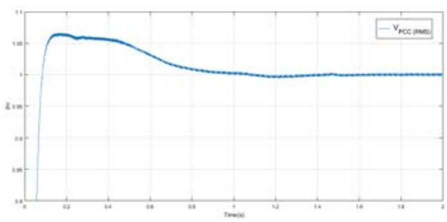

- Control objective 2: Balancing control
  - Preliminary implementation: used an ideal voltage source where Vdc3 = Vdc/3

Simulation

- Control objective 3: Harmonic control

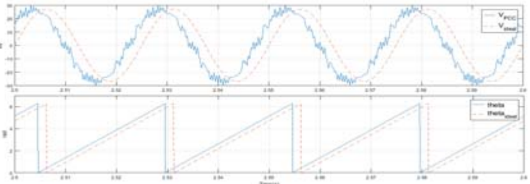

Unfiltered

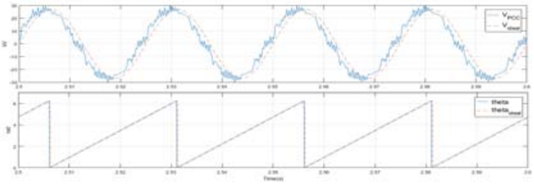

Filtered

Alternative controller

Model-based controller in stationary reference frame:

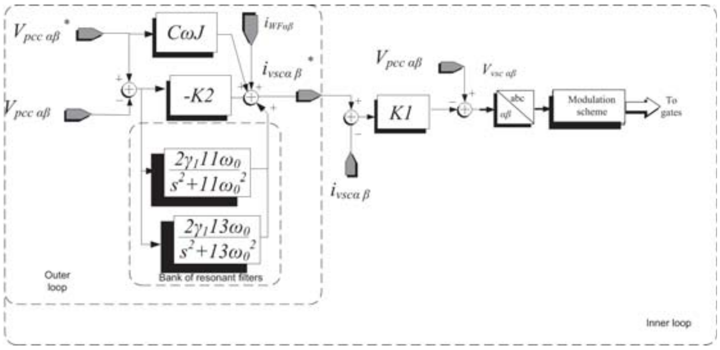

Preliminary results

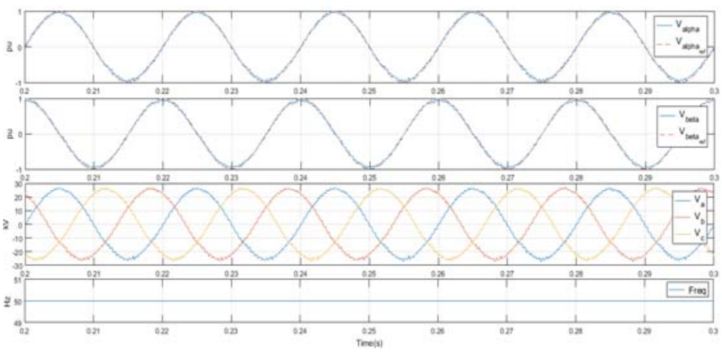

Conclusion

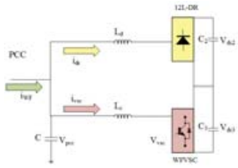

- Challenging controller!
- Reduced number of switching devices
  - More robust
  - Lower switching losses > Higher efficiency
  - Reduced cost of power devices
- Reduced size of filter banks compared with the DR

→ Reduced cost of offshore converter station

Future work: ancillary services

Thank you!

Questions?

[1] T. H. Nguyen, D. C. Lee, and Chan-Ki Kim. "A Series-Connected Topology of a Diode Rectifier and a Voltage-Source Converter for an HVDC Transmission System". In: *Power Electronics, IEEE Transactions on* 29.4 (2014), pp.1579–1584

NTNU – Trondheim
Norwegian University of
Science and Technology

Generator Response Following as a Primary Frequency Response Control Strategy for VSC-HVDC Connected Offshore Windfarms

Ryan McGill
Raymundo Torres-Olguin
Olimpo Anaya-Lara

Full Theoretical System Model:

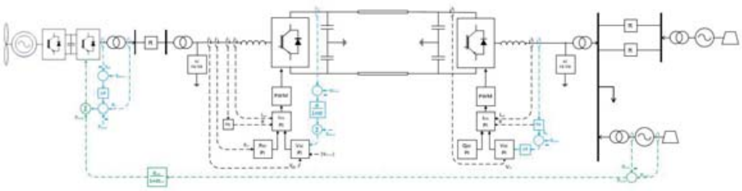

LSG, SSG, Strong Grid, GS-VSC:

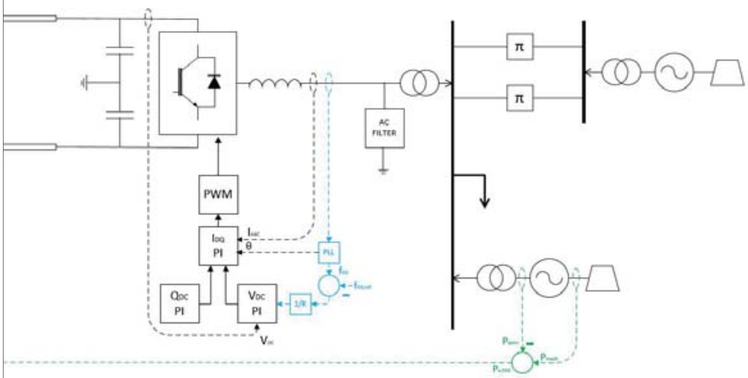

WTG, Weak Grid, WF-VSC:

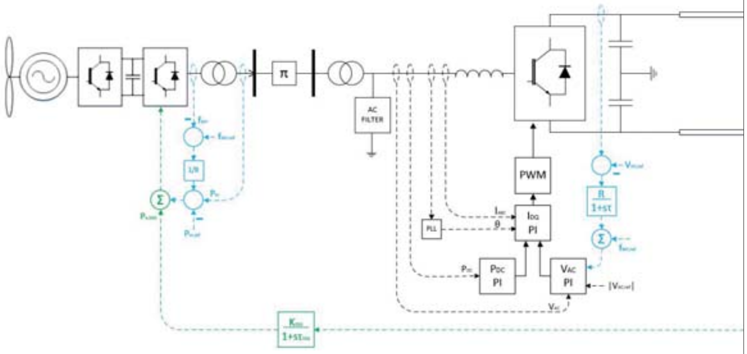

Goals for this Presentation:

- **Provide Background Definitions and Motivation for the Project**
- The effects of inertia are relevant on a dynamic time scale, therefore:
  - Derive Linearized System Equations for Analysis of Synchronous Dynamics
  - Study a Small Signal Disturbance due to a Simple Asynchronous Load Change at the PCC
- **Develop the Theoretical System Model**
- **Describe signal flow of the VSC-HVDC “Communication-less” Method**
- **Describe signal flow of the Fiber Optic Communication Method**
- Time Domain Simulation in PSCAD
- Spectral Analysis of Time Domain Results for Comparison
- Laboratory Test

Outline:

- **Definitions Relevant to AC/DC System Interaction**
- Motivation for Generator Response Following
- Definitions Relevant to Synthetic Inertia and Mechanical Dynamics
- Theoretical System Model
- Practical Modifications
- Other Work

AC System Voltage Strength:

$$SCR_{DC} = \frac{AC\ System\ Short\ Circuit\ Power}{Power\ Rating\ of\ DC\ Link} = \frac{S_{SC,AC}}{P_{DC}} = \frac{E_{AC}^2}{P_{DC}\ Z_{AC}}$$

SCR_{DC}: Effective Short Circuit Ratio is a measure of AC System Short Circuit Strength relative to Capacity of the DC Link

- Strong Voltage AC System has low thevenin equivalent impedance and small voltage variations
- Weak Voltage AC System can result in Dynamic Overvoltage Problems and Harmonic Resonances

Recommended Voltage Strength for an HVDC Connection is:

$$SCR_{DC} \geq 10$$

AC System Frequency Strength:

$$H_{DC} = \frac{AC\ System\ Total\ Rotational\ Inertia}{Power\ Rating\ of\ DC\ Link} = \frac{KE_{LSG}+KE_{SSG}+KE_{WTG}}{P_{DC}}\ [\frac{MWs}{MVA}]$$

H_{DC}: Effective Inertia Constant is a measure of AC System Rotational Inertia relative to Capacity of the DC Link

- Strong Frequency AC System has High Mechanical Inertia. It can absorb dynamic power imbalances leading to shallow frequency gradients and slow frequency variations
- Weak Frequency AC System is unable to absorb power imbalances leading to sharp frequency gradients and faster frequency variations

Recommended Frequency Strength for an HVDC Connection is:

$$H_{DC}\ > 3\ sec$$

AC System X/R Ratio:

Inductive AC System has a high amount of inductance relative to resistance. Therefore:

- exhibits strong dependency between Frequency and Active Power (ie: changes in active power will create changes in frequency)
- exhibits strong dependency between Voltage and Reactive Power (ie: changes in reactive power will create changes in voltage magnitude)

Typical X/R Ratio for 230 kV AC Transmission System:

X/R = 10

AC System Stiffness:

$$\beta = \Sigma \frac{1}{R_i} + D \quad \text{where} \quad \Delta f_{ss} = -\Delta P_L / \beta$$

β: Composite Frequency Response Characteristic: A Measure of System Frequency Sensitivity to Changes in Load (sometimes referred to as stiffness)

$\frac{1}{R_i}$: Individual f-P Regulation Constants: Typical value is 20 to 25

D: Steady state damping effect of all frequency dependant AC loads. Typical value is 1 to 2

- A Stiff AC System has small Steady State Frequency Changes
- β also contributes to Primary Response

AC System Dynamic Stability:

$$\Delta T_e = K_S \Delta\delta + K_D \Delta\omega$$

K_S: Synchronizing Power (Synchronizing Torque) Coefficient: Component of Electrical Power in phase with rotor angle deviation, positive value prevents aperiodic drift of rotor angle

K_D: Damping Power (Damping Torque) Coefficient: Component of Electrical Power in phase with speed deviation, positive value prevents oscillatory instability

HVDC Power Connections do not naturally have these small signal synchronizing or damping components.

Synchronous vs. Asynchronous:

Synchronous Component:

- Inherent to the component and/or contains synchronizing controls
- Contains a Synchronous Power Coefficient for Dynamic Stability
- Example: Synchronous Generator

Frequency Dependent Asynchronous Component:

- Source/Load Changes as a function of frequency
- Example: Simple inductor/capacitor, Induction Machine

Frequency Independent Asynchronous Component:

- Component functions independently of frequency
- Example: Simple resistor, power electronics

Outline:

- Definitions Relevant to AC/DC System Interaction
- **Motivation for Generator Response Following**
- **Definitions Relevant to Synthetic Inertia and Mechanical Dynamics**
- Theoretical System Model
- Practical Modifications
- Other Work

Motivation for Generator Response Following:

Historical Perspective:
- A traditional solution to the problem of low Effective Inertia Constant H_{DC} is to add synchronous condensers to the AC system, increasing the amount of mechanical inertia
- Synchronous Condensers also supply the reactive power requirement of Traditional Load Commutated Converters

Contribution:
- Similarly, this project studies the Mechanical Inertia Response (Electromechanical Power) of a Small Synchronous Generator (SSG) connected at the point of common coupling (PCC)
- A P_e measurement at the SSG can be amplified and superimposed onto the inertia-less Aggregated Wind Turbine Generator (WTG)
- The result is an amplified synchronous dynamic response from the VSC-HVDC Connected Offshore Wind Farm (OWF) at the PCC

Mechanical vs. Synthetic Inertia:

The Swing Equation for Inertial Response:

$$M\frac{df}{dt} = P_m - P_e \text{ [quantities in pu]}$$

Inertia Constant in the Per Unit System ($M = 2H$):

$$H = \frac{KE}{S_{RATED}}, units \left[\frac{MWs}{MVA}\right]$$

Kinetic Energy Associated with Mechanical Inertia:

$$KE = \int J\omega\, d\omega = \frac{1}{2}J\omega^2 \text{ and quantities } P_e \text{ injection}$$

Global Frequency Gradient of Strong AC Grid determined by Composite Inertia Constant:

$$H_{eq} = \frac{KE_{LSG} + KE_{SSG} + KE_{OWF}}{S_{LSG} + S_{SSG} + S_{OWF}}$$

KE_{LSG}, KE_{SSG}: Mechanical Inertia from the SSG and the Aggregated Large Synchronous Generator (LSG) at PCC

KE_{OWF}: Synthetic Inertia from the Power Reserve of the Offshore Windfarm (eg: Turbine Rapid Braking Action, Sub-Optimal MPPT)

Generator Response Following and Synthetic Inertia:

Without Generator Response Following (GRF):

$$H_{OWF} = \frac{KE_{OWF}}{S_{OWF}} \cong \frac{0}{S_{OWF}}$$

With Generator Response Following (GRF) and gain of one:

$$H_{OWF} = H_{SSG}$$

$$\frac{KE_{OWF}}{S_{OWF}} = \frac{KE_{SSG}}{S_{SSG}}$$

$KE_{OWF} = KE_{SSG}\frac{S_{OWF}}{S_{SSG}}$ therefore $H_{eq,GRF} > H_{eq}$

Instantaneous Power Reserve of OWF must also be designed for power injection at all points in time:

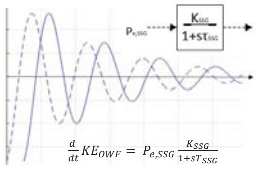

$P_{Reserve}(t) \geq \frac{d}{dt}KE_{OWF}$ where $\frac{d}{dt}KE_{OWF} = P_{e,SSG}\frac{K_{SSG}}{1+sT_{SSG}}$

Communication Channels:

Fiber Optic Communication: Information transmitted via fiber optic cable.

- **Advantage:** Relevant for future development of MTDC networks where direct communication with multiple onshore AC networks may be required
- **Disadvantage:** performance and reliability concerns such as: time delay, reduced data rate, loss of connection

VSC-HVDC Communication-less: V-f proportional cascade used to synthetically couple the strong onshore AC grid to the weak offshore AC grid. Theoretical System Model will elaborate on the signal flow.

- **Advantage:** fast, reliable
- **Disadvantage:** Fiber Optic Communication may be required later as the system grows more complex

Frequency Response:

Inertial Frequency Response:
- Associated with P_e in the swing equation
- Stored energy compensates for temporary power imbalance after load change
- Communicated to OWF via fiber optic channel

Primary Frequency Response:
- Associated with P_m in the swing equation
- Turbine adjusts to meet new demand of load change
- Communicated to OWF via VSC-HVDC communication-less channel

Secondary Frequency Response: System renormalization after primary response steady state has been reached:
- Associated with Power Setpoint or Reference
- Examples: Dynamic Deloading of Wind Turbines, Traditional "Supplementary Control" such as load shedding, etc

Relevant Timescale:

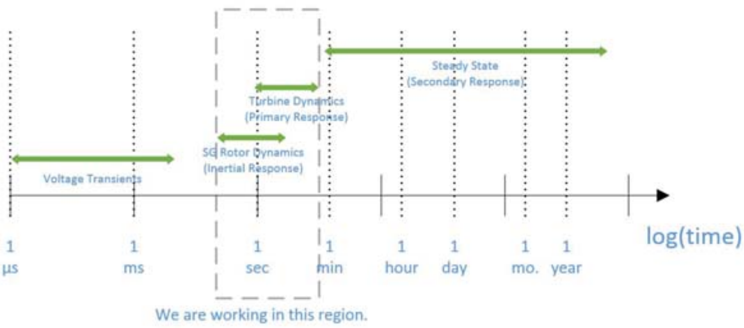

Aggregated Large Synchronous Generator (LSG) and Strong Grid:

- Equivalent pi model with Lumped Parameters
- Strong AC Grid (SCR_{DC} > 10) for Constant Voltage

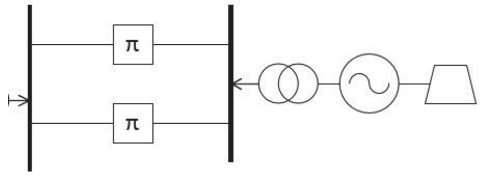

- Strong AC Grid (H_{DC} > 3) for Constant Frequency
- Inductive AC Grid: X/R = 10 (typical) for f-P Load Sharing
- Contribution to Steady State Stiffness: $\beta_{LSG} = 4\,x\,\frac{1}{0.04} = 100$
- Inertia Constant: $H_{LSG} = 3.0$
- Simplifying Assumption: Manual Excitation

LSG, SSG Small Signal Transfer Function:

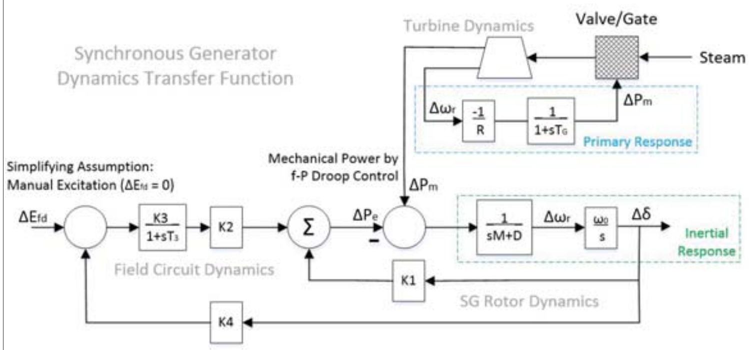

Small Synchronous Generator (SSG):

- Connected at PCC
- Required Power Rating: roughly 5% of HVDC Link
- Contribution to Steady State Stiffness: $\beta_{SSG} = \frac{1}{0.04} = 25$
- Inertia Constant: $H_{SSG} = 3.0$
- Simplifying Assumption: Manual Excitation

P_e: shaft power minus terminal power. Measurement is sent to OWF via **fiber optic channel**

P_m: measured at the shaft

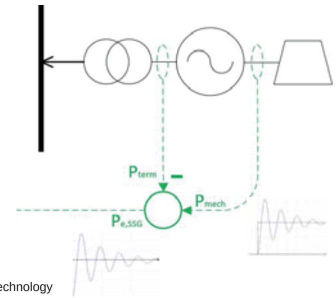

Outline:

- Definitions Relevant to AC/DC System Interaction
- Motivation for Generator Response Following
- Definitions Relevant to Synthetic Inertia and Mechanical Dynamics
- **Theoretical System Model**
- Practical Modifications
- Other Work

Grid Side VSC (GS-VSC):

- Average Model for mechanical dynamics
- Constant Reactive Power Control
- Constant V_{DC} Control modified with Frequency-V_{DC} Droop (**communication-less channel**)

GS-VSC operates independently of Active Power

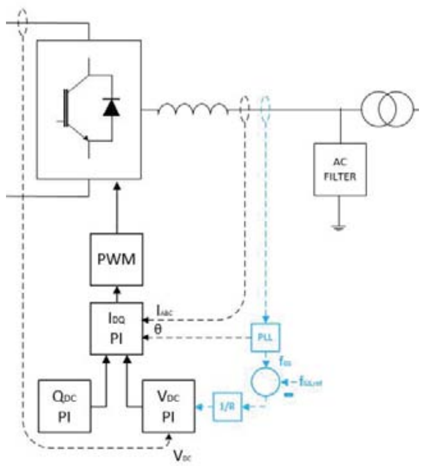

VSC-HVDC Link:

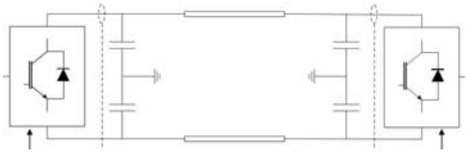

Simplifying Assumptions:

- Uni-Directional Power Flow from OWF to Onshore AC Grid
- No Converter Losses: $P_{AC} = P_{DC}$
- No DC Cable Resistive Losses: $V_{DC,GS} = V_{DC,WF}$ and therefore $f_{GS} = f_{WF}$

Grid side frequency same as Wind Farm Side Frequency (ie: synthetically coupled) with a time delay.

Wind Farm Side VSC (WF-VSC):

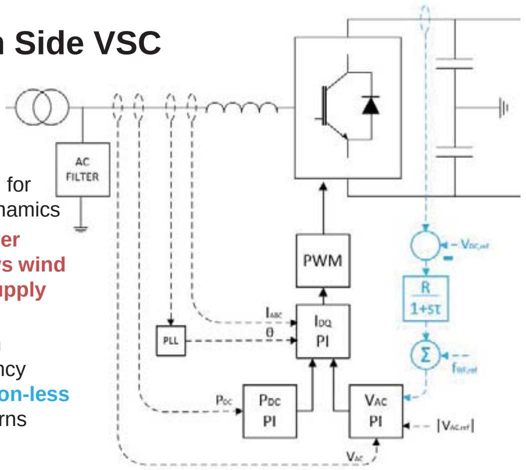

- Average Model for mechanical dynamics
- **Constant Power Control follows wind farm power supply**
- Constant VAC magnitude with varying frequency (**communication-less channel**) governs weak AC grid frequency

Aggregated Wind Turbine Generator (WTG) and Weak Grid:

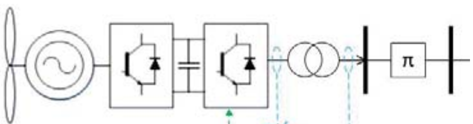

- Equivalent pi model with Lumped Parameters
- Weak AC Collection Grid follows WF-VSC VAC controller amplitude and frequency
  - SCR = 2 (typical)
  - H = 0 (no mechanical inertia)
  - **Low X/R Ratio (decouples f from P)**

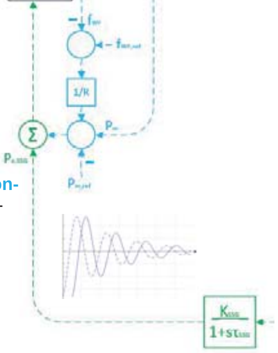

P_m: received by frequency variation (**communication-less channel**) and f-P droop converts to inertia-less primary response

$P_{e,SSG}$: measurement received by **fiber optic channel** and superimposes a synthetic inertia response

Outline:

- Definitions Relevant to AC/DC System Interaction
- Motivation for Generator Response Following
- Definitions Relevant to Synthetic Inertia and Mechanical Dynamics
- Theoretical System Model
- **Practical Modifications**
- **Other Work**

Practical Modifications:

In general, redundancy of communication channels will increase reliability. Below are some other possible communication schemes. System design with a first priority option as well as a second priority option may be desirable.

- Option #1:
  - Small Synchronous Condenser
  - Inertial Response → Pe measurement sent via fiber optic channel
  - Primary Response → Performed by communication-less method
- Option #2:
  - Small Synchronous Condenser
  - Inertial Response → Pe measurement sent via communication-less channel
  - Primary Response → Performed by communication-less method
- Option #3:
  - Nearby Generator/Turbine Installation
  - Inertial & Primary Response → Pe & Pm measurement sent via fiber optic channel
- Option #4:
  - Nearby Generator/Turbine Installation
  - Inertial & Primary Response → Pe & Pm measurement sent via communication-less channel

Other Work:

- Provide Background Definitions and Motivation for the Project
- **The effects of inertia are relevant on a dynamic time scale, therefore:**
  - **Derive Linearized System Equations for Analysis of Synchronous Dynamics**
  - **Study a Small Signal Disturbance due to a Simple Asynchronous Load Change at the PCC**
- Develop the Theoretical System Model
- Describe signal flow of the VSC-HVDC "Communication-less" Method
- Describe signal flow of the Fiber Optic Communication Method
- **Time Domain Simulation in PSCAD**
- **Spectral Analysis of Time Domain Results for Comparison**
- **Laboratory Test**

SCALE MODEL OF MODULAR MULTILEVEL CONVERTER

Kjell Ljøkelsøy

MMC topology

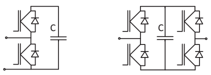

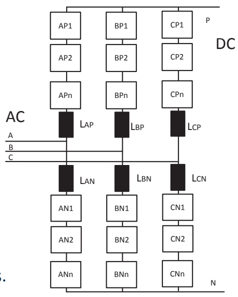

- Halfbridge or fullbridge cells
- Many low voltage cells: (~300 per arm)
- Energy for several periods in cell capacitors
- Good AC voltage control. Small voltage steps.
- Redundancy

Why lab scale models?

- Many components, complex control.
  - Need for experience building.
- Testing on full scale systems not really feasible.
  - Potentially large consequences. Don't get access.
- Simulation models depends on model
  - Gives the answers you expect. Can miss unexpected aspects.
  - Assumptions and simplifications. May omit something important.
- Real converters contains most aspects.
  - Some adaptations and simplifications here too.

HVDC transmission link between France and Spain: HVDC Plus IGBT converter modules for 1000 MW. www.siemens.com/press".

Choice of scale. Power level:

- Full scale: 1000 MW
  - Essentially unmanageable.
- Low power model:
  - Safe. Low cost. Ease of operation.
  - Can behave quite different from full scale reference
  - High series resistances and auxiliary losses give deviations from reference case.
- High power model:
  - Low scaling ratios. Moderate scaling effects, properties close to full-scale reference.
  - Expensive to build. Expensive to run. Difficult and expensive to reconfigure.
  - Safety issues. Large damage potential. Careful planning required.
- Tradeoff: 60 kVA
  - Fits existing laboratory infrastructure.

Scale: Voltage level, etc.

- Depends on power level.
- Three main ranges:
  - < 50V: Considered to be safe. Used for low power models, <1 kW.
  - < 1000V: Governed by low voltage safety regulations
  - > 1000V. Governed by high voltage safety regulations Used for high power models, > 1MW
- Standard supply voltages preferred. 230V AC ,400V AC, 690V AC.
  - 400V AC chosen. Nominal grid voltage in lab.
- Most other parameters determined by power and voltage scaling .
  - Base impedance, Inductance, Capacitance, Transformer ratio.
- Some remaining parameters:
  - Cell number, control system topology.

Series resistance

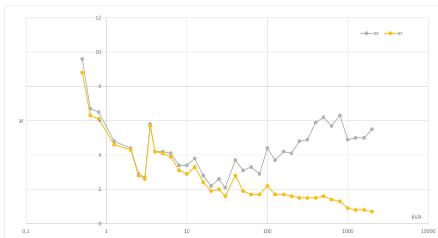

Noratel 3LT series transformers

- Difficult to scale. ESR tend to increase at low power.
- Gives additional damping of oscillations.

Converter specifications

	Reference	18 Halfbridge	12 Fullbridge	6 Halfbridge
Rated power	1059MVA	60 kVA	60 kVA	60 kVA
Rated DC voltage Rated AC voltage	640 kV DC 333 kV	700V 400V	700V 400V	700V 400V
Rated AC current	1836A	85A	85A	85A
Cells per arm Nominal cell voltage	400 2 kV	18 Halfbridge 50V	12 Fullbridge 80V	6 Halfbridge 160V
Arm inductance Cell capacitance	50 mH 10 mF	1,5 mH 20 mF	1,5 mH 15 mF	1,5 mH 7,5 mF
Number of halfbridges	2400	108	144	36

Power cell board

- Common PCB for all variants
  - 50V, 80V 160V, variants
  - Two independent halfbridges,
  - Copper rails for half or fullbridge configuration.
- Low ESR design
  - Thick copper planes in board.
  - Multiple small, low ESR electrolytic capacitors.
- Power circuit domain functions.
  - Transistor drivers, protection and interlock circuits.
  - Generic control signal interface.
  - Voltage and temperature measurements

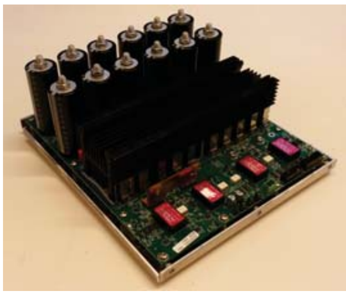

Power transistors

- Scaled cell voltage drop: 100mV
  - MOSFETS, not IGBTs
- 5x parallel MOSFETs
  - 50 and 80V variant: 150V, 5 mOhm => ESR: 1 mOhm
  - 160V variant:: 250V , 15 mOhm => ESR 3 mOhm
  - MOSFETs types with enhanced body diodes required.
- Swiching is fast:
  - Diode reverse recovery snapoff : 20 ns.
  - Little margin for overvoltage transients.
  - Board layout extremely critical.
- Short circuit protection
  - Monitors forward conduction voltage. Trips at 0,8V => 700A

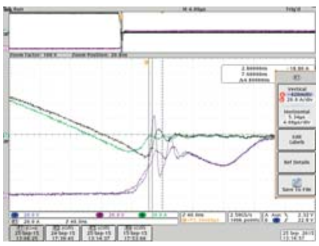

Diode turn off. 5 mm unsymmetry. Ch1,Ch3: uds, Ch4,R1: Id

Control tasks

- Internal
  - Synchronisation of nodes.
  - Protection and state monitoring. Converter fault handling.
  - Cell voltage balancing (within an arm)
  - Arm voltage control (energy balance)
  - Circulating current control
- External
  - Phase current control
  - Active power control/DC voltage control.
  - Reactive power control/ AC voltage control
  - AC phase lock/ Frequency control/ Virtual inertia
  - Harmonic suppression, damping.
  - Grid fault handling, current limiting.

System structure

- Hierarchy:
  - Power cell board
  - Group control board.
  - Converter control board
  - Central control unit
- Optical fiber link
  - 3,75 Gbit/s
  - Chain topology
- Operation modes
  - Normal operation.
  - Development mode. Low level control signals
    - Control algorithms on external unit: OPAL-RT
    - Programming in Matlab/Simulink

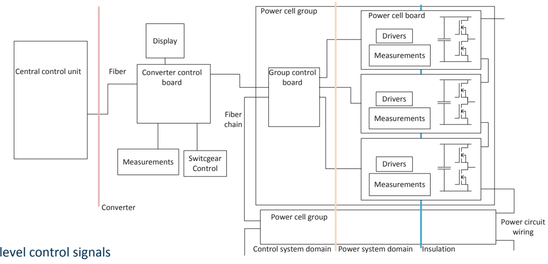

Control electronics

- Group control board.
  - Based on Xilinx Artix FPGA
  - Governs 3-4 power cell boards
  - Gathers measurements.
  - Distributes 24V supply to drivers.
  - Generates, distributes driver signals.
- Converter control board.
  - Designed as general purpose converter control board
  - Based on PicoZed7030 module.
  - Xilinx Zynq 7030 FPGA with ARM A9 processor.
  - 8x 40 MSPS AD converter allows oversampling.
  - Handles converter control and protection functions.

Power cell group module

- 19" subrack 6U height
  - Group control board
  - 3-4 power cell boards: 6 or 8 halfbridges, 4 fullbridges
- All connections at front.
- Power cell modules in front and back of cabinets
- Vertical boards: Convective airflow
  - No fans. Fans may be required in 6 level converter.

19" cabinet

- 18 level halfbridge converter.
- Half filled cabinet: One phase
  - Two phases back to back.
  - Three modules per arm,
  - Two arms per phase.
- Large amount of capacitors.
  - 648 capacitor cans for 18 cell converter.

Complete 12 level fullbridge converter

- Cabinet 1:
  - Switchgear,
  - Arm inductors,
  - Control electronics,
  - Power cells phase A,B
- Cabinet 2:
  - 2: Power cells phase A,B.
- Equal layout for 18 cell halfbridge converter
- Single cabinet for 6 cell fullbridge converter

Single phase test

- Test of 18 level halfbridge converter
  - Open loop, no current control
  - Cell voltage sorting selects to be on or off
  - 100% modulation
  - Single phase RL load
  - Center tap DC capacitor bank
- Waveforms equal to simulations
  - Distorted arm current due to capacitor charging/discharging.

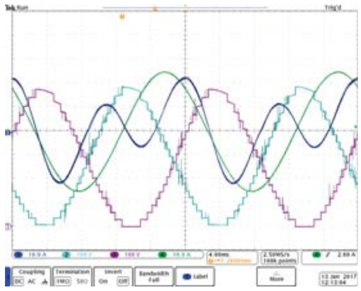

Ch1: Arm current, Ch2, Ch3: Arm voltages, Ch4: Phase current.

It works!

SINTEF

Teknologi for et bedre samfunn

Experimental Validation of High definition Modular Multilevel Converter

Raymundo E. Torres-Olguin†, Michael Smailes, ‡ Chong Ng‡, Pol Paradell□, Jose Luis Domínguez-García□, Giuseppe Guido†, Kjell Ljøkelsøy†, Salvatore D'Arco†
†SINTEF Energy research
‡Offshore Renewable Energy Catapult
□Catalonia institute for energy research IREC

Presenter: Raymundo E. Torres-Olguin

Background

- This work focuses on the experimental validation of the concept proposed by ORE catapult High Definition Modular Multilevel Converter (HD-MMC).
- **SINTEF** and **ORE Catapult** are currently working on MMC. The control algorithm for a HD-MMC was developed at ORE Catapult in a simulation enviroment. MMC units have been developed at SINTEF. **IREC** will act as an impartial referee during the comparison of both techniques C-MMC vs HD-MMC since it has no conflict of interest in the proiect.

Content

- Introduction
- High definition modular Multilevel Converter
- Experimental set-up
- Test procedure
- Some preliminary experimental results
- Conclusions

Introduction

- MMC is emerging topology for offshore wind substations due to its black start capabilities, low Total Harmonic Distortion (THD) and high efficiency.
- The MMC uses a stack of identical modules.
- The multiple voltage steps make the MMC being capable of producing very small harmonic content

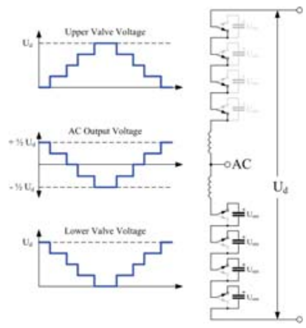

Background

- This work is part of the **1st call for Joint Experiments** organized within the Research Infrastructure WP of IRPWind.
- IRPWind is a European project, which it is aimed to foster better integration of European research activities in the field of wind energy research.
- In Europe, most large research facilities are being devoted to national activities that not necessarily matching the needs of Europe as a whole.
- **1st call for Joint Experiments** has the objective of promoting alignment through joint experiments carried out in European research facilities and its effective use of resources.

Introduction

- In the conventional MMC (C-MMC) each module create one level, so in order to produce a low THD many modules are required.
- What happen if MMC uses an uneven dc values?

Valve	u_c	Logic								
	V	t_0	t_1	t_2	t_3	t_4	t_5	t_6	t_7	t_8
4p	$U_{dc}/4$	1	1	1	1	1	0	0	1	0
3p	$U_{dc}/4$	1	1	1	0	0	0	0	0	1
2p	$U_{dc}/4$	0	1	1	1	1	1	0	0	0
1p	$U_{dc}/4$	0	0	1	1	0	0	0	0	1
1n	$U_{dc}/4$	1	1	0	0	0	1	1	1	0
2n	$U_{dc}/4$	1	0	0	1	1	1	1	1	1
3n	$U_{dc}/4$	0	0	0	0	0	0	1	1	0
4n	$U_{dc}/4$	0	0	0	0	1	1	1	0	1

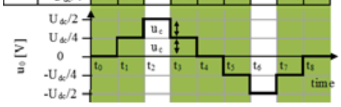

Introduction

By using uneven dc values in the C-MMC, the novel HD-MMC can produce 7 levels using the same number of modules.

Therefore, THD of the convert is reduced.

Some potential advantages:

- It can reduce the number of modules required to produce a required THD
- A more compact converter can be achieved reducing platform size and cost
- the utilisation of the MMC's resources could be improved, since redundant states can be repurposed.

SM	u_c V	t_0	t_1	t_2	t_3	t_4	t_5	t_6	t_7	t_8	t_9	t_{10}	t_{11}	t_{12}
1	u_{c1}	0	1	0	0	1	0	1	1	1	1	0	0	0
2	u_{c1}	1	1	1	0	0	0	0	1	0	1	1	0	1
3	$u_{c2}(2u_{c1})$	0	0	0	0	0	1	1	1	1	1	1	1	0
4	$u_{c2}(2u_{c1})$	1	0	0	0	0	0	0	0	1	1	1	1	1
5	u_{c1}	1	1	1	1	0	0	0	1	0	0	1	0	1
6	u_{c1}	0	1	0	1	1	0	1	1	1	0	0	0	0
7	$u_{c2}(2u_{c1})$	1	1	1	1	1	1	0	0	0	0	0	0	1
8	$u_{c2}(2u_{c1})$	0	0	1	1	1	1	1	0	0	0	0	1	0

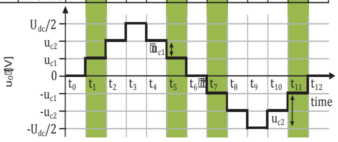

Experimental setup

The single phase 18 module MMC was used for the experiment. The proposed test set-up is shown in Figure.

A RL load is used on the AC bus in place of an AC grid as it is thought to be an unnecessary complication for the test.

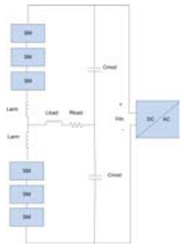

# of cells per arm	18
DC Voltage	700 V
Rated power	60 kVA
Rated current	30 A
Cell capacitance	21.3mF
Arm inductance	1.4 mH

High definition modular Multilevel Converter

The HD-MMC differs from C-MMC primarily though the addition of a control block between the high level power control and the low level module selection and voltage balancing functions.

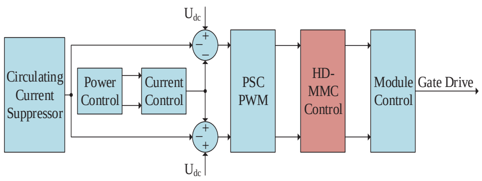

Test procedure

There are 3 main goals of the experiment.

1. Validate the computer models using the test set-up
2. Prove the HD-MMC concept works
3. Compare the performance of the HD-MMC to a C-MMC using THD and efficiency

As THD and efficiency work against each other and the differences between the HD-MMC and C-MMC it would be very difficult to optimise both controls in such a way to ensure a fair test. As a result, several different control combinations for each converter will be tested.

High Definition Modular Multilevel Converter

Since each module is no longer equivalent, the set controller must select the correct combination of modules to create the desired voltage level. The controller must also balance the set voltages to ensure that the step size remains constant, minimizing harmonic generation and aiding in converter control.
This is done using standard module voltage measurements and arm currents, therefore no additional sensors are required.

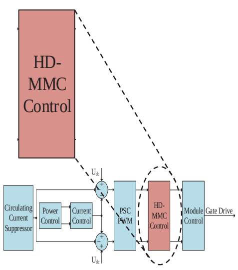

1. Validate the computer models using the test set-up

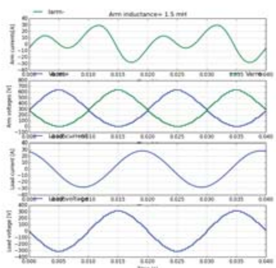

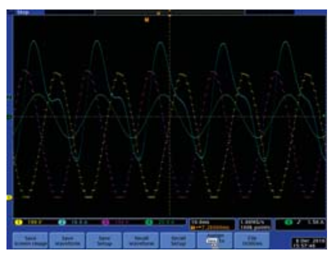

Simulations using NLM

The simulation and experiment match very well

Experiments using NLM

1. Validate the computer models using the test set-up

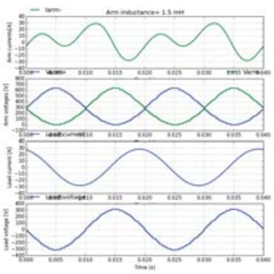

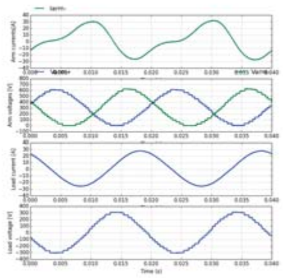

Simulations using NLM

The simulation and experiment match very well

Experiments using NLM

Conclusions

- This work was part of the **1st call for Joint Experiments** organized within The Research Infrastructure WP of IRPWind.
- There were 3 main goals of the experiment.

(i) Validate the computer models using the test set-up. The simulation and experiment match perfectly.

(ii)Prove the HD-MMC concept works. Three cases were proven [9 9], [5,13] [3,15]. The MMC is able to work with uneven dc voltages.

(iii) Compare the performance of the HD-MMC to a C-MMC using THD and efficiency. While the primary goal of HD-MMC is to reduce the THD, however it is important that the losses are not increased significantly as a result.

2. Prove the HD-MMC concept works

Three cases were proven [fully charged half charged]: [9 9], [5,13] [3,15].

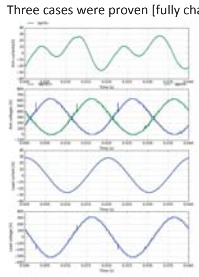

[9 9]

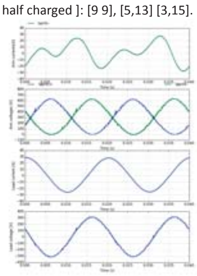

[5 13]

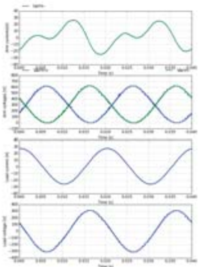

[3 15]

The MMC is able to work with uneven dc voltages as shown in the Figures

THANKS

3. Compare the performance of the HD-MMC to a C-MMC using THD and efficiency

Three cases were proven [9 9], [5,13] [3,15]. Clearly the THD can be improved using the HD-MMC concept. In the case of the efficiency, the input and output power of the converter will also be measured to determine the efficiency. However, the difference between the HD-MMC and C-MMC cases will be very small due in part to the type of switches used, MMC is made using MOSFET. Counting the number of switching operations will therefore provide an easier way to infer the efficiency of each converter.

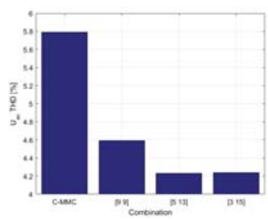

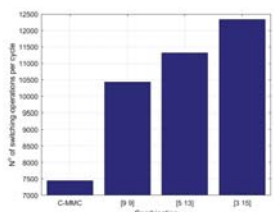

B2) Grid connection and power system integration

Strategies towards an Efficient future North Sea Energy Infrastructure (SENSEI),
F. Papathanasiou, ECN

A hybrid wind-diesel-battery system for fish farming applications, M. Holt, NTNU

Assessing the impact of sampling and clustering techniques on offshore grid expansion planning, P. Härtel, Fraunhofer IWES

Multistage grid investments incorporating uncertainty in offshore wind development – A North Sea case study, H. Svendsen, SINTEF Energi AS

Energy Academy Europe · TNO innovation for life · ECN Your energy. Our passion.

Strategies towards an Efficient future North Sea Energy Infrastructure

Fotis Papathanasiou
EERA DeepWind 2017

Trondheim
19-01-2017

www.ecn.nl

The case of Dutch North Sea region (2/2): ... while offshore gas production is in **decline**

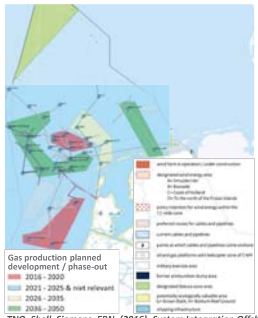

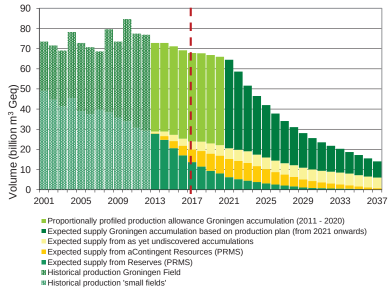

TNO, Shell, Siemens, EBN. (2016). System Integration Offshore Energy: Innovation Project North Sea Energy. Retrieved 11 02, 2016, from https://www.tno.nl/media/8512/system_integration_offshore_energy_final-report_tno_r11234.pdf

Source: Dutch Ministry of Economic Affairs. (2016). Delfstoffen en Aardwarmte in Nederland, revisie 1. Retrieved 12 21, 2016, from http://www.nlog.nl/jaarverslagen

---

Motivation

System integration options
Strategies

Challenges for offshore wind and gas

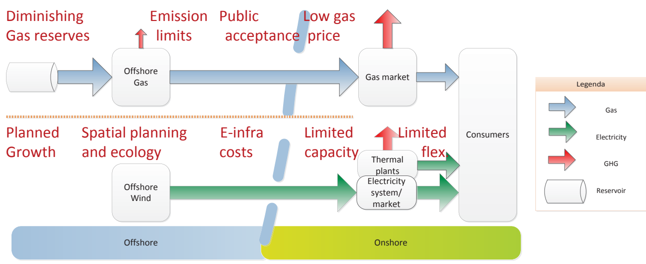

- *Offshore system integration may resolve challenges and bring additional benefits*
- *Systematic overview in the many options is needed*

The case of Dutch North Sea region (1/2): Offshore wind is **growing** rapidly ...

- Designated areas**--> 4.5GW in 2023**

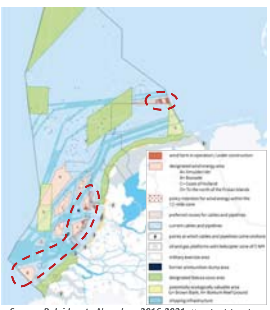

Source: Beleidsnota Noordzee 2016-2021, Noordzeeloket.nl

- Vision beyond 2023: combined offshore wind and transnational grid development

Source: TenneT, 10 June 2016, Retrieved from: tennet.eu/nl/news/article/tennet-presents-hub-and-spoke-concept-for-large-scale-wind-energy-on-the-north-sea.html

---

Support for offshore system integration

- **June 6, 2016, EU Energy Council:**
  "North Sea Declaration" - Regional coordination on offshore energy
- **June 15, 2016, Oil and gas producers (NOGEPA), NWEA, Natuur en Milieu, TenneT, TNO:**
  "Gas meets Wind" - Declaration of Coordination and Cooperation in the North Sea Region
- **June-Dec. 2016:** Project **SENSEI** "Strategies towards an Efficient future North Sea Energy Infrastructure

Project partners:
TNO innovation for life · ECN · Energy Academy Europe — ESTRAC Energy Systems Transition Centre

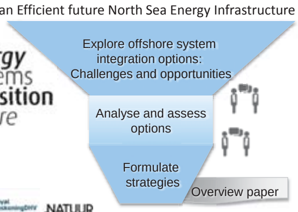

Supported by wind and gas sector and NGOs

TenneT · NOGEPA · TKI Wind op Zee · TKI gas · ENGIE · ebn · NAM · NWEA · Royal HaskoningDHV · SIEMENS · Natuur & Milieu


ECN
Motivation
System integration options
Strategies

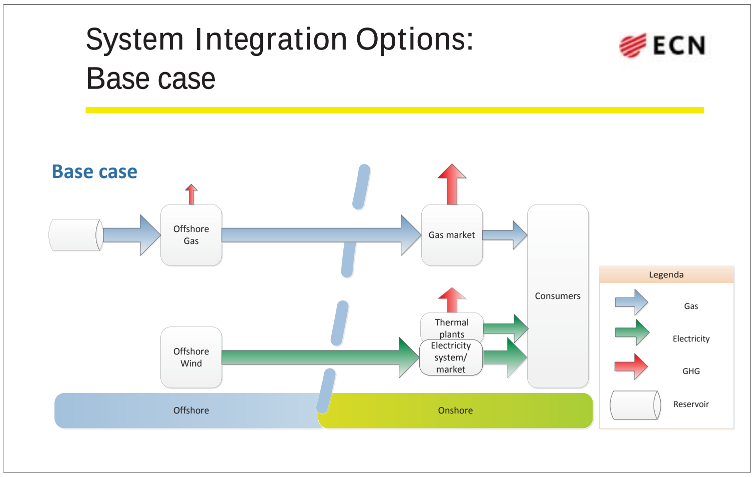
System Integration Options:
Base case
ECN
Base case
Offshore Gas
Gas market
Consumers
Thermal plants
Electricity system/ market
Offshore Wind
Offshore
Onshore
Legenda
Gas
Electricity
GHG
Reservoir

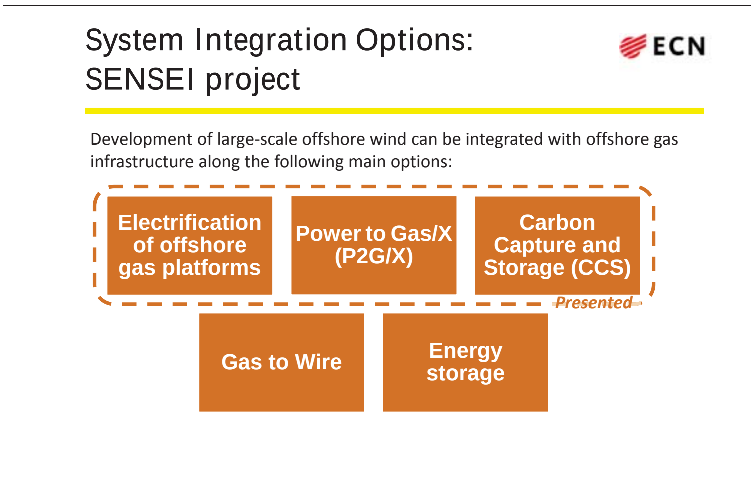
System Integration Options:
SENSEI project
ECN
Development of large-scale offshore wind can be integrated with offshore gas infrastructure along the following main options:
Electrification of offshore gas platforms
Power to Gas/X (P2G/X)
Carbon Capture and Storage (CCS)
Presented
Gas to Wire
Energy storage

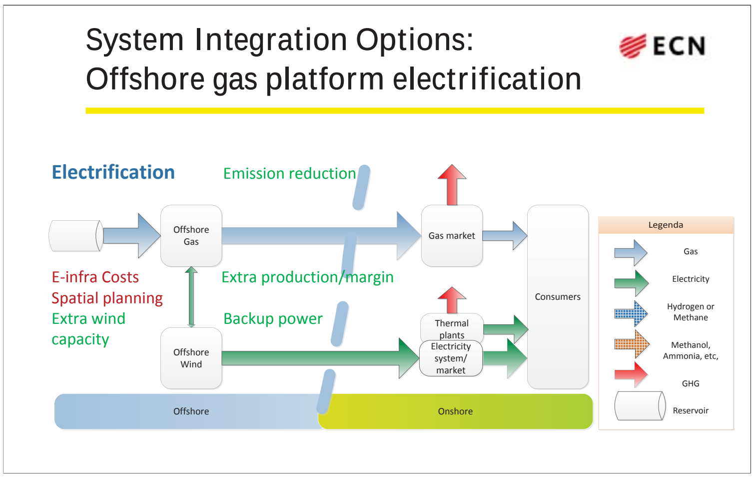
System Integration Options:
Offshore gas platform electrification
ECN
Electrification
Emission reduction
E-infra Costs
Spatial planning
Extra wind capacity
Extra production/margin
Backup power
Offshore Gas
Gas market
Consumers
Thermal plants
Electricity system/ market
Offshore Wind
Offshore
Onshore
Legenda
Gas
Electricity
Hydrogen or Methane
Methanol, Ammonia, etc,
GHG
Reservoir

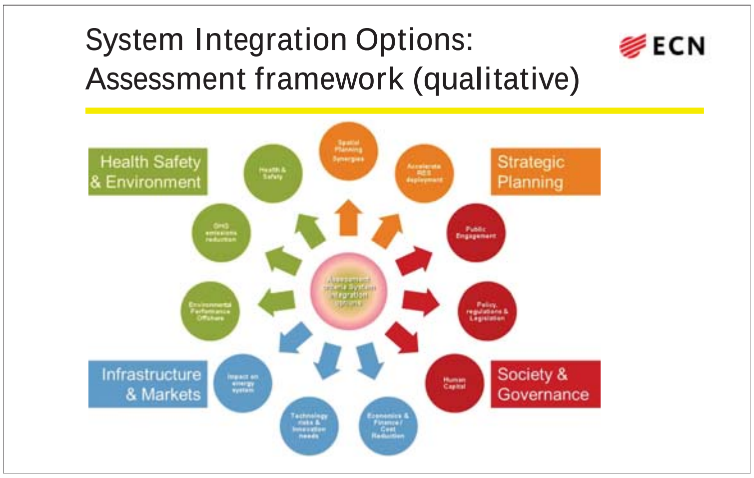
System Integration Options:
Assessment framework (qualitative)
ECN
Health Safety & Environment
Strategic Planning
Infrastructure & Markets
Society & Governance

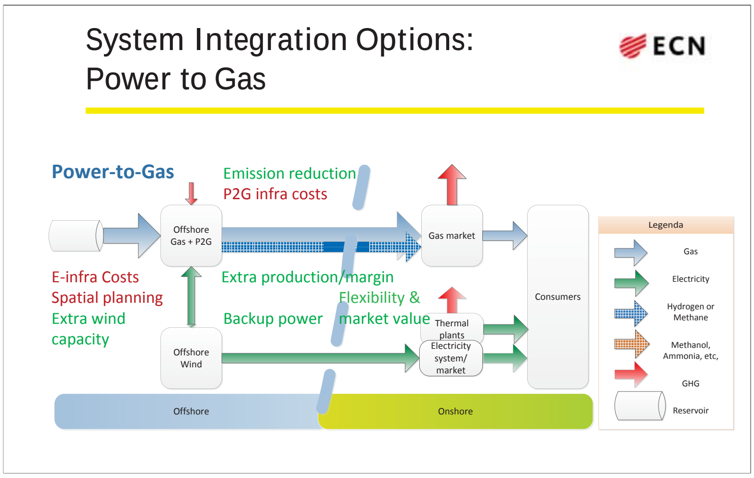
System Integration Options:
Power to Gas
ECN
Power-to-Gas
Emission reduction
P2G infra costs
E-infra Costs
Spatial planning
Extra wind capacity
Extra production/margin
Flexibility & market value
Backup power
Offshore Gas + P2G
Gas market
Consumers
Thermal plants
Electricity system/ market
Offshore Wind
Offshore
Onshore
Legenda
Gas
Electricity
Hydrogen or Methane
Methanol, Ammonia, etc,
GHG
Reservoir

System Integration Options: Offshore CCS

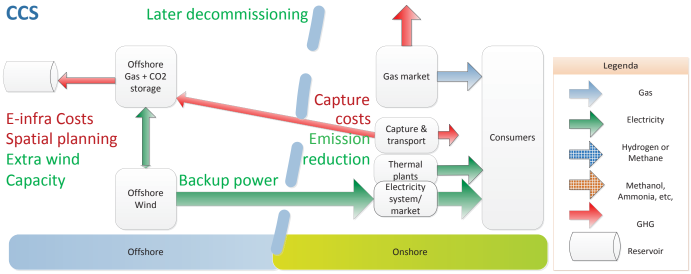

Development strategies (1/2)

Time horizon / System integration options	Short-term <2023	Mid-term 2023 - 2030	Long-term 2030 - 2050
Electrification	Platform electrification near-shore	Platform electrification, far-offshore & stand-alone	Platform electrification, offshore grid
P2G / P2X	Power2Gas, onshore (demo)	Power2Gas, offshore	Power2X, offshore
CCS	CCS + electrification near-shore	CCS + electrification (depleted gas fields)	
GTW	GTW near shore (end-of-field)		GTW far offshore, through offshore grid
Energy storage			Energy storage offshore (H_2, CAES)

- *Electrification is basis for further system integration options (develop in steps)*
- *Favorable short-term options identified, although arranging regulatory issues takes time*

Summary of drivers and barriers

- Main **drivers:**
  - Higher market value for offshore wind from increased flexibility and reliability
  - Lower development costs for offshore wind through savings on grid infrastructure
  - Higher offshore gas production at lower operational costs
  - Reduction of GHG emissions
- Main **barriers:**
  - Regulations (e.g. spatial planning, tight time schedules, support schemes)
  - Uncertainty in market prices (electricity / gas / CO_2) lead to uncertain business case
  - Development needed on offshore conversion technology
  - Public acceptance

Development strategies (2/2)

- **Actions for the short-term:**
  - Set-up **integral strategic vision and roadmap** for North Sea energy transition
  - Identify **shortlist of business cases** that can lead to pilot projects
  - Mobilize **international coordination** (and share experience, e.g. on platform electrification)
  - Develop **regional action plans and strategies** (align investment development)
  - Engage with **stakeholders** (e.g. manage spatial claims, secure value chains)
  - **North Sea Energy project** started, >20 stakeholders, embedded in long-term R&D program
- **R&D needs are broad:**
  - **Technology** development and demonstration -> set-up **pilot projects**
  - System analysis of transition scenarios -> develop **roadmap** with strategic spatial planning
  - **Ecological impact** analysis
  - **Socio-economic, societal** and **governance** analysis -> policy recommendations

Motivation
System integration options
Strategies

Conclusions and recommendations

- **Comprehensive overview** of system integration options in the North Sea is available
- North Sea system integration has **significant economic and ecological potential** and can accelerate energy transition
- Need to quantify benefits and barriers in order to **identify business cases**
- Tight offshore wind planning and accelerated phase-out of offshore gas require **swift action**

Thanks for your attention

Contact: Edwin Wiggelinkhuizen
wiggelinkhuizen@ecn.nl

ECN

Westerduinweg 3	P.O. Box 1
1755 LE Petten	1755 ZG Petten
The Netherlands	The Netherlands
T +31 88 515 49 49	info@ecn.nl
F +31 88 515 44 80	www.ecn.nl

Norwegian University of Science and Technology

NTNU

A hybrid wind-diesel stand-alone system for fish farming applications

Marius Holt, NTNU

NTNU

Overview

- The Norwegian fish farming industry
- Problem definition
- The proposed fish farm
- The hybrid wind-diesel system
- Setting up a long-term performance model in MATLAB
- Case studies and main results
- Shortcomings and further work

NTNU

The Norwegian fish farming industry

- Export 2015: ~47 billion NOK
- Salmon dominates
- Direct employment: Nearly 7000 (per 2015)
- Expected to increase further towards 2050
- Challenges
  - Sea lice
  - Escaping fish
  - Available space
  - Environmental impacts

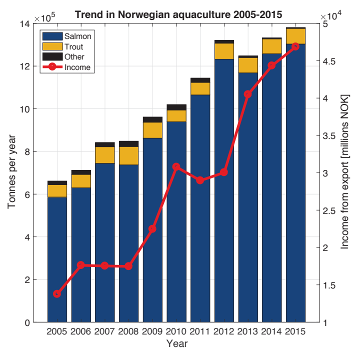

NTNU

Locations with aquaculture

[1] Map from the Norwegian Directorate of Fisheries (2016)

NTNU

Problem definition

- Used today: Diesel aggregates
- Desirable to replace diesel with local renewable sources
- Excessive energy should be used to run:
  - Production of O_2
  - Production of fresh water
  - High pressure washers
- Initiative by Pure Farming
- Co-op. with The National Wind Energy Center Smøla (NVES)
- Objective: *Design a hybrid wind-diesel system in order to reduce diesel fuel consumption as much as possible*

NTNU

A conventional offshore fish farm

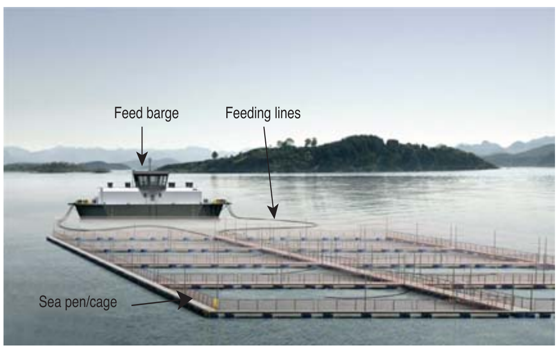

[2] Figure based on AKVA Group's brochure "Cage Farming Aquaculture"

NTNU

The proposed fish farm

- Location: Gråøya, close to Smøla
- 6 feed blowers (each rated at 22 kW)
- 12 cages
- LED lightning of cages
- Expected yearly energy consumption: ~470 000 kWh
- TN-S electrical system

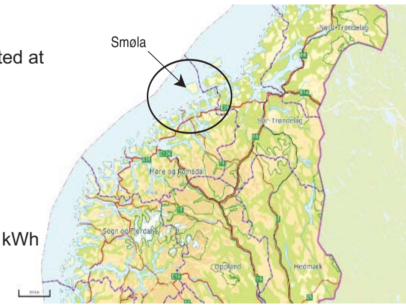

NTNU

The hybrid wind-diesel system

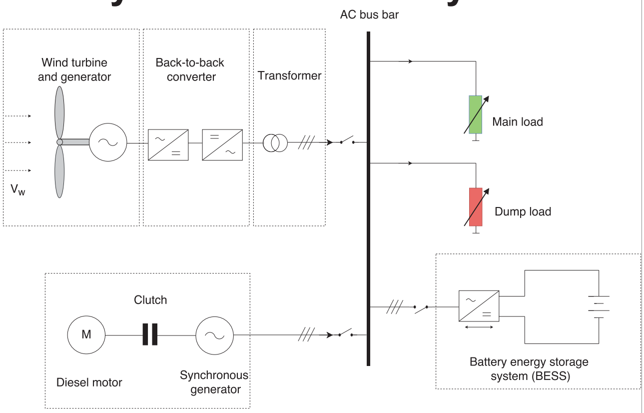

NTNU

System modelling in MATLAB

- Steady state performance model
  - System state is assessed for every half-hour during one year
  - Wind profile
  - Load profile
  - Modelling of the components
  - Control strategy

NTNU

Wind profile

- Based on actual data from Veiholmen (1994-2014)
  - Resolution 1 hour
  - Takes into account seasonal variations
- WAsP used to transform wind speeds to hub height and desired geographical location
- Very good wind conditions
  - Average wind speed: 8.7 m/s (1994-2014)

NTNU

Wind profile

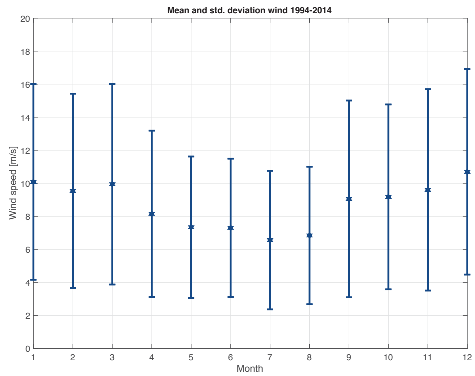

NTNU

Consumption profile

- Expected yearly energy consumption ~470 000 kWh

Deterministic load

- Feed blowers and lightning of cages
- Depends on the day length
  - Blowers run at day-time
  - Lightning at night-time
- Blowers: 72.6 kW
- Lightning: 14.4 kW

Stochastic load

- The feed barge's own consumption
  - Heating
  - Lightning
  - Control system
- Gaussian distribution used
  - Expectation: 9 kW
  - Std. deviation: 2 kW

NTNU

Consumption profile

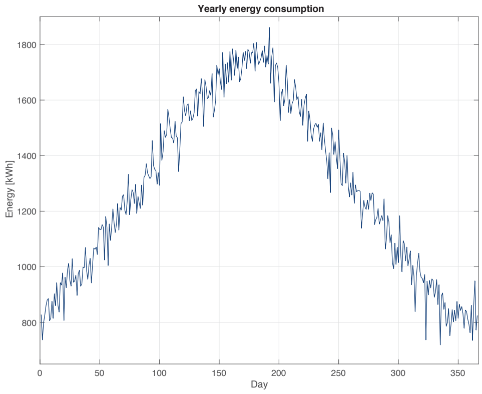

NTNU

The control strategy

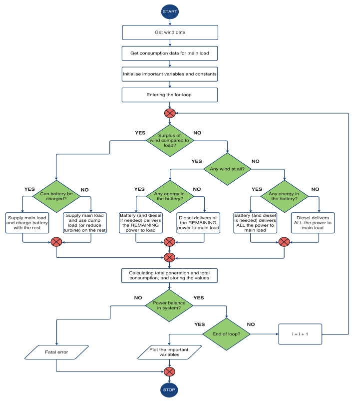

NTNU

Consumption profile

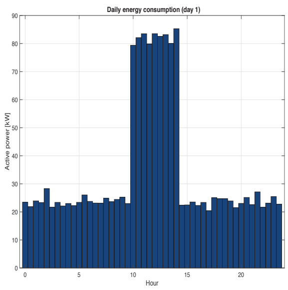

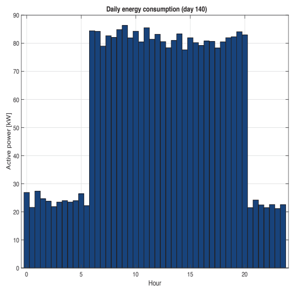

NTNU

Case studies

- Simulated over the year of 2012
- One base case
- Sensitivity cases on
  - Battery size
  - Depth of discharge
  - Max power to/from battery
  - Dump load margins
- Special cases on
  - Wind only
  - Diesel only
  - Wind-diesel

NTNU

Modelling of the components

- Wind turbine: Power curve of an EWT DW52 250 kW turbine used
- Dump load: Max and min power limits
- Battery Energy Storing System (BESS) :
  - Max power capability
  - Max energy capacity
  - Depth of discharge
- Diesel aggregate: Treated as the resolving post
  - Fuel consumption predicted by a simple linear relationship

NTNU

Case studies

Table 5.1: Input data for base case

	Name	Parameter	Value	Unit
Diesel	Diesel fuel constant	A	0.246	l/kWh
	Diesel fuel constant	B	0.08415	l/kWh
	Power rating diesel engine	$P_{D,nom}$	100	kW
BESS	Battery voltage	V_B	520	V
	Battery current capacity	A_B	500	Ah
	Battery depth of discharge	DoD	70	%
	Maximum battery state of charge	$W_{B,max}$	260	kWh
	Minimum battery state of charge	$W_{B,min}$	78	kWh
	Maximum power to/from battery	$P_{B,max}$	100	kW
	Maximum battery through converter	$P_{CONV,max}$	150	kW
Dump	Minimum limit for dump load	$P_{DUMP,min}$	10	kW
	Maximum limit for dump load	$P_{DUMP,max}$	120	kW

NTNU

Main results

- Battery size have largest impact on diesel fuel
- Potential of ~1 500 000 kWh from wind turbine only
  - Dump load margins important
- Wind conditions fairly stable
- More than one diesel aggregate may be desirable
- Reduction in fuel from approx. 170 000 litres to 25 000 litres yearly solely by including a wind turbine (~85 % reduction)
  - More than 1 million NOK yearly in purchase cost only
  - Very large battery may not be needed

NTNU

Shortcomings and further work

- Main goal: form a sound decision basis
- Cost of components and operation not yet surveyed
  - Will be given special focus in the master thesis
- Steady state analyses does not take into account
  - Voltage fluctuations
  - Power quality
  - Other transients
- Detailed component features not included due to the lack of time

Assessing the impact of sampling and clustering techniques on offshore grid expansion planning

14th Deep Sea Offshore Wind R&D Conference, EERA DeepWind'2017

Philipp Härtel, Energy Economy and System Analysis, IWES
Martin Kristiansen, Magnus Korpås, Department of Electric Power Engineering, NTNU

Trondheim, January 19, 2017

Agenda

I	Background and motivation
II	Methodology
III	Case study results
IV	Conclusion

Agenda

I	Background and motivation
II	Methodology
III	Case study results
IV	Conclusion

Increasing variability and uncertainty lead to a growing complexity and present computational challenges for power system models

Rise of power systems underlying variability and uncertainty

- Most power systems experience **increasing share of variable and non-dispatchable generation** in their energy mix
- **Traditional power systems** were **primarily subject** to power **demand variations** and **fault occurrences**
- **Adequate models** for both short- and long-term planning **become more complex**

Crucial task of Transmission Expansion Planning (TEP)

- **Determining** investments in **new transmission lines** or **reinforcements** of the existing transmission network is a **crucial task** in power system planning
- **Long-term** and **capital intensive** decisions having a **long-lasting effect** on expected **market prices** and **power system operation**

Relevance of TEP in European context

- European Union pursuing a **fully integrated internal energy market** in which energy can flow freely across its regions
- **Robust** transmission and distribution **infrastructure**, **well-interconnected European network** key constituents of a successful integration of renewables
- **Spatial levelling effects** of fluctuating renewable energy resources (incl. offshore wind) **make grid reinforcements attractive**

Recent developments make efficient solutions of long-term TEP problems even more necessary, but at the same time increase their complexity

One approach of dealing with computational challenges is to reduce the dimension of the input data through finding representative samples

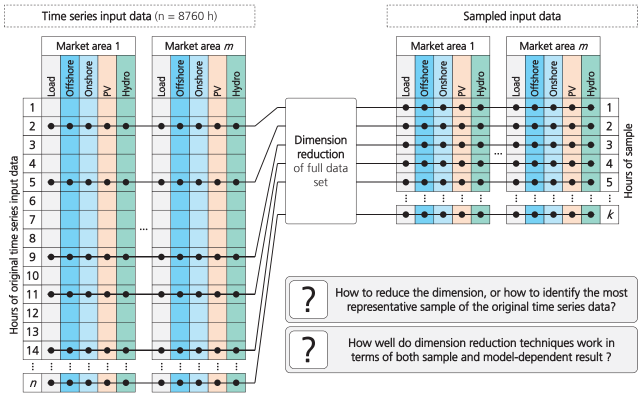

? How to reduce the dimension, or how to identify the most representative sample of the original time series data?

? How well do dimension reduction techniques work in terms of both sample and model-dependent result ?

Agenda

I	Background and motivation
II	Methodology
III	Case study results
IV	Conclusion

5 different sampling & clustering techniques are employed for the dimension reduction – 2 scaling options & heuristic yield 4 variants for each technique & sample size

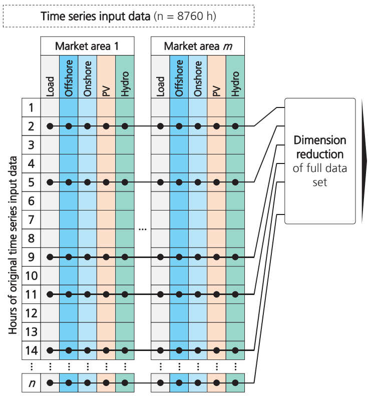

Dimension reduction techniques:

Systematic Sampling	Selects every k^{th} element, k depends on sample size and #observations; Straight-forward but efficient method
k-means clustering	Data-partitioning clustering approach; Subset centroid mean of all measurements
k-medoids clustering	Approach very similar to k-means; Centroids are actual data points (medoid) of the subset
Hierarchical clustering	Agglomerative form of hierarchical clustering analysis; Ward's linkage (minimum variance)
Moment-matching	Sample selection through minimizing a predetermined criterion; Correlation, mean, standard deviation

Two scaling options:

1 Technology-specific scaling

2 Scaling by the highest occurring value

Heuristic:

Moving average heuristic is included as a further variant to capture extreme values (after sampling)

The effect of using the two different scaling options can clearly be seen in the resulting sampling and clustering results

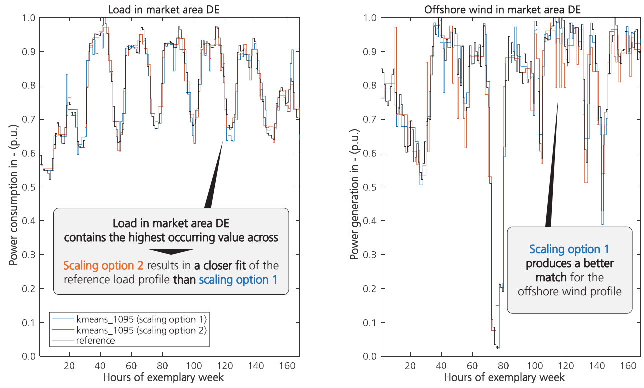

Long-term Transmission Expansion Planning model (PowerGIM) is used for a North Sea offshore grid case study to assess the sampled and clustered input data

Long-term TEP model ("PowerGIM")

- **Two-stage stochastic program** (MILP) co-optimizing investment decisions and market operation in a power system consisting of several market areas
- **Integer variables** used to make **transmission infrastructure investment decisions** (first-stage)
- **Linear program (LP)** reflecting **generator capacity investment** and **market operation** (second-stage)

Case study

- **Offshore grid expansion** in the North Sea region
- **2030 scenario** based on ENTSO-E's **Vision 4**
- **Investment options include combined HVAC and HVDC grids** (both radial- and meshed structures)
- **Considered market areas** are Norway, Great Britain, Denmark, Belgium, Germany and the Netherlands
- Economic investment **lifetime 30 a, 5% discount rate**
- **CO_2-price** of **30 €/tCO_2** is assumed

Mathematical formulation

$$TC = \min_{x} c^T x + E_\xi [\min_{y(\omega)} q(\omega)^T y(\omega)]$$

$$\begin{aligned} &\text{s.t.} \\ &Ax \le b \\ &T(\omega)x + Wy(\omega) \le h(\omega), \quad \forall \omega \in \Omega \\ &x = (x_1, x_2) \ge 0 \\ &x_1 \in \{0,1\}, x_2 \in \mathbb{Z}^+ \\ &y(\omega) = (y_1(\omega), y_2(\omega)) \ge 0, \quad \forall \omega \in \Omega \end{aligned}$$

Premise

- **Static, deterministic version** of stochastic MILP **is used** for comparison study
- **Inter-temporal constraints are not taken into account** by the model (e.g. storage continuity of hydro reservoirs) - allows for an easier sampling of the input data since the **chronological order of occurrence can be omitted**

For almost all techniques, the average load levels tend to be higher than in the reference case – heuristic can partly capture extreme values

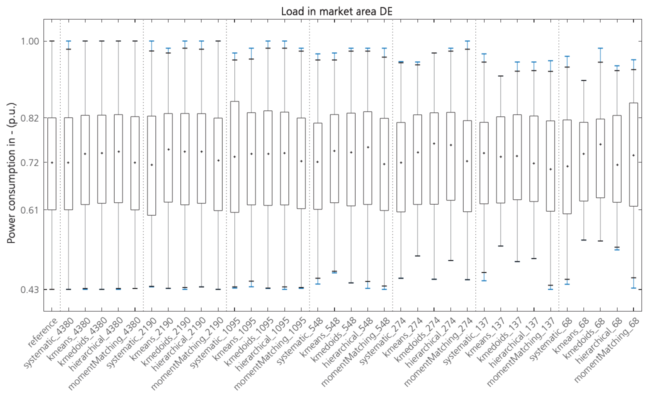

Agenda

I Background and motivation

II Methodology

III **Case study results**

IV Conclusion

Based on the average normalized root-mean-square error, it stands to reason that k-means also yields the most accurate long-term TEP model results

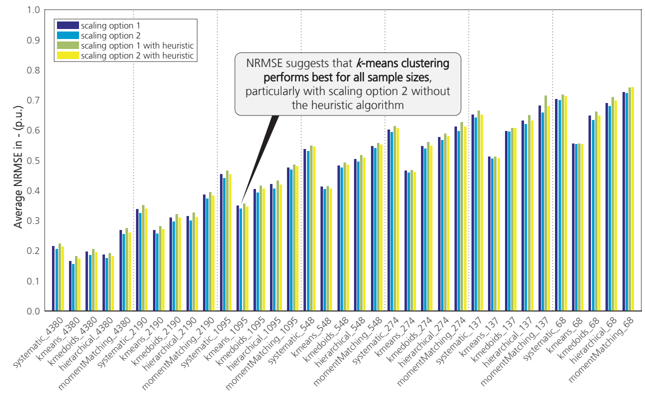

Normalized Root-Mean-Square Error (NRMSE)

Solution time significantly reduced - *k*-means clustering performance not persevering for model-dependent results, Hierarchical and *k*-medoids show good accuracy

	Average reduction in solution time per sample size Solution time as share of full year reference in %							Average cost accuracy Deviation of full year reference in %		
	4380	2190	1095	548	274	137	68	Total (obj.)	Investment	Operation
Systematic	17.83	5.69	2.11	1.03	0.36	0.17	0.09	1.48	0.90	1.51
k-means	23.11	5.75	2.14	0.86	0.62	0.21	0.11	-1.46	-3.36	-1,34
k-medoids	21.23	6.94	2.26	1.05	0.46	0.25	0.09	0.70	-1.63	0.84
Hierarchical	20.52	6.74	2.33	1.16	0.44	0.16	0.09	0.67	-0.23	0.72
Moment-matching	23.47	5.67	2.40	0.83	0.40	0.20	0.10	1.35	2.32	1.29
Reference (abs.)	*2016.1 s*							*473.1 bn€*	*26.9 bn€*	*446.1 bn€*

As expected, **with decreasing sample size** the **average solution time** can be **significantly reduced**

Although showing **best NRMSE**, ***k*-means clustering** exhibits **poor performance** when looking at investment and total cost deviations

Hierarchical clustering shows **highest accuracy**, followed by ***k*-medoids**

Over-investments are mainly limited to one DC cable – under-investments do not occur for sample sizes bigger than 274 h

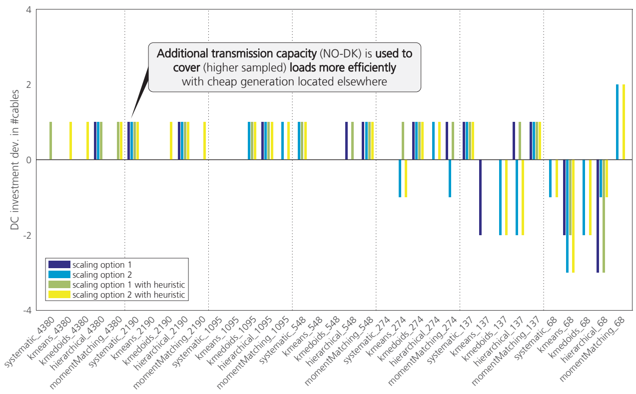

Relative investment and operational cost deviations generally increase with reduced sample size

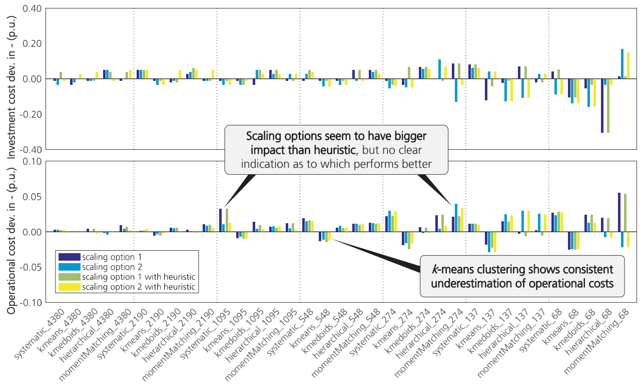

Agenda

I Background and motivation

II Methodology

III Case study results

IV Conclusion

The convergence results of the relative objective value are in line with the previous findings

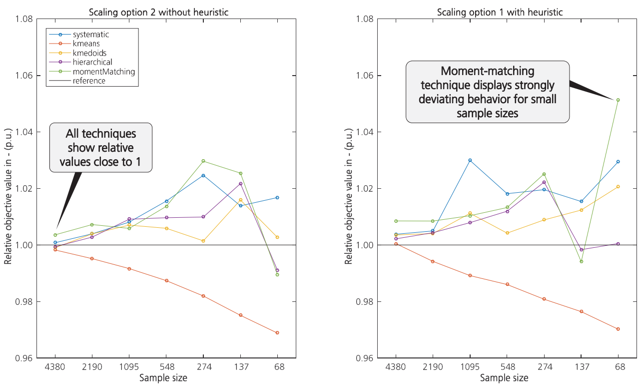

Conclusion

Comprehensive comparison of dimension reduction techniques:

Techniques performing well in the sampling process do not necessarily produce reliable results in the large-scale TEP model which became particularly evident for *k*-means clustering

Agglomerative hierarchical and *k*-medoids clustering show comparatively good results when quantifying both the NRMSE and the effects on offshore grid expansion decisions in the North Sea case study

Scaling options have a greater impact than the applied heuristic but no clear indication can be given as to the more suitable choice of either one, careful attention to different scaling options for the original data set seems appropriate

Future work:

Subsequent analysis of dimension reduction techniques can include the use of more sophisticated heuristics particularly in investment models as they depend on highest occurring values

Ways of incorporating inter-temporal constraints to better capture medium-term dynamics and operational flexibility either by employing dimension reduction approaches or developing alternative solution strategies involving decomposition for the full year problem

Thank you very much for your attention!

Fraunhofer
IWES

M.Sc. Philipp Härtel

Division Energy Economy and Grid Operation
Fraunhofer Institute for Wind Energy
and Energy System Technology IWES

Königstor 59 | 34119 Kassel / Germany
Phone +49 561 7294-471 | Fax +49 561 7294-260
philipp.haertel@iwes.fraunhofer.de

IRPWind NOWITECH Norwegian Research Centre for Offshore Wind Technology

Multistage grid investments incorporating uncertainty in Offshore wind deployment

Presentation by: **Harald G. Svendsen**

Joint work with:
Martin Kristiansen, Magnus Korpås, and Stein-Erik Fleten

SINTEF NTNU

Investment levels in renewables

Annual Investments by Region

Quarterly Investments by Assets (ex. R&D)

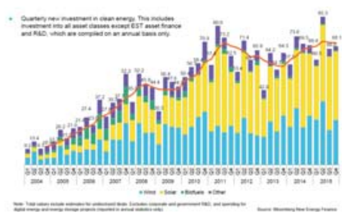

4

SINTEF NTNU

Content

- Transmission expansion planning model
- Incorporating uncertainty in offshore wind deployment
- North Sea 2030 case study

2

Renewable energy resources

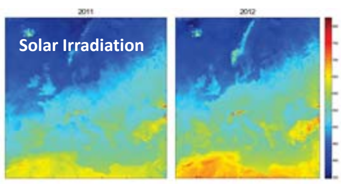

Ref: Tobias Aigner, PhD Thesis, NTNU

Wind Speeds

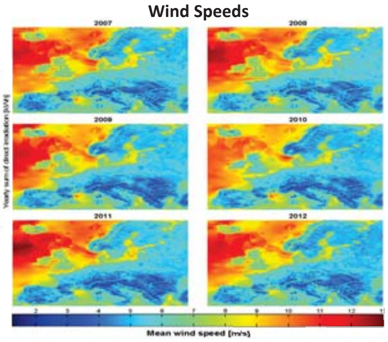

5

Background

SINTEF NTNU

Increasing demand for spatial and temporal flexibility ➡ North Seas Offshore Grid (NSOG)

Ref: www.nature.com

6

SINTEF NTNU

The transmission expansion planning model

Offshore grid – context

- The main drivers are **large-scale integration of non-dispatchable** power generation and multi-national **trade**
- We want a tool to identify **good offshore grid layouts**
  - Useful for strategic planning (TSO's / governments)
  - Proactive in terms of offshore wind integration
- Important aspects
  - Optimal – minimize (socio-economic) costs
  - Robust – not overly sensitive to small changes in parameters
  - Uncertainty – underlying parameters might change
  - Energy policy – national effects in terms of generation portfolio
  - Climate policy – national effects in terms of emissions
  - Risk – investors risk attitude

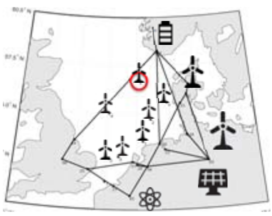

Our approach

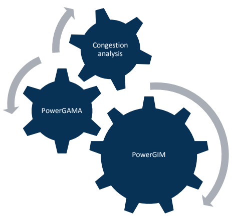

- Linear optimisation
- Take into account:
  - Variability in renewable energy and prices/demand via time-series sampling
  - Different transmission technologies (cost categories)
  - NEW: Uncertain parameters via stochastic programming and scenarios
  - *future: Power flow constraints (not yet)*
- Considering:
  - Capacity investment costs in transmission (cables + power electronics + platforms)
  - Capacity investment costs in generation (per technology)
  - Market operation over sampled hours

PowerGIM

- PowerGIM = Power Grid Investment Module
  - A "proactive" expansion planning model
- Available as part of the open-source grid/market simulation package PowerGAMA
  - https://bitbucket.org/harald_g_svendsen/powergama
- Python-based, modelled with "Pyomo"
  - http://www.pyomo.org/
- Two-stage stochastic mixed-integer linear program (MILP)

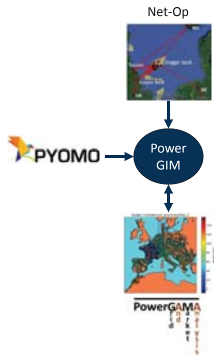

Model formulation

In words..

- Minimize investment cost + operational costs

Subject to

- Market clearing
- Generation limits
- Curtailment
- Load shedding
- Branch flow limits (ATC // DC OPF // PTDFs)
- Capacity investment limits
- (Reserve requirements)
- (Renewable Portfolio Standards)
- (Emission contraints)

In maths..

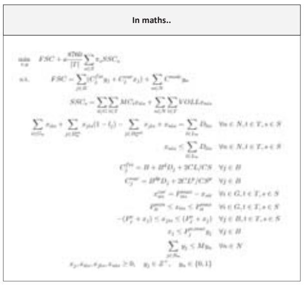

Expansion planning models

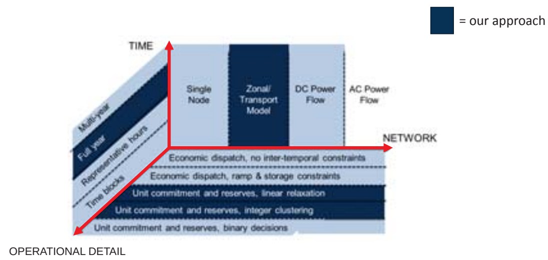

Figure: Jenkins, J., INFORMS, 2016.

Incorporating uncertainty

Two-stage optimization

- Basic idea:
  - When making decisions, some parameters are unknown. The best decision takes into account the probability distribution of those parameters
  - Use scenarios to represent probability distribution for uncertain parameters

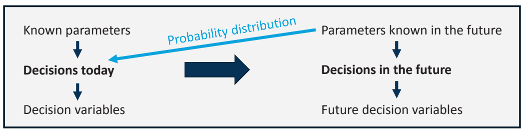

Stochastic programming

- Two-stage problem:

$$\min_{x \in \mathbb{R}^n} \quad g(x) = c^T x + E[Q(x,\xi)]$$
$$\text{subject to} \quad Ax = b$$
$$x \geq 0$$

Expectation value of future (optimal) costs

- x = first stage variables (to decide now)
- ξ = uncertain data
- Q is the optimal value of the second stage problem:

$$\min_{y \in \mathbb{R}^m} \quad q(\xi)^T y$$
$$\text{subject to} \quad T(\xi)x + W(\xi)y = h(\xi)$$
$$y \geq 0$$

- y = second stage variable (to be decided in the future)

Scenario tree

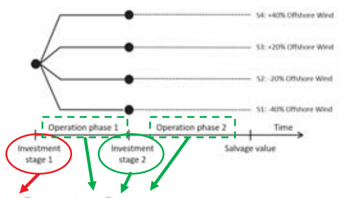

$$TC = \min_x c^T x + E_\xi[\min_{y(\omega)} q^T y(\omega)] \tag{1a}$$

s.t.

$$Ax \leq b \tag{1b}$$

$$T(\omega)x + Wy(\omega) \leq h(\omega), \quad \forall \omega \in \Omega \tag{1c}$$

$$x = (x_1, x_2) \geq 0, x_1 \in \mathbb{Z}^+, y(\omega) = (y_1(\omega), y_2(\omega), y_3(\omega)) \geq 0, y_1(\omega) \in \mathbb{Z}^+ \quad \forall \omega \in \Omega$$

Solution method: progressive hedging

- Stochastic program formulation (deterministic equivalent):

$$\min_x \sum_{s \in S} p_s f_s(x_s)$$
$$x_s \in C_s$$

- Relax non-anticipativity to get scenario-s problem formulation:

$$\min_{x_s} f_s(x_s)$$
$$x_s \in C_s$$

- Add penalty for non-anticipativity

If 1st stage variables are binary, this expression can be linearized

$$\min_{x_s} f_s(x_s) + \left[W^T x_s + \frac{\rho}{2} ||x_s - \hat{x}||^2\right]$$
$$x_s \in C_s$$

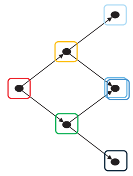

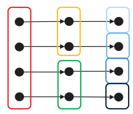

Case study: North Sea 2030 – Energy Revolution (Vision 4)

Base case scenario

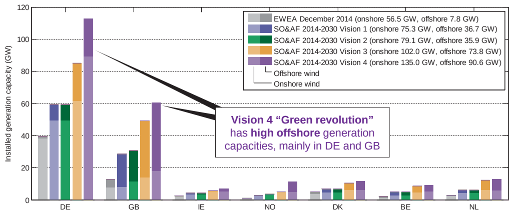

Base case scenario

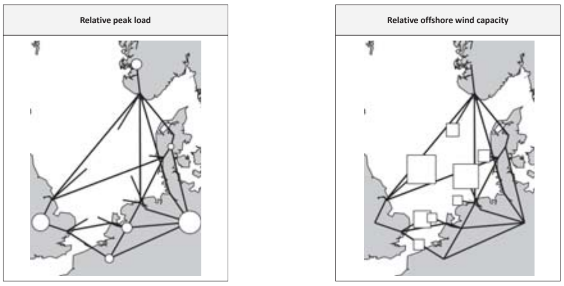

Deterministic: Expected value

No uncertainty taken into account

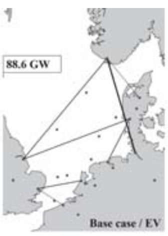

EV solution

Investment: 19.86 bn€
Total cost: 421.21 bn€

But actual operating conditions will not be as expected

Deterministic: Robustness analysis

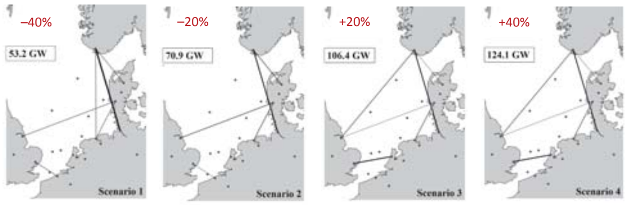

	S1	S2	S3	S4	Expected value
EV solution	487.74	449.22	400.80	384.99	430.69
→ Investment costs	19.86	19.86	19.86	19.86	19.86
Deterministic solution	484.70	447.70	400.11	383.29	428.95
→ Investment costs	12.66	14.85	19.19	19.19	19.86
Value of information	3.04	1.53	0.68	1.70	1.74

With EV solution

With perfect foresight

Expected value of using the EV solution (EEV)

- The WS result might be difficult to interpretate since it contains a set of solutions (one per scenario)
- Tempting to use the EV scenario (only one solution)
- …but the resulting decision is still exposed to future scenarios
- -> EEV:

$$EV = \min_{x} \quad Z(x, \bar{\xi}) \text{ where } \bar{\xi} = E(\xi)$$

$$EEV = E_{\xi}[Z(\bar{x}(\bar{\xi}), \xi)]$$

€430.69 bn (EV €421.21 bn)

Stochastic: one investment stage

RP

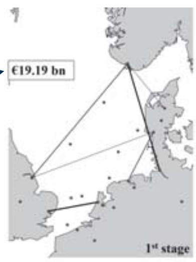

- Uncertain offshore wind capacity taken into account
- No second stage compensating investments considered

Investment: 19.19 bn€
Total cost: 430.668 bn€

Stochastic: two investment stages

Stage 1 investment:
Almost the same as with only one investment stage

5 years later, when wind capacities are known

Expected total investment:
20.16 bn€

25

Expected value of perfect information (EVPI)

- The maximum amount that a system planner would be willing to pay for a "crystal ball"
- Benchmarks
  - Best available tool: a stochastic model (RP)
  - If she knew the future: deterministic solution of those scenarios (WS)
- The EVPI:

$$WS = E_\xi[\min_x Z(x,\xi)] = E_\xi[Z(\bar{x}(\xi),\xi)]$$

$$RP = \min_x \quad E_\xi Z(x,\xi)$$

$$EVPI = RP - WS$$

€1.74 bn (0.40% of RP)

26

Value of stochastic solution (VSS)

- Your best deterministic approach that accounts for some uncertainty: EEV
- Your best alternative that "properly" incorporates uncertainty: RP
- ...which can be used to quantify the cost of ignoring uncertainty (equivalent to the VSS):

$$VSS = EEV - RP$$

€22.30 m (0.0052%)

27

Conclusions

- Deterministic solutions that copes with uncertainty might be hard to evaluate (many solutions) and/or give a cost-inefficient hedge against future scenarios
- Stochastic programs makes it possible to optimize one investment strategy that is cost-efficient against future scenarios (in contrast to EEV)
- Limitations of this study and related metrics (EVPI, EEV, VSS, and ROV)
  - The base case does already contain a strong grid infrastructure for 2030
  - Uncertainty is only represented through offshore wind capacity (wo/ exogenous curtailment cost)
  - A maximum amount of two investment stages limits the value of flexibility (ROV)
  - Last but not least; we use a model…
- "More is better" – eliminate risk and enhance flexibility

28

Real option value (ROV)

- The value of flexibility
- Flexibility is represented with two investment stages
- The system planner can postpone investments in order to learn about the offshore wind deployment

€22.41 m (0.0054%)

(Equivalent to financial options)

29

C1) Met-ocean conditions

Coherent structures in wind measured at a large separation distance,
H. Ágústsson, Kjeller Vindteknikk

Design basis for the feasibility evaluation of four different floater designs, L. Vita, DNV GL

Air-Sea Interaction at Wind Energy Site in FINO1 Using Measurements from OBLEX-F1 campaign, M.B. Paskyabi, University of Bergen

Towards Recommended Practices for Floating Lidar Systems, O. Bischoff, University of Stuttgart

Coherent structures in wind measured at a large separation distance

Hálfdán Ágústsson, Knut Harstveit
and Tuuli Pilvi Miinalainen

Kjeller Vindteknikk AS

halfdan.agustsson@vindteknikk.no

Statens vegvesen

Measurements masts - overview

Site	Fjord	Mast height	Mast type	Data start
Julbø	Julsundet	50 m	Guyed pipe mast	07.02.2014
Midsund	Julsundet	50 m	Guyed pipe mast	06.02.2014
Nautneset	Julsundet	68 m	Lattice tower	07.07.2016
Halsaneset	Halsafjorden	50 m	Guyed pipe mast	26.02.2014
Åkvik	Halsafjorden	50 m	Guyed lattice mast	06.03.2015
Kvitneset	Sulafjorden	96 m	Guyed lattice mast	24.11.2016
Trælboneset	Sulafjorden	78 m	Guyed lattice mast	Spring 2017
Langeneset	Sulafjorden	98 m	Lattice tower	Spring 2017
Kårsteinen	Sulafjorden	62 m	Lattice tower	Spring 2017
Rjåneset	Vardalsfjorden	72 m	Guyed lattice mast	Spring 2017
Synnøytangen	Bjørnafjorden	50 m	Guyed pipe mast	23.02.2015
Svarvehelleholmen	Bjørnafjorden	50 m	Guyed pipe mast	18.03.2015
Ospøya 1	Bjørnafjorden	50 m	Guyed pipe mast	03.12.2015
Ospøya 2	Bjørnafjorden	50 m	Guyed pipe mast	17.12.2015
Landrøypynten	Langenuen	50 m	Guyed pipe mast	06.03.2015
Nesøya	Langenuen	50 m	Guyed pipe mast	24.02.2015

Data coverage: 98- 99%

Experience from 'extreme' bridges

- The Norwegian Public Roads Administration shall bridge the remaining ferry crossings along road E39:
  - Fjord widths 2-7.5 km
  - Fjord depths 300-1300 m
  - High and variable wind, wave and current loads

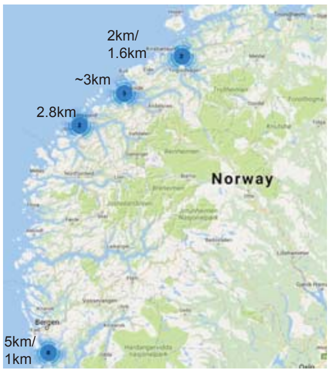


Concept bridge across Bjørnafjorden (5km)

Statens vegvesen
Norwegian Public Roads Administration

Measurement sites in Bjørnafjorden

Design loads and climatic conditions

- Very high resolution (500 m) meso-scale atmospheric simulations
  - Estimating wind climate and extreme winds
  - Input to high-res. wave (ROMS) and current (SWAN) models

- High frequency measurements of wind at several levels in tall meteorological masts:
  - Verification of simulated winds
  - **Assessment of design loads and climatic conditons**

Measurements at Ospøya in Bjornafjørden

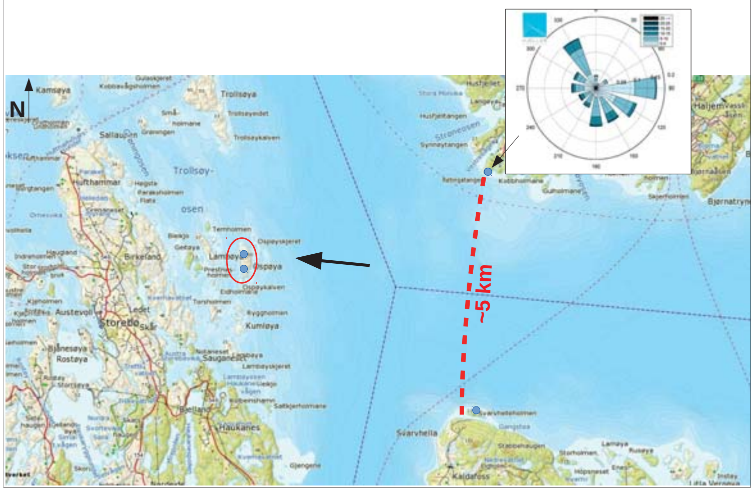

Measurements at Ospøya

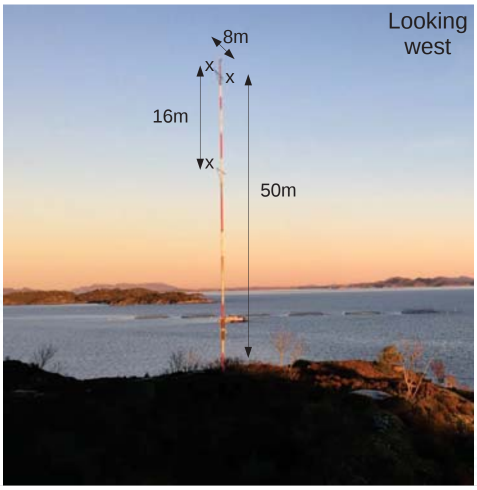

Methodology for analysis of coherence and spectra

- Reference curves for spectra and coherence are based on handbooks H185 and H400, used in the design of bridges.
- Large sets of calculated spectra and coherences are fitted to the models (Davenport) prescribed in the handbooks, for given wind directions and wind speeds U>10 m/s.

The computed turbulence spectras and coherences for measured data were compared to Statens vegvesens guideline book values, referred as "H185". The handbook value for scaled turbulence spectra is computed by

$$\frac{fS_i}{\sigma^2}=\frac{A_i f_i'}{(1+1.5A_i f_i')^{\frac{5}{3}}} \quad ,$$

$$f_i'=\frac{f\,L_u(z)}{U(z)} \quad ,$$

and $U(z)$ is the mean wind speed. The coefficients for different wind components are $A_u=6.8$, $A_v=9.4$ and $A_w=9.4$. Moreover, the length scale $L_u(z)$ for guideline reference is computed by

$$L_i(z)=c*100*(0.1*z)^{0.3},$$

Where one has coefficients $c_i=[1,\frac{1}{4},\frac{1}{12}]$ for u,v and w components.

Coherence series by hand book are computed with Davenport-model,

$$Coh_{185}=\exp\left(-C_{ij}\frac{f\Delta s}{U(z)}\right) \quad ,$$

where $C_{ij}=[10,6.5,3]$ and Δs is the distance between sensors.

Wind measurements

1. Made by group of engineers/technicians at KVT
2. Installed 10 50 m high masts in 2014 - 2015
3. Installed/planned 5 80 - 100 m high masts, for start in 2016 - 2017
4. 3 sensors in each mast, at 2 or 3 levels
5. Data sampling frequency: 10 Hz
6. Wind components: u, v, w
7. Transfer to Kjeller Vindteknikk every hour
8. Driven by batteries with solar cell charging Battery voltages is monitored on daily basis
9. Data availability 95 % - 99 %
10. All raw data also stored for inspection and for spectral and coherence analysis
11. Data are filtered for spike and error removals
12. Twice a year: Reports written including long term statistics and extreme value analysis

Gill WindMaster Pro 3-Axis Anemometer

Example wind series during an easterly event 50 m agl, 22-23 UTC, 9. January 2016

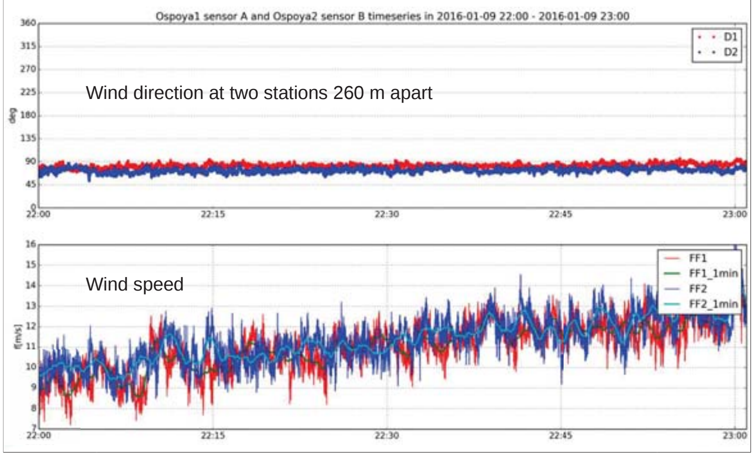

Systematic analysis of coherence and spectra

- All analysis done using python, scipy, numpy, pandas, stats…
- Approximately 1 year of 10 Hz data from 4 synchronized anemometers
- Turbulence spectra, autocorrelation and integral length scales analysed for each 20 minute period
- Coherence analyzed for each:
  - 20 minute period at short distances (8 and 16 m)
  - 60 minute period at long distances (~260 m)
- Data is filtered, detrended and tapered using a Hann-window
- Main wind direction (U) is rotated along the flow
- Spectra based on a periodogram-method with Tukey-windowing, results scaled with frequency and std. dev. of wind.
- Coherence based on cross spectral density and power spectral densities based on Welch's method, with 4 segments and 50% overlap within segments, results scaled with f and σ^2

Example turbulence spectra (easterly wind) 50 m agl, 20 minutes at 22 UTC, 9. January 2016

Ospøya 1 (north) ← 260 m → **Ospøya 2 (south)**

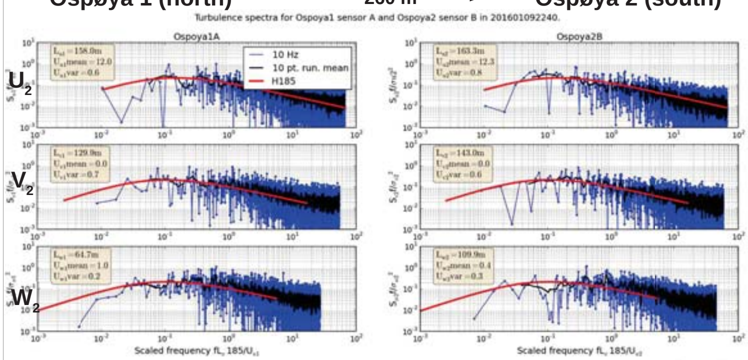

Integral length scales

Systematic analysis based on 20 minute periods (shown for another station than Ospøya)

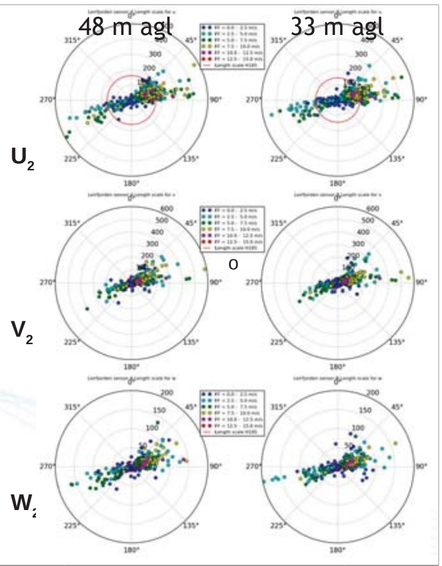

KJELLER VINDTEKNIKK

Horizontal coherence at Ospøya at 260 m (easterly wind) 50 m agl, 60 minutes at 22 UTC, 9. January 2016

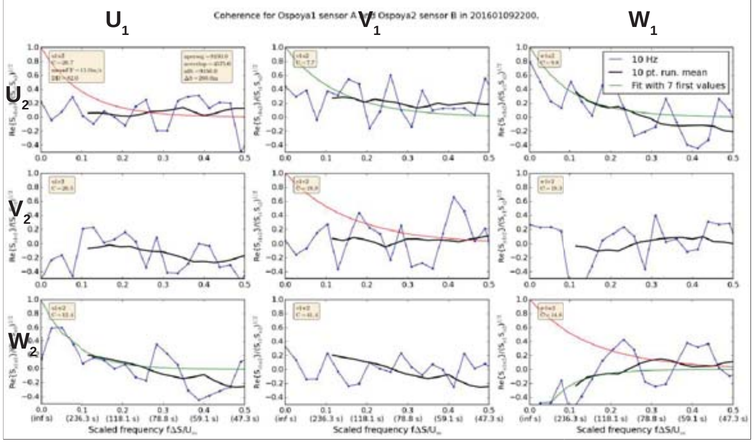

Vertical coherence at Ospøya at 16 m (easterly wind) 33-50 m agl, 20 minutes at 22 UTC, 9. January 2016

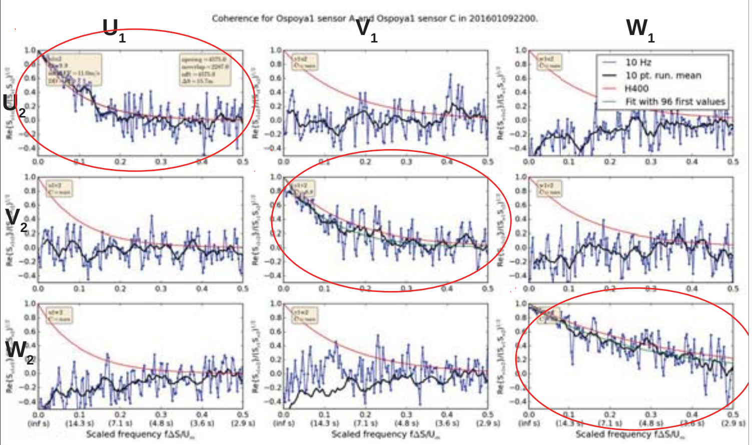

Horizontal coherence at Ospøya at 260 m (easterly wind) 50 m agl, 60 minutes at 23 UTC, 9. January 2016

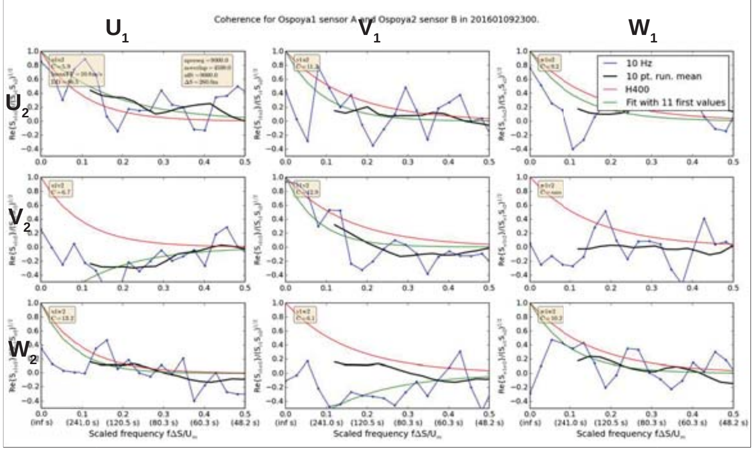

Horizontal coherence at Ospøya at 8 m (easterly wind) 50 m agl, 20 minutes at 22 UTC, 9. January 2016

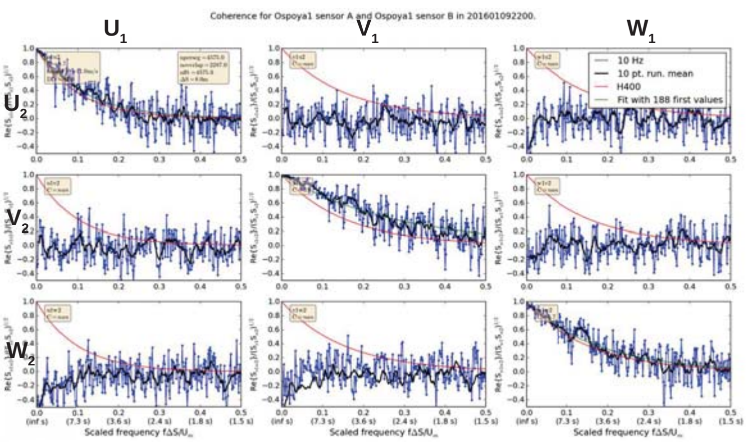

Horizontal coherence at Ospøya at 260 m (easterly wind) 50 m agl, 60 minutes at 4 UTC, 10. January 2016

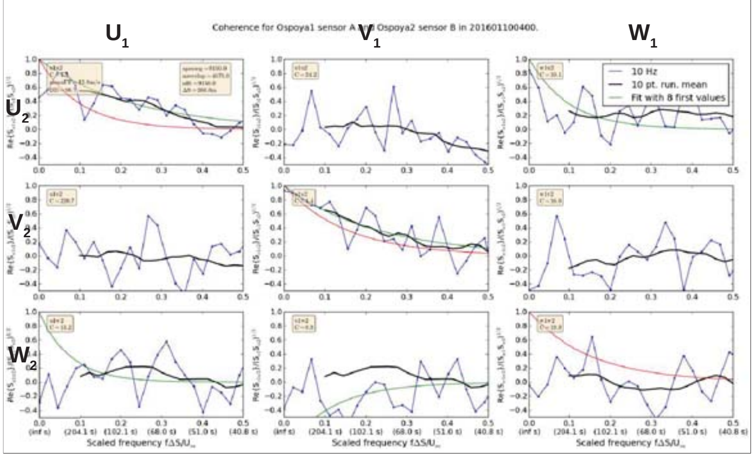

Horizontal coherence at Ospøya at 260 m (westerly wind) 50 m agl, 60 minutes at 11 UTC, 28. January 2016

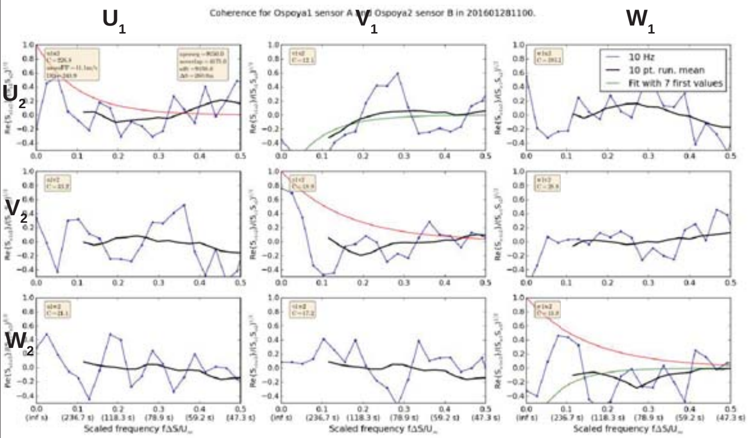

Calculation of coefficients with Davenports cospectra with percentiles of optimized Cij. Effect of lag at one station.

P=0.1	-6s	-3s	0s	1s	3s	6s	9s
ALLE Cij,i=j fra Ø							
EXP(-cij*DS*f/Vm)	5.8	5.9	6.0	5.8	6.0	6.0	6.5
-EXP(-cij*DS*f/Vm)	12.0	12.6	13.5	12.7	17.5	17.5	15.0
ALLE Cij,i=j fra V							
EXP(-cij*DS*f/Vm)	9.4	9.4	9.4	8.4	6.1	6.3	9.1
-EXP(-cij*DS*f/Vm)	13.8	13.2	12.2	11.8	10.1	12.0	10.8
P=0.5	-6s	-3s	0s	1s	3s	6s	9s
ALLE Cij,i=j fra Ø							
EXP(-cij*DS*f/Vm)	11.0	11.0	10.9	10.8	10.0	10.0	11.1
-EXP(-cij*DS*f/Vm)	21.0	19.9	26.6	22.7	69.3	69.3	20.6
ALLE Cij,i=j fra V							
EXP(-cij*DS*f/Vm)	14.6	14.4	14.2	13.8	11.3	9.8	14.6
-EXP(-cij*DS*f/Vm)	82.8	77.1	84.9	83.3	52.6	108.3	81.1

Ospøya horizontal coherens over 260 m distance

From the H400 handbook

Kospektra $S_{i_1 i_2}$ på normalisert form for separasjon normalt på hovedstrømsretningen, horisontalt (y) eller vertikalt (z), er gitt ved:

$$\frac{\mathrm{Re}\,[S_{i_1 i_2}(n, \Delta s_j)]}{\sqrt{S_{i_1}(n) \cdot S_{i_2}(n)}} = \exp\left(-C_{ij} \frac{n \Delta s_j}{v_m(z)}\right) \qquad (5.6)$$

hvor Δs_j er horisontal- eller vertikalavstanden mellom betraktete punkter, og:

$i_1, i_2 = u, v, w$

$j \quad = y, z$

$C_{uy} = C_{uz} = 10{,}0\,,\ C_{vy} = C_{vz} = C_{wy} = 6{,}5\,,\ C_{wz} = 3{,}0$

For horizontal coherence from east and west, Cuy=10, Cvy=6.5 and Cwy=6.5 ifølge håndboken (Davenport model). Here named Cuu, Cvv and Cww in order to not mix up with Cij, i≠j

Coherence is calculated for all 1 hour periods measured, with wind speed > 10 m/s and easterly/westerly flow, and model fitted to the data

Main conclusions and summary

- Present systematic analysis of coherence (and spectra) from a unique measurement site in an open fjord
- 1) The coherence is higher (lower persentiles of Cij) for easterly than for westerly wind
- 2) For easterly wind, no differences in the 0.05, 0.1, and 0.5 percentiles of Cij are seen using -6 sec, -3 sec, 0 sec 1 sec, 3 sec or 6 sec as time lag on Ospøya 1 resp Ospøya 2
- 3) For westerly wind, we find that the coherence are gradually improving from 0 to 6 sec lag.
  - possibly due to the islands west of Ospøya. Wind along 250 - 260 degrees is typically slowd down for one of the stations but not the other.
- The Davenport model is rarely good at large separation distances. Other models are being tested, e.g. Krenk, and analysis methods are being scrutinized.

Calculation of coefficients with Davenports cospectra with percentiles of optimized Cij

				P=0.05	P=0.1	Obs. P=0.5	Handbook H400
U	Cuu	Ø	EXP(-cij*DS*f/Vm)	4.3	5.0	8.7	10
		Ø	-EXP(-cij*DS*f/Vm)	16.3	16.6	42.3	10
		V	EXP(-cij*DS*f/Vm)	10.3	11.1	14.7	10
		V	-EXP(-cij*DS*f/Vm)	11.5	12.2	37.2	10
V	Cvv	Ø	EXP(-cij*DS*f/Vm)	4.4	5.1	9.8	6.5
		Ø	-EXP(-cij*DS*f/Vm)	10.3	10.9	15.9	6.5
		V	EXP(-cij*DS*f/Vm)	8.5	8.8	14.7	6.5
		V	-EXP(-cij*DS*f/Vm)	10.2	12.7	197.0	6.5
W	Cww	Ø	EXP(-cij*DS*f/Vm)	6.4	7.8	14.1	6.5
		Ø	-EXP(-cij*DS*f/Vm)	12.4	13.0	21.6	6.5
		V	EXP(-cij*DS*f/Vm)	8.2	8.4	13.2	6.5
		V	-EXP(-cij*DS*f/Vm)	10.1	11.9	20.6	6.5

Measure masts: Midsund and Nautneset

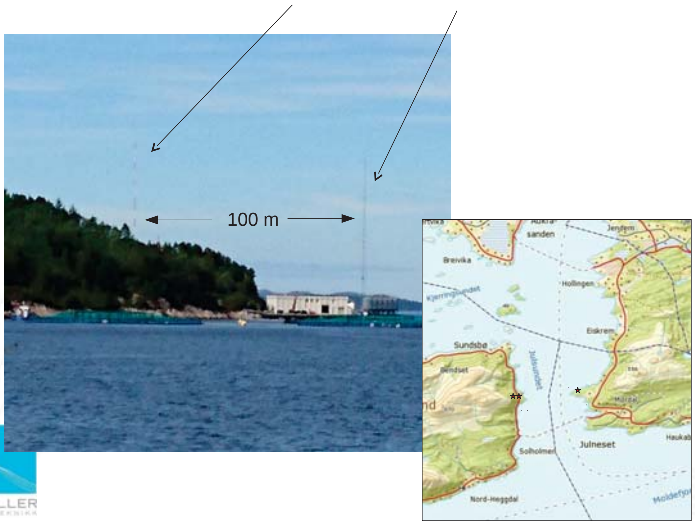

University of Stuttgart Germany DNV·GL

Design basis for the feasibility evaluation of four different floater designs

G K V Ramachandran[a], L Vita[a], A Krieger[a], and K Mueller[b]

[a] DNV GL Renewables Certification

[b] Stuttgart Wind Energy at Institute of Aircraft Design, University of Stuttgart

13 January 2017

Ungraded

Overview

- Introduction
- Floater concepts
- Sites and site conditions
- Wind turbine
- Serviceability Limit States (SLS)
- Design Load Cases (DLCs)
- Sensitivity analysis
- Conclusions

Ungraded

Design Basis

- Design Basis forms the first step towards design
- The European Union-funded project LIFEs50+ as part of Horizon2020 framework.
- Contributors to Design Basis include:
  - *DNV GL*
  - *University of Stuttgart*
  - *Iberdrola IC*
  - *IDEOL*
  - *Nautilus*
  - *Olav Olsen*
  - *Tecnalia*

http://www.statoil.com/

Ungraded

Floater Concepts

- **Four Floater Concepts**
  - Barge platform with moon pool from Ideol
  - Semi-submersible platform from Nautilus
  - OO Star semi-submersible concept from Olav Olsen
  - Tension Leg Platform, TLPWIND, from Iberdrola IC

Introduction – LIFES50+ project

- LIFEs50+ Project Objectives:
  - Optimize and qualify to a TRL of 5, two innovative substructure designs for 10MW turbines
  - Develop a streamlined and KPI-based methodology for the evaluation and qualification process of floating substructures
- The Design Basis serves as the fundamental part for the above process. This provides a generic design basis for the design of floating wind turbines / farm.

Ungraded

Sites and Site Conditions

- Three generic sites are identified
  - Site A – mild sea states (e.g. Golfe de Fos area, France)
  - Site B – moderate sea states (e.g. Gulf of Maine area, USA)
  - Site C – severe sea states (e.g. West of Barra area, Scotland)
  - Site conditions are based on the publicly available data for the example sites blended with the assumptions in the standards (where ever data was lacking)

Sites and Site Conditions (Contd..)

Parameter	Site A	Site B	Site C
Water depth, m	70	130	100
Annual avg. wind speed, $V_{av,h}$, m/s	9.0	6.214	9.089
10 min. mean reference wind speed (50-years return period) at hub height, V_{ref}, m/s	37.0	44.0	53.79
Extreme Sea States (ESS)			
50-year significant wave height, $H_{s50,3h}$, m	7.5	10.9	15.6
50-year peak period range, $T_{p50,3hmin}$ - $T_{p50,3hmax}$, s	8.0 – 11.0	9.0 – 16.0	12.0 – 18.0
Severe Sea States (SSS)*			
Significant wave height up to the rated wind speed, m	4.0	7.7	11.5
Significant wave height beyond the rated wind speed, m	7.5	10.9	15.6

Ungraded

Wind turbine

- **DTU-10MW reference wind turbine**

Parameter	Unit	Value
Rated power	kW	10000 (IEC Class IA)
Rotor diameter	m	178.3
Hub height (w:r:t: MSL)	m	119.0
Rated rotor speed	rpm	9.6
Rated wind speed	m/s	11.4
Rotor mass	Tons	228
Nacelle mass	Tons	446
Tower mass	Tons	628
Life time	Years	25

Comparable with that of NREL-5MW specifications

Ungraded

Sites and Site Conditions (Contd..)

Parameter	Site A	Site B	Site C
Water depth, m	70	130	100
Annual avg. wind speed, $V_{av,h}$, m/s	9.0	6.214	9.089
10 min. mean reference wind speed (50-years return period) at hub height, V_{ref}, m/s	37.0	44.0	~~53.79~~ 50.0
Extreme Sea States (ESS)			
50-year significant wave height, $H_{s50,3h}$, m	7.5	10.9	15.6
50-year peak period range, $T_{p50,3hmin}$ - $T_{p50,3hmax}$, s	8.0 – 11.0	9.0 – 16.0	12.0 – 18.0
Severe Sea States (SSS)*			
Significant wave height up to the rated wind speed, m	4.0	7.7	11.5
Significant wave height beyond the rated wind speed, m	7.5	10.9	15.6

Ungraded

Serviceability Limit States (SLS) – Values

Designers requested to establish SLS limits for the wind turbines.

Values were selected based on previous experience from floating and bottom fixed projects

- **Inclination of tilt**
  - Max. tilt during operational load cases is limited to **5 deg** (mean value) and **10 deg** (max. value)
  - Max. tilt during non-operational load cases is limited to **15 deg** (max. value)
- **Maximum acceleration**
  - Max. acceleration during operational load cases is limited to **0.3g** (max. value)
  - Max. acceleration during non-operational load cases is limited to **0.6g** (max. value)

Ungraded

Sites and Site Conditions (Contd..)

Parameter	Site A	Site B	Site C
Water depth, m	70	130	100
Annual avg. wind speed, $V_{av,h}$, m/s	9.0	6.214	9.089
10 min. mean reference wind speed (50-years return period) at hub height, V_{ref}, m/s	37.0	44.0	50.0
Extreme Sea States (ESS)			
50-year significant wave height, $H_{s50,3h}$, m	7.5	10.9	15.6
50-year peak period range, $T_{p50,3hmin}$ - $T_{p50,3hmax}$, s	8.0 – 11.0	9.0 – 16.0	12.0 – 18.0
Severe Sea States (SSS)*			
Significant wave height up to the rated wind speed, m	4.0	7.7	11.5
Significant wave height beyond the rated wind speed, m	7.5	10.9	15.6

Ungraded

Serviceability Limit States (SLS) – possible limit exceedance

Operational parameters: the wind turbine operations may be curtailed

- It is assumed that an alarm will stop the turbine. However, this capability shall be demonstrated.

Impact of these parameters on loads are quantified and assessed

- Compare the main load components with the design envelope loads when the turbine is in the bottom fixed condition.

Ungraded

Design Load Cases (DLCs) for Preliminary Evaluation – Selection

- **Selection of a subset of load cases for preliminary evaluation of the concepts**
  - In the case of production cases:
    - DLC 1.2 contributes to the major part of fatigue
    - DLC 1.4 – as the deterministic gust is sensitive to the platform period and hence it could be important. Further, it is common that DLC 1.4 drives the critical blade deflection
    - DLC 1.6 – the severe sea states could trigger some of the substructure loads
  - In the case of fault case, DLC 2.3 would be critical as both the amplitude and period of the EOG could be sensitive and might drive the design
  - 6.1/6.2 case for ULS.

Design Load Cases (DLCs) setup

- **For the normal production cases (DLC 1.2)**
  - As per standards, the simulation length => 3 hrs for ULS. Simplification – through sensitivity analysis, for fatigue => 1 hr or les depending on the sensitivity
  - Wind speed bin width => 2 m/s
  - 3 seeds per wind speed
- **For the DLCs dealing with deterministic gusts (DLC 1.4 and 2.3)**
  - ECD – DLC 1.4, gust amplitude, period – most relevant platform period such as yaw period shall be considered.
  - EOG – DLC 2.3, same conditions above + calculate gust amplitude as function of gust period. Timing of grid failure => shall results in conservative loads
- **DLC 1.6**
  - Limited number of wind speeds, 3 seeds per wind speed
  - Simulation length => 3 hrs

DLCs for Preliminary Evaluation (Contd..)

- **DLCs 6.1 and 6.2**
  - Same external conditions for both idling cases with the exception of wind direction and safety factor
  - At least 3 seeds per wind direction
  - Simulation length => 3 hrs
  - In the case of DLC 6.2, a sensitivity analysis can be carried out to evaluate the most severe yaw error and consequently to reduce the number of simulations.

DLCs – Simplified fatigue analysis for preliminary evaluation

- **The FLS verification will include:**
  - RNA loads based on simulations using Ieff for m=4
  - Tower base bending moments
  - Station keeping system – the focus should be on the attachment or the line tension in the moorings / tendons depending on the design.
  - If the design of one of the above parts is driven by FLS, hot spot checks on the floater is recommended.
  - **Assumptions**:
    - Only loads during normal production are considered (DLC 1.2)
    - The wind turbulence are assumed as per type class
    - Normal sea states (NSS) representation is design-independent
    - Only aligned wind / wave conditions

Design Load Cases – SLS and ALS for preliminary evaluation

Only valid for the concepts having a redundant station keeping system

- For the transient load case:
  - Simulation length can be reduced in order to include the transient event
  - Environmental conditions => 1-year return period
  - Both the idling and operational conditions
  - At least 3 seeds per case
- For the post-failure conditions:
  - Simulation length => 3 hrs
  - Environmental conditions => 1-year return period
  - At least 3 seeds per case

Sensitivity Analysis

- Sensitivity analysis for ULS:

  Effect of the following parameters shall be investigated:
  - Wind/wave misalignment
  - Wave peak period/significant wave height
  - Swell (if relevant)
  - Mooring line orientation, with respect to the wave direction
  - Wind direction, with respect to the platform orientation
  - Water depth
  - Gusts and periods
  - Currents
  - Ice, marine growth, or any other factor relevant for the site (but not included in the DLC set up)

Sensitivity Analysis (Contd..)

- Sensitivity analysis for FLS:

  Effect of the following parameters shall be investigated:
  - Wind/wave misalignment
  - Wind direction, with respect to the platform orientation
  - Ice, marine growth, or any other factor relevant for the site (but not included in the DLC set up)

Acknowledgements

We thank the EU and LIFEs50+ project partners for the funding support, providing the data (site conditions and concept details), and allowing us to present the Design Basis part of the project.

Observations / Conclusions

- Key aspects of the design basis for the design (for the 3 generic sites) are detailed.
- Possible simplifications, its consequences, and requirements relevant for a preliminary design and evaluation are discussed.
- Preliminary load cases are identified.
- Potential sensitivity studies are listed.
- Limits for SLS and ALS cases are proposed.
- Recommendations on SLS and ALS load cases are provided.

Thank you for your kind attention..

Luca Vita
Luca.Vita@dnvgl.com
+45-60 35 15 89

www.dnvgl.com

SAFER, SMARTER, GREENER

References

- www.lifes50plus.eu
- DNV-OS-J103, (2013), Design of floating wind turbine structures.
- IEC/TS 61400-3-2 Ed.1.0 Wind turbines – Part 3-2: Design requirements for floating offshore wind turbines.
- www.statoil.com
- Ramachandran G K V, Krieger A, Vita L, Gomez Alonso P, Berque J, and Aguirre G. (2016) Design Basis, LIFES50+ Deliverable D7.2, available at: http://lifes50plus.eu/results/.
- DTU Wind Energy Report-I-0092, (July 2013), Description of the DTU-10MW reference wind turbine.
- DNV-OS-J101, (2014), Design of offshore wind turbine structures.
- IEC 61400-1, Ed.3 (2005), Wind turbines – part 1: Design requirements, incl. Amendment:2010.

Measurement site: FINO1

Offshore **B**oundary **L**ayer **Ex**periment FINO1 (OBLEX-F1)

From June 2015 to September 2016.

Air-sea interaction processes in the presence of offshore platforms: Ge… Fino1 platform and Alpha Ventus offshore wind

Oceanic field work:

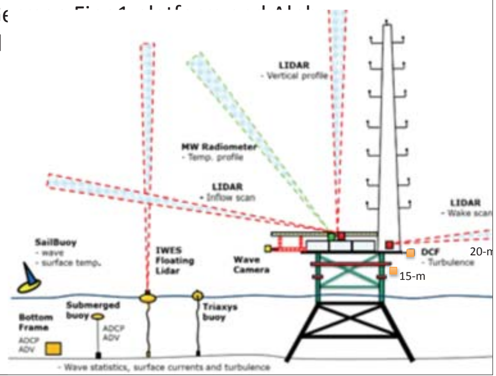

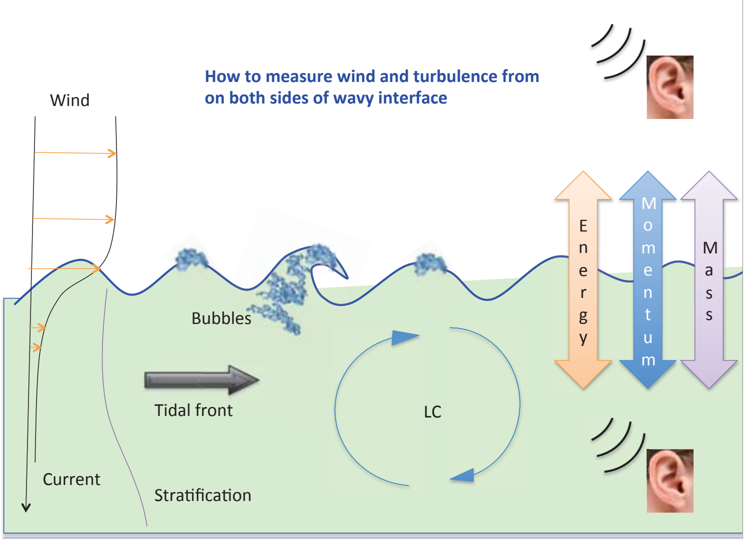

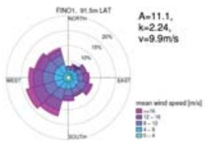

Deployment configuration

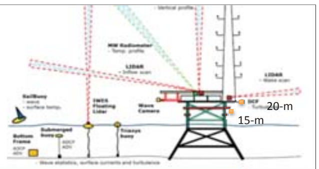

Waverider

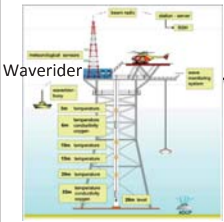

ADCP

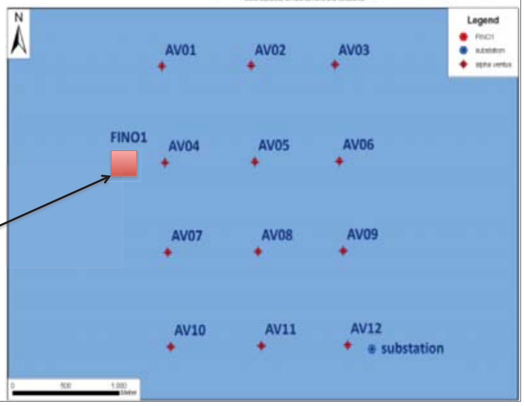

Outline

- Measurement site (FINO1)
- Measuring techniques
- DCF systems and sea waves
- Wind-current interaction
- Conclusions

Fig.1: The FINO1 – Platform in the North Sea

In Fig. 1 the positions of the sensors for wind spe…

Environmental conditions

$$U_{10} = U(z_1) + \frac{u_*}{\kappa}\ln\left(\frac{10}{z_1}\right)$$

Here c_p is the phase speed of the surface waves at the spectral peak.

Friction velocity calculated from cup-anemometer at 33-m height.

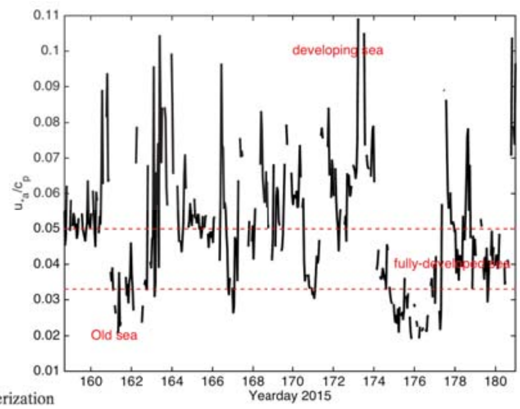

TOGA COARE 3.0 parameterization

DCF system at 15-m

Monin–Obukhov length

$$L = -\frac{u_*^3 \overline{\theta_v}}{\kappa g \overline{w'\theta_v'}},$$

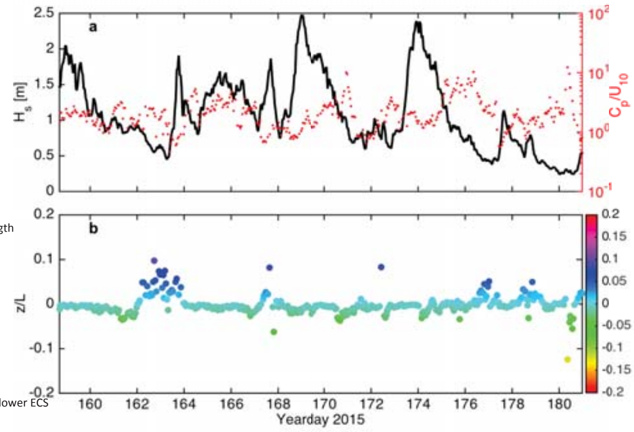

z is the height of the lower ECS

DCF system at 15-m

Wave-wind interaction

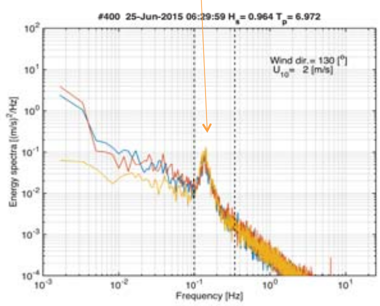

Lidar data to check distorted Flow characteristics

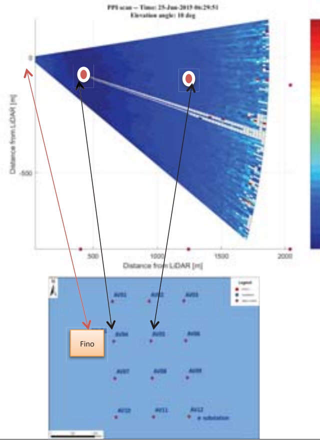

Less influenced by flow distortion.

Wake characteristics: Lidar Data

Distortion assessed at location of AV01

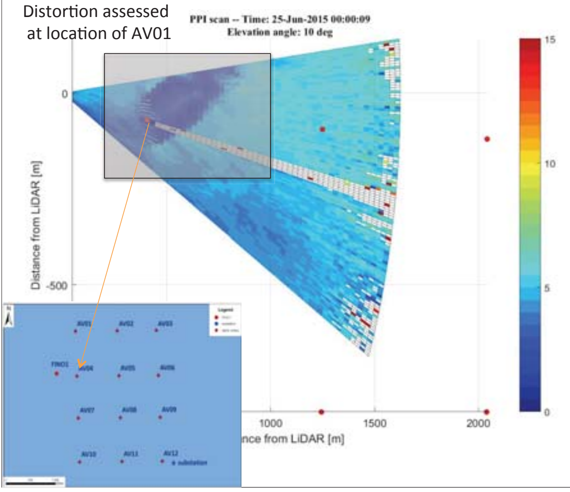

DCF system at 15-m: flow distortion

Effect of distortion on Friction velocity

$$|\tau| = \rho C_z (U_z - U_o)^2,$$

U_o the surface drift speed,

$$\tau = \tau_t + \tau_w + \tau_v,$$

turbulent

viscous

Wave-coherent

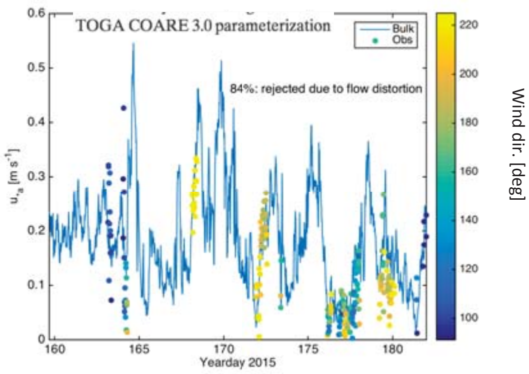

$u_* = (|\tau|/\rho)^{1/2}$ is the friction velocity,

DCF system at 15-m

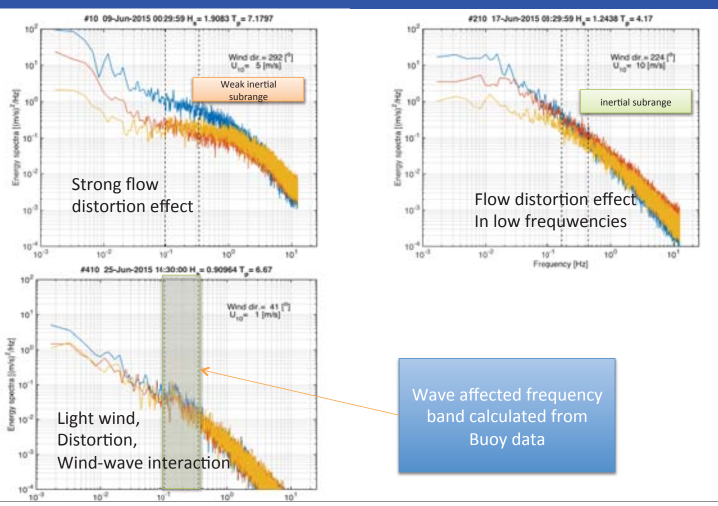

Wave affected frequency band calculated from Buoy data

DCF system at 15-m: friction velocity

$$\tau = -\rho(\overline{u'w'}i + \overline{v'w'}j),$$

$$u_* = (|\tau|/\rho)^{1/2}$$

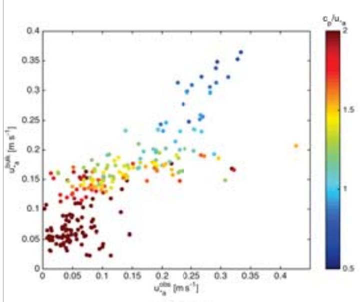

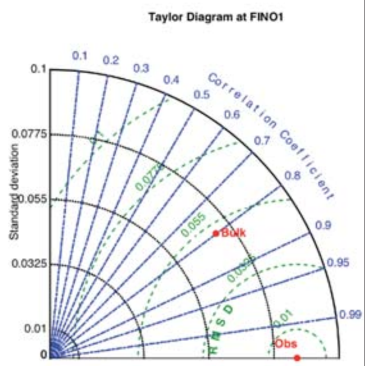

DCF systems: drag coefficient

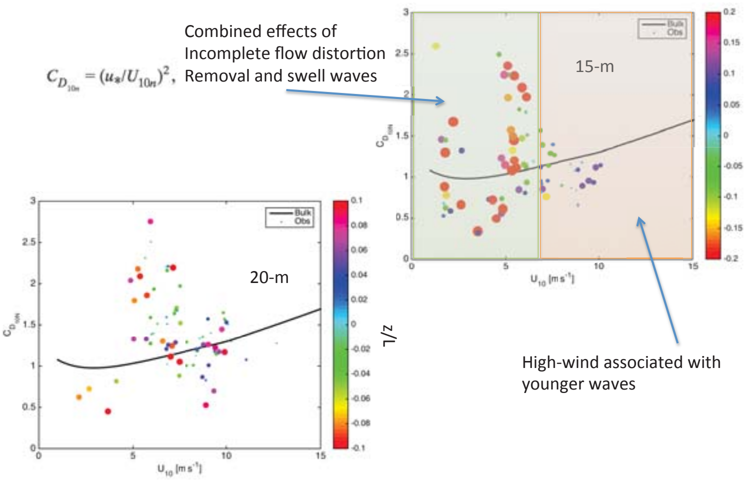

DCF system at 15-m: wind-wave

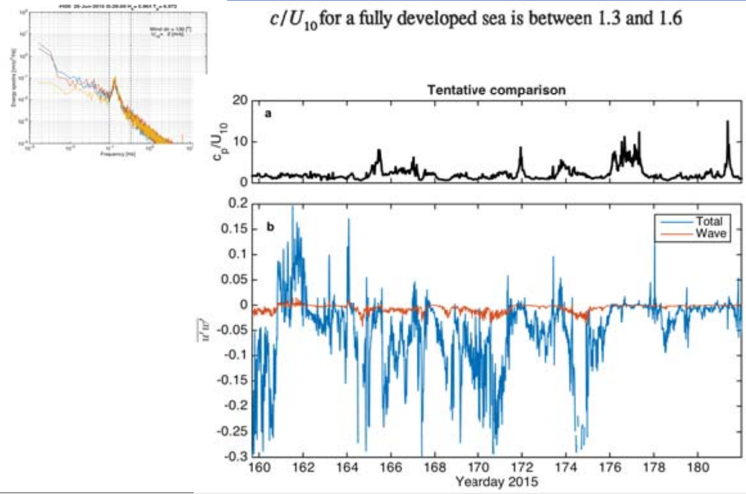

DCF system at 15-m: some statistics

$$f(u_h;b;a) = \frac{a}{b}\left(\frac{u_h}{a}\right)^{b-1} e^{-\left(\frac{u_h}{a}\right)^b},$$

two-parameter Weibull distribution provides a reliable approximation to the probability density function of wind horizontal speed

An analytic expression for the PDF is in Good agreement with the observed one By means of efficiently capturing the behavior of higher moments.

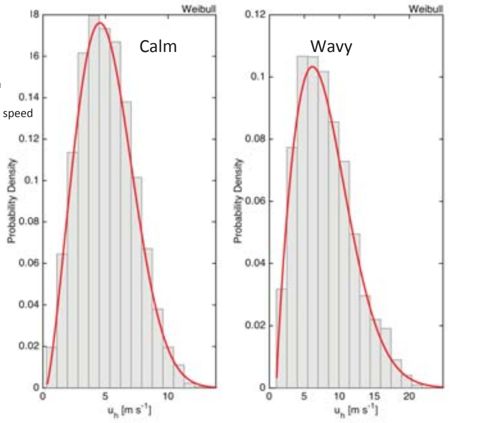

Bakhoday-Paskyabi 2017, under review, OMAE

Ocean currents: uplooking ADCP

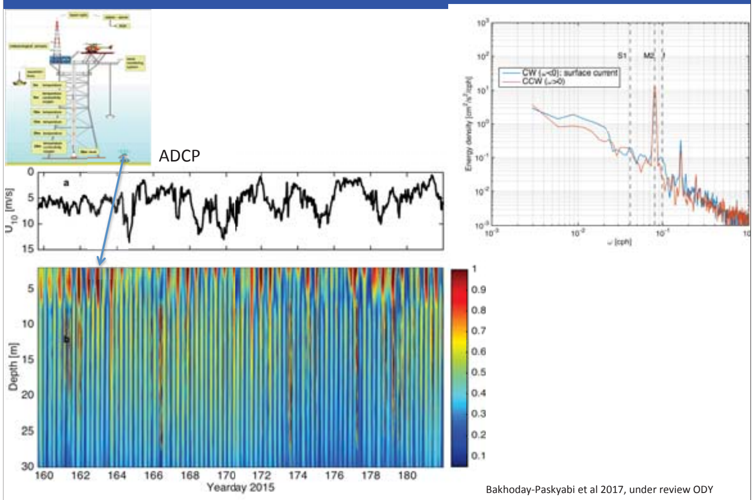

Bakhoday-Paskyabi et al 2017, under review ODY

DCF system at 15-m: wind-wave

horizontal momentum equation in the presence of waves

$$\left[\overline{\tilde{u}\tilde{w}} + \overline{u'w'} + \nu\overline{\frac{\partial u}{\partial z}}\right]_h = \underbrace{\boxed{\frac{1}{\rho_a}\overline{p_\eta\frac{\partial \eta}{\partial x}}}}_{\text{air pressure-wave slope correlation}} + \underbrace{\nu\left(\overline{\frac{\partial u}{\partial z}}\right)_\eta - \nu\overline{\left(\frac{\partial u}{\partial x_i}\right)_\eta\frac{\partial \eta}{\partial x_i}}}_{\text{viscous stress}}$$

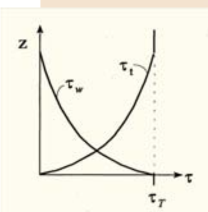

Neglecting viscous terms

$$\rho_a\,\overline{\tilde{u}\tilde{w}}\,|_\eta = \overline{p_\eta\frac{\partial \eta}{\partial x}}$$

It is possible to use the wave-induced air pressure perturbation and wave slope in order to quantify the wave-induced momentum flux.

Due to the lack of sufficient knowledge about the structure of the wave-induced pressure field, we can use either parameterization or measured velocity spectra to estimate wave-induced stress.

Bakhoday-Paskyabi et al 2014
Wetzel 1996

Surface current and wind interaction

At low frequencies, the CW Component seems more energetic, in particular near the inertial frequency.

From rotary cross-spectra, It is possible to assess the phase characteristics between wind and waves and to measure the correlation amplitude.

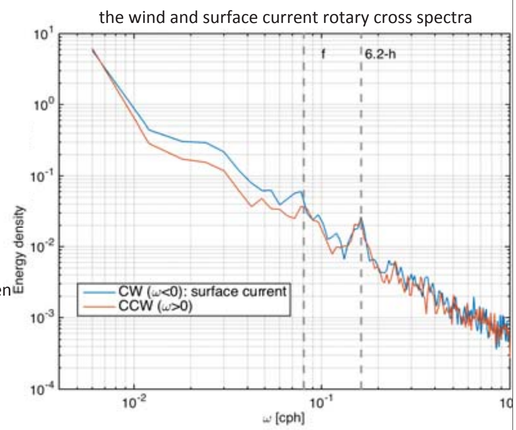

Bakhoda-Paskyabi & Rohre 2017, under preparation

Conclusions

- There are significant scatters for light wind and swell wave conditions which might be explained by the residual effects of flow distortion.
- For high wind conditions, effects of wave-age is more pronounced in DCF measurements at 15-m height.
- Wave signature has been detected in measurements from ECF at 15-m height above MSL.
- Empirical expressions for the probability distribution is in good agreement with the observed ones for both calm and wavy sea-state conditions.
- There exist an almost large deflection angle between wind and surface currents for low frequencies (lower than 1/12 cph).
- All oceanographic data have been successfully analyzed and the first results with focus on processing and farm-wind-current interaction can be found in Bakhoday-Paskyabi et al (2017).

Thanks

Acknowledgment

OBLEX-F1 was coordinated in collaboration between the University of Bergen (Geophysical Institute) and Christian Michelsen Research AS (project executing organization). The Federal Maritime and Hydrographic Agency of Germany (BSH) is acknowledged for providing the FINO1 reference data through the FINO database at http://fino.bshde/. The FINO project (research platforms in the North Sea and Baltic Sea) is funded by the BMU, the German Federal Ministry for the Environment, Nature Conservation, Building and Nu- clear Safety in collaboration with Project Management Ju¨lich GmbH (project no. 0325321). The FINO1 meteorological reference data were provided by Deutsches Windenergi Institut (DEWI) and the FINO1 oceanographic reference data were provided by the BSH. We also thank DEWI for providing the FINO1 high res- olution sonic anemometer data, and the FINO1 platform operator Forschungs- und Entwicklungszentrum Fachhochschule Kiel GmbH (FuE Kiel GmbH) for their support (project no. 0329905E). We thank Steffen Howorek and Andreas Gudi (FuE Kiel GmbH), and Benny Svardal, Stian Stavland for their invaluable support in deploying and maintaining the meteorolog- ical instrumentation during the campaign. We also thank Prof. Ilker Fer the crew of RV H˚akon Mosby, Helge T. Bryhni, and Steinar Myking for their professional deployment and retrieval of the oceanographic instrumentation.

University of Stuttgart
Stuttgart Wind Energy (SWE)
@ Institute of Aircraft Design

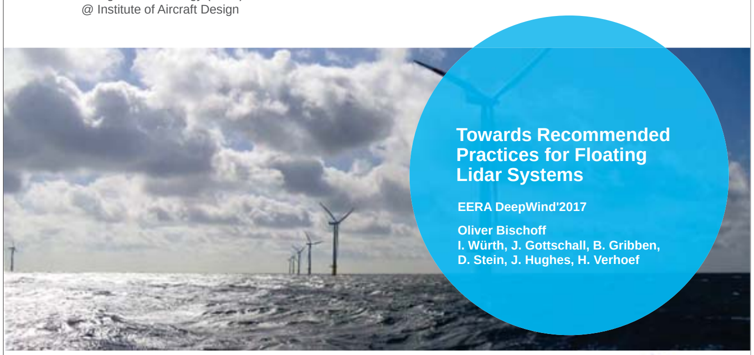

Towards Recommended Practices for Floating Lidar Systems

EERA DeepWind'2017

Oliver Bischoff
I. Würth, J. Gottschall, B. Gribben, D. Stein, J. Hughes, H. Verhoef

What is needed for a succesful operation of Floating Lidar Systems (FLS)?

Variety of concepts and designs available today
(→ picture gallery *and others*)

[Flidar, Fugro Seawatch, SeaZephIR]

Open Questions

- Recommended configuration, mandatory and optional features?
- Requirements of wind industry on systems?
- Maturity of technology
- Present technology gaps?

→ **Need for standards or recommend practices (RP)**
→ **IEA Wind Task 32 activities**
+ Carbon Trust OWA activities

Introduction

Wind lidar technology…

onshore – accepted as (almost) standard tool

… for wind resource assessments

… power curve tests (in flat terrain)

→ cost-efficient, high data quality

OWA Roadmap 2014 2015 2016 2017

Step 0: OWA Roadmap – commercial acceptance of floating lidar

→ *Carbon Trust Offshore Wind Accelerator roadmap for the commercial acceptance of floating lidar technology* (Nov. 2013) …

proposed three stages of maturity:
baseline – pre-commercial – commercial

status linked to a successful (6-months) trial offshore:
meet KPIs for system availability and data accuracy

Introduction

Wind lidar technology…

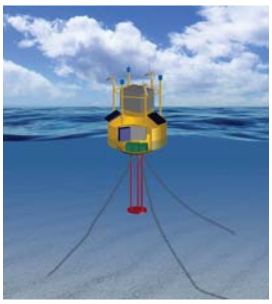

onshore – accepted as (almost) standard tool

… for wind resource assessments

… power curve tests (in flat terrain)

→ cost-efficient, high data quality

offshore – even larger cost benefits (!) –

with lidar devices integrated in / on top of

floating platforms or buoys, resp.

(→ *floating lidar systems*)

OWA Roadmap 2014 2015 2016 2017

Step 0: OWA Roadmap - FLiDAR application example

→ *Carbon Trust Offshore Wind Accelerator roadmap for the commercial acceptance of floating lidar technology* (Nov. 2013) …

[Flidar]

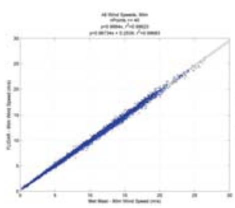

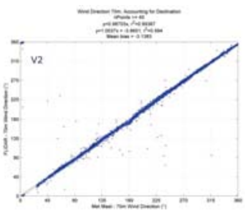

First (almost) pre-commercial floating-lidar system (FLS)

Results of 3-months trial at Gwynt y Mor [presented at EWEA Offshore 2013] show convincing agreement with met mast in wind speed and direction

OWA Roadmap 2014 2015 2016 2017

Step 0: OWA Roadmap - Final document

→ *Carbon Trust Offshore Wind Accelerator roadmap for the commercial acceptance of floating lidar technology* (Nov. 2013) …

Today several FLS with status 'pre-commercial' from different providers, a few more in the pipeline and some even on the way to commercial status

Status 'commercial' gains in importance but is not yet fully defined.



[Axys, IWES, EOLOS]

Online available:
https://www.carbontrust.com/resources/reports/technology/owa-roadmap-for-commercial-acceptance-of-floating-lidar-technologies

2013 2014 2015 Carbon Trust Project 2017

Step 2: OWA Carbon Trust project - Topics

Call for project aiming at further development of RP document, awarded to IEA Wind author team led by Frazer Nash Consulting (FNC)
→ worked on update of report between autumn 2015 and summer 2016
→ 2 workshops with stakeholders OEM's etc.

Topics priorized by workshop participants

- Developing a useable uncertainty framework.
- Guidance on mooring design and assessment
- Making the document more accessible and useful by improved use of drawings and schematics
- Standards for trusted reference system
- Pre-deployment verification - more detailed guidance on when and how much.
- Representativeness / comparisons of wave climates.
- Introduce wind shear as a KPI.

\+

Extensive review process
- author team
- review team
- OWA stakeholders review

2013 IEA Wind Task 32 Phase I WP 1.5 2015 2016 2017

Step 1: IEA Wind Task 32 Phase I WP 1.5 – first step towards Recommended Practices

- IEA Wind Task 32 Phase 1 WP 1.5 on Floating Lidars (initiated in Nov. 2012, 2nd General Meeting in Oldenburg)
- Two actions:
  - create **technology review** document
  - collect **recommended practices** (RP) and prepare document

↓

further discusssions in 2013, start of document production in 2014; formation of author and review groups, focus on RP document

→

Good progress by end of Phase 1
collected recommended Practices (RP) at this stage
published as state-of-the-art report early 2016

2013 2014 2015 Carbon Trust Project 2017

Step 2: OWA Carbon Trust Project – update of state of the art report

OWA Recommended Practices for Floating LiDAR Systems
Issue 1.0 25 October 2016

in total **120 RPs** and some more notes, all with focus on performing wind resource assessment with FLS
\+ **figures**
+ uncertainty framework (!)

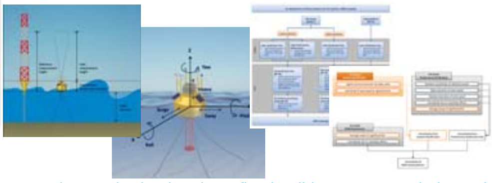

Online available:
https://www.carbontrust.com/resources/reports/technology/owa-floating-lidar-recommended-practice/

2013 IEA Wind Task 32 Phase I WP 1.5 2015 2016 2017

Step 1: IEA Wind Task 32 Phase I WP 1.5 - State of the Art Report

State-of-the-Art Report: Recommended Practices for Floating Lidar Systems
(Issue 1.0, Feb. 2016)

in total 113 RPs and a number of notes, all with focus on performing wind resource assessment with FLS

High interest of OWA (Offshore Wind Accelerator) partners in already before publication of document

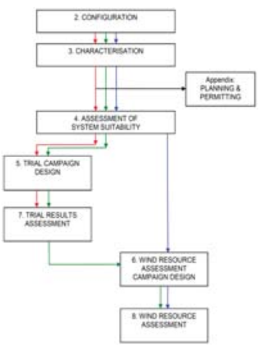

available online:
http://www.ieawindtask32.org/download/task32documents/

2013 2014 2015 IEA Wind Task 32 Phase II 2017

Step 3 IEA Wind Task 32 Phase II - Assessment of stakeholder acceptance

Pre-workshop survey:
answered by participants (incl. OEMs, Consultants, Project developers, Academics)

How would you rate the present level of maturity (in TRL 1-9) of floating-lidar technology in general?
Answer: between TRL 4 and 9 – average 6.9

How do you judge the current acceptance (0 = not at all, 10 = fully) of FLD data to be used quantitatively for finance-relevant wind resource assessments?
Answer: between 2 and 8 – average 5.8

How long will it take for the technology to reach full commercial acceptance?
Answer: 4 out of 18 'already reached', others between 2 and 10 years

Discussion of questions
→ *IEA Wind Task 32 Phase 2 Workshop on Floating Lidar Systems (23-24 Feb. 2016 at ORE Catapult, Blyth)*

2013 2014 2015 IEA Wind Task 32 Phase II 2017

Step 3: IEA Wind Task 32 Phase II - Identification of technology gaps

Outcome of workshop:

Gap 1: well defined uncertainty framework for FLS wind speed measurements

Gap 2: increase of investors' confidence (with appropriate further stakeholder activities)

Gap 3: re-defined validation framework (scope, reference, possibly adjusted to use case)

Gap 4: alternative approaches for validation (?)

Gap 5: turbulence intensity (TI) measurements from FLS (transfer of existing knowledge from Lidar TI data, and further work)

→ **Definition of roadmaps to close the gaps**

Summary & Conclusions

Objectives of this presentation

- Present available documents for application of floating lidar technology
- Elaborate on what is needed for the technology to reach full maturity
- Present activities on floating lidar within IEA Wind Task 32

Current application status

- First commercial WRA campaigns based on FLS are being reported
- The market of FLS providers is still diverse & uncertainty of measurements with FLS requires more consideration

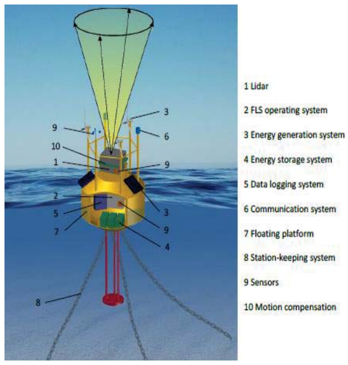

2013 2014 2015 IEA Wind Task 32 Phase II 2017

Step 3: IEA Wind Task 32 Phase II - Example 'uncertainty framework'

'Roadmaps' for gaps/requirements as result from group work

e.g. for Gap 1 – 'uncertainty framework':

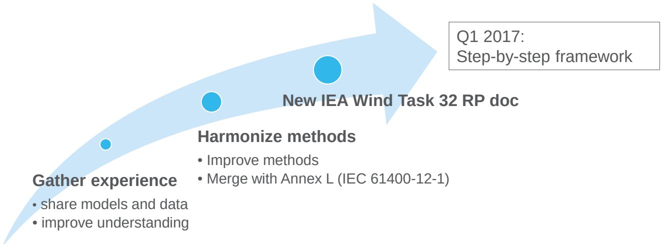

Next steps

- Research FLS for further application (beyond wind resource assessment) e.g
  - → assessment of turbine performance (incl. loads)
  - → use of TI data from FLS
  - → Power curve tests – higher demand on uncertainties and their estimation
- further workshops are planned in IEA Wind Task 32 to identify and to mitigate barriers to the use of the lidar technology in wind energy applications

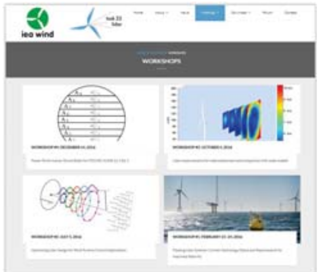

http://www.ieawindtask32.org/meetings/workshops/

Final Step: Submission of updated RP document to IEA Wind ExCo for review and consideration as IEA Wind RP doc.

Overview about currently available documents

Different projects & work in the field of Floating Lidar Systems (FLS) since 2013

→ Outcome: 3 relevant documents regarding commercial use of FLS

→ Final goal: IEA Recommended Practices

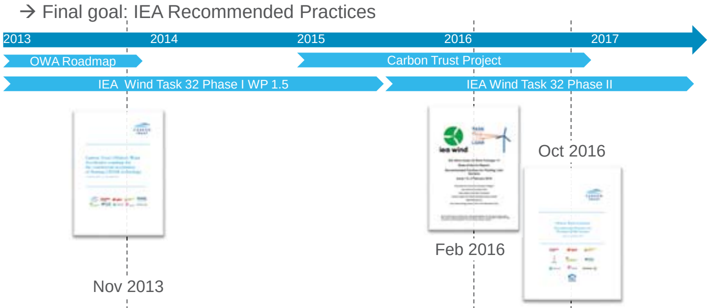

Acknowledgements

J. Gottschall (Fraunhofer IWES)
B. Gribben (Frazer Nash Consultancy)
J. Hughes (ORE Catapult)
D. Stein (DNV GL)
I. Würth, O. Bischoff, D. Schlipf (University of Stuttgart)
H. Verhoef (ECN)
A. Clifton (NREL)

University of Stuttgart

Thank you!

Oliver Bischoff

e-mail bischoff@ifb.uni-stuttgart.de
phone +49 (0) 711 685-68213
fax +49 (0) 711 685-

University of Stuttgart

C2) Met-ocean conditions

Spectral characteristics of offshore wind turbulence, E. Cheynet, University of Stavanger

Offshore Wind Turbine Wake characteristics using Scanning Doppler Lidar, J. Jakobsen, UiS

LiDAR capability to model robust rotor equivalent wind speed, J.R. Krokstad, NTNU

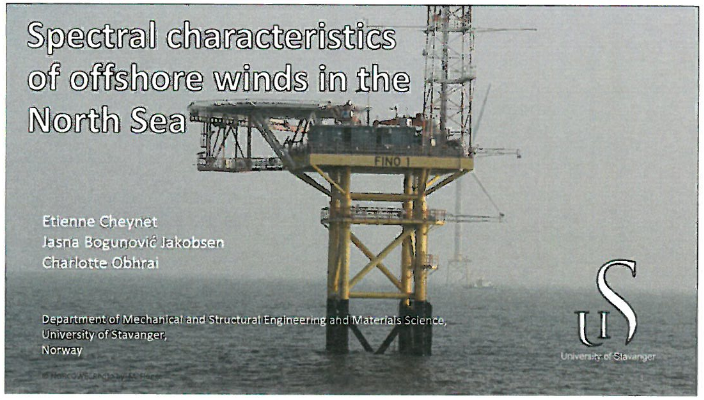

Organisation of the presentation

1. Wind spectra studied
2. Data processing
3. Comparison of the wind spectra in the field and those in standards

Wind spectral models for offshore wind turbines

$$u_* = [(uw)^2 + (uv)^2]^{\frac{1}{4}}$$

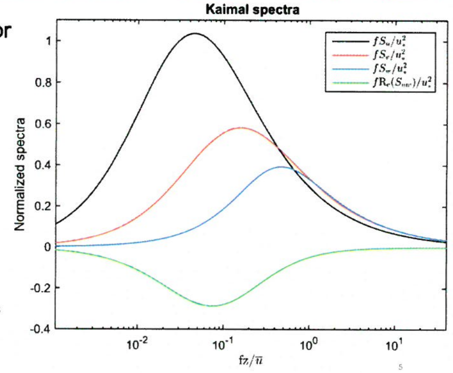

Kaimal, J. C., Wyngaard, J., Izumi, Y., & Coté, O. R. (1972). Spectral characteristics of surface-layer turbulence. *Quarterly Journal of the Royal Meteorological Society*, *98*(417), 563-589.

Do the wind spectra proposed in IEC 61400 [1,2] apply well in the North sea ?

1. *IEC 61400-1 Wind turbines Part 1: Design requirements; 2005*
2. *IEC 61400-3, . Wind Turbines Part 3: Design Requirements for Offshore Wind Turbines; 2009.*

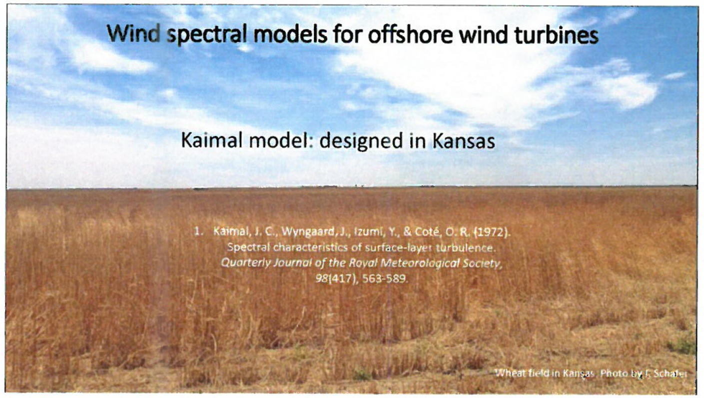

"Original Kaimal spectrum"
For *u* component

$$\frac{f\,S_u}{u_*^2} = \frac{105\,n}{(1+33\,n)^{5/3}}$$

$$n = \frac{fz}{\bar{u}}$$

"IEC Kaimal spectrum"
For *u* component

$$\frac{\cdot\,S_u}{\sigma_u^2} = \frac{4\,f_r}{(1+6\,f_r)^{5/3}}$$

$$f_r = \frac{f L_u}{\bar{u}}$$

$$L_u = 8.1\,\Lambda_1$$

$$\Lambda_1 = 42\text{ m (at } z = 80\text{ m)}$$

Wind spectral models for offshore wind turbines

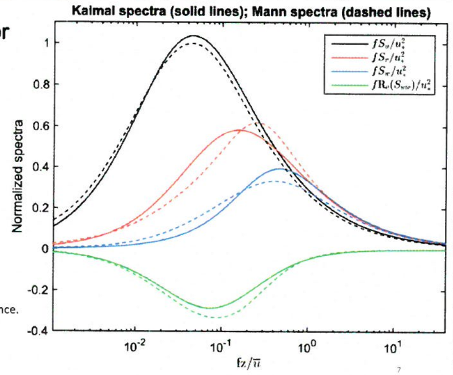

Mann, J. (1994). The spatial structure of neutral atmospheric surface-layer turbulence. *Journal of fluid mechanics*, *273*, 141-168.

Data pre-processing

Non-stationary wind model with time-varying mean extracted using the Empirical model decomposition (EMD).

+

Stationary test conducted with Reverse arrangement test [1]

[1] Bendat, J. S., & Piersol, A. G. (2011). *Random data: analysis and measurement procedures* (Vol. 729). John Wiley & Sons.

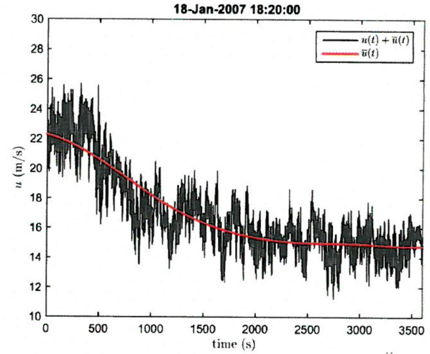

NORSOK standard

$$S_u(f) = 320 \left(\frac{\bar{u}}{10}\right)^2 \left(\frac{z}{10}\right)^{0.45} (1 + A^m)^{-\frac{5}{3m}}$$

$$A = 172 f \left(\frac{\bar{u}}{10}\right)^{-0.75} \left(\frac{z}{10}\right)^{2/3}$$

$$m = 0.468$$

Andersen, O. J., & Løvseth, J. (2006). The Frøya database and maritime boundary layer wind description. *Marine Structures*, *19*(2), 173-192.

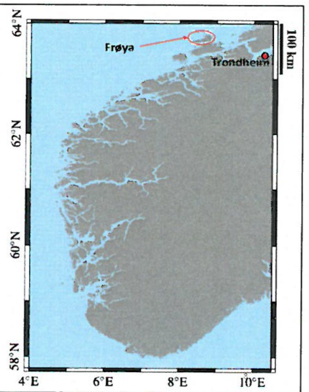

Wind measurement overview

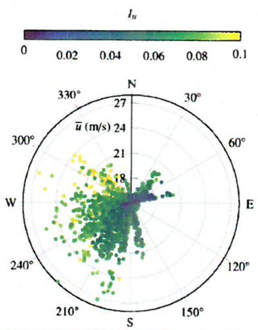

14 m/s $\leq \bar{u} \leq 28$ m/s

Averaging time: 1 h

2 years of data (2007-2008)

u, *v* and *w* are studied

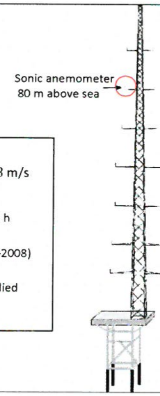

Selection of neutral wind conditions

Source: Kaimal, J. C., Wyngaard, J., Izumi, Y., & Coté, O. R. (1972). Spectral characteristics of surface-layer turbulence. *Quarterly Journal of the Royal Meteorological Society*, *98*(417), 563-589.

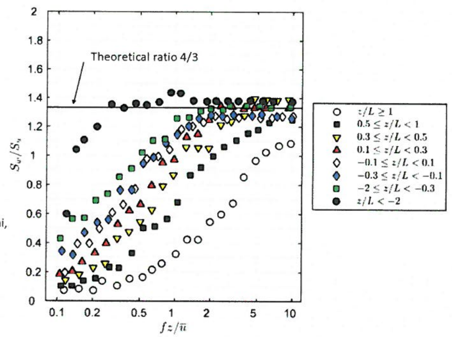

Selection of neutral wind conditions

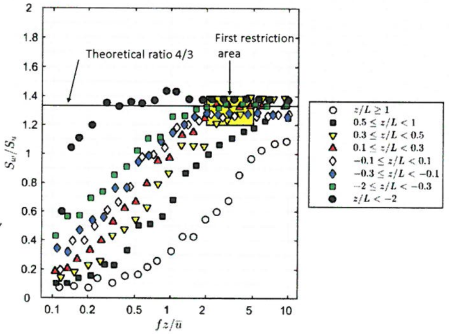

Source: Kaimal, J. C., Wyngaard, J., Izumi, Y., & Coté, O. R. (1972). Spectral characteristics of surface-layer turbulence. *Quarterly Journal of the Royal Meteorological Society, 98*(417), 563-589.

Measured vs Kaimal spectra

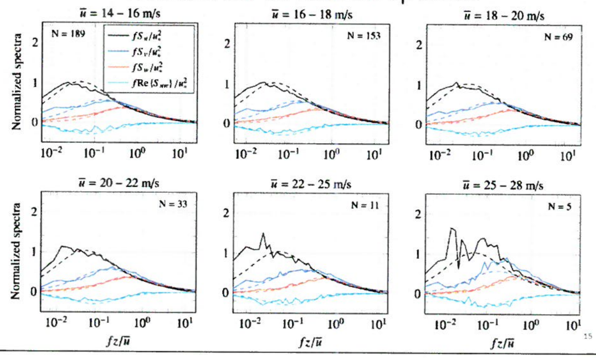

Measured vs fitted Mann spectral model

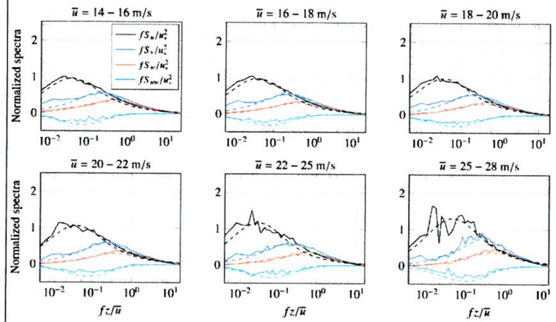

Fitted parameters:
$\Gamma = 3.7$
L = 70 m
$\alpha\varepsilon^{2/3}$ = 0.04 $m^{4/3}s^{-2}$

Selection of neutral wind conditions

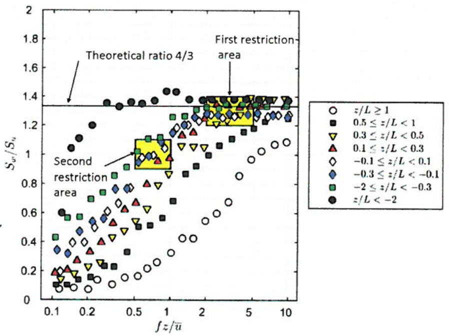

Source: Kaimal, J. C., Wyngaard, J., Izumi, Y., & Coté, O. R. (1972). Spectral characteristics of surface-layer turbulence. *Quarterly Journal of the Royal Meteorological Society, 98*(417), 563-589.

Original Kaimal spectrum
For
along wind component

$$\frac{f\,S_u}{u_*^2} = \frac{a\,n}{(1+b\,n)^{5/3}}$$

a = 105
b = 33

Fitted spectral model
For
along wind component

$$\frac{f\,S_u}{u_*^2} = \frac{a\,n}{(1+b\,n)^{5/3}}$$

a = 148
b = 45

Measured vs NORSOK vs IEC Kaimal spectra

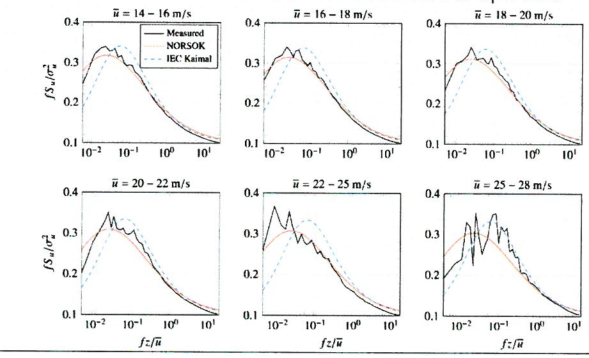

IEC Kaimal spectrum
For
along wind component

$$\frac{f\,S_u}{\sigma_u^2} = \frac{4\,f_r}{(1+6\,f_r)^{5/3}}$$

$$f_r = \frac{f\,L_u}{\bar{u}}$$

$L_u = 8.1\,\Lambda_1$

$\Lambda_1 = 42$ m (at $z = 80$ m)

Modified IEC Kaimal spectrum
For
along wind component

$$\frac{f\,S_u}{\sigma_u^2} = \frac{4\,f_r}{(1+6\,f_r)^{5/3}}$$

$$f_r = \frac{f\,L_u}{\bar{u}}$$

$L_u = 8.1\,\Lambda_1$

$\Lambda_1 = 73$ m (at $z = 80$ m)

Conclusions

- 2 year of wind measurement conducted at FINO 1 platform, 80 m above sea level
- Single-point wind spectra were measured and compared to:
  1. Kaimal spectral model
  2. IEC Kaimal model (IEC 61400)
  3. NORSOK standard
  4. Mann spectral model
- Larger energy content at low frequency than predicted
- A good overall agreement with Kaimal spectrum is observed
- > 80 % of wind data detected as "non-neutral" conditions

Offshore Wind Turbine Wake Characterization using Scanning Doppler Lidar

R. Krishnamurthy[a], J. Reuder[b], B. Svardal[c], H.J.S. Fernando[a], J. B. Jakobsen[d]

[a] University of Notre-Dame, Notre-Dame, Indiana 46545, USA
[b] University of Bergen, Bergen, Norway
[c] Christian Michelson's Research Institute, Bergen, Norway
[d] University of Stavanger, Stavanger, Norway

The College of Engineering at the University of Notre Dame

Offshore Wind Turbine Wakes

- Knowledge of wind turbine wakes is crucial to improve modelling of:
  - Power production and
  - Wind turbine loading in wind farms.
- Scanning Doppler Lidars:
  - Can capture the spatial and temporal characteristic of the wind turbine wakes and their dependency on the inflow characteristics
  - Can assist in wind farm control strategies (wake redirection...)

The College of Engineering at the University of Notre Dame

OBLEX-F1 Experimental setup

- Focus on:
  - Improved the knowledge of the marine atmospheric boundary-layer (MABL)
  - Turbulence generation processes in the water column
  - Offshore wind turbine wake propagation effects...

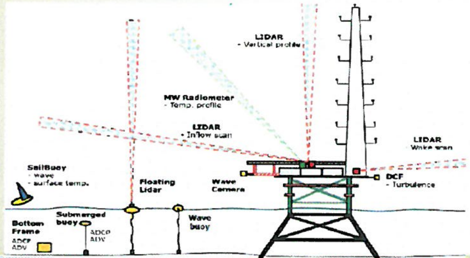

The College of Engineering at the University of Notre Dame

Outline

- Offshore Wind Turbine Wakes
- OBLEX-F1 Experimental Setup
- Methodology
- Alpha Ventus Wind Turbine Wake Characteristics
- Conclusions

The College of Engineering at the University of Notre Dame

Time and Length Scales of Interest in Wind Energy

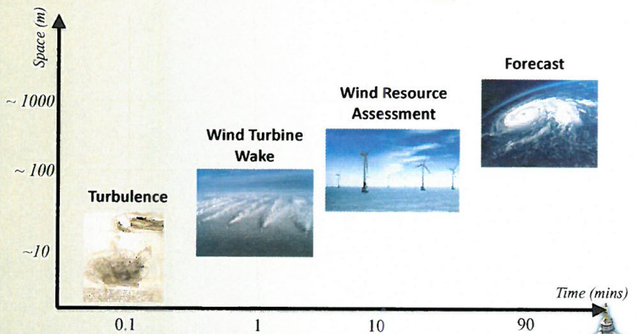

The College of Engineering at the University of Notre Dame

Adapted from A. Santiago, Leosphere

Site Conditions

- Wake characterization study period: Aug-Sept 2016

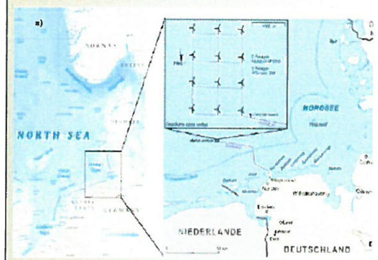

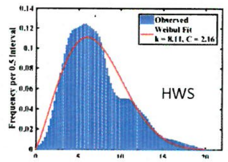

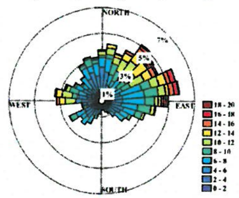

- Alpha Ventus wind turbines
- 5 MW, D=116/126 m, d=30 m

The College of Engineering at the University of Notre Dame

LIDAR – LIght Detection And Ranging

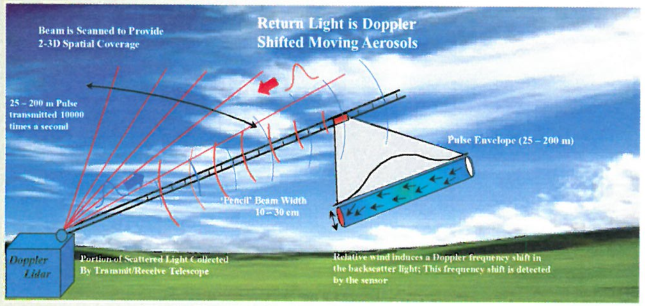

$$v_r(R,\phi,\theta) = U\sin\phi\cos\theta + V\cos\phi\cos\theta + W\sin\theta$$

V_r =Radial Velocity, ϕ = Azimuth Angle , θ = Elevation angle; U, V, W = Components of wind speed

Adapted from Calhoun, ASU

Scanning modes

DBS/VAD

What: Velocity Azimuth Displays

How: Conical scan or variation

Why: Vertical profile of the horizontal and vertical velocity

RHI

What: Range-Height Indicator

How: Elevation changes, azimuth fixed

Why: Vertical cross sections, wind shear (wind changes with height) and wind overturning events (wind direction changes with height)

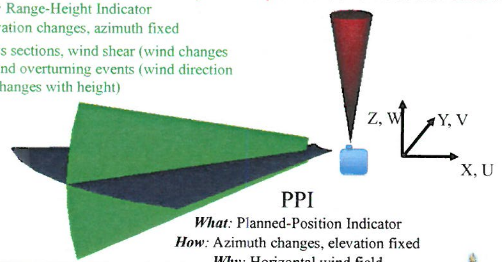

PPI

What: Planned-Position Indicator

How: Azimuth changes, elevation fixed

Why: Horizontal wind field

Wake Scan Pattern

Data analyzed:

Scan	Azimuth (deg)	Elevation (deg)	Scan rate (deg/sec)	Averaging (secs)	Repetitions in 10 minutes (#)
PPI	131.5 –179.5	4.62	1	1	12

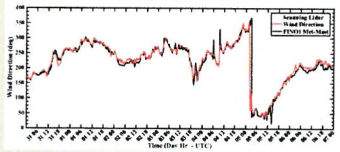

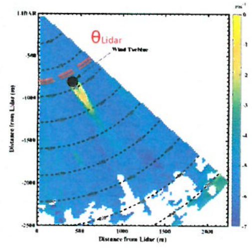

Scanning Lidar Specifications

WindCube 100S

Lidar Specifications	Value
Eye Safety	Class 1M
Wavelength (μm)	1.54
Pulse Energy (μJ)	100
PRF (Hz)	10000
Pulse Averaged	10000
Pulse Duration (ns)	150
Range-gate interval (m)	25
Velocity Precision (cm s^{-1})	< 20
Minimum Range (m)	50
Maximum Range (m)	3000

Wake Scan Pattern

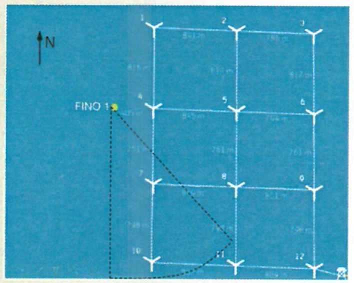

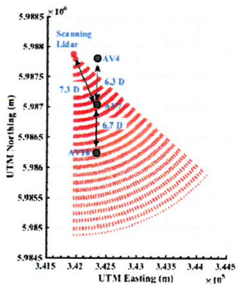

Methodology

- Wind turbine velocity deficit is defined as

$$VD\,(R,x) = \left(1 - {U(R,x)}/{U_A(R,x')}\right) \times 100\%$$

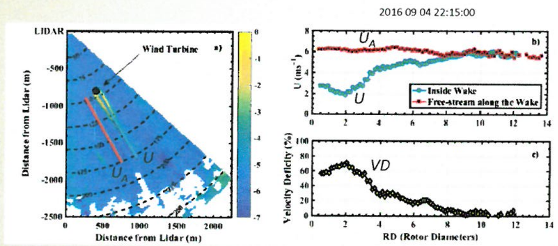

Adapted from Smalikho et al., 2013

Methodology

- To account for the wake centerline deviation from the WT axis:
  - A Gaussian curve fit was applied to the velocity deficit data

$$VD_{fit}(R,x) = a\, e^{-\left[\frac{x-b}{c}\right]^2}$$

where R is the downwind distance, x is the lateral distance and a, b & c are fit parameters

  - Wake centerline (W_c) was defined as

$$W_c(R) = max[VD_{fit}(R,x)]$$

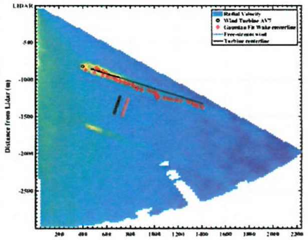

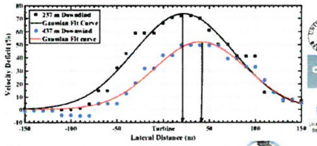

Wake length as a function of time of the day

- (Daytime – 0700 hrs to 1800 hrs & night time – 1800 hrs to 0700 hrs)
  - Day-time wakes have 4-11% lower velocity deficits
  - Night-time wakes have 60% larger wake lengths

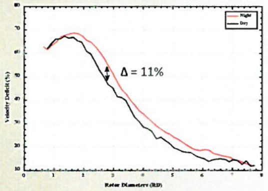

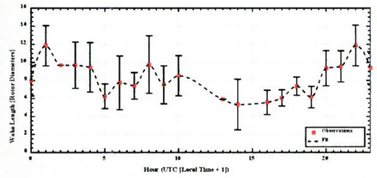

The College of Engineering at the University of Notre Dame

Conclusions

Alpha Ventus wind turbine wake studied (252 samples, 5 min) shows:

- A higher velocity deficit compared to previous studies (up to 20%).
- Higher velocity deficits during night time than at the daytime (11% higher) and larger wake lengths (up to 60%).
- Wake centerline deviation from the WT axis up to 25°.

Scanning lidar is a valuable tool to characterize wind field within a wind farm and thereby contribute to an improved wind power extraction and the wind turbine design.

The College of Engineering at the University of Notre Dame

Average velocity deficit over the duration of the campaign

Higher deficit than reported in literature (Barthelmie et al., 2006 & Hirth et al., 2013 etc...) , likely due to differences in:

- Measurement techniques
- Ambient wind conditions
- WT operation mode

$$\frac{\Delta U}{U_A} = 1.50x^{-1.12}$$

*R2 of the model – 87.45%

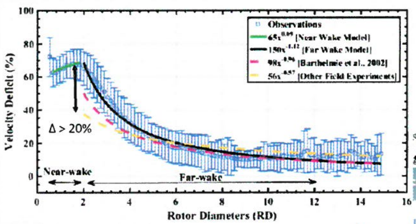

*Averaged over 252 samples

The College of Engineering at the University of Notre Dame

Wind Turbine Wake Characteristics

- Deviation of the wake center from turbine location
  - Significant wake centerline deviation from the WT axis, maximum deviation of greater than 25 degrees at 8 Rotor Diameters
  - Important to understand for wind turbine siting and wind farm control strategies.

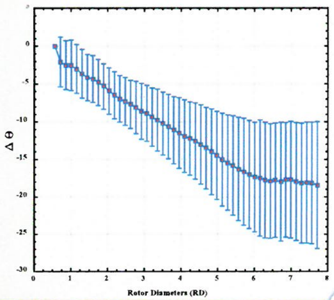

The College of Engineering at the University of Notre Dame

EERA DeepWind'2017

LIDAR capability to model robust rotor equivalent wind speed

by
Jørgen R. Krokstad (Fugro/NTNU)
Vegar Neshaug (Fugro)
Birgitte Furevik (NMI)
Knut Helge Midtbø (NMI)
Teresa Valkonen (NMI)

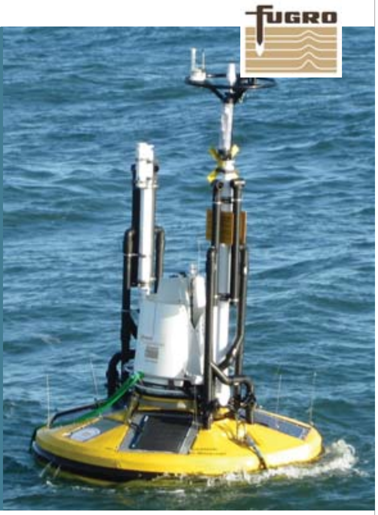

New requirements using REWS

- Wind Resource Assessment is sensitive to small % changes in AEP (annual energy production)
- IEC – 61400-12 – CD2 is not publically available but used as a reference for measurement campaigns – consequence?
- IEC - 61400-12 – CD2 is a drive from metmast based to LiDAR based power curve and AEP estimation
- Ref: Wagner et al – *Rotor equivalent wind speed for power curve measurements – comparative exercise for IEA Wind Annex 32*

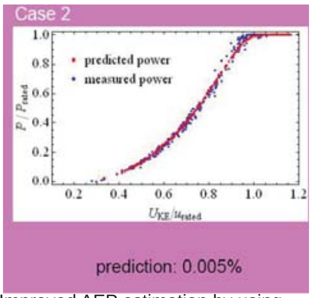

Improved AEP estimation by using REWS compared with measured power
DTU – Risø – Rozenn Wagner

The Seawatch Wind LiDAR Buoy – status - 2017

- Integrate wind and metocean measurements
- Many operational projects in Europa – Netherland, UK and Poland
- Wind profiling capability up to 300m
- May utilize wind profiles «above» hub heights
- IEC 61400-12, CD-2 will allow wind measurements to be based on LiDAR only
- Current profiling capability down to 1000m
- Directional wave measurements
- Measurement of a wide range of met-ocean parameters
- Flexible energy system
- A fraction of the cost of a traditional offshore met-mast

Causes of wind shear in the coastal zone and offshore

- Surface friction
- Stability effects, internal boundary layers
- Convection, rain cells
- Atmospheric fronts
- Low level jets

Motivation for looking at REWS (Rotor Equivalent Wind Speed)

- May utilize data above hub height – metmast always truncated
- Improved accuracy of Power estimates

  U_{hub} versus U_{eq}

- More important for large rotor diameter turbines (D=150-180 meter) than standard (D=110–150 meter)
- Reduced uncertainty in AEP (annual energy production) estimates
- Prepare for ratification of IEC-61400-12 CD2

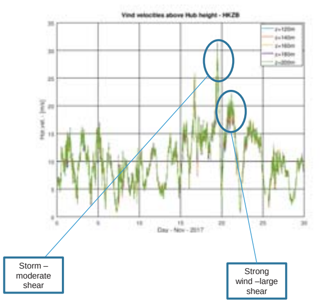

MET Norway weather forecast model AROME 2.5km x 2.5km grid spacing

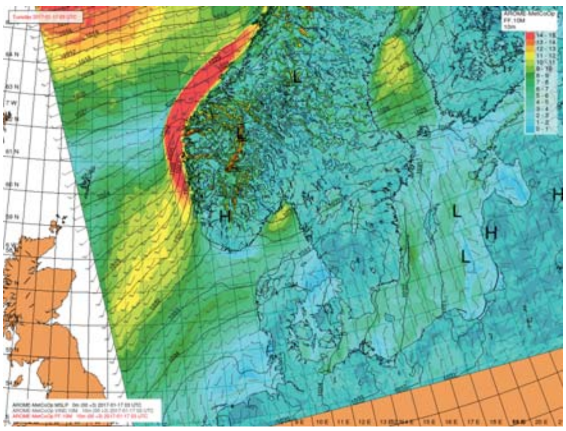

Sola airport 2013

NORCOWE Lidar measurements at Sola airport showing diurnal variation in wind speed and direction (*Lidar measurement campaign field report*, Kumer, 2014)

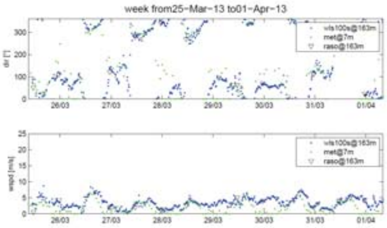

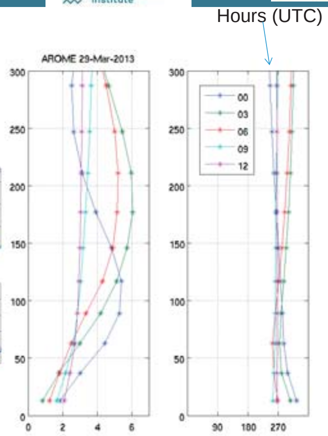

AROME model 3-hr profiles

NREL – 5 MW turbine , DTU – 10 MW turbine

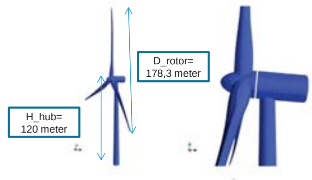

10 MW – scaled from 5 MW NREL

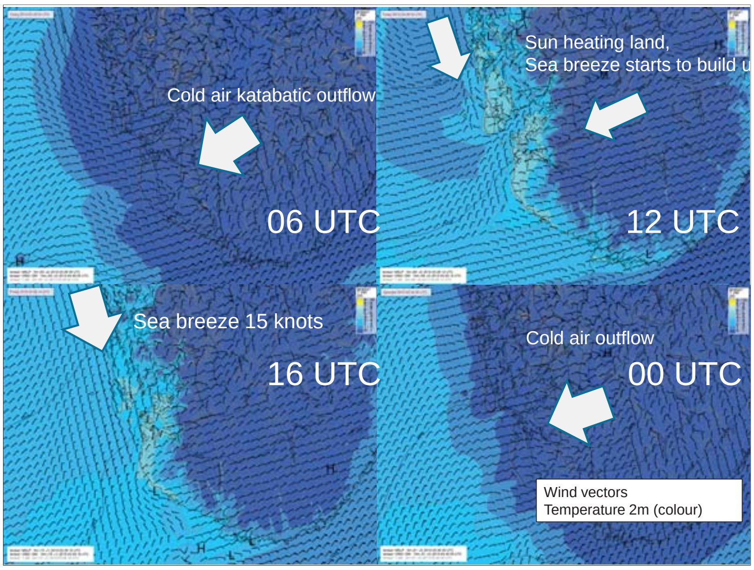

Power curves – 5 MW NREL , 10 MW DTU

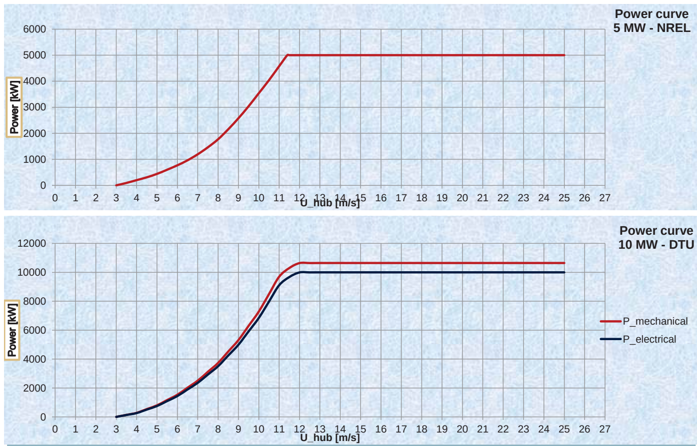

REWS principles for calculation

$$A_i = \int_{z_i}^{z_{i+1}} c(z)dz$$

$$c(z) = 2\sqrt{R^2 - (z - H)^2}$$

Where H is hub height – R is rotor radius

$$u_{eq} = \left(\sum_{i=1}^{n} u_i^3 \frac{A_i}{A}\right)^{\frac{1}{3}}$$

$$AEP = N_h \sum_{i=1}^{N} [F(u_i) - F(u_{i-1})] \left(\frac{P_{i-1} + P_i}{2}\right)$$

$$F(u) = 1 - e^{-\frac{\pi}{4}\left(\frac{u}{u_{ave}}\right)^2}$$

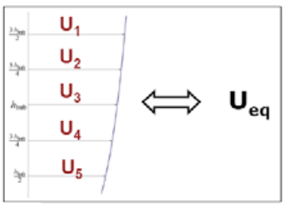

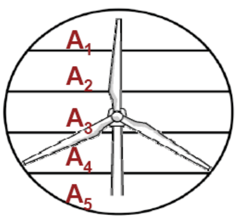

Hollandse Kust Wind Farm Zone

2 SW Wind Lidar buoys deployed June 2016

Parameters:

- Mooring at 23 m water depth
- Wave height, period and direction
- Current profile (22 m) and water temperature
- Wind speed and direction
- Wind speed and direction profile
- Air pressure
- Air humidity and temperature
- Water level (tide)

Wind observations

Wind speed and direction, turbulence intensity, inflow angle and wind shear/veer

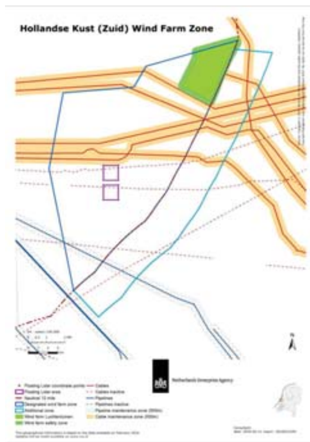

Hollandse Kust Wind Farm Zone, RVO 2016

Norwegian Meteorological Institute · FUGRO

Environmental conditions experienced at Hollandse Kust Wind Farm Zone

Parameter		Value	
Highest Significant Wave height	m	5.20	20th Nov2016
Max wave height	m	7.74	20th Nov 2016
Highest 10 min Average Wind speed (30 m)	m/s	29.1	20th Nov 2016
Highest 10 min Average Wind speed (200 m)	m/s	33.7	20th Nov 2016

Ratio between energy production - AEP

Norwegian Meteorological Institute · FUGRO

- Average(u_eq/u_hub)^3 < 1 for the monthly dataset – 10 MW turbine
- Spikes due to sudden changes in heading of the profile
- AEP ratios calculated as follows

Turbine	Ratio P_rews/P_hub
5 MW	0,99
10 MW	0,98

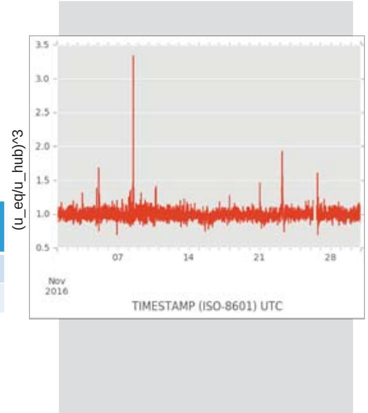

Hollandse Kust Wind Farm Zone, 2016 - *Ongoing*

Norwegian Meteorological Institute · FUGRO

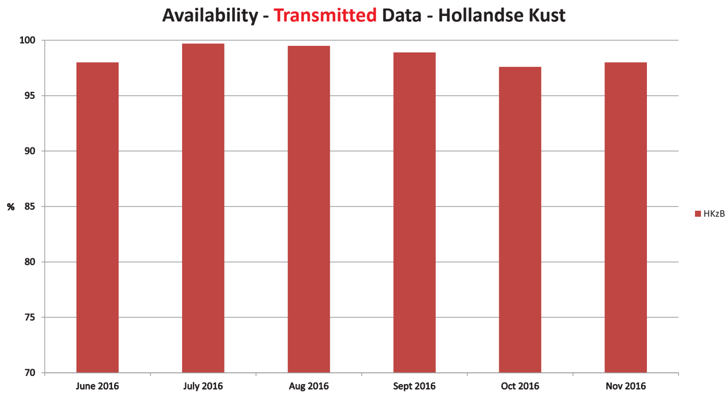

Conclusions

Norwegian Meteorological Institute · FUGRO

- **Floating LiDAR** – the first choice for measuring offshore wind resource
- **Data** from the Hollandse Kust zuid is used – the data is publically available
- Different **shear profiles** are presented, Holland, and from the LiDAR based Sola airport project (near offshore conditions) in 2013
- A **weather front driven change** in wind share is shown
- **Rotor Equivalent Wind Speed is introduced** and applied for two «theoretical» turbines with medium and large rotor diameter's, NREL 5MW and DTU 10 MW.
- From prelimenary results – The ratio between hub height and equivalent wind speed - **larger than 1 for some speed ranges** and largest for 10 MW.
- **Small reduction effects in AEP** – reduced production with the use of REWS - but limited confidence in data basis for the conclusion.

Wind profiles – against ratio between (u_eq/u_hub)^3

Norwegian Meteorological Institute · FUGRO

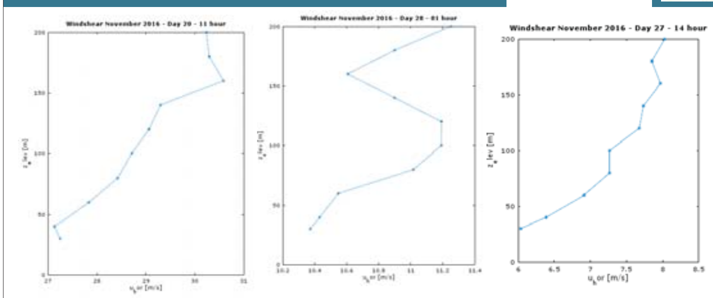

Above cut-out
10 MW
(u_eq/u_hub)^3 = 1,005
5 MW
(u_eq/u_hub)^3 = 0,982

Close to rated
10 MW
(u_eq/u_hub)^3 = 1,066
5 MW
(u_eq/u_hub)^3 = 1,013

Below rated

FUGRO · Norwegian Meteorological Institute

Thank you for your time

EERA DeepWind 2017

D1) Operations & maintenance

A metaheuristic solution method for optimizing vessel fleet size and mix for maintenance operations at offshore wind farms under uncertainty, E.Halvorsen-Weare, SINTEF Ocean

Optimizing Jack-up vessel strategies for offshore wind farms, M. Stålhane, NTNU

Short-Term Decision Optimization for Offshore Wind Farm Maintenance,
C. Stock-Williams, ECN

Improved short term decision making for offshore wind farm vessel routing,
R. Dawid, Strathclyde University

A METAHEURISTIC SOLUTION METHOD FOR OPTIMIZING VESSEL FLEET SIZE AND MIX FOR MAINTENANCE OPERATIONS AT OFFSHORE WIND FARMS UNDER UNCERTAINTY

EERA DEEPWIND'2017, TRONDHEIM, 18 JANUARY 2017

Elin E. Halvorsen-Weare[1], Inge Norstad[1], Magnus Stålhane[2], Lars Magne Nonås[1]

[1]Department of Maritime, SINTEF Ocean
[2]Department of Industrial Economics and Technology Management, NTNU

Outline

1 Setting the scene
2 Vessel fleet optimization model
3 Solution method
4 Application on a reference case
5 Summary

Outline

1 Setting the scene
2 Vessel fleet optimization model
3 Solution method
4 Application on a reference case
5 Summary

Deep sea offshore wind O&M logistics - Challenges

- Large number of turbines
  - Many maintenance tasks
- Large distances
- Marine operations
- Accessibility to wind farm and turbines
  - Weather restrictions

O&M at offshore wind farms

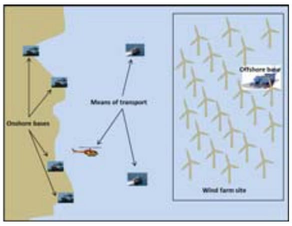

Focus on the maritime transportation and logistic challenges:

- Need to execute maintenance tasks at wind turbines
  - Preventive maintenance tasks
    - Scheduled tasks
  - Corrective maintenance tasks
    - Component failure requiring repair or replacement
- Need to transport technicians, spare parts etc. from a maintenance base to the turbines
  - From which maintenance ports/bases?
  - By which vessel resources?

Which vessel resources are most promising for a given offshore wind farm?

Evaluating all possible vessel fleets is impractical and time consuming, and often impossible

10 vessel types, 0-3 vessels each → $2^{20} \approx 1$ million combinations

Outline

1 Setting the scene
2 Vessel fleet optimization model
3 Solution method
4 Application on a reference case
5 Summary

SINTEF

Vessel fleet optimization model for O&M

Main idea:

- Create a decision support tool for selecting the best logistical resources, i.e. vessels, infrastructure and related resources, and the best deployment of these resources to execute maintenance tasks at offshore wind farms

Why?

- Many options for vessels and infrastructure configurations, maintenance strategies, and site specific considerations makes it difficult to get a good overview without strategic analytical tools to evaluate the solution space
- Offshore wind farms at deep sea locations creates the need to develop new technology and logistics strategies, that need to be evaluated from an economical perspective

SINTEF

Development of vessel fleet optimization model

Vessel fleet optimization model – developed through various research projects:

NOWITECH (2010 – 2017)
Initialization of development
Development of stochastic mathematical model for vessel fleet optimization

FAROFF (2012 – 2013)
Developed first prototype of vessel fleet optimization model

- Deterministic mathematical model for vessel fleet optimization

LEANWIND (2013 – 2017)
Development of heuristic solver for the stochastic vessel fleet optimization model

SINTEF

Stochastic mathematical optimization model

- Pattern-based mathematical formulation
  - Candidate patterns generated for vessel and base combinations
  - Based on vessel characteristics and compatibility with maintenance tasks
- Patterns are input to the mathematical model
  - Two-stage stochastic model formulation
- Stochastic parameters
  - Weather conditions (wind and wave)
  - Corrective maintenance tasks (generated based on failure rates)

SINTEF

Stochastic mathematical optimization model

- Variables:
  - Which vessels to use
    - Short-term or long-term charter?
  - Which maintenance patterns vessels should execute
  - Which maintenance ports/bases to use
- Objective: Minimize total cost
  - Time charter costs
  - Port/base costs
  - Fuel costs – and other voyage related costs
  - Downtime cost
- All maintenance tasks should be executed within the planning horizon, or they are given a penalty cost

SINTEF

Stochastic mathematical optimization model

$$\min \sum_{k\in K} C_k^F \delta_k + \sum_{k\in K}\sum_{v\in V_k} C_v^F x_{kv}^L + \sum_{k\in K}\sum_{v\in V_k}\sum_{t\in P^T} C_{vt}^F x_{kvt}^S +$$
$$\sum_{s\in S} P_s \Bigg[\sum_{v\in V}\sum_{i\in N^C\cap N_v}\sum_{j\in N_{is}^C}\sum_{p\in P_{vijs}} C_{ijps}^D y_{vijps} + \sum_{k\in K}\sum_{v\in V_k}\sum_{w\in W_{kv}}\sum_{i\in N^P\cap N_v}\sum_{p\in P_{kvws}} C_{ips}^D A_{iw}\lambda_{kvwps} +$$
$$\sum_{k\in K}\sum_{v\in V_k}\sum_{w\in W_{kv}}\sum_{p\in P_{kvws}} C_{kvwps}\lambda_{kvwps} + \sum_{i\in N^P} C_i^P z_{is} + \sum_{i\in N^C}\sum_{j\in N_{is}^C} C_i^P z_{ijs}\Bigg]. \quad (1)$$

Objective function

SINTEF

Stochastic mathematical optimization model

$$x^L_{kv} + x^S_{kvt} \le Q_{kv}\delta_k, \quad k \in K, v \in V_k, t \in P^T, \quad (2)$$
$$\delta_{k1} + \delta_{k2} \le 1, \quad (k1, k2) \in K^C, \quad (3)$$
$$\delta_k \ge E_k, \quad k \in K, \quad (4)$$
$$x^L_{kv} \ge E_{kv}, \quad k \in K, v \in V_k, \quad (5)$$
$$\sum_{k \in K} x^S_{kvt} \le Q^{MX}_{vt}, \quad v \in V, t \in P^T, \quad (6)$$
$$\delta_k \in \{0,1\}, \quad k \in K, \quad (7)$$
$$x^L_{kv} \in Z^+, \quad k \in K, v \in V_k, \quad (8)$$
$$x^S_{kvt} \in Z^+, \quad k \in K, v \in V_k, t \in P^T. \quad (9)$$

First stage constraints

SINTEF

Metaheuristic solution framework

Greedy randomized adaptive search procedure – GRASP

1. Construct an initial feasible solution to the problem by a greedy randomized algorithm
2. Improve the initial feasible solution by a local search procedure
3. Continue until stopping criterion is met

All candidate solutions are evaluated by a simulation procedure taking into account uncertainty in weather conditions and corrective maintenance tasks

SINTEF

Stochastic mathematical optimization model

$$\sum_{k \in K} \sum_{v \in (V_k \cap V_i)} \sum_{w \in W_{kv}} \sum_{p \in P_{kvws}} A_{iw}\lambda_{kvwps} + z_{is} = A_i, \quad i \in N^P, s \in \mathcal{S}, \quad (10)$$
$$\sum_{v \in V_i} \sum_{p \in P_{vijs}} y_{vijps} + z_{ijs} = 1, \quad i \in N^C, s \in \mathcal{S}, j \in N^C_{is}, \quad (11)$$
$$\sum_{k \in K} \sum_{w \in W_{kv}} A_{iw}\lambda_{kvwps} - \sum_{j \in N^C_{is}} y_{vijps} = 0, \quad v \in V, i \in N^C \cap N_v, p \in P_v, s \in \mathcal{S}, \quad (12)$$
$$\sum_{w \in W_{kv}} \lambda_{kvwps} \le x^L_{kv} + x^S_{kvt}, \quad k \in K, v \in V_k, p \in P_v, t \in P^T | p \in t, s \in \mathcal{S}, \quad (13)$$
$$\sum_{v \in V} \sum_{w \in W_{kv}} M_v\lambda_{kvwps} \le M_k\delta_k, \quad k \in K, p \in P, s \in \mathcal{S}, \quad (14)$$
$$\lambda_{kvwps} \in Z^+, \quad k \in K, v \in V_k, w \in W_{kv}, s \in \mathcal{S}, p \in P_{kvws}, \quad (15)$$
$$y_{vijps} \in \{0,1\}, \quad v \in V, i \in N^C \cap N_v, s \in \mathcal{S}, j \in N^C_{is}, p \in P_{vijs}, \quad (16)$$
$$z_{is} \in Z^+, \quad i \in N^P, s \in \mathcal{S}, \quad (17)$$
$$z_{ijs} \in \{0,1\}, \quad i \in N^C, s \in \mathcal{S}, j \in N^C_{is}. \quad (18)$$

Second stage constraints

SINTEF

Local search algorithm

Explore neighborhood solutions to an initial solution:

- Add vessel long-term
- Remove vessel long-term
- Add vessel short-term
- Remove vessel short-term
- Remove base
- Swap bases
- Swap vessels long-term
- Swap vessels short-term

SINTEF

Outline

1 Setting the scene
2 Vessel fleet optimization model
3 Solution method
4 Application on a reference case
5 Summary

SINTEF

Evaluation of candidate solutions

- Scenario generator
  - Generates a number of weather data sets and corrective maintenance tasks sets
- Calculator
  - Calculates the objective function value of a solution for a given weather data and corrective maintenance task set

SINTEF

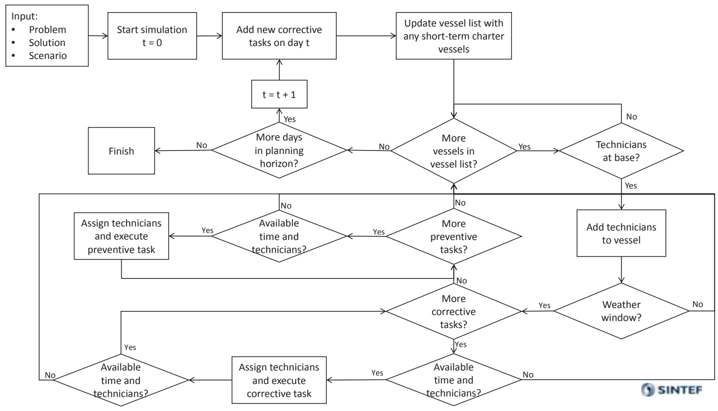

Outline

1 Setting the scene
2 Vessel fleet optimization model
3 Solution method
4 Application on a reference case
5 Summary

Overview metaheuristic framework

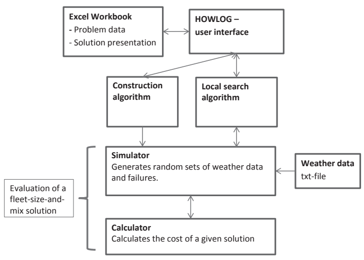

Application on a reference case
(Sperstad et al. 2016)

- Wind farm with 80 3MW turbines
- 50 km distance to onshore maintenance base
- One type of preventive maintenance: 60 hours work x 80 turbines
- Three types of corrective maintenance: Failure rates 7.5, 3 and 0.825
- Weather data from FINO1 metocean platform
- Electricity price 90 GBP/MWh

Configuration of vessel fleet optimization tool

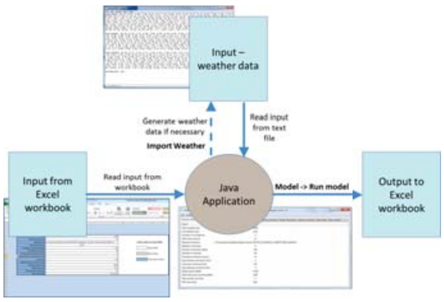

Available vessel resources

Vessel type name	Hs limit [m]	Transfer speed [knots]	Day rate [GBP]	Technician transfer space	Access time [min]	# available vessels
Crew transfer vessel (CTV)	1.5	20	1 750	12	15	5
Surface effect ship (SES)	2.0	35	5 000	12	15	5
Small accommodation vessel (SAV)	2.0	20	12 500	12	15	1
Mini mother vessel (MM)	2.5	14	25 000	16	30	1
Daughter vessel (DM)	1.2	16	N/A	6	15	2

Results

	GRASP	EXACT
Vessel fleet	**2 SES**	**2 SES**
Expected total cost	13 438 089	13 318 186
Vessel cost	3 650 000	3 650 000
Voyage cost	2 098 533	2 016 700
Downtime cost	7 689 544	7 651 486
Electricity based availability	92.96 %	93.02 %
Computational time [s]	144	7 961

GRASP method has been implemented in Java, number of simulations on each candidate solution was 30. EXACT method has been implemented in the Mosel language and solved by FICO™ Xpress, number of scenarios was 5, and optimality gap was set to 1.0%.

Summary

- Determining optimal vessel fleets for maintenance operations at offshore wind farms is challenging
- We have developed a vessel fleet optimization model for decision support
- An efficient metaheuristic solution procedure has been implemented
  - Greedy randomized adaptive search procedure
  - Uncertainty in weather conditions and corrective maintenance tasks considered by a simulation procedure
  - Reports optimal vessel fleet compared with exact solution method
- Decision support tool can aid many actors in the offshore wind industry

Application areas

- Offshore wind farm developers
  - Which are the optimal maintenance vessel resources?
  - Which are the optimal maintenance ports/bases and what type of characteristics should they have?
  - When should the maintenance activities be scheduled?
- Maintenance vessel developers and innovators
  - Cost/benefit analysis for evaluating/choosing among existing vessels
  - Early phase feedback for design of new vessels
- Maintenance concept developers and innovators
  - Cost/benefit analysis of new concepts and the potential effects on the logistic systems

References

- Cradden, L.; Gebruers, C.; Halvorsen-Weare, E.E.; Irawan, C.; Nonås, L.M.; Norstad, I.; Pappas, T.; Schäffer, L.E. (2016), "Mathematical optimisation models and methods for transport systems". LEANWIND Deliverable 5.6.
- Sperstad, I.B.; Stålhane, M.; Dinwoodie, I.; Endrerud, O.-E.V.; Martin, R.; Warner E. (2016), "Testing the Robustness of Optimal Vessel Fleet Selection for Operation and Maintenance of Offshore Wind Farms". (Unpublished.)
- Stålhane, M.; Halvorsen-Weare, E.E.; Nonås, L.M. (2014), "FAROFF Optimization model technical report", MARINTEK Report MT2014 F-097.
- Stålhane, M.; Halvorsen-Weare, E.E.; Nonås, L.M. (2016), "A decision support system for vessel fleet analysis for maintenance operations at offshore wind farms", Working paper. (Unpublished.)

Outline

1 Setting the scene
2 Vessel fleet optimization model
3 Solution method
4 Application on a reference case
5 Summary

SINTEF

Technology for a better society

NTNU
Norwegian University of Science and Technology

Optimizing Jack-Up Vessel Chartering Strategies for Offshore Wind Farms

Andreas Jebsen Mikkelsen
Odin Kirkeby
Marielle Christiansen
Magnus Stålhane

Outline

- Motivation
- Problem description
- Mathematical model
- Preliminary results
- Further research

Jack-up vessel

Motivation

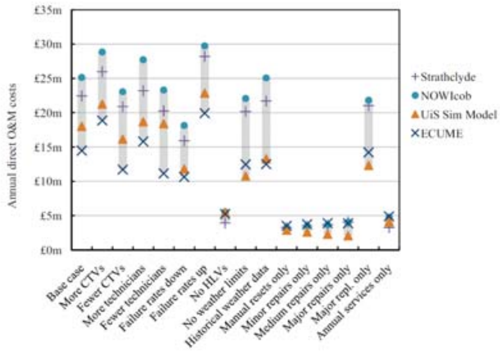

*from Dinwoodie et al (2015)

Motivation

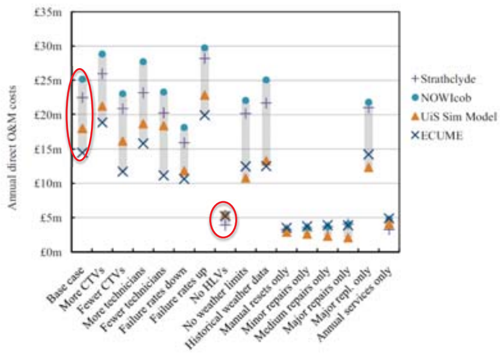

*from Dinwoodie et al (2015)

Jack-up vessel charter rates

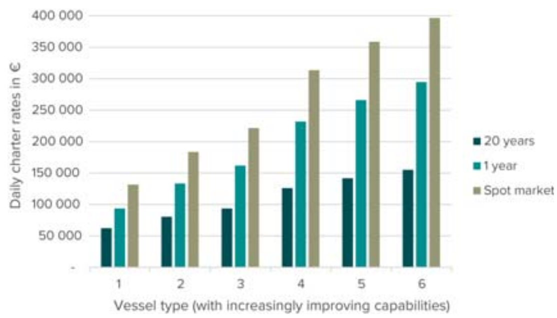

*Based on data from Dalgic et al (2013)

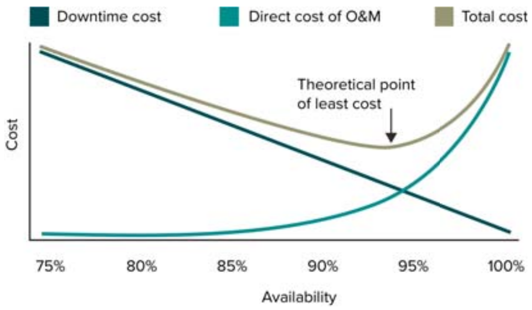

Current Jack-Up Charter Practices

- Options:
  - Annual charter
  - Fix-on-fail
  - Batch-repair
- Difficult to determine best option
- Obstacles:
  - Inflexibility
  - Expensive
  - Determining optimal batch
  - Uncertainty

Optimal jack-up strategy depends on:

- Size of the wind farm
- Weather conditions at the wind farm site
- Failure rate of the components
- Charter rate for jack-up vessels
- Capabilities of the jack-up vessels

- Goal: To determine when, and for how long, to charter in a jack-up vessel in order to minimize expected total O&M cost.

Mathematical model

- Uncertain parameters:
  - When failures that require jack-up vessels occur
  - The weather conditions at the wind farm site each day of the planning horizon
- Two-stage stochastic optimization model
  - First stage: Decide when, and for how long, to charter a jack-up vessel
  - Second stage: Given first stage decision, how to deploy the jack-up vessel in order to minimize the downtime cost

First stage model

$$\min \sum_{v\in\mathcal{V}}\sum_{t\in\mathcal{T}} C^P_{vt} y_{vt} + \sum_{v\in\mathcal{V}}\sum_{t\in\mathcal{T}} C^M_v v_{vt} + E_\xi[Q(y,\xi)]$$

$$\begin{aligned}
& y_{vt} - y_{v(t-1)} \le v_{vt}, && v\in\mathcal{V}, t\in\mathcal{T}\setminus\{1\},\\
& y_{v1} - y_{|\mathcal{T}|} \le v_{vt}, && v\in\mathcal{V},\\
& \sum_{\tau=t}^{t+\underline{T}^L-1} y_\tau \ge \underline{T}^L v_t, && v\in\mathcal{V}, t\in\mathcal{T} : t \le |\mathcal{T}| - \underline{T}^L + 1,\\
& \sum_{\tau=t}^{|\mathcal{T}|} y_\tau + \sum_{\tau=1}^{t+\underline{T}^L-|\mathcal{T}|-1} y_\tau \ge \underline{T}^L v_t, && v\in\mathcal{V}, t\in\mathcal{T} : t \ge |\mathcal{T}| - \underline{T}^L,\\
& y_{vt} \in \{0,1\}, && v\in\mathcal{V}, t\in\mathcal{T},\\
& v_{vt} \in \{0,1\}, && v\in\mathcal{V}, t\in\mathcal{T}.
\end{aligned}$$

First stage model

Daily charter rate

$$\min \sum_{v\in\mathcal{V}}\sum_{t\in\mathcal{T}} C^P_{vt} y_{vt} + \sum_{v\in\mathcal{V}}\sum_{t\in\mathcal{T}} C^M_v v_{vt} + E_\xi[Q(y,\xi)]$$

$$\begin{aligned}
& y_{vt} - y_{v(t-1)} \le v_{vt}, && v\in\mathcal{V}, t\in\mathcal{T}\setminus\{1\},\\
& y_{v1} - y_{|\mathcal{T}|} \le v_{vt}, && v\in\mathcal{V},\\
& \sum_{\tau=t}^{t+\underline{T}^L-1} y_\tau \ge \underline{T}^L v_t, && v\in\mathcal{V}, t\in\mathcal{T} : t \le |\mathcal{T}| - \underline{T}^L + 1,\\
& \sum_{\tau=t}^{|\mathcal{T}|} y_\tau + \sum_{\tau=1}^{t+\underline{T}^L-|\mathcal{T}|-1} y_\tau \ge \underline{T}^L v_t, && v\in\mathcal{V}, t\in\mathcal{T} : t \ge |\mathcal{T}| - \underline{T}^L,\\
& y_{vt} \in \{0,1\}, && v\in\mathcal{V}, t\in\mathcal{T},\\
& v_{vt} \in \{0,1\}, && v\in\mathcal{V}, t\in\mathcal{T}.
\end{aligned}$$

First stage model

Mobilisation rate

$$\min \sum_{v\in\mathcal{V}}\sum_{t\in\mathcal{T}} C^P_{vt} y_{vt} + \sum_{v\in\mathcal{V}}\sum_{t\in\mathcal{T}} C^M_v v_{vt} + E_\xi[Q(y,\xi)]$$

$$\begin{aligned}
& y_{vt} - y_{v(t-1)} \le v_{vt}, && v\in\mathcal{V}, t\in\mathcal{T}\setminus\{1\},\\
& y_{v1} - y_{|\mathcal{T}|} \le v_{vt}, && v\in\mathcal{V},\\
& \sum_{\tau=t}^{t+\underline{T}^L-1} y_\tau \ge \underline{T}^L v_t, && v\in\mathcal{V}, t\in\mathcal{T} : t \le |\mathcal{T}| - \underline{T}^L + 1,\\
& \sum_{\tau=t}^{|\mathcal{T}|} y_\tau + \sum_{\tau=1}^{t+\underline{T}^L-|\mathcal{T}|-1} y_\tau \ge \underline{T}^L v_t, && v\in\mathcal{V}, t\in\mathcal{T} : t \ge |\mathcal{T}| - \underline{T}^L,\\
& y_{vt} \in \{0,1\}, && v\in\mathcal{V}, t\in\mathcal{T},\\
& v_{vt} \in \{0,1\}, && v\in\mathcal{V}, t\in\mathcal{T}.
\end{aligned}$$

First stage model

Expected total downtime cost

$$\min \sum_{v\in\mathcal{V}}\sum_{t\in\mathcal{T}} C^P_{vt} y_{vt} + \sum_{v\in\mathcal{V}}\sum_{t\in\mathcal{T}} C^M_v v_{vt} + E_\xi[Q(y,\xi)]$$

$$\begin{aligned}
& y_{vt} - y_{v(t-1)} \le v_{vt}, && v\in\mathcal{V}, t\in\mathcal{T}\setminus\{1\},\\
& y_{v1} - y_{|\mathcal{T}|} \le v_{vt}, && v\in\mathcal{V},\\
& \sum_{\tau=t}^{t+\underline{T}^L-1} y_\tau \ge \underline{T}^L v_t, && v\in\mathcal{V}, t\in\mathcal{T} : t \le |\mathcal{T}| - \underline{T}^L + 1,\\
& \sum_{\tau=t}^{|\mathcal{T}|} y_\tau + \sum_{\tau=1}^{t+\underline{T}^L-|\mathcal{T}|-1} y_\tau \ge \underline{T}^L v_t, && v\in\mathcal{V}, t\in\mathcal{T} : t \ge |\mathcal{T}| - \underline{T}^L,\\
& y_{vt} \in \{0,1\}, && v\in\mathcal{V}, t\in\mathcal{T},\\
& v_{vt} \in \{0,1\}, && v\in\mathcal{V}, t\in\mathcal{T}.
\end{aligned}$$

First stage model

$$\min \sum_{v\in\mathcal{V}}\sum_{t\in\mathcal{T}} C^P_{vt} y_{vt} + \sum_{v\in\mathcal{V}}\sum_{t\in\mathcal{T}} C^M_v v_{vt} + E_\xi[Q(y,\xi)]$$

Must mobilize vessel to have it available

$$\begin{aligned}
& && v\in\mathcal{V}, t\in\mathcal{T}\setminus\{1\},\\
& && v\in\mathcal{V},\\
& \sum_{\tau=t}^{t+\underline{T}^L-1} y_\tau \ge \underline{T}^L v_t, && v\in\mathcal{V}, t\in\mathcal{T} : t \le |\mathcal{T}| - \underline{T}^L + 1,\\
& \sum_{\tau=t}^{|\mathcal{T}|} y_\tau + \sum_{\tau=1}^{t+\underline{T}^L-|\mathcal{T}|-1} y_\tau \ge \underline{T}^L v_t, && v\in\mathcal{V}, t\in\mathcal{T} : t \ge |\mathcal{T}| - \underline{T}^L,\\
& y_{vt} \in \{0,1\}, && v\in\mathcal{V}, t\in\mathcal{T},\\
& v_{vt} \in \{0,1\}, && v\in\mathcal{V}, t\in\mathcal{T}.
\end{aligned}$$

First stage model

$$\min \sum_{v\in\mathcal{V}}\sum_{t\in\mathcal{T}} C^P_{vt} y_{vt} + \sum_{v\in\mathcal{V}}\sum_{t\in\mathcal{T}} C^M_v v_{vt} + E_\xi[Q(y,\xi)]$$

Must keep vessel for a minimum number of days, if mobilised

$$\begin{aligned}
& y_{vt} - y_{v(t-1)} \le v_{vt}, && v\in\mathcal{V}, t\in\mathcal{T}\setminus\{1\},\\
& y_{v1} - y_{|\mathcal{T}|} \le v_{vt}, && v\in\mathcal{V},\\
& && v\in\mathcal{V}, t\in\mathcal{T} : t \le |\mathcal{T}| - \underline{T}^L + 1,\\
& \sum_{\tau=t}^{|\mathcal{T}|} y_\tau + \sum_{\tau=1} y_\tau \ge \underline{T}^L v_t, && v\in\mathcal{V}, t\in\mathcal{T} : t \ge |\mathcal{T}| - \underline{T}^L,\\
& y_{vt} \in \{0,1\}, && v\in\mathcal{V}, t\in\mathcal{T},\\
& v_{vt} \in \{0,1\}, && v\in\mathcal{V}, t\in\mathcal{T}.
\end{aligned}$$

Second stage model

$$Q(y^*,\xi) = \min \sum_{v\in\mathcal{V}}\sum_{c\in\mathcal{C}}\sum_{f\in\mathcal{F}_c(\xi)}\sum_{t_2\in\mathcal{T}} C^D_{vct(f)t_2}(\xi) x_{vft_2} + \sum_{c\in\mathcal{C}}\sum_{f\in\mathcal{F}_c(\xi)} C^P z_f,$$

$$\begin{aligned}
& \sum_{c\in\mathcal{C}}\sum_{f\in\mathcal{F}_c(\xi)}\sum_{t\in\mathcal{T}} A_{vct\tau}(\xi) x_{vft} \le y^*_{v\tau}, && v\in\mathcal{V}, \tau\in\mathcal{T},\\
& \sum_{v\in\mathcal{V}}\sum_{t\in\mathcal{T}} x_{vft} + z_f = 1, && c\in\mathcal{C}, f\in\mathcal{F}_c,\\
& x_{vft} \in \{0,1\}, && v\in\mathcal{V}, f\in\mathcal{F}, t\in\mathcal{T},,\\
& z_f \in \{0,1\}, && f\in\mathcal{F},.
\end{aligned}$$

Second stage model

Downtime cost of fixing a failure on a given day

$$Q(y^*,\xi) = \min \sum_{v\in\mathcal{V}}\sum_{c\in\mathcal{C}}\sum_{f\in\mathcal{F}_c(\xi)}\sum_{t_2\in\mathcal{T}} C^D_{vct(f)t_2}(\xi) x_{vft_2} + \sum_{c\in\mathcal{C}}\sum_{f\in\mathcal{F}_c(\xi)} C^P z_f,$$

$$\begin{aligned}
& \sum_{c\in\mathcal{C}}\sum_{f\in\mathcal{F}_c(\xi)}\sum_{t\in\mathcal{T}} A_{vct\tau}(\xi) x_{vft} \le y^*_{v\tau}, && v\in\mathcal{V}, \tau\in\mathcal{T},\\
& \sum_{v\in\mathcal{V}}\sum_{t\in\mathcal{T}} x_{vft} + z_f = 1, && c\in\mathcal{C}, f\in\mathcal{F}_c,\\
& x_{vft} \in \{0,1\}, && v\in\mathcal{V}, f\in\mathcal{F}, t\in\mathcal{T},,\\
& z_f \in \{0,1\}, && f\in\mathcal{F},.
\end{aligned}$$

Second stage model

Penalty cost applied if a failure is not fixed

$$Q(y^*,\xi) = \min \sum_{v\in\mathcal{V}}\sum_{c\in\mathcal{C}}\sum_{f\in\mathcal{F}_c(\xi)}\sum_{t_2\in\mathcal{T}} C^D_{vct(f)t_2}(\xi)x_{vft_2} + \sum_{c\in\mathcal{C}}\sum_{f\in\mathcal{F}_c(\xi)} C^P z_f,$$

$$\sum_{c\in\mathcal{C}}\sum_{f\in\mathcal{F}_c(\xi)}\sum_{t\in\mathcal{T}} A_{vct\tau}(\xi)x_{vft} \le y^*_{v\tau}, \qquad v\in\mathcal{V}, \tau\in\mathcal{T},$$

$$\sum_{v\in\mathcal{V}}\sum_{t\in\mathcal{T}} x_{vft} + z_f = 1, \qquad c\in\mathcal{C}, f\in\mathcal{F}_c,$$

$$x_{vft}\in\{0,1\}, \qquad v\in\mathcal{V}, f\in\mathcal{F}, t\in\mathcal{T},,$$

$$z_f\in\{0,1\}, \qquad f\in\mathcal{F},.$$

Second stage model

$$Q(y^*,\xi) = \min \sum_{v\in\mathcal{V}}\sum_{c\in\mathcal{C}}\sum_{f\in\mathcal{F}_c(\xi)}\sum_{t_2\in\mathcal{T}} C^D_{vct(f)t_2}(\xi)x_{vft_2} + \sum_{c\in\mathcal{C}}\sum_{f\in\mathcal{F}_c(\xi)} C^P z_f,$$

Faliures can only be fixed in time periods the vessel is chartered. Repair time is weather dependent

$$\sum_{c\in\mathcal{C}}\sum_{f\in\mathcal{F}_c(\xi)}\sum_{t\in\mathcal{T}} A_{vct\tau}(\xi)x_{vft} \le y^*_{v\tau}, \qquad v\in\mathcal{V}, \tau\in\mathcal{T},$$

$$\sum_{v\in\mathcal{V}}\sum_{t\in\mathcal{T}} x_{vft} + z_f = 1, \qquad c\in\mathcal{C}, f\in\mathcal{F}_c,$$

$$x_{vft}\in\{0,1\}, \qquad v\in\mathcal{V}, f\in\mathcal{F}, t\in\mathcal{T},,$$

$$z_f\in\{0,1\}, \qquad f\in\mathcal{F},.$$

Second stage model

$$Q(y^*,\xi) = \min \sum_{v\in\mathcal{V}}\sum_{c\in\mathcal{C}}\sum_{f\in\mathcal{F}_c(\xi)}\sum_{t_2\in\mathcal{T}} C^D_{vct(f)t_2}(\xi)x_{vft_2} + \sum_{c\in\mathcal{C}}\sum_{f\in\mathcal{F}_c(\xi)} C^P z_f,$$

All failures must be fixed, otherwise a penalty is added

$$\sum_{c\in\mathcal{C}}\sum_{f\in\mathcal{F}_c(\xi)}\sum_{t\in\mathcal{T}} A_{vct\tau}(\xi)x_{vft} \le y^*_{v\tau}, \qquad v\in\mathcal{V}, \tau\in\mathcal{T},$$

$$\sum_{v\in\mathcal{V}}\sum_{t\in\mathcal{T}} x_{vft} + z_f = 1, \qquad c\in\mathcal{C}, f\in\mathcal{F}_c,$$

$$x_{vft}\in\{0,1\}, \qquad v\in\mathcal{V}, f\in\mathcal{F}, t\in\mathcal{T},,$$

$$z_f\in\{0,1\}, \qquad f\in\mathcal{F},.$$

Solution method

- The two-stage stochastic programming model is solved using scenario generation and then solving the deterministic equivalent
- Each scenario represents one realisation of one year

Scenario

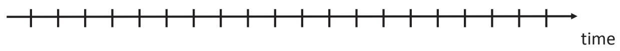

Scenario

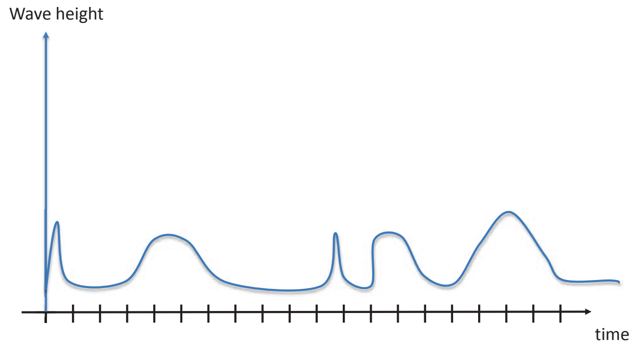

Scenario

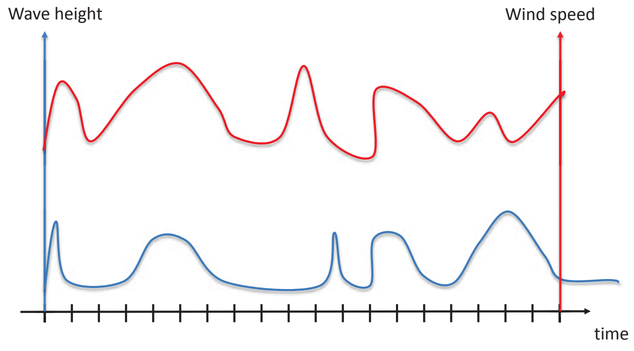

Scenario

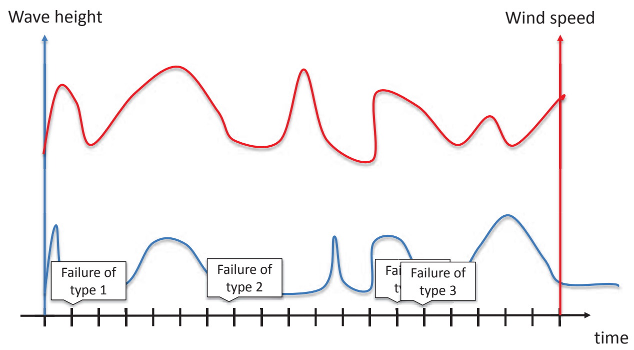

Scenarios

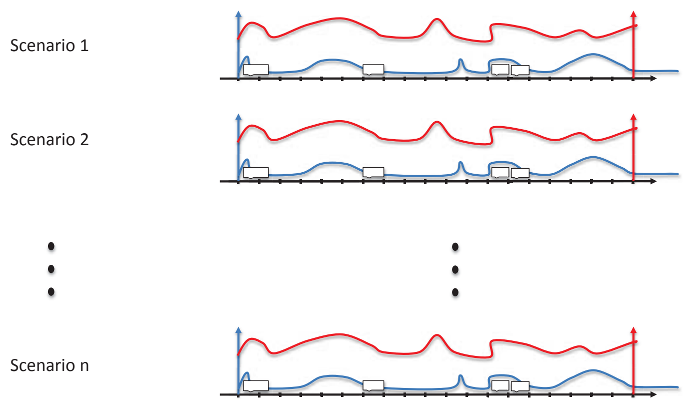

Scenarios

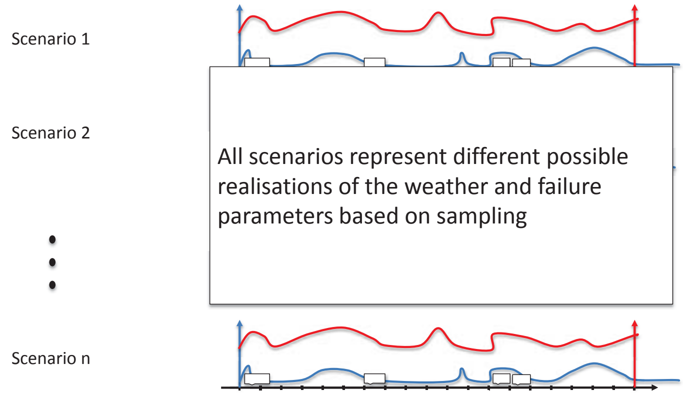

Scenarios

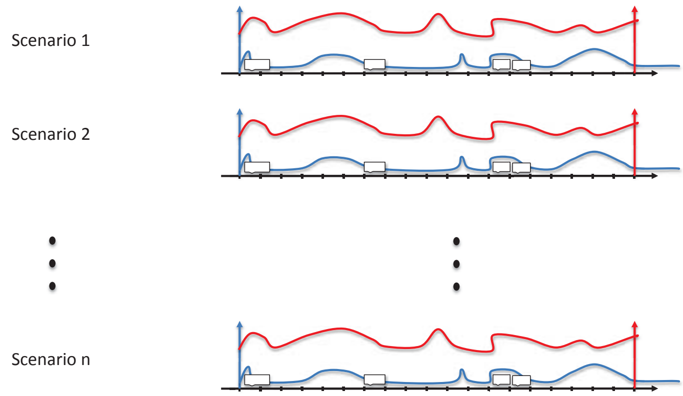

First stage decisions – must be the same in all scenarios

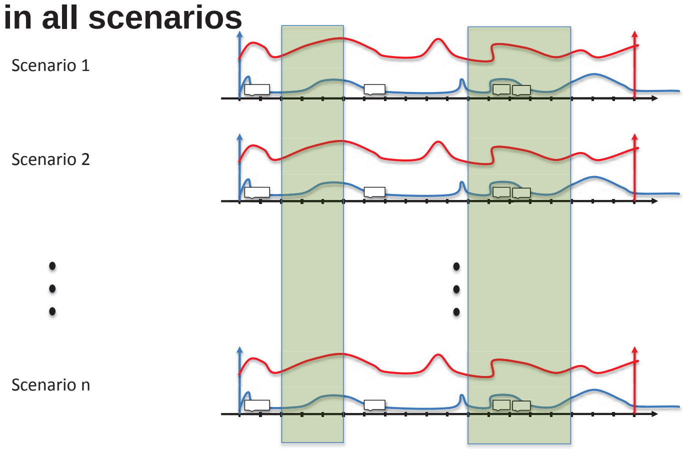

First stage decisions – must be the same in all scenarios

Scenario 1

Scenario 2

•
•
•

Scenario n

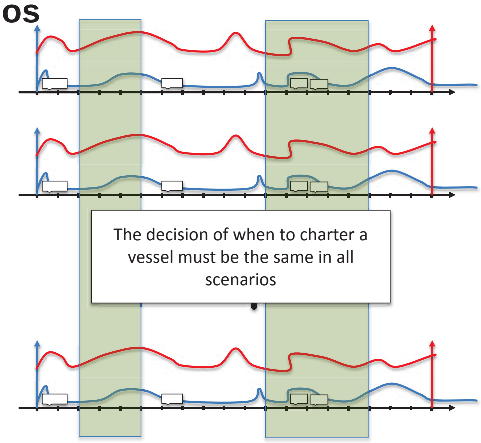

Second stage decisions – different for each scenario

Scenario 1

Scenario 2

•
•
•

Scenario n

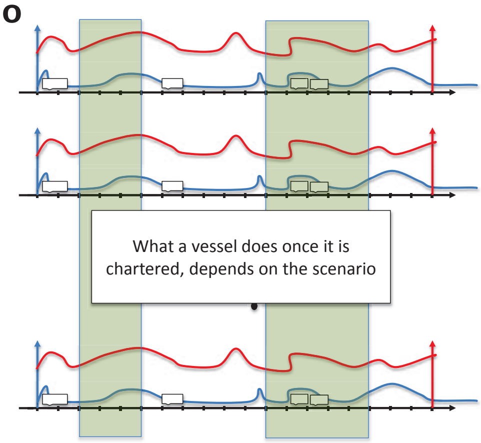

Second stage decision – when to fix a given failure

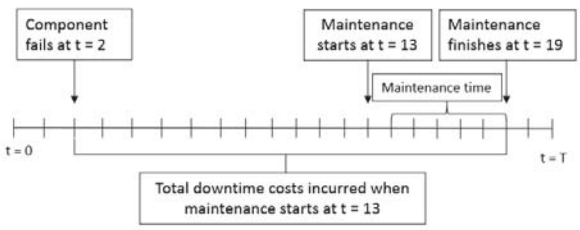

Second stage decision – when to fix a given failure

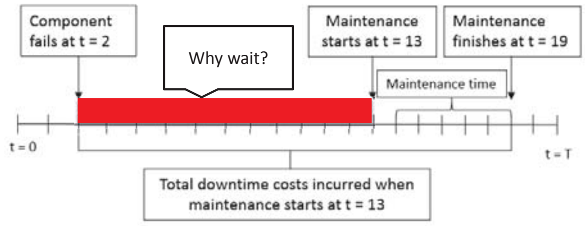

Second stage decision – when to fix a given failure

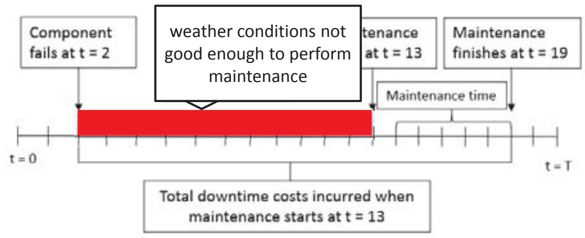

Second stage decision – when to fix a given failure

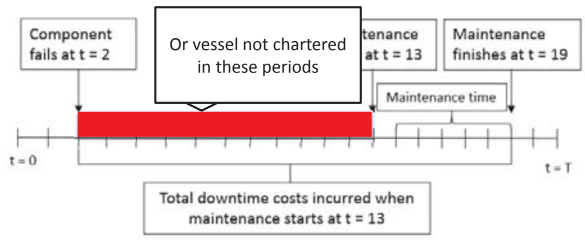

Downtime costs – depends on wind speed

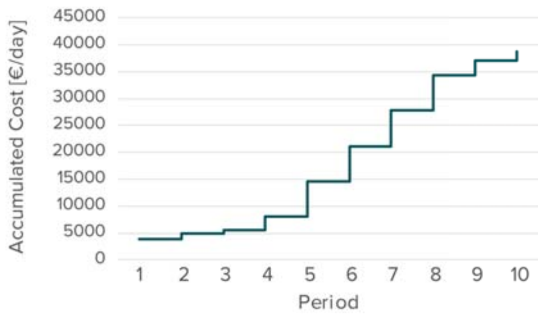

NTNU
Norwegian University of Science and Technology

Optimizing Jack-Up Vessel Chartering Strategies for Offshore Wind Farms

Andreas Jebsen Mikkelsen
Odin Kirkeby
Marielle Christiansen
Magnus Stålhane

Preliminary Results

- The model is able to solve one-year problems with 100 scenarios
- Weather conditions at site and vessel capabilities greatly affect results
- Anything from 50 to 200 days of charter for a 80-100 turbine wind farm

NTNU
Norwegian University of Science and Technology

Optimizing Jack-Up Vessel Chartering Strategies for Offshore Wind Farms

Andreas Jebsen Mikkelsen
Odin Kirkeby
Marielle Christiansen
Magnus Stålhane

Future reasearch

- Ensure realistic data
  - Huge differences in values used in different research
- Verify model results in a cost of energy simulation model
- Compare strategy with batch-repair strategy
- Add possibility of sub-leasing

NTNU
Norwegian University of Science and Technology

Optimizing Jack-Up Vessel Chartering Strategies for Offshore Wind Farms

Andreas Jebsen Mikkelsen
Odin Kirkeby
Marielle Christiansen
Magnus Stålhane

NTNU
Norwegian University of Science and Technology

Optimizing Jack-Up Vessel Chartering Strategies for Offshore Wind Farms

Andreas Jebsen Mikkelsen
Odin Kirkeby
Marielle Christiansen
Magnus Stålhane

Short-Term Decision Optimisation for Offshore Wind Farm Maintenance

Clym Stock-Williams
Bhargav Ravindranath
Ashish Dewan

DeepWind, Trondheim
19 January 2017

www.ecn.nl

ECN IO&M Team Activities

We are building the world's most powerful strategic simulation tools for offshore wind farms

Contents

- Overview of ECN's activities
- The Offshore Wind Farm Manager's challenge
- How does ECN Despatch^{TM} help the Farm Manager make better decisions?
- Example results
- How to get involved

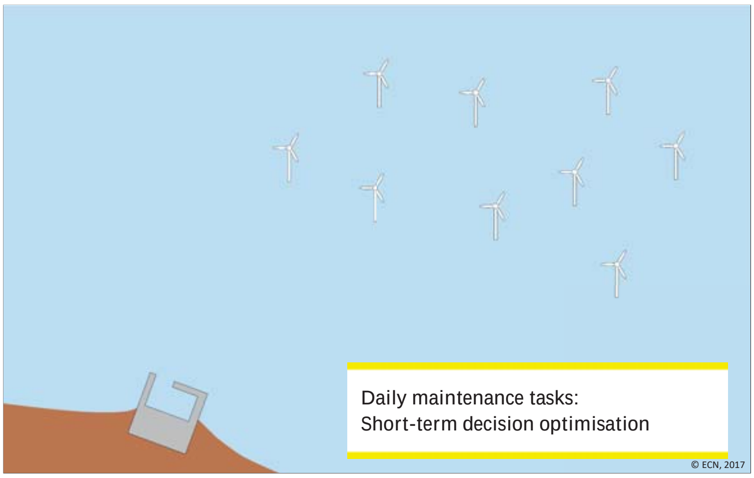

Daily maintenance tasks:
Short-term decision optimisation

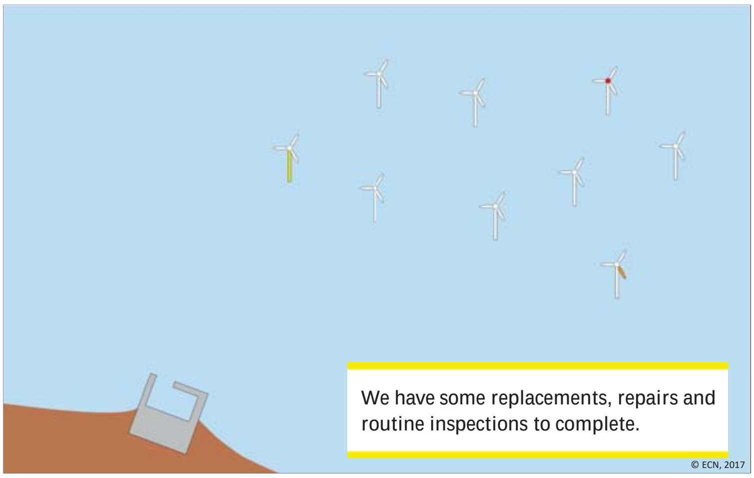

We have some replacements, repairs and routine inspections to complete.

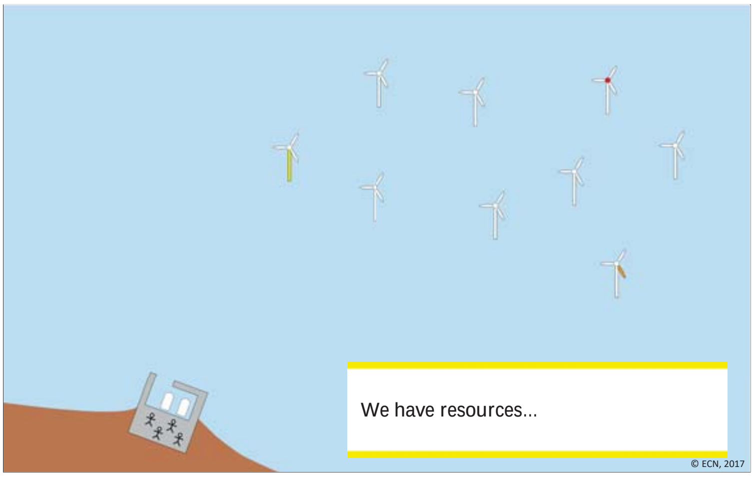

Input and Output Summary

- List of service orders
- Vessel availability
- Technician availability
- Spares availability
- Weather forecast (winds + waves)

- Service order definition:
  - Vessel, technician and spares requirements
  - Time requirements*
- Turbine and port locations
- Operational weather limits
- Vessel speed and capacity

- Objective for optimisation:
  - Minimum downtime
  - Minimum cost?
  - Maximum utilisation?
  - Maximum energy output**
  - Maximum income***

Time:	7	9	11	13	15	17
Service Order 1						
Service Order 4						
Service Order 5						
Service Order 2						

* We have obtained this from historical data.
** Need turbine power curve to estimate.
*** Need energy prices and fixed/variable costs.

Main Challenges To Solve

1. Prioritise the Service Orders.
2. Create feasible vessel and technician schedules.
3. Run quickly.
4. Use resources wisely: do less or more, earlier or later.
5. Consider weather forecast and task uncertainties.

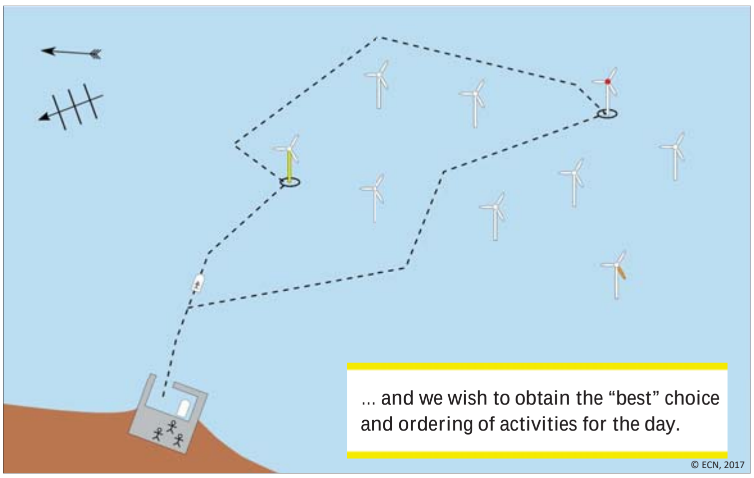

The Optimiser

- Exhaustive Search is clearly not a realistic option:
  - 5 Service Orders: 120 solutions
  - 10 Service Orders: 3,628,800 solutions
  - 15 Service Orders: 1,307,674,368,000 possible solutions
- Genetic Algorithm
  1. Permutation representation for Service Orders: “Travelling Salesman Problem”
     - Mutation rate: 15%
     - Population size: 100
     - Converges for 20 cities in 3000-3500 evaluations

  - Intra-day scheduling takes Service Order priority and works out the time-domain solution.

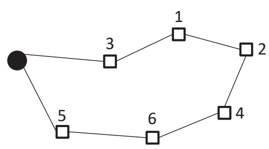

Main Challenges To Solve

1. Prioritise the Service Orders.
2. Create feasible vessel and technician schedules.
3. Run quickly.
4. Use resources wisely: do less or more, earlier or later.
5. Consider weather forecast and task uncertainties.

The ECN Despatch™ Concept

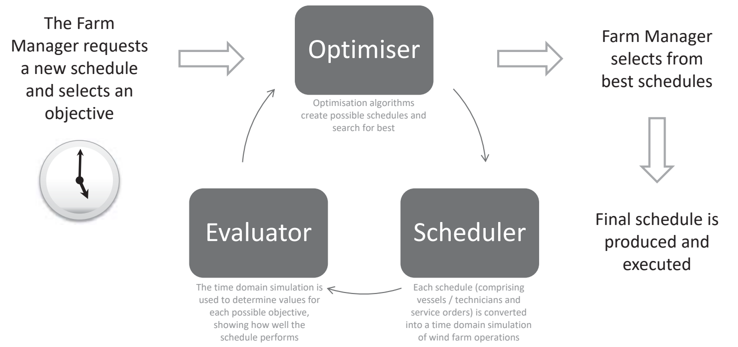

"Travelling Merchant Problem"

- Instead of just "visiting" each city, why not use limited time available to spend time selling?!

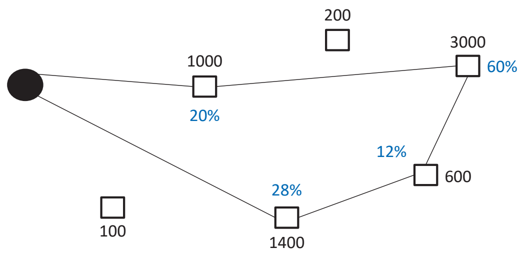

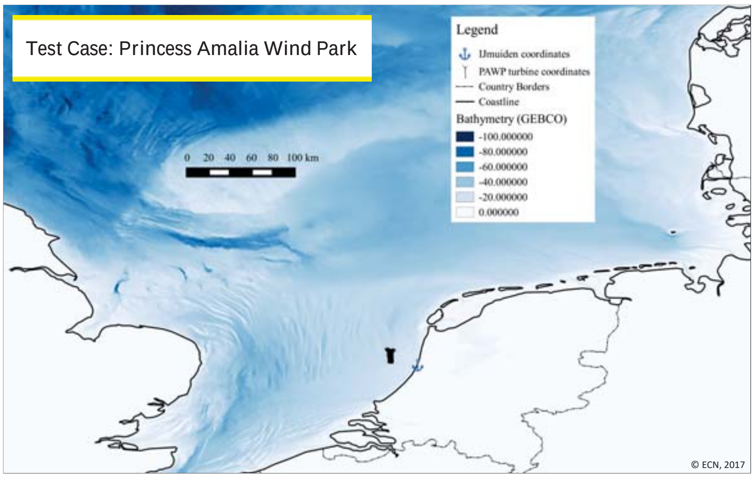

Removing End Effects

- The Evaluator and Scheduler are also used to assign a value to tasks not performed.

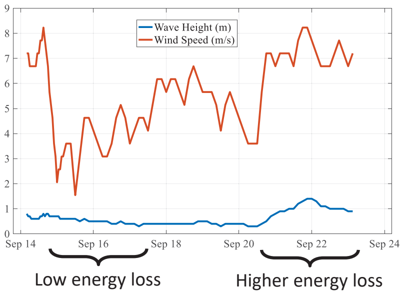

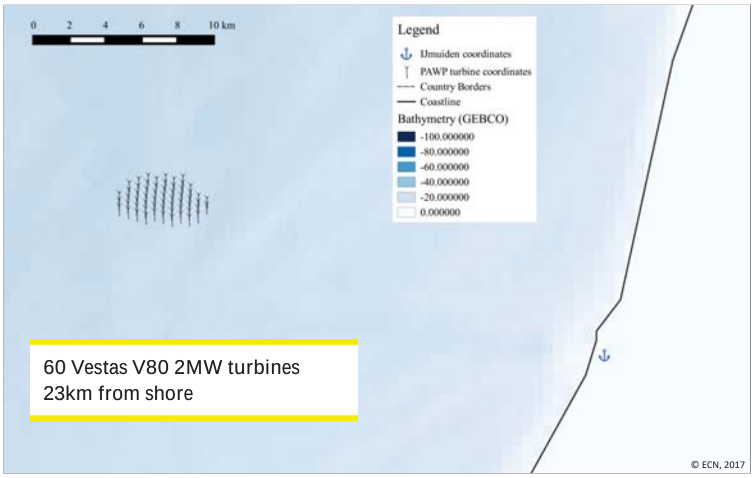

Example Prioritisation: Inputs

- 9 open orders:

WTG #	Type	Man Hours Required	Technicians Used
9	Run	8.5	2
10	Stop	14	2
13	Run	0.5	2
13	Run	1	1
14	Stop	4.5	2
14	Stop	8.25	2
24	Run	19.74	3
34	Run	1	1
44	Run	1.5	2

Example Prioritisation: Inputs

- Weather forecast:

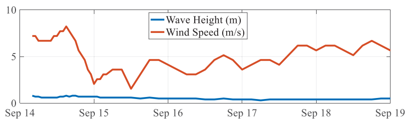

- Transit / transfer limit: 2.5m Hs
- Technicians Available: 12
- Shift times: 06:30 – 17:30

Example Prioritisation: Output 1

- Fixed at 12 technicians available, no future valuation.

WTG #	Type	Man Hours Required	Technicians Used	Day 1 Completion %
9	Run	8.5	**2**	**100**
10	Stop	14	**1**	**50**
13	Run	0.5	**1**	**100**
13	Run	1	**1**	**100**
14	Stop	4.5	**2**	**100**
14	Stop	8.25	**2**	**79**
24	Run	19.74	**1**	**25**
34	Run	1	**1**	**100**
44	Run	1.5	**1**	**100**

69.8MWh lost

Example Prioritisation: Output 2

- Fixed at 12 technicians available, **including future valuation**.

WTG #	Type	Man Hours Required	Technicians Used	Day 1 Completion %
9	Run	8.5	**2**	**100**
10	Stop	14	**1**	**50**
13	Run	0.5	**1**	**100**
13	Run	1	**1**	**100**
14	Stop	4.5	**2**	**100**
14	Stop	8.25	**2**	**79**
24	Run	19.74	**1**	**30**
34	Run	1	**1**	**100**
44	Run	1.5	**1**	**100**

71.7MWh lost

Example Prioritisation: Output 3

- Fixed at 12 technicians available, **both days scheduled**.

WTG #	Type	Man Hours Required	Technicians Used	Day 1 Completion %
9	Run	8.5	**2**	**100**
10	Stop	14	**1**	**50**
13	Run	0.5	**1**	**100**
13	Run	1	**1**	**100**
14	Stop	4.5	**2**	**100**
14	Stop	8.25	**2**	**79**
24	Run	19.74	**1**	**25**
34	Run	1	**1**	**100**
44	Run	1.5	**1**	**100**

71.0MWh lost

Example Prioritisation: Output 4

- Fixed at 7 technicians available, **both days scheduled**.

WTG #	Type	Man Hours Required	Technicians Used	Day 1 Completion %
9	Run	8.5	**0**	**0**
10	Stop	14	**1**	**54**
13	Run	0.5	**1**	**100**
13	Run	1	**1**	**75**
14	Stop	4.5	**1**	**100**
14	Stop	8.25	**1**	**79**
24	Run	19.74	**0**	**0**
34	Run	1	**1**	**100**
44	Run	1.5	**1**	**100**

55.1MWh lost

ECN

Interested in Getting Involved?

- ECN is developing a powerful capability for daily offshore wind farm decision making.
- Paper to be submitted mid-2017, **including valuation methodology**.
- Does your company operate a wind farm?
  - We are looking for new partners to input into the design.
  - Conduct an “offline” study to apply ECN Despatch™ to historic wind farm operations and build a business case for implementation.
  - Implement into an operational wind farm.

Acknowledgement: All work so far funded by TKI through the Daisy4Offshore project

ECN

Example Prioritisation: Reality

- What they actually did...

WTG #	Type	Man Hours Required	Technicians Used	Day 1 Completion %
9	Run	8.5	**0**	**0**
10	Stop	14	**0**	**0**
13	Run	0.5	**0**	**0**
13	Run	1	**0**	**0**
14	Stop	4.5	**2**	**100**
14	Stop	8.25	**0**	**0**
24	Run	19.74	**0**	**0**
34	Run	1	**0**	**0**
44	Run	1.5	**0**	**0**

45.5MWh lost

ECN

The Optimiser (2)

- Move to a new representation:
  - For each vessel, for each day, a Service Order is assigned a real number.
  - Service Orders < 0 are not done.
  - Service Orders > 0 are assigned a *proportion* of the available technicians.

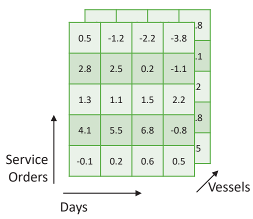

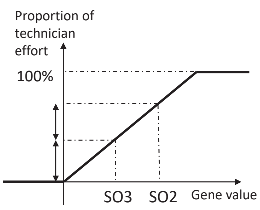

IMPROVED SHORT-TERM DECISION MAKING FOR OFFSHORE WIND FARM VESSEL ROUTING

Rafael Dawid

University of Strathclyde
Rafael.dawid@strath.ac.uk

Outer problem – heuristic method

- Cluster matching algorithm
- Procedure:
  - Generate all possible clusters with up to 4 turbines per vessel
  - Calculate value (and feasibility) of each cluster
    - Rank each cluster by value (or value per technician used, or a combination of those)
  - Pick best cluster
  - Pick next best that meets constraints
  - Repeat the above as many times as there is time for

Introduction

- On the day planning maintenance actions at an offshore wind farm:
  - Which vessels to use?
  - Which turbines to visit?
  - In what order should repairs be carried out?
- Vessel routing is still planned without the use of decision support tools
- Low accessibility during winter
- High uncertainties (failure diagnosis, repair duration, human error, transfer onto turbine not always possible)

Inner problem: logic flowcharts

- Computationally effective & accurate
- Objective: minimise time taken by a policy & no. of technician used
- More advanced solution may be required if more than 5 turbines can be visited by one vessel
- Example: logic for 1 vessel, 2 turbines (both "lengthy" repairs)

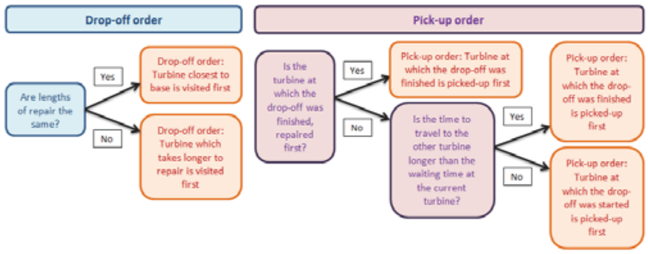

Methodology

- Inner and outer problem approach
- Heuristic method: Cluster matching algorithm
- Value = Rewards – costs
- Simulation running time: user dependent

What is not modelled

- Different grades of technicians
- Vessel stays with turbine during repair

What is modelled

- Multiple O&M bases
- Constraints:
  - Time
  - Number of technicians available
  - Vessel capacity (technicians and load)
- Variable vessel speed (slower when at farm)
- One day planning horizon only
- Up to 4 turbines per vessel
- One crew can visit maximum of 2 turbines per day
- Costs: fuel, vessel hire, repair cost
- Probabilities

Model inputs

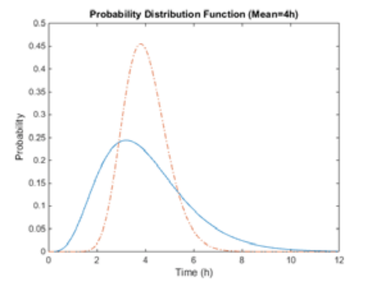

1	0.8	0.5	
1	0.8	0.5	
1	1	0.75	0
1	1	0.75	0

Repairs	Time required (h)	Technicians required
Manual reset	2	2
Minor repair	4	3
Medium repair	6	3
Annual service	6	2

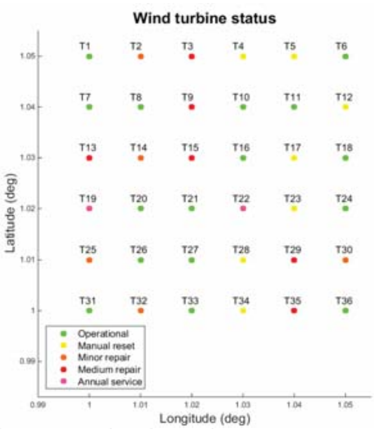

Output: Vessel dispatch strategy

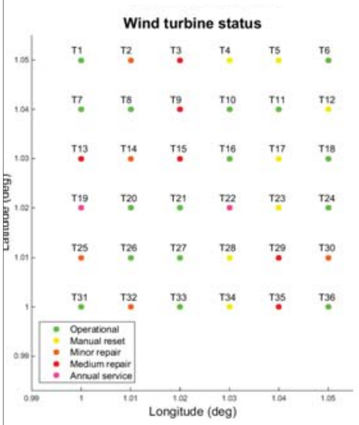


```
OPTIMAL POLICY:
Dispatch vessel 1 to:
Wind turbine T29    (Medium repair)
Wind turbine T30    (Minor repair)
Wind turbine T34    (Manual reset)
Gantt Chart is located in Sheet 6.
Probability of successfully carrying out this policy is 1.9177%
Vessel 1 order:
    'T29'    'T30'    'T34'    'T34'    'T30'    'T29'
Dispatch vessel 2 to:
Wind turbine T14    (Minor repair)
Wind turbine T15    (Medium repair)
Gantt Chart is located in Sheet 3.
Probability of successfully carrying out this policy is 5.9895%
Vessel 2 order:
    'T15'    'T14'    'T14'    'T15'
Dispatch vessel 3 to:
Wind turbine T19    (Annual service)
Wind turbine T22    (Annual service)
Wind turbine T25    (Minor repair)
Wind turbine T28    (Manual reset)
Gantt Chart is located in Sheet 10.
Probability of successfully carrying out this policy is 11.0523%
Vessel 3 order:
    'T22'    'T19'    'T25'    'T28'    'T28'    'T22'    'T19'    'T25'
Dispatch vessel 4 to:
Wind turbine T2    (Minor repair)
Wind turbine T3    (Medium repair)
Wind turbine T4    (Manual reset)
Wind turbine T5    (Manual reset)
Gantt Chart is located in Sheet 8.
Probability of successfully carrying out this policy is 3.3079%
Vessel 4 order:
    'T5'    'T3'    'T2'    'T5'    'T4'    'T2'    'T4'    'T3'
```

Probability

- Probability of successfully carrying out a policy is calculated. Factors considered (user inputs):
  - Probability of successful transfer from a given vessel onto turbine
  - Probability of each individual repair not taking longer than the expected duration + slack time
  - Probability of correct diagnosis
- Should a value be placed on this probability to influence the process of selecting the optimal decision?

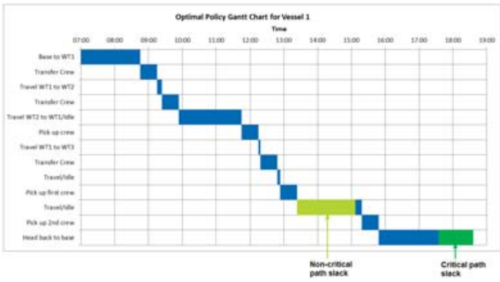

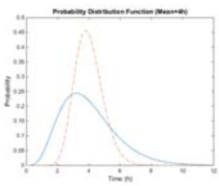

Output: Gantt chart

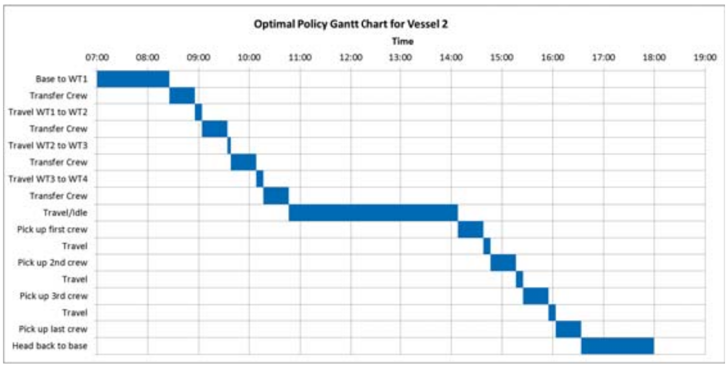

Summary

Conclusions

Other models in academia solve the theoretical rather than the practical problem

Assumptions & inputs verified by offshore O&M operator

User-friendly outputs

Computational time can be changed depending on the desired accuracy

“Repair probability” variable can be used to discourage policies which are highly unlikely to be successful

Future Work

Assess the importance of getting the estimated time of repair right

Does encouraging low-risk policies work?

More in-depth real life case studies

Practical application/commercialisation

Output: Value function

- In some instances, only a handful of policies can visit the maximum number of turbines

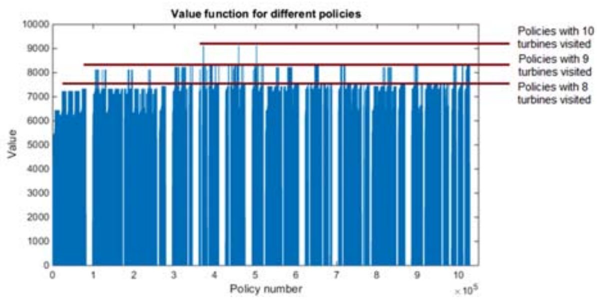

Questions?

Contact:
Rafael Dawid

Wind & Marine Energy Systems CDT

Floor 4 | Technology & Innovation Centre
99 George Street | Glasgow | G1 1RD

Office: +44 (0) 0141 444 7227
Mobile: +44 (0)74 1137 4431
Email: rafael.dawid@strath.ac.uk

University of Strathclyde Engineering

D2) Operations & maintenance

Experience from RCM and RDS-PP coding for offshore wind farms, R.Sundal, Maintech

Enhance decision support tools through an improved reliability model,
S. Faulstich, Fraunhofer IWES

Technology for a real-time simulation-based system monitoring of wind turbines,
D. Zwick, Fedem Technology/SAP SE

Experience from RCM and RDS-PP coding for offshore wind farms

EERA DeepWind 2017,
Trondheim 19th of January 2017

roger.sundal@maintech.no

MainTech

MainTech

Man
forty-seven
most uneven age ever

Roger Sundal

MainTech

52 655 Tags

609 Tags for each turbine

88 turbine

7531 transmissions Tags

RDS-PP on turbines

IEC 61346 on transmission assets

MainTech

Reelle løsninger på reelle problem. Alltid.

www.maintech.no
#maintechkonferansen

MainTech

Reliability-Centered Maintenance

MainTech

An analytical process used to determine appropriate **failure management** strategies to ensure safe and cost-effective operations of a physical asset in a specific operating environment.

MainTech

Distribution of tasks on task types

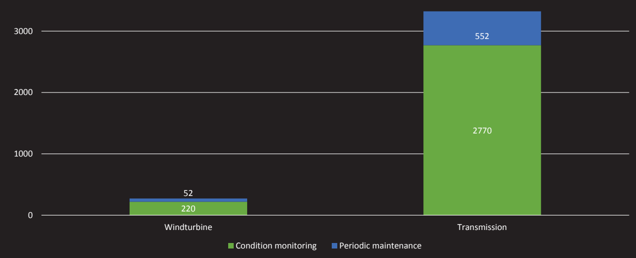

MainTech

Failure management can be to create preventive maintenance tasks, or to run the asset to failure

MainTech

Failure management decision

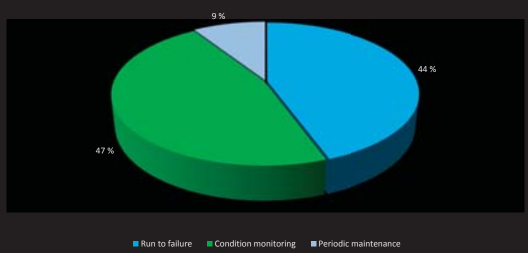

MainTech

The main goal of RCM is to avoid or reduce failure CONSEQUENCES - Not necessarily to avoid failures

IEC 60300-3-11	Application guide Reliability-Centered maintenance
SAE JA 1011	Evaluation criteria for Reliability-Centered Maintenance processes

MainTech

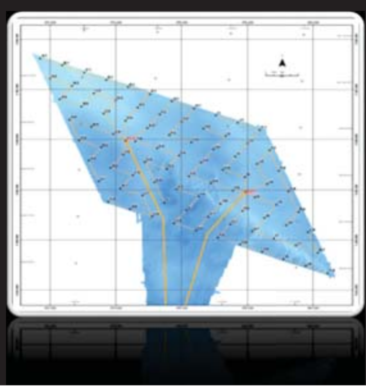

88 similar turbines

MainTech

Logistics are different offshore

Thank you for your attention!

roger.sundal@maintech.no
www.maintech.no
#maintechkonferansen

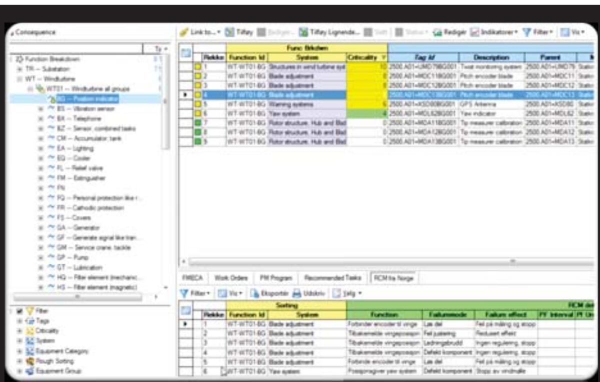

Benefit from others work – apply a standard

RDS-PP – find your level

Remember: Failures you want to register on a low level, preventive work on a higher level

ENHANCE DECISION SUPPORT TOOLS THROUGH AN IMPROVED RELIABILITY MODEL

Dipl.-Ing. M.Sc. Stefan Faulstich,
Volker Berkhout, Jochen Mayer, David Siebenlist
Fraunhofer Institute for Wind Energy and Energy System Technology (IWES)

ENHANCE DECISION SUPPORT TOOLS THROUGH AN IMPROVED RELIABILITY MODEL

Contents

- Fraunhofer IWES
- Decision support tools
- Reliability model
  - Requirements
  - Approach
- Failure categories
- Parameter estimation
- Simulation results
- Conclusion and Outlook

Fraunhofer IWES

Introduction
Fraunhofer Institute for Wind Energy and Energy System Technology

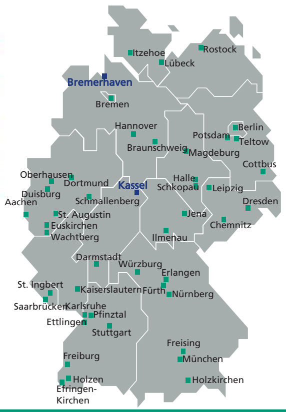

- Personal: approx. 310
- Annual budget: approx. 20 Mio EUR
- Director: Prof. Dr. Clemens Hoffmann

www.energiesystemtechnik.iwes.fraunhofer.de

Fraunhofer IWES

Introduction
Research group „Reliability & Maintenance strategies"

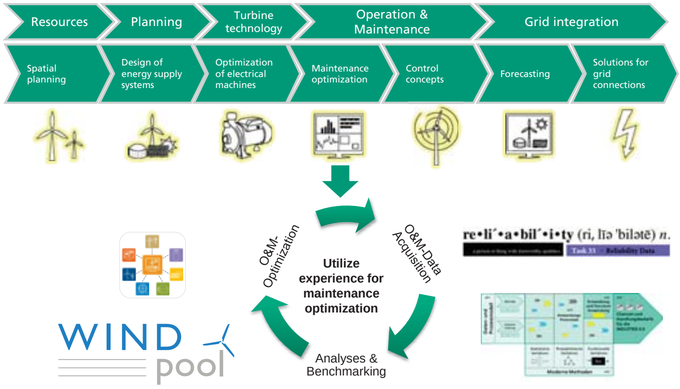

Fraunhofer IWES

Decision support tools
Variety of tools

Table 1: Overview of models reviewed

	Name	Organisation	Year	Project Phase: Construction	Project Phase: Operation	Aspects Considered: Turbine	Support Structure	Electrical Infrastructure	Transport/ Installation	Weather/ Wind/Waves	Wake	Maintenance Strategy	Failures	Total Project Perspective	Features: Uncertainty	Offshore	Commercial	Simulation/ Optimization	Software	Time Horizon	Model Output	Source
Total Project Cost	Rambølls tool	Rambøll	2003	x	x	x	x	x	x	x		x		x	yes	yes	(yes)	Sim	Excel, RiskSim	Life cycle	Net present value	[14, 15]
	IEA recommendation	IEA	1994	x	x	x	x	x				x		x	yes	no	no	Sim	Excel	Life cycle	Levelized production cost	[16]
	Extend simulation of DNV	DNV	2010		x	x		x	x	x	x	x	x	x	yes	yes	(yes)	Sim	Extend	Life cycle	Net present value and others	[17] and direct contact
	Fingersh et al.	NREL	2006	x	x	x	x	x						x	no	yes	no	Sim	Excel	long term	Cost of energy	[18]
	OFWIC	George Washington University	2010	x	x	x	x	x	x	x	x			x	yes	yes	no	Sim/ Opt	Excel, Palisade, Frontline	Life cycle	Cost of energy	[19, 20]
Operation and Maintenance	RECOFF-model	ECN	2004		x	x			x	x		x	x		yes	yes	no	Sim	Excel, @Risk	long term	Costs	[21]
	ECN O&M Tool	ECN	2007		x	x			x	x		x	x		yes	yes	yes	Sim	Excel, @Risk	long term	Costs	[22]
	OMCE	ECN	2009		x	x			x	x		x	x		?	yes	no	Sim	(MatLab)	long term	Costs	[23]
	CONTO FAX	TU Delft	1997		x	x			x	x		x	x		yes	yes	no	Sim	Excel	long term	Costs, availability, energy produced	[24, 25]
	O2M	Garrad Hassan	2007		x	x			x	x		x	x		no	yes	(yes)	Sim/ Opt	not specified	long term	Costs, lost production	[26]
	MWCOST	BMT	2009	x	x	x	x		x	x		x	x		yes	yes	(yes)	Sim	not specified	long term	Net present value	[27, 28]
	Maros	DNV	2010		x	x		x	x	x		x	x		yes	(yes)	yes	Sim	Own development	long term	Net present value	[29]

Source: Hofmann. 2011 [1]

Fraunhofer IWES

Decision support tools
@Fraunhofer IWES

- MAS-ZIH – Multi-Agent Simulation as support for a reliability oriented maintenance of offshore wind farms
- Offshore-TIMES - Offshore Transport, Inspection and Maintenance Software

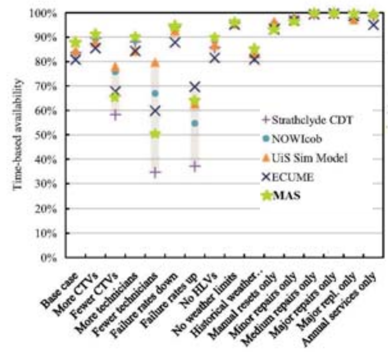

Figure 1. Average value for the time-based availability for the models for the reference cases

Source: MAS-ZIH, adopted from Dinwoodie 2015 [2]

Fraunhofer IWES

Reliability model
Requirements

FAILURE INPUT	Manual reset	Minor repair	Medium repair	Major repair	Major replacement	Annual service
Repair time	3 hours	7.5 hours	22 hours	26 hours	52 hours	60 hours
Required technicians	2	2	3	4	5	3
Vessel type	CTV	CTV	CTV	FSV	HLV	CTV
Failure rate	7.5	3.0	0.275	0.04	0.08	1
Repair cost [19]	0	£ 1000	£ 18 500	£ 73 500	£ 334 500	£ 18 500

Source: Dinwoodie 2015 [2]

Stakeholder Workshop

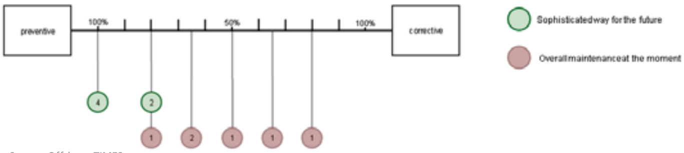

Source: Offshore-TIMES

Reliability model
Requirements

Stakeholder Workshop

Level of detail

Have the use-case of the simulation in mind.
For strategic purposes the focus should be on the main components.

Influencing parameters

Cluster	Parameter
Time	Age of component
	Time
Stress	Full load hours
	Shear modus
	Deviations
Environment	AMB temperature
	Wind speed
	Wave height
	Wake effect
Maintenance	Crane/non-crane components
	Rate/degree/effort of maintenance
	Human factor

Reliability model
Approach

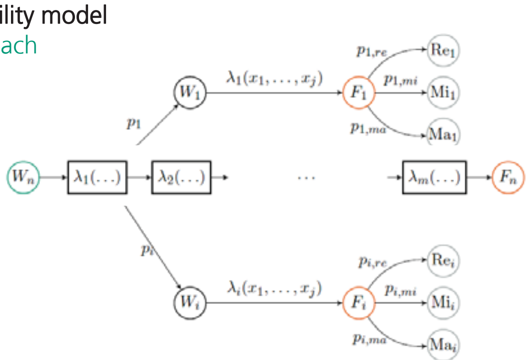

Share of failure categories | Mathematical description | Failure consequence

Component reliability

Turbine reliability

Failure categories
Time

- Early failures
- Aging failures

$$f(t) = \begin{cases} 0 & t < 0 \\ \frac{\beta}{\eta}\left(\frac{t-t_0}{\eta}\right)^{\beta-1} e^{-\left(\frac{t-t_0}{\eta}\right)^{\beta}} & 0 < t < t_{max} \end{cases}$$

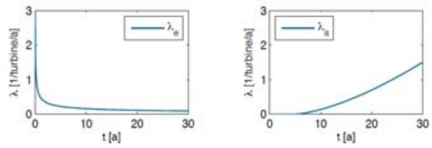

Failure categories
Stress

- Early failures
- Aging failures
- Fatigue failures

$$f(E) = \begin{cases} 0 & E < 0 \\ \frac{\beta}{\eta}\left(\frac{E}{\eta}\right)^{\beta-1} e^{-\left(\frac{E}{\eta}\right)^{\beta}} & E \geq 0 \end{cases}$$

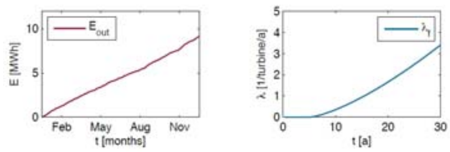

Failure categories
Environment

- Early failures
- Aging failures
- Fatigue failures
- Overload failures

$$\lambda_{overload}(v_{wind}) = \begin{cases} 0 & v < v_{wind} \\ m * (v - v_{wind}) & v_{min} < v < v_{max} \\ 0 & v > v_{max} \end{cases}$$

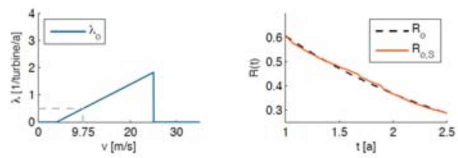

Failure categories
Environment

- Early failures
- Aging failures
- Fatigue failures
- Overload failures
- System-specific failures

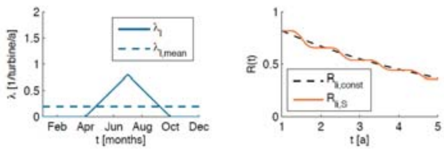

Failure categories
Other

- Early failures
- Aging failures
- Fatigue failures
- Overload failures
- System-specific failures
- Random failures

Parameter estimation
Failure statistics

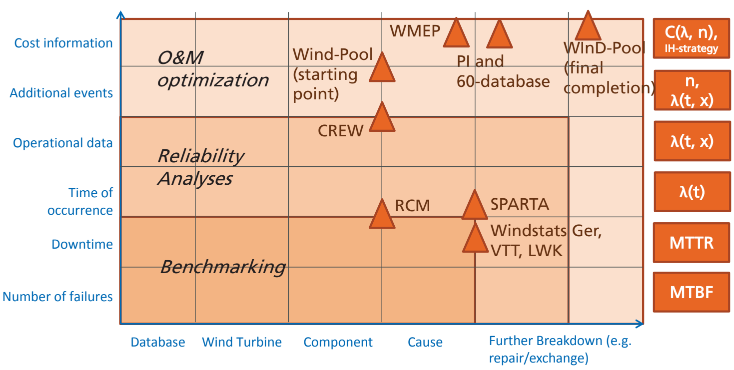

Parameter estimation
Approach

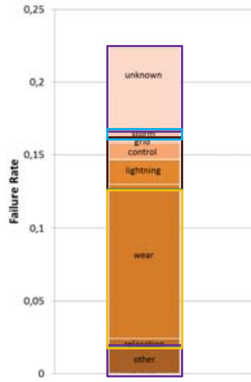

1. Determine the total number of failures for the simulation period
2. Weighting of failure categories

i	Failure category	Share of total failures (%)
1	Random	15%
2	Early	5%
3	Aging	15%
4	Fatigue	55%
5	Overload	10%

Parameter estimation
Approach

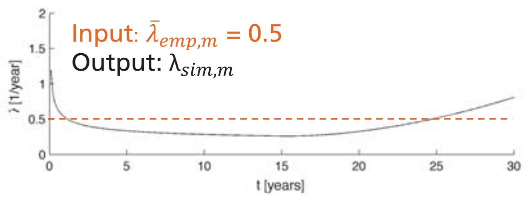

1. Determine the total number of failures for the simulation period
2. Weighting of failure categories
3. Initialize parameters
4. Calculate deviation $e_{sim,m} = \bar{\lambda}_{emp,m} - \bar{\lambda}_m$
5. Optimize Simulation parameter $e_{sim,m} \approx 0$

Simulation results
Component reliability

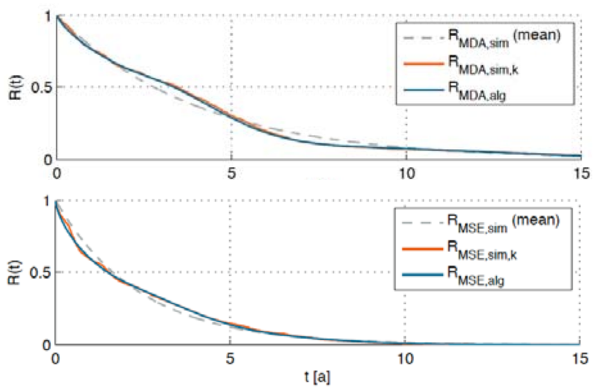

Simulation results
Validation

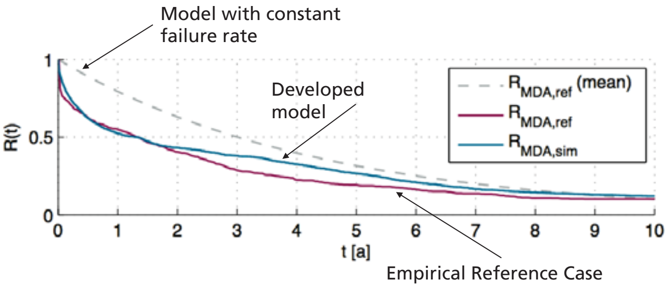

Simulation results
Overload failures

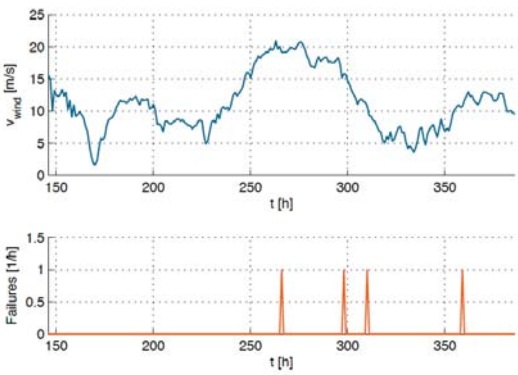

Simulation results
Overload failures

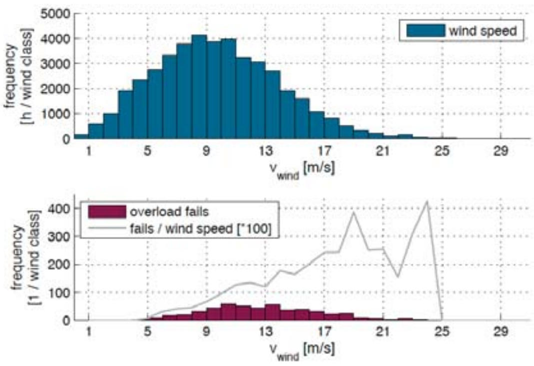

Simulation results
Lightning strikes

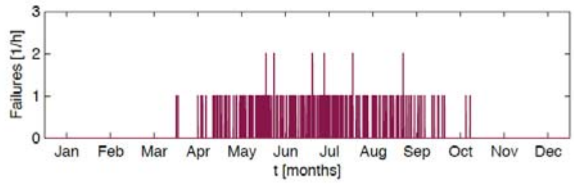

Conclusion

- Modelling the failure behaviour of wind turbines is an essential part of offshore simulation software
- failure model based on a reliability-block-diagram has been proposed
- incorporates different failure categories
- essential for better including preventive maintenance strategies
- include increased failure rates at higher wind speed and seasonal effects on failures due to lightning or icing
- Failure statistics using a systematic approach of gathering reliability information are indispensable

Fraunhofer IWES

Dipl.-Ing. Stefan Faulstich M. Sc.
Reliability and maintenance strategies
Wind farm planning and operation
Fraunhofer Institute for Wind energy and energy system technology (Fh IWES)
Königstor 59 | 34119 Kassel
stefan.faulstich@iwes.fraunhofer.de
www.iwes.fraunhofer.de

from Things
Technology for a real-time simulation-based system monitoring of wind turbines
Daniel Zwick, Tomáš Mánik, Asle Heide Vaskinn, Jon Tøndevoldshagen
(all Fedem Technology AS / SAP SE)
EERA DeepWind'2017, 14th deep sea offshore wind R&D conference, 18 - 20 January 2017
SAP
to Outcomes

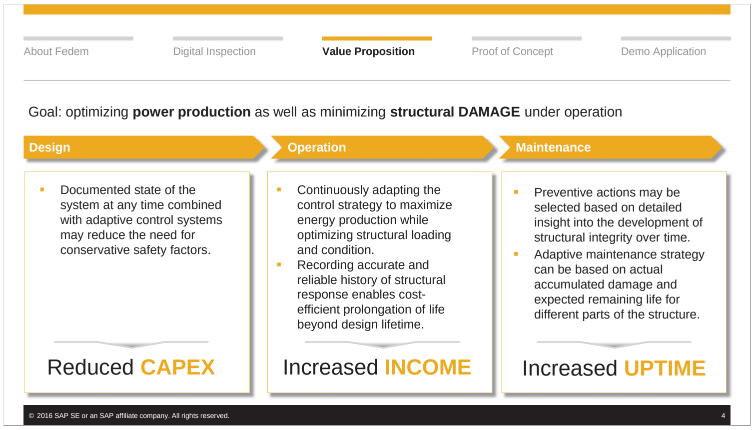

About Fedem
Digital Inspection
Value Proposition
Proof of Concept
Demo Application
Goal: optimizing power production as well as minimizing structural DAMAGE under operation
Design
Operation
Maintenance
Documented state of the system at any time combined with adaptive control systems may reduce the need for conservative safety factors.
Continuously adapting the control strategy to maximize energy production while optimizing structural loading and condition.
Recording accurate and reliable history of structural response enables cost-efficient prolongation of life beyond design lifetime.
Preventive actions may be selected based on detailed insight into the development of structural integrity over time.
Adaptive maintenance strategy can be based on actual accumulated damage and expected remaining life for different parts of the structure.
Reduced CAPEX
Increased INCOME
Increased UPTIME
© 2016 SAP SE or an SAP affiliate company. All rights reserved.
4

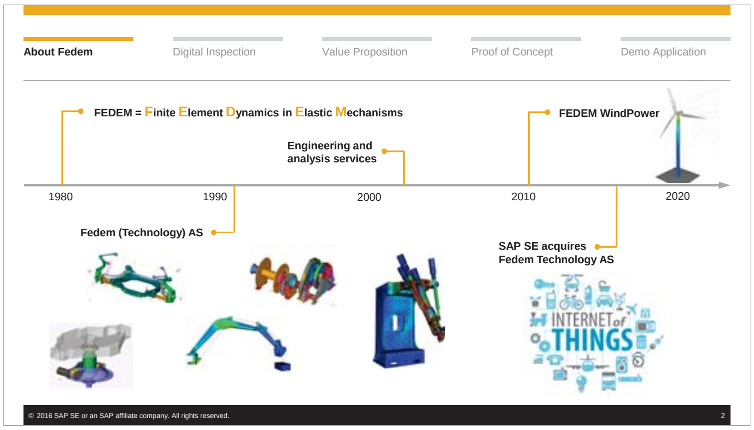

About Fedem
Digital Inspection
Value Proposition
Proof of Concept
Demo Application
FEDEM = Finite Element Dynamics in Elastic Mechanisms
FEDEM WindPower
Engineering and analysis services
1980
1990
2000
2010
2020
Fedem (Technology) AS
SAP SE acquires Fedem Technology AS
INTERNET of THINGS
© 2016 SAP SE or an SAP affiliate company. All rights reserved.
2

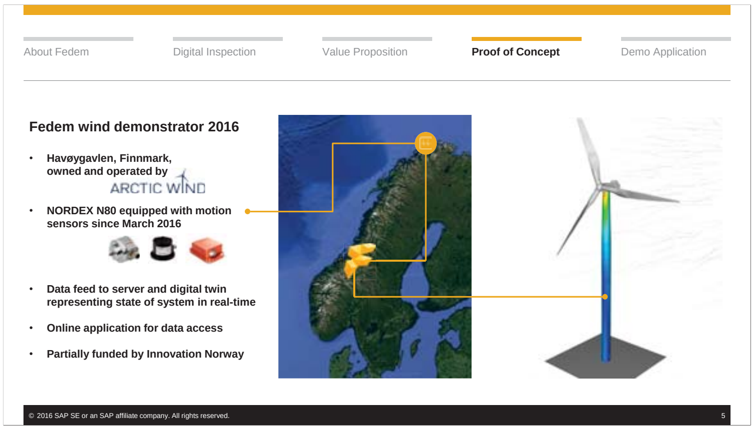

About Fedem
Digital Inspection
Value Proposition
Proof of Concept
Demo Application
Fedem wind demonstrator 2016
Havøygavlen, Finnmark, owned and operated by
ARCTIC WIND
NORDEX N80 equipped with motion sensors since March 2016
Data feed to server and digital twin representing state of system in real-time
Online application for data access
Partially funded by Innovation Norway
© 2016 SAP SE or an SAP affiliate company. All rights reserved.
5

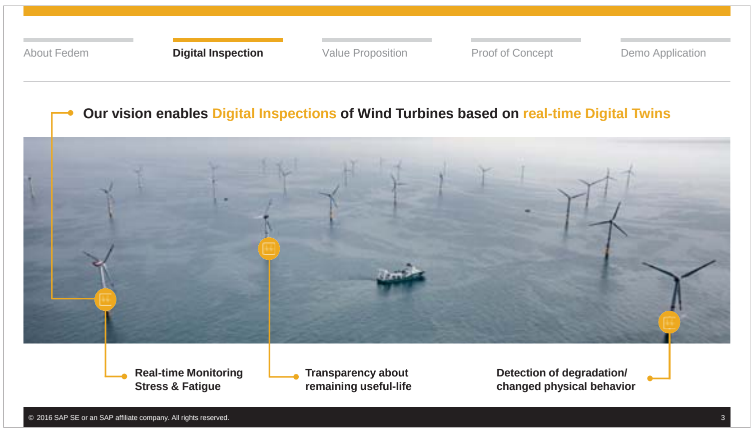

About Fedem
Digital Inspection
Value Proposition
Proof of Concept
Demo Application
Our vision enables Digital Inspections of Wind Turbines based on real-time Digital Twins
Real-time Monitoring Stress & Fatigue
Transparency about remaining useful-life
Detection of degradation/ changed physical behavior
© 2016 SAP SE or an SAP affiliate company. All rights reserved.
3

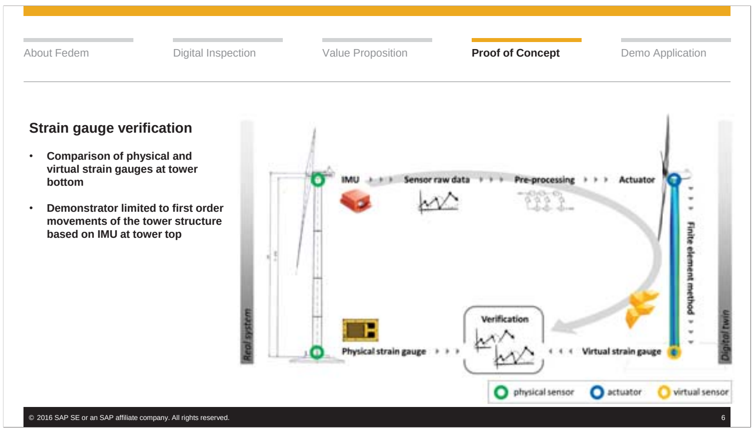

About Fedem
Digital Inspection
Value Proposition
Proof of Concept
Demo Application
Strain gauge verification
Comparison of physical and virtual strain gauges at tower bottom
Demonstrator limited to first order movements of the tower structure based on IMU at tower top
IMU
Sensor raw data
Pre-processing
Actuator
Finite element method
Verification
Physical strain gauge
Virtual strain gauge
Real system
Digital twin
physical sensor
actuator
virtual sensor
© 2016 SAP SE or an SAP affiliate company. All rights reserved.
6

Strain gauge verification

- Production to stop scenario
- Tower structure oscillates in its first eigenmode for several minutes
- Data compliance in both amplitude and period achieved by virtual strain gauges

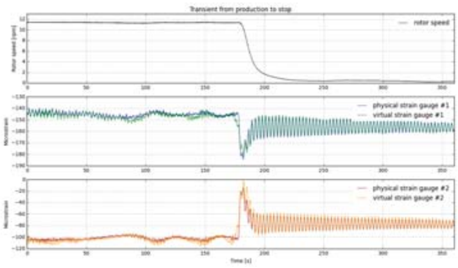

Digital twin based structural integrity monitoring

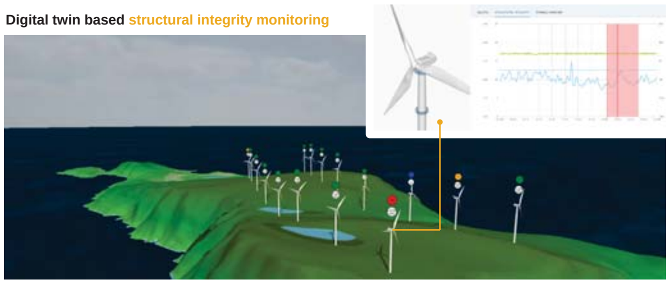

Fatigue analysis

- Simulation study on the contribution of structural modes to fatigue
- Number of recorded structural modes by sensors determines the accuracy that can be achieved in the fatigue analysis

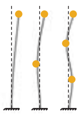

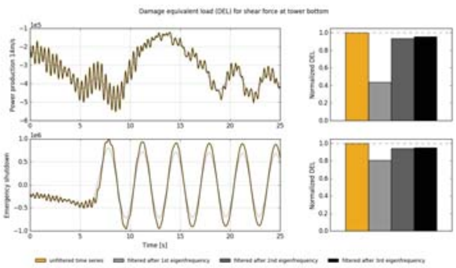

Simulation studies and further work

- Bottom-fixed and floating offshore wind turbine
- Extending the solution to cover complete wind turbine system
- Transferring technology into other industries

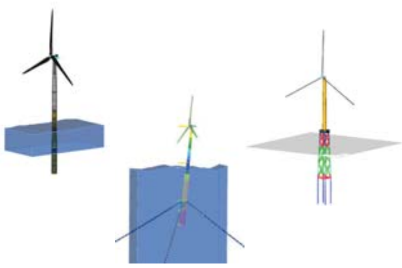

E1) Installation and sub-structures

Results of a comparative risk assessment of different substructures for floating offshore wind turbines, R. Proskovics, ORE Catapult

Conceptual optimal design of jackets, K. Sandal, DTU

Fatigue behavior of grouted connections at different ambient conditions and loading scenarios, A. Raba, ForWind – Leibniz University Hannover

Analysis of experimental data: The average shape of extreme wave forces on monopile foundations, S. Schløer, DTU Wind Energy

Results of a comparative risk assessment of different substructures for floating offshore wind turbines

Roberts Proskovics (ORE Catapult)
Matti Niclas Scheu, Denis Matha (Ramboll)

19/01/2017 –EERA DeepWind'2017 (Trondheim)

Qualification of innovative floating substructures for 10MW wind turbines and water depths greater than 50m

The research leading to these results has received funding from the European Union Horizon2020 programme under the agreement H2020-LCE-2014-1-640741.

Contents

- Introduction
  - Project background
  - Task at hand
- Methodology used
  - Background
  - Challenges and solutions
- Results
- Future work

Introduction: Project background

- Overview
  - Horizon 2020 project, 12 partners, 7+ M€
  - 40 months, started 06/2015
- Objectives
  - Development of a methodology for evaluation and qualification of floating wind substructures
  - Progressing two designs to TRL 5 for 10MW wind turbines

Introduction: Project background

- 4 substructures for floating wind turbines
  - TLPWIND (steel TLP)
  - IDEOL (concrete barge)
  - NAUTILUS (steel semi-sub)
  - OO-STAR (concrete semi-sub)
- More info at
  - http://lifes50plus.eu/

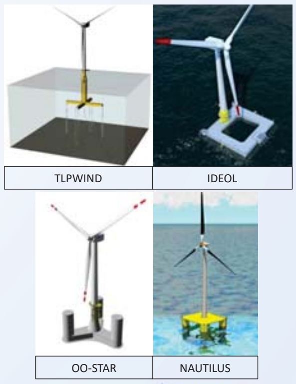

Introduction: Task at hand

- Technology risk assessment
  - of 4 very different systems
  - of 3 locations with different legislations and environment
  - as a comparative study
  - across 4 consequence categories
    - cost, availability, H&S, environment
  - part of a wider substructure evaluation
    - financial (LCoE), technical (KPIs) and life cycle assessments (GWP, AdP and PE)

Methodology: Background

- Based on methodology developed in LIFES50+
- Based on standard techniques

- Uses functional decomposition (as opposed to structural), novelty categorisation
- A highly iterative process

Methodology: Background

- 'Medium-level' flow diagram

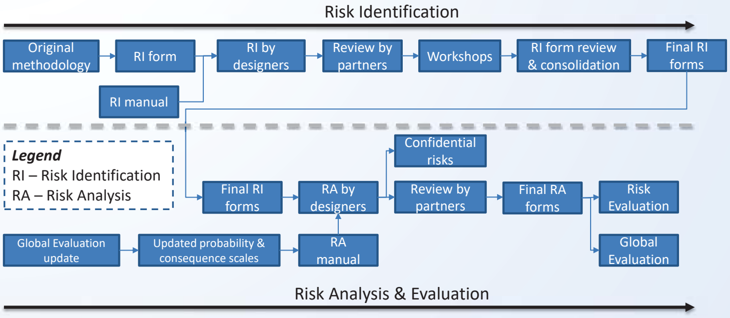

Methodology: Challenges & solutions

- Differentiation between designs
  - Conditional probability (aka β-factor)
    - Modified risk calculation formula
- Level playing field
  - Predefined failure effect, HAZID form consolidation, manual development
- Data confidentiality
  - 1-2-1 workshops, data anonymisation
- Risk part of a wider evaluation
  - MCDM with weighting factors, modified probability and consequence scales

Methodology: Challenges & solutions

- A hypothetical example

Design	Hazard	Potential Failure Cause	Failure Effect	Current Control	Probability	Conditional Probability (β-factor)	Consequence			
							Cost	Availability	H&S	Environment
A	Mooring line failure	Underestimated fatigue loading	Loss of stability resulting in loss of structure	• Design to standard • Wave tank tests • Numerical simulations • Independent 3rd party review	1	Possible	5	5	1	5
B				• All from the above (A) + • Redundancy	1	Highly unlikely	5	5	1	5

(Assumes direct link between *Potential Failure Cause* and *Hazard)*

Results: Risk identification

- ~80 risks identified after risk identification response consolidation
- Functions used in risk identification
  - Buoyancy, stability, station keeping, structural integrity, power transmission, RNA interfacing, monitoring and communications
- Good spread of risks across all functions
  - Fewest for buoyancy, and monitoring and communications
  - Most for station keeping
- Majority of risks seen as being of a low novelty categorisation
  - Proportionally, station keeping and power transmission are seen as having higher novelty associated with them

Results: Risk identification

- Life cycle phases used in risk identification
  - Design, manufacturing (construction and assembly), transportation and installation, O&M, decommissioning
- Risks spread across life cycle phases
  - Fewer risks for decommissioning
  - Most for design and O&M
- Importance of clear life cycle phase definition
  - Inception vs materialisation of hazard

Results: Risk analysis

- Very similar average risk scores across all functions and life cycle phases
- The highest average risk scores are
  - for functions that fall under direct remit of designers (e.g. structural integrity, buoyancy)
  - associated with severe failure effects
- The lowest average risk scores are
  - functions that aren't under direct remit of designers
  - associated with loss of power production or inadequate working environment (shows high confidence in OEMs, installers and operators)

Results: Risk analysis

- Developed a generic list of risks for floating wind turbines (currently confidential)
  - Includes a list of various possible control measures

Function	Element	Hazard	Life Cycle Phase	Potential Failure Cause	Failure Effect	Control Measures
Buoyancy	Main buoyant body	Flooding of main buoyant body	O&M	Collision	Compromised buoyancy	• Compartamentalisation • Review and quality control • Periodic inspection • Signalling • Design for vessel impact resistance
Structural Integrity	Primary material	Insufficient structural capacity	Design	Design error (underestimation of extreme loading)	Collapse of the structure	• Detailed environmental studies • Design to standard • Independent 3rd party review and certification • Monitoring • Wave tank experiments
Stability	Passive ballasting	Unequal distribution of permanent ballast (solid or liquid)	Installation	Installation error	Compromised stability	• Compartamentalisation • Review and quality control • Experience from other industries

Results: Risk analysis

Source: Wind Power Offshore (Pic: Yumiuri Shimbun)

Results: Risk analysis

Function	Element	Hazard	Life Cycle Phase	Potential Failure Cause	Failure Effect	Control Measures
Station Keeping	Mooring lines	Mooring line(s) failure	Manufacturing	Manufacturing error (e.g. exceedance of tolerances)	Compromised station keeping capabilities	• Review and quality control • Inspection • Component testing • Redundancy
RNA Interfacing	Full structure (transition piece + tower + RNA)	Excessive motions	Design	Underestimation of inclinations, accelerations and vibrations	Damage to RNA	• Design to standard • Use of proven numerical simulation tools • Wave tank experiments • Collaboration with OEMs • Independent 3rd party review and certification • Monitoring • Inspection
Power Transmission	Dynamic cable / umbilical	Damage to dynamic cable / umbilical	O&M	Unintended interaction / collision with foreign objects (e.g. vessels, debris)	Loss of power production	• Collaboration with OEMs • Layout redundancy • Experience from other industries
Monitoring and Communication	Structural monitoring	Partial or complete loss of structural hull stress monitoring information	O&M	Expected failure of sensors during operation	Collapse of the structure	• Sensor redundancy • Monitoring • Inspection

Results: Risk evaluation

- Risk evaluation helps in the decision of risk treatment (risk analysis vs risk criteria)
- Risk treatment not part of risk assessment (falls under risk management)
- Risk criteria is highly internal context dependent

Results: Risk evaluation

- A hypothetical example using average risk scores to show importance of well defined risk criteria

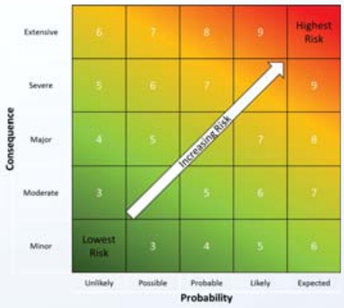

	Case 1		Case 2	
Category	Scale	No. of risks	Scale	No. of risks
Low	risk < 4	27	risk < 3.8	22
Medium	4 ≤ risk ≤ 7	50	3.8 ≤ risk ≤ 6	34
High	risk > 7	23	risk > 6	44

Future work

- H&S risk assessment for all life cycle phases
- O&M risk assessment
- Commercialisation risk assessment
- Revised technology risk assessment after optimisation of the substructures
- Combination of all of the above into a wider substructure evaluation
- Update of the original methodology

Thank You!

Questions?

LIFES50+

Investigating Optimal Leg Distance, using Conceptual Design Optimization

DTU

Kasper Sandal
Alexander Verbart
Mathias Stolpe
Technical University of Denmark,
Dept. of Wind Energy

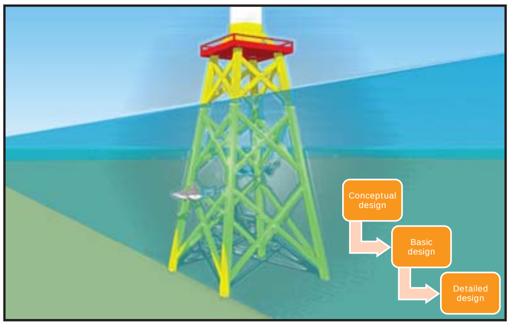

This talk presents conceptual design optimization of jacket structures for offshore wind turbines

DTU

Design considerations

$$\begin{aligned} &\text{minimize} && f(x) \\ &\text{subject to} && \mathbf{K}(x)u - \Delta P = \mathbf{0} \\ &&& \underline{\sigma} \leq \sigma(x) \leq \overline{\sigma} \\ &&& \underline{\omega} \leq \omega(x) \leq \overline{\omega} \end{aligned}$$

Optimal design problem

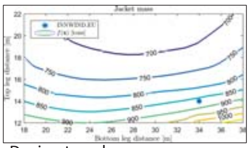

Design trends

A good jacket design has low mass to minimize material, transportation, and installation costs

DTU

Photo: Iberdrola

To avoid resonance, the natural frequency must lie in the soft-stiff range between the 1p and 3p rotor frequencies

DTU

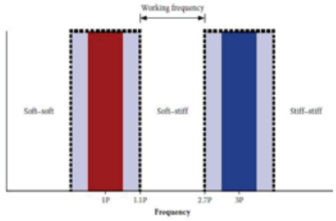

Photo: W S van Zyl; G P A G van Zijl

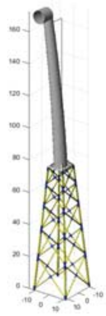

Reference jackets in the literature have very different leg distances

DTU

OC4 jacket

Designed for NREL 5 MW

8 m

12 m

INNWIND.EU jacket
Designed for DTU 10 MW

14 m

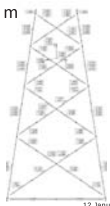

34 m

Placing the same tower and turbine on two jackets allows us to compare them

DTU

OC4 jacket

Designed for NREL 5 MW

8 m

12 m

JADOP models with DTU 10 MW tower & turbine

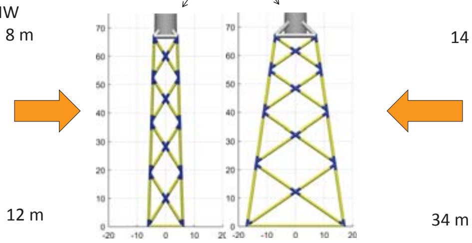

INNWIND.EU jacket
Designed for DTU 10 MW

14 m

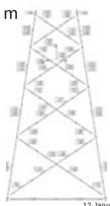

34 m

When cross sections are equal, a slender jacket will have a lower mass and a lower frequency than a bulky jacket

JADOP models with DTU
10 MW tower & turbine
Diameters = 1 m
Thicknesses = 50 mm

Slender
1060 tons
0.20 Hz

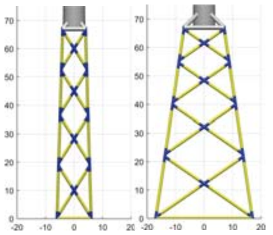

Bulky
1510 tons
0.27 Hz

Damage equivalent loads are used to make an approximate fatigue constraint using static stress constraints

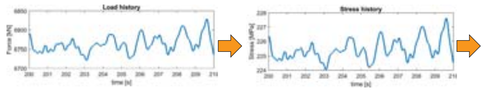

Rainflow counting: $\Delta\sigma_i, n_i$
$D = \sum_i \frac{n_i(\Delta\sigma_i)^m}{\bar{a}} \leq D^{max}$

To satisfy the fatigue and ultimate limit states, the cross sections have to change when the slenderness change

JADOP models with DTU
10 MW tower & turbine
Diameters = 1 m
Thicknesses = 50 mm

Slender
1060 tons
0.20 Hz

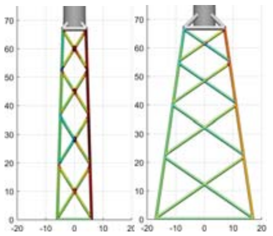

Bulky
1510 tons
0.27 Hz

Damage equivalent loads are used to make an approximate fatigue constraint using static stress constraints

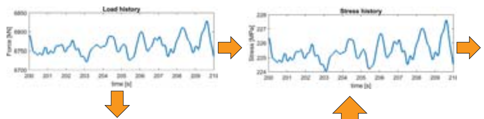

Rainflow counting: $\Delta\sigma_i, n_i$
$D = \sum_i \frac{n_i(\Delta\sigma_i)^m}{\bar{a}} \leq D^{max}$

Rainflow counting: $\Delta P_i, n_i$

$n_T(\Delta P^{1Hz})^m = \sum_i n_i(\Delta P_i)^m$

$\Rightarrow \Delta P^{1Hz} = \left(\frac{1}{n_T}\sum_i n_i(\Delta P_i)^m\right)^{\frac{1}{m}}$

Equal
fatigue
damage

$\Delta\sigma^{1Hz}$

Quasi-static behaviour
1 degree of freedom load
High-cycle SN-curve

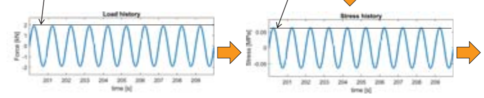

$D = \frac{n_T(\Delta\sigma^{1Hz})^m}{\bar{a}} \leq D_{max}$

$\Delta\sigma^{1Hz} \leq \overline{\Delta\sigma} = \left(\frac{D_{max}\bar{a}}{T^{life}}\right)^{\frac{1}{m}}$

The optimization problem for conceptual design is formulated with static loads, and constraints on stress, buckling, and frequency

x = cross sections

minimize	$f(x)$
subject to	$\mathbf{K}(x)\boldsymbol{u} - \boldsymbol{f}(x) = \mathbf{0}$
	$\underline{\sigma} \leq \sigma(x) \leq \overline{\sigma}$
	$\underline{\omega} \leq \omega(x) \leq \overline{\omega}$

Jacket mass
Stress
Frequency

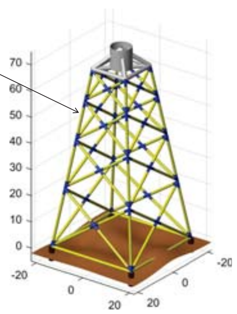

The problem is solved using the JAcket Design OPtimization tool JADOP and the open source optimization solver IPOPT

```
% Specify settings
S                                   = settings;

% Specify DTU 10 MW turbine and INNWIND.EU jacket without piles
S.Geometry.Piles     = 0;     % 1 for piles, 0 for clamped.
S.Geometry.LegdistB  = 24;    % Leg distance at seabed
S.Geometry.LegdistT  = 14;    % Leg distance at transition piece
S.Geometry.Sections  = 4;     % Number of sections
S.Geometry.Height    = 67;    % Jacket height (bottom of transition piece)
S.Geometry.MSL_h     = 50;    % Mean sea level
S.Geometry.Turbine   = 1;     % 1-DTU10MW, 2-NREL5MW

% Optimization settings
S.Optimization.flag                 = 1;
S.Optimization.sand_flag            = 0;
S.Optimization.maxIter              = 500;
S.Optimization.constraints          = {'SCF-validity';'Stress ULS';'Buckling';
                                       'Equivalent fatigue';'Frequency'};
S.Optimization.variable_linking = '4nv';
S.Optimization.scale_obj            = 1;
S.Optimization.con_lim.disp         = 10;
S.Optimization.scale_stress         = 1e-6;
S.Optimization.con_lim.stress       = 350e6;
S.Optimization.con_lim.FLSstress= 11.5e6;
```

DTU 10 MW: Tower, turbine, and loads

- Parametric input
- Analytic sensitivities
- Many types of constraints

With leg distances from the INNWIND.EU jacket, the mass was minimized to 870 tons in 2 minutes on a laptop

DTU

Top leg distance	= 14 m
Bottom leg distance	= 34 m
Jacket mass	= 870 tons
Natural frequency	= 0,264 Hz
Computation time	= 118 s

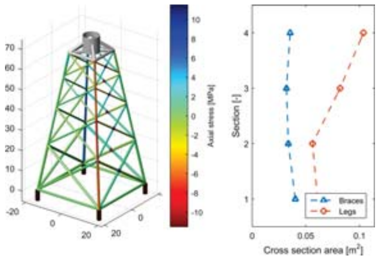

High leg distances at both bottom and top increase the natural frequency

DTU

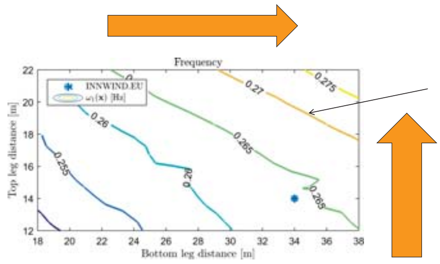

Upper bound on soft-stiff range

Optimization of 400 jackets indicate that an increased top leg distance reduces the jacket mass with about 20 percent

DTU

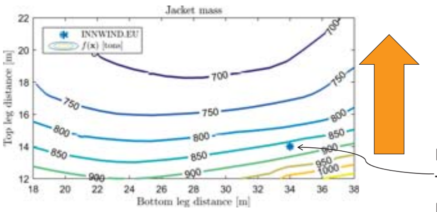

INNWIND.EU leg distances

Top leg distance	= 14 m
Bottom leg distance	= 34 m

Reducing the bottom leg distance of the INNWIND.EU jacket from 34 to 24 meters, reduces both overall mass and frequency

DTU

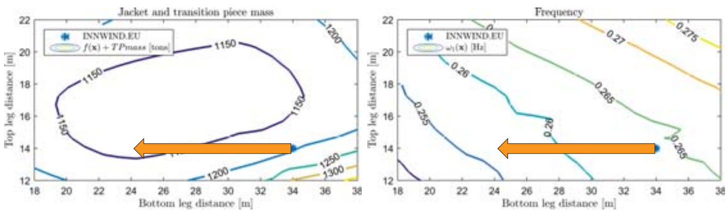

Since transition piece mass increases with larger top leg distance, the overall mass reduction is much less

DTU

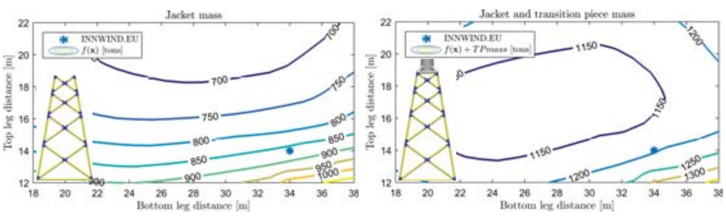

In conclusion, the conceptual design optimization is a fast and useful tool for investigating key parameters such as leg distance

DTU

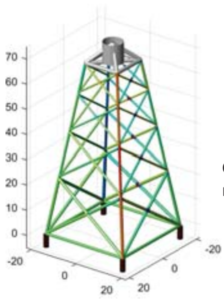

Bottom leg distance:	34 m ➔ 24 m
Mass:	-6.7 percent
Frequency:	-2.8 percent

Can also be used for pile stick-up, number of sections, height, etc.

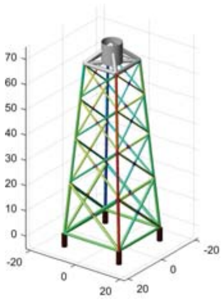

In conclusion, the conceptual design optimization is a fast and useful tool for investigating key parameters such as leg distance

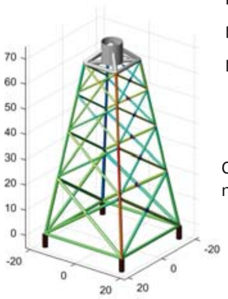

Bottom leg distance: 34 m → 24 m

Mass: -6.7 percent

Frequency: -2.8 percent

Can also be used for pile stick-up, number of sections, height, etc.

Questions?

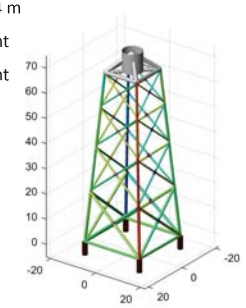

EXTRA SLIDES

Design according to DNVGL offshore standard and recommended practices

DNVGL-OS-C101 Design of offshore steel structures

DNVGL-RP-C203 Fatigue design of offshore steel structures

DNV-RP-C202 Buckling strength of shells

Optimal design problem

$$
\begin{aligned}
\underset{\mathbf{v}\in\mathbf{R}^{n_v},\mathbf{u}\in\mathbf{R}^{dn_l}}{\text{minimize}} \quad & f(\mathbf{v}) = \rho\sum_{e=1}^{n} A_e(d_e,t_e)l_e \\
\text{subject to} \quad & \mathbf{A}\mathbf{v} \leq \mathbf{b} \\
& \mathbf{K}(\mathbf{v})\mathbf{u}^l - \mathbf{f}^l(\mathbf{v}) = \mathbf{0}, && l = 1,\dots,n_l \\
& \underline{\sigma} \leq \sigma^{scf}_{ehl}(\mathbf{v},\mathbf{u}^l,\gamma_h) \leq \overline{\sigma}, && e = 1,\dots,n, h = 1,\dots,n_h, l = 1,\dots,n_{FLS} \\
& \sigma^b(\mathbf{v}) - \sigma_{ehl}(\mathbf{v},\mathbf{u}^l,\gamma_h) \leq 0, && e = 1,\dots,n, h = 1,\dots,n_h, l = n_{FLS}+1,\dots,n_l \\
& \underline{\omega_i} \leq \omega_i(\mathbf{v}) \leq \overline{\omega_i}, && i = 1,\dots,n_f \\
& g_e(\mathbf{v}) \leq 0, && e = 1,\dots,n \\
& \underline{\mathbf{v}} \leq \mathbf{v} \leq \overline{\mathbf{v}},
\end{aligned}
\tag{16}
$$

Load cases

Table 3: Description of static load cases

	Load type	Limit state	Rotation [deg]	Tower top load
1	Thrust	Fatigue	0	$F_x + M_y + \frac{1}{3}M_z$ from Δp^{1Hz}
2	Thrust	Fatigue	45	$F_x + M_y + \frac{1}{2}M_z$ from Δp^{1Hz}
3	Torsion	Fatigue	0	$\frac{1}{3}F_x + \frac{1}{3}M_y + M_z$ from Δp^{1Hz}
4	Torsion	Fatigue	45	$\frac{1}{2}F_x + \frac{1}{2}M_y + M_z$ from Δp^{1Hz}
5	Thrust	Ultimate	0	$F_x^{max} + M_y^{max}$ from [5]
6	Thrust	Ultimate	45	$F_x^{max} + M_y^{max}$ from [5]
7	Torsion	Ultimate	0	M_z^{max} from [5]

Shell buckling

$$\sigma^b(\mathbf{v}) - \sigma_{ehl}(\mathbf{v},\mathbf{u}^l,\gamma_h) \leq 0, \tag{31}$$

where the shell buckling capacity in compression $\sigma^b(\mathbf{v})$, is defined as

$$\sigma^b(\mathbf{v}) = \frac{-\sigma^y}{\gamma_M\sqrt{1+\left(\frac{\sigma^y}{f_{Em}}\right)^2}}, \qquad f_{Em} = C\frac{\pi^2 E}{12(1-\nu^2)}\left(\frac{t_e}{L_e}\right)^2, \qquad C = \sqrt{1+(\rho\xi)^2} \tag{32}$$

$$\rho = \frac{1}{2\sqrt{1+\frac{d_e}{600t_e}}}, \qquad \xi = 1.404\frac{L_e^2}{d_e t_e}\sqrt{1-\nu^2}, \tag{33}$$

Column buckling

Column buckling need only be assessed for element e if

$$\frac{(kL_e)^2 A_e}{I_e} \geq \frac{2.5E}{\sigma^y}. \tag{34}$$

where $k = 0.7$ is the effective column length. To avoid assessing column buckling, the inverse of equation (34) can be formulated as a non-linear constraint $g_e(\mathbf{v}) \leq 0$, where

$$g_e(\mathbf{v}) = \sqrt{\frac{3.2\sigma^y}{E}} kL_e - d_e^2 + 2d_e t_e - 2t_e^2. \tag{35}$$

SCF validity constraints

The linear constraints $\mathbf{Ax} \leq \mathbf{b}$ enforce the SCF validity range [2], which states that for a joint where a brace is welded onto a leg, the dimensions should satisfy the following relations:

$$0.2d_{Leg} - d_{Brace} \leq 0 \tag{17}$$
$$d_{Brace} - d_{Leg} \leq 0 \tag{18}$$
$$0.2t_{Leg} - t_{Brace} \leq 0 \tag{19}$$
$$t_{Brace} - t_{Leg} \leq 0, \tag{20}$$

and that for all elements, the following should hold

$$16t - d \leq 0 \tag{21}$$
$$d - 64t \leq 0. \tag{22}$$

Stress & SCF

In the analysis of the offshore wind turbine structure, we assume that only normal stress $\sigma(\mathbf{v}, \mathbf{u}, \xi, \eta, \zeta) \in \mathbb{R}$ is significant. The normal stress in element e, position h, is computed as

$$\sigma_{eh}(\mathbf{v}, \mathbf{u}_e^g, \gamma_h) = E\mathbf{b}(\mathbf{v}, \gamma_h)\mathbf{T}_e \mathbf{u}_e^g, \tag{12}$$

where $\mathbf{b}(\mathbf{v}, \gamma_h) \in \mathbb{R}^{1\times12}$ is the strain displacement vector for normal stress at postition h, and E is the materials Youngs modulus.

To account for stress concentrations in welded tubular joints, the recommended practice [2] provides a method using stress concentration factors (SCFs). This method assumes superposition of the normal stress components coming from axial forces (ax), moments in plane (mi) and moments out of plane (mo). We decompose the normal stress $\sigma_{eh}(\mathbf{v}, \mathbf{u}_e^g, \gamma_h)$ by decomposing the strain displacement vector:

$$\mathbf{b}(\mathbf{v}, \gamma_h) = \mathbf{b}^{ax}(\mathbf{v}, \gamma_h) + \mathbf{b}^{mi}(\mathbf{v}, \gamma_h) + \mathbf{b}^{mo}(\mathbf{v}, \gamma_h) \tag{13}$$

The recommended practice then provides coefficients that are to be multiplied onto each stress component. These coefficients are functions of diameter and thickness of all elements in the joint, as well as joint geometry, and the position h along the element circumference. The number of hot spots n_h in each element should be at least eight. The scf-stress $\sigma_{eh}^{scf}(\mathbf{v}, \mathbf{u}_e^g, \gamma_h)$ in element e, hot spot h is computed as

$$\sigma_{eh}^{scf}(\mathbf{v}, \mathbf{u}_e^g) = \mathbf{b}_{eh}^{scf}(\mathbf{v}, \gamma_h)\mathbf{T}_e \mathbf{u}_e^g \tag{14}$$
$$\mathbf{b}_{eh}^{scf}(\mathbf{v}, \gamma_h) = SCF_{eh}^{ax}(\mathbf{v})\mathbf{b}_{eh}^{ax}(\mathbf{v}, \gamma_h) + SCF_{eh}^{mi}(\mathbf{v})\mathbf{b}_{eh}^{mi}(\mathbf{v}, \gamma_h) + SCF_{eh}^{mo}(\mathbf{v})\mathbf{b}_{eh}^{mo}(\mathbf{v}, \gamma_h) \tag{15}$$

EERA DeepWind'2017

Fatigue behaviour of grouted connections at different ambient conditions

Prof. Peter Schaumann
Alexander Raba
Anne Bechtel

Trondheim, 19/01/2017

Leibniz Universität Hannover
Institute for Steel Construction Prof. Dr.-Ing. Peter Schaumann
ForWind Center for Wind Energy Research

Grouted connections

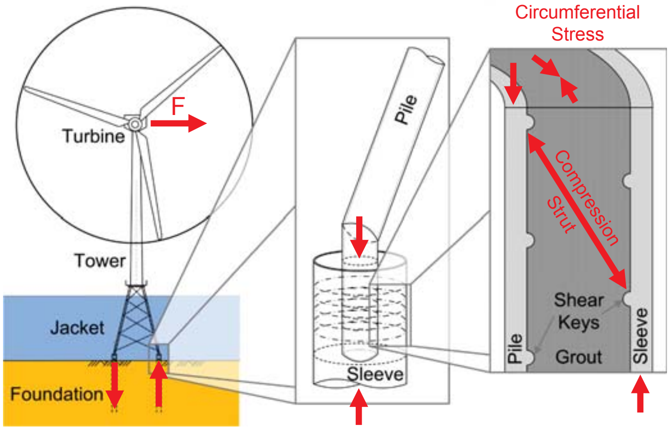

Outline

- Grouted connections
- Submerged fatigue tests
  - Small-scale
  - Large-scale
- Damage mechanisms
- Summary and Outlook

Small-scale tests – setup

- 1 Geometry
- 2 Grout materials
  - f_c = 90 N/mm² / 140 N/mm²
- 2 Load levels
  - constant amplitude
  - F_{max} = 50% F_{ULS} / 20% F_{ULS}
  - R = 20
- 2 Ambient conditions
  - dry / wet
- 5 Loading frequencies
  - 0.3 – 10 Hz

Geometry

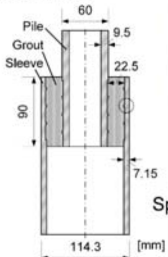

Shear key

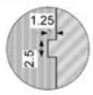

MFL – Test-Rig

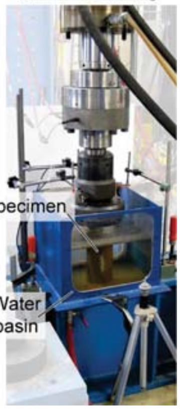

Grouted connections

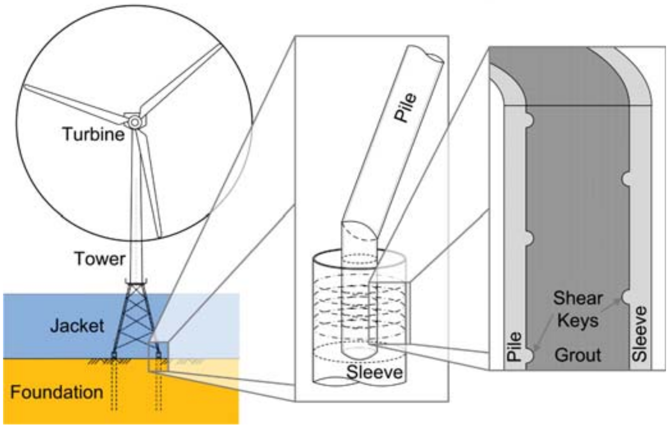

Small-scale tests – endurable load cycles

- Water leads to significant reduction of N
  N_{dry} = 2 m. (runner) N_{wet} ~ 50'000 N_{dry}/N_{wet} = 40
- Lower loading frequency increases N

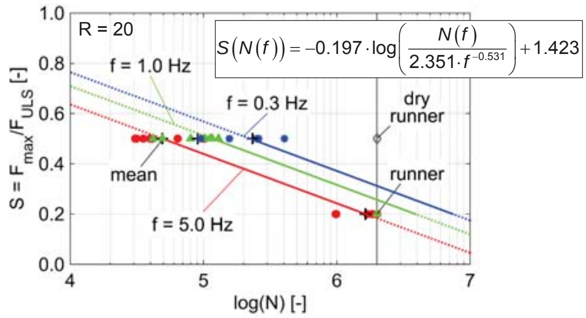

Small-scale tests – damage patterns

- Water introduces
  - Grout flushing
  - Early stage cracking

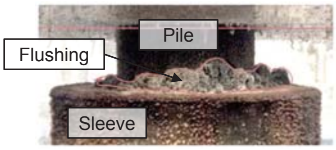

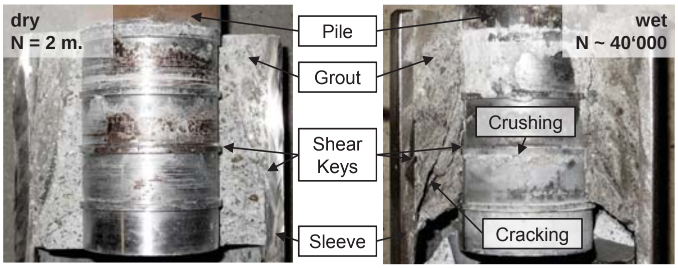

Large-scale tests – load scenarios

- Objective: fatigue damage
  - F_{max} < F_{FLS} (ISO 19902) < F_{ULS} (ISO 19902, DNVGL-ST-0126)
  - Damage expected ≥ LS 3

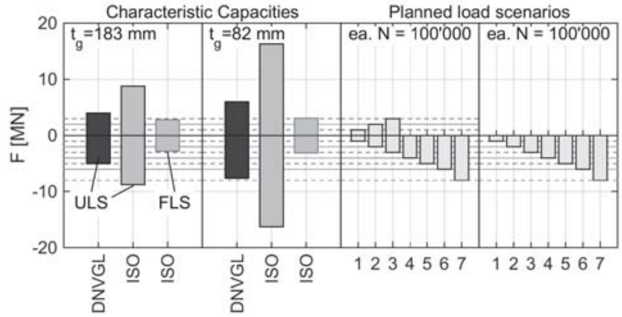

Large-scale tests – setup

- 2 Geometries
  - G1: t_g = 183 mm
  - G2: t_g = 82 mm
- 1 Grout-Material
  - f_c = 140 N/mm²
  - f_t = 8.6 N/mm²
  - E = 50'900 N/mm²
- 2 Loading scenarios
  - R = -1 / R = ∞
- 2 Ambient conditions
  - dry / wet

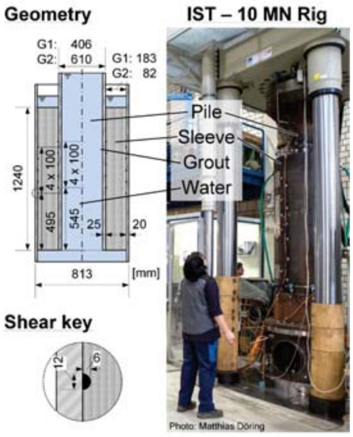

Large-scale tests – endurable load cycles

- Failure t_g = 183 mm D1 (R = -1 / dry) LS7 (N ~ 200)
  W1 (R = -1 / wet) LS1 (N ~ 95'000)

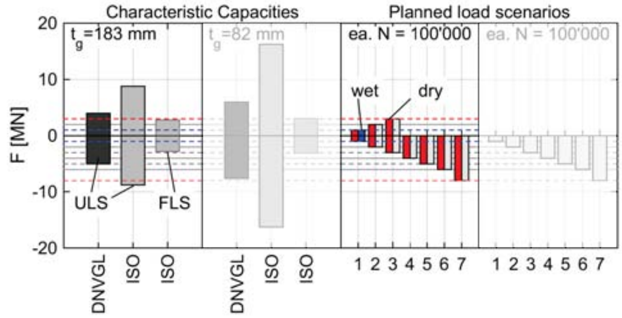

Large-scale tests – load scenarios

- Objective: fatigue damage
  - F_{max} < F_{FLS} (ISO 19902) < F_{ULS} (ISO 19902, DNVGL-ST-0126)

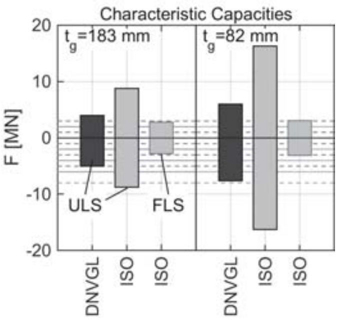

Large-scale tests – endurable load cycles

- Failure t_g = 183 mm D1 (R = -1 / dry) LS7 (N ~ 200)
  W1 (R = -1 / wet) LS1 (N ~ 95'000)
  W3 (R = ∞ / wet) LS2 (N ~ 45'000)

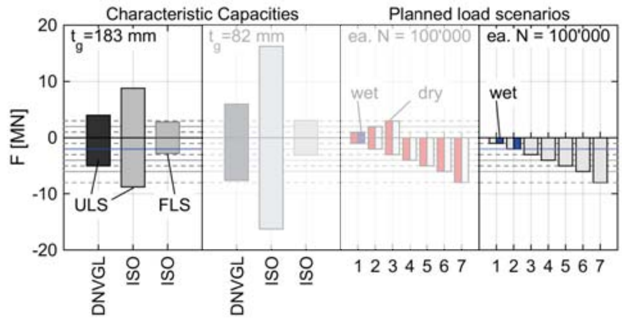

Large-scale tests – deformation behaviour t_g = 183 mm

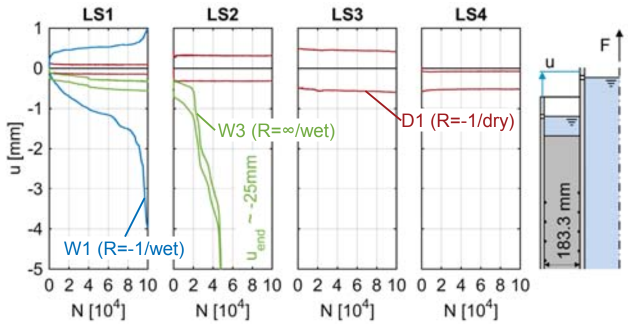

- Water provokes instable load bearing behaviour

Large-scale tests – damage patterns t_g = 183 mm (W1)

- Grinding marks on grout
- Connection backlash established during test
- Grout crushing around shear keys (sleeve-grout)

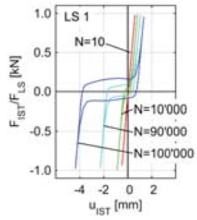

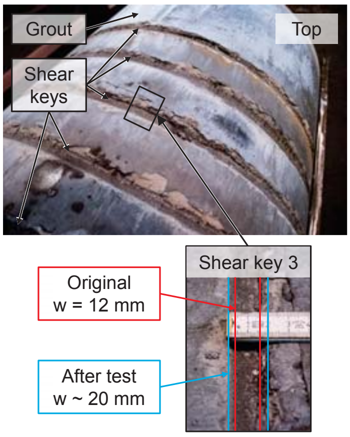

Large-scale tests – flushing

- Filterbasin to detect flushing and particle sizes

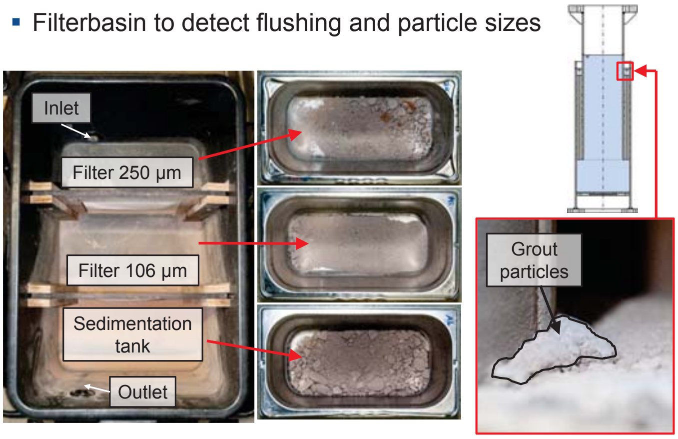

Large-scale tests – damage patterns t_g = 183 mm (W3)

- Compression strut cracking
- Grout crushing around shear keys
- Water passages
- Flushed grout particles

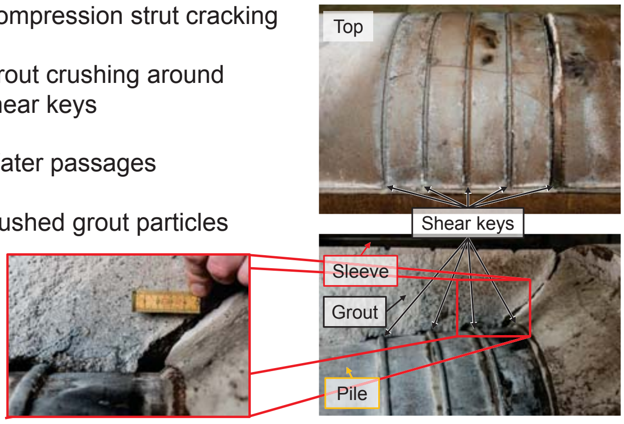

Large-scale tests – dismantling

Summary and Outlook

- Parameter influence
  - AC wet → N ↘
  - Load ↘ → N ↗
  - Load ratio R > 0 → N ↗
  - Loading frequency ↘ → N ↗
  - Grout annulus t_g ↘ → N ↗

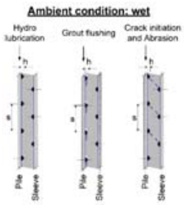

- Additional damage mechanisms
  - Grout crushing and flushing
  - Early stage cracking
- Comparable results for small- and large-scale tests

Summary and Outlook

- Parameter influence
  - AC wet → N ↘
  - Load ↘ → N ↗
  - Load ratio R > 0 → N ↗
  - Loading frequency ↘ → N ↗
  - Grout annulus t_g ↘ → N ↗

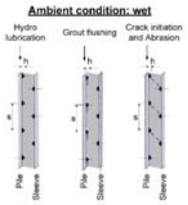

- Additional damage mechanisms
  - Grout crushing and flushing
  - Early stage cracking
- Comparable results for small- and large-scale tests
- Future tests with OPC in preparation

Thank you to our project partners and supporters!
Thank you for your attention!

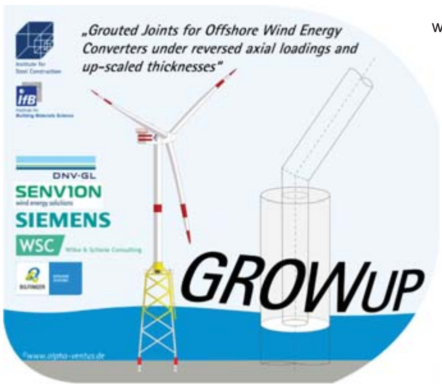

www.stahlbau.uni-hannover.de
www.forwind.de

Supported by:
Federal Ministry for Economic Affairs and Energy
on the basis of a decision by the German Bundestag

Raba – Fatigue behaviour of grouted connections
at different ambient conditions and loading scenarios
ForWind Center for Wind Energy Research

Innovation Fund Denmark
RESEARCH, TECHNOLOGY & GROWTH

Analysis of experimental data: The average shape of extreme wave forces on monopile foundations compared to the New Force model

EERA Deepwind '2017

Signe Schløer, Henrik Bredmose, Amin Ghadirian

DHI · DONG energy · Statkraft · Statoil
DTU Wind Energy, Department of Wind Energy
DTU Mechanical Engineering, Department of Mechanical Engineering
DTU Compute, Department of Applied Mathematics and Computer Science

Outset of the anaysis
Extreme load cases

$$\frac{F}{\rho g h R^2} = f\left(\frac{H_s}{gT_p^2}, \frac{h}{gT_p^2}, \gamma, \frac{R}{gT_p^2}, \frac{\nu}{\sqrt{ghR^2}}, \frac{t}{T_p}, \{x_j\}\right)$$

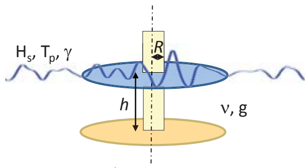

$$P\left(\frac{F_i}{\rho g h R^2} \le \frac{F}{\rho g h R^2}\right) = f_1\left(\frac{H_s}{gT_p^2}, \frac{h}{gT_p^2}, \gamma, \frac{R}{gT_p^2}, \frac{\nu}{\sqrt{ghR^2}}\right)$$

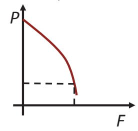

$$\frac{F}{F_i} = f_2\left(\frac{F_i}{\rho g h R^2}, \frac{H_s}{gT_p^2}, \frac{h}{gT_p^2}, \gamma, \frac{R}{gT_p^2}, \frac{\nu}{\sqrt{ghR^2}}, \frac{t}{T_p}\right)$$

DeRisk – De-risking of ULS wave loads on offshore wind turbine structures

Outset of the anaysis
Extreme load cases

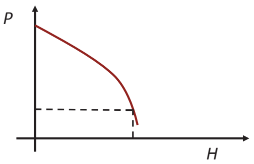

f=ρRC$_D$u^2+ρAC$_M$u$_t$

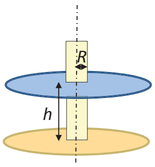

DeRisk – De-risking of ULS wave loads on offshore wind turbine structures

Outset of the anaysis
Extreme load cases

$$\frac{F}{\rho g h R^2} = f\left(\frac{H_s}{gT_p^2}, \frac{h}{gT_p^2}, \gamma, \frac{R}{gT_p^2}, \frac{\nu}{\sqrt{ghR^2}}, \frac{t}{T_p}, \{x_j\}\right)$$

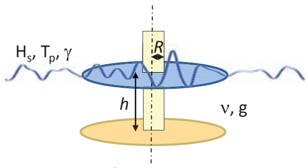

$$P\left(\frac{F_i}{\rho g h R^2} \le \frac{F}{\rho g h R^2}\right) = f_1\left(\frac{H_s}{gT_p^2}, \frac{h}{gT_p^2}, \cancel{\gamma}, \cancel{\frac{R}{gT_p^2}}, \cancel{\frac{\nu}{\sqrt{ghR^2}}}\right)$$

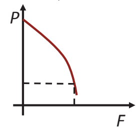

$$\frac{F}{F_i} = f_2\left(\frac{F_i}{\rho g h R^2}, \frac{H_s}{gT_p^2}, \frac{h}{gT_p^2}, \cancel{\gamma}, \cancel{\frac{R}{gT_p^2}}, \cancel{\frac{\nu}{\sqrt{ghR^2}}}, \frac{t}{T_p}\right)$$

DeRisk – De-risking of ULS wave loads on offshore wind turbine structures

Outset of the anaysis
Extreme load cases

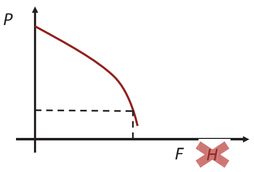

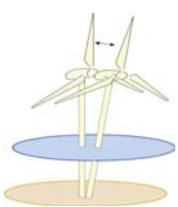

Shape of force?

DeRisk – De-risking of ULS wave loads on offshore wind turbine structures

Outset of the anaysis
Extreme load cases

$$\frac{F}{\rho g h R^2} = f\left(\frac{H_s}{gT_p^2}, \frac{h}{gT_p^2}, \gamma, \frac{R}{gT_p^2}, \frac{\nu}{\sqrt{ghR^2}}, \frac{t}{T_p}, \{x_j\}\right)$$

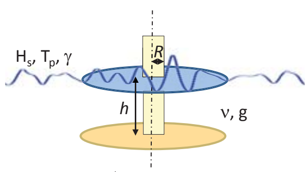

$$P\left(\frac{F_i}{\rho g h R^2} \le \frac{F}{\rho g h R^2}\right) = f_1\left(\frac{H_s}{gT_p^2}, \frac{h}{gT_p^2}\right)$$

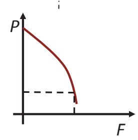

$$\frac{F}{F_i} = f_2\left(\frac{F_i}{\rho g h R^2}, \frac{H_s}{gT_p^2}, \frac{h}{gT_p^2}, \frac{t}{T_a}\right)$$

DeRisk – De-risking of ULS wave loads on offshore wind turbine structures

Outset of the anaysis
Extreme load cases

$$\frac{F}{\rho g h R^2} = f\left(\frac{H_s}{gT_p^2}, \frac{h}{gT_p^2}, \gamma, \frac{R}{gT_p^2}, \frac{\nu}{\sqrt{ghR^2}}, \frac{t}{T_p}, \{x_j\}\right)$$

$$P\left(\frac{F_i}{\rho g H_s R^2} \le \frac{F}{\rho g H_s R^2}\right) = f_1\left(H_s \ldots\right.$$

$$\frac{F}{F_i} = f_2\left(\frac{F_i}{\rho g h R^2}, \ldots, \frac{h}{gT_p^2}, \frac{t}{T_a}\right)$$

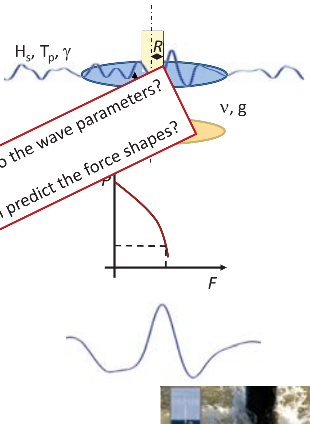

Functional dependencies of f_1 and f_2 to the wave parameters?

How well can the New Force model predict the force shapes?

DeRisk – De-risking of ULS wave loads on offshore wind turbine structures

The New Force model

$$\eta_{\text{New Wave}} = \frac{\alpha_\eta}{\sigma_\eta^2}\sum_j \mathrm{Re}\left\{S_\eta(\omega_j)\Delta\omega \exp\left(i\left(\omega_j(t-t_0)-k_j(x-x_0)\right)\right)\right\}$$

$$\Gamma(\omega) = i\rho\pi R^2 C_M \omega^2/k \qquad S_F(\omega) = |\Gamma(\omega)|^2 S_\eta(\omega)$$

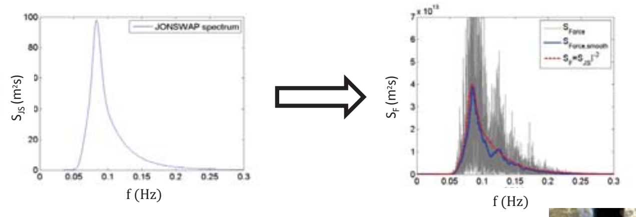

DeRisk – De-risking of ULS wave loads on offshore wind turbine structures

Agenda

- The New Force model
- Experimental data
- Exceedance probability distributions of the free surface elevation and force signal
- Average shape of measured inline forces
- Comparison to the New Force model
- Conclusion

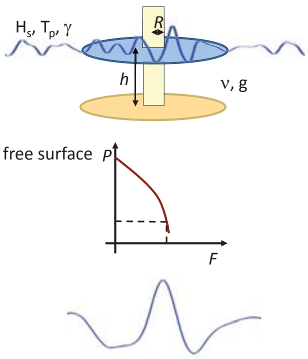

DeRisk – De-risking of ULS wave loads on offshore wind turbine structures

The New Force model

$$\eta_{\text{New Wave}} = \frac{\alpha_\eta}{\sigma_\eta^2}\sum_j \mathrm{Re}\left\{S_\eta(\omega_j)\Delta\omega \exp\left(i\left(\omega_j(t-t_0)-k_j(x-x_0)\right)\right)\right\}$$

$$\Gamma(\omega) = i\rho\pi R^2 C_M \omega^2/k \qquad S_F(\omega) = |\Gamma(\omega)|^2 S_\eta(\omega)$$

$$F_{\text{New Force}} = \frac{\alpha_F}{\sigma_F^2}\sum_j \mathrm{Re}\left\{|\Gamma(\omega_j)|^2 S_\eta(\omega_j)\Delta\omega \exp\left(i\left(\omega_j(t-t_0)-k_j(x-x_0)\right)\right)\right\}$$

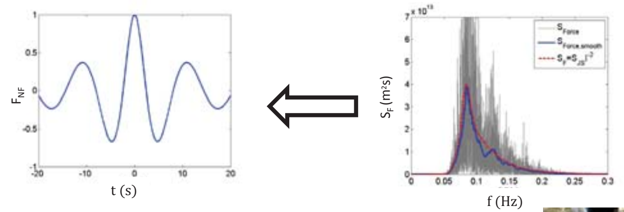

DeRisk – De-risking of ULS wave loads on offshore wind turbine structures

The New Force model

$$\eta_{\text{New Wave}} = \frac{\alpha_\eta}{\sigma_\eta^2}\sum_j \mathrm{Re}\left\{S_\eta(\omega_j)\Delta\omega \exp\left(i\left(\omega_j(t-t_0)-k_j(x-x_0)\right)\right)\right\}$$ [Lindgren (1976), Boccotti (1983), Tromans (1991)]

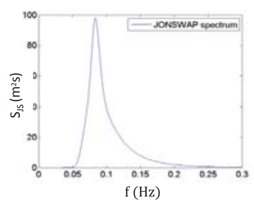

DeRisk – De-risking of ULS wave loads on offshore wind turbine structures

The New Force model

$$\eta_{\text{New Wave}} = \frac{\alpha_\eta}{\sigma_\eta^2}\sum_j \mathrm{Re}\left\{S_\eta(\omega_j)\Delta\omega \exp\left(i\left(\omega_j(t-t_0)-k_j(x-x_0)\right)\right)\right\}$$

$$\Gamma(\omega) = i\rho\pi R^2 C_M \omega^2/k \qquad S_F(\omega) = |\Gamma(\omega)|^2 S_\eta(\omega)$$

$$F_{\text{New Force}} = \frac{\alpha_F}{\sigma_F^2}\sum_j \mathrm{Re}\left\{|\Gamma(\omega_j)|^2 S_\eta(\omega_j)\Delta\omega \exp\left(i\left(\omega_j(t-t_0)-k_j(x-x_0)\right)\right)\right\}$$

$$\eta_{\text{New Force}} = \frac{\alpha_F}{\sigma_F^2}\sum_j \mathrm{Re}\left\{\Gamma^*(\omega_j) S_\eta(\omega_j)\Delta\omega \exp\left(i\left(\omega_j(t-t_0)-k_j(x-x_0)\right)\right)\right\}$$

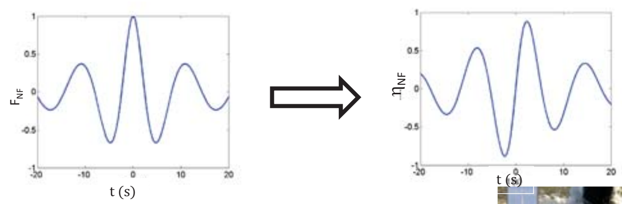

DeRisk – De-risking of ULS wave loads on offshore wind turbine structures

The New Force model – 2nd order contribution

$F^{(1)+(2)}=+F^{(1)}+F_M^{(2)}$

$$F_M^{(2)} = \rho\pi R^2 C_M \int_{-h}^{0} (u_t^{(2)} + u^{(1)}u_x^{(1)} + w^{(1)}u_z^{(1)})dz + \rho R C_D \int_{-h}^{0} u^{(1)}|u^{(1)}|dz$$
$$+\rho\pi R^2 (C_M-1)\int_{-h}^{0} (u^{(1)}w_z^{(1)})dz + \rho\pi R^2 C_M \eta_{NF}^{(1)} u_t^{(1)}.$$

Second order wave kinematics based on second order wave theory of Sharma and Dean (1981)

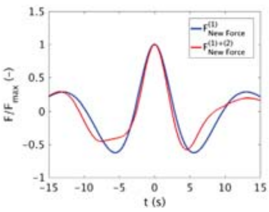

Exceedance probability distributions of the free surface elevation and force signal

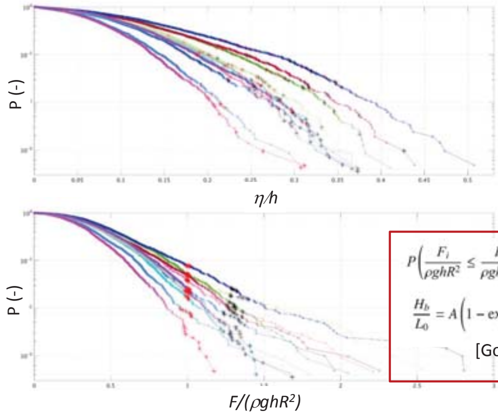

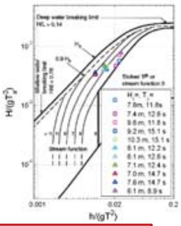

$$P\left(\frac{F_i}{\rho g h R^2} \le \frac{F}{\rho g h R^2}\right) = f_1\left(\frac{H_s}{gT_p^2}, \frac{h}{gT_p^2}\right)$$

$$\frac{H_b}{L_0} = A\left(1-\exp\left(-1.5\pi\frac{h}{L_0}\right)\right)$$

[Goda et al. 1976]

Model tests

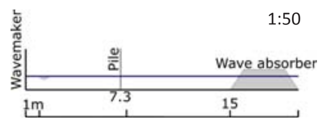

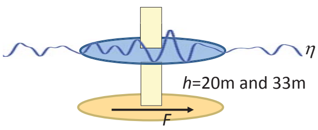

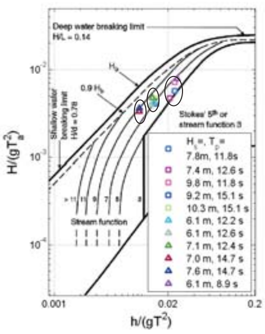

Exceedance probability distributions of the free surface elevation and force signal

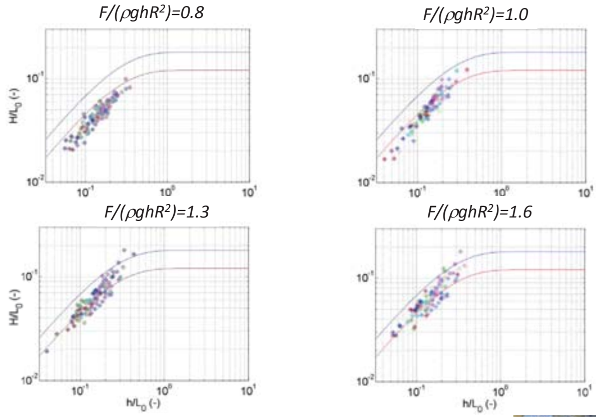

Exceedance probability distributions of the free surface elevation and force signal

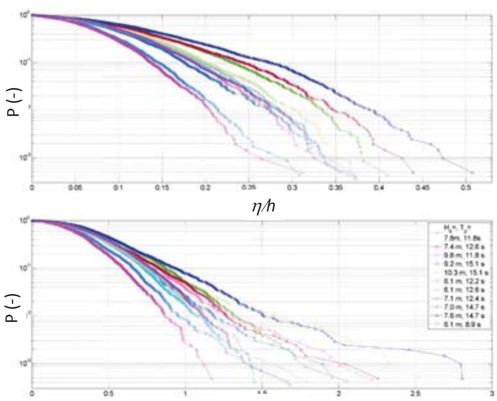

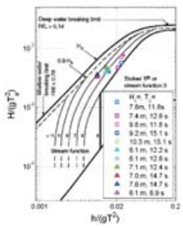

The average force shape

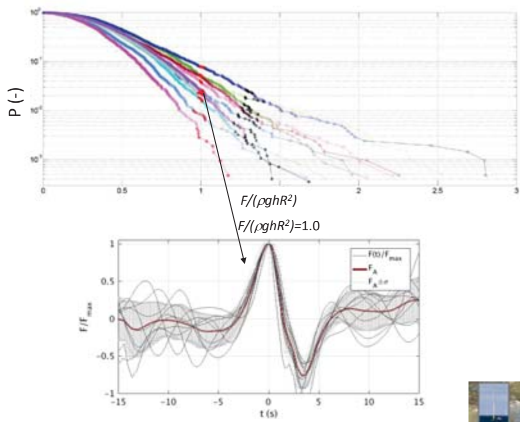

The average force shape

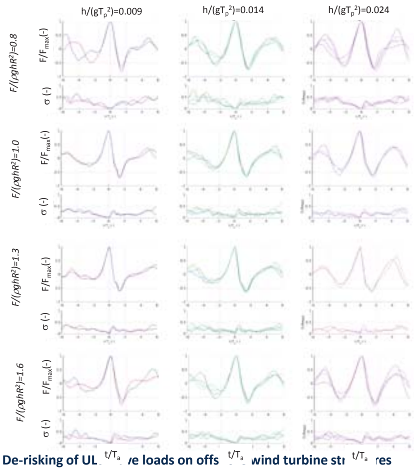

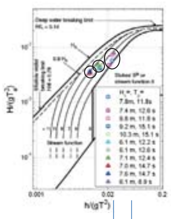

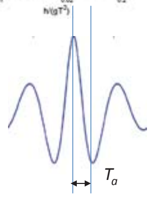

Thank you

sigs@dtu.dk

Acknowledgment

DeRisk is funded by a research project grant from Innovation Fund Denmark, grant number 4106-00038B. Further funding is provided by Statoil and the participating partners. All funding is gratefully acknowledged.

The average force shape

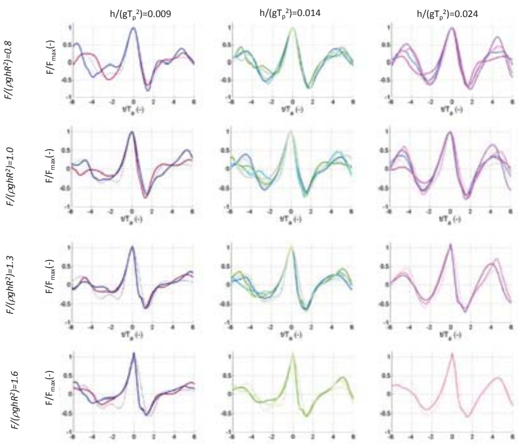

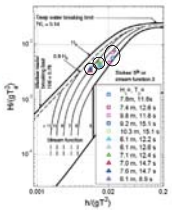

Conclusion

For the considered sea states

- The probability distributions of the force peaks are function of $F/(\rho ghR^2)$, $H_s/(gT_p^2)$, $h/(gT_p^2)$ → possible to estimate the probability distributions of the force peaks from stocastic variables of the sea states.

- The normalised force shapes are function of $F/(\rho ghR^2)$, $h/(gT_p^2)$, t/T_a.
- For moderate nonlinear waves The New Force model of second order predicts the shapes of well.

Planned future work

- To predict force shapes of more nonlinear waves, more advanced wave models should be used together with the New Force model.
- Include multidirectional waves in the analysis

E2) Installation and sub-structures

Fatigue Crack Detection for Lifetime Extension of Monopile-based Offshore Wind Turbines, L. Ziegler, Ramboll

Fabrication and installation constraints for floating wind and implications on current infrastructure and design, D. Matha, Ramboll

TELWIND- Integrated Telescopic tower combined with an evolved spar floating substructure for low-cost deep water offshore wind and next generation of 10 MW+ wind turbines, B. Counago, ESTEYCO SAP

RAMBØLL

DeepWind 2017
Trondheim: January 19th, 2017

AWESOME
PhD'S IN WIND POWER O&M

Fatigue crack detection for lifetime extension of monopile-based offshore wind turbines

Jutta Stutzmann[1,2], **Lisa Ziegler[3,4]**, Michael Muskulus[4]

[1] University of Stuttgart, Germany
[2] Chalmers University of Technology, Sweden
[3] Rambøll, Germany
[4] Norwegian University of Science and Technology

This project has received funding from the European Union's Horizon 2020 research and innovation programme under the Marie Sklodowska-Curie grant agreement No 642108

Agenda

1. Inspection of fatigue cracks
2. Simulation of fatigue cracks
3. How to link inspections and simulations: Bayes Theorem
4. Results: Reduction of uncertainty

AWESOME

Why lifetime extension?

- Design lifetime at least 20 years
- Lifetime extension possible if structural reserves are left
- Increases profit and reduces environmental impact

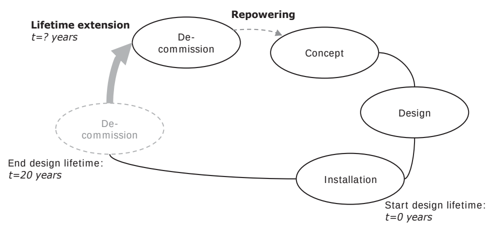

Inspection for fatigue cracks

- Probability of detection
  - Inspection method (eddy current, visual inspection,…)
  - Ease of access
  - Crack size

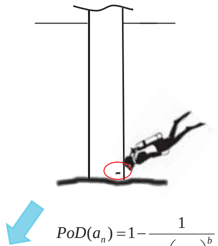

$$PoD(a_n) = 1 - \frac{1}{1 + \left(\frac{a_n}{X_0}\right)^b}$$

PoD parameters given in DNVGL RP-C210

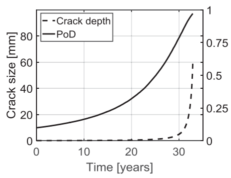

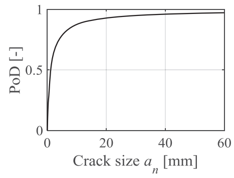

What do we need for lifetime extension?

We need to…

- keep the target safety level
- know structural reserves and remaining useful lifetime

This can be done by…

- analytical assessments
- practical assessments

Problems of inspections are…

- access
- safety risks
- costs
- detection uncertainty

➡ *Is it worth to do inspections?*

AWESOME

Simulation of fatigue cracks

- DeepWind 2016:
  Load sequence is negligible using Paris law
- Integration of Paris law now possible ☺

$$\frac{da}{dN} = C(\Delta K_I)^m \quad \text{with} \quad \Delta K_I = \Delta S Y \sqrt{\pi a}$$

$$CS^m \Delta N = \int_{a_0}^{a_n} \frac{da}{Y^m (a\pi)^m}$$

a : crack depth [mm]
N : number of cycles [-]
ΔK_I : stress intensity factor
ΔS : stress range [MPa]
Y : geometry factor [-]
C, m : material constants

- Variable amplitude loading
  ➡ bins of 1MPa

Simulation of fatigue cracks

- Why integration of Paris Law?
  - Because it is fast
- Why do we need it fast?
  - Monte Carlo Simulation

Monte Carlo Simulations

- Uncertainties: C, Y, a_0
- Deterministic loads from case study
- Distribution of crack size in year 20

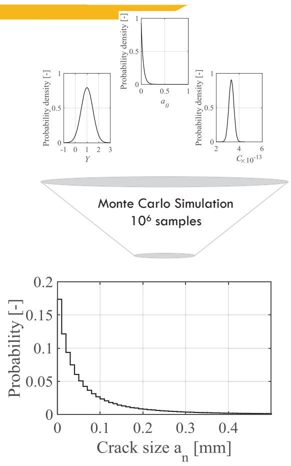

Simulation of fatigue cracks

- Why integration of Paris Law?
  - Because it is fast
- Why do we need it fast?
  - Monte Carlo Simulation

Monte Carlo Simulations

- Uncertainties: C, Y, a_0
- Deterministic loads from case study
- Distribution of crack size in year 20

Remaining useful lifetime

- Time until a_n reaches a_{fail}

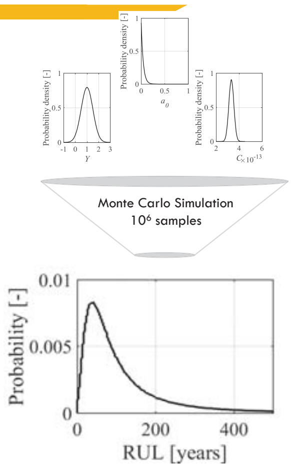

How to link inspections and simulations: Bayes Theorem

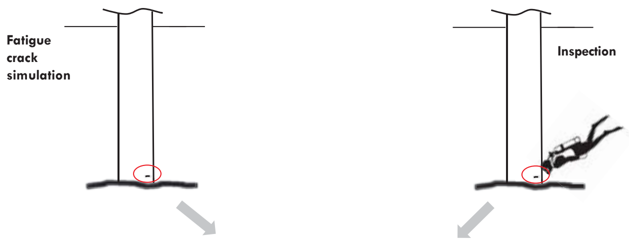

How to link inspections and simulations: Bayes Theorem

$$P(a_n \mid z) = \frac{P(a_n)P(z \mid a_n)}{P(z)}$$

$P(a_n)$: Probability of crack size a_n

$P(z \mid a_n)$: Probability of detection (POD)

P(z): Probability of inspection outcome

$$P(z) = \sum_{a_{min}}^{a_{max}} POD(a_n)P(a_n)$$

Inspection outcomes and Bayesian updating

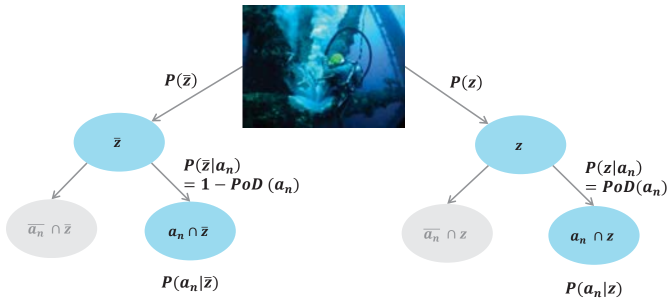

$P(a_n)$: Probability of crack size a_n

P(z): Probability of detection

$\bar{x}$: complement of x

$P(z \mid a_n)$: Probability of detection (POD)

$P(a_n \mid z)$: Updated probability of crack size

Results: Reduction of uncertainty

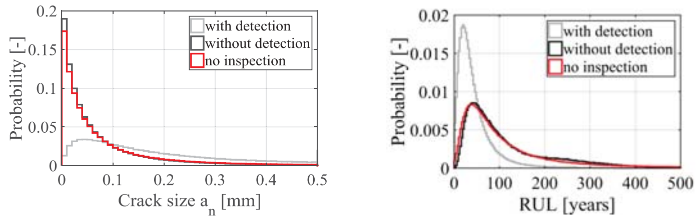

	Median crack size an [mm]	Median RUL [years]	Standard deviation RUL [years]
No inspection	0.04	78	446
With detection	0.20	33	47
Without detection	0.04	83	103

Results: Reduction of uncertainty

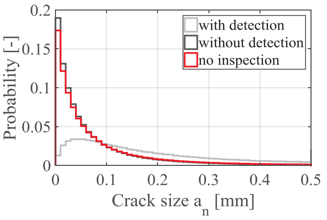

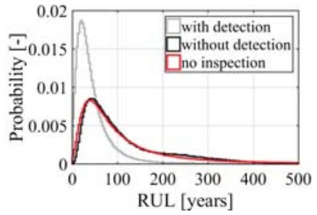

- Results influenced by tails of distribution
- Case with detection: 10% of RUL is below 10 years
- Case without detection: 10% of RUL is below 30 years
- Larger reduction of uncertainty in case of detection
- Individual results for every structural detail – Where is the hot spot?

AWESOME

AWESOME PHD'S IN WIND POWER O&M

- AWESOME = Advanced wind energy systems operation and maintenance expertise
- Marie Skłodowska-Curie Innovative Training Networks
- 11 PhD's
- O&M
  - Failure diagnostic and prognostic
  - Maintenance scheduling
  - Strategy optimization

www.awesome-h2020.eu

Conclusion

Inspections are costly and risky.
Is it worth to do it?

We showed the value of inspections is:
- Reduction of uncertainty
- Eliminate risks of large cracks

Conclusion:
- A trade-off between costs and benefits necessary!
- Is the safety level without inspections acceptable?
  ➡ Design fatigue factor of 3 = inspection free
- Alternative: Structural health monitoring

Lifetime extension – a future problem?

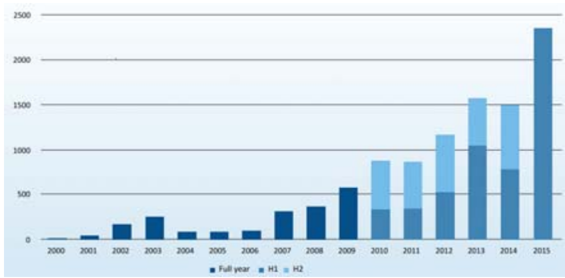

Annual installed offshore wind capacity in Europe (MW). Source: EWEA 2015.

Acknowledgements to Kolja Müller and Ursula Smolka for input and support on the study project.

AWESOME PHD'S IN WIND POWER O&M

Thanks for your attention

Lisa Ziegler
PhD researcher
lisa.ziegler@ramboll.com
+49 (0) 151 44 006 445

Rambøll Wind
Hamburg, Germany
www.ramboll.com/wind

RAMBOLL

Jutta Stutzmann
Student MSc Sustainable Energy
jutta@stutzmann.de
+49 (0) 160 81 34 855

University of Stuttgart
Chalmers University of Technology

Lifetime extension assessment

Analytical assessment
- Renewed simulations with focus on fatigue
- Calculate remaining useful lifetime

Practical assessment
- Inspections, maintenance history
- Foundations are one component
- Cracks as fatigue damage
- Other failure modes: corrosion, scour,…

Case study

- NREL 5MW and monopile from OC3 project
  (Nichols et al. 2009)
- Met-ocean data from Upwind project
  (Fischer et al. 2010)
- Fatigue load cases: power production, idling
- Structural response to aerodynamic and hydrodynamic loading (impulse-based substructuring)

➡ Simulation of fatigue crack growth with Paris law

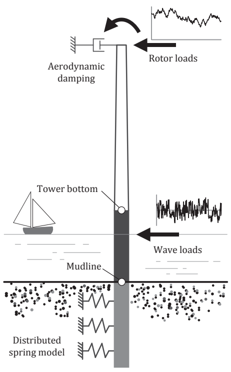

Model of offshore wind monopile.

Fabrication and installation constraints for floating wind and implications on current infrastructure and design

Denis Matha, Alexander Mitzlaff
Christopher Brons-Illing, Ron Scheffler
Ramboll

Qualification of innovative floating substructures for 10MW wind turbines and water depths greater than 50m

The research leading to these results has received funding from the European Union Horizon2020 programme under the agreement H2020-LCE-2014-1-640741.

INTRODUCTION

Floating Wind Projects
Already in planning phase [INNOSEA]:

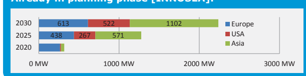

- Large offshore floating wind farm projects expected by 2025
- EU H2020 LIFES50+ scenario:
  - 10 MW Wind Turbine
  - 500 MW wind farms at 3 sites
- Fabrication and Installation Constraints need to be identified and addressed before large scale deployment

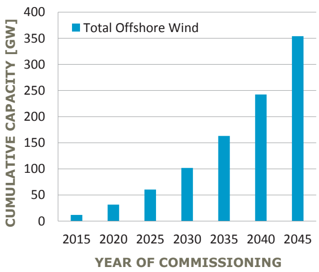

Forecast based on IRENA 2016, "INNOVATION OUTLOOK **OFFSHORE WIND**"

RAMBOLL 2

NOTE: All data/results present herein are generic/hypothetical and not related to LIFES50+ concepts from Olav Olsen, Iberdrola, Nautilus and Ideol

FABRICATION
STEEL

- Pre-fabrication
  - Typically in shipyards
  - Many ports do not provide capability
- Transport (if not in shipyard)
  - Accessibility to Cargo vessels, Rail, Road
  - Size restrictions
- Storage for mass production
  - Space required for pre-fabricated parts
  - Bearing capacity & weather restrictions
- Assembly
  - Dry dock or Quayside (water depth)
  - Bearing capacity & crane restrictions
  - Weather restrictions for welding

Photo – Principle Power, WindFloat 1

Photo – Navantia, Hywind Scotland

RAMBOLL 3

NOTE: All data/results present herein are generic/hypothetical and not related to LIFES50+ concepts from Olav Olsen, Iberdrola, Nautilus and Ideol

FABRICATION
CONCRETE

- *Precast*
  - *Concrete factory*
  - *No weather dependence*
  - *Transport to assembly port*
- In-situ
  - Local concrete plant or mobile batching plant
  - Weather restrictions apply (drying)
  - Longer production periods
  - Cast in one part
- Bearing capacity of construction site (for assembly crane and/or structure)

Photo by IDEOL
IDEOL Floatgen

Photo by MT Højgaard
Cranefree® Gravity foundation

RAMBOLL 4

NOTE: All data/results present herein are generic/hypothetical and not related to LIFES50+ concepts from Olav Olsen, Iberdrola, Nautilus and Ideol

FABRICATION
SUMMARY

Steel

Advantages	Challenges
• **Established** in the offshore wind industry: ○ Know-how existing ○ Proven solutions and standards exist to avoid issues related to corrosion due to saltwater and salty air, wind turbine load, etc. • **Assembly** can be executed **relatively fast** if components are pre-fabricated (consists of welding operations and positioning of the parts only) • **Lighter substructures** are possible (compared with concrete)	• Expensive material, **price fluctuating**, planning difficult • **Specialized equipment** (e.g. large scale welding machines and cranes with sufficient lift capacity) required, shipyard preferable • Large dimension **components/parts**: ○ Need to be built at shipyards/factories, typically not at construction site, which is a challenge for mass production ○ Heavy/large parts need to be transported to construction site, suitable access (road, railways, waterways) required ○ Suitable storage area at port required

RAMBOLL 5

NOTE: All data/results present herein are generic/hypothetical and not related to LIFES50+ concepts from Olav Olsen, Iberdrola, Nautilus and Ideol

FABRICATION
SUMMARY

Concrete

Advantages	Challenges
• **Concrete local supply** adaptable to local conditions and project requirements: ○ Ready-mix concrete ○ Mobile batching plant ○ Installation of a stationary batching plant at the construction site • **No specialized equipment**, like large scale welding machines, required (construction at lower costs) • **Low costs of concrete** as a raw material • Ready-mix concrete only: **less storage area required** (no raw material has to be stored for batching at port)	• **Limited use in offshore wind** industry • **(Often) larger dimensions of concrete floaters** require large construction area for mass production • **High weight of concrete floaters** (restrictions to the bearing capacity and space) • Concrete cannot bear **tension loads**, therefore additional procedures (e.g. pre-tensioning, avoiding of upending actions) necessary • Wide range of **weather restrictions** for construction/drying process (e.g.no construction during frost or heavy rain) • Mixing process at the construction site possibly more inaccurate (additional quality assurance necessary)

RAMBOLL 6

NOTE: All data/results present herein are generic/hypothetical and not related to LIFES50+ concepts from Olav Olsen, Iberdrola, Nautilus and Ideol

LIFES50+ SITES
RELEVANT PORTS

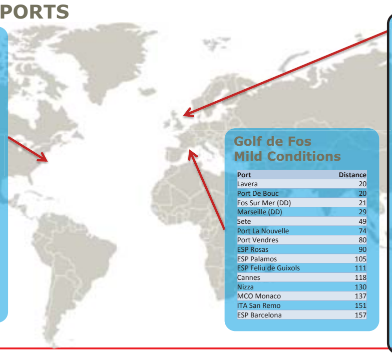

Gulf of Maine
Medium Conditions

Port	Distance
Port Clyde	23
Bath	28
Yarmouth	33
Portland	35
Rockland	42
Belfast	58
Bucksport	71
Bar Harbor	79
Gloucester	82
Bangor	85
Salem	90
Boston (DD)	102
Provincetown	104
Plymouth	110
Sandwich	118
Eastport	139
Hyannis Harbor	140
Nantucket Harbor	140
CAN Yarmouth	143
CAN Port Maitland	145
CAN Meteghan	147
CAN Beaver Harbor	150
Oak Bluff	151
CAN Bayside	154
CAN Weymouth	159

Golf de Fos
Mild Conditions

Port	Distance
Lavera	20
Port De Bouc	20
Fos Sur Mer (DD)	21
Marseille (DD)	29
Sete	49
Port La Nouvelle	74
Port Vendres	80
ESP Rosas	90
ESP Palamos	105
ESP Feliu de Guixols	111
Cannes	118
Nizza	130
MCO Monaco	137
ITA San Remo	151
ESP Barcelona	157

West of Barra
Severe Conditions

Port	Distance
Castlebay	18
Lochboisdale	35
Lochmaddy	62
Mallaig	69
Lochaline	75
Glensanda	87
Kyle of Lochalsh	87
Kishorn	88
Crinan Canal	94
Port Askaig	94
Coleraine	100
Loch Gairloch	100
Arnish	105
Stornoway	106
Corpach	107
IRL Rathmullen	110
IRL Moville	112
Port Ellen	114
IRL Burtonport	117
Londonderry	121
Ullapool	121
Campbeltown	130
Carnlough	132
Larne	141
Cairnryan	152
Girvan	152
IRL Killybegs	152
Kilroot	154
Stranraer	156
Belfast (DD)	159

RAMBOLL

7

NOTE: All data/results present herein are generic/hypothetical and not related to LIFES50+ concepts from Olav Olsen, Iberdrola, Nautilus and Ideol

STORAGE SPACE AND SIMULTANEOUS INSTALLATION
CHALLENGES

Kishorn
- Former fabrication of O&G platforms
- Heavy lift capacities
- Quays: 3.5m - 10m depth 80m & 120m length
- Dry-dock: 8m (LAT), 12m (HAT) 150m gate
- Concrete casting facility on site

Challenges for 10MW Floating + Simultaneous Installation
- Significant space limitations
- No cranes

>> Significant investments in infrastructure is likely required

RAMBOLL

10

NOTE: All data/results present herein are generic/hypothetical and not related to LIFES50+ concepts from Olav Olsen, Iberdrola, Nautilus and Ideol

STORAGE SPACE AND SIMULTANEOUS INSTALLATION
INVESTIGATED PORTS

Well-suited, high potential manufacturing ports with short distance to LIFES50+ Site C:

Arnish (Distance: 105 NM)

Kishorn (Distance: 88 NM)

RAMBOLL

8

NOTE: All data/results present herein are generic/hypothetical and not related to LIFES50+ concepts from Olav Olsen, Iberdrola, Nautilus and Ideol

INSTALLATION
SUMMARY

Start
Substructure and wind turbine at construction/launch site

Dep. on distance

8h – 55h

Float Out (Tide)
Hook up of harbor tug boats; Float out from construction/launching site; Ballasting of substructure (and removing of temporary buoyancy modules, if used); Dis- and reconnecting of towing lines to sea-going tugs; Towing of the floater towards open sea

11h

Transit (Hs 2.5m)
Transit to wind farm; Positioning of floater at exact position (dynamic positioning); Deployment of teams onto floater

11h

Installation (Hs 1.5m)
Work preparation for installation (including power supply); Anchor Supply Vessel takes over messenger line; Messenger and mooring line pulled in; Mooring handed over to floater; Pre-tensioning of mooring, locked by chain stoppers; Ballasting

22h

Dynamic Cable Installation (1.5m)
Positioning of Cable Lay Vessel/or other suitable vessel; Crew transfer and work preparation; Cable inspection and pick up of messenger line; Pull in of cable; Installation of temporary security modules (e.g. hang off clamp) for connection; Tests to confirm the functionality

Termination (1.5m)
Crew transfer and work preparation; Removing armoring, preparation of conductors; Cable connection, test preparation and conduct; Permanent hang off; Clean up and disembarking

Dep. on distance

Return
Transit back to coast and port; Unload of equipment

RAMBOLL

11

NOTE: All data/results present herein are generic/hypothetical and not related to LIFES50+ concepts from Olav Olsen, Iberdrola, Nautilus and Ideol

STORAGE SPACE AND SIMULTANEOUS INSTALLATION
CHALLENGES

Arnish (Distance: 105 NM)
- Former oil and gas fabrication
- 80t/m² heavy lift
- In redevelopment for fabrication of jacket subcomponents

Challenges for 10MW Floating + Simultaneous Installation
- Quay length 100m (+200m)
- Space 48ha (10ha developed)
- Water depth 6.5m (intended to 8,5-9m depth)
- No large cranes

>> Significant investments in infrastructure is likely required

>> Belfast with shipyard (156nm)

RAMBOLL

9

NOTE: All data/results present herein are generic/hypothetical and not related to LIFES50+ concepts from Olav Olsen, Iberdrola, Nautilus and Ideol

INSTALLATION
ANALYSIS METHOD

SETUP

SITE Setup
- Site Selection
- Port Selection
- Minimum Weather Window

PROJECT Setup
- Vessel Types
- Vessel Numbers
- Vessel Properties
- Project Data
  - Starting Dates
  - Dimensions

CALCULATION

DATABASES
- Vessel Properties
- Weather Data
- Port Properties
- Work Break-Down

CALCULATION
- Required Time
  - Weather Window
  - Installation Time
- Estimated Costs
  - Use of Vessels

RESULTS

REQUIRED TIME
- Site/Port-specific
- One FOWT and whole Farm
- Operational Time and Stand-by Time

ESTIMATED COSTS
- Indicative Results
- Fixed Costs and Variable Costs

RAMBOLL

12

NOTE: All data/results present herein are generic/hypothetical and not related to LIFES50+ concepts from Olav Olsen, Iberdrola, Nautilus and Ideol

INSTALLATION
LIMITATIONS OF ANALYSIS METHOD

- Limitations
  - Generic installation non-optimized procedure assumed
    >> with real substructures differences are expected
  - Weather persistence data was estimated and no accurate persistence data available for all 3 sites
  - Vessel cost fluctuation is high
    >> influences the conclusions on key aspects
  - No consideration of availability of vessels
    >> only possible in commercial setting with specific timelines
  - Calculation is static and not suited for short term planning
    >> here time-domain Installation/O&M planning tools are required

RAMBØLL

13

NOTE: All data/results present herein are generic/hypothetical and not related to LIFES50+ concepts from Olav Olsen, Iberdrola, Nautilus and Ideol

INSTALLATION
PORT LOCATION

Port Distance & Towing speed

Scenario
Site C (West of Barra)

- Option 1:
  Max. Towing Speed = 3 NM/h
- Option 2:
  Max. Towing Speed = 8 NM/h
- ***4 FOWT installed simultaneously***

- **Minor influence of towing speed**
- **Large influence of distance to port**
- **50 Floaters in 4m required!**

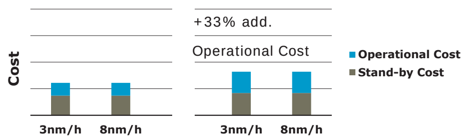

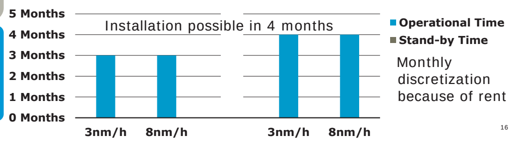

RAMBØLL

16

NOTE: All data/results present herein are generic/hypothetical and not related to LIFES50+ concepts from Olav Olsen, Iberdrola, Nautilus and Ideol

INSTALLATION
ASSUMPTIONS

Vessel [Abbreviation]	[Name]	Bollard Pull	[Figs. By DAMEN]	Fix Costs [average €/d]	Variable Costs [average €/d]
HT	Harbor Tug	BP: 40 t		7000	1000
AHTS-280BP	Anchor Handling Tug Supply Vessel (A-Type)	BP: 280 t		130000	20000
AHTS-180BP	Anchor Handling Tug Supply Vessel (C-Type)	BP: 180 t		64000	6000
AHTS-85BP	Anchor Handling Tug/ Offshore Supply Vessel	BP: 85 t	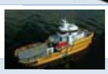	36000	4000
OT-80BP	Offshore Tug	BP: 80 t		17000	3000
OT-50BP	Offshore Tug	BP: 50 t		8500	1500
CTV	Crew Transfer Vessel			3000	500
(CLV)	Cable Lay Vessel			55000	5000

Strong variation in fixed costs

RAMBØLL

14

NOTE: All data/results present herein are generic/hypothetical and not related to LIFES50+ concepts from Olav Olsen, Iberdrola, Nautilus and Ideol

INSTALLATION
WEATHER WINDOWS

Installation Start & Weather at Site

Scenario
Distance Port to Windfarm approx. 70 NM

- Option 1:
  Operation start in January
- Option 2:
  Operation start in May
- *3 FOWTs installed simultaneously*

- **Start of Operation more important for severe weather sites**
- **Major influence of Site (Weather Windows)**
- **No securing for floaters**

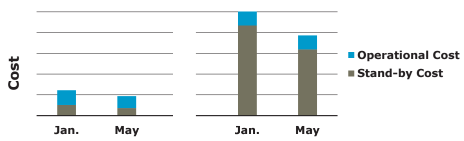

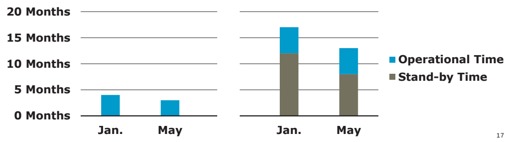

RAMBØLL

17

NOTE: All data/results present herein are generic/hypothetical and not related to LIFES50+ concepts from Olav Olsen, Iberdrola, Nautilus and Ideol

INSTALLATION
PORT LOCATION

Port Distance & Towing speed

Scenario
Site C (West of Barra)

- Option 1:
  Max. Towing Speed = 3 NM/h
- Option 2:
  Max. Towing Speed = 8 NM/h
- ***1 FOWT installed simultaneously***

- **Towing speed important for small fleets and large distance**
- **Considerable influence of dist., but more weather dominated**

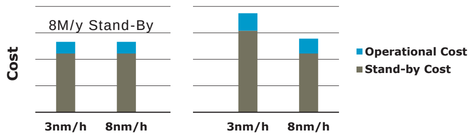

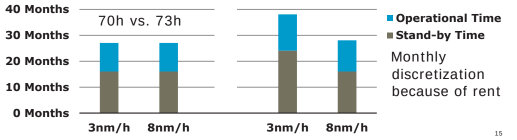

RAMBØLL

15

NOTE: All data/results present herein are generic/hypothetical and not related to LIFES50+ concepts from Olav Olsen, Iberdrola, Nautilus and Ideol

INSTALLATION
FLEET SIZE

Fleet Size & Req. Vessels

Scenario
Site B (Gulf of Maine)
70 NM distance

- Option 1:
  Req. number of Vessels x2
- Option 2:
  Regular Number of Vessels
- Operation starts in May

- **Usage of more fleets decreases primarily time**
- **Vessel requirements have large influence on cost >> Optimization potential for floaters**

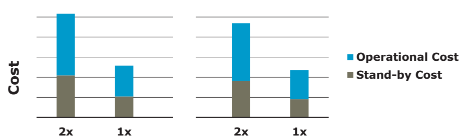

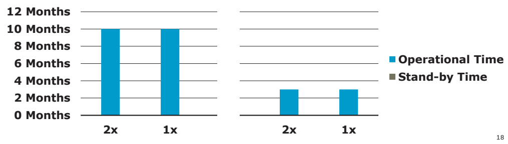

RAMBØLL

18

NOTE: All data/results present herein are generic/hypothetical and not related to LIFES50+ concepts from Olav Olsen, Iberdrola, Nautilus and Ideol

INSTALLATION
SUMMARY

- Installation Port
  - Major influence of distance -> Transit times & Cost
  - Towing speed important for small fleets and large distance
  - More fleets massively improve cost and time -> Req. fast supply of floaters
  - Min. requirements for selection: Water Depth, Fabrication, Cranes, Space & Bearing Capacities
- Weather Windows
  - Start of Operation more important for severe weather sites
  - Major influence of Weather Windows if distance to port is high
  - Forecasts more important: Challenging to secure structures in case of bad weather (no jack-up)
- Required Vessels and Fleet Size
  - Usage of more fleets decreases primarily time
  - Vessel requirements have large influence on cost -> Optimization potential for floaters

RAMBOLL

NOTE: All data/results present herein are generic/hypothetical and not related to LIFES50+ concepts from Olav Olsen, Iberdrola, Nautilus and Ideol

OUTLOOK
RECOMMENDATIONS & NEXT STEPS IN LIFES50+

Recommendations for large wind farm projects at specific sites:

- Early involvement of manufacturer & early review of installation port restrictions
- Selection of port is of high importance
- Adapt design to capabilities of manufacturer, port and installation procedure

Next steps Phase 2 of LIFES50+:

- Detailed analysis of fabrication and installation procedures of selected designs
- Usage of the tool for installation (&fabrication) strategy optimization (automatic)
- Support to designers in detailing the F&I processes for the LIFES50+ sites and 50 unit wind farms
- Extension of analysis beyond installation to O&M phase

RAMBOLL

NOTE: All data/results present herein are generic/hypothetical and not related to LIFES50+ concepts from Olav Olsen, Iberdrola, Nautilus and Ideol


EERA DeepWind
Deep Sea Offshore Wind R&D Conference
TELWIND: Evolved Spar combined with telescopic tower
ESTEYCO
TELWIND
PROJECT
TELWIND: funded by the European Union's Horizon 2020 research and innovation programme under grant agreement No 654634
TELWIND-WP8-PPT-TD-002 Status: In Progress Preliminary Checked Issued


Main Objectives
ESTEYCO ENERGIA
TELWIND BACKGROUND: THE TELESCOPIC TOWER
TELWIND TECHNOLOGY
MAJOR FINDINGS
EERA Deepwind. Trondheim 2017
2


INDEX
1. ESTEYCO WHO WE ARE
2. BACKGROUND: THE TELESCOPIC TOWER TECHNOLOGY
3. TELWIND FUNDAMENTALS
4. SEAKEEPING & TANK TESTING
5. CHALLENGES & NEXT STEPS
ESTEYCO
TELWIND
PROJECT
EERA DeepWind
Deep Sea Offshore Wind R&D Conference
3

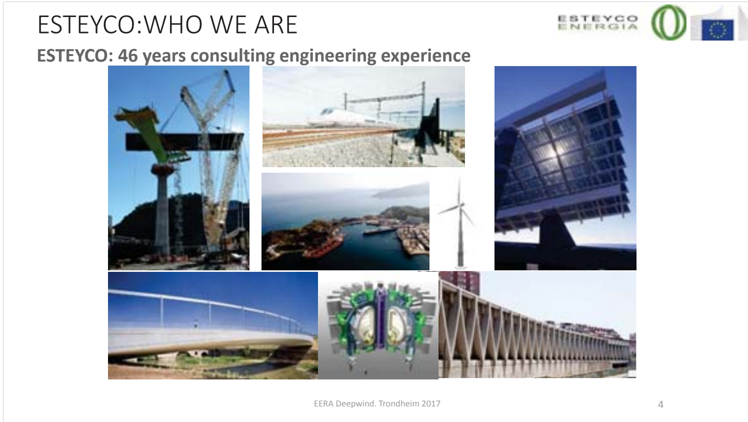
ESTEYCO:WHO WE ARE
ESTEYCO ENERGIA
ESTEYCO: 46 years consulting engineering experience
EERA Deepwind. Trondheim 2017
4


ESTEYCO:WHO WE ARE
ESTEYCO ENERGIA
Evolution to Renewable Energy
Leaders in civil works in wind energy sector
EERA Deepwind. Trondheim 2017
5

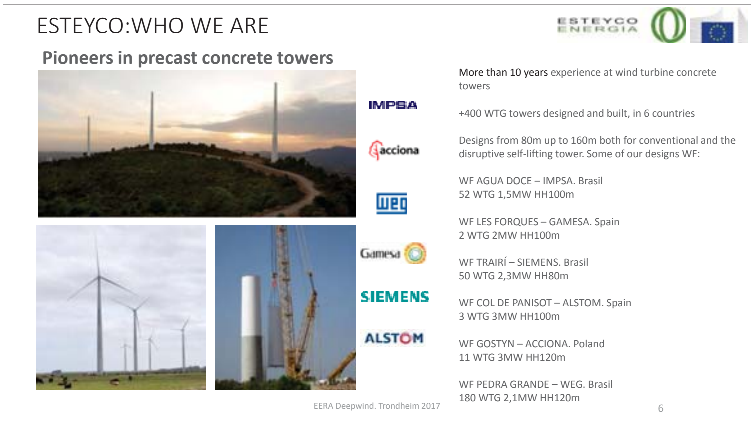
ESTEYCO:WHO WE ARE
ESTEYCO ENERGIA
Pioneers in precast concrete towers
IMPSA
acciona
WEG
Gamesa
SIEMENS
ALSTOM
More than 10 years experience at wind turbine concrete towers
+400 WTG towers designed and built, in 6 countries
Designs from 80m up to 160m both for conventional and the disruptive self-lifting tower. Some of our designs WF:
WF AGUA DOCE – IMPSA. Brasil
52 WTG 1,5MW HH100m
WF LES FORQUES – GAMESA. Spain
2 WTG 2MW HH100m
WF TRAIRÍ – SIEMENS. Brasil
50 WTG 2,3MW HH80m
WF COL DE PANISOT – ALSTOM. Spain
3 WTG 3MW HH100m
WF GOSTYN – ACCIONA. Poland
11 WTG 3MW HH120m
WF PEDRA GRANDE – WEG. Brasil
180 WTG 2,1MW HH120m
EERA Deepwind. Trondheim 2017
6

INDEX

1. ESTEYCO WHO WE ARE
2. **BACKGROUND: THE TELESCOPIC TOWER TECHNOLOGY**
3. TELWIND FUNDAMENTALS
4. SEAKEEPING & TANK TESTING
5. CHALLENGES & NEXT STEPS

TELWIND PROJECT

EERA DeepWind
Deep Sea Offshore Wind R&D Conference

THE TELESCOPIC TOWER

VIDEO-H2020 ELISA/ELICAN- 5MW GBS-TOWER ASSEMBLY JANUARY 2017

THE TELESCOPIC TOWER

VIDEO- CONSTRUCTIVE PROCESS FULL SCALE PROTOTYPE. MADRID. SPAIN. Mar – Oct 2014

THE TELESCOPIC TOWER

ELISA/ELICAN 5MW GBS + TELESCOPIC TOWER

DEMONSTRATION PROJECT IN PLOCAN. GRAN CANARIA. SPAIN. Sept15– May17 (Expected)

THE TELESCOPIC TOWER

ONSHORE-FULL SCALE PROTOTYPE OF THE TELESCOPIC TOWER

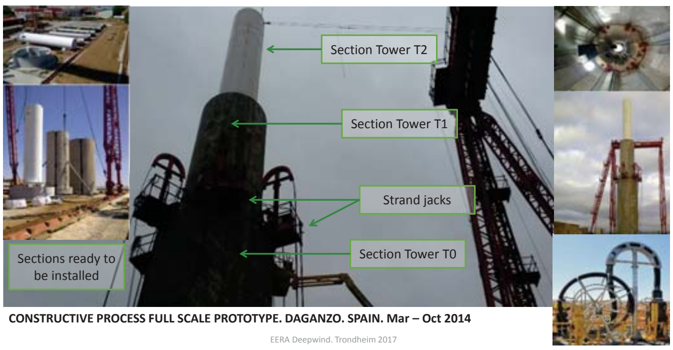

CONSTRUCTIVE PROCESS FULL SCALE PROTOTYPE. DAGANZO. SPAIN. Mar – Oct 2014

INDEX

1. ESTEYCO WHO WE ARE
2. **BACKGROUND: THE TELESCOPIC TOWER TECHNOLOGY**
3. **TELWIND FUNDAMENTALS**
4. SEAKEEPING & TANK TESTING
5. CHALLENGES & NEXT STEPS

TELWIND PROJECT

EERA DeepWind
Deep Sea Offshore Wind R&D Conference

TELWIND FUNDAMENTALS

FUNDAMENTALS

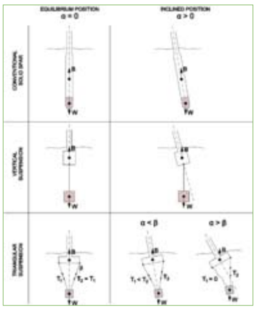

MAIN COMPONENTS

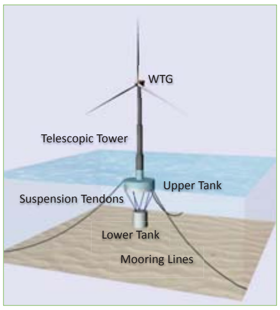

PRELIMINARY DESIGN

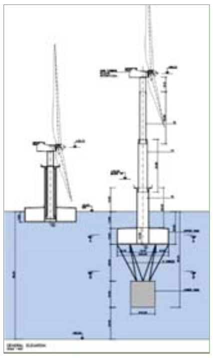

Parameter	Value	
Wind Turbine	5	MW
Water depth	80	m
Hub Height above MSL	86	m
Nacelle Weight	273	t

Parameter	Value	
Overall Draft	60	m
Upper Tank draft	20.50	m
Upper Tank diameter	32.00	m
Lower Tank diameter	15.35	m
Metacentric height inplace (GM)	>3m	m
Metacentric height transport (GM)	>2m	m
Tilt static angle (θ_{STA})	<10º	º
Overall heave period (T3)	>30s	s
Overall pitch period (T5)	>35s	s

TECHNOLOGY DEVELOPMENT & DEMONSTRATION

H2020 TELWIND PROJECT: Integrated telescopic tower and evolved spar floating substructure for low-cost deep offshore wind and next generation of 10MW+ turbines

EU Contribution: **3,498,530.00 €**

Consortium: **Esteyco**, ALE Heavylift R&D, ACS-Cobra, CEDEX, Dywidag Systems International, Mecal WTD, TUM, UC-IHC.

EU Horizon 2020 – Low Carbon Energy Call LCE-2015
Number of Proposals vs. Evaluation (Phase 1)

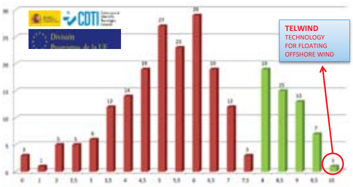

ESTEYCO is also currently collaborating with DNVGL in the project:

JOINT INDUSTRY PROJECT (JIP)
COUPLED ANALYSIS OF FLOATING WIND TURBINES

INSTALLATION STORYBOARD

Transport configuration. Preferred alternative-Multi tow configuration (work in progress)

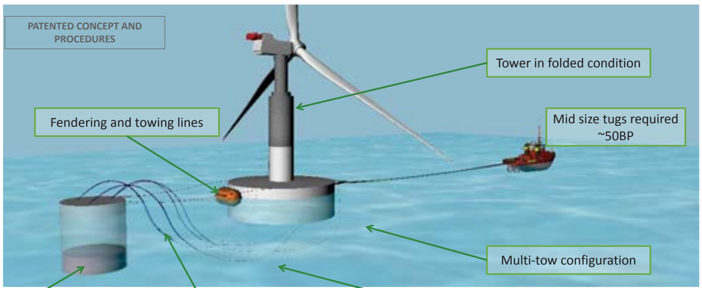

MAIN OBJECTIVES

- Design a 5MW WTG from conceptual to detail-constructive engineering.
- Study the concept **scalability** for a 12 MW WTG.
- Build a **fully coupled aero-hydro-servo-elastic** Floating Wind Turbine model and investigate coupling effects in the overall wind turbine performance
- **Model Basin Tests** in operating, extreme and installation conditions
- Perform **laboratory tests** to study the performance of the suspension **tendons**
- **CapEx and OpEx** estimate. **Viability** analysis of a single installation and integration in a multi-megawatt floating wind farm
- Obtain the **Certification** of the design
- Project **dissemination** in general and technical forums and conferences

INSTALLATION STORYBOARD

Offshore Installation

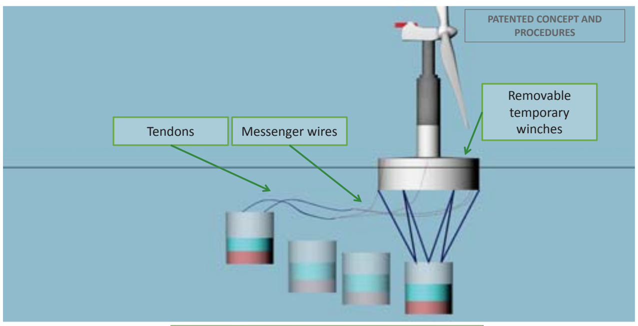

LT CONTROLLED BALLASTING & SINKING

INSTALLATION STORYBOARD

Offshore Installation

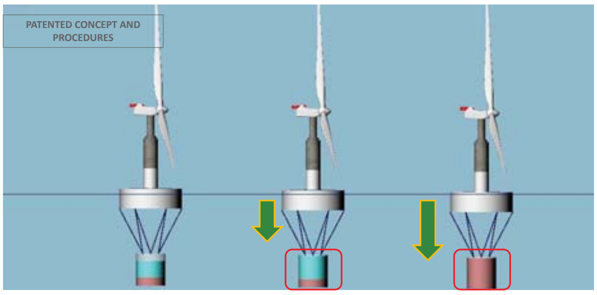

Final Pull in and fine adjustment of tendons
Progressive ballasting of LT internals

LT Fully flooded.
Tendons in position

Solid Ballast
Installation

INSTALLATION STORYBOARD

Offshore Installation

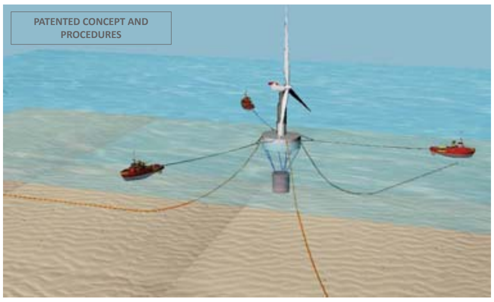

Mooring Installation

INSTALLATION STORYBOARD

Offshore Installation

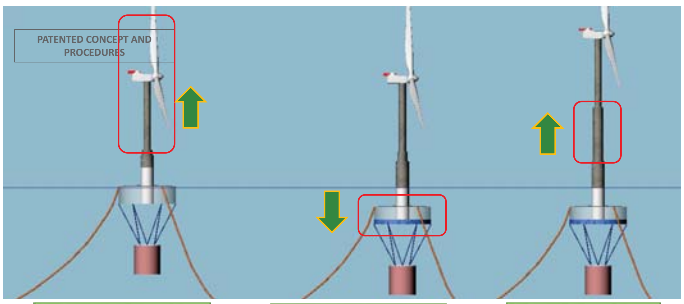

Jacking up tower first section (T2)

UT ballasting until targeted position

Jacking up tower second section (T1)

INSTALLATION STORYBOARD

Offshore Installation

PATENTED CONCEPT AND PROCEDURES

JOINTS termination. Removal of equipment (strand jacks, generators, power packs etc)
WTG Comissioning.
Platform inplace

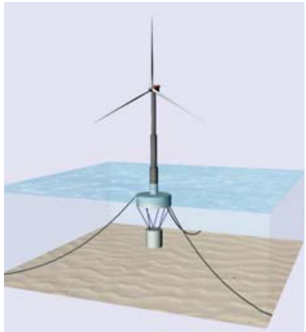

INDEX

1. ESTEYCO WHO WE ARE
2. BACKGROUND: THE TELESCOPIC TOWER TECHNOLOGY
3. TELWIND FUNDAMENTALS
4. **SEAKEEPING & TANK TESTING**
5. CHALLENGES & NEXT STEPS

TELWIND PROJECT

PROJECT TODAY

IHCantabria tank testing facilities

- Two tank testing campaigns expected
- IHCANTABRIA has extensive experience on floating platforms and singular floating devices
  - http://www.ihcantabria.com/es/
  - http://ccob.ihcantabria.com/
  - https://vimeo.com/183657521
- OBJECTIVES
  - Proof of TELWIND fundamentals: solidary motion between LT and UT
  - To quantify Hydrodynamic Damping
  - RAO´s
  - Response in irregular waves
  - First test for coupling wind (multifan) + waves

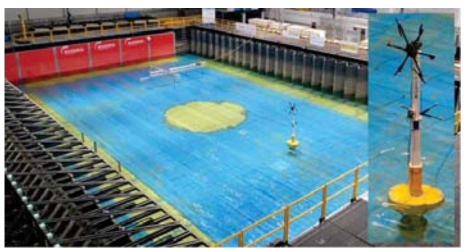

PROJECT TODAY
TELWIND SCALED MODEL

Basin tests performed during first campaign

- Dry characterization tests
- Basin characterization tests
- Wave only tests
- Wind only tests
- Current only tests
- Wave + wind tests
- Wave + wind + current tests

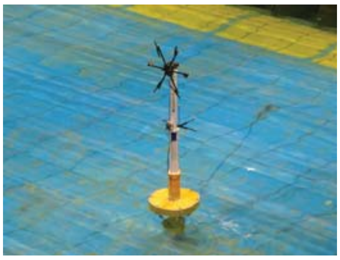

First set of results expected by end of Jan-2016

TIME DOMAIN SOLUTIONS

Preliminary pitch motion time series

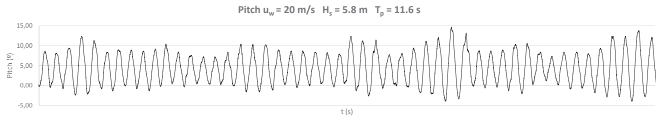

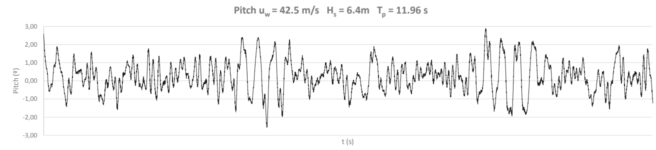

FREE DECAY TESTS

Preliminary decay tests of pitch and heave DOFs with mooring

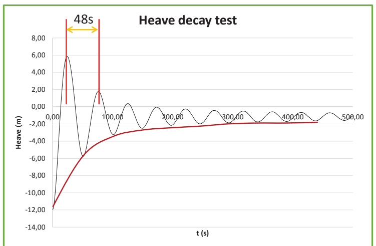

Heave

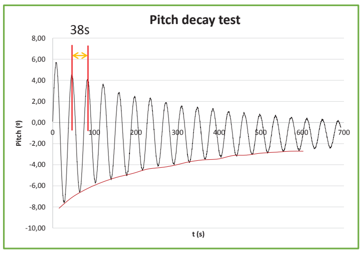

Pitch

TIME DOMAIN SOLUTIONS

Accelerations X-direction at the naccelle

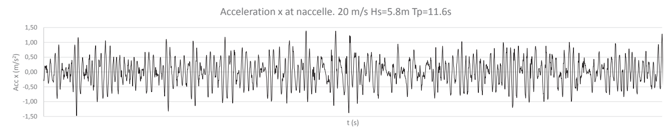

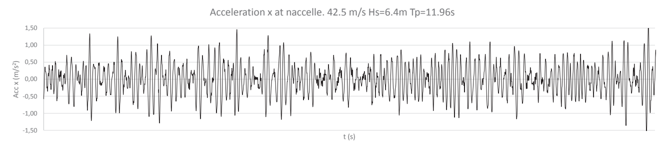

RESPONSE AMPLITUDE OPERATORS (RAO´s)

Preliminary RAOs of heave and pitch DOF´s

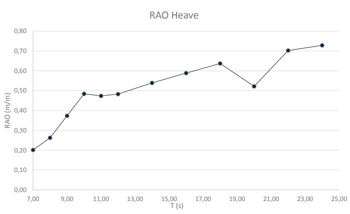

Heave

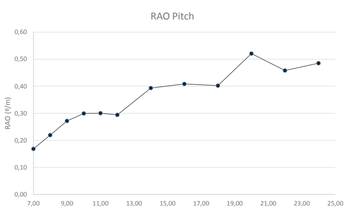

Pitch

A FEW DEMONSTRATIVE VIDEOS

Videos

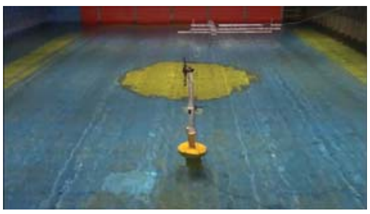

PARKED
PLOCAN 50 yr storm-ULS H_s = 6.4 m T_p = 11,96 m

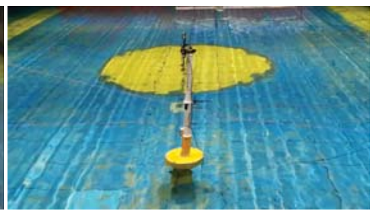

OPERATING
PLOCAN extreme operating conditions
U_w = 20 m/s H_s = 5,8 m T_p = 11,6 s

COMING SOON…

Next remarkable steps

WP2 ESTEYCO
- Design Basis Final Version
- Design certification
- Active Ballast system design
- Scalability to 12MW WTG

WP3 MEC-IHC
- Calibration of Numerical models based on tank testing results
- Ad hoc WTG control for TELWIND floating platform

WP4 ESTEYCO-DSI
- Laboratory tests campaign
- Detailed definition of connections and guides
- Tendon Fatigue design

WP5 IHC
- Optimization of mooring system
- Selection of anchoring

WP6 ESTEYCO-CEDEX
- Installation method statements
- Installation storyboards

WP7 IHC-CEDEX
- Installation tank tests
- Full implementation of software in the loop (SiL) strategy during the second test campaign

WP8 COBRA-ESTEYCO
- CapEx and OpEx estimate for a large scale wind farm
- Financial Model-Feasibility Analysis
- Set up a commercial business plan based on the feasibility analysis

CONCLUSIONS

TELWIND BACKGROUND: THE TELESCOPIC TOWER
- Proven technology
- WTG fully assembled onshore
- No HLV and Jack up required

TELWIND TECHNOLOGY
- Spar type solution
- Solidary motions between LT and UT
- Cost savings: material and installation

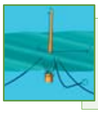

MAIN FINDINGS
- Tank tests alligned with numerical models and telwind fundamentals
- Very good response in waves

TELWIND: funded by the European Union´s Horizon 2020 research and innovation programme under grant agreement No 654634

F) Wind farm optimization

Influence of turbulence intensity on wind turbine power curves, L.M. Bardal, NTNU

A test case of meandering wake simulation with the Extended-Disk Particle model at the offshore test field Alpha Ventus, J. Trujillo, University of Oldenburg

A comprehensive multiscale numerical framework for wind energy modelling, A. Rasheed, SINTEF ICT

Application of a Reduced Order Wind Farm Model on a Scaled Wind Farm, J. Schreiber, Technische Universität München

Influence of turbulence on wind turbine power curves

-Experimental evaluation of IEC 61400-12-1 CD1 Annex M

Lars Morten Bardal
Department of Energy and Process Engineering
Norwegian University of Science and Technology

24.01.2017

2

Outline

- Background
- Measurement site and methods
- Results
- Summary and conclusion

3

Turbulence influence on a power curve

- Time averaging of non-linear function
- Direct aerodynamic influence on rotor performance

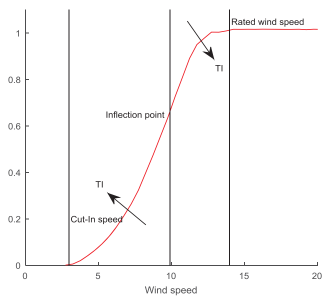

4

Taylor series expansion around $\bar{v}$

$$P(v) = P(\bar{v}) + \frac{1}{2}\frac{dP}{dv}\bigg|_{\bar{v}}(v-\bar{v}) + \frac{1}{2}\frac{d^2P}{dv^2}\bigg|_{\bar{v}}(v-\bar{v})^2 + \cdots$$

and averaging

$$\overline{P(v)} = P(\bar{v}) + \frac{1}{2}\frac{d^2P}{dv^2}\bigg|_{\bar{v}}\sigma_v{}^2 + \cdots$$

5

Standards for performance testing of wind turbines

- IEC 61400-12-1 1.ed (2005)
  - Site dependent
    - Wind shear
    - Wind veer
    - Turbulence intensity
  - 10 minute averaging period
- IEC 61400-12-1 2.ed (exp. Feb 2017)
  - Equivalent wind speed addresses wind shear and veer
  - Remote sensing wind speed measurement
  - Zero turbulence power curve normalization addresses turbulence and time averaging

6

Zero turbulence power curve

IEC 61400-12-1 2.ed CD Annex M

Normalize measured power curve to zero turbulence conditions

⇩

Simulate new power curve for different turbulence conditions assuming a gaussian wind speed distribution

$$\overline{P_{sim}(v)} = \int_{v=0}^{\infty} P_{TI=0}(v) f(v) dv$$

Mainly addresses effect of 10-minute averaging

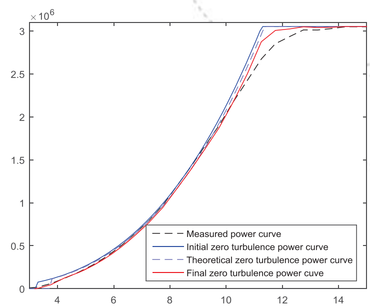

7

Valsneset wind turbine test site

NTNU Det skapende universitet

www.ntnu.no

8

Valsneset wind turbine test site

NTNU Det skapende universitet

www.ntnu.no

9

Valsneset wind turbine test site

NTNU Det skapende universitet

www.ntnu.no

10

Measurements

- IEC 61400-12-1 1.ed with modifications
- Leosphere Windcube v2 lidar
  - 3D from wind turbine
  - Wind speed, wind direction and turbulence intensity*
- 3MW wind turbine
  - Pitch regulated HAWT
  - Hub height: 92 meters
  - Rotor diameter: 100,6 meters
  - Direct drive
  - Net electrical power, status, air temperature
- Short met-mast
  - Air pressure
  - Verification of lidar measurements

*Turbulence measurement with a lidar involves high uncertainty for small time scales

NTNU Det skapende universitet

www.ntnu.no

11

Valsneset wind turbine test site

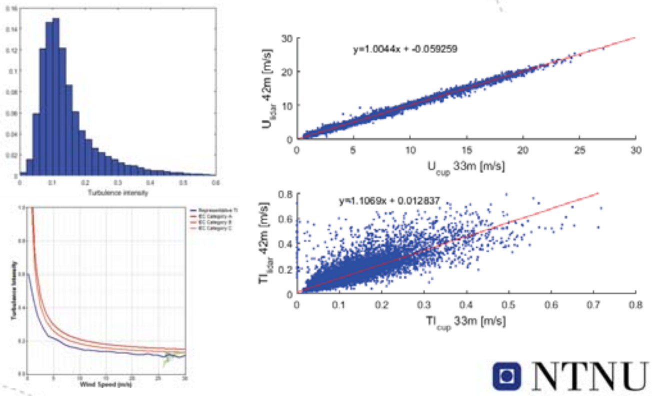

NTNU Det skapende universitet

www.ntnu.no

12

Results – TI and power

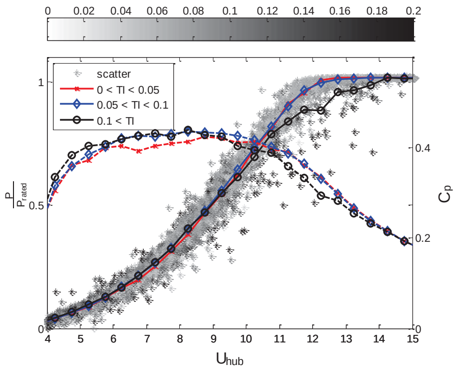

NTNU Det skapende universitet

www.ntnu.no

13

Results – Turbulence normalization: High TI to low TI

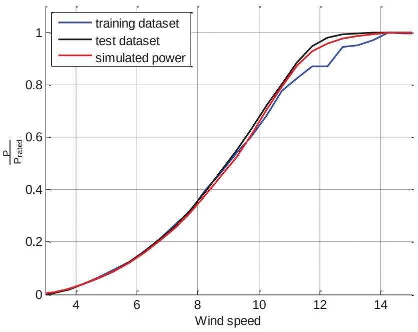

Training dataset: TI > 10%
Test dataset: TI < 10%

NTNU Det skapende universitet

14

Results – Turbulence normalization: Low TI to high TI

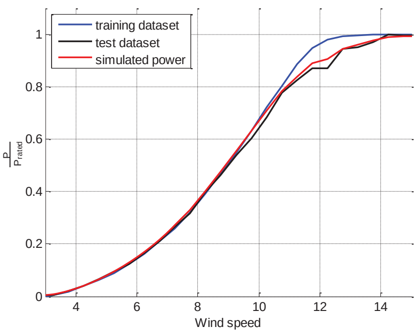

Training dataset: TI < 10%
Test dataset: TI > 10%

NTNU Det skapende universitet

15

Results – Influence on AEP

	TI low->high	TI high ->low
AEP training data [MWh]	11774	11490
AEP test data [MWh]	11490	11774
AEP simulated [MWh]	11652	11619

ΔAEP = 2.5%

AEP difference reduced by ~ 50%

NTNU Det skapende universitet

16

Summary & Conclusion

- Time averaging and turbulence causes a bias in the measured power curve depending on the curvature of the power curve and wind speed variance
- Using the zero turbulence power curve AEP difference between different datasets was reduced by ~50%. This in accordance to the estimate in the IEC standard
- Ground based lidar turbulence measurements involves increased uncertainty and scatter

NTNU Det skapende universitet

Questions or comments?

A test case of meandering wake simulation with the Extended-Disk Particle model at alpha ventus

Juan-José Trujillo[1], Hauke Beck[1], Kolja Müller[2], Po Wen Cheng[2], Martin Kühn[1]

[1] ForWind - University of Oldenburg, Institute of Physics, Germany

[2] SWE - University of Stuttgart, Institute of Aircraft Design, Germany

EERA DeepWind – 14th Deep Sea Offshore Wind R&D Conference
Trondheim, 20th of January, 2017

Why do we care about large-scale wake dynamic models?

The wake deficit sweeping in front of the turbine affects its performance

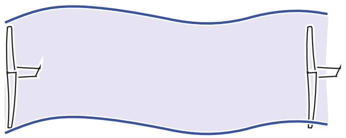

Areas of application

- Fatigue loads
- Wind farm control

How does the EDPM approaches the meandering problem?

Summary

Discrete volumes (extended disks) advect downstream independently and make up the meandering flow

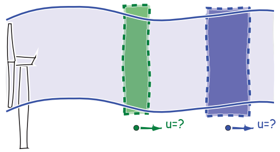

Main characteristics

- Passive advection of the disks
- The disks *contain/transport* a mean wake deficit
- and also wake turbulence

We aim a detailed validation of meandering models

Objective

Perform direct validation of the main assumptions of meandering models

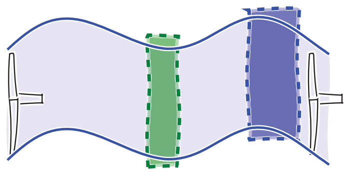

By which means?

- Long range lidar measurements
- Wake tracking techniques
- Wind field reconstruction techniques

Key parameters of meandering simulation

Wake meandering

Time series of transversal wake movement from wake tracking

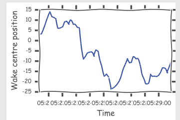

Wake deficit

Wind speed estimated in the meandering frame of reference

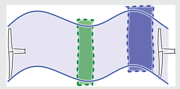

Wake turbulence

Turbulence in the meandering frame of reference not measured by the scanning pulsed lidar

Summary of lidar data processing

Capturing large scale wake movements

1. Lidar wake measurements

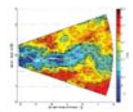

2. Wake tracking by fitting axi-symmetrical template

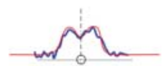

3. Time series of wake position at a downstream station

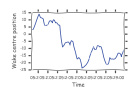

4. Stacking aligned wake profiles → Wake in meandering frame of reference

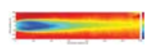

Long range lidar campaign at alpha ventus
Experimental setup

Data sources

- Meteorological mast FINO1
- Leosphere Windcube 200s at FINO1 platform
- SCADA and load data at AV04

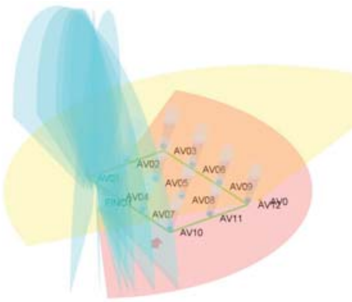

Long range lidar campaign at alpha ventus
Six-hour test case

Wind farm inflow conditions

- 19th August 2013 0:18h – 5:50h
- Southerly wind
- $u_o = 3.5\,\mathrm{m/s}$ to $6.5\,\mathrm{m/s}$
- $\phi_{wind} = 165^\circ$ to 185°

Lidar scanning

- Plan Peripheral Indicator (PPI)
- 3.4° elevation angle from FINO1
- Scan time of 154 s

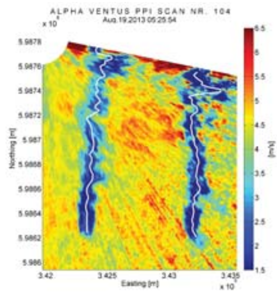

Six-hour test case
Single wake on AV04

- Turbine AV04 experiences meandering single wake from AV10
- Downstream distance approx. $13\mathcal{D}$ ($\mathcal{D}$: rotor diameter)
- FINO1 platform remains *unaffected*

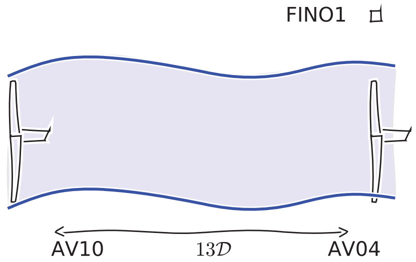

Six-hour test case
Wake position time series $2\mathcal{D}$ in front of AV04

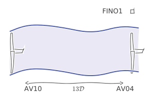

- Wake tracking with fit of Gaussian template function
- Over-sampling via reconstruction with a passive advection method

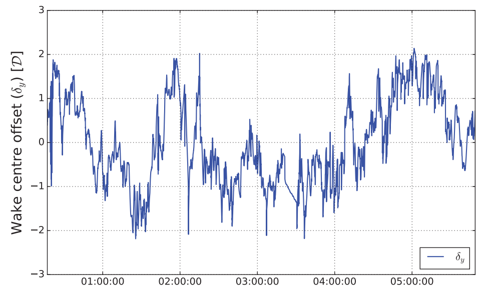

Six-hour test case
Wake position time series $2\mathcal{D}$ in front of AV04

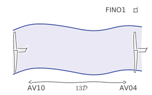

- Wind direction from ultrasonic anemometer at 40m (FINO1)
- Low-pass filter with an approximate $2\mathcal{D}$ length scale

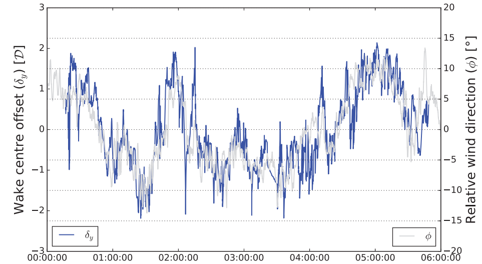

Six-hour test case
Wake position time series $2\mathcal{D}$ in front of AV04

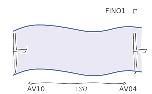

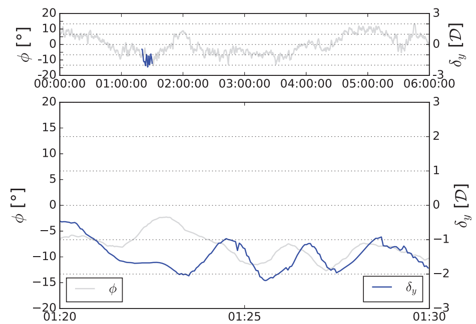

Six-hour test case
Modelled wake position time series $2\mathcal{D}$ in front of AV04

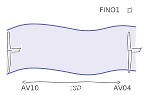

- Straight advection with identical initial conditions as at FINO1
- RMSE $= 0.78\mathcal{D}$

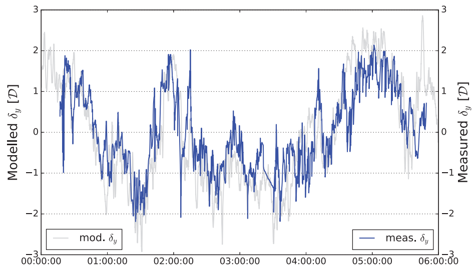

Six-hour test case
Wake of AV10 estimated from lidar measurements[1]

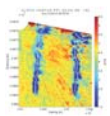

Fixed frame of reference

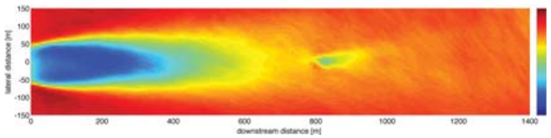

Meandering frame of reference

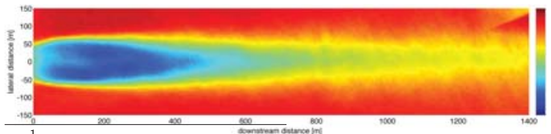

[1] H. Beck et al., "Analysis of wake sweeping effects based on load and long-range lidar measurements." German Wind Energy Conference – DEWEK, Bremen, 2015.

Six-hour test case
Planned simulation experiment of AV04

- Flex5 + Poseidon
  - Integrated approach
  - Coupled turbine, substructure and foundation model
  - Validated model of AV04[2]
- Inflow conditions for six hours
  - Free
  - Frandsen effective turbulence
  - Constrained to lidar meas.
  - DWM proxy
  - EDPM extended disk particle

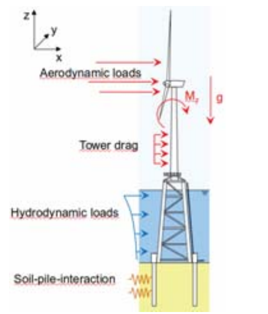

[2] D. Kaufer et al. "Validation of an Integrated Simulation Method with High Resolution Load Measurements of the Offshore Wind Turbine REpower 5M at Alpha Ventus." 23rd International Offshore and Polar Engineering Conf.

Final remarks

Preliminary observations

- Long range lidar measurements provide unique data for direct validation of wake meandering models.
- Preliminary results suggest an acceptable correlation of lateral wake position estimated by simplified EDPM and by lidar wake tracking

Outlook

- Analysis of fatigue loads from the aero-elastic simulations with meandering models and comparison against measurements

Acknowledgements

We would like to thank Senvion for the access to the wind turbine data and the permission to perform the simulations of the wind turbine AV04.

This research was carried out in the frame of the RAVE (Research at Alpha Ventus) projects «OWEA Loads»and «GW Wakes», funded by the German Federal Ministry for Economic Affairs and Energy (BMWi) based on a decision of the Parliament of the Federal Republic of Germany (grant numbers 0325577B and 0325397A, respectively).

Federal Ministry for Economic Affairs and Energy

A Comprehensive Multiscale Numerical Framework For Wind Energy Modelling

FLUID-STRUCTURE INTERACTION FOR WIND TURBINES (FSI-WT project 2012 - 2017)

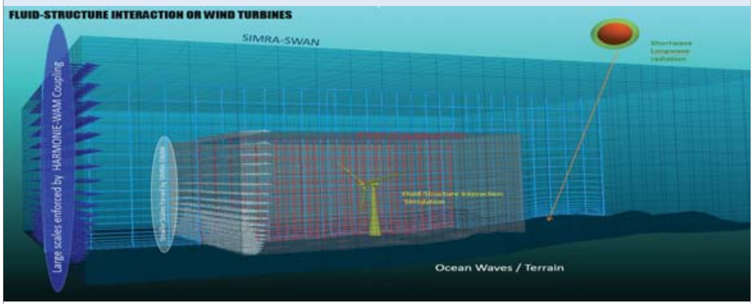

SINTEF DIGITAL (Formerly ICT), MATHEMATICS AND CYBERNETICS DEPARTMENT.
ADIL RASHEED , MANDAR TABIB, TROND KVAMSDAL, KARL MERZ, JOHN TANDE.

CONTENT

- MOTIVATION
- MUTLI-SCALE METHOD
  - APPROACH AND TOOLS USED/DEVELOPED
  - MULTI-SCALE COUPLINGS
- CASE STUDY AND VALIDATION EXAMPLES
  - NREL 5 MW –TOOL DEVELOPMENT
  - BESSAKER ONSHORE WIND FARM
  - MET-OCEAN INTERACTION FOR OFFSHORE WIND FARM
- FUTURE WORK TOWARDS ROMs (OPWIND)

MOTIVATION

- Develop efficient methods for real-time simulation for industrial needs.
  - Approach - From High-fidelity simulation to faster reduced order methods.
- Aim of FSI-WT project – High fidelity tools in a multi-scale framework in order to resolve wide-range of spatio-temporal scales and to accurately determine influence of key variables on wind-farm performance (onshore and offshore).
  - Meso-scale atmospheric phenomena and stratification – Marine and Atmospheric boundary layer.
  - Ocean-atmospheric interactions for offshore wind farms
  - Terrain influence on wind
  - Influence of blade geometry
  - Wake dynamics.
  - **A single model cannot resolve all the spatio-temporal scales and hence need to embed several models in a multi-scale framework.**
  - These hi-fidelity models can be used later to develop reduced order models for faster simulation.

TOOLS USED/DEVELOPED FOR MULTISCALE MODEL

Physics	Tool Coupling and Resolution of use
Mesoscale atmospheric flow.	Mesoscale weather forcasting model - **HARMONIE - 1 Km x 1 Km** resolution.
Microscale wind model with terrain impact.	**SIMRA (inhouse code) – 50 m x 50 m** resolution.
Supermicroscale - Wind Farm resolved with Turbine model Influence of wake with terrain features and stratification.	**SIMRAFOAM** with Actuator line method (SIMRA + SOWFA). Finest mesh resolution – **3m x 3m x 3m** = (*Turbine diameter/20*) . Turbine not explicitly resolved and needs turbine data.
Turbine blade resolving models	Turbine geometry resolved. Mesh resolution in *μm* to *mm* near boundary of turbine. **Flow over airofoil (IFEM), Sliding mesh and MRF.**
Ocean Wave models	WAM and SWAN.

MULTI-SCALE COUPLING - OFFSHORE

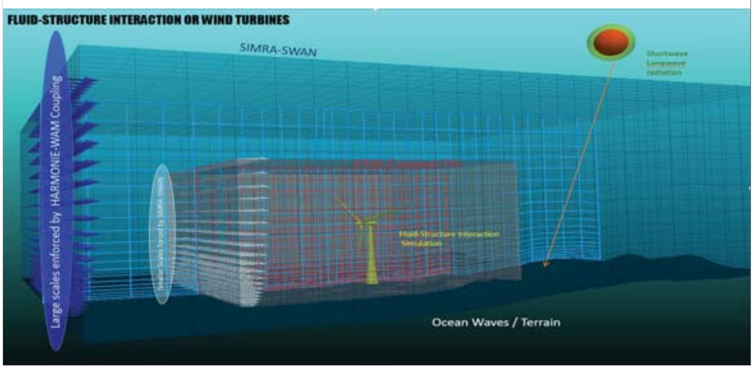

MULTI-SCALE COUPLING - ONSHORE

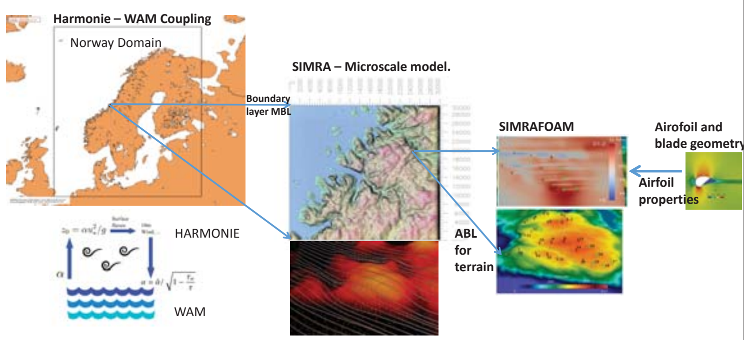

CASE STUDY AND VALIDATION EXAMPLE

CONTINUED … VALIDATION OF MULTISCALE FRAMEWORK FOR OFFSHORE CONDITIONS – WAM-HARMONIE.

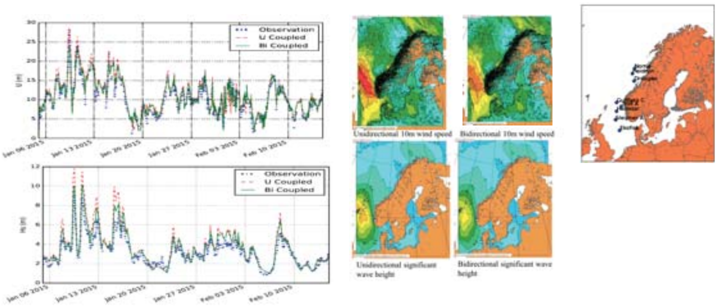

Comparison of wind speed (U) and wave height (Hs) as predicted by Uni and Bi coupled approaches over a month with observations measured on Sleipner platform.

NREL 5 MW FOR TESTING - 2D Vs Q3D Vs 3D Blade Models. Flow At Different Sections.

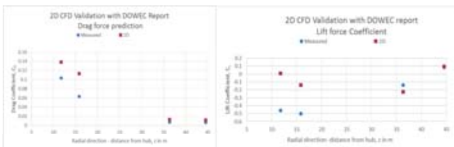

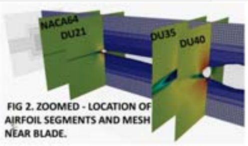

As one moves away from hub towards the tip, the flow begins to loose its 3D characteristics and can be reasonably well represented by efficient 2D simulations.

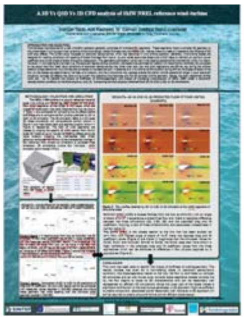

CONTINUED … VALIDATION OF MULTISCALE FRAMEWORK FOR OFFSHORE CONDITIONS – WAM-HARMONIE

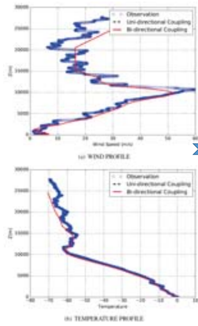

MBL AS INPUT TO SIMRA/ SIMRAFOAM for wind-farm.

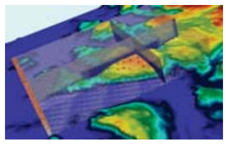

VALIDATION OF MULTISCALE FRAMEWORK FOR OFFSHORE CONDITIONS – WAM-HARMONIE AND SIMRA-SWAN.

MET OCEAN INTERACTIONS

HARMONIE-WAM	SIMRA-SWAN
Resolution ~1km	Resolution ~50m for air flow, 5m for wave modeling
Unsteady mode	Steady mode
Accounts for sensible and latent heat flux	Accounts for only sensible heat flux
Not good close to the coast in shallow water	Idea for shallow water and close to the coast

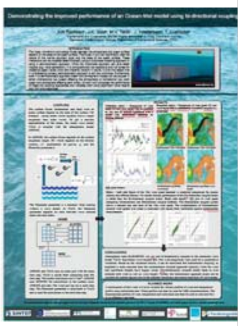

CONTINUED … VALIDATION OF MULTISCALE FRAMEWORK FOR ONSHORE BESAKKER WIND FARM – HARMONIE-WAM-SIMRA-SIMRAFOAM.

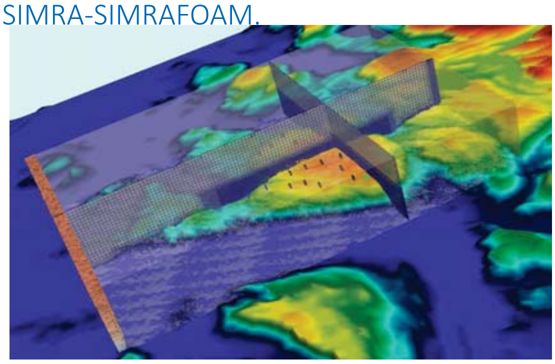

25 Turbine farm

Altitude - Sea-level to 400 m.

Domain:
6.8km X 4.5 km X 1.5km

Boundary condition from the coupled **HARMONIE-SIMRA** provided to **SIMRAFOAM.**

Mesh: 13 million grid cell with 3m resolution close to the TURBINE location

CONTINUED … VALIDATION OF MULTISCALE FRAMEWORK FOR ONSHORE BESAKKER WIND FARM – STRATIFICATION INFLUENCE AND TERRAIN INFLUENCE.

Velocity in Neutral condition

Velocity in Stable stratification

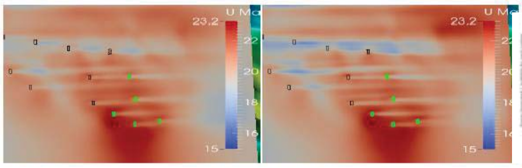

Terrain Influence. Flat and Complex Terrain with neutral flow.

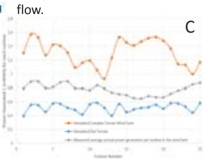

FUTURE WORK - 2017 – 2020 WITH OPWIND (SINTEF Energy)

- ROM MODEL DEVELOPMENT FOR INDUSTRY.
  - GENERATE DATABASE
  - Generate Reduced order model

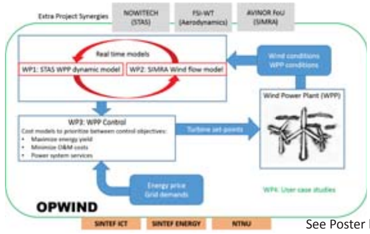

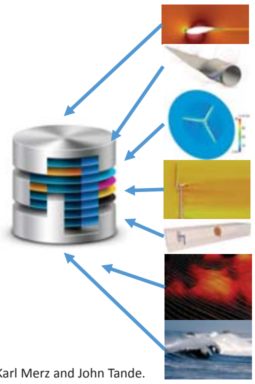

See Poster by Karl Merz and John Tande.

CONTINUED … VALIDATION OF MULTISCALE FRAMEWORK FOR OFFSHORE CONDITIONS – SIMRA-SWAN.

Location	Obs Hs (m)	Standalone Model Hs (m)	Coupled Model Hs (m)
1	4.16	4.30	4.27
2	4.54	4.80	4.87
5	4.17	4.59	4.5
6	4.01	4.06	4.00
7	2.13	2.40	2.45
8	2.03	2.60	2.60
9	2.57	2.80	2.85
10	2.68	2.90	2.92

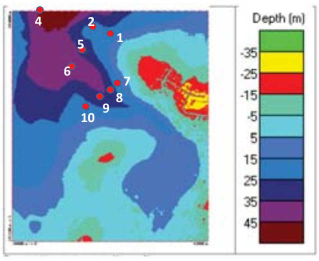

Flow accelerates in the fjord due to channeling effect as a result of which the source term (wind induced) increases which in turn results in an increased significant wave height in the coupled model.

Demonstration of Usability of ROMS

Analysis of dominant flow structures and their flow dynamics in chemical process equipment using snapshot proper orthogonal decomposition technique. M. V. Tabib and J. B. Joshi. Chemical Engineering Science, 63 (14), 2008, 3695-3715.

Proper Orthogonal Decomposition

Energy Distribution as a function of modes for different kinds of rotating machinery. It is clear that only first 4-5 modes contribute most of the energy.

μ can be any parameter like pitch, yaw, angle of attack, surface roughnes, scales of turbine

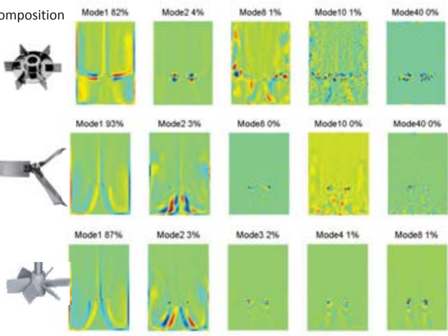

Disc Turbine (Radial Flow)

HE3

PBDT

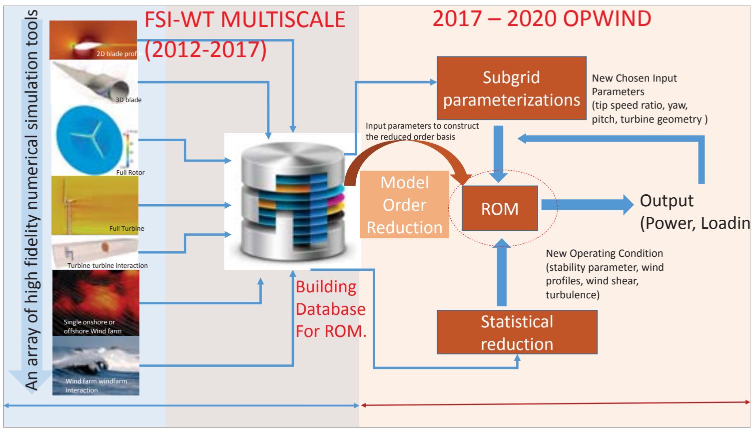

APPLICATION TO RECONSTRUCT WAKE.

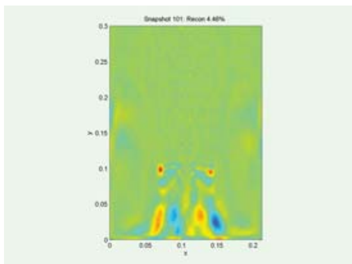

Rolling off blade tip vortices is seen

ACKNOWLEDGEMENTS

- Financial support from the Norwegian Research Council and support from the industrial partners of the FSI-WT (http://www.fsi-wt.no) project (Kjeller Vindteknikk, Statoil, Trønder Energi AS and WindSim).

THANK YOU

Queries?

MULTISCALE APPROACHES
MULTDOMAIN
EMBEDDED – DOWNSCALING AND UPSCALING.
PARALLEL MULTISCALE
SERIAL SIMPLIFICATION TRANSFORMATION ONE WAY COUPLING.

Technische Universität München
Wind Energy Institute

Application of a Reduced Order Wind Farm Model on a Scaled Wind Farm

J Schreiber[1], C L Bottasso[1,2]

johannes.schreiber@tum.de

[1] Wind Energy Institute, Technische Universität München, Germany
[2] Dipartimento di Scienze e Tecnologie Aerospaziali, Politecnico di Milano, Italy

DeepWind 2017
Trondheim, Germany

January 20th 2017

Supported by: Federal Ministry for Economic Affairs and Energy
on the basis of a decision by the German Bundestag

This research was supported by the German Federal Ministry of Economic Affairs and Energy (BMWi) within the CompactWind project.

Motivation

Wind Farm Control:

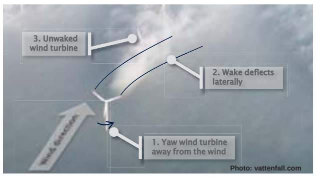

Wake steering/deflection:

Yawing a wind turbine out of the wind, deflects the wake.

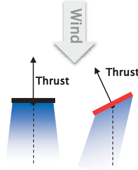

non-yawed and yawed wind turbine ►

How to find the optimum yaw configuration for a wind farm?
- Engineering wake models (based on operating conditions, wind speed, turbulence and direction)

How to deal with model mismatch and disturbance?
- Wind observer and wake detectors (based on turbine rotor loads)

Outline

- Motivation
- Reduced Order Wind Farm Model (ROWFM)
- Scaled Wind Farm Experiments
- Wake Position Observer
- Conclusions and Outlook

Outline

- Motivation
- **Reduced Order Wind Farm Model (ROWFM)**
- Scaled Wind Farm Experiments
- Wake Position Observer
- Conclusions and Outlook

Outline

- **Motivation**
- Reduced Order Wind Farm Model (ROWFM)
- Scaled Wind Farm Experiments
- Wake Position Observer
- Conclusions and Outlook

ROWFM

Reduced order wind farm model (ROWFM), FLORIS-like [1]

11 independent parameters to model:
- Reduction
- Expansion
- Deflection

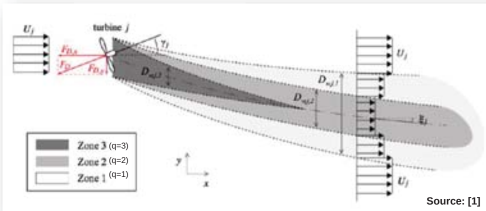

Reduction
- Jensen Wake Model like
- Small asymmetric effect due to yawing
- k_e as parameter to be changed for different TI

$$U_{w,q}(x) = U_\infty(1-r)$$

$$r = 2a\left(\frac{D}{D + 2k_e\Delta x \frac{m_{U,q}}{\cos(a_U + b_U\gamma)}}\right)^2$$

Reduction Identified Parameter	
k_e	0.6
$m_{U,1}$	0.1894
$m_{U,2}$	0.3603
$m_{U,3}$	0.0978
a_U	0.9631°
b_U	2.0105

[1] P. M. Gebraad, F.W. Teeuwisse, J.W. van Wingerden, P. A. Fleming, S. D. Ruben, J. R. Marden, and L. Y. Pao, "A data-driven model for wind plant power optimization by yaw control," 2014.

ROWFM

Reduced order wind farm model (ROWFM), FLORIS–like [1]

11 independent Parameters to model:
- Reduction
- Expansion
- Deflection

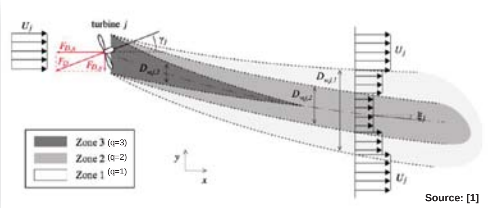

Expansion
- Jensen Wake Model like
- Linear
- Negative coefficient in inner wake zone (near wake)
- k_e as parameter to be changed for different TI

$$D_{w,q}(x) = 2k_e m_{e,q}\Delta x$$

Expansion Identified Parameter	
k_e	0.6
$m_{e,1}$	0.0040
$m_{e,2}$	0.0374
$m_{e,3}$	-0.0549

[1] P. M. Gebraad, F.W. Teeuwisse, J.W. van Wingerden, P. A. Fleming, S. D. Ruben, J. R. Marden, and L. Y. Pao, "A data-driven model for wind plant power optimization by yaw control," 2014.

Wake Parameter Identification

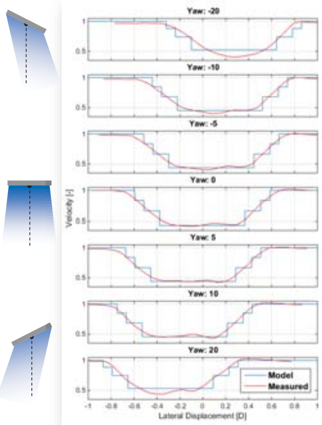

Wake measurements
- Hot wire probes
- At hub height of isolated turbine
- Below rated wind speed
- Low TI (<1%)
- Different turbine yawing
- Identification of wake parameters θ by solving:

$$\min_{\theta} \int [V_{measured}(x) - V_{model}(x,\theta)]^2 dx$$

Process:
1. Identify linear wake deflection parameters ($\gamma = 0, \Delta x = 4D, 7D, 8D, 11D$)
2. Identify all other parameters ($\gamma = -20°\ to + 20°, \Delta x = 4D$)

◄ Wake at 4D longitudinal distance. Comparison between measurements and identified model for different turbine yawing.

ROWFM

Reduced order wind farm model (ROWFM), FLORIS–like [1]

11 independent Parameters to model:
- Reduction
- Expansion
- Deflection

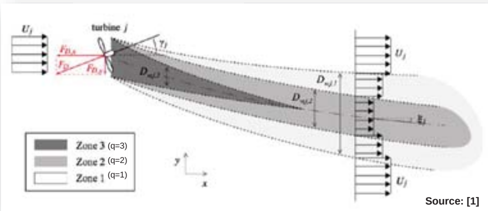

Deflection
- Wake rotation induced (linear)
- Yaw induced (Jiménez et al.)

$$y_w(c) = \delta_{w,rot}(x) + \delta_{w,yaw}(x)$$

$$\delta_{w,rot}(x) = a_d + b_d\Delta x$$
$$\delta_{w,yaw}(x) = f(\gamma, a, C_T, k_d)$$

Deflection Identified Parameter	
k_d	0.1280
a_d	0.0108
b_d	-0.0036

[1] P. M. Gebraad, F.W. Teeuwisse, J.W. van Wingerden, P. A. Fleming, S. D. Ruben, J. R. Marden, and L. Y. Pao, "A data-driven model for wind plant power optimization by yaw control," 2014.

Wake Parameter Identification

Wake measurements at higher TI (~5%)
- k_e re–identification ($\gamma = 0, \Delta x = 4D$)

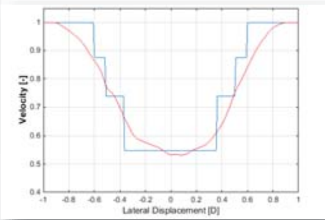

▲ Wake at 4D longitudinal distance (used for re–identification)

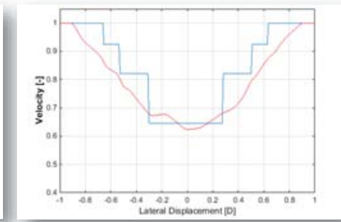

▲ Wake at 6D longitudinal distance

Wake model parameter summary:
- All wake parameter identified at low TI (<1%)
- Only k_e adaped for operation at higher TI (~5%), k_e=0.6549

Model
Measurements

G1 – Generic Scaled Wind Turbine

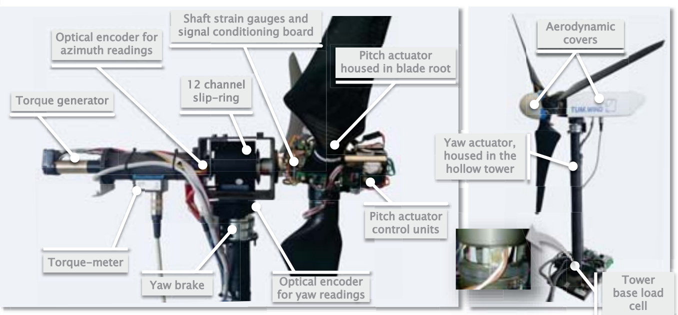

Rotor diameter:	1.1 m	Design TSR:	8
Tower height:	0.8 m	Rated rotor speed:	850 rpm

Campagnolo F, Petrović V, Schreiber J, Nanos E M, Croce A and Bottasso C L 2016 Wind tunnel testing of a closed-loop wake deflection controller for wind farm power maximization *Journal of Physics: Conference Series* **753** 32006

Power Model

Power Calculation

$$P = \frac{1}{2}\rho A V^3 C_P(\gamma)$$

Measured and modeled $C_P(\gamma)$ ►

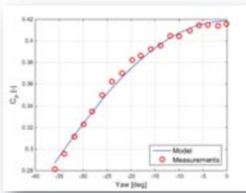

Power Coefficient

$$C_P(\gamma) = C_{P,0}\cos(\gamma)^{p_p}$$

Power Identified Parameter	
p_p	1.787

Multiple wake interaction
- Overlapping wakes

$$V = U_\infty \Pi(1 - r_i)$$

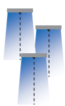

Flow at turbine affected by two wakes ►

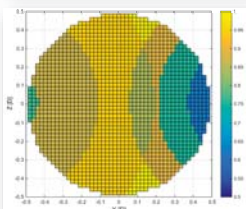

Outline

- Motivation
- Reduced Order Wind Farm Model (ROWFM)
- **Scaled Wind Farm Experiments**
- Wake Position Observer
- Conclusions and Outlook

Scaled Experiments – Layout 2

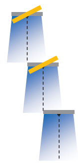

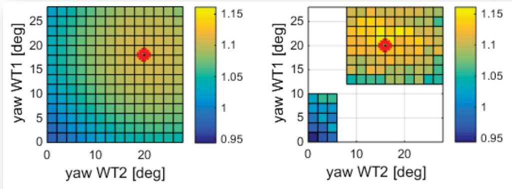

▲ **Model** total WF–Cp ▲ **Experiment** total WF–Cp

- Model determines roughly the optimum yaw configuration:
  - Optimum model: Yaw WT 1: 18° Yaw WT 2: 20°
  - Optimum experiment: Yaw WT 1: 20° Yaw WT 2: 16°
- Both show **power increase > 10%** (w.r.t. not yawing)
- But what happens in case of disturbances (i.e. wrong wind direction as model input)?

Scaled Experiments – Layout 1

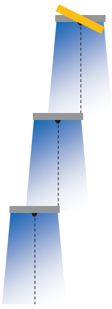

Layout 1

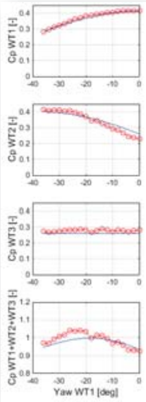

Wind farm with three wind turbines:

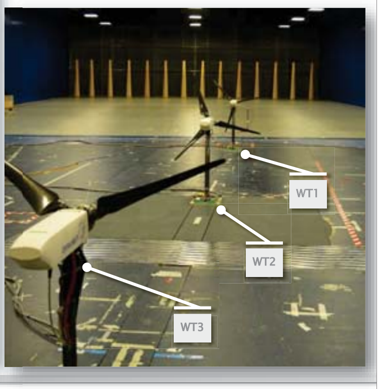

▲ Boundary layer wind tunnel at Politecnico di Milano (cross section 14x4m)

Outline

- Motivation
- Reduced Order Wind Farm Model (ROWFM)
- Scaled Wind Farm Experiments
- **Wake Position Observer**
- Conclusions and Outlook

Scaled Experiments – Layout 2

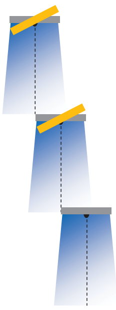

Layout 2

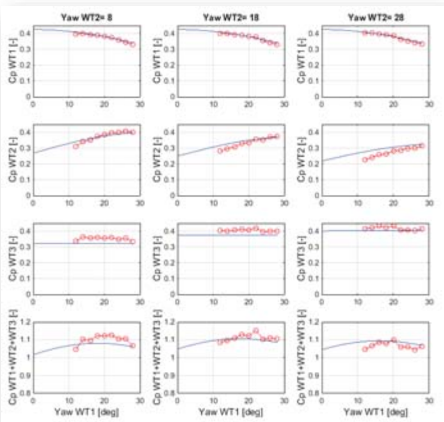

Wake Position Estimation from Rotor Loads

Using blade out of plane loads the **wind speed at each blade position** (blade effective wind speed V_{BE}) can be estimated through the cone–coefficient:

$$C_{m_0}(\lambda_{\mathrm{LE}},\beta,q) = \frac{m(\psi)}{\frac{1}{2}\rho A R {V_{\mathrm{BE}}}^2}$$

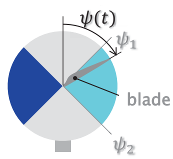

The estimated blade effective wind speed gives velocity at different parts of the rotor disk or the **horizontal wind shear.**

By comparing the

- **observed** horizontal wind shear and rotor speed at a wind turbine and
- **expected** properties (based on a wake deficit model)

one can estimate the wake position.

See also: J Schreiber, S Cacciola, F Campagnolo, V Petrović, D Mourembles and C L Bottasso 2016 Wind shear estimation and wake detection by rotor loads — First wind tunnel verification *Journal of Physics: Conference Series* **753** 32027

Wake Position Estimation from Rotor Loads

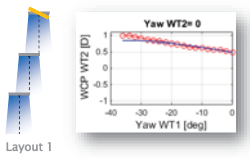

- Difference between modeled and observed wake center position (WCP < 0.2D)
- Modeled wake positions base on isolated wake measurement at low TI
- 0.2D also corresponds to a wrong wind direction of only 3°

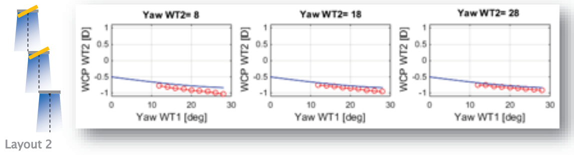

Conclusions & Outlook

Conclusions:
- **ROWFM parameter identified** for scaled wind turbine G1 (at low TI)
- Simple (single) parameter adaptation for higher TI
- Sucessful **prediction of approx. optimum yaw configuration** in scaled experiments
- Wake position observer can **improve knowledge on wind farm flow**

Outlook:
- Study of further experiments in additional layouts
- Employ wind observer and/or wake position observer
  - to **improve knowledge of model input** (ambient wind direction)
  - as **feedback in closed loop wind farm control**

Thank you for your attention!

Wake Position Estimation: An Experiment

Disturbance in wind direction:
- No error in ROWFM-wind direction: Model predictions are good (upper subplot)
- Error in ROWFM-wind direction: Model predictions fail completely (lower subplots)

Using Wake Position Estimator:
- Instead of ROWFM-wake position, the observed wake position is used in the model (Model corrected)
- Much better power prediction in all cases

Wake position estimation can be valuable information in wind farm control!

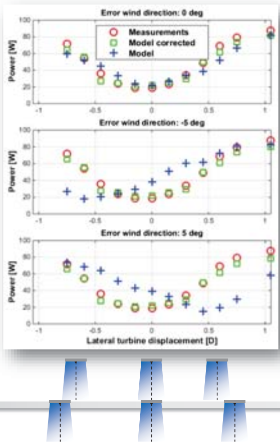

Note: A different turbine model (G2) has been used in those experiments.

Outline

- Motivation
- Reduced Order Wind Farm Model (ROWFM)
- Scaled Wind Farm Experiments
- Wake Position Observer
- **Conclusions and Outlook**

G1) Experimental Testing and Validation

Model testing of a floating wind turbine including control, F. Savenije, ECN

The Tripple Spar campaign: Model tests of a 10MW floating wind turbine with waves, wind and pitch control, H. Bredmose, DTU

Validation of a time-domain numerical approach for determining forces and moments in floaters by using measured data of a semi-submersible wind turbine model test,
C. Luan, NTNU

Nacelle Based Lidar Measurements for the Characterization of the Wake on an Offshore Wind Turbine under Different Atmospheric Conditions, D. Trabucchi, University of Oldenburg

ECN
Your energy. Our passion.

Model testing of a floating wind turbine including control

Feike Savenije (ECN)

EERA DeepWind'2017

Trondheim, 2017/01/19

www.ecn.nl

Introduction (2)

ECN

Earlier studies showed the large impact of the wind turbine controller on the floating wind turbine behavior:

- Operational curve (thrust)
- Limit cycling with closed loop blade pitch control

Several methods to included the wind turbine (with controller) are under investigation:

- Model scale wind turbine
- Hardware in the loop (tension rod / fan)

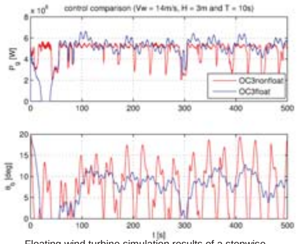

Floating wind turbine simulation results of a stepwise increasing wind speed with two different controllers; one conventional and one tuned for floating to prevent limit cycling due to interaction with floater pitch motion.

Contents

ECN

1. Introduction
2. Controller design at model scale
3. Model test campaign setup
4. Model test results
5. Conclusions
6. Questions

Introduction (3)

ECN

A model test campaign of the Tri-Floater concept (GustoMSC, MARIN, ECN) in 2011 showed:

- Importance of the correct wind turbine characteristics at model scale
- Wind turbine control that mimics full scale behavior is possible, but there are challenges to further investigate

New model test campaign in the TO2 project 'Floating Wind Energy', with focus on:

- Effects of narrow wave basin on system behavior in the dominant direction
- Floating wind turbine control at model scale

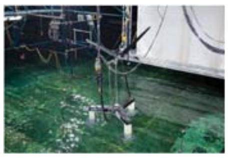

GustoMSC Tri-Floater campaign in MARINs Offshore wave basin

TO2 federatie

Introduction (1)

ECN

Physical model test of floating offshore structures are common practice:

- Calibration of the numerical model
- To investigate phenomena that are difficult to capture with numerical methods
- (Visual) feedback on the behavior of the total system in wind and waves

Breaking wave on monopile foundation from MARINs WiFi model test campaign

Control design at model scale (1)

ECN

Challenges when moving to model scale:

- How to determine the rotor characteristics?
- How to deal with low Reynolds number, low power coefficient, highly 3D flow on the blades

Basic PI-controller design to mimic full scale behavior, including:

- Gain scheduling
- Peak shaving
- Stall shaving
- Controller gains

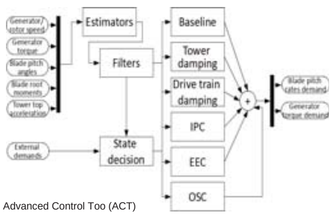

ECN Advanced Control Too (ACT)

Control design at model scale (2)

How to capture the rotor characteristics:

- Measure on the actual system
- Calculate with numerical model

(low Reynolds number!)

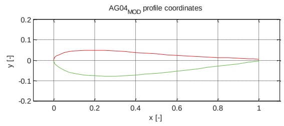

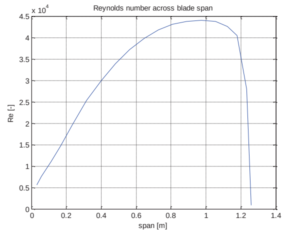

Control design at model scale (3)

RFOIL calculations show laminar seperation for low Re (45k)

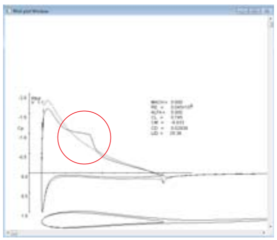

RFOIL calculation with clean AG04mod airfoil

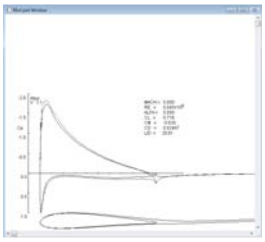

RFOIL calculation with 5% tripped AG04mod airfoil

Control design at model scale (4)

Predicted, derived[1] and measured characteristics:

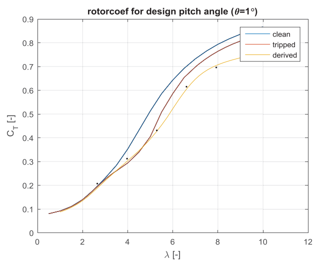

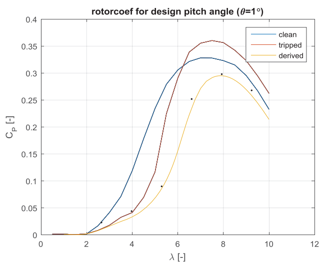

[1] Goupee, A. J.; Kimball, R. W.; de Ridder, E.; Helder, J.; Robertson, A. N.; Jonkman, J. M. (2015). "A Calibrated Blade-Element/Momentum Theory Aerodynamic Model of the MARIN Stock Wind Turbine". OMAE Conference, June 2015.

Control design at model scale (5)

Full scale

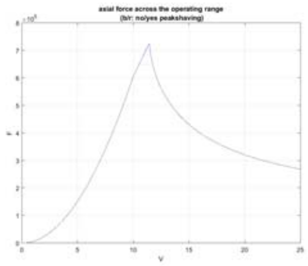

Model scale

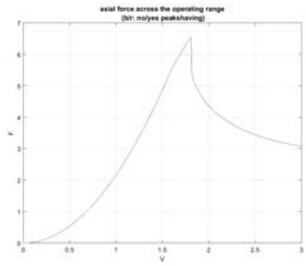

Control design at model scale (6)

Stability analysis of bottom-fixed controller

(full scale)

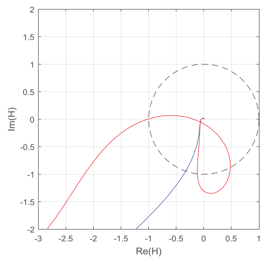

(model scale)

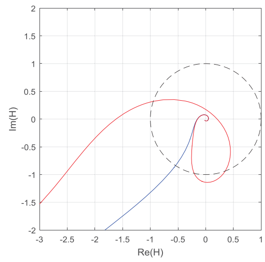

Nyquist plot to assess system stability (red: open loop, blue: closed loop with bottom-fixed controller)

Control design at model scale (7)

Similar solution for full scale and model scale (detune for lower bandwidth)

(full scale)

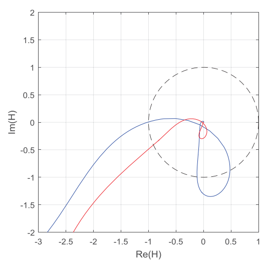

(model scale)

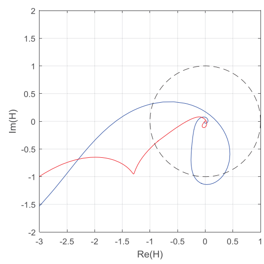

Nyquist plot to assess system stability (blue: closed loop with bottom-fixed controller, red: closed loop with detuned controller)

Model test campaign setup (1)

ECN

Overview of the campaign:

- Two weeks of testing November 2015
- MARIN concept basin, equipped with new wave and wind generators
- OC4 semi-submersible with the MSWT
- Dedicated mooring layout for narrow basin
- Three different controllers to be tested

Model test results (2)

ECN

Staircase to verify:

- Wind speed estimation
- Partial/full load switching

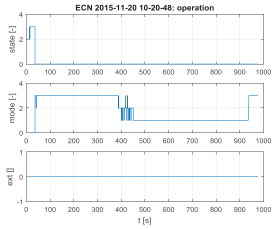

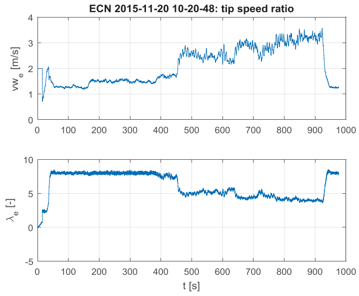

Model test campaign setup (2)

ECN

Test cases with focus on controller interaction:

- Wind and wave calibration
- Constant and staircase wind
- Decay tests with and without control
- Limited number of operational cases (stochastic wind and irregular waves at rated and above rated)

Three different controllers have been tested:

[C1] fixed rotor speed, blade pitch scheduled with power

[C2] variable rotor speed, pitch to vane (tuned for bottom-fixed wind turbine)

[C3] variable rotor speed, pitch to vane (tuned for floating wind turbine)

Model test results (3)

ECN

Staircase to verify:

- Floater motions
- Tower top acceleration
- Floater motion observer

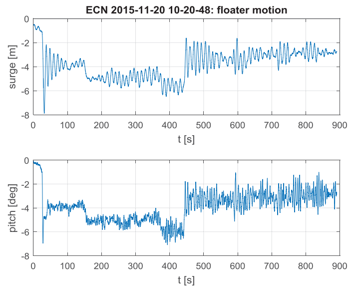

Model test results (1)

ECN

Staircase to verify:

- Rotor speed regulation
- Operational curve

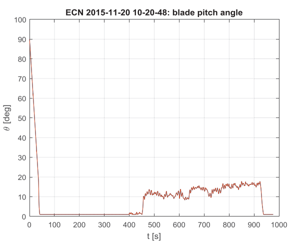

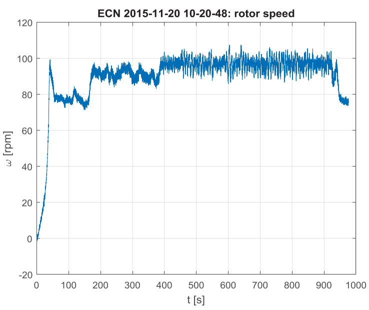

Model test results (4)

ECN

Limit cycling occurs with bottom-fixed controller!

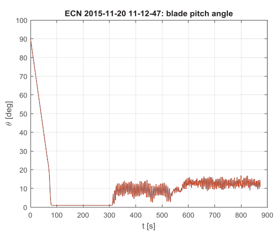

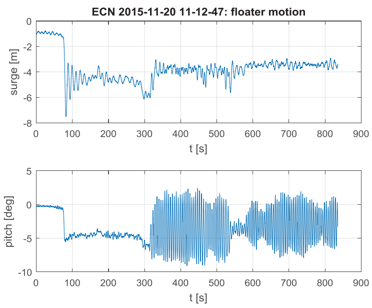

Model test results (5)

Decay test to see influence of different controllers:

- Detuning of the controller prevents limit cycling
- Damping can be increased by feedback of floater motions

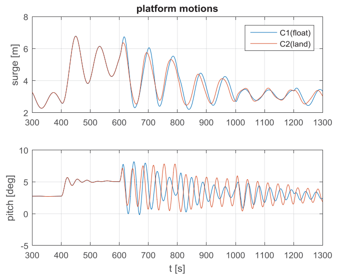

Conclusion

Design of a controller for floating wind turbine model testing is feasible, given:

- Proper rotor characteristics
- Minor adjustments in the design (prevent early stall, gain scheduling etc)

This setup mimics full scale behavior of a floating wind turbine with controller.

The results from floating wind turbine model tests including control can be used to:

- Better calibrate the numerical models
- Evaluate the behavior and improve the design of the floating wind turbine and controller.

Control design at model scale

Full scale (OC4)

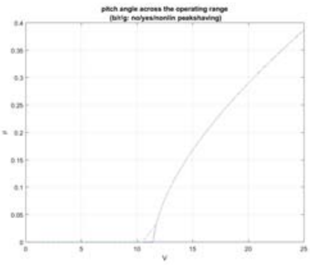

Model scale (OC5)

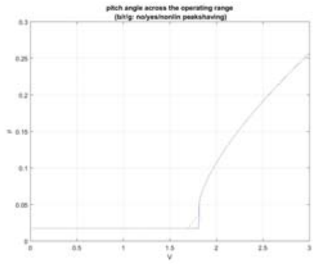

Thank you for your attention

This work has been carried out within the Dutch R&D project 'Floating Wind Energy' funded by the TO2 federation. Sebastien Gueydon, Haite van der Schaaf and Erik-Jan de Ridder from MARIN are acknowledged for the contribution.

ECN
Westerduinweg 3 | P.O. Box 1
1755 LE Petten | 1755 ZG Petten
The Netherlands | The Netherlands

T +31 88 515 49 49 | info@ecn.nl
F +31 88 515 44 80 | **www.ecn.nl**

Control design at model scale

Full scale (OC4)

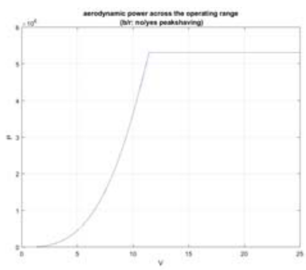

Model scale (OC5)

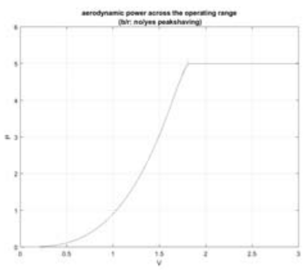

Control design at model scale

Full scale (OC4)

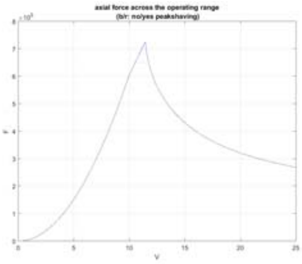

Model scale (OC5)

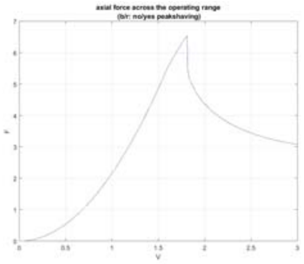

Control design at model scale

Full scale (OC4)

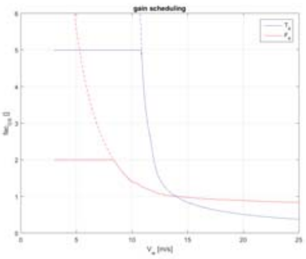

Model scale (OC5)

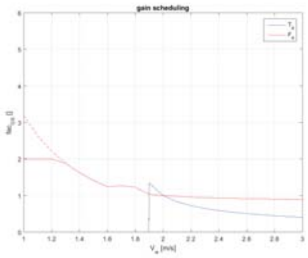

The Triple Spar campaign: Experiments with a floating wind turbine in wind, waves and blade pitch control

Henrik Bredmose, Frank Lemmer, Michael Borg, Antonio Pegalajar Jurado, Robert Mikkelsen, Troels Stoklund Larsen, Tobias Fjeldstrup, Yu Wei, Anders Kjær Lomholt, Lasse Boehm, José Azcona Armendariz

DTU Wind Energy
University of Stuttgart
CENER

Pitch instability for floating WT

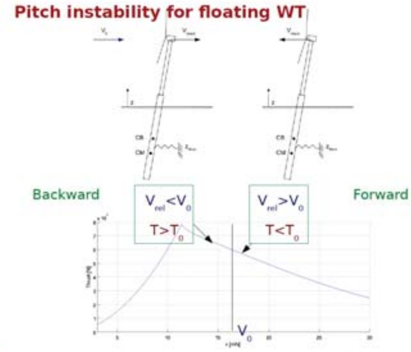

The Triple Spar campaign: Experiments with a floating w… waves and blade pitch contro…

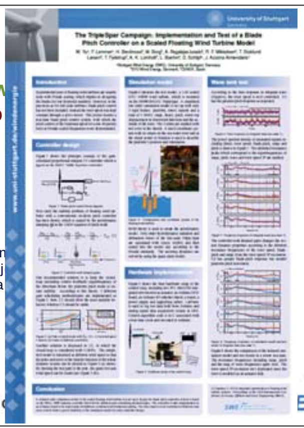

Henrik Bredmose, Frank Lemmer, Michael Borg, An…
Robert Mikkelsen, Troels Stoklund Larsen, Tobias Fj…
Kjær Lomholt, Lasse Boehm, José Azcona Armenda…

DTU Wind Energy
University of Stuttgart
CENER

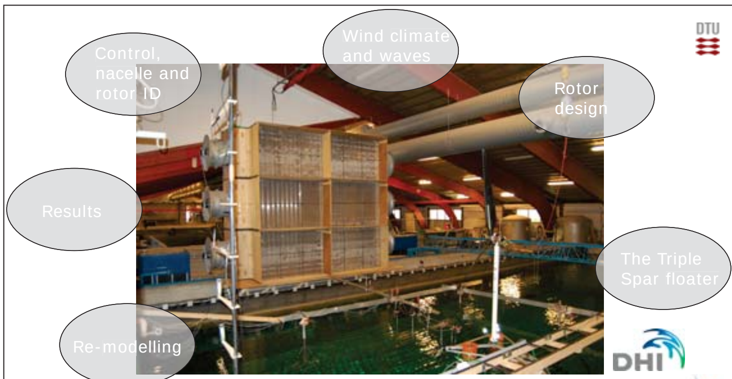

Floating wind turbine tests

DeepCWind consortium

Marin + ECN

Ulsan

Mitsubishi Heavy Industries

University of Maine

Marintek

DTU

University of Stuttgart

Politecnico di Milano

Hansen et al (2014) Sandner et al (2015) Bredmose et al (2015) Pegalajar-Jurado et al (2016)

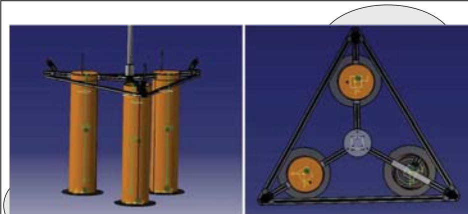

Dimension	Prototype Scale	Froude Model Scale	Actual Model Scale (incl. instrumentation)
Platform			
Draft	54.5m	908mm	918mm
Elevation of tower base above MSL	25.0m	417mm	333mm
Column diameter	15.0m	250mm	250mm
Column length	65.0m	1083mm	1100mm
Deck elevation above MSL	10.5m	175mm	182mm
Centre offset from tower centerline	26.3m	438mm	430mm
Tripod overall height	15.0m	250mm	-
Heave plate diameter	22.5m	375mm	375mm
Heave plate thickness	0.5m	8.3mm	3mm
Displaced volume	29224m³	0.1353m³	0.1357m³
Platform mass	28229t	130.69kg	129.35kg
Centre of mass below MSL	36.02m	600mm	646mm

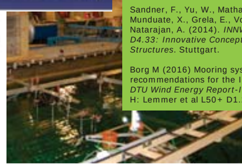

Designed in the INNWIND.EU project.

Hybrid of semi-sub and spar.

Heave plates and catenary mooring

Lemmer, F., Amann, F., Raach, S., & Schlipf, D. (2016). Definition of the SWE-TripleSpar platform for the DTU10MW reference turbine. http://www.ifb.uni-stuttgart.de/windenergie/downloads

Sandner, F., Yu, W., Matha, D., Azcona, J., Munduate, X., Grela, E., Voutsinas, S., Natarajan, A. (2014). *INNWIND.EU D4.33: Innovative Concepts for Floating Structures*. Stuttgart.

Borg M (2016) Mooring system analysis and recommendations for the INNWIND Triple Spar concept. *DTU Wind Energy Report-I-0448*, Kgs. Lyngby, Denmark.
H: Lemmer et al L50+ D1.2: Simplified models

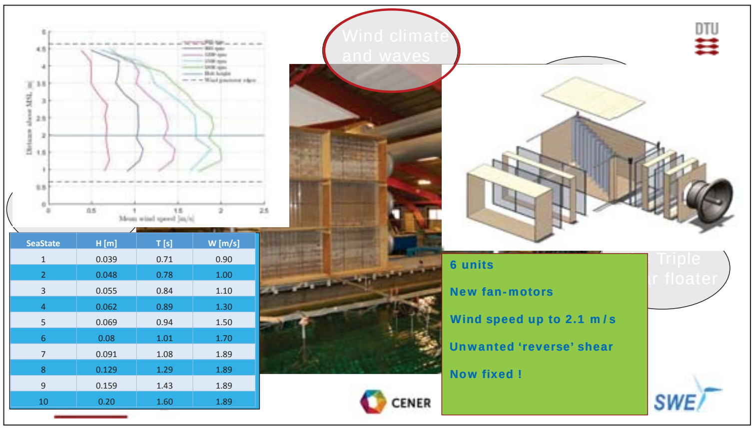

SeaState	H [m]	T [s]	W [m/s]
1	0.039	0.71	0.90
2	0.048	0.78	1.00
3	0.055	0.84	1.10
4	0.062	0.89	1.30
5	0.069	0.94	1.50
6	0.08	1.01	1.70
7	0.091	1.08	1.89
8	0.129	1.29	1.89
9	0.159	1.43	1.89
10	0.20	1.60	1.89

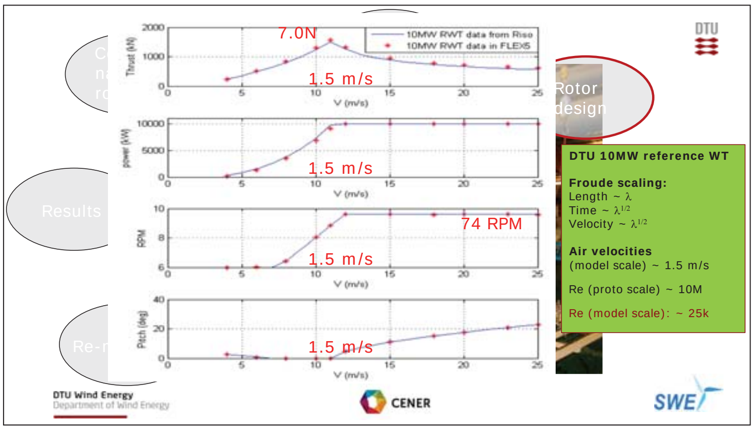

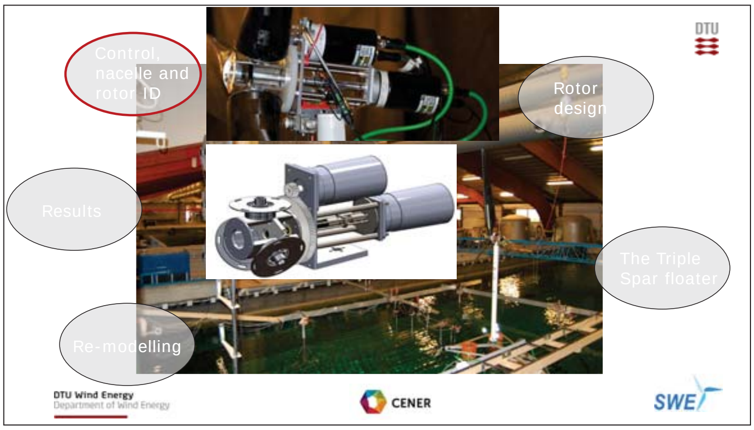

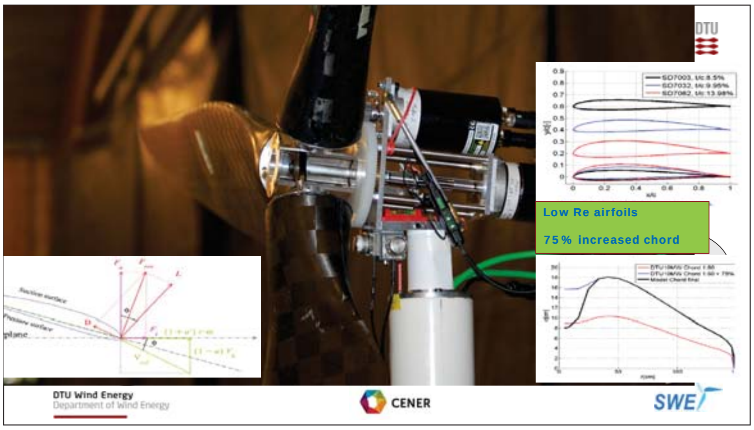

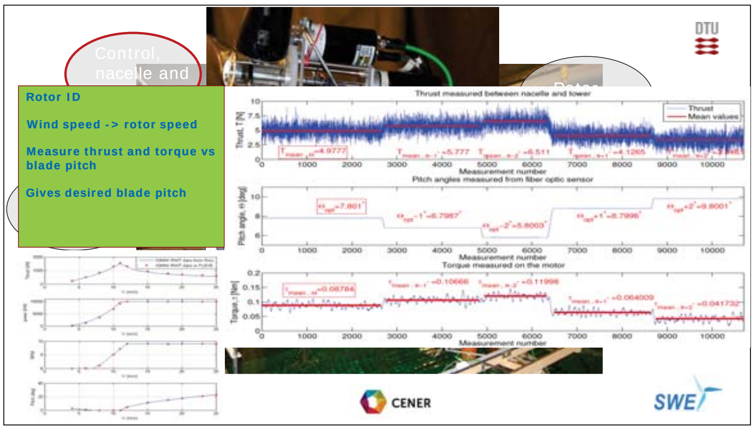

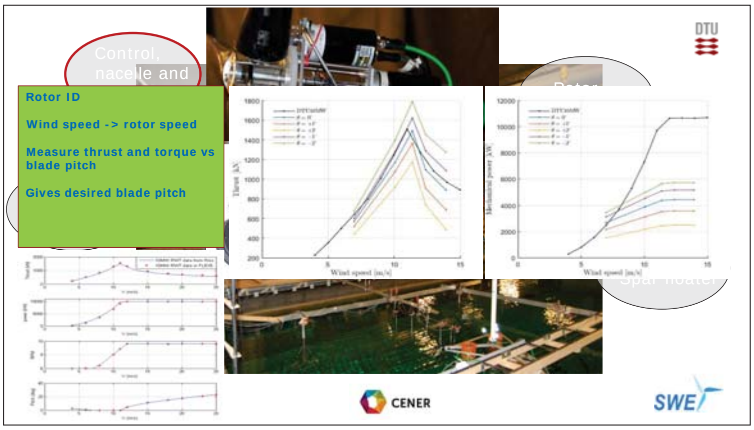
Control, nacelle and
Rotor ID
Wind speed -> rotor speed
Measure thrust and torque vs blade pitch
Gives desired blade pitch
Thrust [kN]
Wind speed [m/s]
Mechanical power [kW]
CENER
SWE

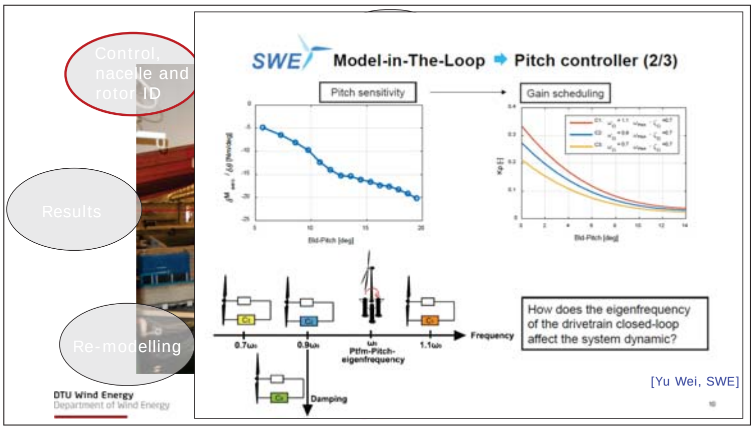
Control, nacelle and rotor ID
Results
Re-modelling
SWE
Model-in-The-Loop
Pitch controller (2/3)
Pitch sensitivity
Gain scheduling
Bld-Pitch [deg]
Frequency
Damping
Ptfm-Pitch-eigenfrequency
How does the eigenfrequency of the drivetrain closed-loop affect the system dynamic?
[Yu Wei, SWE]
DTU Wind Energy
Department of Wind Energy

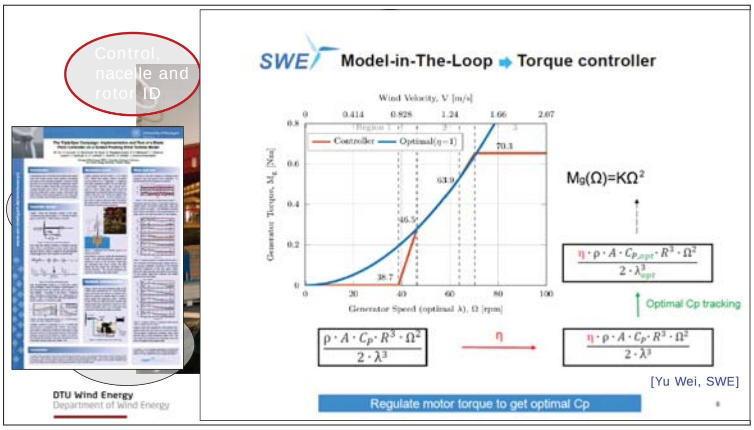
Control, nacelle and rotor ID
Re-modelling
SWE
Model-in-The-Loop
Torque controller
Wind Velocity, V [m/s]
Generator Torque, M_g [Nm]
Generator Speed (optimal λ), Ω [rpm]
Controller
Optimal(η=1)
$M_g(\Omega)=K\Omega^2$
$\frac{\eta \cdot \rho \cdot A \cdot C_{p,opt} \cdot R^3 \cdot \Omega^2}{2 \cdot \lambda_{opt}^3}$
Optimal Cp tracking
$\frac{\rho \cdot A \cdot C_p \cdot R^3 \cdot \Omega^2}{2 \cdot \lambda^3}$
η
$\frac{\eta \cdot \rho \cdot A \cdot C_p \cdot R^3 \cdot \Omega^2}{2 \cdot \lambda^3}$
[Yu Wei, SWE]
Regulate motor torque to get optimal Cp
DTU Wind Energy
Department of Wind Energy

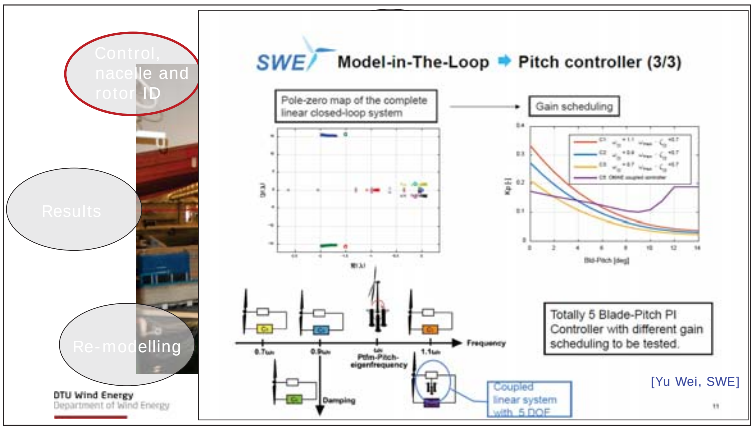
Control, nacelle and rotor ID
Results
Re-modelling
SWE
Model-in-The-Loop
Pitch controller (3/3)
Pole-zero map of the complete linear closed-loop system
Gain scheduling
Bld-Pitch [deg]
Frequency
Damping
Totally 5 Blade-Pitch PI Controller with different gain scheduling to be tested.
Coupled linear system with 5 DOF
[Yu Wei, SWE]
DTU Wind Energy
Department of Wind Energy

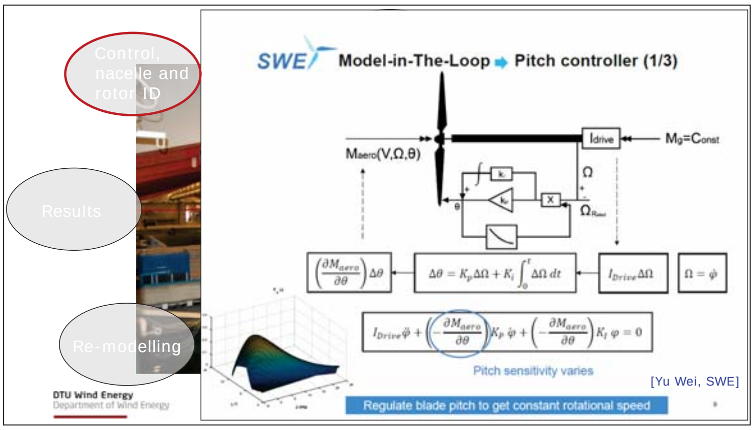
Control, nacelle and rotor ID
Results
Re-modelling
SWE
Model-in-The-Loop
Pitch controller (1/3)
$M_{aero}(V,\Omega,\theta)$
I_{drive}
$M_g=Const$
$\left(\frac{\partial M_{aero}}{\partial \theta}\right)\Delta\theta$
$\Delta\theta = K_p\Delta\Omega + K_i\int_0^t \Delta\Omega\, dt$
$I_{Drive}\Delta\dot{\Omega}$
$\Omega = \dot{\varphi}$
$I_{Drive}\ddot{\varphi} + \left(-\frac{\partial M_{aero}}{\partial \theta}\right)K_p\dot{\varphi} + \left(-\frac{\partial M_{aero}}{\partial \theta}\right)K_I\varphi = 0$
Pitch sensitivity varies
[Yu Wei, SWE]
Regulate blade pitch to get constant rotational speed
DTU Wind Energy
Department of Wind Energy

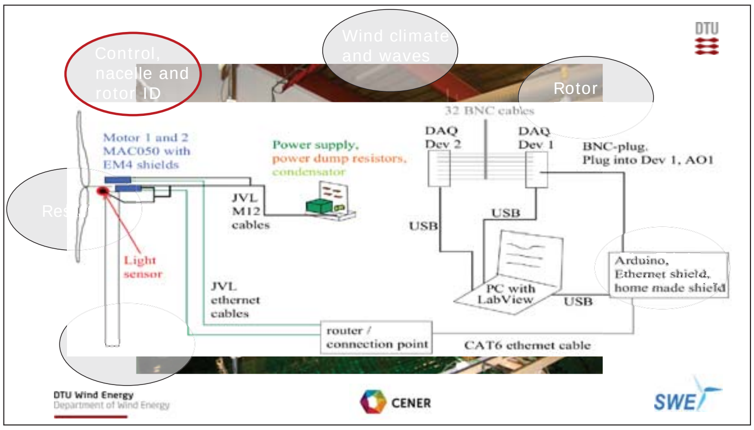
Control, nacelle and rotor ID
Wind climate and waves
Rotor
32 BNC cables
Motor 1 and 2 MAC050 with EM4 shields
Power supply, power dump resistors, condensator
DAQ Dev 2
DAQ Dev 1
BNC-plug. Plug into Dev 1, AO1
JVL M12 cables
USB
USB
Light sensor
JVL ethernet cables
PC with LabView
USB
Arduino, Ethernet shield, home made shield
router / connection point
CAT6 ethernet cable
DTU Wind Energy
Department of Wind Energy
CENER
SWE

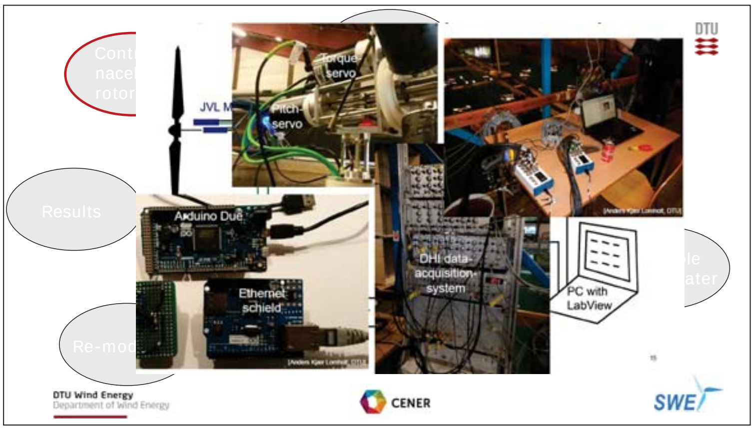
Torque servo
Pitch-servo
Arduino Due
Ethernet schield
DHI data-acquisition system
PC with LabView
Results
DTU
DTU Wind Energy
Department of Wind Energy
CENER
SWE

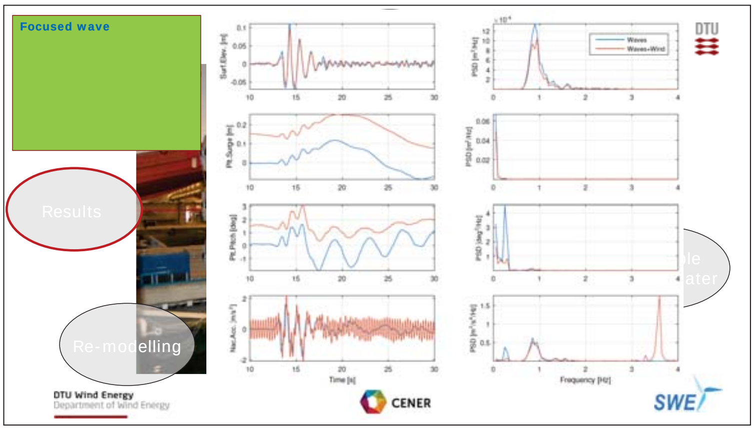
Focused wave
Results
Re-modelling
Time [s]
Frequency [Hz]
DTU
DTU Wind Energy
Department of Wind Energy
CENER
SWE

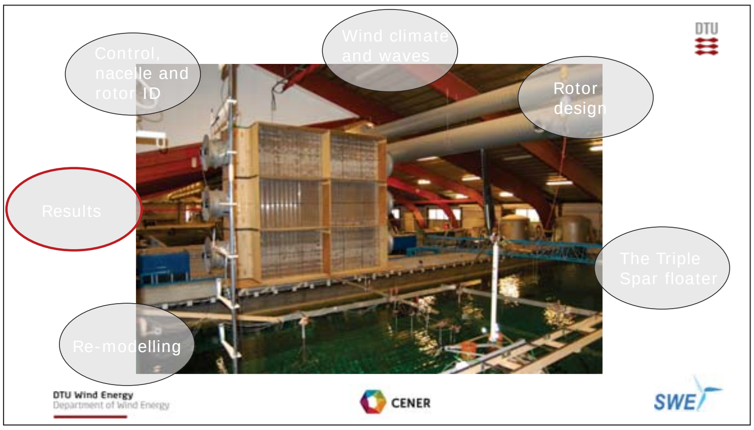
Control, nacelle and rotor ID
Wind climate and waves
Rotor design
Results
The Triple Spar floater
Re-modelling
DTU
DTU Wind Energy
Department of Wind Energy
CENER
SWE

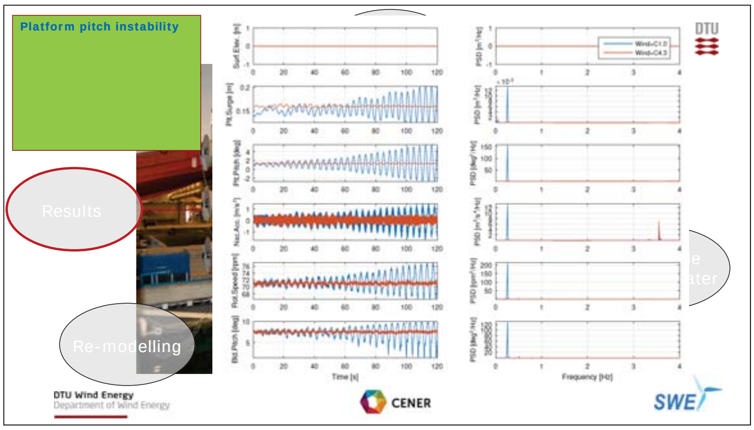
Platform pitch instability
Results
Re-modelling
Time [s]
Frequency [Hz]
DTU
DTU Wind Energy
Department of Wind Energy
CENER
SWE

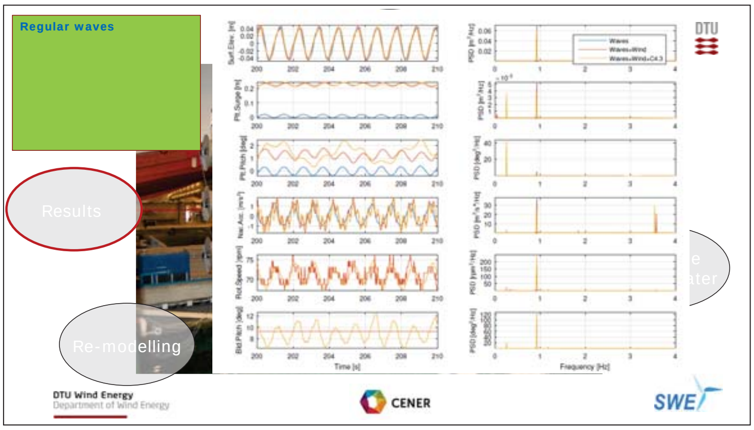
Regular waves
Results
Re-modelling
Time [s]
Frequency [Hz]
DTU
DTU Wind Energy
Department of Wind Energy
CENER
SWE

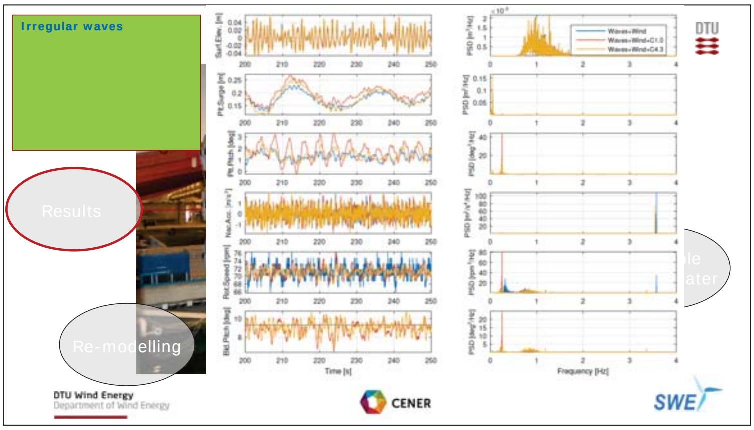
Irregular waves
Results
Re-modelling
Time [s]
Frequency [Hz]
DTU
DTU Wind Energy
Department of Wind Energy
CENER
SWE

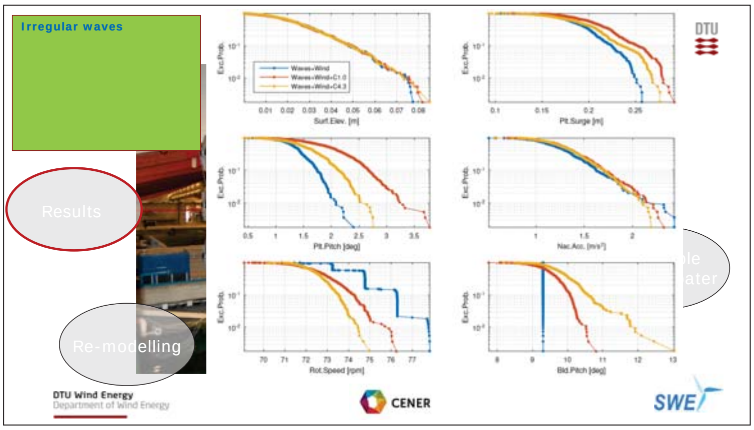
Irregular waves
Results
Re-modelling
Exc.Prob.
Waves+Wind
Waves+Wind+C1.0
Waves+Wind+C4.3
Surf.Elev. [m]
Plt.Surge [m]
Plt.Pitch [deg]
Rot.Speed [rpm]
Bld.Pitch [deg]
DTU
DTU Wind Energy
Department of Wind Energy
CENER
SWE

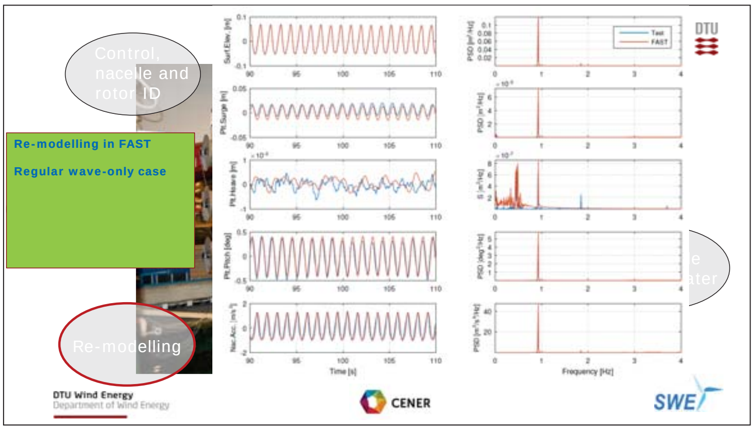
Control, nacelle and rotor ID
Re-modelling in FAST
Regular wave-only case
Re-modelling
Test
FAST
Time [s]
Frequency [Hz]
DTU
DTU Wind Energy
Department of Wind Energy
CENER
SWE

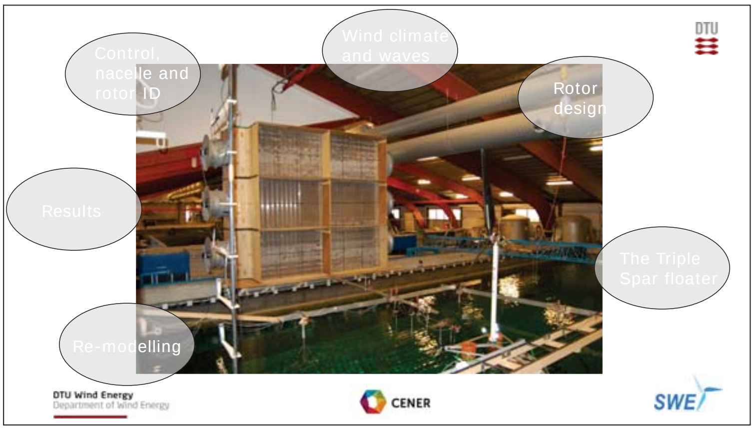
Control, nacelle and rotor ID
Wind climate and waves
Rotor design
Results
The Triple Spar floater
Re-modelling
DTU
DTU Wind Energy
Department of Wind Energy
CENER
SWE

NTNU
Norwegian University of Science and Technology

CENTRE FOR ENVIRONMENT-FRIENDLY ENERGY RESEARCH

Validation of a time-domain numerical approach for determining forces and moments in floaters by using measured data of a semi-submersible wind turbine model test

Chenyu Luan[a,b,c], Valentin Chabaud[a,d], Erin E. Bachynski[b,c,d], Zhen Gao[b,c,d] and Torgeir Moan[a,b,c,d]

[a]Norwegian Research Centre for Offshore Wind Technology (NOWITECH)
[b]Centre for Ships and Ocean Structures (CeSOS), NTNU
[c]Centre for Autonomous Marine Operations and Systems (AMOS), NTNU
[d]Department of Marine Technology, NTNU

19.01.2017

Content

- Development of a time-domain numerical approach for determining forces and moments in floaters [2]
- Real-time hybrid testing of a braceless semisubmersible wind turbine [3, 4]
- Validation

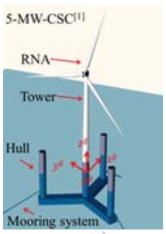

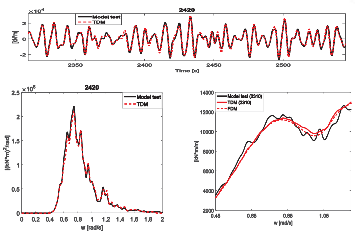

Development of a time-domain numerical approach for determining forces and moments in floaters

A beam element finite element model for the hull

External and inertial loads on the structural component 1

External and inertial loads on the structural component *i*

External and inertial loads on the structural component *d*

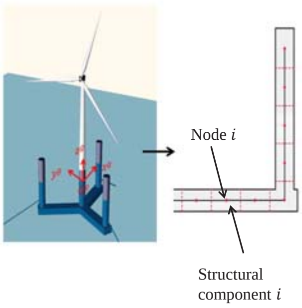

Development of a time-domain numerical approach for determining forces and moments in floaters

A beam element finite element model for the hull

External and inertial loads on the structural component 1

External and inertial loads on the structural component *i*

External and inertial loads on the structural component *d*

Inertia loads

Drag forces

Gravity loads

Hydro loads (Potential-flow theory)

Relevant approaches are developed to derive the corresponding coefficients for modeling the external and inertial loads on each structural component. Details are available in [2].

Real-time hybrid testing

The Hybrid System

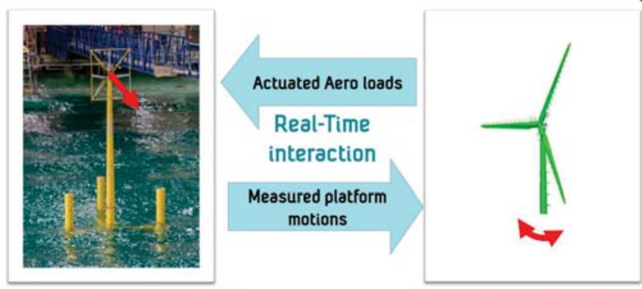

Physcial waves and current

Froude Scale: 1/30

Simulated aerodynamic loads

- Thrust
- Aerodynamic sway force
- Aerodynamic pitch and yaw moment
- Generator torque

Real-time hybrid testing

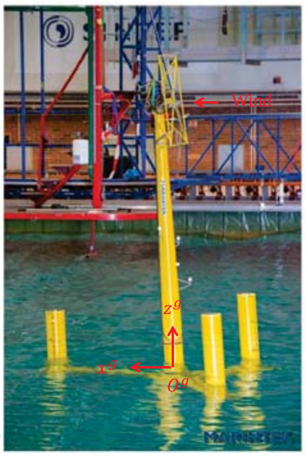

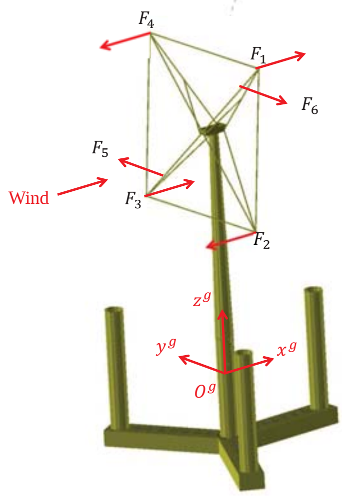

Real-time hybrid testing

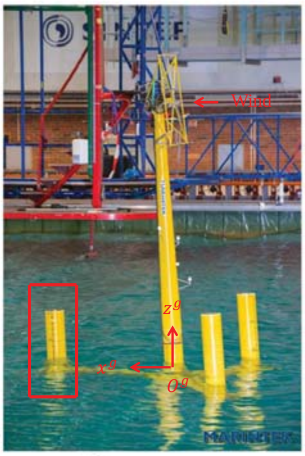

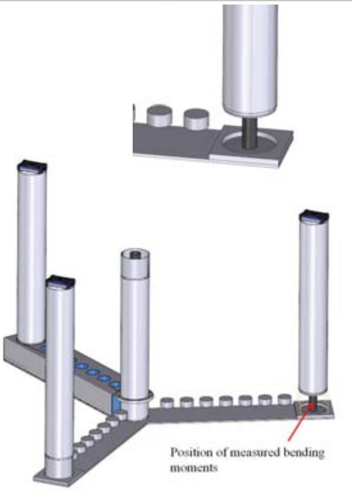

Provided by Mr. Fredrik Brun from SINTEF Ocean

Wave induced transfer function moduli

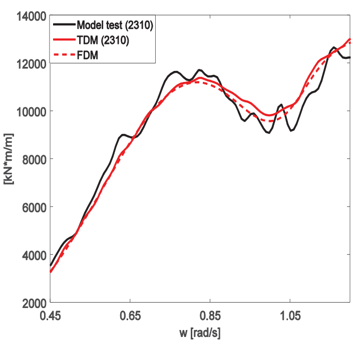

Fore-aft bending moment (M_y) 0-degree-wave in Pink noise model test, $\mathrm{H_s} = 2$ m

- 6 d.o.f.s rigid-body motions
- Fore-aft and side-to-side bending moments
- Good agreement
- Non-linear effects, noise and uncertainties

Wave kinematics

	2310	2321	2331	2340	2410	2420	4121	4221	4310	4410
Std	0.47	1.00	0.99	0.98	3.79	0.92	1.48	1.40	0.92	1.35
Std	0.47	0.99	0.99	0.97	3.78	0.92	1.47	1.40	0.92	1.35
Max	1.89	3.89	4.79	4.35	17.93	4.00	6.37	5.39	3.99	6.31
Max	1.78	3.15	4.26	4.34	18.36	3.89	5.94	5.30	3.88	6.15
Min	-1.62	-3.08	-3.44	-3.02	-12.39	-3.03	-5.48	-4.44	-3.03	-4.48
Min	-1.63	-3.33	-3.42	-3.05	-11.64	-3.02	-5.41	-4.52	-3.01	-4.46

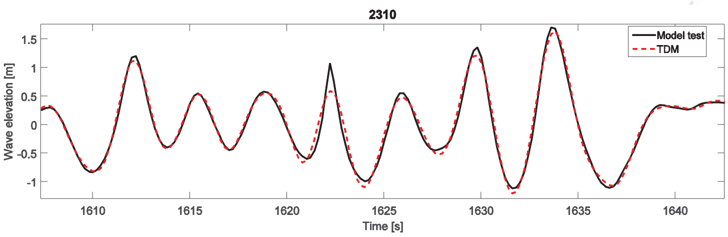

Airy wave theory v.s. measured realizations of wave elevation

Wave induced transfer function moduli

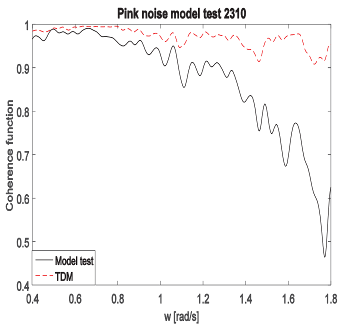

Coherence function: 1-hour wave elevation and the fore-aft bending moment (M_y) . Pink noise model test , $\mathrm{H_s} = 2$ m

- Non-linear effects, noise and uncertainties

$$\gamma^2_{x_i y_i}(\omega) = \frac{|G_{x_i y_i}(\omega)|^2}{G_{x_i x_i}(\omega) G_{y_i y_i}(\omega)}$$

$$0 \le \gamma^2_{x_i y_i} \le 1$$

Responses in moderate waves

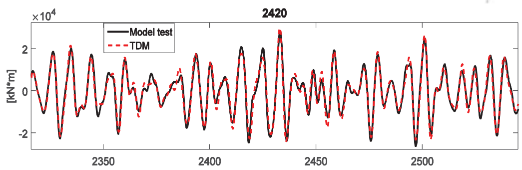

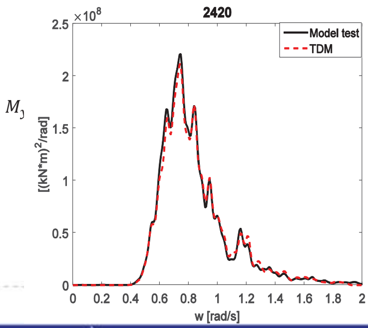

Moderate waves

Good agreement

$\mathrm{H_s} = 3.6$ m and $\mathrm{T_p} = 10.2$ s.

Responses in extreme waves

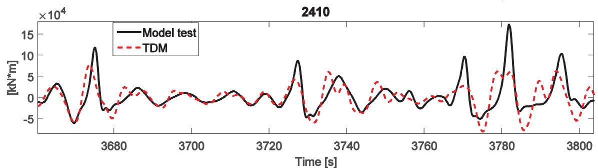

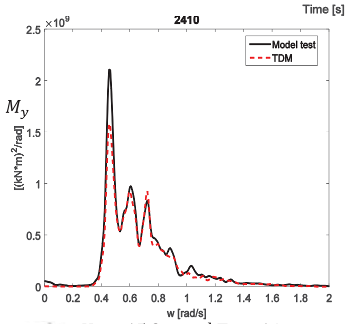

$\mathrm{H_s} = 15.3$ m and $\mathrm{T_p} = 14$ s.

Extreme waves

2nd and higher order wave loads
(not included in the TDM)

Non-linear wave kinematics
(not included in the TDM)

Responses in wind and waves

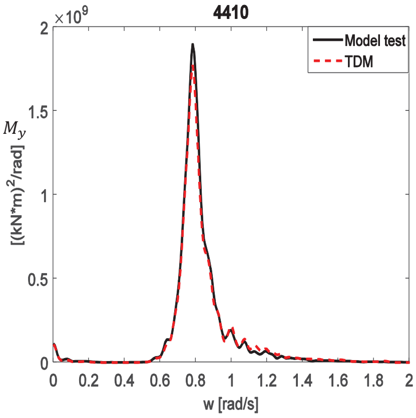

Turbulent winds, mean wind speed = 8 m/s
H_s = 5.2 m and T_p = 8 s.

2nd and higher order wave loads
(not included in the TDM)

Aerodynamic damping [5]

Drag forces

Transfer function modulus curves for the fore-aft bending moment and components of the corresponding external and inertial loads

Base of the side column 1

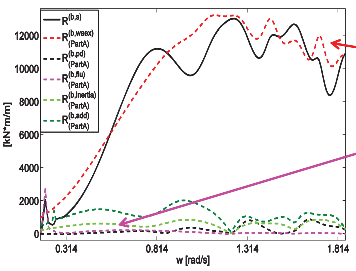

$$R^{b,s}(\omega,t) = R^{b,inertia}_{PartA}(\omega,t) + R^{b,add}_{PartA}(\omega,t) + R^{b,pd}_{PartA}(\omega,t) + R^{b,flu}_{PartA}(\omega,t) - R^{b,waex}_{PartA}(\omega,t)$$

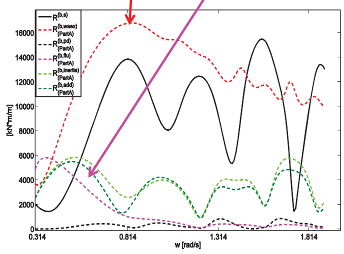

A given cross section in the Pontoon 1

Conclusions

- The time-domain approach has been validated.
- Good agreement between simulations and measurements
- Non-linear effects (e.g. 2nd and higher order wave loads and wave kinematics)
- Uncertainties, noise and unknown errors in the measurements
- Comparisons of the simulated and measured global forces and moments in the pontoons and the central column are considered future work.
- Achieving consistent aerodynamic damping in the experimental and numerical model is challenging

ACKNOWLEDGEMENT

The authors acknowledge Mr. Fredrik Brun from SINTEF Ocean for providing the figures in the slide 7 and the financial support provided by the Research Council of Norway through the Centre for Ships and Ocean Structures; the Norwegian Research Centre for Offshore Wind Technology (NOWITECH), NTNU; and the Centre for Autonomous Marine Operations and Systems (AMOS), NTNU.

REFERENCE

[1] Luan, C., Gao, Z., and Moan, T., (2016). "Design and analysis of a braceless steel 5-mw semi-submersible wind turbine". Proceedings of the 35th International Conference on Ocean, Offshore and Arctic Engineering, OMAE2016-54848, Busan, Korea, June 19–24.
[2] Luan, C., Gao, Z. and Moan, T., (2017), "Development and verification of a time-domain approach for determining forces and moments in structural components of floaters with an application to floating wind turbines". Marine Structures. vol. 5 pp 87-109.
[3] Bachynski, E. E., Thys, M., Chabaud, V., and Sauder, T., (2016). "Realtime Hybrid Model Testing of a Braceless Semi-submersible Wind turbine. Part II: Experimental Results". In 35th International Conference on Ocean, Offshore and Arctic Engineering, no OMAE2016-54437.
[4] Sauder, T., Chabaud, V., Thys, M., Bachynski, E. E., and Sæther, L. O., (2016). "Real-time hybrid model testing of a braceless semi-submersible wind turbine: Part I: The hybrid approach". In 35th International Conference on Ocean, Offshore and Arctic Engineering, no. OMAE2016-54435.
[5] Stewart, G. and Muskulus, Michael., (2016). "Aerodynamic Simulation of the MARINTEK Braceless Semisubmersible Wave Tank Tests". WindEurope Summit. Journal of Physics: Conference Series 749 (2016) 012012.

Thank you for your attention

Real-time hybrid testing

Model Test program:

- Tests without hybrid system
  Decay, Regular waves, Irregular waves
- Tests with zero wind
  Decay, Regular waves, Irregular waves
- Tests with constant wind
  Decay and Regular waves
- Tests with turbulent wind
  -Wind-only
  -Irregular waves
    -Below rated, rated, above rated
    -One test with current
    -Misaligned waves
  -Fault conditions

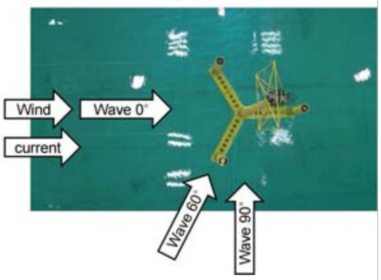

Step by step increase in complexity with repetitions and decomposed conditions

Environmental conditions of selected model tests

Reference No.	Mean wind speed at nacelle height [m/s]	H_s [m]	T_p [s]	Wind direction [degree]	Wave direction [degree]	Model test duration [hour]	Note
1713	11	-	-	0	-	3	Turbulent wind only
1733	25	-	-	0	-	3	
2310	-	2	3.5-22	-	0	3	Pink noise tests Wave only
2321	-	4	4.5-22	-	0		
2331	-	4	4.5-16	-	60		
2340	-	4	4.5-16	-	90		
2410	-	15.3	14	-	0	3	JONSWAP spectrum Wave only
2420	-	3.6	10.2	-	0	3	
4121	25	5.9	11.3	0	0	3	Turbulent wind JONSWAP spectrum
4221	25	5.9	11.3		60		
4310	11	3.6	10.2		0		
4410	8	5.2	8		0		

Development of a time-domain numerical approach for determining forces and moments in floaters

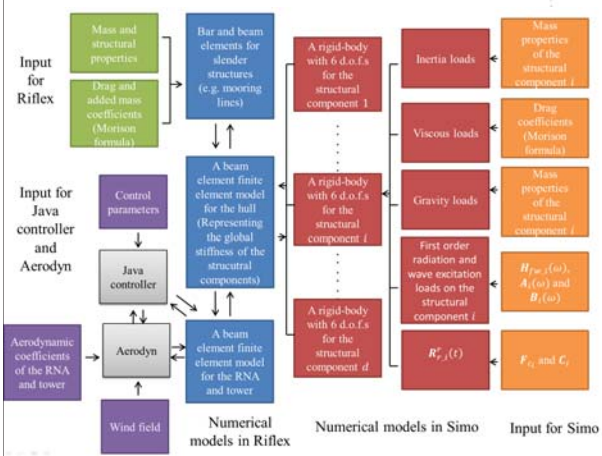

A flow chart

Simo/Riflex/ Aerodyn

A generic horizontal axis floating wind turbine

Nacelle Based Lidar Measurements for the Characterisation of the Wake of an Offshore Wind Turbine under Different Atmospheric Conditions

Davide Trabucchi, Juan-José Trujillo, Katrin Ritter, Jorge Steiner and Martin Kühn
ForWind - University of Oldenburg, Institute of Physics

14th Deep Sea Offshore Wind R&D Conference, EERA DeepWind 2017
18-20 January 2017, Trondheim, Norway

davide.trabucchi@uni-oldenburg.de

Wake losses and wake models

50% uncertainties on prediction of **wake losses** for offshore wind farm projects

Negative influence on external investors

Wake models need to be improved

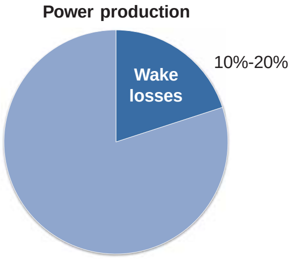

Objective

Show how full-field lidar data can be applied to the verification of wake models

Outline

1. Measurements
2. Wake model
3. Parameter fit
4. Results

Measurements
Experimental setup in Nordsee Ost

- 48x Senvion 6.2M126
- Mast with cup anemometers and vane at hub height
- Nacelle based long range scanning lidar on NO48
- Operational data of NO48

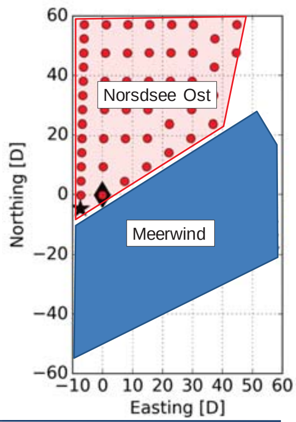

Measurements
Lidar principles & settings

- Light pulses illuminate a thin volume
- Doppler effect from aerosol backscatter

⇒ Measurement of **radial wind component** as **volume average**

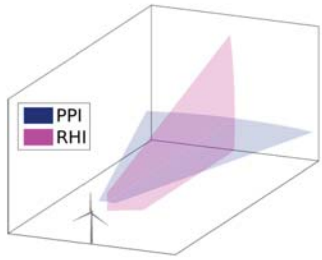

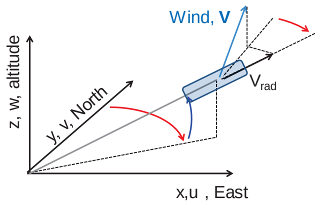

Scanning parameters	
Cycle (≈200s)	5PPI+1RHI
Sector	-15° → +15° (0.5° res.)
Speed	1°/s
Accumulation time	0.5s
Range	100 m → 1000m (100 m → 2500m)
Range spacing	15m (25m)

Measurements
Lidar data

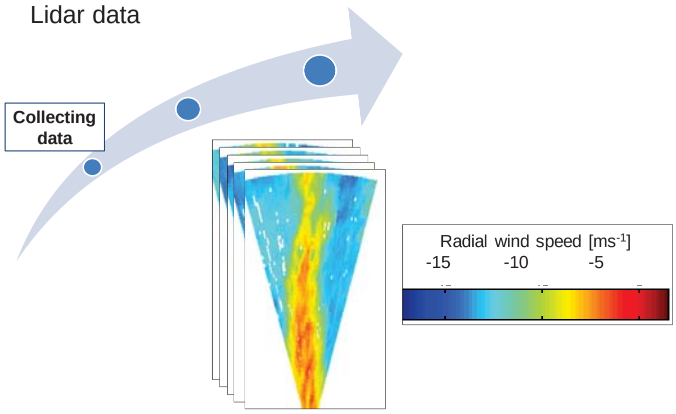

Measurements
Lidar data

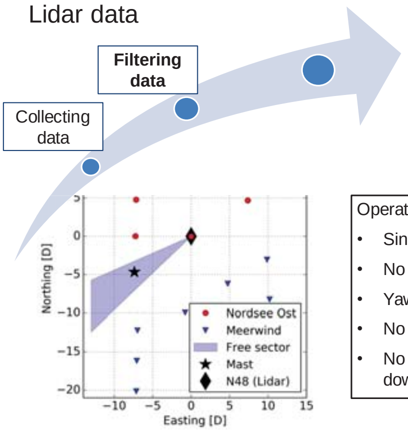

Operation	Lidar data
• Single wake sector • No nacelle yaw • Yaw misalignment < 3° • No near wake • No influence of downstream turbine	• Hard target • High noise • Outliers

Measurements
Lidar data

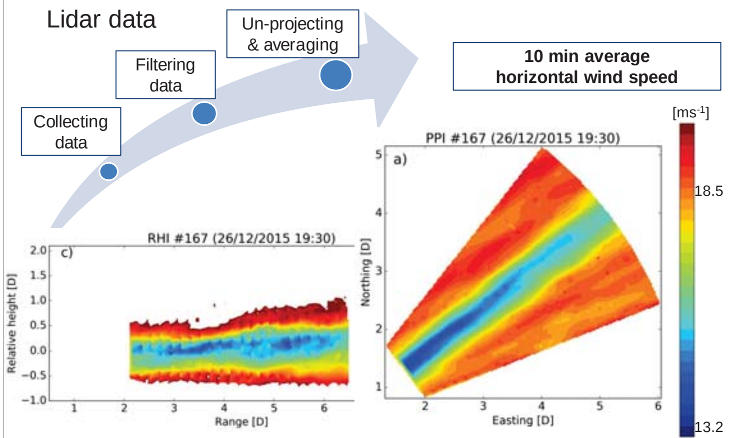

Analytical wake model
Profile

Wake deficit

$$V_D = 1 - \frac{V_{hor}}{V_{hub}}$$

Wake deficit model

$$V_{DM} = A(x_w, C_T)\exp\left(-\frac{y_w^2 + z_w^2}{2\sigma(x_w)^2}\right)$$

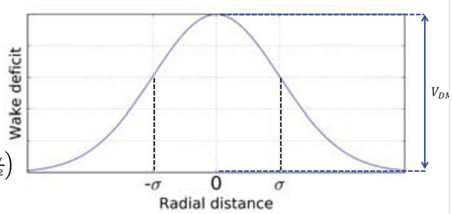

Rotation according to wind direction φ

$$x_w = x\sin(90-\gamma) + y\cos(90-\varphi)$$
$$y_w = y\cos(90-\gamma) - x\cos(90-\varphi)$$

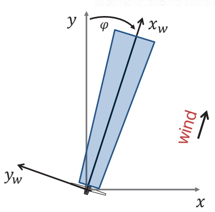

Analytical wake model
Downstream development [1]

- Linear wake expansion
  $\sigma = \varepsilon + k^* x_w$
- From
  1. Thrust coefficient C_T
  2. Mass conservation
  3. Momentum balance

  $\Rightarrow\ \varepsilon \approx 0.2\sqrt{\beta}$ with $\beta = \frac{1}{2}\frac{1+\sqrt{1-C_T}}{\sqrt{1-C_T}}$

  $\Rightarrow\ A = \left(1 - \sqrt{1 - \frac{C_T}{8\sigma^2}}\right)$
- From scaled experiment LES[2]

  $\Rightarrow k^* = 0.3837\ TI\ +\ 0.003678$

$$V_{DM} = A(x_w, C_T)\exp\left(-\frac{y_w^2 + z_w^2}{2\sigma(x_w)^2}\right)$$

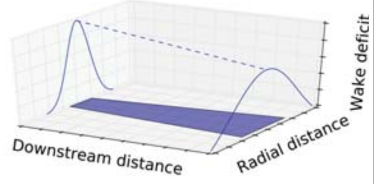

1:Batankhah 2014
2:Niayifar 2016

Results
Fit to the data

$$V_{DM} = \left(1 - \sqrt{1 - \frac{C_T}{8(\varepsilon + k^* x_w)^2}}\right)\exp\left(-\frac{y_w^2 + z_w^2}{2(\varepsilon + k^* x_w)^2}\right)$$

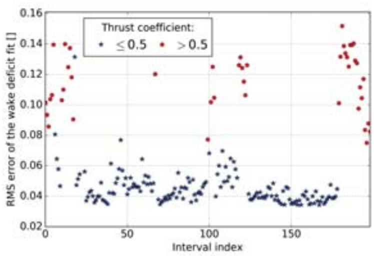

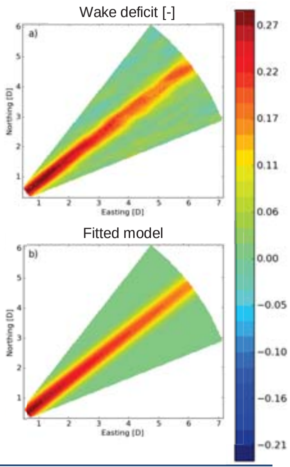

- Better fit for lower thrust coefficient
- Only few time intervals excluded after visual inspection

Results
Wake and wind direction

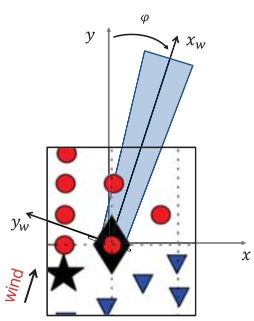

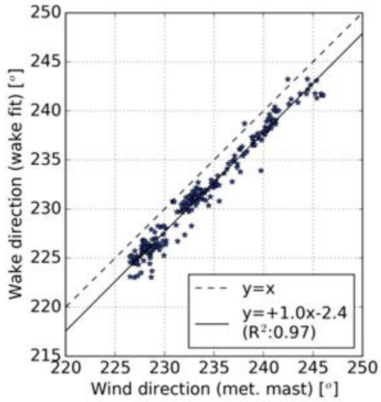

- Good agreement
- Small offset

Results
Expansion rate

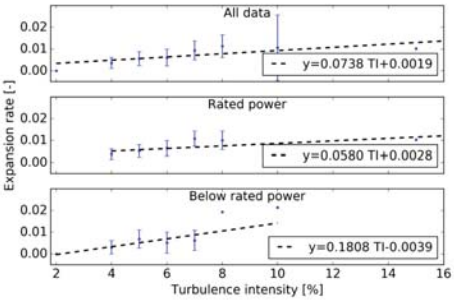

- Very small offset similar as Niayfar et al. 2016
- Smaller slope than Niayfar et al. 2016
- Improved agreement for cases below rated power

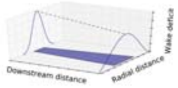

- Linear wake expansion: $\sigma = \varepsilon + k^* x_w$
- From scaled experiment and LES[2] : $k^* = 0.3837\, TI + 0.003678$

[2:Niayifar 2016]

Nacelle Based Lidar Measurements for the Characterisation of the Wake of an Offshore Wind Turbine under Different Atmospheric Conditions

Thanks
for the attention!

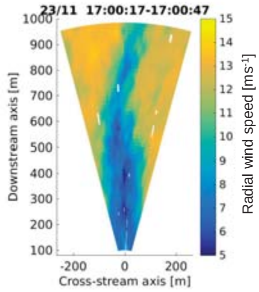

Acknowledgements. The authors would like to acknowledge RWE for providing the access to wind turbine and the meteorological mast data, Senvion for providing support during the measurement campaign and the colleagues from the University of Oldenburg who contributed to the realization of the experimental campaign. The measurement campaign was funded by the european project FP7-Energy-2011 283145/ClusterDesign.

Results
Initial width

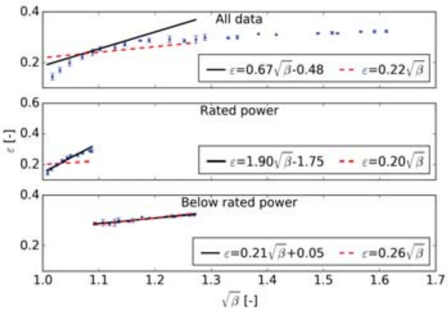

- Agreement with expectations when the offset is forced to 0
- Improved agreement for cases below rated power

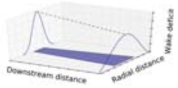

- Linear wake expansion: $\sigma = \varepsilon + k^* x_w$
- From theoretical study[1,2] : $\varepsilon \approx 0.2\sqrt{\beta}$ with $\beta = \frac{1}{2}\frac{1+\sqrt{1-C_T}}{\sqrt{1-C_T}}$

[1:Batankhah 2014
2:Niayifar 2016]

References

[1] Bastankhah, M. & Porté-Agel, F. A new analytical model for wind-turbine wakes Renewable Energy , 2014, 70, 116 – 123

[2] Niayifar, A. & Porté-Agel, F. Analytical Modeling of Wind Farms: A New Approach for Power Prediction Energies, 2016, 9, 741

Conclusions

- **Nacelle based measurements** of wind turbine wakes are a **suitable source** of data **for verification of wake models**
- **Full-field experiments** may provide **different calibration** of analytical wake models from test cases **from wind tunnel or high fidelity simulation**
- **Full-field results** are in **good agreement with theoretical expectations** from the conservation of mass and momentum when the turbine is operating below rated power

G2) Experimental Testing and Validation

Testing philosophies for floating wind turbines in coupled model tests, E.L. Walter, DNV GL

On the impact of non-Gaussian wind statistics on wind turbines – an experimental approach, J. Schottler, ForWind – University of Oldenburg

Wind Tunnel Wake Measurements of Floating Offshore Wind Turbines,
I. Bayati, Politecnico di Milano

Lidars for Wind Tunnels – an IRPWind Joint Experiment Project, M. Sjöholm, DTU Wind Energy

DNV·GL

ENERGY

JIP on Coupled analyses of FOWTs

Testing philosophies for floating offshore wind turbines

E. L. Walter, S. Gueydon, P. A. Berthelsen
19 January 2017

MARIN
SINTEF

JIP on Coupled Analysis of FOWTs

- DNV GL joint industry project (JIP) together with thirteen global partners
- Developing a Recommended Practice (RP) for coupled analysis of floating offshore wind turbines
- Building on the experience from the application of the Offshore Standard DNV-OS-J103
- Work package 6, consisting of DNV GL, MARIN and SINTEF Ocean (fmr. MARINTEK), considers model tests of FOWTs.

Purpose of this presentation

- Present on overall level
  - Why perform model tests?
  - Challenges with testing FOWT
  - Methods for testing FOWT
- Get your input to the RP development:
  - What kind of model tests are preferred?
  - What challenges have been experienced?
  - What simplifications have been necessary?

Why perform model tests?

- DNV-OS-J103 clause 6.2.1 states:

  "Model tests shall be carried out to validate software used in design, to check effects which are known not to be adequately covered by the software, and to check the structure if unforeseen phenomena should occur."

- Validation of numerical and analytical models
- Calibration of hydrodynamic coefficients
- Study of global behaviour or other special effects

General challenges of coupled hydro-aero testing of FOWTs

- Froude scaling is usually applied in hydrodynamic tests.

  ⇒Too low Reynolds number for aerodynamic loads on the rotor

	Definition	Description
Froude	$Fr = \frac{U}{\sqrt{gL}}$	Ratio inertia force to gravity force
Reynolds	$Re = \frac{UL}{\nu}$	Ratio inertia force to viscous force

- Representation of aerodynamic loads
- Generation of wind fields with high quality
- Size of rotor

Representation of aerodynamic loads

Introduction

- For FOWTs, both hydrodynamic and aerodynamic loads can be significant for global behaviour and design driving loads
- With Froude scaling, which is necessary to scale wave loads correctly, Reynolds number is wrong and aerodynamics are not reproduced correctly
- Representation of aerodynamic loads in such low Reynolds regime is key to reliable model tests of FOWTs in model basins
- What methods are applicable for different purposes?

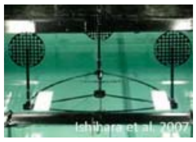

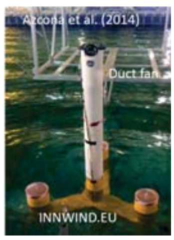

Testing philosophies for hydrodynamic model tests of FOWTs

- Three main philosophies:
  - Passive methods (simplified)
  - Physical wind turbine
  - Hybrid test methods
- Tests in wind tunnels are not considered here (c.f. presentation by I. Bayati from Politecnico di Milano later today)

Quick survey

Quick survey

How many of you have performed or been involved in (as e.g. stakeholder) a model tests campaign?

Quick survey

Do you favour passive methods?

Do you favour active methods?

Quick survey

Particular challenges you experienced in your campaigns?

What did work / what did not work?

Passive Method: Wire applying constant force

- Wire applying constant horizontal force on the tower
- Mean thrust
- Drawbacks include:
  - Only steady thrust is modelled (variation of thrust and aero-hydro-coupling are deficiently modelled)
  - Other aerodynamic loads neglected
- Examples: AFOSP/Windcrete - Matha et. al (2014) and Molins et. al (2014)

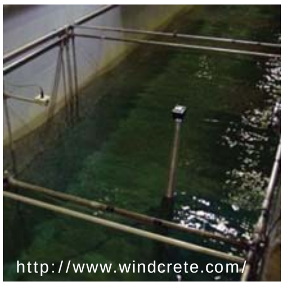

Passive method: Obstructing disk

- Solid or perforated disc
- Wind generated by fans
- Size of disc adjusted to give correct mean force
- Gyroscopic loads included if the disc can spin, or by rotating a rod with proper mass distribution

- Drawbacks:
  - Blade/tower interactions (tower shadow) omitted
  - Aerodynamic torque omitted
  - Varying drag loads due to flow issues around disc

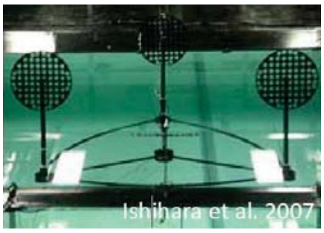

Refined methodology: Physical wind turbine

- Scaled down functional rotors
- Wind field generated by fans (Froude scaled)
- **Performance scaling** of blades
- Includes many more effects than the passive methods

- Challenges and limitations:
  - Mass distribution (heavy turbine)
  - Accuracy of generated wind field
  - Other aerod. load comp. than thrust
  - Validity of performance scaling outside calibrated range of wind velocities
  - Redesign of the blades is not easy and it results in a different rotor

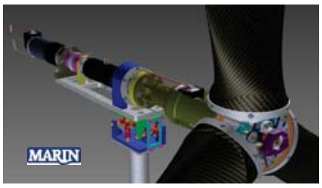

Generation of wind

- Wind field can change rapidly in space as it circulates in the model basin

- Shear with water surface, walls and ceiling

- Low wind speeds required for Froude scaled wind - see e.g. Koch et. al (2016)

- Wind field characteristics should be documented before tests are initiated

- Common ways to improve wind field:
  - Nozzles and honeycomb grid
  - Larger basins are advantageous for recirculation of the air flow

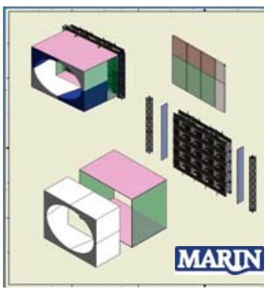

Hybrid testing methods

- Floating foundation tested physically at model scale, while virtual model of wind turbine simulated in real-time on computer
- Real and virtual model connected by sensors and actuators, e.g.:
  - Small fans mounted in a matrix layout
  - Cable-driven robots

- Challenges and limitations:
  - Complexity of interface between real and virtual model, e.g.
    - Time delays
    - Application of high frequency loads
    - Dynamic response of actuators
  - Aerodynamic loads 'as good as' numerical model

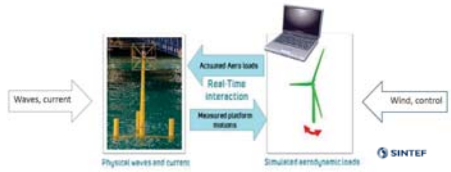

Summary – Mitigation of Froude/Reynolds scaling issues for model tests of FOWTs

Method	Mitigation strategy
Passive wire, obstructing disc or fan/jet	Calibrate thrust load rather than wind speed
Physical wind rotors	Redesign blades
Hybrid methods	Aerodynamic loads are calculated in software at full-scale, and resulting loads are applied by actuators at model scale

Experience from the industry

The following items are being discussed in the JIP work package, but we are interested in hearing experiences made by the industry (both from the JIP participants and the general industry)

- What model scales have been applied in your tests?

- What important simplifications was necessary in your tests?

- Did you use a passive or active system to model aerodynamic loads? Are tests with passive solutions of any value?

- Was a blade pitch controller included in your tests? Was the controller changed after the model tests – and do you plan to perform new tests with the updated controller?

Experience from the industry ctd.

- What was the reason for performing the model test? Calibration/validation of model/software or verification of concept/design?
- Has the concept changed after the model tests – and are the model tests deemed valid for the updated concept?
- What is your opinion on the value of full scale tests versus controlled model scale tests?
- What is important when selecting the format of model tests?
  - Methodologies for testing FOWT
  - Quality of tests
  - Simplicity of tests
  - Expertise and experience

Literature

- de Ridder, E.-J., Otto, W., Zondervan, G.-J., Huijs, F., Vaz, G., 2014, Development of a Scaled-Down Floating Wind Turbine for Offshore Basin Testing, Proc. 33th Int. Conf. on Ocean, Offshore and Arctic Engineering, California, USA.
- Ishihara, T., Phuc, P.V., Sukegawa, H., Shimada, K., Ohyama, T. (2007). A study on the dynamic response of a semi-submersible floating offshore wind turbine system Part 1: A water tank test. ICWE12, Cairns, Australia.
- Koch, C.; Lemmer, F.; Borisade, F.; Matha, D.; Cheng, P.W. „Validation of INNWIND.EU Scaled Model Tests of a Semi-submersible Floating Wind Turbine", ISOPE 2016, Rhodes, Greece
- Matha, D., Sandner, F., Molins, C., Cheng, P.W.; "Efficient preliminary floating offshore wind turbine design and testing methodologies and application to a concrete spar design", Phil. Trans. R. Soc. A, 373(20140347)
- Molins, C., Campos, A., Sandner, F., Matha, D.; "Monolithic concrete offshore floating structure for wind turbines", Proceedings of EWEA, Barcelona, Spain 2014
- Sandner, F.; Amann, F.; Matha, D.; Azcona, J.; Munduate, X.; Bottasso, C.; Campagnolo, F.; Bredmose, H.; Manjock, A.; Pereira, R.; Robertson, A. "Model Building and Scaled Testing of 5MW and 10MW Semi-Submersible Floating Wind Turbines", 12th Deep Sea Offshore Wind R&D Conference, EERA DeepWind'2015, Trondheim, Norway
- Sauder T., Chabaud V., Thys M., Bachynski E.E., and Sæther L.O., 2016, Real-time hybrid model testing of a braceless semi-submersible wind turbine. Part I: The hybrid approach. Proc. 35th Int. Conf. on Ocean, Offshore and Arctic Engineering, Busan, Korea

Please join us for a chat after the session

Erik Løkken Walter
Erik.Lokken.Walter@dnvgl.com

www.dnvgl.com

SAFER, SMARTER, GREENER

On the impact of non-Gaussian wind statistics on wind turbines - an experimental approach

Jannik Schottler, N. Reinke, A. Hölling, J. Peinke, M. Hölling

ForWind, Center for Wind Energy Research
University of Oldenburg, Germany

jannik.schottler@forwind.de

Motivation

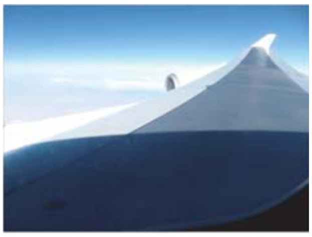

source: youtube.com

- wind turbines are subjected to **atmospheric turbulence**!
- potential impact on...
  - ...power output: grid fluctuations [Carrasco et al., 2006; Sørensen et al., 2007]
  - ...torque: drive train failure [Musial et al., 2007; Feng et al., 2013]
  - ...loads: lifetime [Burton et al., 2001]

$€ - cost of energy

Motivation

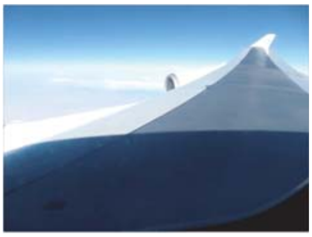

source: youtube.com

Motivation

Field measurements

- expensive
- limited availability
- uncontrolled boundary conditions

Motivation

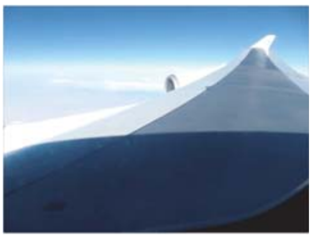

source: youtube.com

- wind turbines are subjected to **atmospheric turbulence**!
- potential impact on...
  - ...power output: grid fluctuations [Carrasco et al., 2006; Sørensen et al., 2007]
  - ...torque: drive train failure [Musial et al., 2007; Feng et al., 2013]
  - ...loads: lifetime [Burton et al., 2001]

Motivation

Field measurements

- expensive
- limited availability
- uncontrolled boundary conditions

Numerics

- turbulence models
- computational costs
- validation?

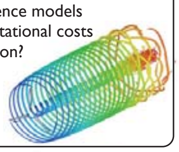

Motivation

Field measurements

- expensive
- limited availability
- uncontrolled boundary conditions

Numerics

- turbulence models
- computational costs
- validation?

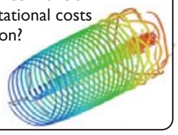

Experiments

- inexpensive
- controlled environment
- **tunable boundary conditions**
- upscaling?

Describing turbulence

- industry standard for wind field description:

  10 min mean values, turbulence intensity

$$TI = \sigma_u / \langle u \rangle$$

Motivation

Field measurements

- expensive
- limited availability
- uncontrolled boundary conditions

Numerics

- turbulence models
- computational costs
- validation?

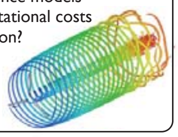

Experiments

- inexpensive
- controlled environment
- **tunable boundary conditions**
- upscaling?

Describing turbulence

- industry standard for wind field description:

  10 min mean values, turbulence intensity

$$TI = \sigma_u / \langle u \rangle$$

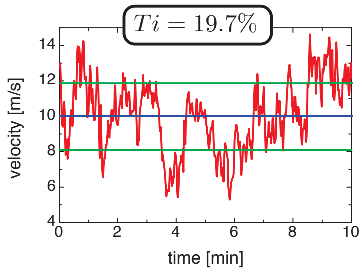

Motivation

Field measurements

- expensive
- limited availability
- uncontrolled boundary conditions

Numerics

- turbulence models
- computational costs
- validation?

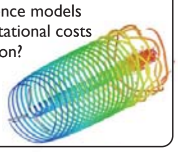

Experiments

- inexpensive
- controlled environment
- **tunable boundary conditions**
- upscaling?

Describing turbulence

- industry standard for wind field description:

  10 min mean values, turbulence intensity

$$TI = \sigma_u / \langle u \rangle$$

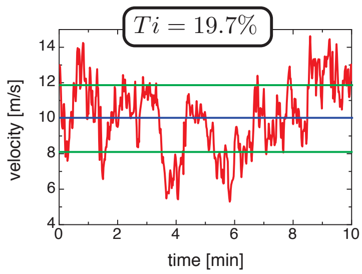

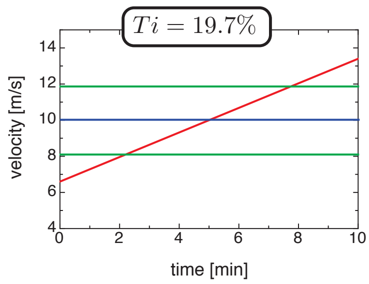

Increment statistics

time series

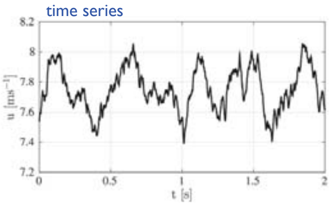

Increment statistics

time series

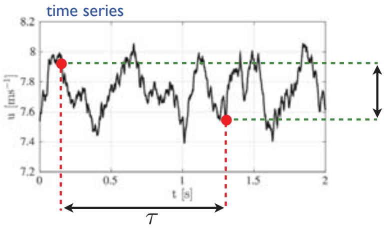

velocity increment

$u_\tau := u(t+\tau) - u(t)$

time series of increments

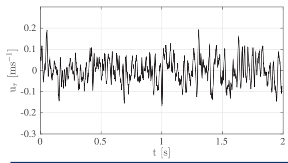

Increment statistics

time series

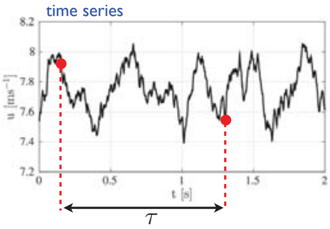

Increment statistics

time series

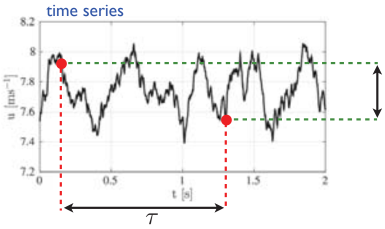

velocity increment

$u_\tau := u(t+\tau) - u(t)$

increment PDF

time series of increments

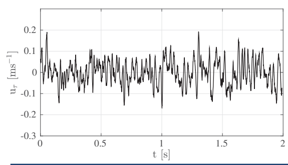

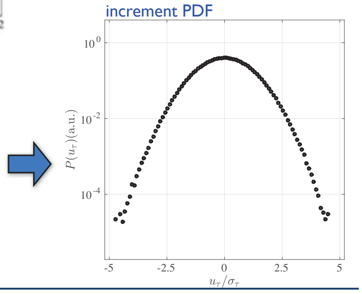

Increment statistics

time series

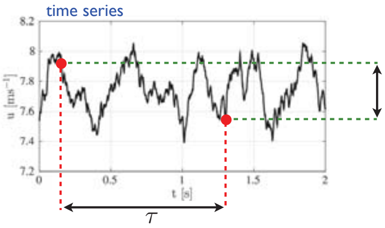

velocity increment

$u_\tau := u(t+\tau) - u(t)$

Industry standards

IEC 61400-1-ED3, 2005 wind turbines, design requirements

turbulence: Mann model (1998) / Kaimal model (1972)

Industry standards

IEC 61400-1-ED3, 2005 wind turbines, design requirements

turbulence: Mann model (1998) / Kaimal model (1972)

Increment PDF according to IEC-Norm (TurbSim, Kaimal model)

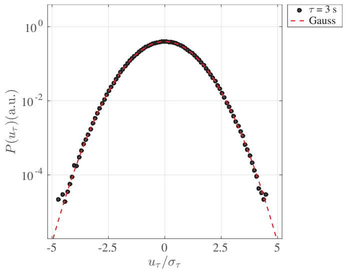

Field data vs model

Time series	$\langle u \rangle$ [m s^{-1}]	σ_u [m s^{-1}]	TI [%]
Kaimal	7.51	0.54	7.21
FINO1	7.50	0.54	7.18

- datasets nearly equal acc. to mean + TI

Industry standards

IEC 61400-1-ED3, 2005 wind turbines, design requirements

turbulence: Mann model (1998) / Kaimal model (1972)

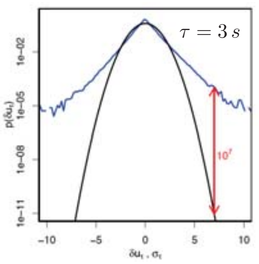

- offshore wind data
- non-Gaussian, intermittent increments
- underestimation of extreme events

[Wächter et al. 2012]

Field data vs model

Time series	$\langle u \rangle$ [m s^{-1}]	σ_u [m s^{-1}]	TI [%]
Kaimal	7.51	0.54	7.21
FINO1	7.50	0.54	7.18

- datasets nearly equal acc. to mean + TI

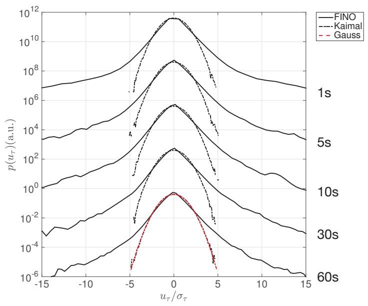

- strongly different regarding increment PDF
- intermittency not reflected correctly by Kaimal model

Industry standards

IEC 61400-1-ED3, 2005 wind turbines, design requirements

turbulence: Mann model (1998) / Kaimal model (1972)

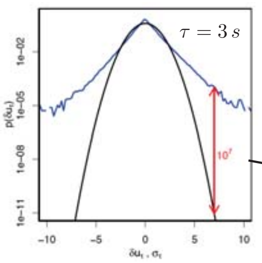

- offshore wind data
- non-Gaussian, intermittent increments
- underestimation of extreme events

once a year ➡ every 5 minutes!

[Wächter et al. 2012]

Field data vs model

Time series	$\langle u \rangle$ [m s^{-1}]	σ_u [m s^{-1}]	TI [%]
Kaimal	7.51	0.54	7.21
FINO1	7.50	0.54	7.18

- datasets nearly equal acc. to mean + TI

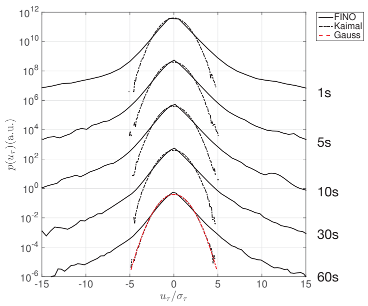

- strongly different regarding increment PDF
- intermittency not reflected correctly by Kaimal model

Impact on wind turbines?

Setup

[Schottler et al., 2017]

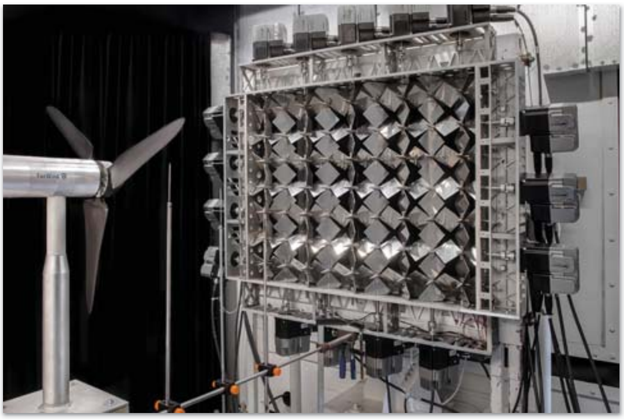

Turbulence generation

- 16 axes w/ stepper motors
- individually tunable
- defined, turbulent flows
- reproducible:
  - time series
  - statistics

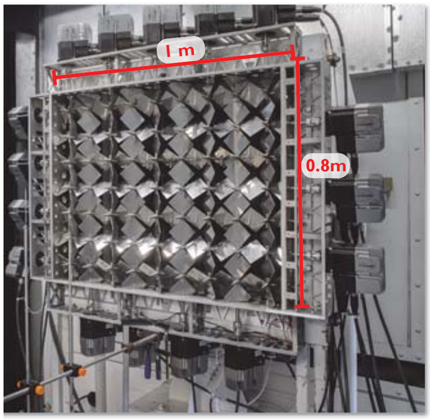

Turbulence generation

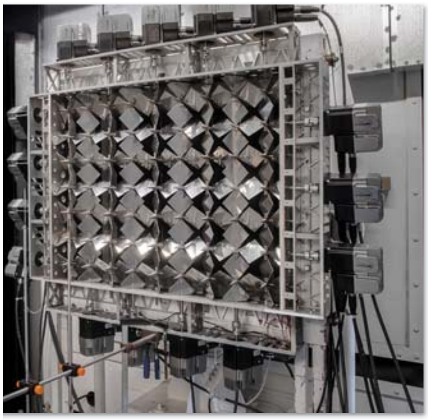

Turbulence generation

- 16 axes w/ stepper motors
- individually tunable
- defined, turbulent flows
- reproducible:
  - time series
  - statistics

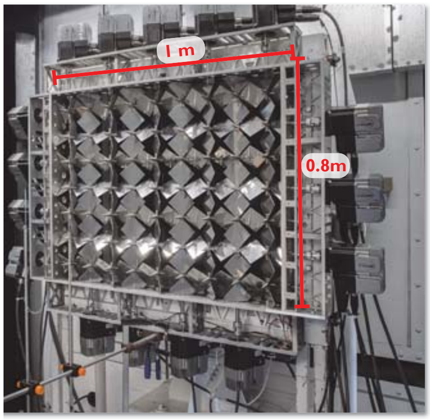

Turbulence generation

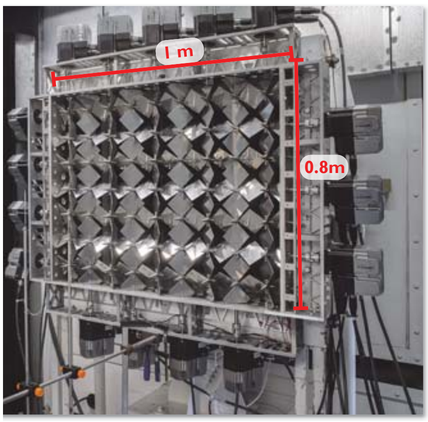

Setup

- model wind turbine
- D=58cm
- active load control
- hot wire measurements upstream of rotor
- TSR = 7
- turbine data:
  - thrust (load cell)
  - torque (generator current)
  - power (electric)

Setup

- model wind turbine
- D=58cm
- active load control
- hot wire measurements upstream of rotor
- TSR = 7
- turbine data:
  - thrust (load cell)
  - torque (generator current)
  - power (electric)

Main idea

Inflow A) Inflow B)

equal according to mean+ TI

Gaussian increments

Main idea

Inflow A) Inflow B)

Main idea

Inflow A) Inflow B)

equal according to mean+ TI

Gaussian increments intermittent flow

Main idea

Inflow A) Inflow B)

equal according to mean+ TI

Main idea

Inflow A) Inflow B)

equal according to mean+ TI

Gaussian increments intermittent flow

Does the turbine ‚see' the difference?

Inflow

- hot wire data
- measured at rotor plane
- no turbine installed

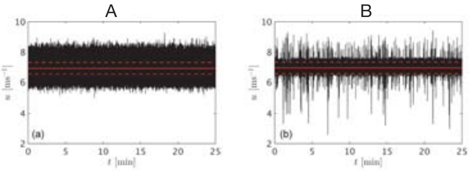

[Schottler et al. 2017]

Inflow

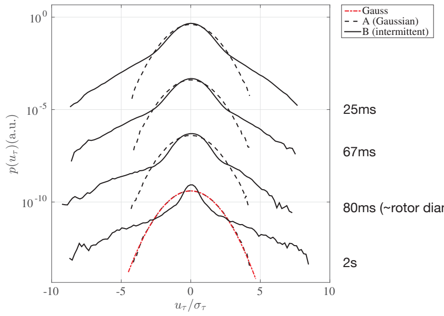

25ms

67ms

80ms (~rotor diameter)

2s

Inflow

- hot wire data
- measured at rotor plane
- no turbine installed

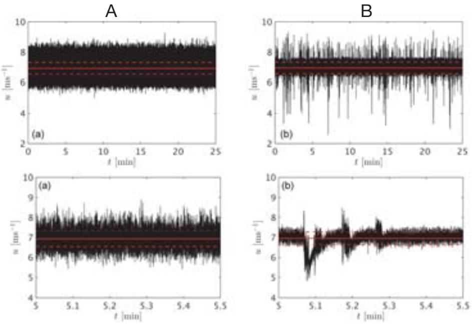

[Schottler et al. 2017]

Inflow

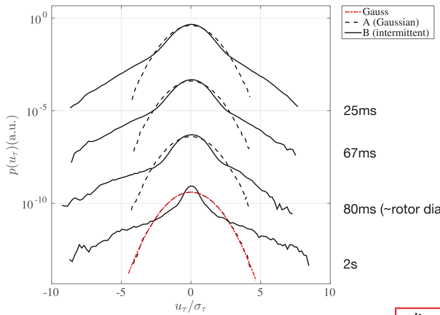

Time series	$\langle u(t)\rangle$ [m s^{-1}]	σ_u [m s^{-1}]	TI [%]
A	6.92	0.39	5.59
B	6.96	0.38	5.50

25ms

67ms

80ms (~rotor diameter)

2s

- discrepancy between Gaussian assumption and intermittency reproduced in the lab!
- effect of properties beyond mean + TI (intermittency) isolated

Inflow

- hot wire data
- measured at rotor plane
- no turbine installed

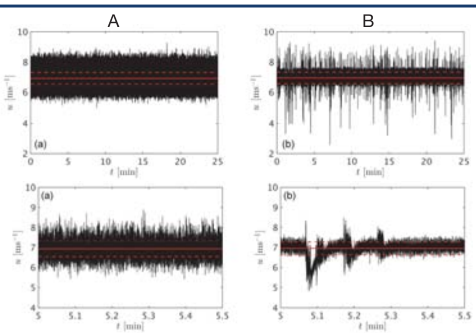

Time series	$\langle u(t)\rangle$ [m s^{-1}]	σ_u [m s^{-1}]	TI [%]
A	6.92	0.39	5.59
B	6.96	0.38	5.50

[Schottler et al. 2017]

Turbine reaction - thrust

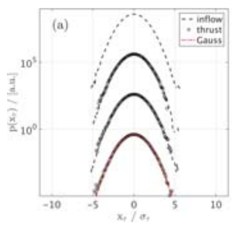

25ms (~blade length)

67ms

80ms (~rotor diameter)

2s

Turbine reaction - thrust

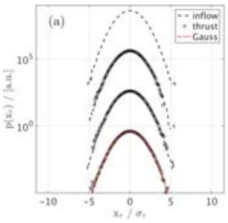

25ms (~blade length)

67ms

80ms (~rotor diameter)

2s

Gaussian inflow
↓
Gaussian thrust

Turbine reaction - all quantities

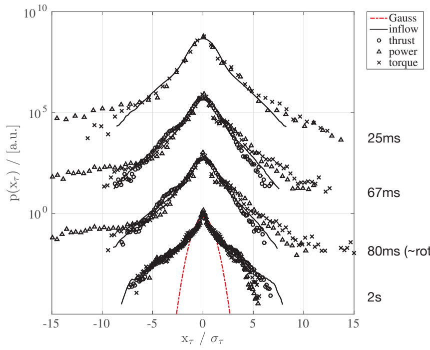

25ms

67ms

80ms (~rotor diameter)

2s

Turbine reaction - thrust

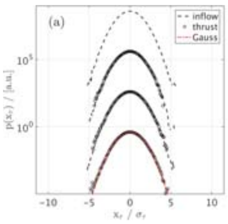

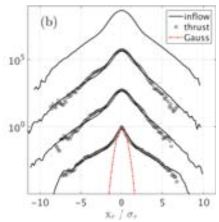

25ms (~blade length)

67ms

80ms (~rotor diameter)

2s

Gaussian inflow
↓
Gaussian thrust

intermittent inflow
↓
intermittent thrust

Turbine reaction - all quantities

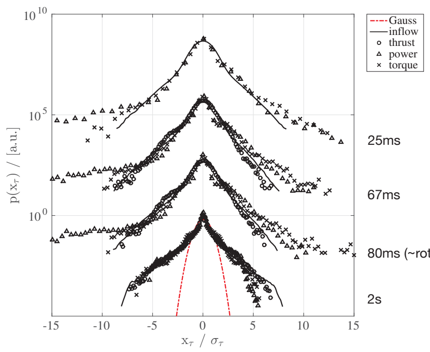

25ms

67ms

80ms (~rotor diameter)

2s

Intermittent characteristics remain present in turbine data !

Turbine reaction - thrust

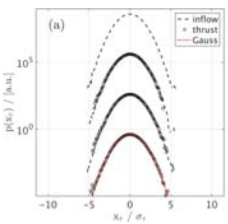

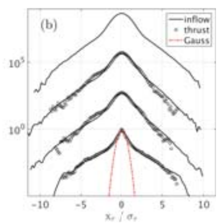

25ms (~blade length)

67ms

80ms (~rotor diameter)

2s

Gaussian inflow
↓
Gaussian thrust

intermittent inflow
↓
intermittent thrust

no ‘filtering’ of intermittency by the turbine

Impact on wind turbine

One second data, multi MW nearshore turbine

[P. Milan]

Impact on wind turbine

One second data, multi MW nearshore turbine

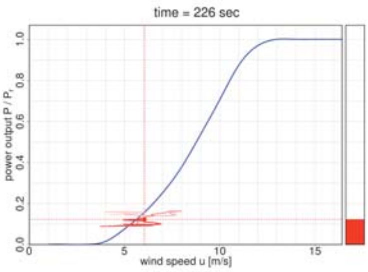

[P. Milan]

Load Control

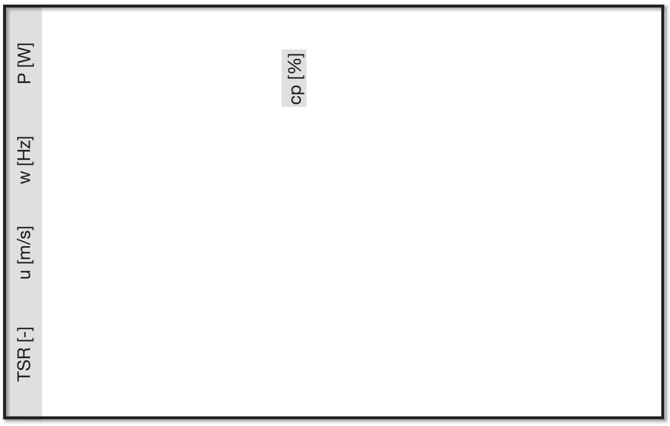

Impact on wind turbine

One second data, multi MW nearshore turbine

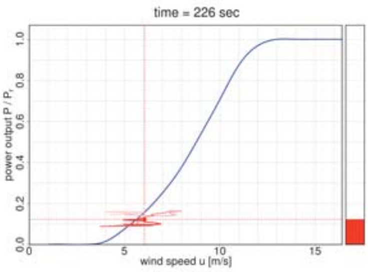

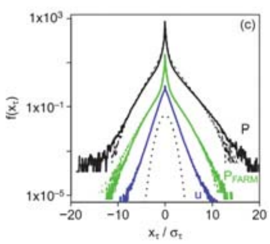

[Milan et al. 2013]

[P. Milan]

Load Control

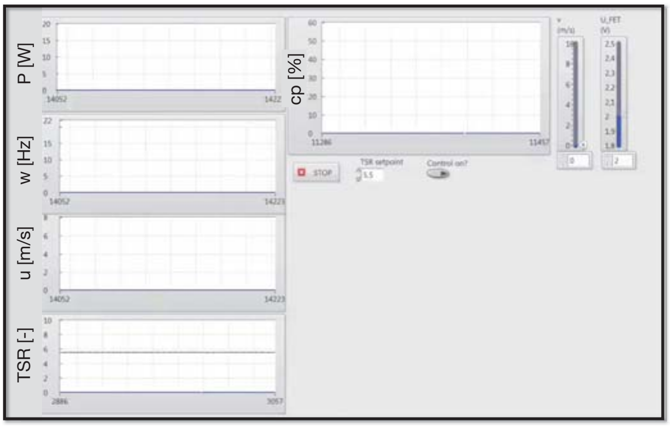

Thank you for your attention!

REINER LEMOINE STIFTUNG

Funded by the Reiner Lemoine Stiftung

Further information:

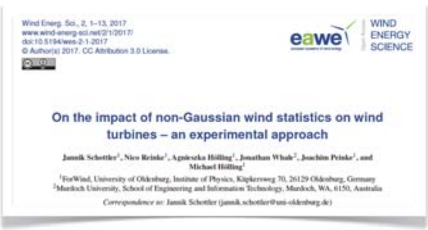

Wind Energ. Sci., 2, 1–13, 2017
www.wind-energ-sci.net/2/1/2017/
doi:10.5194/wes-2-1-2017

eawe WIND ENERGY SCIENCE

On the impact of non-Gaussian wind statistics on wind turbines – an experimental approach

Jannik Schottler[1], Nico Reinke[1], Agnieszka Hölling[1], Jonathan Whale[2], Joachim Peinke[1], and Michael Hölling[1]

[1]ForWind, University of Oldenburg, Institute of Physics, Küpkersweg 70, 26129 Oldenburg, Germany
[2]Murdoch University, School of Engineering and Information Technology, Murdoch, WA, 6150, Australia

Correspondence to: Jannik Schottler (jannik.schottler@uni-oldenburg.de)

Eera Deepwind'2017, 14th Deep Sea Offshore Wind
R&D Conference, 18 - 20 January 2017

Wind Tunnel Wake Measurements of Floating Offshore Wind Turbines

I. Bayati, M. Belloli, L. Bernini, A. Zasso

Politecnico di Milano, Department of Mechanical Engineering

Ongoing analysis of unsteady aerodynamics of FOWTs @ PoliMi

From experiments, unsteadiness depends on:

- Tip Speed Ratio
- "Wake Reduced Velocity" V_w^*

$$\boxed{V_w^* = \frac{U}{f \cdot D}}$$

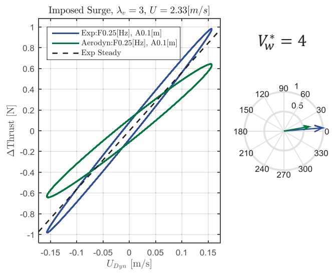

V_w^* *N* of rotor **diameters *D*** "travelled " by the air with a **drift (mean) velocity *V*** within **one cycle** of **platform motion** of **frequency *f***

$V_w^* > 5$ Quasi-steady behaviour

$V_w^* < 5$ Non-linear behaviour: the rotor re-enters its wake

Presentation's outline

- Motivations and goals
- Ongoing analysis of unsteady aerodynamics of FOWTs @ PoliMi
- Experimental Setup and Tests
- Results
- Conclusions

Experimental Setup and Tests

Experimental Setup

- Downwind Hot-wire anemometer
- Upwind Pitot Anemometer
- 6 Components balances
- Imposed Surge Motion

Tests

- **2D Map** (*Y-Z* plane)
  - @ Rated
- **1D Map** (*Y*, Hub's height)
  - @ Below Rated
  - @ Rated
  - @ Above Rated

  +
  - Different Amplitudes & frequencies

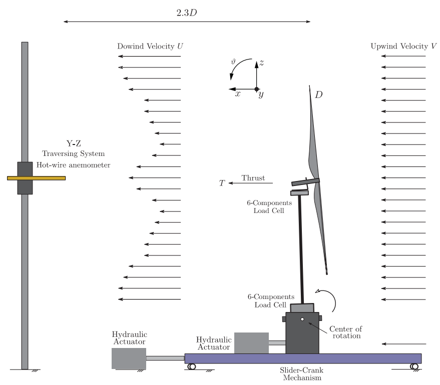

Motivations and goals

- Support side activity of LIFES50+ project Hybrid tests in Wave Basin
- Understanding unsteady aerodynamics due to platform's motion
- Calibration of numerical models

Imposed Surge motion @ different amplitudes and frequencies

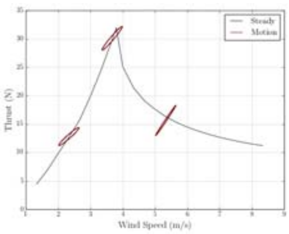

Steady 2D map @ Rated Wind Speed

- Wind speed *U*=3.67 m/s scale factor (1/3)
- Rotor Diameter D =2.38 m scale factor (1/75)
- Expected/measured Thrust ≈ 28 N scale factor (1/50594)
- Recomputed Thrust ≈ 28 N from wake deficit

$$T = \int_A \rho U (U_\infty - U) dA$$

(Mass conservation + Momentum loss)

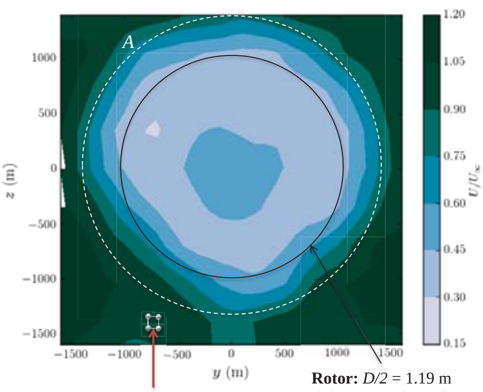

Meshgrid unit 0.1 x 0.1 m

Rotor: *D*/2 = 1.19 m (1/75 DTU 10 MW)

No Motion: the effect of *Ct* on the mean wake velocity

- High Ct = great momentum loss (Below/Low Rated)
- Low Ct = low wake deficit (Above Rated)

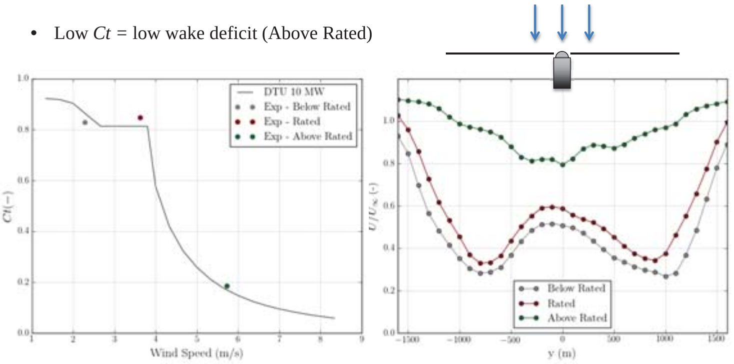

Imposed Motion: Surge frequency in the wake

- **Same operational conditions**
- **Normalization** of the FFT by the maximum peak amplitude
- Clear evidence of the **surge motion** frequency f
- Rotational frequency still evident (where present from no motion)

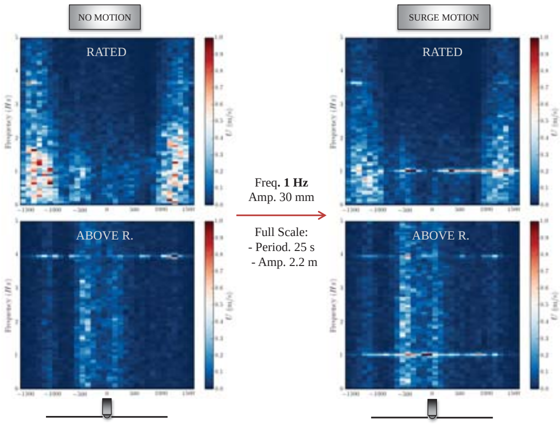

No Motion: turbulence in the wake

- Higher turbulence
- Tip vortices

- Lower turbulence
- Clear visibility of the rotational frequency (4 Hz)

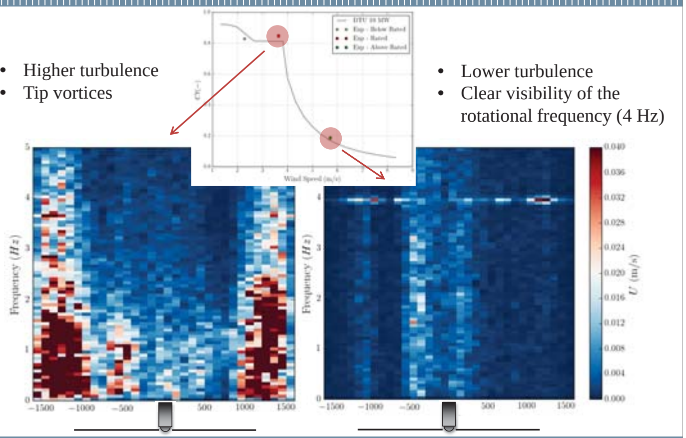

Imposed Motion: Surge frequency in the wake (Changing V_w^*) @Rated

Towards quasi-steady dynamic conditions (higher V_w^*), Surge frequency more visible in the wake…

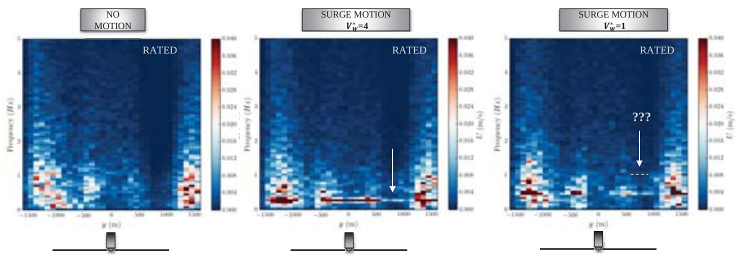

$$V_w^* = \frac{U}{f \cdot D}$$

Freq. **0.25 Hz**
Amp. 100 mm

Surge frequency visible in the wake

Freq. **1 Hz**
Amp. 30 mm

…missing Surge frequency in the wake!!

Imposed Motion: Wake dynamic component at the frequency of the imposed motion

- Mean wake velocity influences the entity of **wind oscillation** at surge frequency f

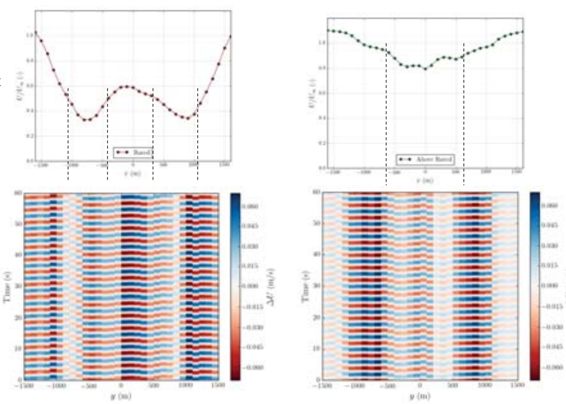

Imposed Motion: Surge frequency in the wake (depending on V_w^*) @Above rated

This dependency on V_w^* is however affected by the corresponding steady spectral content (Ct)

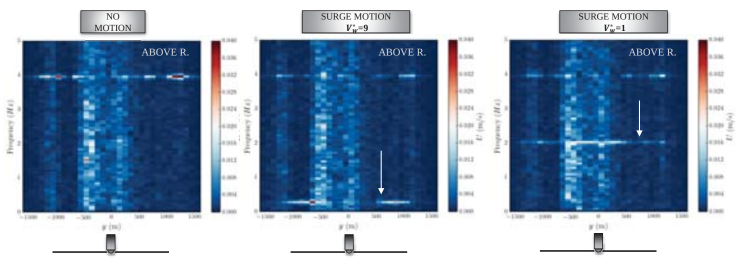

$$V_w^* = \frac{U}{f \cdot D}$$

Freq. **0.25 Hz**
Amp. 100 mm

Surge frequency visible in the wake

Freq. **2 Hz**
Amp. 15 mm

Surge frequency **still visible** in the wake

Conclusions and on-going work

- No motion, steady 2D map @ rated:
  correspondence between force measurements and wake deficit analysis
- No Motion: visible effect of *Ct* on the mean wake velocity
- No Motion: visible turbulence in the wake linked to the aerodynamic efficiency (*Ct*)
- With Motion, different wave reduced velocity V_w^* test cases:
  - Towards quasi-steady dynamic conditions (higher V_w^*), Surge frequency more visible in the wake
  - This dependency on V_w^* is however affected by the corresponding steady spectral content (*Ct*)
- Overall confirmation of the **dual dependency** of the unsteadiness on the **steady aerodynamic efficiency** and the **wake reduced velocity V_w^***
- Measurements at different downwind distances

Imposed Motion: Test Matrix, different V_w^* test cases

Full Scale			Wind Tunnel			V_W^*
U (m/s)	Amp x_0 (m)	Period T (s)	U (m/s)	Amp x_0 (m)	Frequency f (Hz)	(-)
7	7.5	100	2.3	0.1	0.25	≈ 4
	2.25	25		0.03	1	≈ 1
	1.125	12.5		0.015	2	≈ 0.5
11	7.5	100	3.6	0.1	0.25	≈ 6
	2.25	25		0.03	1	≈ 1.5
	1.125	12.5		0.015	2	≈ 0.8
16	7.5	100	5.3	0.1	0.25	≈ 9
	2.25	25		0.03	1	≈ 2.2
	1.125	12.5		0.015	2	≈ 1

NTNU
Norwegian University of Science and Technology

VTT

SINTEF

DTU

Lidars for Wind Tunnels – an IRPWind Joint Experiment Project L4WT

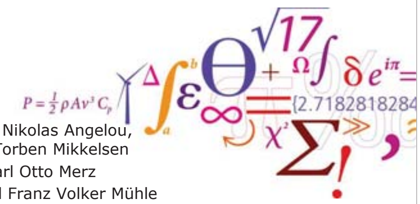

DTU: Mikael Sjöholm, Andrea Vignaroli, Nikolas Angelou, Morten Busk Nielsen, Jakob Mann, and Torben Mikkelsen
SINTEF: Hans Christian Bolstad, and Karl Otto Merz
NTNU: Lars Roar Sætran, Jan Bartl, and Franz Volker Mühle
VTT: Mikko Tiihonen, and Ville Lehtomäki

DTU Wind Energy
Department of Wind Energy

EERA

IRPWind

The European WindScanner Facility

DTU

The WindScanner, a distributed mobile research infrastructure

DTU

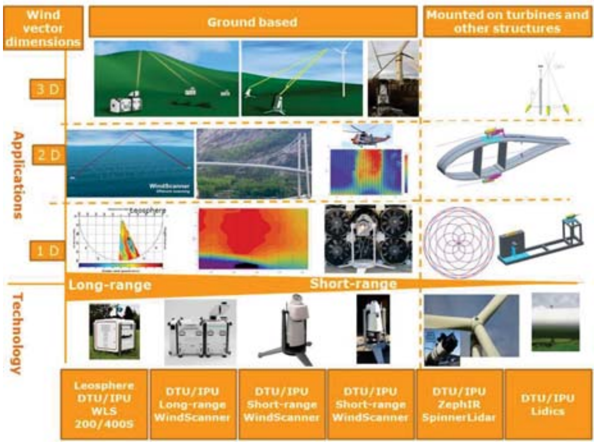

The WindScanner, a distributed mobile research infrastructure

DTU

http://www.windscanner.eu/

The Blade Lidar (Lidic)

DTU

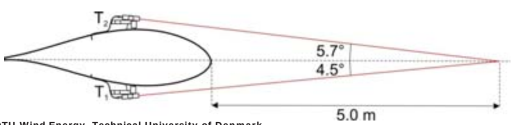

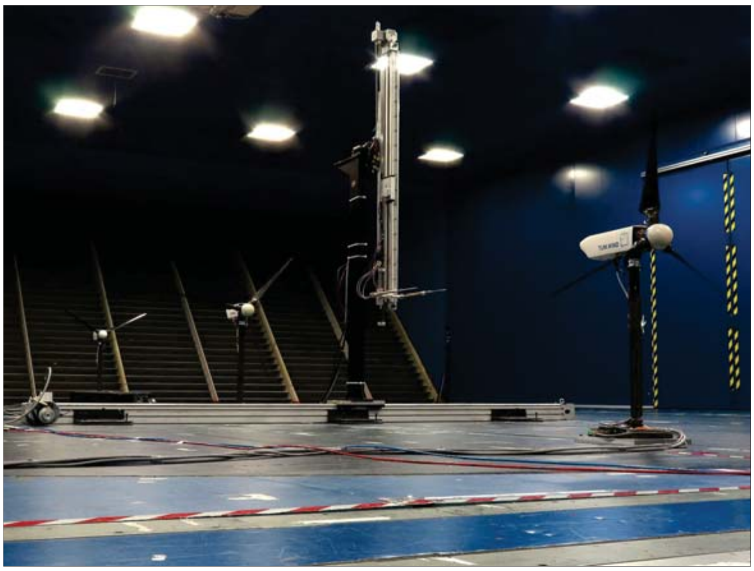

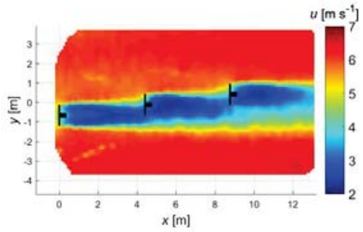

van Dooren, MF, Kühn, M, Petrovic, V, Bottasso, CL, Campagnolo, F, Sjöholm, M, Angelou, N, Mikkelsen, TK, Croce, A & Zasso, A, 2016, *"Demonstration of synchronised scanning Lidar measurements of 2D velocity fields in a boundary-layer wind tunnel"*, **Journal of Physics: Conference Series** (Online), vol 753, 072032. DOI: 10.1088/1742-6596/753/7/072032

Cold Climate Definition

Wind Energy in Cold Climates (CC) refers to sites that may experience frequent icing events, temperatures below the operational limits of standard wind turbines (WT), or both.

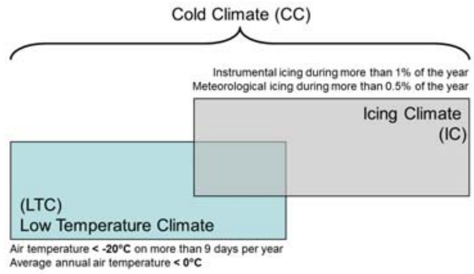

https://www.ieawind.org/task_19.html

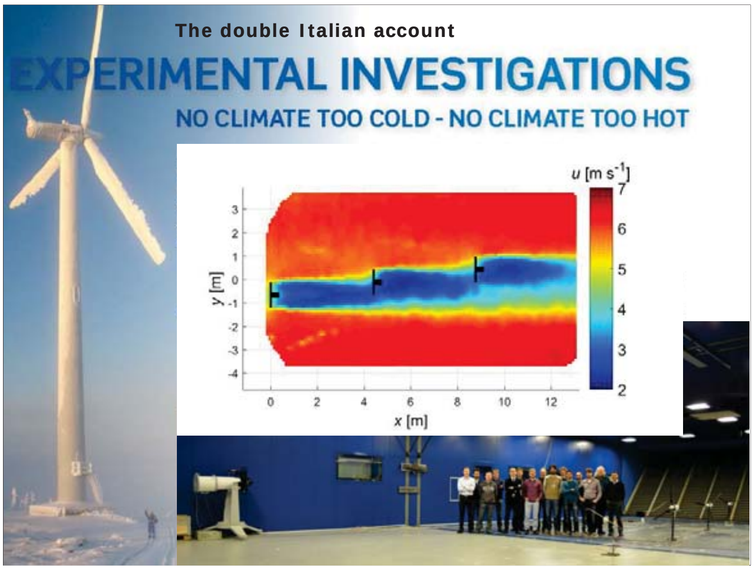

Atmospheric Icing Phases

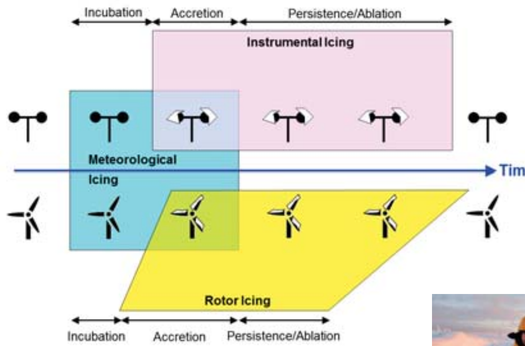

Wind Energy Capacity in Cold Climate

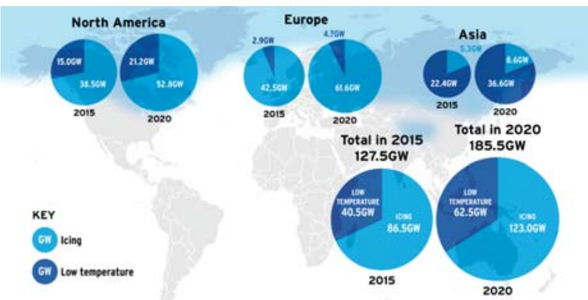

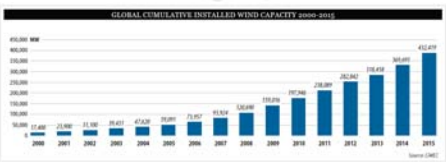

http://www.windpowermonthly.com/article/1403504/emerging-cold

Remote Sensing of Icing Conditions

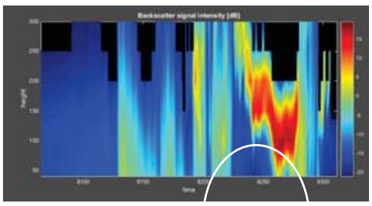

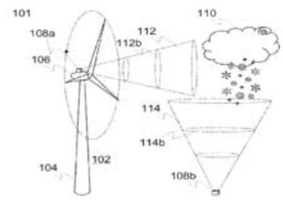

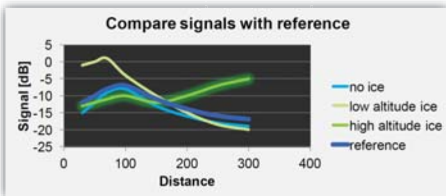

US Patent 2014/0192356: Arrangement and method for icing detection (Esa Peltola, Petteri Antikainen, and Andrea Vignaroli)

Slide extract from: Karlsson et al, Lidar as ice detector, Winterwind 2015

The IRPWind

DTU Wind Energy, Technical University of Denmark

http://www.irpwind.eu/

NTNU Boundary-Layer Wind Tunnel

Test section: 11 m long
2 x 3 m cross section
30 m/s max velocity
http://www.ntnu.edu/ept/laboratories/aerodynamic

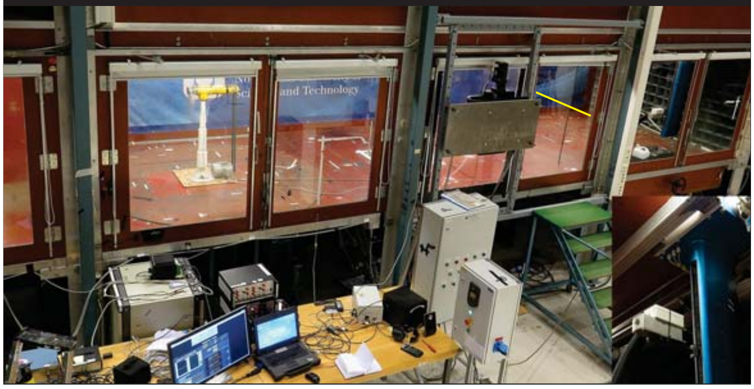

IRPWIND Relevant Networks

1. Research Wind Turbines
2. Wind Tunnels
3. Grid Integration

NTNU
Boundary-Layer Wind Tunnel
Trondheim, Norway

VTT
Icing Wind Tunnel (IWT)
Espoo, Finland

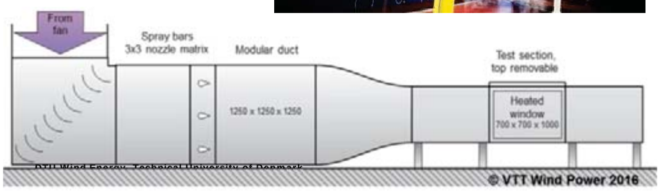

DTU Wind Energy, Technical University of Denmark

Short-range WindScanners

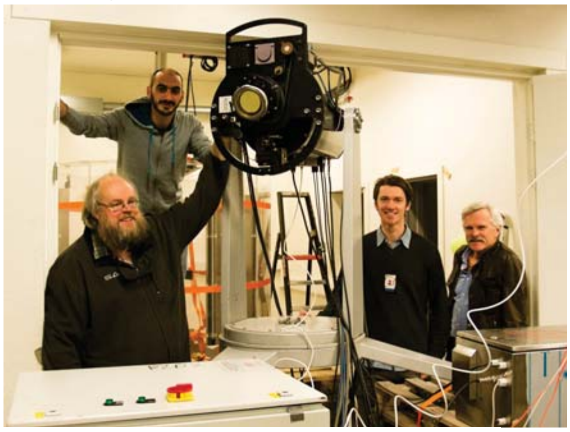

http://www.ntnutechzone.no/2016/12/siste-skrik-i-visualisering-av-vind/

DTU Wind Energy, Technical University of Denmark

NTNU Norwegian University of Science and Technology
VTT
SINTEF

Lidars for Wind Tunnels – an IRPWind Joint Experiment Project L4WT

The aim of L4WT
is
to gain and share knowledge
about the possibilities and limitations
with lidar instrumentation in wind tunnels
and
to foster collaboration
in a prospective Nordic wind tunnel network
for
alignment of research activities
relevant to
wind conditions in cold climate

DTU Wind Energy
Department of Wind Energy
EERA
IRPWind

Blog dissemination

http://blog.sintefenergy.com/vindkraft/spennende-malinger-i-vindtunnel-laben-til-ntnu/

DTU Wind Energy, Technical University of Denmark

Renewable Energy 50 (2013) 325–333

Contents lists available at SciVerse ScienceDirect

Renewable Energy

journal homepage: www.elsevier.com/locate/renene

"Blind test" calculations of the performance and wake development for a model wind turbine

Per-Åge Krogstad*, Pål Egil Eriksen

Department of Energy and Process Engineering, Norwegian University of Science and Technology NTNU, 7491 Trondheim, Norway

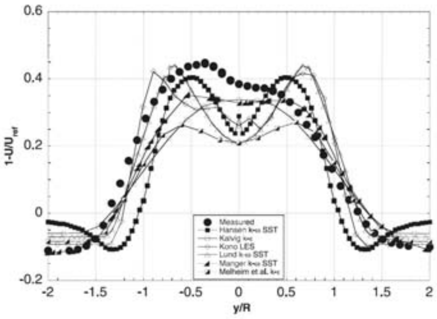

Blind Test Comparison With Lidar Lidic Inside the Tunnel

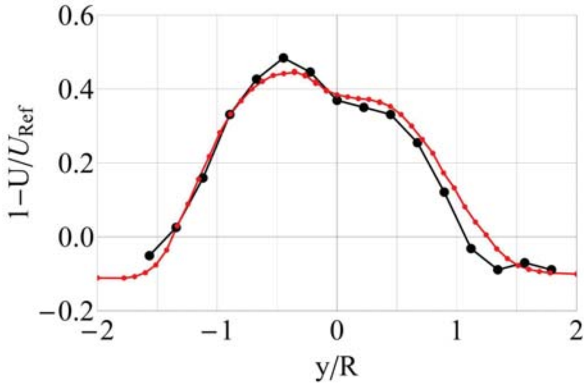

Blind Test Comparison With Lidar Outside the Tunnel

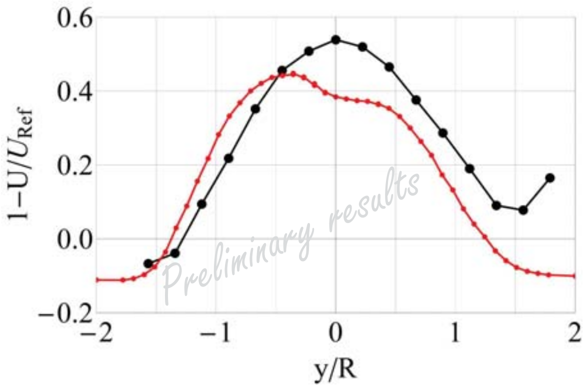

Blind Test Comparison With Lidic Inside the Tunnel

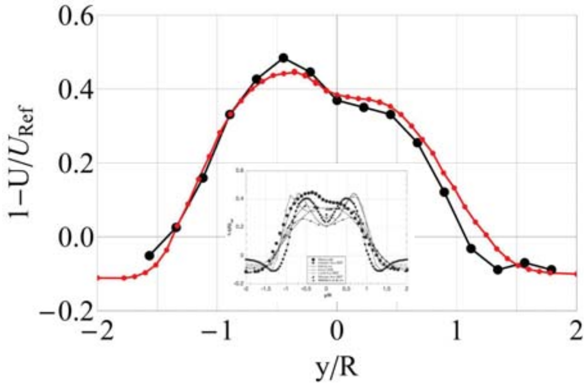

Blind Test Comparison With Lidar Scanner Outside the Tunnel

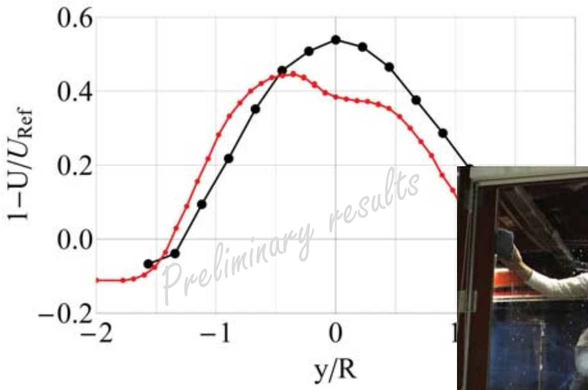

Doppler Spectra in The Wake

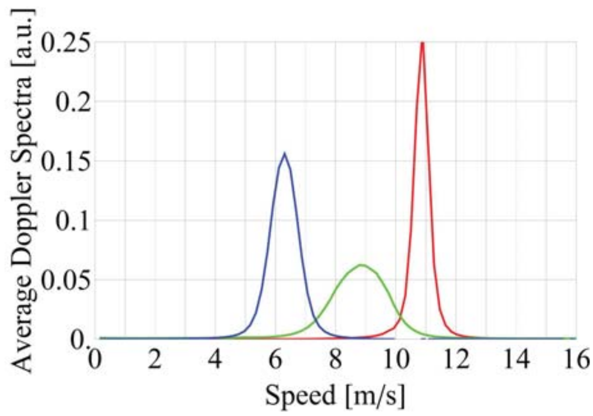

VTT Icing Wind Tunnel

http://www.vttresearch.com..

Property	Range in the facility	VTT's Reference conditions	
		In-cloud icing, stationary components	In-cloud icing, wind turbine rotor blades
Temperature [°C]	-20…+30	-5	-5
Wind speed [m/s]	0…45	7	40
Water content [g/m³]	0.1…1.0	0.2	0.2
Droplet size, MVD [µm]	20…50	20	20

Droplet size and wind speed profile have been verified using shadow imaging.

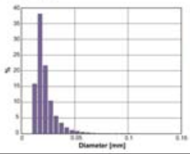

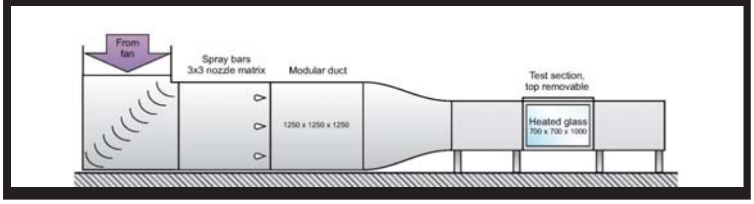

The sampling volume at 1.5 meter

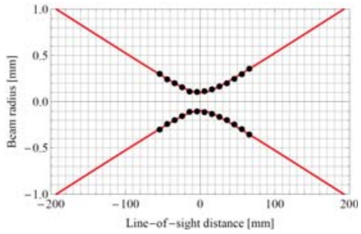

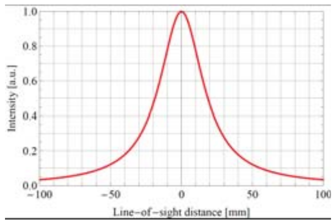

DTU Wind Energy, Technical University of Denmark

Measurement Campaign in VTT Icing Wind Tunnel

Lidar high frequency time series along the wind

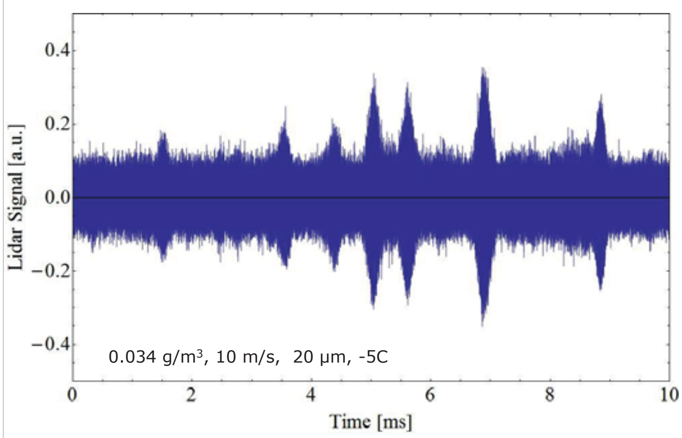

DTU Wind Energy, Technical University of Denmark

Protective measures in the Icing Wind Tunnel

DTU Wind Energy, Technical University of Denmark

Lidar signal strength distributions

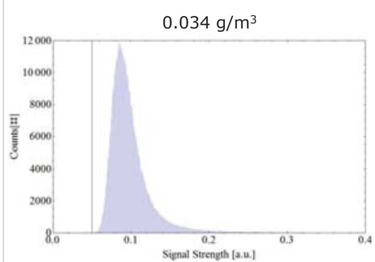

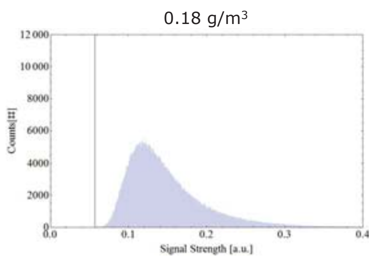

DTU Wind Energy, Technical University of Denmark

This very morning at the ECN test site in The Netherlands in another IPRWind Joint Experiment called ScanFlow

DTU Wind Energy, Technical University of Denmark

X) Floating wind turbines

Sensitivity Analysis of Limited Actuation for Real-time Hybrid Model Testing of 5MW Bottom-fixed Offshore Wind Turbine, M. Karimirad, SINTEF Ocean

OC5 Project Phase II: Validation of Global Loads of the DeepCwind Floating Semisubmersible, A. N. Robertson, NREL

Joint industry project on coupled analysis of floating wind turbines, L. Vita, DNV GL

Using FAST for the design of a TLP substructure made out of steel reinforced concrete composite components, P. Schünemann, University of Rostock

Sensitivity Analysis of Limited Actuation for Real-time Hybrid Model Testing of 5MW and 10MW Monopile Offshore Wind Turbines

Madjid Karimirad (SINTEF Ocean)
Erin Bachynski (NTNU)

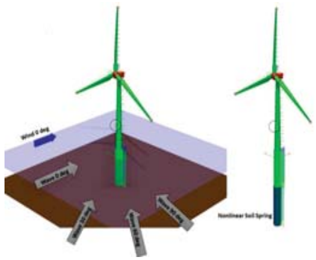

SINTEF

Outline

- Computational methodology
- Wind turbine models
- Load cases
- Sensitivity to
  - Aerodynamic loading in parked condition
  - Aerodynamic pitch moment
  - Aerodynamic sway force
  - Aerodynamic yaw moment
- Outlook

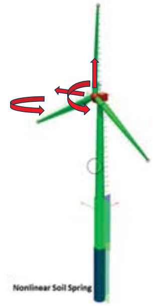

 SINTEF

Computational methodology: aerodynamic force modification

Rigid body dynamics: Jacobian matrices used for transformation of forces and velocities between frames

rotor frame, local frame, Aero forces/moments, Jacobian

$$\tau_a^R = J_{BR}^F \tau_a^B$$

$$\hat{\tau}_a^R = \tau_a^R + modifications$$

$$\cancel{\hat{\tau}_a^B = {J_{BR}^F}^{-1} \hat{\tau}_a^R}$$

$$\hat{\tau}_a^B = {J_{BR}^F}^{-1} \frac{\sum_{i=1}^{N_b} \sum_{j=1}^{N_e} \hat{\tau}_{a\,ij}^R}{N_e N_b}$$

 SINTEF

Context

- Design of ReaTHM® tests of large monopile wind turbines
  - Physical hydrodynamic loads
  - Virtual aerodynamic/turbine loads, applied in an integrated manner
- How important are each of the turbine load components?
- How important are aerodynamic effects in parked, extreme conditions?

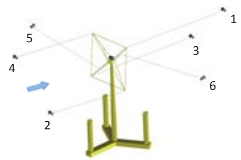

 SINTEF

Computational methodology

Source: NREL/Wind power today, 2010.

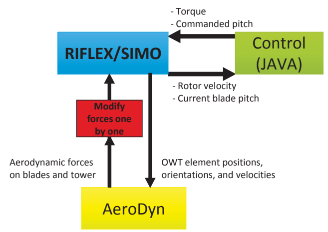

Present limitation: rigid blades (elastic blades in near future)

 SINTEF

5MW and 10MW monopile wind turbine models

- 30 m water depth
- 5MW: based on OC3, but extended due to deeper water
- 10MW: new design, soil-pile characteristics assumed same as OC3 despite larger diameter
- Sensitivity study is carried out with torsional spring (as in lab) rather than soil springs

	5MW	10MW
Turbine	NREL 5MW	DTU 10MW
Monopile	OC3	Representative
Soil stiffness	OC3*	OC3*
Rated thrust (kN)	710	1500
Hub height (m)	90	119
Monopile diameter (m)	7	10
Thickness (cm)	6	8
Embedded length (m)	46	56

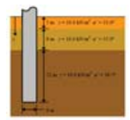

 SINTEF

Eigenfrequencies and eigenmodes

	Mode	Linear distributed springs (below the seabed)	Single torsional spring (at seabed)
5 MW	1st bending (Hz)	0.261	0.261
	2nd bending (Hz)	1.239	1.423
10 MW	1st bending (Hz)	0.262	0.261
	2nd bending (Hz)	1.219	1.365

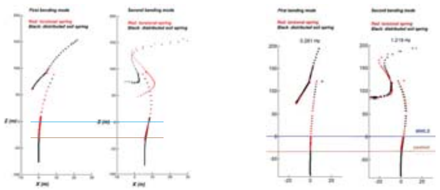

Madjid Karimirad and Erin Bachynski

SINTEF

Fault cases

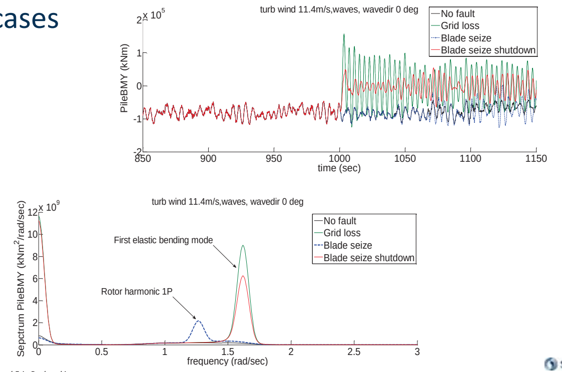

Madjid Karimirad and Erin Bachynski

SINTEF

Sensitivity study results: summary

	5MW, normal	5MW, fault	10MW, normal	10MW, fault
Aerodynamic damping, parked	100%	N/A	100%	N/A
Aerodynamic pitch	<5%	20-30%	10-30%	25-40%
Aerodynamic sway	<7%	<5%	<5%	<10%
Aerodynamic yaw	60% *	100% *	90% *	100% *
Dynamic torque	<5%	<5%	<20%	<10%

*only for torsion/yaw

- Key observations:
  - Only effects on "responses of interest" are shown
  - 10 MW is generally more sensitive to limited actuation
  - Aerodynamic yaw is important for torsion/yaw responses, but largely decoupled from other responses
  - Aerodynamic pitch moment is less important for bottom-fixed concept compared to NOWITECH FWT

Madjid Karimirad and Erin Bachynski

SINTEF

Load cases

- Based on hindcast data for 29m water depth, North Sea site (Li et al., 2013)
- 3 operational cases, one storm (parked)
- EC 2 cases repeated with fault
  - Grid loss (with shutdown)
  - Blade seize (without shutdown)
  - Blade seize (with shutdown)

	EC 1	EC 2	EC 3	EC 4
Uw (m/s)	8	11.4	20	31.5
Hs (m)	1.2	1.8	3.6	9.5
Tp (s)	5.8	6.5	8.2	12.3
I% (NTM)	17.1	14.0	11.5	11.0

Madjid Karimirad and Erin Bachynski

SINTEF

Aerodynamic loading in parked condition

- Aerodynamic **damping** is important even in parked conditions for the dynamic bending moment response
  - 100% difference
- Dynamic shear force is less affected
- Similar results for 5 MW and 10 MW

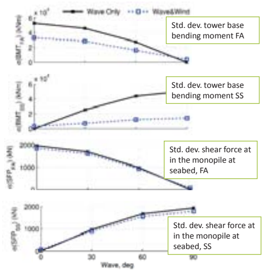

Madjid Karimirad and Erin Bachynski

SINTEF

Aerodynamic pitch moment

- Different effects for 5 MW vs 10 MW.
- Less important for 5 MW monopile than for 5 MW floating.

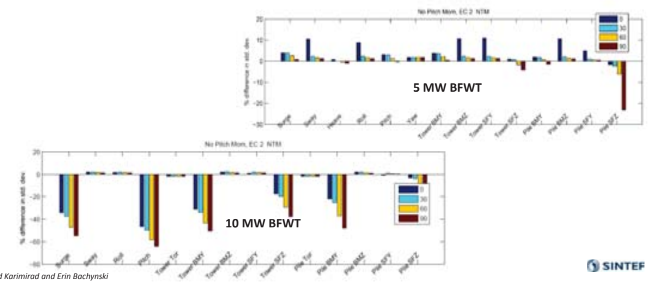

Madjid Karimirad and Erin Bachynski

SINTEF

Aerodynamic yaw moment: fixed vs. floating

- Natural periods in yaw/torsion:
  - Bottom-fixed: <2s
  - CSC 5MW: 62s
- Aerodynamic yaw is primarily a low-frequency excitation, so it can excite yaw resonant response in the floating concept, but only quasi-static response for the bottom-fixed turbines

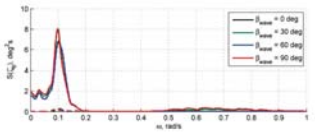

5 MW CSC results for yaw, above-rated wind speed

SINTEF

Teknologi for et bedre samfunn

Conclusions/outlook

- Monopile wind turbine designs for basin tests, including torsional stiffness
- Preliminary response analysis for physical test design
- Application of a methodology developed for FWT to bottom-fixed concepts, and to a new turbine
- Aerodynamic damping should be included in tests with extreme waves (in some way)
- Aerodynamic pitch moment is important in fault cases and for the 10 MW concept
- Aerodynamic yaw moment is only important for torsional responses
- Aerodynamic sway and dynamic torque have minor effects

- Future work:
  - Extension to flexible blades
  - Sensitivity to other limitations (frequency, delays)
  - NOWITECH tests in 2017

OC5 Project Phase II: Validation of Global Loads of the DeepCwind Floating Semisubmersible Wind Turbine

DeepWind Conference – Trondheim, Norway

Amy Robertson

January 20, 2017

Co-Authors

- ***Fabian F. Wendt*** - National Renewable Energy Laboratory, Colorado, USA
- ***Jason M. Jonkman*** - National Renewable Energy Laboratory, Colorado, USA
- ***Wojciech Popko*** - Fraunhofer IWES, Germany
- **Habib Dagher** - University of Maine, USA
- ***Sebastien Gueydon***, MARIN, Netherlands
- ***Jacob Qvist*** - 4Subsea, Norway
- ***Felipe Vittori***, CENER, Spain
- **José Azcona**, CENER, Spain
- ***Emre Uzunoglu***, CENTEC, Portugal
- ***Carlos Guedes Soares***, CENTEC, Portugal
- ***Rob Harries*** - DNV GL, England
- ***Anders Yde*** - DTU, Denmark
- ***Christos Galinos***, DTU, Denmark
- ***Koen Hermans***, ECN, Netherlands
- ***Jacobus Bernardus de Vaal***, IFE, Norway
- ***Pauline Bozonnet*** - IFP Energies nouvelles, France
- ***Ludovic Bouy*** - PRINCIPIA, France
- ***Ilmas Bayati*** - Politecnico di Milano, Italy
- ***Roger Bergua*** - Alstom Wind, Spain
- ***Josean Galvan***, Tecnalia, Spain
- ***Iñigo Mendikoa***, **Tecnalia, Spain**
- ***Carlos Barrera Sanchez*** - Universidad de Cantabria – IH Cantabria, Spain
- ***Hyunkyoung Shin*** - University of Ulsan, Korea
- ***Sho Oh***, University of Tokyo, Japan
- ***Climent Molins***, Universitat Politècnica de Catalunya, Spain
- **Yannick Debruyne**, WavEC Offshore Renewables, Portugal

IEA Wind Tasks 23 and 30 (OC3/OC4/OC5)

- Verification and validation of coupled offshore wind modeling tools are need to ensure their accuracy, and give confidence in their usefulness to users.
- Three research projects were initiated under IEA Wind to address this need:

OC3 = Offshore Code Comparison Collaboration (2005-2009)

OC4 = Offshore Code Comparison Collaboration, Continuation (2010-2013)

OC5 = Offshore Code Comparison Collaboration, Continuation, with Correlation (2014-2017)

OC5 Project Phases

- OC3 and OC4 focused on ***verifying*** tools (tool-to-tool comparisons)
- OC5 focuses on ***validating*** tools (code-to-data comparisons)

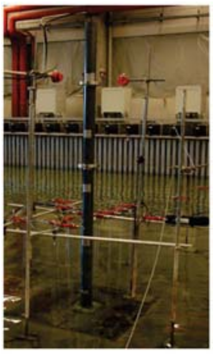

Phase I: Monopile - Tank Testing

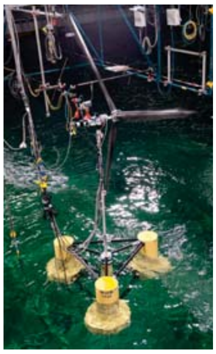

Phase II: Semi - Tank Testing

Phase III: Jacket/Tripod – Open Ocean

OC5 Phase II

- **Objective**: validate ultimate and fatigue loads in tower/moorings
- Test Data from **DeepCwind** project**:**
  - Carried out by the DeepCwind consortium, led by the University of Maine
  - MARIN wave basin - 2013
  - 1/50th-scale floating semisubmersible
  - MARIN Stock Wind Turbine
  - Same platform as OC4, but different turbine
  - **Thank you to:** Andrew Goupee and Habib Dagher for allowing us to use the data in the OC5 project

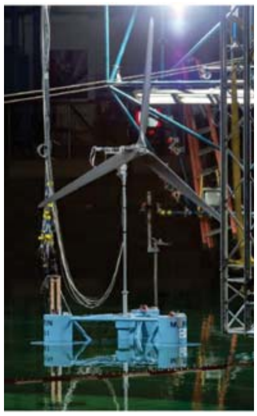

Instrumented OC5-DeepCwind model in the MARIN offshore basin

Test Summary

- **Tests:**
  - Free-decay
  - Wind-only
  - Wave-only
  - Wind/wave
- **Recorded data:**
  - Rotor torque and position
  - Tower-top and -base forces an moments
  - Mooring line tensions
  - 6DOF platform motions
  - Accelerations on the nacelle, tower, and platform

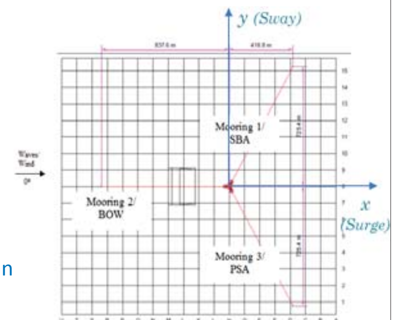

Layout of the floating wind system in the tank

Summary of Tools and Modeling Approach

Participant	Code	Aero-dynamics		Hydrodynamics							Moorings		
		Dyn. Wake	Unst. Airfoil	2nd+ WK	1st PF	2nd PF	ME	Meas. Wave	Stretch	Inst. Pos.	Dyn.	Hydro Exc.	Seabed Fric.
4Subsea	OrcaFlex-FAST v8												
CENER	FAST v6 + OPASS												
CENTEC	FAST v8												
DNV GL	Bladed 4.8												
DTU ME	HAWC2												
DTU PF	HAWC2												
ECN-MARIN	aNySIM-PHATAS v10												
IFE	3DFloat												
IFP_PRI	DeepLinesWind V5R2												
NREL PF	FAST v8												
NREL ME	FAST v8												
POLIMI	FAST v8.15			Diff									
Siemens PLM	Samcef Wind Turbine												
Tecnalia F7O	FAST v7 + OrcaFlex 9.7												
Tecnalia F8	FAST v8.16												
UC-IHC	Sesam												
UOU	UOU + FAST v8												
UPC	UPC + FAST												
UTokyo	NK-UTWind												
WavEC FAST	FAST v8												
WavEC FF2W	FF2W												

Calibration – Wave-Only Tests

- **Regular wave tests used to:**
  - Tune mooring properties
  - Assess heave excitation
- **Some models are missing critical elements of heave excitation**
  - Dynamic pressure on base columns for Morison solutions
  - Relative fluid velocity for viscous drag calculation
- **Also showed issues related to using a quasi-static mooring model**

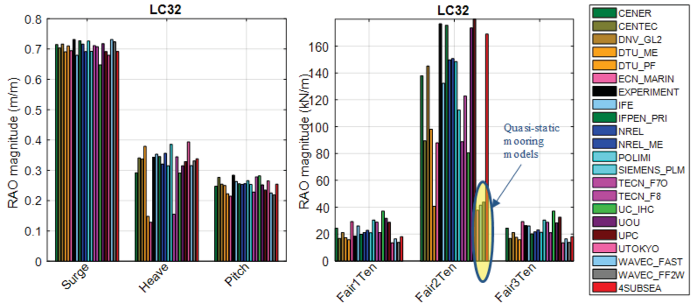

Calibration

- **Static Equilibrium -** position and loads (tower/moorings)
  - Tuning of nacelle CM to achieve near 0 pitch
  - System properties needed adjustment for 0 heave equilibrium
- **Mooring Offsets** – load/displacement curve for moorings
  - Adjustment to mooring line length/stiffness properties
- **Free Decay** – eigen-frequencies and damping
  - Adjustment of C_D and C_A, or calculation of damping matrix
  - Additional linear damping matrix
  - Additional stiffness in surge/pitch to match natural frequencies (cable bundle influence?)

DOF	Frequency (Hz)	Period (s)	Damping Coeff. (linear, p) (quadratic, q)
Surge	0.00937	107	0.1095 0.1242
Sway	0.00890	112	0.0795 0.1265
Heave	0.0571	17.5	0.0094 0.2733
Roll	0.0305	32.8	0.0648 0.0625
Pitch	0.0308	32.5	0.0579 0.0686
Yaw	0.0124	80.8	0.1446 0.0165
Tower Bending Fore/Aft (F/A)	0.315	3.18	
Tower Bending Side/Side (S/S)	0.325	3.08	

Validation Tests

Load Case	Description	RPM	Blade Pitch (deg)	Wave Condition	Wind Condition	Sim. Length (min)
3.3	Operational Wave	0	90	Irregular: H_s = 7.1 m, T_p = 12.1 s, γ=2.2, JONSWAP	N/A	176
3.4	Design Wave	0	90	Irregular: H_s = 10.5 m, T_p = 14.3 s, γ=3.0, JONSWAP	N/A	180
3.5	White Noise Wave	0	90	White noise: H_s = 10.5 m, T_{range} =6-26 s	N/A	180
4.1	Oper. Wave Steady Wind 1	12.1	1.2	Irregular: H_s = 7.1 m, T_p = 12.1 s, γ=2.2, JONSWAP	$V_{hub,x}$= 12.91 , $V_{hub,z}$= -0.343 σ_x = 0.5456, σ_z = 0.2376	180
4.2	Oper.Wave Steady Wind 2	12.1	15.0	Irregular: H_s = 7.1 m, T_p = 12.1 s, γ=2.2, JONSWAP	$V_{hub,x}$= 21.19, $V_{hub,z}$= -0.600 σ_x = 0.9630, σ_z = 0.4327	180
4.3	Oper. Wave Dynamic Wind	12.1	1.2	Irregular: H_s = 7.1 m, T_p = 12.1 s, γ=2.2, JONSWAP	NPD spectrum, μ = 13.05	180
4.4	Design Wave Steady Wind 1	12.1	1.2	Irregular: H_s = 10.5 m, T_p = 14.3 s, γ=3.0, JONSWAP	$V_{hub,x}$= 12.91 , $V_{hub,z}$= -0.343 σ_x = 0.5456, σ_z = 0.2376	180
4.5	White N. Wave Steady Wind 1	12.1	1.2	White noise: H_s = 10.5 m, T_{range} = 6-26 s	$V_{hub,x}$= 12.91 , $V_{hub,z}$= -0.343 σ_x = 0.5456, σ_z = 0.2376	180

Calibration – Wind-Only Tests

- **Check aerodynamic properties**
  - Tuning done by UMaine, and used by all participants
  - Modification of wind model to better match tests (shear, coherence, turbulence)
  - Variations in individual blade mass and pitch to create 1P, 2P, and 4P excitation

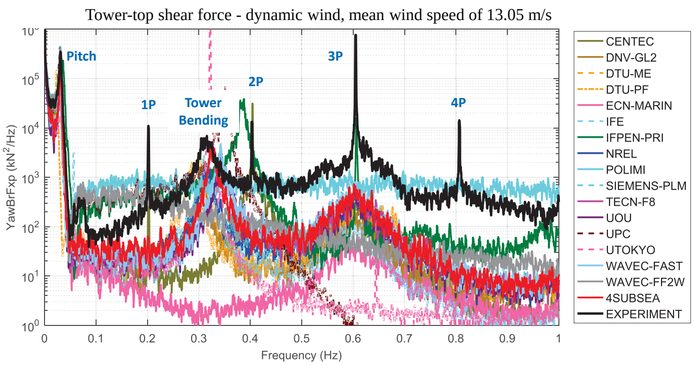

Validation – Ultimate and Fatigue Loads

- **Validation assessed by comparing ultimate and fatigue loads for the:**
  - Tower-top shear force
  - Tower-base shear force
  - Upwind mooring line
- **Simulations generally underestimated these loads**
  - Error greater for fatigue
  - When wind is included, tower loads are higher, fatigue error greater, ultimate error smaller
  - Error generally larger at tower bottom compared to tower top (only bottom shown here)
  - Not a significant change for different wind/wave conditions

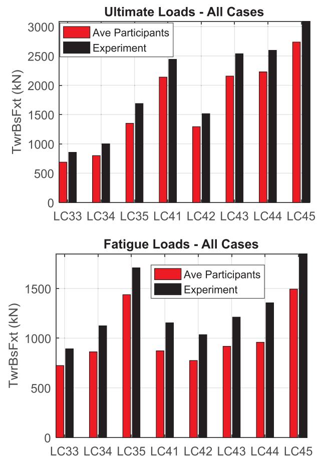

Exceedance Probability Plots

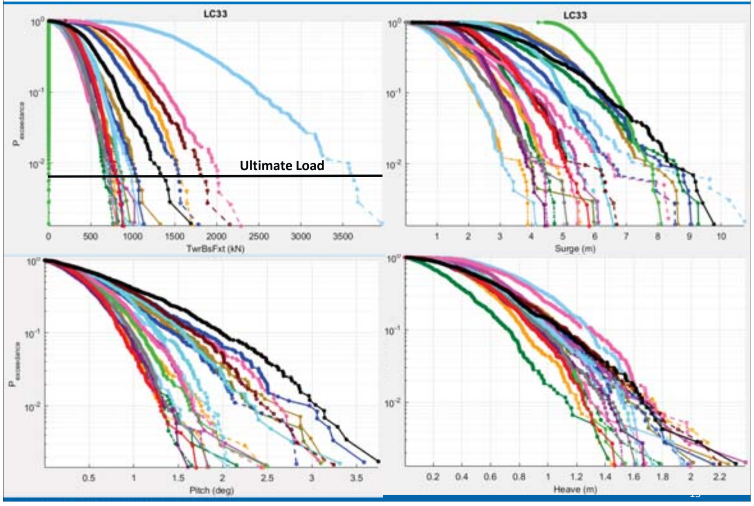

Tower Base PSD – LC 4.1 – Waves + Wind

- **With wind added:**
  - Pitch/Tower peaks decrease for all
  - Experiment response to waves increases ??
- **For PF-models,** error about the same for pitch as linear wave region
- **For ME-only models**, most still have largest error at tower bending frequency
- 3P excitation apparent, but does not significantly affect ultimate/fatigue loads

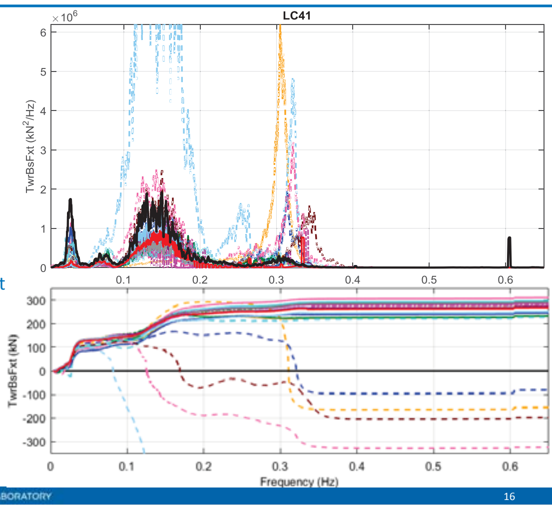

Ultimate/Fatigue Loads – LC 3.3 and 4.1

- **Colors:**
  - Red = PF-only
  - Green = ME-only
  - Blue = PF+ME
- Most PF models under-predicting loads
- Without wind, most ME-only models over-predicting loads

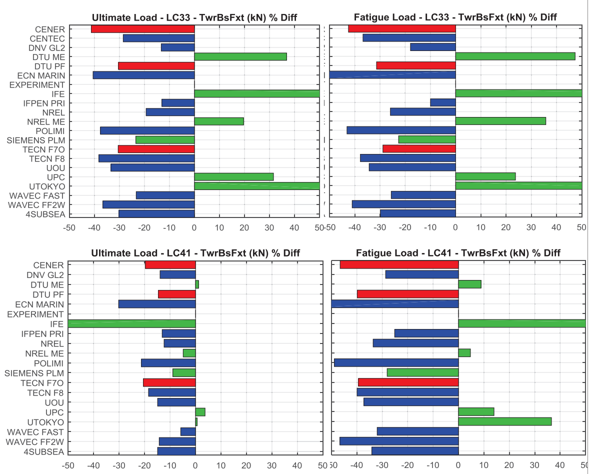

Conclusions

- **Fairly consistent under-prediction of ultimate/fatigue loads**
  - Seeing an average of about 20% under-prediction
  - Not bad, but would like to better understand reasons
  - See this level of error for wave-only, so not just due to wind
- **Saw some issues with the test data:**
  - Wind: large broad-band frequency excitation and 1P/2P/3P/4P excitation
  - Instruments and cabling could be adding influence
  - Hysteresis of mooring lines
- **Modeling approach influences:**
  - Nonlinear wave forces (2nd-order PF, 2nd-order wave kin., wave stretching, etc.)
  - Axial excitation on heave plates
  - Dynamic mooring models
  - Not much focus on aerodynamics
  - Most ME-only models – large tower bending excitation
- **Uncertainty**
  - Difficult to determine if differences caused by modeling error or test uncertainties
  - Uncertainty not assessed here, but examined in ISOPE paper by Robertson, 2017
- **Future Recommendations:**
  - Address uncertainty in model tests
  - Use CFD to assess modeling errors

Robertson, A. et al. "Uncertainty Analysis of OC5-DeepCwind Floating Semisubmersible Offshore Wind Test Campaign". To be presented at The International Society of Offshore and Polar Engineers Conference, June 2017.

Tower Base PSD – LC 3.3 – Waves Only

- **Line Style:**
  - Solid = PF+ME
  - Dash = ME-only
  - Dash-Dot = PF-only
- **Distinct peaks:** pitch, waves, tower bending
- **Cumulative PSD Difference**
  - Sum integrated PSD difference from low to high frequencies
  - Shows where largest model error occurs

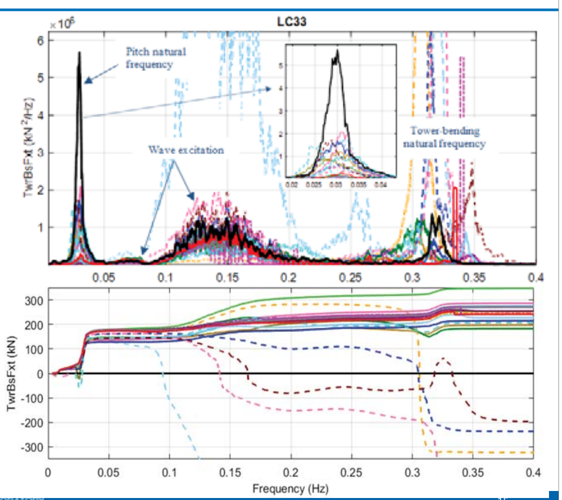

DNV·GL

ENERGY

JIP coupled analyses of FOWTs

Towards a new Recommended Practice

L. Vita, E. L. Walter , R. Harries

RAMBØLL · ideol · DR. TECHN. OLAV OLSEN · EDF · Glosten · NREL · ATKINS · MARIN · stx France · GICON · ESTEYCO ENERGIA · SINTEF

Presentation overview

- Project rationale
- Overview & Status
- Timeline & collaborations

DNV-OS-J103 Design of Floating Wind Turbine Structures

- Published June 2013
- Can be downloaded for free on www.dnvgl.com
- Developed through a Joint Industry Project (JIP) during 2011 – 2013
- Industry hearing April 2013
- Participants:

Statoil · Sasebo Heavy Industries · ALSTOM · IBERDROLA · PRINCIPLE renewable energy delivered · NIPPON STEEL & SUMITOMO METAL · Navantia · THE GLOSTEN ASSOCIATES · stx · Gamesa

---

JIP scope

JIP main scope

- The main scope of the project is to produce a Recommended Practice (RP) on Coupled Analysis of Floating Wind Turbines

Challenges

- Maturity of the industry
- Clear conclusions

What the project IS

- Collecting experience
- Verifying methodologies
- Concluding on best practices for a given scope

What the project IS NOT

- NOT Numerical code benchmark
- NO New model tests
- NO developing new methods

Analysis of floating wind turbines

Experience used by three working groups

TLP · Spar · Semi · Barge

- Practical experience
- Numerical model
- Validation data

Modelling & validation · Model Test · Analysis

Industrial agreed recommended practices, based on:

- Experience from the selected case studies
- Experience from all participants
- New analysis run during the project to validate/integrate the state of art experience

Analysis of floating wind turbines

Modelling and validation

Modelling & validation · Model Test · Analysis

- Environmental Conditions
- Dynamic Models
- Validation

Modelling – Environmental conditions

Recommendations For Modelling Environmental Conditions

- **Wind**
- Waves
- **Current**
- Wave current interaction
- **Tide**
- Seismic
- **Tsunamis**
- Ice

- Building on available standards, e.g. DNV-RP-C205
- Clarify applications for floating wind

Controller – other items considered

- Nonlinearity due to large system motions
- Lightly damped yaw motion
- Rotor harmonic clashes with structural frequencies (strategy to avoid)
- Monitoring
- Fidelity

Modelling of environmental conditions – turbulence wind

Turbulence model	No. dimensions	Developed for offshore conditions ?	Industry Source	Additional comments
Kaimal	3D			
Frøya	1D			
API				
Von Karman	3D			
ESDU	3D			
Mann	3D			

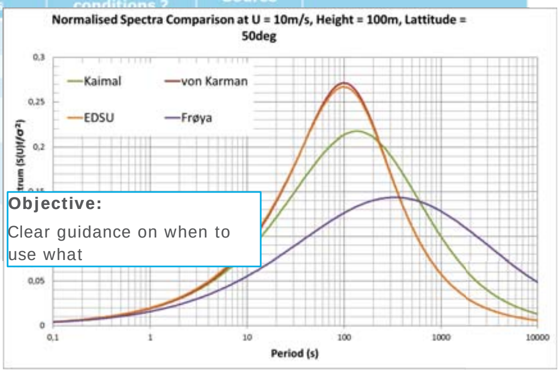

Objective:
Clear guidance on when to use what

Modelling and validation

Modelling & validation

Model Test

- When to do the testing
- Available Methods
- What to test

Analysis

Possible controller instabilities and strategis

Many existing methods to decouple the rotor speed control loop from the platform motions.

Three groups identified:

- Reduce bandwidth of the speed control loop
- Explicitly remove pitch actuation at platform frequencies
- Introduce explicit platform stabilisation loops

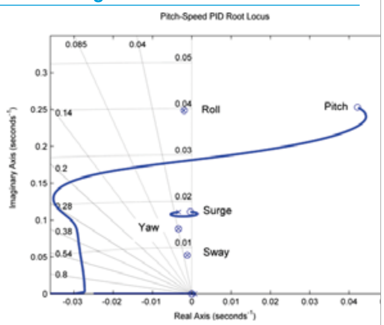

Model Tests - methods

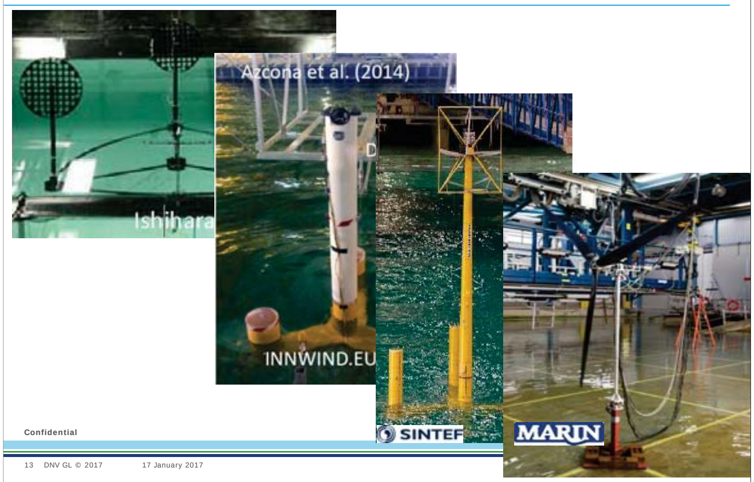

Model Tests - methods

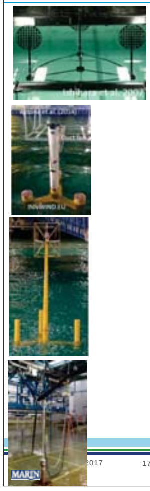

Pro:
Contra:
Purpose

Pro:
Contra:
Purpose

Pro:
Contra:
Purpose

Pro:
Contra:
Purpose

Load analysis - Database

TLP | Spar | Semi | Barge

Database from NREL

New simulations

Data from other partners

Large dataset to validate load methods and assumptions

Model test – DLCs and validation

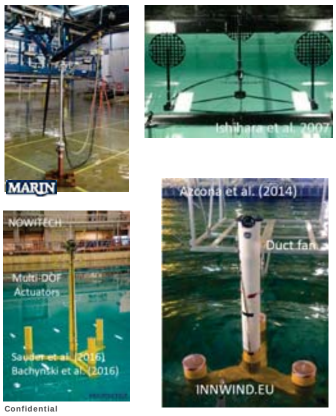

+ Purpose

Load cases for model testing	
DLC1	
…….	
….	

Design specific considerations still to be made!

Possible conclusions from anaysis of database

From existing data
- Duration of time series
- Number of seeds
- Miaslignment
- Partial cycles
- Number of bins (wave direction and wave Tp)
- Methods for wave lumping
- Possible use of regional classes (e.g. J103, section 3.6)

From additional simulations
- Extending the conclusions to TLP and barge
- Relative importance of idling cases to fatigue
- Yaw error
- Platform orientation
- Swell
- Wave spectrum (gamma)
- ULS characteristic loads

Modelling and validation

Modelling & validation

Model Test

Analysis

Setup for the analysis

Load cases reduction

Conclusions and collaborations

- **Comments on the contents?**
- **Methodos to be considered?**
- Timeline:
  – Work completed by September 2017
  – Final draft by end 2017
  – External hearing Q2 2018

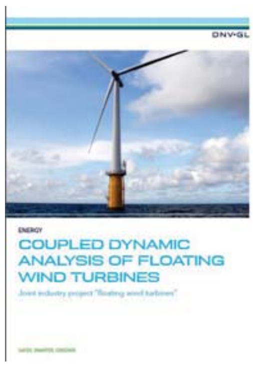

Thanks for your attention

RAMBØLL

ESTEYCO ENERGIA

ATKINS

ideol

eDF

DR. TECHN. OLAV OLSEN

GICON®

nautilus floating solutions

MARIN

stx France

SINTEF

NREL NATIONAL RENEWABLE ENERGY LABORATORY

Glosten

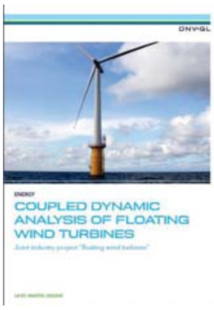

Luca Vita
Luca.vita@dnvgl.com

www.dnvgl.com

SAFER, SMARTER, GREENER

Confidential

Universität Rostock Traditio et Innovatio

LWET Stiftungslehrstuhl Windenergietechnik

Using FAST for the design of a TLP substructure made out of steel reinforced concrete composite components

Paul Schünemann
University of Rostock,
Endowed Chair of Wind Energy Technology
- in collaboration with GICON® Group -

EERA DeepWind'2017
14th Deep Sea Offshore Wind R&D Conference
18 - 20 January 2017, Trondheim, Norway

Universität Rostock Traditio et Innovatio

LWET Stiftungslehrstuhl Windenergietechnik

1. Introduction to the new GICON® TLP
2. Description of the Wind Turbine
3. Simulation Results
4. Outlook

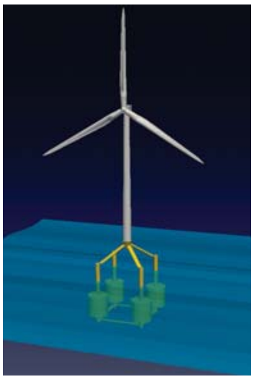

Universität Rostock Traditio et Innovatio

LWET Stiftungslehrstuhl Windenergietechnik

General Concept of the GICON® TLP

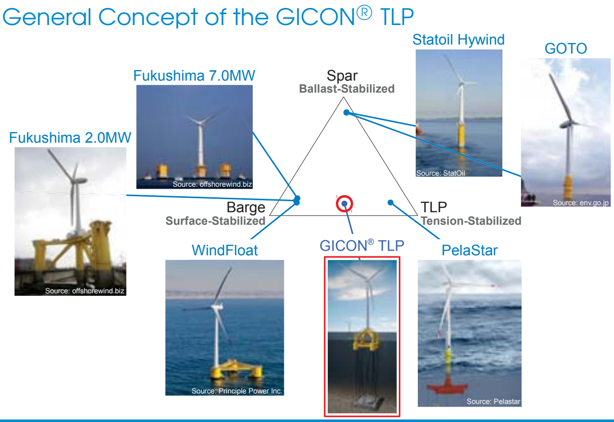

Universität Rostock Traditio et Innovatio

LWET Stiftungslehrstuhl Windenergietechnik

Key Features of the GICON® TLP

- Water depths: 30 m - 500 m
- One step installation
- High modularity
- Reinforced concrete components with Ultra High Performance Concrete (UHPC)

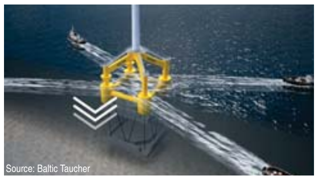

⇒ reduced fabrication time + reduced CO_2 emissions + reduced costs

Universität Rostock Traditio et Innovatio

LWET Stiftungslehrstuhl Windenergietechnik

Components of the GICON® TLP

- Prestressed concrete columns (UHPC)
- Reinforced concrete shell segments
- Steel cover and bottom plate
- Steel TP and nodes

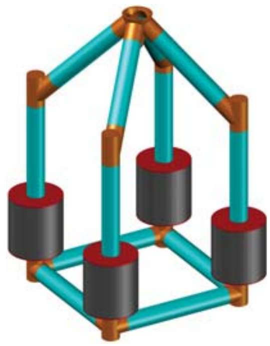

Universität Rostock Traditio et Innovatio

LWET Stiftungslehrstuhl Windenergietechnik

1. Introduction to the new GICON® TLP
2. Description of the Wind Turbine
3. Simulation Results
4. Outlook

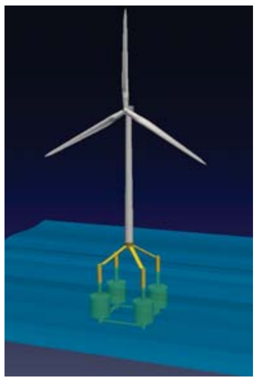

Universität Rostock Traditio et Innovatio — LWET Stiftungslehrstuhl Windenergietechnik

Summary of Wind Turbine Properties

- Based on the 6 MW turbine of the DOWEC project

Rotor	Upwind, 3 Blades
Rotor Diameter	129 m
Hub Height, Overhang	114 m (above MSL), 5 m
Cone, Shaft Tilt	4.5°, 5°
Drivetrain	Gearbox
Control	Variable Speed, Collective Pitch
Rated Wind Speed	12.1 m/s
RNA Mass	416 658 kg
Tower Mass	345 080 kg

Universität Rostock Traditio et Innovatio — LWET Stiftungslehrstuhl Windenergietechnik

1. Introduction to the new GICON® TLP
2. Description of the Wind Turbine
3. Simulation Results
4. Outlook

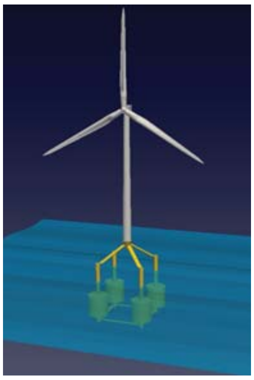

Universität Rostock Traditio et Innovatio — LWET Stiftungslehrstuhl Windenergietechnik

General Settings of the Simulation

- Aerodynamics ⇒ AeroDyn v15
- Structural Dynamics ⇒ ElastoDyn
- Control Dynamics ⇒ ServoDyn (DLL)
- Hydrodynamic Loads ⇒ HydroDyn (only strip-theory solution)
- Mooring System ⇒ MoorDyn

⇓

- 2 Load Cases $\begin{cases}\text{LC 1: Power Production at Rated Conditions } (\approx \text{DLC 1.1}) \\ \text{LC 2: Parked Turbine at 50-Years-Storm } (\approx \text{DLC 6.1a})\end{cases}$

Universität Rostock Traditio et Innovatio — LWET Stiftungslehrstuhl Windenergietechnik

Definition of LC 1 - Power Production at Rated Cond.

- Structural Model
  - No rotor mass imbalance, no aerodynamic imbalance (pitch error), no yaw error
  - All DOFs enabled
- Wind
  - Turbulent wind with $u_{ref} = 12.1$ m/s (rated)
  - NTM with turbulence category „A" (IEC 61400-1, ed3)
  - Wind direction: 0°
- Waves
  - Water Depth: 200 m
  - Irregular Waves based on JONSWAP-Spectrum ($H_s = 1.92$ m, $T_p = 7.29$ s $\rightarrow L_0 \approx 83$ m, $\gamma = 3.3$)
  - Wave direction: 0°
  - Without Current, 2nd order waves and marine growth

Universität Rostock Traditio et Innovatio — LWET Stiftungslehrstuhl Windenergietechnik

LC 1: Platform Motion

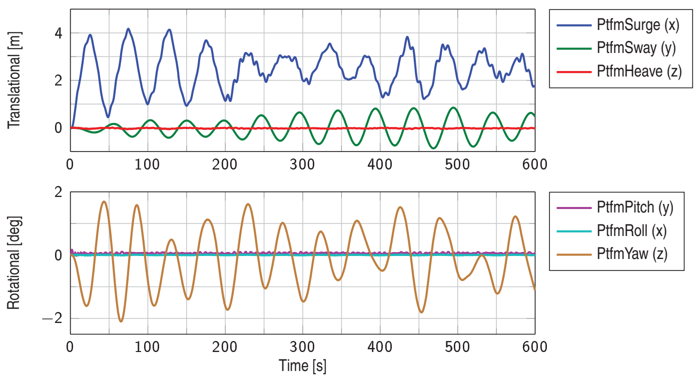

Universität Rostock Traditio et Innovatio — LWET Stiftungslehrstuhl Windenergietechnik

LC 1: Tower-Top Motion

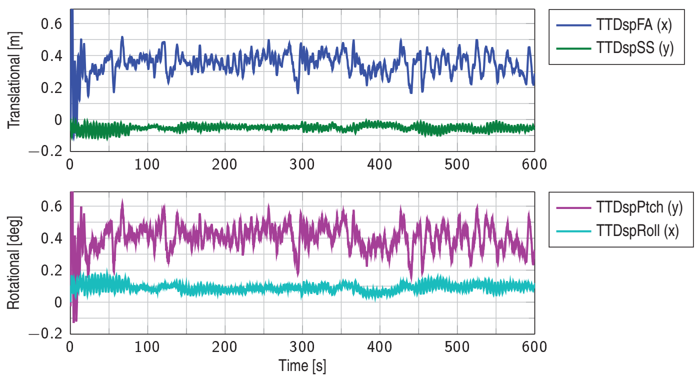

LC 1: Tower-Top Acceleration

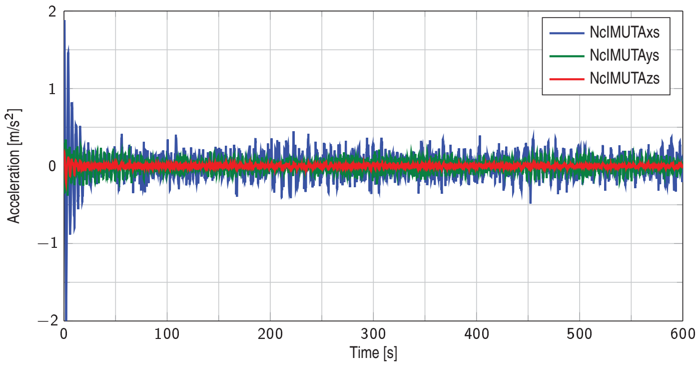

LC 1: Tower-Base Loads

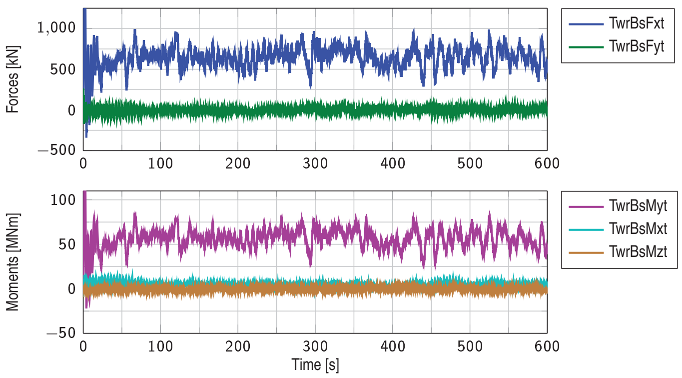

Definition of LC 2 - Parked Turbine at 50-Years-Storm

- Structural Model
  - No rotor mass imbalance, no aerodynamic imbalance (pitch error), no yaw error
  - All DOFs, except of Generator DOF, enabled; Pitch angle fixed at 90°
- Wind
  - Turbulent wind
  - EWM for wind turbine class „IIA“ (IEC 61400-1, ed3)
  - Wind direction: 0°
- Waves
  - Water Depth: 200 m
  - Irregular Waves based on JONSWAP-Spectrum (50-year-storm) ($H_s = 9.72$ m, $T_p = 17.72$ s $\rightarrow L_0 \approx 490$ m, $\gamma = 3.3$)
  - Wave direction: 0°
  - Without Current, 2nd order waves and marine growth

LC 2: Platform Motion

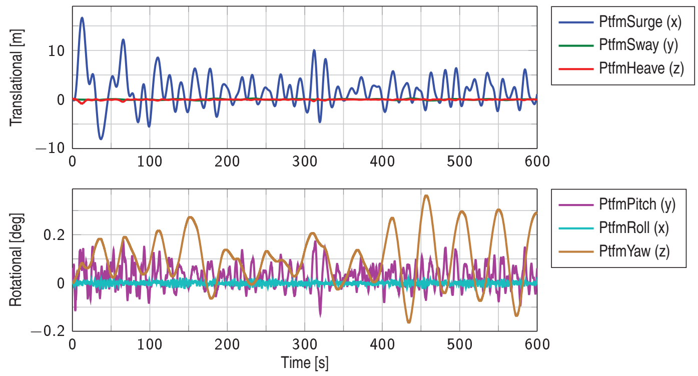

LC 2: Tower-Top Motion

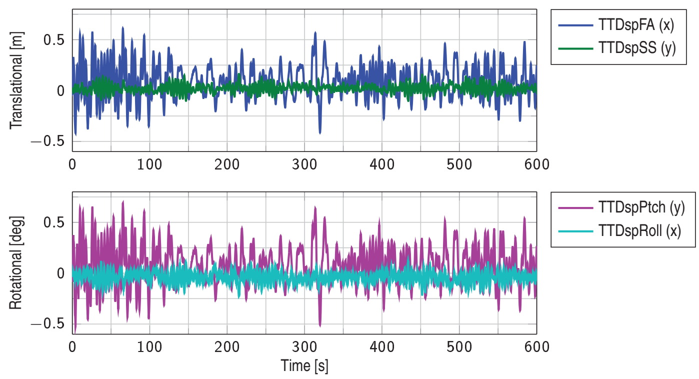

LC 2: Tower-Top Acceleration

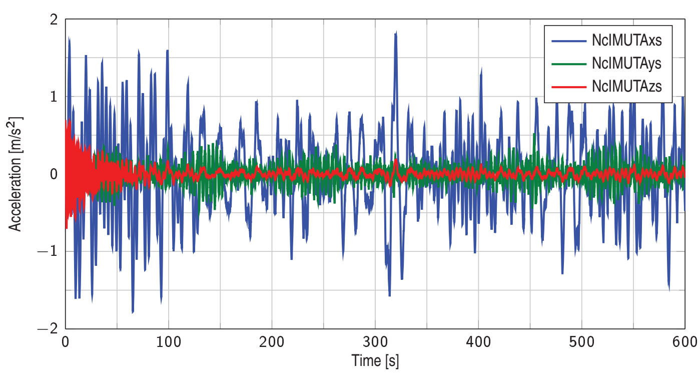

Universität Rostock Traditio et Innovatio

LWET STIFTUNGSLEHRSTUHL WINDENERGIETECHNIK

LC 2: Tower-Base Loads

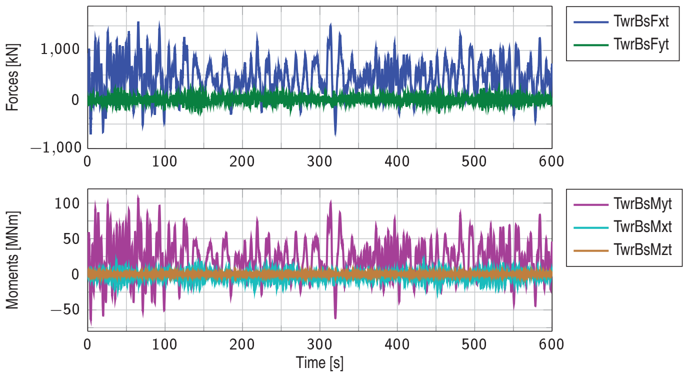

Universität Rostock Traditio et Innovatio

LWET STIFTUNGSLEHRSTUHL WINDENERGIETECHNIK

1. Introduction to the new GICON® TLP

2. Description of the Wind Turbine

3. Simulation Results

4. Outlook

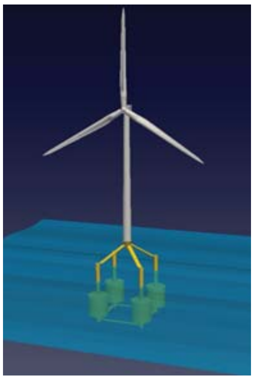

Universität Rostock Traditio et Innovatio

LWET STIFTUNGSLEHRSTUHL WINDENERGIETECHNIK

Outlook

- Improving the used Model (e.g. including potential flow solution)
- Investigate more load cases (e.g. with imbalances, wind-wave-misalignment, special events, ...)
- Detailed design of the substructures components with the dynamic loads from the coupled simulations
- Calibration of simulation results with tank tests planned this summer

Universität Rostock Traditio et Innovatio

LWET STIFTUNGSLEHRSTUHL WINDENERGIETECHNIK

Thank you very much for your attention!

Contact:
Endowed Chair of Wind Energy Technology
Albert-Einstein-Str. 2
D-18059 Rostock

paul.schuenemann@uni-rostock.de
+ 49 381 498 9575

EUROPEAN UNION EUROPEAN REGIONAL DEVELOPMENT FUND We like to express our sincere gratitude to the German Federal State of Mecklenburg-Vorpommern for the financial support from the European Regional Development Fund (project number: TBI-V-1-071-VBW-025).

Closing session – Strategic Outlook

ETIP wind Strategic Research and Innovation Agenda, Aidan Cronin, Siemens Wind Power

Bringing trust to the Internet of Things – When valuable insights can be gained from data to support critical decisions in industry, issues such as the quality and integrity of the data has to be included in the risk picture, M.R. de Picciotto, S. George, DNV GL

A new approach for going offshore, Frank Richert, SkyWind

ETIP Wind
EUROPEAN TECHNOLOGY & INNOVATION PLATFORM ON WIND ENERGY

ETIPWind a common forum with common goals and a common message

EERA DeepWind 2017, Trondheim

Aidan Cronin, ETIPWind Chairman

etipwind.eu

January 20, 2017

What are ETIPs?

Advanced Fossil Fuel Power Generation	Bioenergy	Biofuels
Carbon Capture Utilisation and Storage	Cogeneration of Heat and Power	Concentrated Solar Power
Electricity Storage in the Power Sector	Energy Efficiency in the Cement Industry	Energy Efficiency in the Iron and Steel Industry
Energy Efficiency in the Pulp and Paper Industry	Fuel Cells and Hydrogen	Geothermal Power
Heating and Cooling Technologies	Hydropower	Nuclear Fission Power
Nuclear Fusion Power	Ocean Energy	Road Transport Efficiency
Smart Electricity Grids	Solar Photovoltaic	Wind Energy

ETIP Wind

etipwind.eu

Agenda

- Structure
- The importance of collaboration
- Progress to date
- Current ETIPWind aspirations

ETIP Wind

etipwind.eu

ETIPWind Structure

27 steering committee members 1/3 academia remainder industrials

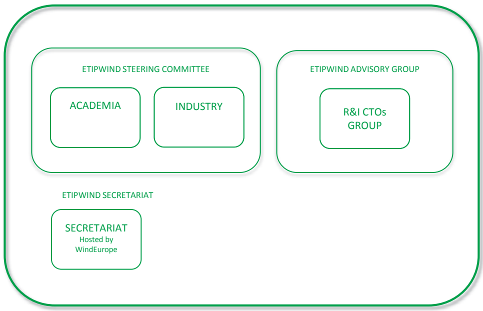

ETIP Wind

etipwind.eu

What are ETIPs?

European Technology and Innovation Platforms are industry-led stakeholder fora recognised by the European Commission

Goals

- Drive innovation, knowledge transfer and European competitiveness
- Develop research and innovation agendas and roadmaps for action at EU and national levels

ETIP Wind

etipwind.eu

Turbine Manufacturers

Vestas, MHI Vestas, SIEMENS, SENVION

Utilities and developers

IBERDROLA RENEWABLES, edp renewables, EDF energies nouvelles, DONG energy, e.on, res, enel, Statoil, VATTENFALL

Universities, research institutes and consultants

DTU Wind Energy, ECN, DNV·GL, Fraunhofer, SINTEF

Others

ABB, LM WIND POWER

ETIP Wind

etipwind.eu

Objectives

ETIP Wind etipwind.eu

Example of policy push, Horizon2020 timeline

ETIP Wind etipwind.eu

How does ETIPWind work?

A two years cycle…

Align on priorities

- **Define** the next challenges for the wind energy sector
- **Align** on priorities relevant for both industry and academia
- **Write** a Strategic Research and Innovation Agenda

Push to policymakers

- Make sure the EC and member states are aware of our priorities
- Help and **provide advice** in the writing of calls for projects

ETIP Wind etipwind.eu

Available budget of the H2020 Energy Challenges

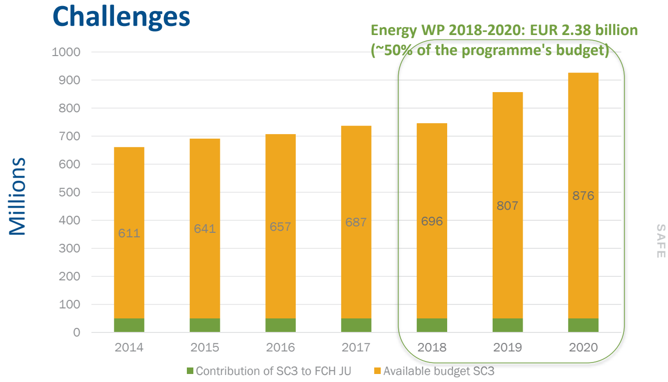

ETIP Wind etipwind.eu

SET-Plan

Towards an Integrated Strategic Energy Technology (SET) Plan: Accelerating the European Energy System Transformation C(2015) 6317

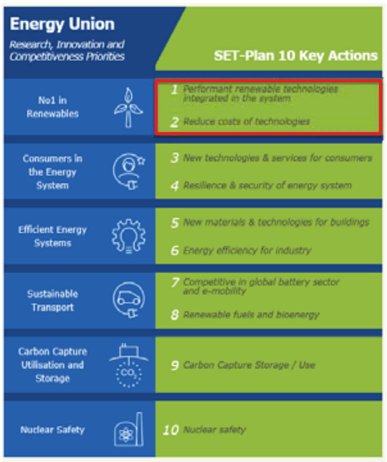

ETIP Wind

ETIP Wind

EUROPEAN TECHNOLOGY & INNOVATION PLATFORM ON WIND ENERGY

The importance of collaboration "Whats in it for all of us"

etipwind.eu

One view of the world

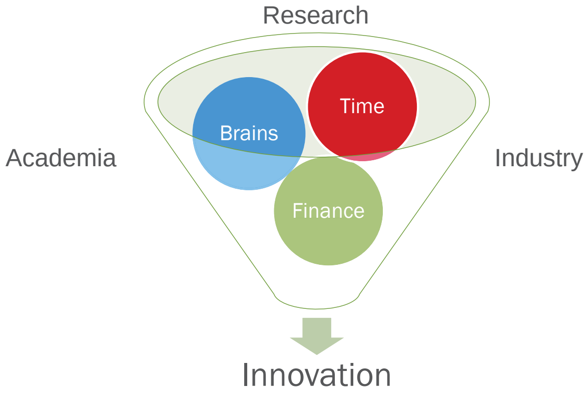

ETIP Wind

etipwind.eu

ETIP Wind

EUROPEAN TECHNOLOGY & INNOVATION PLATFORM ON WIND ENERGY

Progress to date

etipwind.eu

November, 2016

A second view of the world

ETIP Wind

etipwind.eu

Chairmen are nasty people

- Race against the clock
- Passionate discussions
- Frayed tempers

  - Consensus reached in the SRIA
  - Submitted on time and professionally
  - Submitted 30 project areas to Commission
  - Cooked 30 projects down to 15

Perfect process no - but a really good result ☺

ETIP Wind

etipwind.eu

Pitfalls to be avoided

- The messiah complex
- Pre-concieved opinions
- Two worlds apart – how many companies are here?
- Avoid being divided by ST policy makers
- Specific not to yield to the fuzzy general
- Divorces are messy - parties are fun

ETIP Wind

etipwind.eu

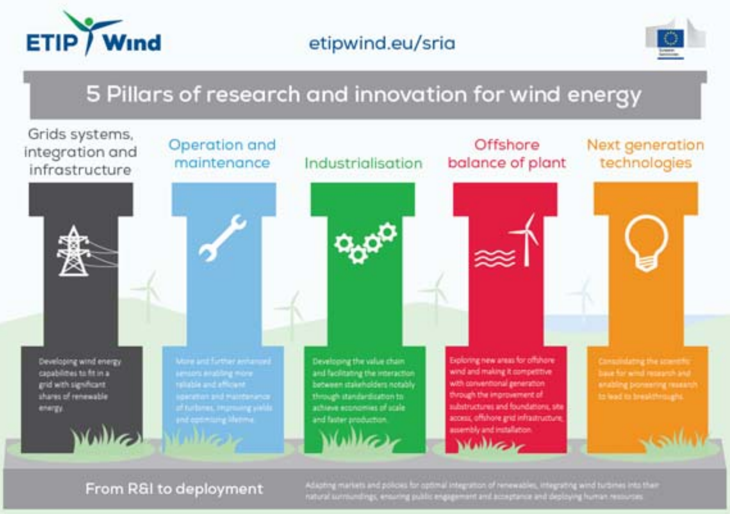

Scope of the discussion

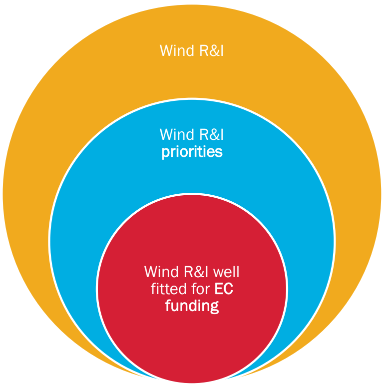

ETIP Wind etipwind.eu

Projects proposal for the European Commission

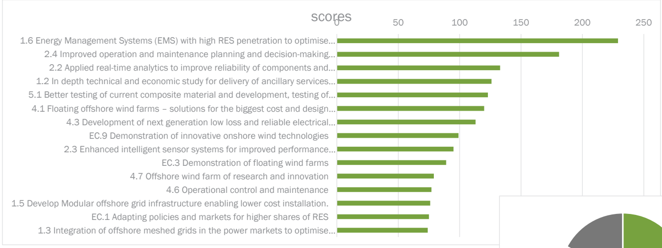

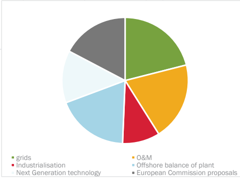

ETIP Wind etipwind.eu

ETIP Wind

EUROPEAN TECHNOLOGY & INNOVATION PLATFORM ON WIND ENERGY

Current ETIPWind Aspirations

etipwind.eu

The life cycle of a progressive society

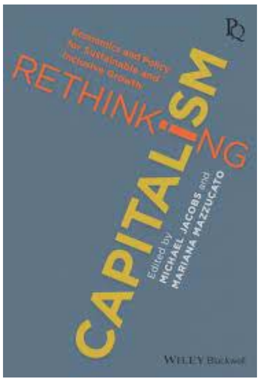

Specifically chapters

1. Introduction
4. Costs of Short-termism
5. The Innovative Enterprise
6. Innovation, the State and **Patient Capital**

ETIP Wind etipwind.eu

Projects proposal for the European Commission

- **Definition** of more than 30 projects of interest for the academia and the industry
- **Submission** to the European Commission for feed-back
- **Reception** of EC's feed back, including proposition of new topics
- **Survey** of the wind energy community on which are the most attractive projects (~15)
- **Analysis** of the best topics to fulfil our objectives
- **Final submission** to the EC

Creation of a common future vision with PV and other renewable technologies.

ETIP Wind etipwind.eu

ETIP Wind

EUROPEAN TECHNOLOGY & INNOVATION PLATFORM ON WIND ENERGY

Thank you for listening
& a special thank you to my hard working Steering Committee & Secretariat

etipwind.eu

DNV·GL

ENERGY

Bringing trust to the Internet of Things

Valuable insights from data to support critical decisions in industry

Marte Riiber de Picciotto, Scott George DNV GL

20 January 2017

Ungraded

Digital transformation of the largest man made system on earth

Ungraded

Data are becoming the new raw material of business

Craig Mundie
Senior Advisor to the CEO of Microsoft

Ungraded

Toward data-driven decision making, rules and standards

Ungraded

The value of combined data sets

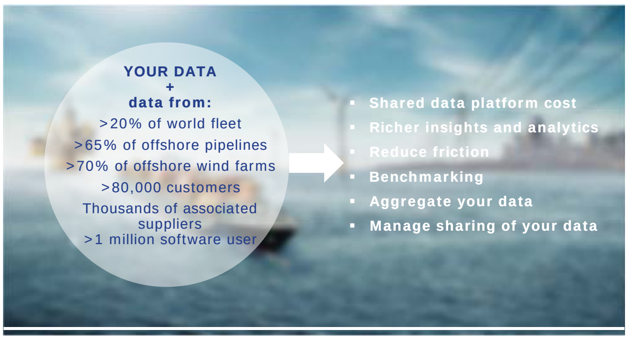

YOUR DATA
+
data from:
>20% of world fleet
>65% of offshore pipelines
>70% of offshore wind farms
>80,000 customers
Thousands of associated suppliers
>1 million software user

- Shared data platform cost
- Richer insights and analytics
- Reduce friction
- Benchmarking
- Aggregate your data
- Manage sharing of your data

Ungraded

Open platform for trusted data

We provide trusted integration, profiling, benchmarking, quality assurance and management of data between providers and consumers

OUR UNIQUE PLATFORM ELEMENTS

ASSET DATA	DATA QUALITY	ANALYTICS
Ingest, storage and integration	Assessment	DNV GL and third-party analytics providers

Ungraded

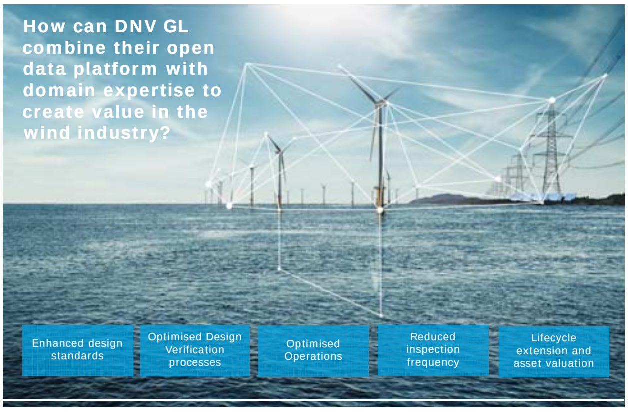

Risk Based Inspections: Informed by Modelling

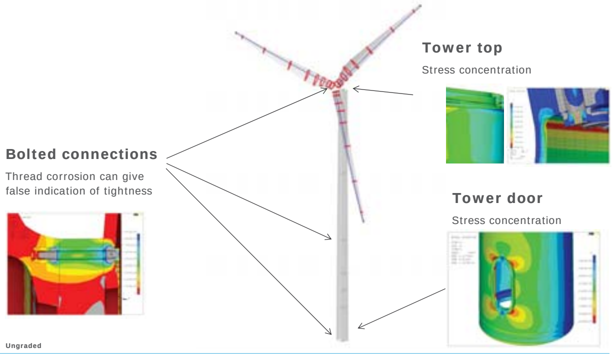

Enhanced Design Standards

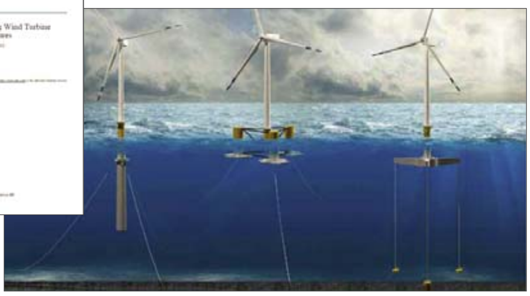

Lifetime extension; Evaluating asset health from data

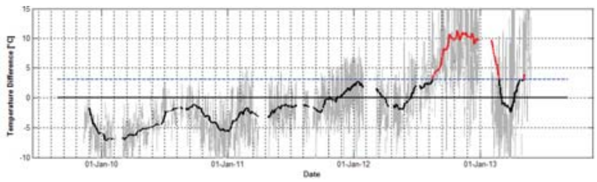

Digital twin for “what if?” analysis

Operations

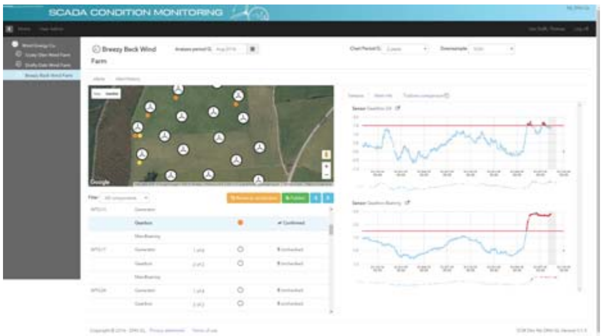

Optimizing performance

- 3 years of 10 minute average data for a commercial MW scale turbine

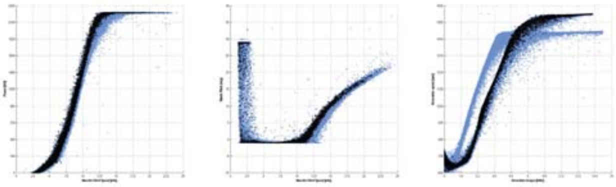

Power Vs wind speed	Pitch Vs wind speed	Rotational speed Vs torque

Ungraded

Asset and data life cycle

Ungraded

Scott A. George, Marte Riiber de Picciotto
Scott.George@dnvgl.com
Marte.de_picciotto@dnvgl.com

+47 920 22 420

www.dnvgl.com

SAFER, SMARTER, GREENER

Ungraded

Developing the Future
from Vision to Reality

SkyWind

CAPEX and turbine components' contribution

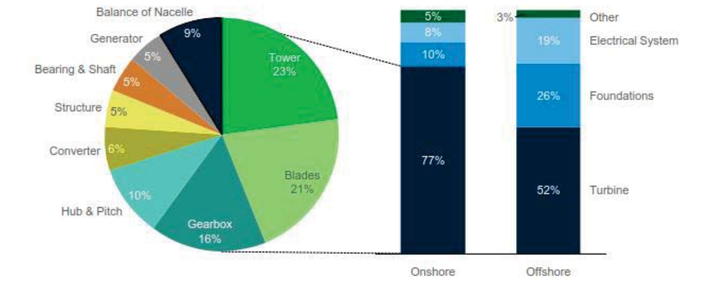

Source: MAKE
Note: Baseline Turbine: 2-2.5MW, 90-110m rotor glass blades, DFIG electrical system, 80m steel tubular tower
Onshore wind plant: 100MW, flat terrain, 33 kV interarray, 220 kV collector. Wind turbine = 2.0MW, 80m towers
Offshore wind plant: 396MW, 50m depth, 30km from shore, 33kV interarray, 2x 220 kV collector, 1 substation. Wind turbine = 6.0MW, quadrapod foundation

Forecasting Wind Energy Costs and Cost Drivers

The Views of the World's Leading Experts

	ONSHORE (LAND-BASED)	FIXED-BOTTOM OFFSHORE	FLOATING OFFSHORE
LEVELIZED COST OF ENERGY (median estimates for median scenario & 1st-3rd quartile range)	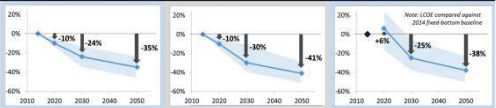		
DRIVERS FOR COST REDUCTION IN 2030 (median estimates; median scenario)	Capacity factor: +10% Project life: +10% CapEx: -12% OpEx: -9% WACC: no Δ	Capacity factor: +4% Project life: +15% CapEx: -14% OpEx: -9% WACC: -10%	Capacity factor: +9% Project life: +25% CapEx: -5% OpEx: -8% WACC: -5%
TURBINE SIZE IN 2030 (typical projects)	 3.25 MW 115 m hub height 135 m rotor diameter	 11 MW 125 m hub height 190 m rotor diameter	 9 MW 125 m hub height 190 m rotor diameter
TOP-FIVE IMPACT CATEGORIES	• Larger rotors, reduced specific power • Rotor design advancements • Taller towers • Reduced financing costs • Component durability / reliability	• Larger turbine capacity • Foundation / support structure design • Reduced financing costs • Economies of scale via project size • Component durability / reliability	• Foundation / support structure design • Installation process efficiencies • Foundation / support manufacturing • Economies of scale via project size • Installation / transport equipment

NREL
iea wind
2016

Cost barriers for larger rotor MW-scale turbines

	Units	<2010 Turbine	>2010 Turbine	Next Gen 1.X
Color Code				
Turbine Rating	(MW)	1.8	1.8	1.8
Rotor Diameter	(meters)	82	100	124
Specific Rating	(W/m²)	340	230	150*

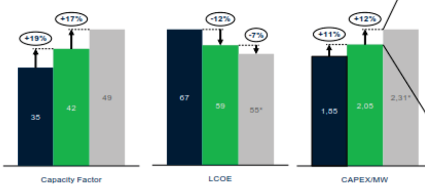

Added Cost components

Blades
- 12 meters longer
- Adds ~5 tons per blade

Tower
- 10-12 meters taller
- 80m → 90/95m
- Adds ~35 tons of steel

Machine structure
- Weight increase
- Gearbox redesign
- Main shaft redesign
- Hub redesign
- Bedplate redesign

Foundations
- Weight increase ~30%

Roads
- Road length increase by ~7.5km

Interarray cabling
- Cables increase by ~10km

Source: MAKE
Note: * Indicates target values
100MW U.S. wind plant, PTC
OPEX cost = USD 60K/Turbine/year Full Service Agreement
Finance: 20-year life, WACC = 8%, 70/30 Debt/Equity, Debt Rate = 5%, 10 year tenor

Relative Impact of Drivers for LCOE Reduction in 2030

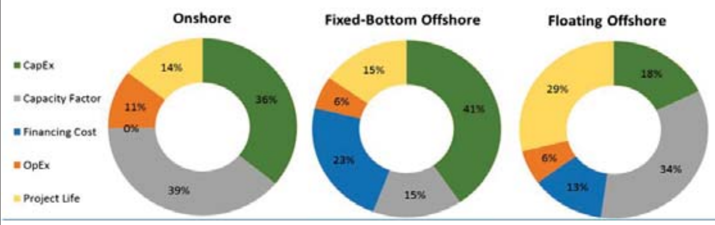

NREL
iea wind
2016

Turbine Weight and Cost „Scaling Laws“

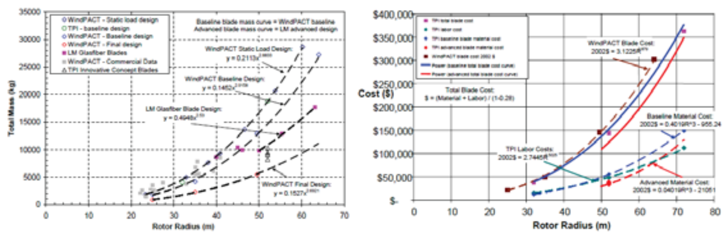

U.S. Department of Energy's (DoE's) Wind Partnership for Advanced Component Technologies (WindPACT)

Scaling means:
Extending existing systems and technology

We talk about Power Plants!

SkyWind

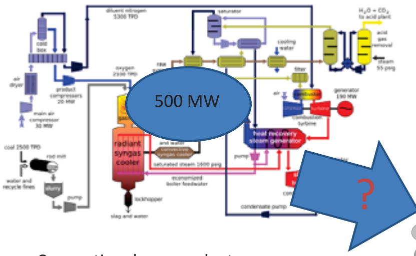

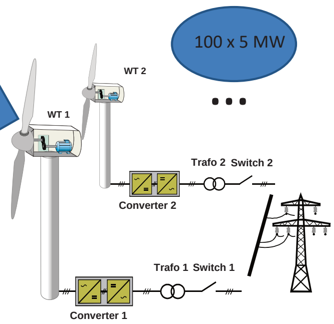

Conventional power plants consists out of several generators, which work together with specific devices for grid connection, whereas each wind turbine has its own grid connection system.

Is this a setup for a economic (wind) power plant?

Background of SkyWind

SkyWind

20 Years Experience

GEO WEST cmc BZEE Academy GmbH

- Planning, realization and operation of wind farms (250 turbines, all types, all manufactures)
- Design, service, education and training

Development Approach

- Born from experience (eliminate / improve failure areas)
- Change point of view (supplier-> operator, manufacturer -> user)

Aim of the development

- Minimize the Life Cycle Costs of Energy of wind turbines
- Bundling of wind turbines to Wind Power Plant (WPP/RPP)

Wind Power Plant with Grid Connection Unit

SkyWind

Single Wind Turbines

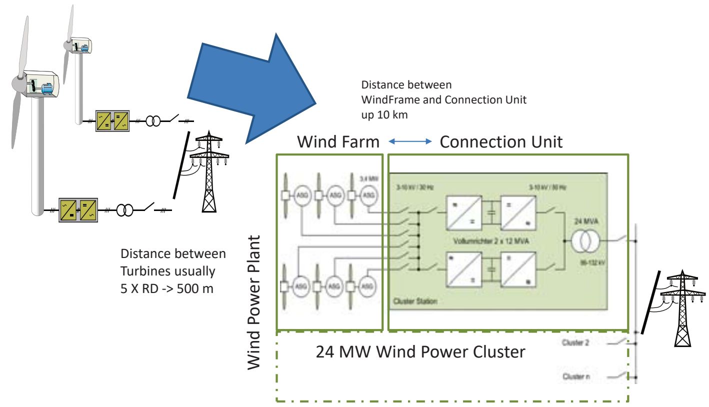

Wind turbine

SkyWind

Built in separate modules

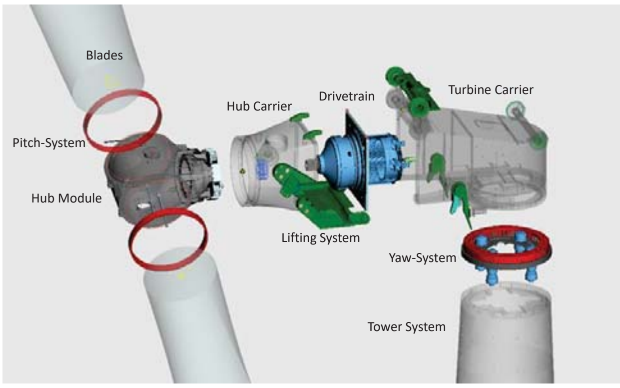

Built in Modules

SkyWind

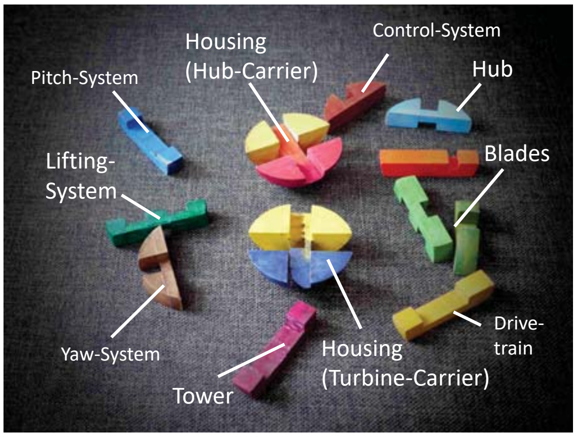

Prozess WindPowerPlant

SkyWind

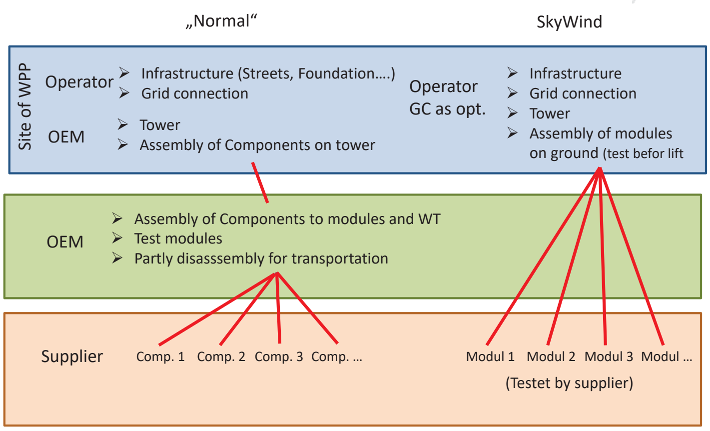

Assembly

SkyWind

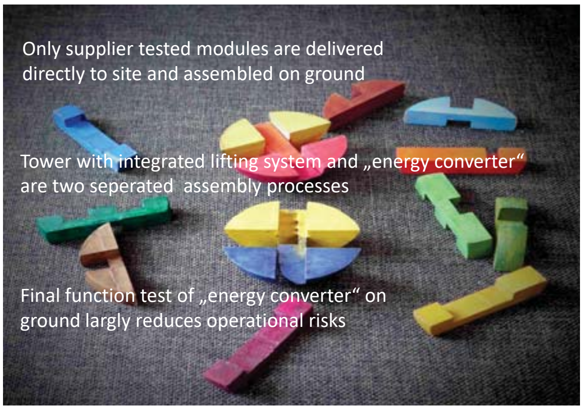

WETEC Lifting

SkyWind

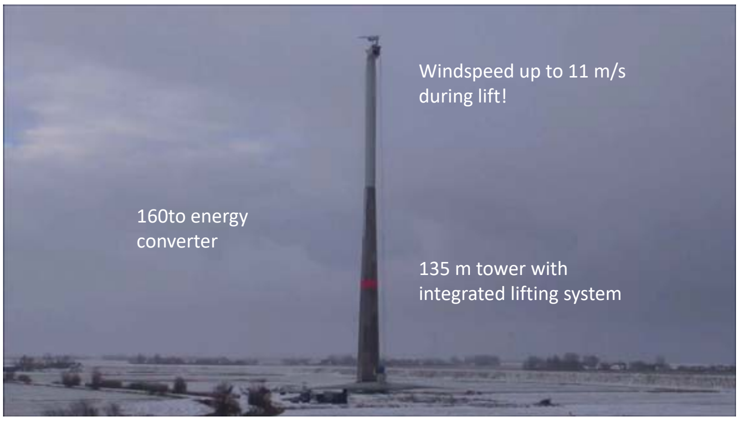

Installation

SkyWind

WETEC Operation

SkyWind

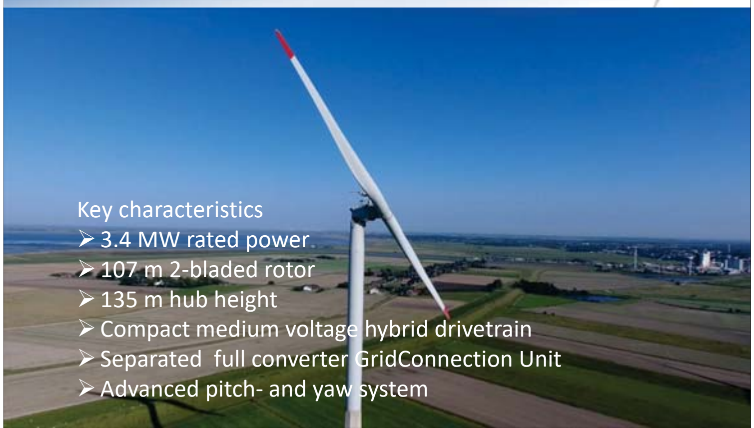

Installation (onshore)

SkyWind

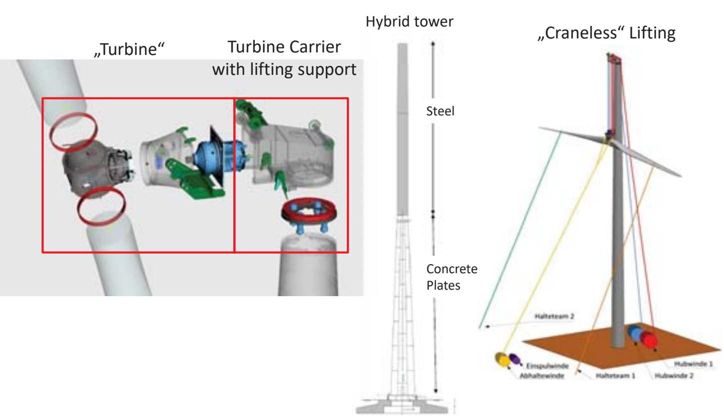

Scaling up ?

SkyWind

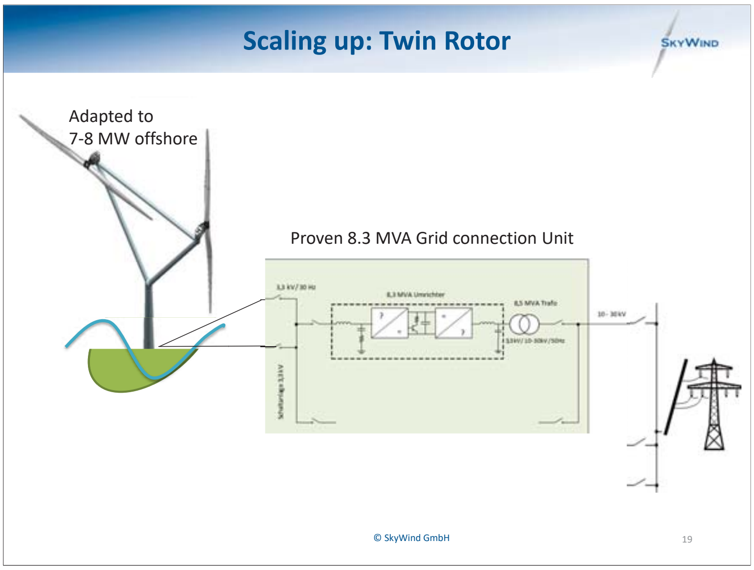
Scaling up: Twin Rotor
SkyWind
Adapted to
7-8 MW offshore
Proven 8.3 MVA Grid connection Unit
© SkyWind GmbH
19

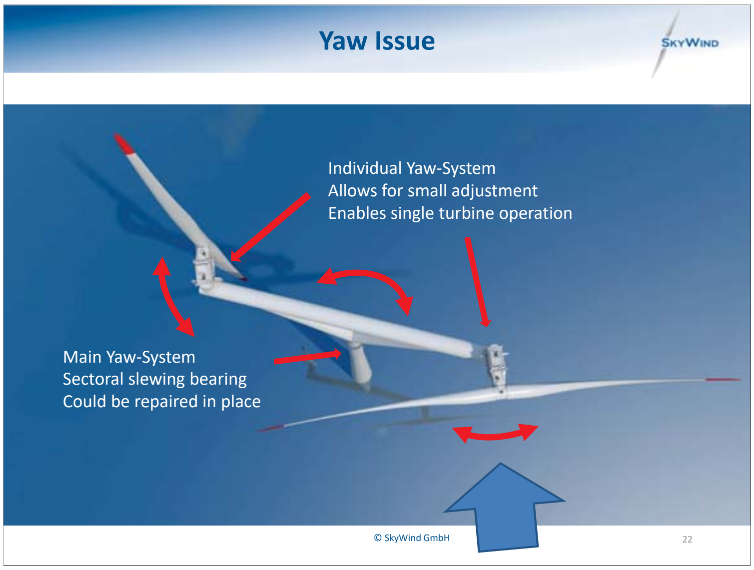
Yaw Issue
SkyWind
Individual Yaw-System
Allows for small adjustment
Enables single turbine operation
Main Yaw-System
Sectoral slewing bearing
Could be repaired in place
© SkyWind GmbH
22


Multirotor
SkyWind
Size, time line?
How to install and maintain?
Electrical integration?
4 X 100 kW Lagerwey 1976
4 X 225 kW Vestas 2016
© SkyWind GmbH
20

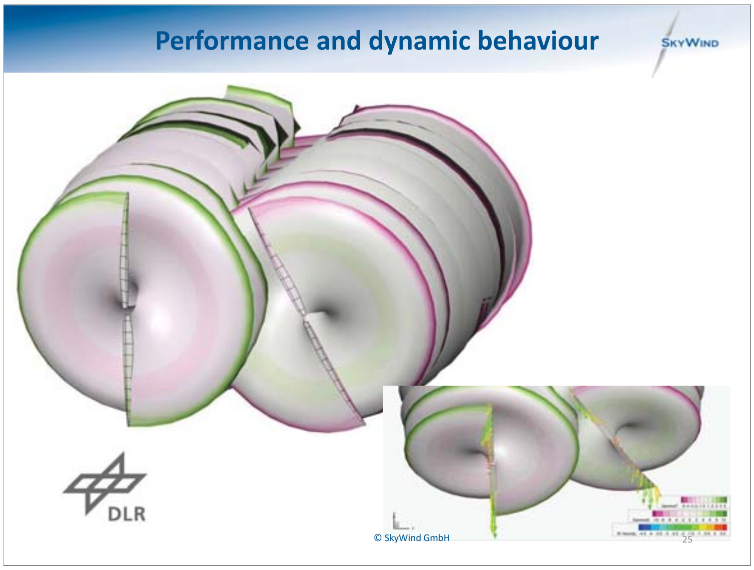
Performance and dynamic behaviour
SkyWind
DLR
© SkyWind GmbH


Adapt onshore to offshore
SkyWind
© SkyWind GmbH
21

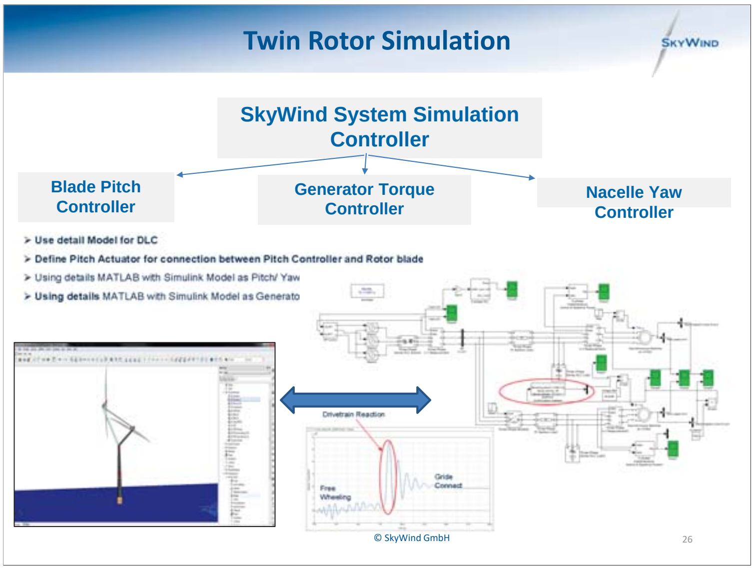
Twin Rotor Simulation
SkyWind
SkyWind System Simulation
Controller
Blade Pitch
Controller
Generator Torque
Controller
Nacelle Yaw
Controller
Use detail Model for DLC
Define Pitch Actuator for connection between Pitch Controller and Rotor blade
Using details MATLAB with Simulink Model as Pitch/ Yaw
Using details MATLAB with Simulink Model as Generato
Drivetrain Reaction
Free Wheeling
Grids Connect
© SkyWind GmbH
26

Windprofile and Rotorsize

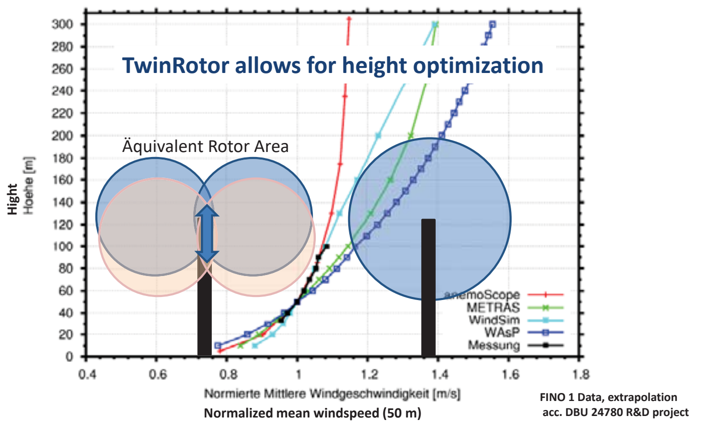

FINO 1 Data, extrapolation acc. DBU 24780 R&D project

Thank You

SkyWind

Husum, Kiel, München
Bergen (N)

www.skywind.de
www.skywind.no

mailto@skywind.de

+49 4841 77255 0

Mass- and Cost Potential

According to WindPACT und Jamieson scaling laws

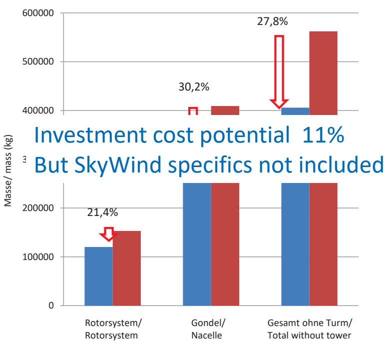

Investment cost potential 11%
But SkyWind specifics not included

Further cost reduction potential
- Supply Process
- 20 m lower tower
- Installation method (also for maintenance !)
- Same turbine on- and offshore
  - Serial production
  - Stuff education
  - Common SCADA
  - Spare parts

Target: 30 %

Summary- SkyWind for offshore wind farms

- Scaling up with two "known" turbines per foundation
- Installation is controlled with winches on DP vessel - no large cranes needed
- Substructure / foundation needs to be developed and total system to be optimized (eg. controller)

➡ Invitation for Norwegian R&D

Pilot options Karmøy Metcentre (or onshore)

Potential that turbine(s)
with lowest CoE
could be manufactured
in Norway!!

Poster session

Session A

1. *Power quality studies of a Stand-Alone Wind Powered Water Injection System without Physical Inertia, A. Gaugstad, NTNU*
2. *Multibody Analysis of Floating Offshore Wind Turbine System, Y. Totsuka, Wind Energy Institute of Tokyo Inc.*
3. *Investigation of design driving load cases for floating VAWT with pitched blades, F. Savenije, ECN*
4. *SKARV – Preventing bird strikes through active control of wind turbines, K. Merz, SINTEF Energi AS*
5. *An elemental study of optimal wind power plant control, K. Merz, SINTEF Energi AS*

Session B

6. *Inertia Response from HVDC connected Full Converter Wind Turbines, J. Ødegård, Statnett*
7. *Investigation of power sharing solutions for offshore wind farms connected by diode rectifier for HVDC grid, I. Flåten, NTNU*
8. *Offshore Wind Power Plants with 66 kV Collection Grids – Study of Resonance Frequencies, A. Holdyk, SINTEF Energi*
9. *Grid Integration of offshore wind farms using a hybrid composed by an MMC with an LCC-based transmission system*, R. Torres-Olguin, SINTEF Energi
10. *Review of Investment Model Cost Parameters for VSC HVDC Transmission Infrastructure*, T.K. Vrana, SINTEF Energi

Session C

11. *Meteorological Phenomena Influences on Offshore Wind Energy, S. Ollier, Loughborough University*
12. *Availability of the OBLO infrastructure for wind energy research in Norway, M. Flügge, CMR*
13. *Demonstrating the improved performance of an Ocean-Met model using bi-directional coupling, A. Rasheed, SINTEF ICT*
14. *A comparison of short-term weather forecast with the measured conditions at the Hywind Demo site, L. Sætran, NTNU*

Session D

15. *Diagnostic monitoring of drivetrain in a 5-MW spar type floating wind turbine using frequency domain analysis, M. Ghane, NTNU*
16. *Risk-based planning of operation and maintenance for offshore wind farms, M. Florian, Aalborg University*
17. *Improving fatigue load estimation of wind turbines using a neural network trained with short-duration measurements, J. Seifert, University of Oldenburg*
18. *Recommended practices for wind farm data collection and reliability assessment for O&M optimization, T. Welte, SINTEF Energi*
19. *Integration of Degradation Processes in a Strategic Offshore Wind Farm O&M Simulation Model, T. Welte, SINTEF Energi*
20. *Experiences from Wind Turbine Pilot Test of a Remote Inspection System, Ø. Netland, NTNU*
21. *A Framework for Reliability-based Controller Scheduling in Offshore Wind Turbines, J-T H. Horn, NTNU*
22. *Key performance indicators for wind farm operation and maintenance, H. Seyr, NTNU*
23. *Optimization of data acquisition in wind turbines with data-driven conversion functions for sensor measurements, L. Colone, DTU Denmark*

Session E

24. *Design and Fatigue Analysis of Monopile Foundations to Support the DTU 10 MW Offshore Wind Turbine, J.M Velarde, NTNU*
25. *Design load basis of a 10MW floating wind turbine: substructure modelling effects, M. Borg, DTU Wind Energy*
26. *New Foundation Models for Integrated Analyses of Offshore Wind Turbines, A.M. Page, NTNU*
27. *Damage assessment of floating offshore wind turbines using latin hypercube sampling, K. Müller, University of Stuttgart*
28. *Development and validation of an engineering model for floating offshore wind turbines, A.Pegalajar-Jurado, DTU Wind Energy*
29. *Improved estimation of extreme wave loads on monopiles using First Order Reliability Method, A. Ghadirian, DTU*
30. *A 3D fem model for wind turbines support structures, C. Molins, Universitat Politecnica de Catalunya*
31. *Fully integrated load analysis included in the structural reliability assessment of a monopile supported offshore wind turbine, J. Peeringa, ECN*
32. *Parametric study of mesh for fatigue assessment of tubular joints using numerical methods, J. Mendoza, NTNU*
33. *Lifetime extension for large offshore wind farms: Is it enough to reassess fatigue for selected design positions? C. Bouty, NTNU*
34. *Optimization of offshore wind farm installations, S. Backe, University of Bergen*
35. *Modelling of Marine Operations in the Installation of Offshore Wind Farms, A. Dewan, ECN*
36. *Effect of irregular second-order waves on the fatigue lifetime of a monopile based offshore wind turbine in shallow waters, F. Pierella, IFE*
37. *A review of slamming load application to offshore wind turbines from an integrated perspective, Y. Tu, NTNU*

Session F

38. *Offshore Turbine Wake Power Losses: Is Turbine Separation Significant?, P. Argyle, CREST, Loughborough University*
39. *Experimental study on the optimal control of three in-line turbines, J. Bartl, NTNU*
40. *A step towards a reduced order modelling of flow characterized by wakes using Proper Orthogonal Decomposition, E. Fonn, SINTEF ICT*
41. *Explaining the Torque vs TSR curve of a 5MW NREL reference turbine, M.S. Siddiqui, SINTEF ICT*
42. *A 3D Vs 2.5D Vs 2D CFD analysis of 5MW NREL reference wind-turbine to study impact of bluff sections, M. Tabib, SINTEF ICT*
43. *Simulating Single turbine and associated wake development - comparison of computational methods (Actuator Line Vs Sliding Mesh Interface Vs Multiple Reference Frame) for an industrial scale wind turbine, M.S. Siddiqui, SINTEF ICT*

44. *2D VAR single Doppler LIDAR vector retrieval and its application in offshore wind energy, R. Calhoun, Arizona State University*

Session G

45. *IRPWIND ScanFlow project, C. Hasager, DTU Wind Energy*
46. *Comparison of Numerical Response Predictions for a Bottom Fixed Offshore Wind Turbine, S.H. Sørum, NTNU*
47. *Comparison of the effect of different inflow turbulences on the wake of a model wind turbine, I. Neunaber, University of Oldenburg*
48. *IRPWIND ScanFlow Public database, J.W. Wagenaar, ECN*
49. *Wind Tunnel Hybrid/HIL Tests on the OC5/PhaseII Floating System, I. Bayati, Politecnico di Milano*
50. *Calibration and Validation of a FAST model of the MARINTEK Hybrid Semisubmersible Experiment, G. Stewart, NTNU*
51. *The TripleSpar campaign: Implementation and test of a blade pitch controller on a scaled floating wind turbine model, W. Yu,, University of Stuttgart*
52. *A computational fluid dynamics investigation of performance of tip winglets for horizontal axis wind turbine blades, K. Sagmo, NTNU*
53. *Numerical study of irregular breaking wave forces on a vertical monopile for offshore wind turbines*, A. Aggarwal, NTNU
54. *Modelling of the Viscous Loads on a Semi-Submersible Floating Support Structure Using a Viscous-Flow Solver and Morison Formulation Combined with a Potential-Flow Solver, S. Burmester, MARIN*

POWER QUALITY STUDIES OF A STAND-ALONE WIND-POWERED WATER INJECTION SYSTEM WITHOUT PHYSICAL INERTIA

Alexander Gaugstad, Santiago Sanchez, Elisabetta Tedeschi, Muhammad Jafar, Yongtao Yang
alexantg@stud.ntnu.no, santiago.sanchez@ntnu.no, elisabetta.tedeschi@ntnu.no, muhammad.jafar@dnvgl.com, yongtao.yang@dnvgl.com

Abstract
A model of a wind-powered microgrid for applications in oil & gas industries is presented in this poster. The model is used to simulate the power quality during common wind scenarios and important aspects as black start and Fault Ride-Through (FRT) capability. The controller tuning has been carefully chosen in order to maximize power production while minimizing fluctuations.

Concept: Wind-powered Water Injection [1]

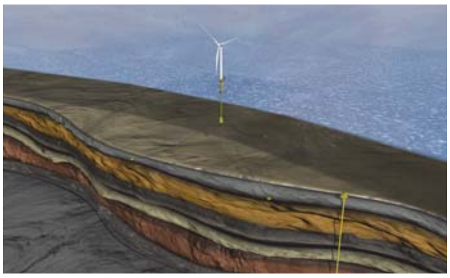

Proposed topology

- 6 MW offshore Permanent Magnet Synchronous Generator (PMSG) wind turbine [2].
- The main load: centrifugal pump driven by a 3 MW Induction Motor Drive.
- 0.5 MW fixed critical load: pitch and yaw drives, control- and communication systems and lightning and climate conditioning systems.
- A battery storage is responsible for supplying the critical loads during low wind conditions, and the control of main bus voltage magnitude and frequency.
- The VSC control systems utilize Field Oriented Control based upon [3][4][5].

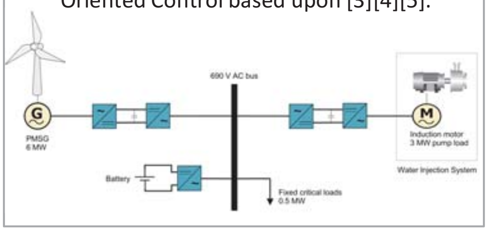

Control strategies

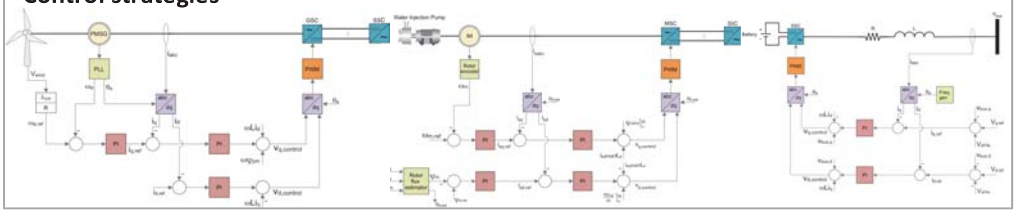

Wind Turbine simulations

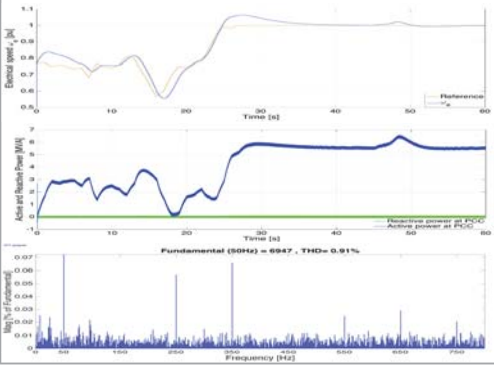

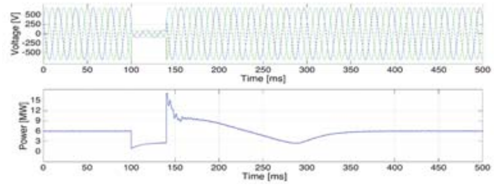

1. The ability of PMSG to follow the optimal speed.
2. The corresponding output power.
3. The harmonic current distortion provided by the PMSG at PCC.
4. Fault ride-through analysis: 40 ms fault, 0.15 pu voltage.

Water Injection System simulations

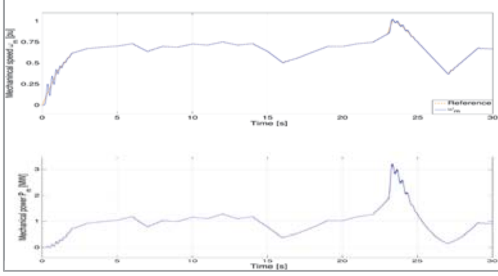

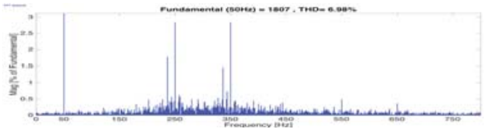

1. The ability induction machine to follow the optimal speed during power fluctuations.
2. The corresponding mechanical output power
3. The harmonic distortion of the VSD input current.

Battery System simulations

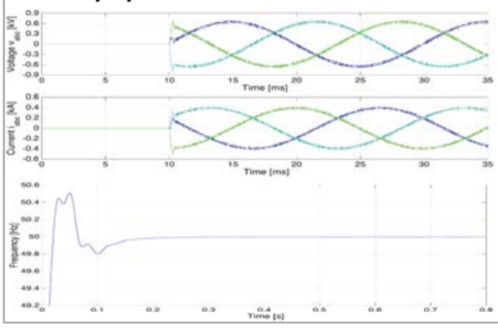

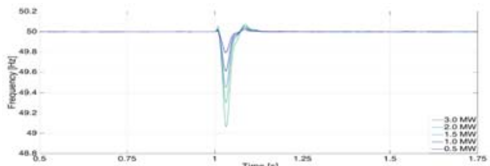

1. Voltage and current when the battery performs a black start after 10 ms.
2. The voltage frequency during the black start.
3. Voltage frequency response during a sudden load change in the system which occurs after 1 s.

Conclusions

- Simulations have shown the generator to be able to follow a rapidly changing speed reference, with a close to optimal power production. Note that the pitch controller limits the speed of the wind turbine after 48 s when the wind speed rises above the base speed.
- The total current harmonic distortion of the PMSG is measured to be 0.91%, which is clearly within the IEEE 519 recommendations.
- A fault ride-through analysis showed that the PMSG can withstand a 40 ms fault with 0.15 pu voltage at the point of common coupling. The power peak after fault clearing is due to increased current.
- The induction motor is to able to follow a rapidly changing speed reference, which represents the fluctuating power production from the wind turbine. Some oscillations are observed at very large fluctuations, but this is expected due to the fast dynamics of the high speed motor.
- The total current harmonic distortion at the point of common coupling of the main bus and the VSD is measured to be within the distortion limit of 8% in IEEE 519.
- A black start of the system has been proven possible through simulations. The voltage magnitude and frequency is rapidly set to the rated values by the battery when the black start is initiated.
- The battery is able to keep the rated voltage magnitude and frequency in case of rapid load change or sudden loss of wind power.
- Simulations at rated conditions suggest a current up to 3.0 kA at the PCC that the battery must be able to absorb.

References

[1] DNV GL, «WIN WIN Joint Industry Project: Wind-powered water injection,» DNV GL, Høvik, 2016.

[2] Siemens AS, *Wind Turbine SWT-6.0-154,* Hamburg, 2016.

[3] A. Årdal, *Feasibility studies on integrating offshore wind power with oil platforms.* Master's thesis, Department of Electrical Engineering, NTNU, Trondheim, 2011.

[4] R. Nilsen, TET4120 Electric Drives, Department of Electrical Engineering, NTNU, Trondheim, 2016.

[5] N. Mohan, Advanced Electric Drives, John Wiley & Sons, Inc, Hoboken, 2014.

Multibody Analysis of Floating Offshore Wind Turbine System

Yoshitaka Totsuka, Hiroshi Imamura and Fuminori HIOKI
Wind Energy Institute of Tokyo Inc.

Introduction

As waters around Japan is mostly deeper, deployment of floating offshore wind turbine is necessary. Toward widespread use of floating offshore wind turbine in Japan, authors focus on load analysis of drivetrain components on floating offshore wind turbine. This research is performed under Development of next-generation floating offshore wind turbine systems in NEDO and project scope is development of low cost floating wind turbine for shallow water.

Analysis model

In our research, four different floater concepts (TLP, semi-sub, pontoon and spar [see Figure 1]) are analyzed and the obtained results are compared with the result on land based wind turbine. Specification of RNA and tower is summarized in Table 1. We revised the NREL 5MW model[1] as the common RNA and tower model which is used for all floater concepts.

To identify critical drivetrain components on design process of floating offshore wind turbine, we constructed ADAMS multibody drivetrain dynamics model. The model structure and its topology are shown in Figure 2.

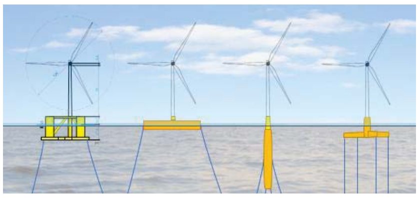

Figure1 Four different floater concepts in this study

Specification of 5MW RNA and tower（red font is revised part from NREL 5MW baseline model）

Rated Power	5 [MW]
Rotor	Upwind , 3Bladed
Control	Variable speed, Collective Blade pitch
Drivetrain	High Speed, Multiple-Stage Gearbox
Rotor diameter and Hub diameter	126, 3 [m]
Hub Height	83.1（=80.7+2.4） [m]
Cut-in, rated and Cut-out WSP	3.0, 11.4, 25.0 [m/s]
Cut-in and rated rotor speed	6.9, 12.1 [rpm]
Circumferential speed	80 [m/s]
Overhang, Tilt and Precone	5 [m] 5（tilt）, 2.5（precone） [deg.]
Rotor, Nacelle and Tower mass	110,000, 240,000, 514,000 [kg]

Table 1 RNA Specification

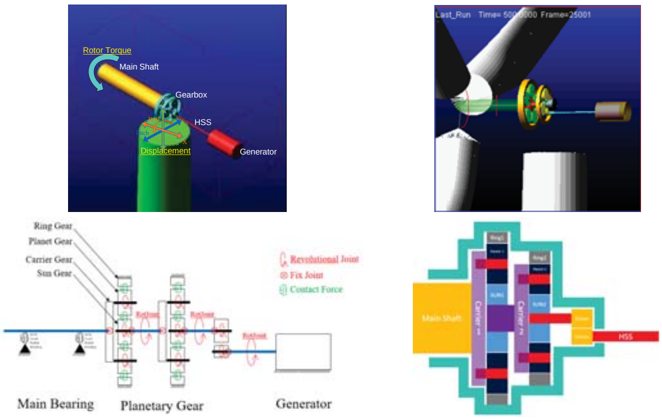

Figure2 Drivetrain analysis model

Analysis condition

For our comparison study, DLC1.2 of rated WSP condition which is most likely to have the large load fluctuation, was chosen as analysis condition. Wind and wave condition are summarized in Table 2. We have two steps for our drivetrain analysis. The first step is FAST[2] simulation for the whole system of floating type offshore wind turbine. In the next step ADAMS drivetrain dynamics simulation is performed and the obtained FAST time series result of tower top displacement and hub load is used as boundary condition of ADAMS Drivetrain model.

Wave		Wind	
water depth	150 [m]	Hub height WSP	12 [m/s]
wave model	NSS (Normal Sea State)	TI : Iref	Class IB
wave spectrum	Pierson-Moskowitz	inclination angle	0 [deg]
current	NA [m/s]	wind shear	0.14
Significant wave height	1.73 [m]	yaw misalignment	0 [deg]
peak spectral period	6.6 [sec]	Turbulence model	Kaimal

Table2 Analysis condition in FAST

Results

Normal operation condition with average WSP of 12[m/s] is analyzed and the results are compared between four different FOWT(TLP, semi-sub, pontoon and spar) and land based WT.

As seen from FAST result of rotor torque and speed fluctuation indicates in Figure 4, controller is suitably tuned for FOWT. Different order of Sun-gear bending moment fluctuation is obtained due to the platform pitch motion of FOWT in Figure 6.

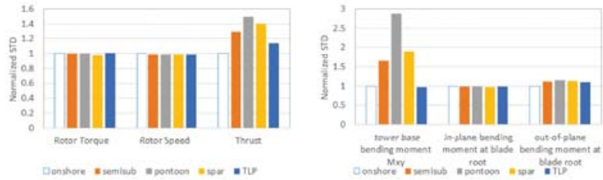

Figure 3 Fluctuation on Rotor Torque, Thrust, Rotor Speed and Moment by FAST

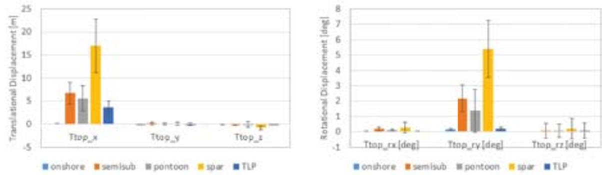

Figure 4 Comparison of tower top motion by FAST

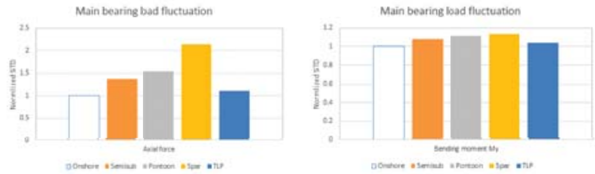

Figure 5 Load fluctuation of main bearing by ADAMS

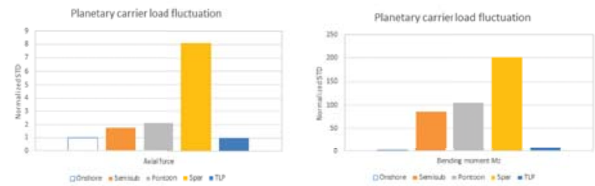

Figure 6 Load fluctuation of sun gear by ADAMS

Conclusion

Multibody simulation model of floating offshore wind turbine system is constructed and we carried out load analysis of Drivetrain components for floating offshore wind turbine. Different order of bending moment fluctuation is obtained due to the platform pitch motion of floating offshore wind turbine.

Verification work for new load reduction concept is continued for further advanced drivetrain model of floating offshore wind turbines.

Acknowledgement

This research is performed under the Development of next-generation floating offshore wind turbine systems (Development of fundamental technologies) in NEDO (New Energy and Industrial Technology Development Organization).

Reference

1. J. Jonkman et. al., Definition of a 5-MW Reference Wind Turbine for Offshore System Development, NREL/TP-500-38060, 2009.
2. J.M. Jonkman and M. L. Buhl Jr., FAST User's Guide, NREL/EL-500-38230, 2005.

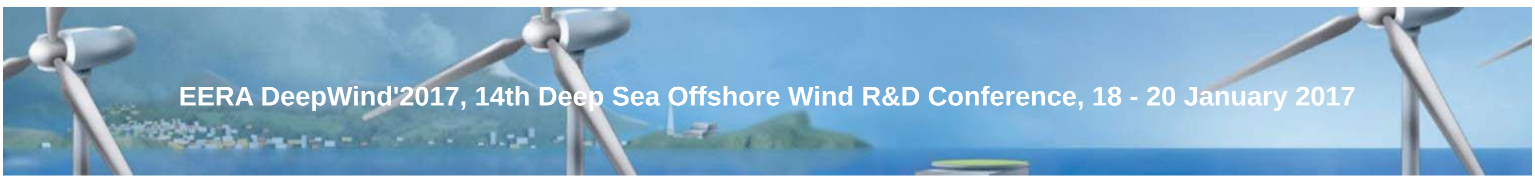

A cormorant (skarv)

SKARV

Preventing bird strikes through active control of wind turbines

(Norwegian: Slippe fuglekollisjoner med aktiv regulering av vindturbiner)

Karl Merz (karl.merz@sintef.no) and John Olav Tande, SINTEF Energy Research
Amund Skavhaug and Dag Sjong, Norsk Automatisering AS

- Detect the presence of birds with sensors such as low-cost digital video cameras or radars.
- Based on these measurements perform a probabilistic estimate of the birds' flight path.
- Control the rotational speed of the wind turbine to minimize the probability of collision.

The wind turbine remains in normal operation. The rotor speed is only perturbed by a moderate amount. This requires that the birds be detected and tracked at least several seconds before they cross the rotor plane.

In contrast to existing technologies which employ deterrents such as sounds and lights, the proposed system is entirely benign, avoiding disturbances to the birds and surrounding nature. If successful, the proposed active bird-avoidance control strategy would prevent most bird-blade collisions, with a negligible impact on annual energy production.

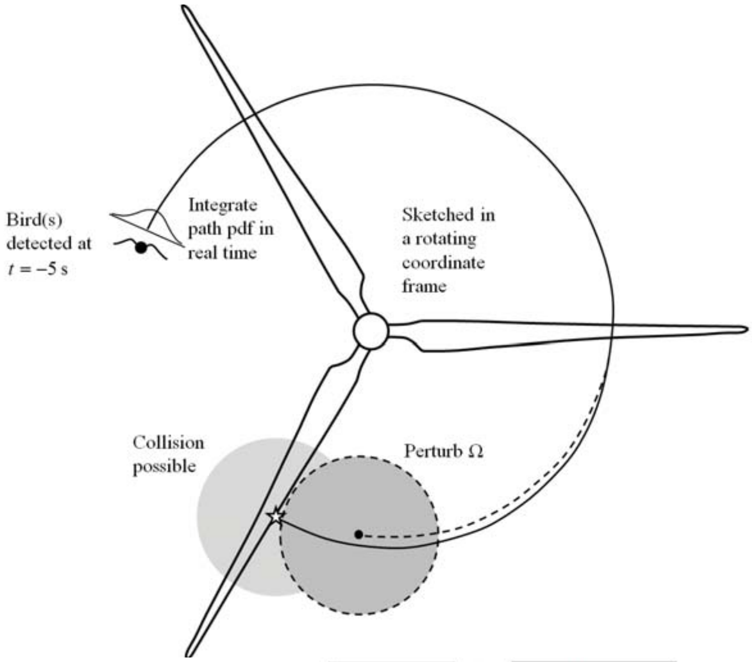

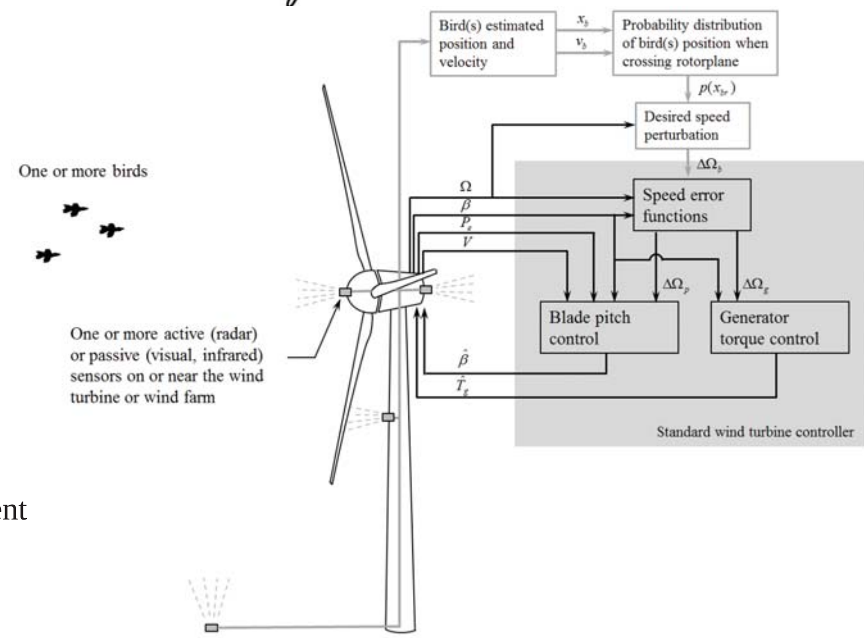

Challenges:

Detecting Birds Approaching the Rotor: Detection and tracking must be done with equipment that is cheap on a per-turbine basis. There are two strategies which could be feasible: installing inexpensive instrumentation on every turbine, or installing a small number of more expensive sensor systems to cover an entire wind farm.

Predicting flight path: The proposed concept requires that the flight path of a bird be characterized mathematically by a probability density function which can be integrated over time, to obtain the probability distribution of the location of the bird at some future time. The model of bird flight does not need to be highly sophisticated, since the computed estimates are continually updated by the tracking data. An initial case for study will be white-tailed eagles at Smøla, for which satellite tracking data has been collected. Radar tracking data of migrating species, in the vicinity of offshore wind farms, is also available, as are some observations on the behaviour of birds near wind turbine rotors.

Preventing bird strikes: The success of the idea hinges upon the ability to detect and predict the probability distribution of the flight paths of birds far enough ahead of time that a small correction to the rotational speed is sufficient to provide an effective reduction in the probability of collision.

Keeping dynamic loads low: The dynamic response of the turbine places constraints on the type of control actions that are feasible. Abrupt acceleration and deceleration of the rotor implies large fluctuating forces in the pitch actuators and turbine structures. Thus the earlier that the bird is detected, the fewer the number of false alerts, and the earlier that the control action is initiated, the more benign the consequences for fatigue of turbine components.

Elements of real-time optimal wind power plant control

Karl Merz (karl.merz@sintef.no) and John Olav Tande, SINTEF Energy Research
Adil Rasheed, SINTEF Digital

Aeroelastic model

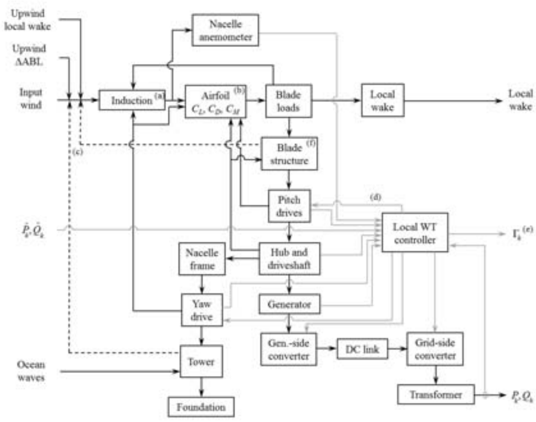

Modal reduction of the system

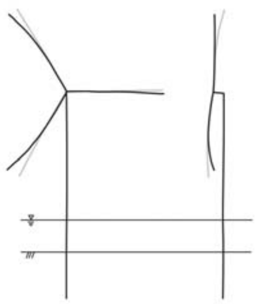

Engineering methods for turbulent wake flow

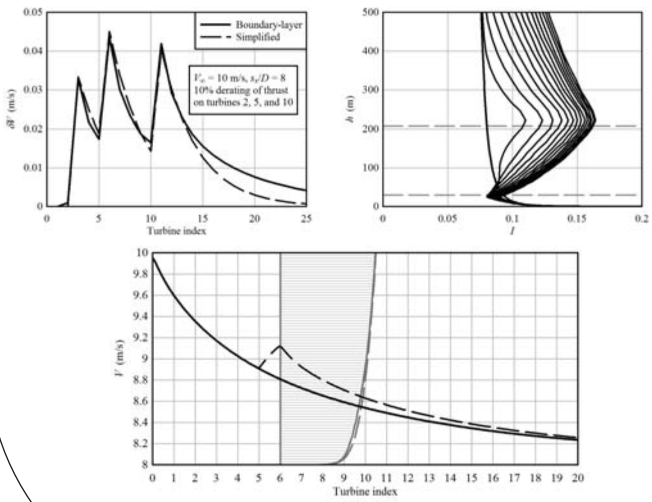

Full suite of control functions

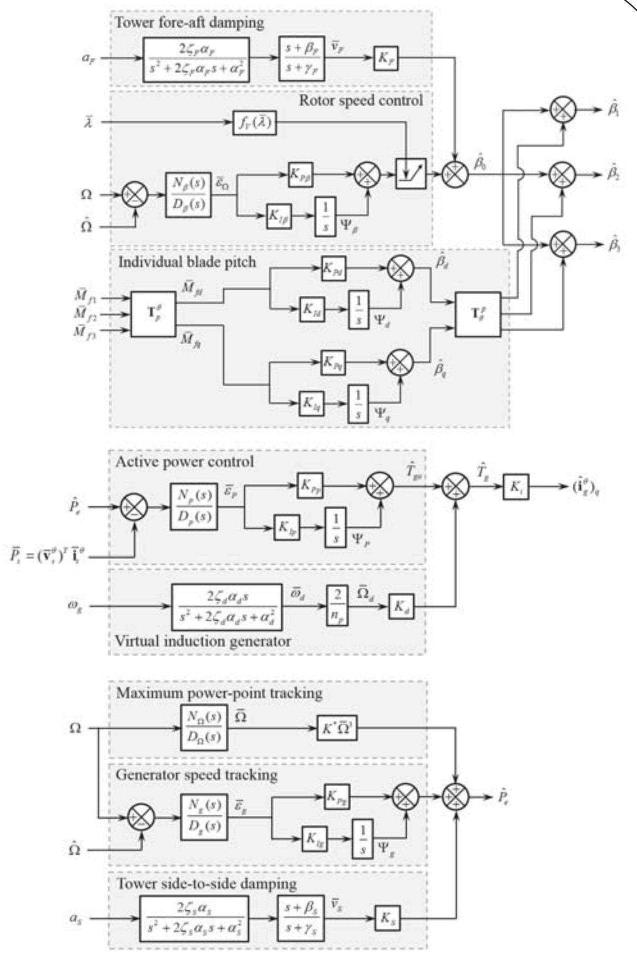

Electrical components and systems

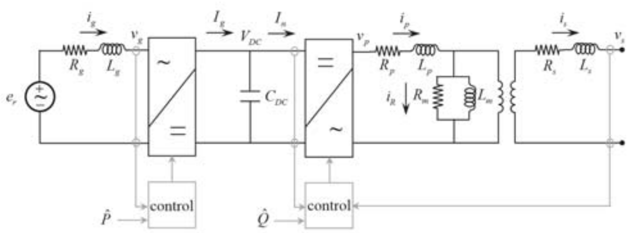

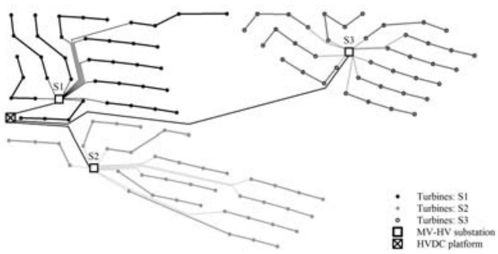

Unified state-space/observer model (STAS)

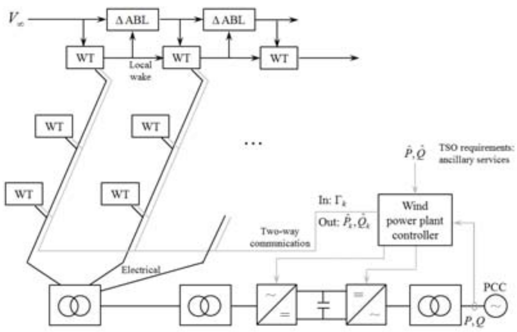

The OPWIND project (2017-2021)

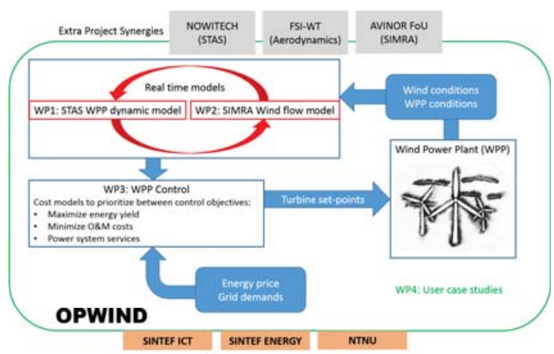

Inertia Response from HVDC connected Full Converter Wind Turbines

14th Deep Sea Offshore Wind R&D Conference, EERA DeepWind 2017

Jon Ødegård, Statnett, Power System Functionality - jon.odegard@statnett.no **Atle Rygg, NTNU, dept. of Engineering Cybernetics – atle.rygg@itk.ntnu.no**

Introduction

The state of art in wind turbine technology features a fully rated frequency converter, allowing the generator side to operate asynchronously from the grid. The Voltage Source Converters, VSC, utilizes extremely rapid switching of semiconductors in order to synthesize the sinusoidal voltage at any frequency. These provide great opportunities with regard to efficiency and flexibility in maximizing power and regulating voltage at the terminals. In addition, VSC-HVDC-links allow the wind parks to be placed offshore, out of sight and in stable wind conditions. A challenge with such installations however, is that the asynchronous operation decouples them from the residual grid, meaning that their equivalent inertia seen from the onshore grid is zero. Adding the fact that power system in general has an increasing amount of distributed power generation (smaller units), the system as a whole has a lower inertia, and is therefore more prone to frequency variations following loss of generation or loads.

System

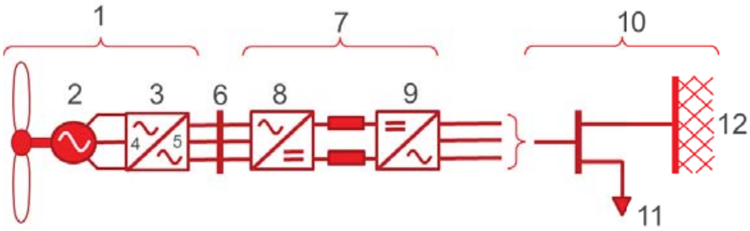

System configuration and notation:

1. Full Converter Wind Turbine (FCWT), 2. Wind Turbine Generator, 3. Turbine Frequency Converter, 4. Generator Drive Converter, 5. Wind Turbine Grid Converter, 6. Offshore Grid, 7. VSC-HVDC-link, 8. HVDC Offshore Grid Converter, 9. HVDC Onshore Grid Converter, 10. Power system, 11. Load , 12. Residual Grid

The wind turbines are assumed run at optimal power (no reserves) and the system has about 1/3 wind power.

Laboratory set up, National Smartgrids Laboratory at NTNU and SINTEF

Auxilliary control

Principles:

- Energy can be absorbed or supplied by change of rotor speed (kinetically stored)
- Wind turbines must return to its initial rotational speed
- The control should account for lack of primary control (reduced damping)
- Rotational speed drop limits must be kept
- HVDC-voltage limits must be kept

By modifying the reference values of relevant controls in the classical wind turbine converter and HVDC-converter, the frequency deviation of the power system is coupled with the rotational speed of the turbines by electrical qualities, allowing them to contribute with inertia response.

The control design should account for lack of primary control (which dampens the oscillations following a frequency response). This can be explained in two ways; 1. the power flow from the system changes direction when returning to nominal speed (inertial energy can only be lent). 2. The primary control of the residual system must act on a greater mass, its own and the wind turbines.

Control: DC-voltage control — Offshore frequency control — Speed control

Measure: Power system frequency — DC-voltage (HVDC) — Offshore grid frequency — Turbine speed

Notation: SDM—Scaled Deviation Mirroring (controller for frequency deviation to be mirrored onto turbine speed), WTS—Wind Turbine Stabilizer (controller for improved damping)

Results

Performance of system with auxiliary controllers. The system is imposed with a 0,0588 p.u. load step in all tests:

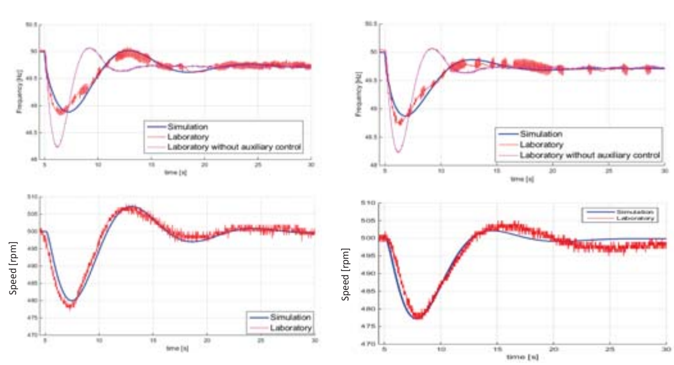

Auxiliary Turbine Controllers	Δf [Hz]	Δf-reduction [%]	$\Delta\omega_{WT}$ [rpm]	Overshoot [Hz]	Overshoot reduction [%]	Sustained Oscillations [s]
None	$1.7\ Hz$	-	-	$0.4\ Hz$	-	10 s
SDM	$1.1\ Hz$	35.3 %	$20\ rpm$	$0.35\ Hz$	12.5 %	20 s
SDM and WTS, $K_T = 0.66$	$1.2\ Hz$	29.4 %	$20\ rpm$	$0.15\ Hz$	62.5 %	15 s

Additional results:

By changing the relative contribution from the SDM and WTS control designs, the timing of the inertial contribution is altered, and consequently the frequency response, amplitude and damping.

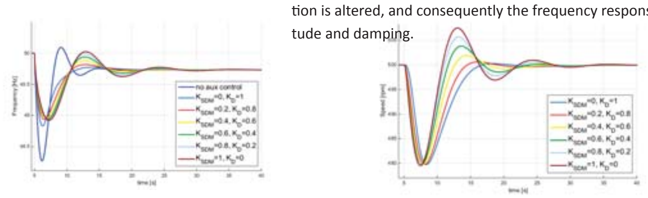

Speed-power characteristics of the wind turbine:

Results show a 4% reduction of speed for the wind turbines. Investigation of the aerodynamic performance of a wind turbine gave these results:

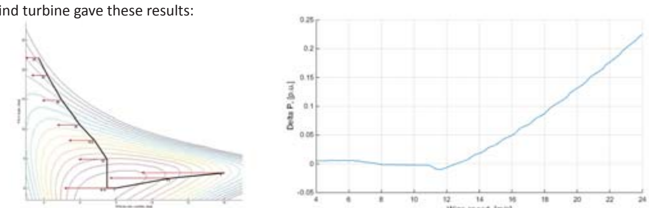

Conclusions

The following points have been demonstrated successfully in simulations and laboratory:

- Frequency response can be improved by inertia response from wind turbine control
- Net energy can not be extracted from a governorless power generated unit.
- Added mass in the system, without added primary response, increases oscillations.
- Asynchronous power generation can have its response phase shifted an arbitrary amount, giving possibilities for performance improvement with regard to damping.
- The power coefficient is not critically influenced by the response

The presented material is a selection of the results from the master thesis by Jon Ødegård from NTNU, 2015. The work does not represent Statnett SFs work or research on inertia response, even though it is now Jon Ødegårds current employer and is attending the conference as a representative of Statnett.

NTNU Statnett Fremtiden er elektrisk

Control of HVDC systems based on diode rectifier for offshore wind farm applications

Ida L. Flåten, Gilbert Bergna-Diaz, Santiago Sanchez, Elisabetta Tedeschi

Department of Electrical Power Engineering
Norwegian University of Science and Technology

Introduction

The integration of offshore wind energy into the power system, has led to progressive research in HVDC-converters where a possible solution is diode rectifier. The potential advantages with diode rectifier compared to conventional converters as Line Commutated Converter (LCC) and Voltage Source Converter (VSC) are:

- lower conduction losses
- reduced installation costs
- reduced converter size
- higher reliability

System model

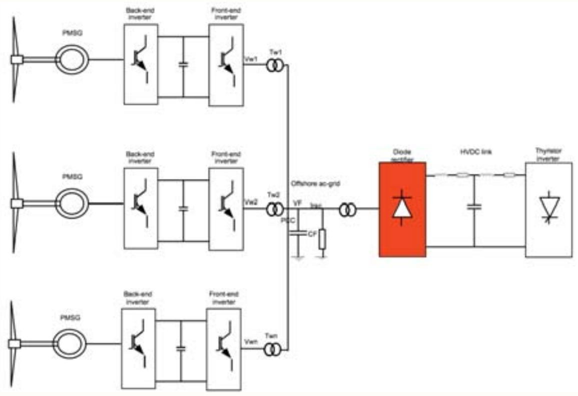

Figure 1: The system model studied

Objectives

- Examine the main adaptations of the control system with the system topology with diode rectifier
- Since the diode rectifier is uncontrolled, another part of the system will have to overtake the control of the ac-grid voltage and frequency, conventionally conducted by the HVDC converter
- The main field of reseach is the front end converters of the wind turbines, which can overtake the control of the ac-grid

Control system

Figure 1 can be described by equation 1-4 in a synchronous reference frame with $V_{Fq} = 0$, and makes the base for the control system. An extensive deduction of the control system based on these equations can be found in [1].

$$\frac{dI_{Fdi}}{dt} = -\frac{R_{Twi}}{L_{Twi}} I_{Fdi} + \omega_F I_{Fqi} + \frac{V_{Wdi}}{L_{Twi}} - \frac{V_{Fd}}{L_{Twi}} \tag{1}$$

$$\frac{dI_{Fqi}}{dt} = -\frac{R_{Twi}}{L_{Twi}} I_{Fqi} - \omega_F I_{Fdi} + \frac{V_{Wqi}}{L_{Twi}} \tag{2}$$

$$\frac{dV_{Fd}}{dt} = \frac{1}{C_F} \sum_{i=1}^{n} I_{Fdi} - \frac{1}{C_F} I_{Racd} \tag{3}$$

$$\omega_F V_{Fd} = \frac{1}{C_F} \sum_{i=1}^{n} I_{Fqi} - \frac{1}{C_F} I_{Racq} \tag{4}$$

Phase Locked Loop

- The Phase Locked Loop (PLL) extracts the voltage signal at the point of common coupling (PCC) to determine the phase angle and frequency of the ac-grid
- The system model has unidirectional power flow, and the traditional PLL can not achieve its function
- A fixed reference signal of the phase angle and frequency was proposed in [2]
- Another solution is to modify the traditional PLL with an integrated phase angle reference [3]. This PLL is shown in equation 5.

$$\frac{d\theta}{dt} = \omega^* + \Delta\omega = \omega^* + K_P(V_{Fq} - V_{Fq}^*) + K_I \int (V_{Fq} - V_{Fq}^*)dt \tag{5}$$

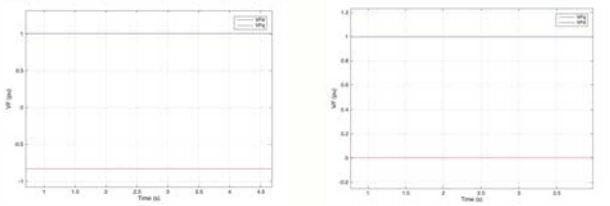

Figure 2: The voltage V_F, at PCC, using fixed reference signal and modified PLL respectively

Droop control

The droop control can be constructed from P/V and Q/f relations as seen from the system equations with output/input terminology. The latter can also be shifted to a f/Q droop where the output of this droop control then can be used as the input to the modified PLL.

Figure 3: Conventional solution: P/V and Q/f droop | Our solution: P/V and f/Q droop

With P/V and Q/f droop method the frequency, voltage and current control loop is following its reference, but with a large steady state error. In addition V_{Fq} is no longer zero.

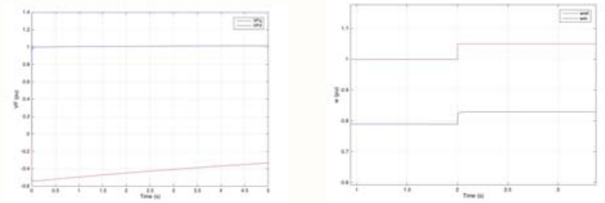

Figure 4: (a) V_F at PCC (b) frequency control, both with P/V and Q/f droop control

The P/V droop is maintained while the Q/f curve is shifted and the frequency is used as the integrated phase angle in the PLL. With this method $V_{Fq} = 0$

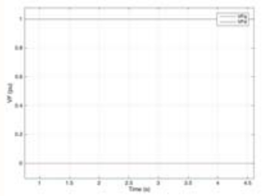

Figure 5: The voltage, V_F, at PCC in the distributed model with P/V and f/Q droop control

Summary and conclusions

- The PLL was found as a crucial part of the control strategy since the control method was based upon the assumption that $V_{Fq} = 0$
- The conventional PLL could not serve its function together with diode rectifier as HVDC converter
- Fixed reference signal of frequency was attempted applied, but V_{Fq} was not zero
- PLL with integrated phase angle reference was chosen for further simulations
- Droop control relating ω^* to the modified PLL was successfully implemented
- Reactive power sharing among the turbines was achieved
- Active power control was implemented in a master-slave technique
- Further work will include improving the active power control to also obtain active power sharing among the turbines

References

[1] R. Blasco-Gimenez et al., "Distributed voltage and frequency control of offshore wind farms connected with a diode based HVDC link", Nov. 2010

[2] H.Eckel et al., "FixRef: A control strategy for offshore wind farms with different wind turbine types and diode rectifier HVDC transmission", June 2016

[3] S. Sanchez "Stability Investigation of Power Electronic Systems", March 2015

Offshore Wind Power Plants with 66 kV Collection Grids
Study of Resonance Frequencies

Andrzej Hołdyk, SINTEF Energy Research, andrzej.holdyk@sintef.no,
Łukasz Hubert Kocewiak, DONG Energy Wind Power A/S, LUKKO@dongenergy.dk

Introduction

Nowadays, large offshore wind power plants (OWPPs) are characterized by a complex electrical infrastructure comprising of a number of wind turbines with step-up transformers, offshore transformers and large offshore array collection cable grid which is typically connected to the grid via HVAC transmission cable. Such a system creates challenges in analysis and design covering harmonic propagation and transient studies. Standard voltage level of collection grids of large OWPPs is approximately 33 kV. Doubling it might provide technical or economic benefits; therefore, it is foreseen that a part of the large offshore wind power plants in the future will be at 66 kV level. This change might influence harmonic and transient behaviour of an OWPPs as compared to those known today. It is therefore important to analyse how the increase of the collection grid voltage level changes characteristic of the electrical environment of a wind power plant in a wide range of frequencies.

Procedure

In this study, a comparison is made between elements of frequency- - dependent, wide-band admittance matrix of an OWPPs with 66 kV collection grid and one with corresponding power and at 33 kV collection grid:

- Wide-band models (20 Hz – 1 MHz) are developed in Matlab and represented as admittance matrix using state-of-the-art component models
- Cables (33 kV and 66 kV) represented based on design information using traveling-wave model with frequency dependency of all parameters
- Transformers (33 kV): black box model based on sweep frequency response measurements of real turbine and park transformers; accuracy at lower frequencies improved by incorporation of 50 Hz manufacturer's information
- Transformers (66 kV): models based on data manipulation of 33 kV models
  - Adjusted voltage ratio (positive sequence)
  - Adjusted winding resonance frequencies

Wind farm structure and main assumptions (33 kV and 66 kV models)

Transformers: wind park: 90 MVA, wind turbines: 6.8 MVA
Number of turbines per string: 8
Cables: three-core submarine cables with armour

- Same cable cross-section in whole string:
  - 66 kV: 95 mm2
  - 33 kV: 500 mm2
- Length per section: 1000 m

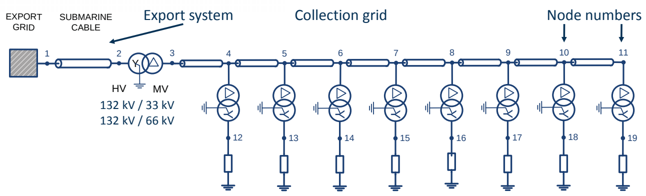

Results

Driving point admittance at selected nodes of the collection grid

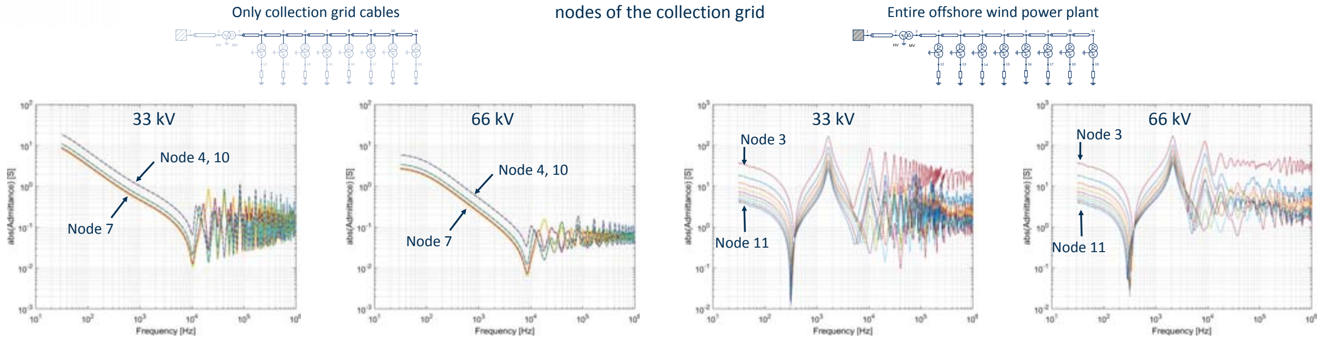

Change of voltage level in transformers

Approximation of winding resonance frequency: $f(\mathrm{kHz}) = C_1 \cdot \frac{MVA^{C_2}}{kV^{C_3}}$

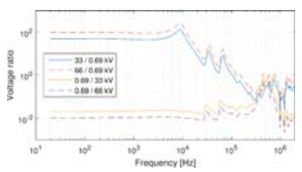

Positive sequence voltage ratios of 6.8 MVA transformer. 66/0.69 kV and 33/0.69 kV

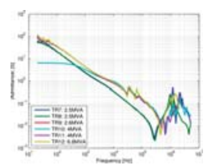

Wide-band characteristic of LV winding on wind-turbine and distribution transformers (measured)

Change of voltage level in cables

$$C = \frac{2\pi\epsilon}{\ln \frac{OuterDiam_{insul}}{InnerDiam_{insul}}}$$

Quarter wave resonance frequency:

$$f = \frac{1}{4l\sqrt{LC}}$$

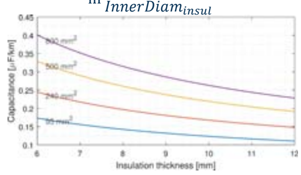

Cable capacitance for different conductor cross-sections and insulation thickness (33kV: 8mm, 66kV: 9mm)

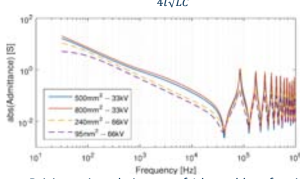

Driving point admittance of 1 km cables of various conductor cross-sections and voltage levels

Conclusions

- Keeping the same power in a radial but increasing the voltage level causes the use of cables with different conductor cross-sections, what changes capacitance, inductance and damping of cables. This influences both harmonic and transient behaviour of a wind farm.
- Depending on construction, increasing voltage level might shift resonance frequency of transformer winding to lower values.
- Changing voltage level influences cable capacitance and therefore, its resonance frequency.

Grid Integration of offshore wind farms using a Hybrid HVDC composed by an MMC with an LCC-based HVDC system

Raymundo Enrique Torres-Olguin* & Alejandro Garces+

SINTEF Energy Research* & Universidad Tecnológica de Pereira+

SINTEF

Universidad Tecnológica de Pereira

Objective

This paper presents a hybrid HVDC-transmission system composed by a Full-Bridge Modular Multilevel Converter (FB-MMC) and a Line-commutated Converter (LCC) to integrate offshore wind farms into the main grid. The operational characteristics of a three-terminal hybrid-HVDC system, two LCC stations and one MMC station, is investigated using PSCAD/EMTDC.

Introduction

In recent literature, the feasibility of grid integration of offshore wind farms using hybrid HVDC systems composed by voltage source converters (VSC) and line-commutated converters (LCC), have been investigated. Such a hybrid HVDC systems are attractive mainly because their low power losses compared to a VSC-based HVDC systems. However, hybrid HVDC systems have serious limitations when an ac fault occurs at the LCC inverter.

System description

The proposed configuration is shown in Fig. 1. It consists of two ac grids (AC1 and AC2) interconnected by a bipolar HVDC system with 12-pulse line-commutated converters. This HVDC transmission line is interconnected to an FB-MMC by means of a T-connection. This FB-MMC integrates offshore resources along the transmission line.

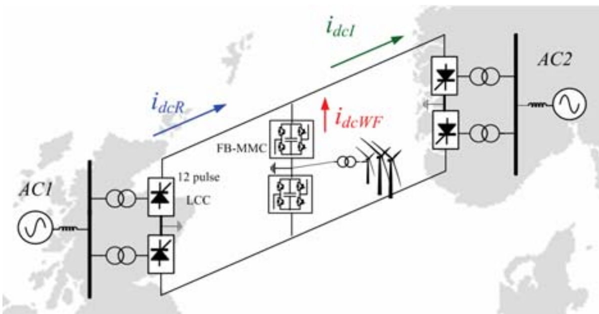

Figure: Proposed Hybrid HVDC for integration of OWF.

Proposed control design

The design of the controllers is divided into four sections: the LCC rectifier, the LCC inverter, the MMC, and the offshore wind farm.

- The LCC rectifier regulates the power extracted from one grid to another. In normal operation, the LCC rectifier operates in a constant DC current mode.
- The LCC inverter control objective is to regulate the DC link voltage.
- As power control is performed by the wind turbines, the main responsibility of the MMC is to establish the offshore ac voltage.
- Generally, a commutation failure (CF) occurs in LCC inverters when there is a significant voltage drop on the ac side. FB-MMC topologies can clear dc fault currents since they are build using full-bridge sub-modules which are able of suppressing the fault current against dc faults as shown as follows.

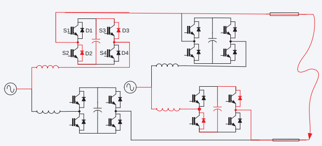

Figure: Full bridge MMC DC fault response

Simulation Results

The simulations were conducted under different conditions to investigate the operating characteristics of the proposed system. These conditions include start-up procedure, and ac and dc faults.

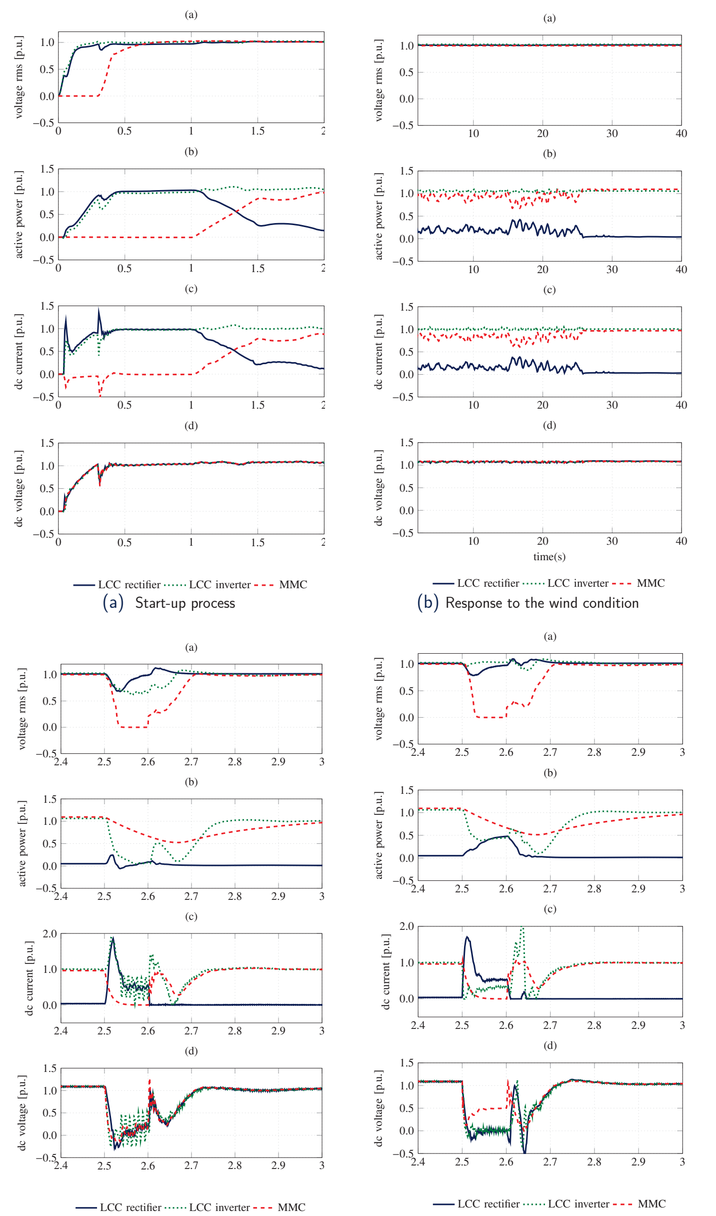

(a) Start-up process

(b) Response to the wind condition

(c) Response to ac fault (inverter side)

(d) Response to dc fault

Figure: [Top to bottom] (a) ac voltages (rms), (b) dc currents, (c) active powers, (d) dc voltages

Conclusions

AC fault is a very serious condition in a hybrid configuration because the commutation failure in line-commutated converters is translated into a dc fault in the voltage source converters. Full bridge MMC can provide a solution to this problem since they provide an available current path through the series connected capacitors of each MMC sub-modules.

Contact email: raymundo.torres-olguin@sintef.no

Review of Investment Model Cost Parameters for VSC HVDC Transmission Infrastructure

Til Kristian Vrana, Philipp Härtel,

Tobias Hennig, Michael von Bonin, Edwin Jan Wiggelinkhuizen, Frans D.J. Nieuwenhout

The Linear Cost Model

$$C^k_{\mathrm{est},i} = \sum_f^{F_i} B^k_f(l_f, p_f) + \sum_g^{G_i} N^k_g(p_g) + \sum_h^{H_i} S^k_h(p_h) \quad (1)$$

$$B^k_f(l_f, p_f) = B^k_{lp} \cdot l_f \cdot p_f + B^k_l \cdot l_f + B^k_0 \quad (2)$$

$$N^k_g(p_g) = N^k_p \cdot p_g + N^k_0 \quad (3)$$

$$S^k_h(p_h) = S^k_p \cdot p_h + S^k_0 \quad (4)$$

$$l_f = l_{\mathrm{SMC},f} + \frac{5}{4} l_{\mathrm{UGC},f} + \frac{2}{3} l_{\mathrm{OHL},f} \quad (5)$$

The Collected Cost Parameter Sets

- RealiseGrid
- Windspeed
- ENTSO-E's technology cost report
- Ergun et al. (KU Leuven)
- ETYS13 (the Electricity Ten Year Statement)
- North Sea Transnational Grid
- North Sea Offshore Grid
- Imperial College
- North Sea Grid
- OffshoreDC
- Madariaga et al. (ORE Catapult)
- ETYS15
- Torbaghan (TU Delft)

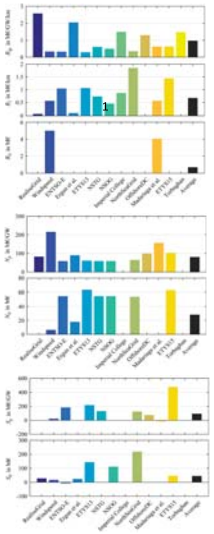

Parameter	Value	Unit
B^{avg}_{lp}	0.97	M€/GW·km
B^{avg}_{l}	0.68	M€/km
B^{avg}_{0}	0.70	M€
N^{avg}_{p}	80.88	M€/GW
N^{avg}_{0}	28.38	M€
S^{avg}_{p}	93.45	M€/GW
S^{avg}_{0}	44.81	M€

The Collected Reference Projects

Back-to-Back

Project name	Rated power MW	Contracted cost ($C^{\mathrm{ref}}_{\mathrm{con},i}$) Converters M€*	Source
TresAmigas	750	150.0	[36]
Mackinac	350	68.0	[37]
KriegersFlak	500	125.7	[38]

Interconnector

Project name	Rated power MW	Line length: SMC+ km	UGC+ km	OHL+ km	Contracted cost ($C^{\mathrm{ref}}_{\mathrm{con},i}$): Line M€*	Converters M€*	Total M€*	Source(s)
EstLink1	350	74	31	-	84.8		84.8	[19]
EWIC	500	186	76	-	291.1	130.6	421.7	[20], [21]
NordBalt	700	400	13	40	268.7	169.9	438.6	[22], [23]
Åland	100	158	-	-	99.1		99.1	[24]
Skagerrak4	700	138	92	12	127.0	131.9	258.9	[25], [26], [27]
NordLink	1,400	516	54	53	936.5[a]	395.9[a]	1,332.3	[28], [29]
NorthSeaLink	1,400	720	7	-	890.0	408.9	1,298.9	[30], [31], [32]
COBRA	700	299	26	-	250.0	170.0	420.0	[33], [34]

Offshore Wind Connections

Project name	Rated power MW	Line length: SMC+ km	UGC+ km	OHL+ km	Contracted cost ($C^{\mathrm{ref}}_{\mathrm{con},i}$): Line M€*	Converters M€*	Platform M€*	Total M€*	Source(s)
BorWin1	400	125	75	-	422.8[a]			422.8	[39]
BorWin2	800	125	75	-	300.0	445.3[a]		745.3	[40], [41]
HelWin1	576	85	45	-	150.0	595.3[a]		745.3	[41], [42]
DolWin1	800	75	90	-	682.4[a]			682.4	[43], [44]
SylWin1	864	160	45	-	250.0	495.3[a]		745.3	[45], [46], [47]
DolWin2	916	45	92	-	479.6		353.0[a]	832.6	[48], [49]
HelWin2	690	85	45	-	200.0	645.3[ab]		845.3	[50], [51]
DolWin3	900	83	79	-	350.0	800.0		1,150.0	[52], [53], [54]
BorWin3	900	132	29	-	250.0	1000.0		1,250.0	[55], [56], [57]

Estimation of Overhead-Cost

$$C^{\mathrm{ref}}_{\mathrm{inv},i} = \frac{11}{10} C^{\mathrm{ref}}_{\mathrm{con},i} \qquad \forall i \in I_{\mathrm{B2B}}$$

$$C^{\mathrm{ref}}_{\mathrm{inv},i} = \frac{5}{4} C^{\mathrm{ref}}_{\mathrm{con},i} \qquad \forall i \in I_{\mathrm{IC}}$$

$$C^{\mathrm{ref}}_{\mathrm{inv},i} = \frac{5}{4} C^{\mathrm{ref}}_{\mathrm{con},i} \qquad \forall i \in I_{\mathrm{OWC}}$$

Cost Parameter Set Evaluation

Project- and Category-Deviation

$$D^k_i = \log_2\left(\frac{C^k_{\mathrm{est},i}}{C^{\mathrm{ref}}_{\mathrm{inv},i}}\right) \qquad D^k_j = \frac{1}{|I_j|}\sum_i^{I_j} D^k_i$$

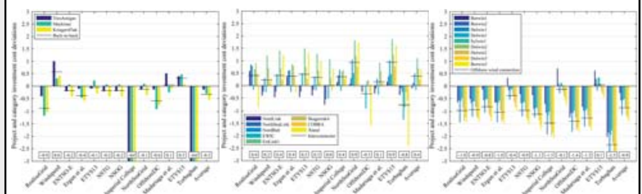

Category- and Overall-Error

$$E^k_j = \sqrt{\frac{1}{|I_j|}\sum_i^{I_j}\left(D^k_i\right)^2} \qquad E^k = \sqrt{\frac{1}{|J|}\sum_j^{J}\left(E^k_j\right)^2}$$

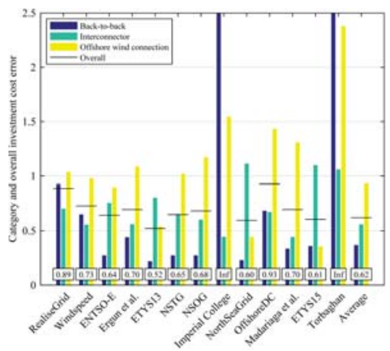

Conclusion

- High level of uncertainty (large differences between project cost data and between cost parameter sets)
- Few reference projects, many influencing factors (market situation/power, fast progress, steel/copper price, risk perception, type of client, weather dependence, location aspects,...)
- Large differences between cost estimates (different purposes, different foci, different assuptions, level of simplification,..)

Future Work

- Better cost estimates are needed for grid planning studies
- This review laid a solid basis
- All the collected information will be used to generate an improved cost parameter set

Centre for renewable Energy Systems Technology, CREST

Sarah Ollier, Simon Watson
s.ollier@lboro.ac.uk

Loughborough University

Wind Phenomena: Impacts on Power Output

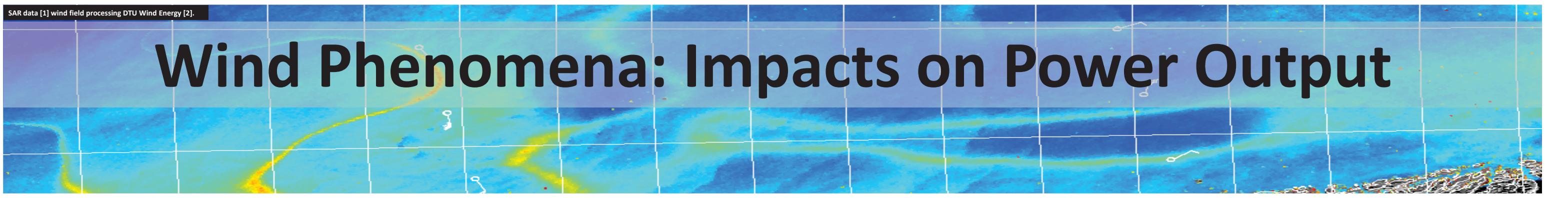

1… Introduction

We investigate the impact of meteorological phenomena on wind energy using:

- Synthetic Aperture Radar (SAR) examples of phenomena Greater Gabbard wind farm, UK (fig. 1-3)(sections 1.1 – 1.4).
- Estimation of power output estimation for an individual turbine and across a wind farm during these events.

1.1. Roll Vortices (RV):

Counter-rotating turbulent rolls which form and persist. In [4] RV led to periodic turbine loading and power output variations in onshore wind farms, frequent RV are expected in stable offshore wind farm regions (fig. 1).

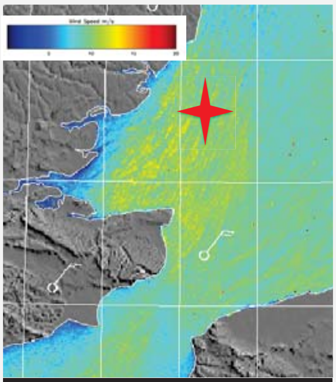

Fig.1. Roll Vortices over Greater Gabbard. SAR data [1] wind field processing DTU Wind Energy [2]. Red cross - approx. location of Greater Gabbard wind farm.

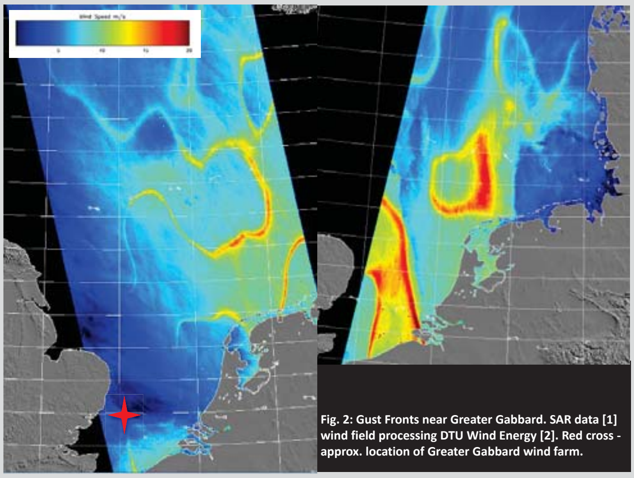

Fig. 2: Gust Fronts near Greater Gabbard. SAR data [1] wind field processing DTU Wind Energy [2]. Red cross - approx. location of Greater Gabbard wind farm.

1.2 Mesoscale gust fronts:

localised high speed wind gusts and precipitation. In [6] gust associated increases in ocean wave height impacted turbine structures, whilst intermittent wind speeds reduced energy capture efficiency (Fig.2).

1.3 Atmospheric Gravity Waves (AGW)

Topographic obstacles displace coast-sea flow and waves persist in stable conditions. In [5] 0.6 ms^{-1} decreases in wind speed were associated with AGW across a theoretical wind farm; small AGW were created by turbines unlike the larger scale AGW in fig. 3.

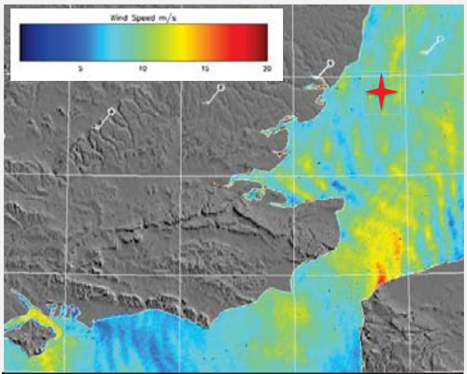

Fig. 3: Atmospheric Gravity Waves over Greater Gabbard. SAR data [1] wind field processing DTU Wind Energy [2]. Red cross - approx. location of Greater Gabbard wind farm.

2. Gust front event, estimated single turbine diurnal power output

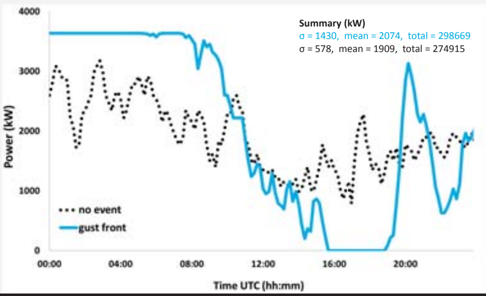

Fig. 4: Estimated power output for a single turbine at Greater Gabbard during the gust front event (fig. 2.)(blue line) compared with a day with no event (dotted line) at the same locatioh. Wind speed data inputs obtained from the Marine Data Exchange [9].

Estimated power output was calculated for a single Siemens 3.6 turbine at Greater Gabbard using meteorological mast data [9].

During the gust event power output is more variable and total power output higher than for a non-event day with a similar average wind speed (fig. 4).

3. Gravity Wave event, estimated spatial variation in power output across a theoretical wind farm

Fig. (5a) shows spatial power variation across a theoretical windfarm based on Greater Gabbard during the AGW event (fig. 3.).

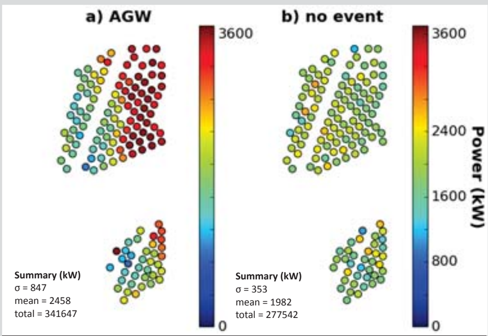

Fig. 5: Power output over theoretical wind farm, each dot represents a turbine and the colour coding represents the power output from an individual turbine. SAR data [1] wind field processing DTU Wind Energy [2].

The theoretical farm uses Greater Gabbard layout in a location clear of turbines to avoid errors in wind speed estimation from SAR introduced by scattering from the turbines.

There is considerably higher spatial variation in power output and a higher total power output for the farm compared with a non-event day with a similar average wind speed (b).

4… Future directions

- SAR and mesoscale model (WRF) based climatology of phenomena around wind farms.
- Analysis of turbine condition monitoring data (SCADA) during events.
- 3D modelling of phenomena-turbine interaction to assess fatigue loading.

[1] ESA, "What is Sentinel-1," 2016. [Online]. Available: https://earth.esa.int/web/guest/missions/esa-operational-eo-missions/sentinel-1.
[2] DTU-WE, "ENVISAT surface wind field processing." Danish Technical University (DTU) Department of Wind Energy, 2016.
[3] W. Gutierrez, *et al.,* "Structural impact assessment of low level jets over wind turbines,", 2016.
[4] A. Smedman, "Occurrence of roll circulations in a shallow boundary layer," *Boundary-Layer Meteorol.*, vol. 57, no. 4, pp. 343–358, 1991.
[5] R. B. Smith, "Gravity wave effects on wind farm efficiency," *Wind Energy*, vol. 13, no. 5, pp. 449–458, 2010.
[6] S. Brusch, *et al.,* "Synergetic Use of Radar and Optical Satellite Images to Support Severe Storm Prediction for Offshore Wind Farming," 2008.
[7] K.-F. Dagestad, *et al.,* "Wind retrieval from synthetic aperture radar -an overview,", 2013. [8] ESA, "What is Envisat?," European Space Agency, 2016
[9] Marine Data Exchange, Greater Gabbard Offshore Windfarm Ltd, Meteorological Mast Data (IGMMZ) http://www.marinedataexchange.co.uk/

CATAPULT Offshore Renewable Energy
NERC SCIENCE OF THE ENVIRONMENT

Availability of the OBLO infrastructure for wind energy research in Norway

Martin Flügge[1,3], Joachim Reuder[2,3], Mostafa Bakhoday Paskyabi[2,3], Benny Svardal[1,3]
[1] Christian Michelsen Research AS, Bergen, Norway
[2] University of Bergen, Bergen, Norway
[3] Norwegian Centre for Offshore Wind Energy (NORCOWE)

Christian Michelsen Research

norcowe Norwegian Centre for Offshore Wind Energy

Background

The Offshore Boundary-Layer Observatory (OBLO) infrastructure is part of the Research Council of Norway founded NOWERI (Norwegian Offshore Wind Energy Research) project, which is intended to provide and operate state-of-the-art instrumentation and measurement capabilities for a wide range of atmospheric and oceanographic parameters relevant for offshore wind energy applications. The objective of the OBLO project is to increase the knowledge and understanding of the physical processes relevant for offshore wind energy, such as wind turbine wakes and their interactions with the boundary-layer, atmospheric stability, vertical wind profile relationships and turbulence parameter estimations. The infrastructure is available for public and private research institutions dealing with wind energy in Norway. Between May 2015 – September 2016, instruments of the OBLO infrastructure were deployed at the German wind energy research platform FINO1 during the Norwegian Centre for Offshore Wind Energy (NORCOWE) Offshore Boundary-Layer Experiment (OBLEX-F1). Usage of the OBLO instrumentation allowed NORCOWE scientists to collect a unique data set including both atmospheric and oceanographic measurements. This poster presents some of the OBLO infrastructure and its application at FINO1 during the OBLEX-F1 field campaign.

Meteorological OBLO instrumentation deployed at the German research platform FINO1 in the North Sea.

Radial wind speed measurements

The OBLO portfolio includes two WindCubes100s systems. One additional WindCube100s system is available through Christian Michelsen Research AS. The LiDAR's have a scan range of up to 3000 m and a longitudinal resolution of 25 m. The WindCube100s is able to record the radial wind speed over the azimuth range [0° 360°] and elevation range [-10° 190°]. During the OBLEX-F1 campaign, the two LiDAR systems performed both stand alone and combined scans in order to investigate wind turbine wake effects, wake turbulence and wake extensions.

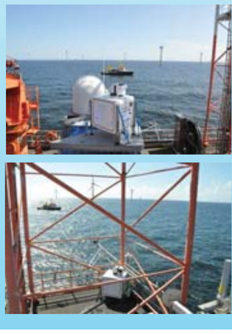

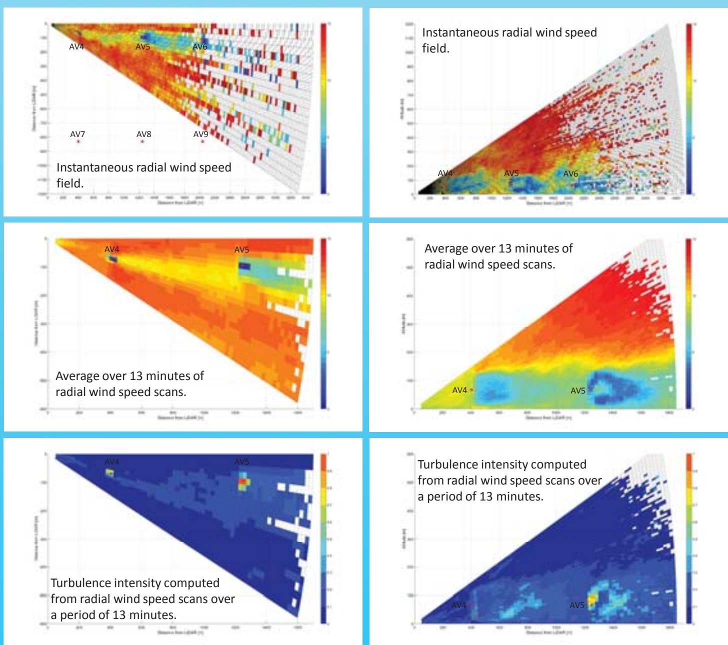

Example of Plan Position Indicator (left column) and Range Height Indicator (right column) scan scenarios directed towards the AV 4 and AV5 wind turbines (denoted by the red dots).

Passive microwave measurements

Two RPG HATPRO-R4 passive microwave radiometers are available through the OBLO project. A passive microwave radiometer measures atmospheric radiation in the K-band and V-band and transforms this information into vertical profiles of temperature and humidity. The accuracy of the temperature measurements with this instrument is comparable to measurements from meteorological masts. Measurements of the absolute humidity are reasonable comparable to mast measurements. Combining the data from the radiometer and the LiDAR systems provides information on the atmospheric stability and boundary-layer height. During the OBLEX-F1 campaign, it was the first time that such an instrument was deployed in the vicinity of an offshore wind farm.

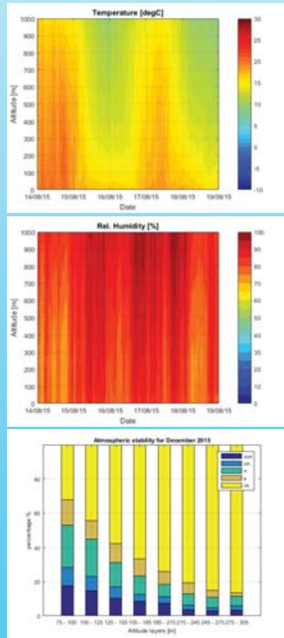

Example of Hovmøller diagrams for temperature (upper panel) and relative humidity (middle panel), and computed atmospheric stability (lower panel).

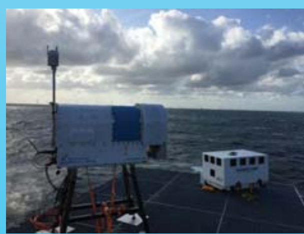

Passive microwave radiometer deployed at FINO1, next to a WindCube V1.

Oceanographic equipment

The OBLO project also offers access to oceanographic equipment which provides information on the current profile and surface wave field. Such measurements are highly required to quantify the impact of the wave field on the vertical wind profile, and can also contribute to estimate sediment transport around wind turbine foundations. The portfolio for the oceanographic equipment includes one Fugro Oceanor Wavescan buoy, two (sea) bottom frames, two Acoustic Doppler Velocimeters (ADV) and two advanced 5-beam Acoustic Doppler Current Profilers (AD2CP). Additionally, a submergible buoy at which oceanographic instruments can be mounted is available through the University of Bergen.

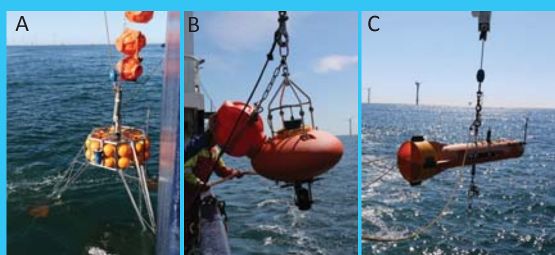

Oceanographic equipment deployed during OBLEX-F1 to collect data on the wave field and current profile for air-sea interaction studies. A) bottom frame, B) submergible buoy equipped with AD2CP and C) submergible buoy equipped with ADV and shear-probes.

Infrastructure access

As national infrastructure, the OBLO instrumentation is in general available for public and private research institutions dealing with wind energy in Norway. Applications for the use of the instrumentation will be prioritized after the following criteria:

- NORCOWE/NOWITECH partners (fully open projects)
- NORCOWE/NOWITECH partners (closed/partly closed projects)
- Others with data sharing agreements
- Others without data sharing agreements

It is expected that the pricing for the various user groups also will be reflected by this prioritization.

A complete list of available OBLO instrumentation can be found at http://oblo.uib.no .

The OBLO project also offers services for planning and execution of field deployments and post-analysis of the gathered data through the University of Bergen and Christian Michelsen Research AS. For more information and access to the infrastructure, please contact Joachim.Reuder@uib.no, University of Bergen or Martin.Flugge@cmr.no , Christian Michelsen Research AS.

Demonstrating the improved performance of an Ocean-Met model using bi-directional coupling

Adil Rasheed[1], J.K. Süld[2], M.V. Tabib[1], J, Kristiansen[2], T. Kvamsdal[3]
[1]Mathematics and Cybernetics, SINTEF Digital, Strindveien 4, 7035, Trondheim, Norway.
[2]Norwegian Meteorological Institute, [3]Department of Mathematical Sciences, NTNU

INTRODUCTION

The mass, momentum and energy fluxes between the atmosphere and ocean surface depend on the state of the ocean surface. The fluxes in turn can significantly alter the nature of the marine boundary layer and the state of the ocean surface. These interactions can be modelled deterministically using a multiphase modelling approach or using a semi-stochastic approach. While the multiphase approach can give better insights (e.g. wave generation), it is computationally too expensive and not suited for modelling ocean waves which are inherently random in nature. It is for this reason that in a forecasting context, semi-stochastic approach is still the workhorse. Furthermore, even in a semi-stochastic approach ocean and atmospheric models can be coupled in either unidirectional way (ocean affecting the atmosphere) or bidirectional way (both ocean and atmosphere affecting each other). Current work compares the performance of these two coupling approaches and validates them using Significant wave heights and 10m wind magnitude.

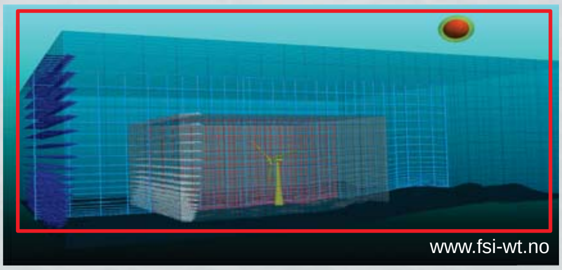

COUPLING

The surface fluxes (momentum and heat) over an ocean surface depend on the state of the surface. For example, young ocean waves typically have a larger roughness than older waves. To get a realistic representation of the ocean, the ocean wave model WAM is coupled with the atmospheric model AROME.

In AROME, the surface fluxes depends on the surface roughness length, Z0, which depends on the friction velocity, u*, acceleration of gravity, g, and the Charnock parameter α

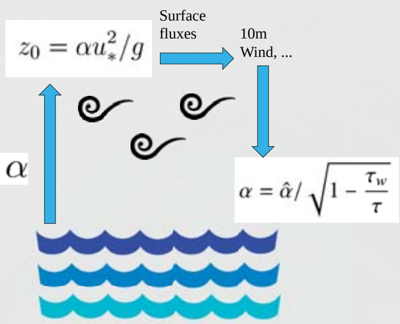

The Charnock parameter is a constant when running without a wave model. In WAM, the Charnock parameter depends on ratio between wave induced stress and total stress.

AROME

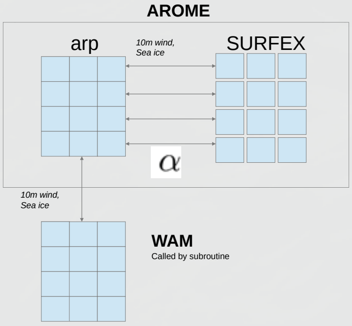

AROME and WAM runs on same grid with the same time step. WAM is called from subroutine each 60s time step. The model resolutions are 2.5 km^2. AROME uses SURFEX for calculations in the surface layer. AROME provides 10m wind and sea ice in each time step. The Charnock parameter is calculated in WAM and is used for calculations in the next time step.

RESULTS

Validation below - Comparison of wind speed (U) and wave height (Hs) as predicted by Uni and Bi coupled approaches over a month with observations measured on Sleipner platform.

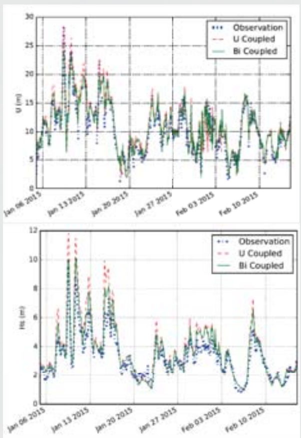

Snapshots below - Comparison of wind speed (U) and wave height (Hs) as predicted by Uni and Bi coupled at a given time.

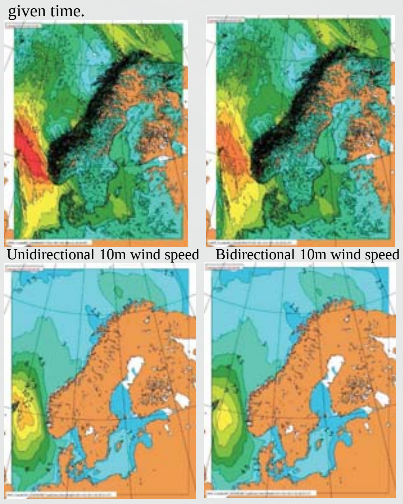

Unidirectional 10m wind speed | Bidirectional 10m wind speed

Unidirectional significant wave height | Bidirectional significant wave height

QQ plots below.

Below - **Left side figure** of the 10m wind speed recorded vs modelled comparison for coastal stations and offshore stations. For coastal stations performance of the Uni-directional coupled model is better than the Bi-directional coupled model. **Right side figure** - QQ plot of wind speed comparing Unidirectional and Bidirectional coupled methods. The Bidirectional coupled system shows a reduced bias and error of the 10m wind speed. The overestimation of Unidirectional coupled wind speeds over ocean is consistent with results from verification against scatterometer measurements.

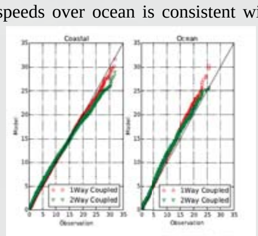

FIGURE 3. QQ PLOT FOR COASTAL AND OFFSHORE STATIONS

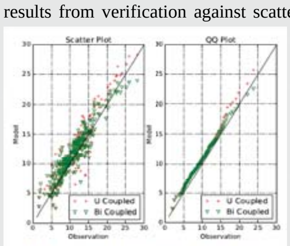

FIGURE SCATTER AND QQ PLOTS FOR WIND SPEED

CONCLUSIONS

Atmospheric code HARMONIE was uni and bi-directionally coupled to the stochastic wave model WAM. Significant wave heights and 10m wind magnitude were used for a quantitative validation. Based on the validation results, it can be concluded that bidirectional coupling, as expected is more accurate than the unidirectional coupled approach specially when the wind and significant heights have bigger values. Uni-directionally coupled model tends to over estimate both wind as well as wave height. Further, the bidirectional approach might not be valuable for coastal regions due to the inherent limitations and coarse resolution of wave model.

PLANNED WORK

A continuation of this work will be to validate the vertical profiles of wind and temperature profile using radiosonde data. These profiles can then be used for MBL characterization. The characterized profiles of wind, temperature and turbulence can then be used to simulate flow in an offshore wind farm.

The authors acknowledge the financial support from the Norwegian Research Council and the industrial partners of the FSI-WT-project (216465/E20) and the EU project MyWave | Contact: jakobks@met.no

SINTEF | NTNU Norwegian University of Science and Technology | FFI Forsvarets forskningsinstitutt | Meteorologisk institutt | TrønderEnergi | windsim | Statoil | KJELLER | Forskningsrådet

A comparison of short-term weather forecast with the measured conditions at the Hywind Demo site

Marit Stokke, Lars Sætran*
Norwegian University of Science and Technology
Department of Energy and Process Engineering
*lars.satran@ntnu.no

Abstract

Operations at the floating wind turbine Hywind Demo site have been challenging due to weather forcast that fails, especially for strength and direction of the ocean current. This work is comparing short-term weather forecast with measured data from a Seawatch buoy. It is found a low correlation for currents. For wind and waves the correlations are relatively good. It is shown that one year of weather forecast data give a reasonable estimate of which loads an object will experience at the site. Exceptions are that stronger surface currents will most likely occur and lower waves are to be expected.

Forecast methods

The weather forecast are provided by the Norwegian Meteorological Institute (MET Norway). The predicted data are result of short-term forecast models that have been run once a day for currents, and twice a day for wind and waves. All the models predict the weather +1, +2, +3 etc. hours ahead.

- *The atmospheric model* is called UM1 and covers the Hywind area on a 1 km scale.
- *The wave model* Simulating Waves Nearshore (SWAN) is used at this site. The model has a mesh size of 500 m x 500 m.
- *The ocean model* MET Norway used was a version of The Princeton Ocean Model (POM), called MI-POM, having a mesh size of 1.5 km.

The Seawatch buoy

In 2009, the Seawatch buoy was installed 200 m west of Hywind Demo, positioned southwest of Karmøy. The following metocean parameters are measured by the sensors printed in italics.

- Wind speed, direction and gust at 3.5 m above the sea level. *Yound, 85106-19 Ultrasonic*
- Wave height, period and direction relative to mean sea level. *Seatex, MRU-4*
- Current speed and direction, from 3 to 180 m depth. *RDI, ADCP 150 kHz - Sentinel*

Offshore operation

To perform an operation at the Hywind Demo site, a significant wave height of 1.5 m is the upper, permissible limit. A common practise is an upper limit of wind speed at 12 m/s. For comparison has current speed below 0.7 m/s been plotted.

Result

Parameter	r_{+3}	r_{+24}
Wind speed 10 m	0.88	0.82
Significant wave height	0.94	0.92
Current speed 10 m	0.34	0.34

Table 1: ***The correlation coefficients between the weather forecast +3/+24 and the measured values.***

Wind

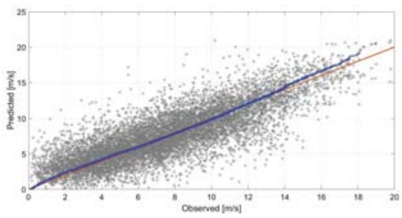

Figure 1 : ***A comparison of wind speed data at 10 m height, forecast +24 (UM1). Grey dots - scatter plot, blue dots - q-q plot and red line - observation equal to forecast.***

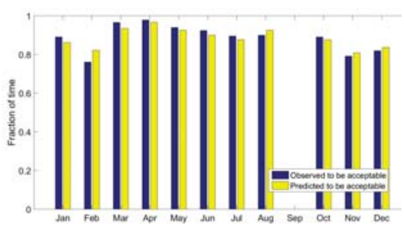

Figure 2 : ***The fraction of time the wind speed at 10 m height is less than 12 m/s, forecast +24 (UM1).***

Wave

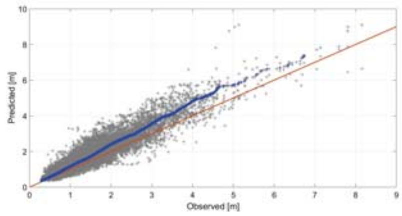

Figure 3 : ***A comparison of significant wave height data, forecast +24 (SWAN). Grey dots - scatter plot, blue dots - q-q plot and red line - observation equal to forecast.***

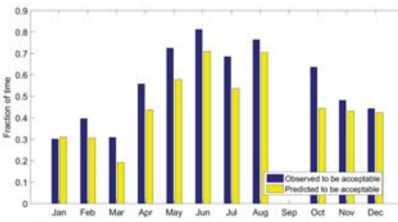

Figure 4 : ***The fraction of time the significant wave height is less than 1.5 m, forecast +24 (SWAN).***

Ocean current

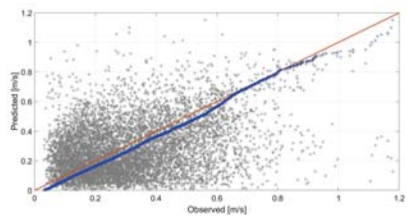

Figure 5 : ***A comparison of current speed data at 10 m depth, forecast +24 (POM). Grey dots - scatter plot, blue dots - q-q plot and red line - observation equal to forecast.***

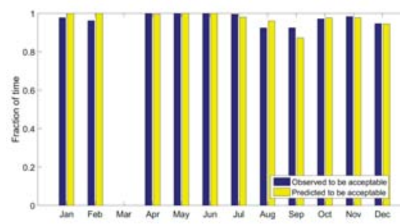

Figure 6 : ***The fraction of time the current speed at 10 m depth is less than 0.7 m/s, forecast +24 (POM).***

Conclusions

- The forecast of wind is relatively good.
- The forecast of waves is relatively good, but lower waves are to be expected.
- The ocean model POM is unreliable and struggles with estimating strong currents.

References

[1] DNV-RP-C205. *Environmental conditions and environmental loads.* Det Norske Veritas, April 2007.

[2] Sætre, R., Ed. *The Norwegian Coastal Current - Oceanography and Climate.* Tapir Academic Press, 2007.

[3] Stewart, R. H. *Introduction To Physical Oceanography.* Department of Oceanography, Texas A&M University, Texas, United States, September 2008.

[4] Torsethaugen, K. *Simplified double peak spectral model for ocean waves.* SINTEF, Fisheries and Aquaculture, Trondheim, 2004.

Acknowledgements

The author would like to thank Statoil, Fugro OCEANOR and MET Norway by Birgitte Furevik for acquisition of data and general information.

Diagnostic monitoring of drivetrain in a 5 MW spar-type floating wind turbine using Hilbert spectrum

NTNU

Mahdi Ghane[1], Amir R. Nejad[1], Mogens Blanke[1,2], Zhen Gao[1], Torgeir Moan[1]

[1]Center for Autonomous Marine Operations and Systems (AMOS), Dept. of Marine Technology and Dept. of Engineering Cybernetics, Norwegian University of Science and Technology (NTNU), Trondheim, Norway.

[2]Dept. of Electrical Engineering, Technical University of Denmark (DTU), DK 2800 Kgs. Lyngby, Denmark

Abstract

The objective of this paper is to investigate the frequency-based fault detection in a 5MW spar-type floating wind turbine (WT) gearbox using the global response. It is extremely costly to seed managed defects in real WT gearbox; t using analytical tools, therefore, is one of the promising approaches in this regard. Forces and moments on the main shaft are obtained from the global response analysis using an aero-hydro-servo-elastic code, SIMO-RIFLEX-AeroDyn. Then, they are utilized as inputs to a high fidelity model developed using a multi-body simulation software (SIMPACK). The main shaft bearing is one of the critical components, since it protects gearbox from axial and radial loads. Six different fault cases with different severity in this bearing were investigated using power spectral density (PSD). It was shown that in severe degradation of this bearing the first stage dynamic of the gearbox is dominant in the main shaft vibration signal. Inside the gearbox, the bearings on the high speed side are those often with high probability of failure, thus, one fault case in IMS-B bearing was also considered. Based on the earlier studies, the angular velocity error function is considered as residual for this fault. The Hilbert transform was used to determine the envelope of this residual. Information in the amplitude of this residual properly indicate wear in this bearing.

Introduction

- Wind energy is a rapidly growing renewable energy source, and the trend is toward applications further offshore in order to access higher wind and to avoid acoustic noise.
- Maintenance and repair costs constitute an important portion of the operating costs particularly for offshore wind turbines.
- Condition monitoring can play a crucial role in managing the operation and maintenance by:
- ✓ Preventing component failure and system shutdown by early detection of incipient degradation.
- ✓ Moving from planned maintenance to condition -based maintenance.
- Drivetrain, in particular, the gearbox, is among the most critical subsystems due its high repair downtime.
- This paper deals with fault detection of main shaft bearing of 5 MW gearbox, which its health is critical to other components, and one bearing inside the gearbox using:
- ✓ Main shaft acceleration measurement and angular velocity error function
- ✓ Power spectral density and The Hilbert transform

Wind turbine and drivetrain model

Fault detection in main shaft bearing of a 5-MW reference gearbox installed on the OC3 Hywind floating spar structure is studied using a de-coupled approach.

- De-coupled Approach & Environmental Condition
- The forces and moments on the main shaft are first obtained from the global response analysis using an aero-hydro-servo-elastic code, SIMO-RIFLEX-AeroDyn. Simulations are carried out at:
- ✓ The rated wind speed (11.4 m/s)
- ✓ Significant wave height HS = 5 m and peak period TP = 12 s The turbulence intensity factor is taken as 0.15 according to IEC 61400-1.

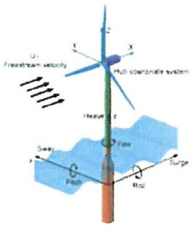

Global analysis in SIMO-RIFLEX-AeroDyn

Parameter	Value
Type	Upwind/3 blades
Cut-in wind speed (m/s)	3
Rated wind speed (m/s)	11.4
Cut out wind speed (m/s)	25
Hub height (m)	87.6
Rotor diameter (m)	126
Hub diameter (m)	3
Rotor mass (1000 kg)	110
Nacelle mass (1000 kg)	240
Hub mass (1000 kg)	56.8

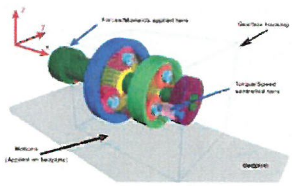

Global Loads are applied on a detailed gearbox model in Multibody Dynamics (MBD)

Parameter	Value
Type	2 Planetary + 1 Parallel
1st stage ratio	1:3.947
2nd stage ratio	1:6.167
3rd stage ratio	1:3.958
Total ratio	1:96.354
Designed power (kW)	5000
Rated input shaft speed (rpm)	12.1
Rated generator shaft speed (rpm)	1165.9
Rated input shaft torque (kN.m)	3946
Rated generator shaft torque (kN.m)	40.953
Total dry mass (1000 kg)	53
Service life (year)	20

Simulation results

- Fault cases and fault detection results
- Physical meaning of fault cases in the main shaft bearing (INP-B) according to ISO 10816-1 standard:

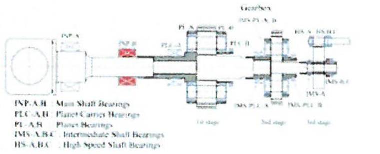

Fault cases	$\frac{K_{y}}{K_{yf}} \times 100\%$	r.m.s (mm/s)	vibration zone boundary
FC0	100	0.8	A
FC1	95	0.9	A
FC2	85	0.9	A
FC3	70	2.2	B
FC4	50	2.4	B
FC5	30	8.3	C
FC6	10	7.7	C

- Residual: Main shaft axial acceleration - nacelle acceleration

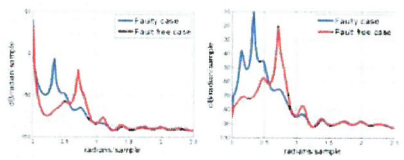

Subtraction acts similar to a high pass filer, making residual robust to wave and winds

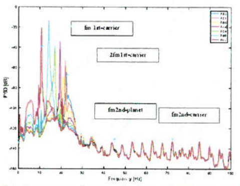

PSD of seven fault cases in the main shaft bearing

- Fault in IMS-B bearing
- Residual: Angular velocity error function

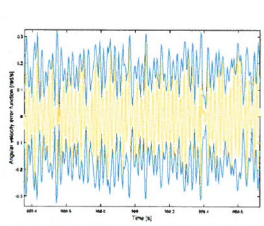

The angular velocity error function and its envelope

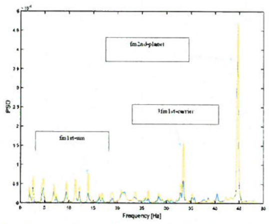

Envelope spectrum of the angular velocity error function.

Methodology

- Envelope analysis using the Hilbert transformation
- Unlike the Fourier transform and Laplace, Hilbert transform does not involve a change of domain. The Hilbert transform of a signal in time (frequency) is another signal in time (frequency). The Hilbert transform of a real value time-domain signal, x(t), is defined by:

$$H[x(t)] = \frac{1}{\pi}\ \text{p.v.} \int_{-\infty}^{\infty} \frac{x(t)}{t-\tau}\, d\tau$$

- H[x(t)] is a complex time series, where the magnitude of this complex signal represents the envelop of a signal, an estimate of the amplitude modulation.

Conclusion

- This paper has employed frequency analysis for fault detection in the main shaft bearing and a bearing inside gearbox. Relative axial acceleration and Angular velocity error function were the residuals, respectively.
- ✓ Global analysis was obtained using SIMO-RIFLEX-AeroDyn
- ✓ Global Loads were applied on a detailed gearbox model in Multibody Dynamics (MBD)
- Gearbox first stage dynamics and 2nd stage dynamics are dominant in the main shaft bearing and IMS-B bearing faults, respectively.

Special thanks to

This work has been carried out at the Center for Autonomous Marine Operations and Systems (AMOS) and the Center for Ships and Ocean Structures (CeSOS). The Norwegian Research Council is acknowledged as the main sponsor of AMOS and CeSOS. This work was supported by the Research Council of Norway through the Centers of Excellence funding scheme, project number 223254-AMOS.

Contact information

Mahdi Ghane
Centre for Autonomous Marine Operations and Systems (AMOS)
Otto Nielsens veg 10 , Department of Marine Technology, NTNU, 7491 Trondheim

Office : (+47) 73 59 56 06
Mobile: (+47) 48 34 3616
Email: Mahdi.Ghane@ntnu.no

Risk and Reliability based O&M Planning of Offshore Wind Farms

M. Florian[1], J.D. Sørensen[1]

1) Aalborg University (AAU), Department of Civil Engineering, Denmark

Introduction

Operational costs of offshore wind farms are one of the main contributors to the high cost of energy and can be significantly reduced by using an optimal maintenance strategy to support the wind farm operator in short-term decision making and long-term O&M planning.

During the PhD project an optimal risk and reliability O&M model is being developed to minimize the total operational costs by balancing the amount of corrective and preventive maintenance efforts, considering all system effects.

The developed O&M model consists of a risk based decision and cost model, which are using deterioration models, inspection results, SCADA data, condition monitoring data and climate data as inputs.

The model output is the long-term O&M planning of the wind farm and decision support to the wind farm operator in daily wind farm operation.

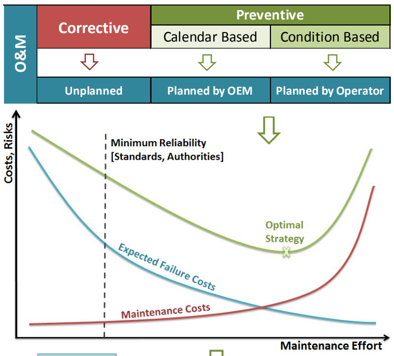

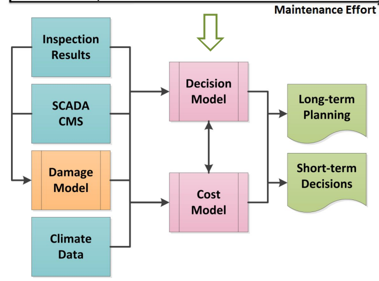

Risk based decision model

By having all the input data it's possible to develop a decision model including decision rules and criteria. The model is formulated as a Bayesian decision tree.

In predictions, unknown results from future inspections are included as the expected value in the deterioration model.

Inspection planning and decisions are chosen to minimize expected cost for the remainder of the blades lifetime

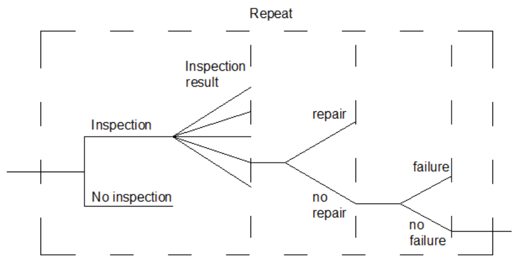

$$C_{total}(t) = \sum_{t=t_0}^{t_L} \left(\sum_{i=thr}^{5} P_i(t|IP)C_i + P_F(t|IP)C_F + P_{ins}(t|IP)C_{ins}\right)$$

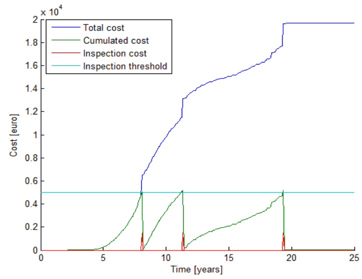

Decision rules for repair threshold and for time of inspection based on cumulated cost/risk

The lifetime cost is determined as a function of the decision plan and the one leading to the minimum expected cost is chosen

After an inspection is made, the information is used to update the degradation model and the optimization is remade for the reminder of the blades life. Therefore, the maintenance policy is updated after every inspection.

Deterioration model and cost model

Based on an existing database of crack sizes and consultation with industry members, a cost model is set up for wind turbine blades.

Category	Repair Priority	Blade Inspection Description/Findings	Continue to Run / Take Offline?	Action
1	None	Blade is in good working condition typical for it's age with possible signs of minor wear	Continue to Run	No action necessary
2	None	Blade shows early signs of wear or damage	Continue to Run	Monitor & Repair within 1 year
3	Low	Blade shows significant signs of wear or damage	Continue to Run	Monitor & Repair within 6 months
4	Medium	Blade shows advanced signs of wear or damage and should be scheduled to be repaired before	Continue to Run	Monitor & Repair within 3 months
5	High	Blade has failed or must be taken out of service to prevent further damage	Take Offline	Repair or Replace Immediately

Category	1	2	3	4	5	Fail
Size [m]	< 0.05	0.05 - 0.2	0.2 - 0.5	0.5 - 1	1 – 3	>3

Degradation is modeled using a continuous probabilistic fracture mechanics model, calibrated to the *guide-to-defect* database.

$$\frac{da}{dt} = \frac{A(\Delta K)^m}{(1-R)^{m(1-\lambda_W)}}$$

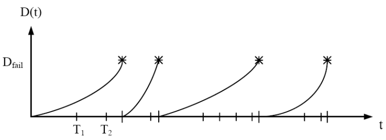

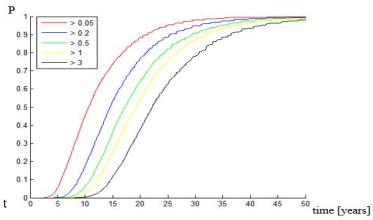

Updating the deterioration model

Since deterioration are associated with significant uncertainty, deterioration model is updated using direct information from indicators using inspection techniques and Bayesian statistics.

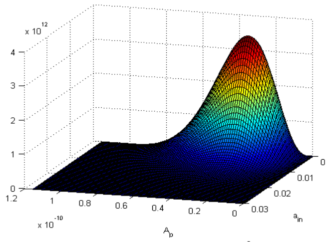

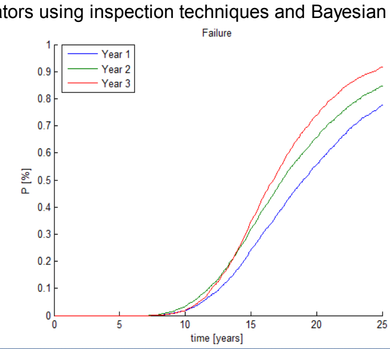

$$f''_{(q,v|a_m)} = \frac{f(a_m|q,v)f'(q,v)}{\int\int f(a_m|q,v)f'(q,v)\,dq\,dv}$$

Demonstration of risk-based model

Using Monte Carlo simulations, the "exact" cost of maintenance over 25 a year lifetime is determined for a single blade. This is compared to traditional condition based strategies.

Condition based

Mean Annual O&M cost [euro]	CoV of mean cost [%]
1451	61

Risk based

Mean Annual O&M cost [euro]	CoV of mean cost [%]
1125	71

A reduction of 22.5 [%] in expected annual cost is obtained using risk-based maintenance strategies

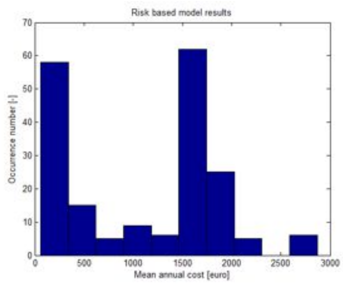

Application on NORCOWE wind farm

For demonstration of practical applicability, the risk based maintenance model for blades is included into a discrete event simulator similar to ones developed for commercial/research purposes (ECN O&M tool, NOWIcob, Maintsys™).

25 year lifetimes are simulated for the 80 turbine wind farm using 3 [h] time steps and wind/wave measurements for weather conditions

Maintenance is split in blade maintenance, using the risk model and corrective/condition based maintenance for other components.

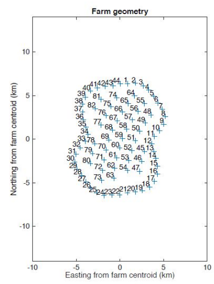

Acknowledgments

The work presented here is supported by Aalborg University and NORCOWE.

EERA DeepWind'2017
Radisson Blu Royal Garden Hotel, Trondheim
January 18-20, 2017

ForWind Center for Wind Energy Research — Bremen Hannover Oldenburg

Research Alliance Wind Energy

Carl von Ossietzky universität Oldenburg

Training requirements of a neural network used for fatigue load estimation of offshore wind turbines

J. Seifert *, L. Vera-Tudela, M. Kühn

ForWind, Institute of Physics, Carl von Ossietzky University of Oldenburg, 26129 Oldenburg, Germany

* email: janna.seifert@forwind.de

Introduction

Background

To estimate fatigue loads, neural networks (NNs) have been proven to be a reliable method [1-3]. After training the neural network with a set of load measurements and SCADA signals it is able to predict the loads with SCADA signals solely. However, load measurements are costly [2].

Objectives

- assess the minimum needed length of consecutive load measurements
- investigate the time dependence of the training samples (seasonal effects)
- check the representativeness of the training samples to validate the processed samples sizes

Measurements

- Baltic 1: 21 Siemens 2.3-93 wind turbines
- Examined wind turbines:
  B01 (mainly free flow)
  B08 (predominantly in wake)
- Period: Mar2013 - Mar2014
- Sampling rate: 10-minute statistics
- Availability:
  B01: 60.83% (32062 records)
  B08: 56.81% (29943 records)

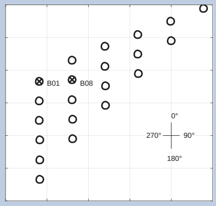

Fig. 1: Layout of Baltic 1.

Methods

Feed forward neural network

- One hidden-layer
- 30 neurons
- Estimator: 8 SCADA statistics
- Target: flapwise blade root bending moment

Prediction error

- relative mean squared error
- $rMSE = \frac{1}{n}\sum_{i=1}^{n}\left(\frac{\hat{y}_i - y_i}{y_i}\right)^2$

number of records n, estimated loads $\hat{y}_i$, measured loads y_i

Statistical testing

- K-fold cross validation (with overlap)
- Smallest size: about two days (144 records)
- Largest size: about 45 days (4032 records)
- Step size: about two days (144 records)

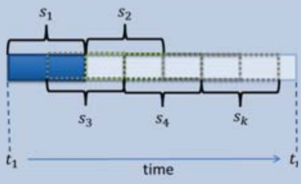

Fig. 2: Scheme of k-fold cross validation with overlap.

Representativeness of training samples

- Filling degree of capture matrix of training sample compared to filling degree of capture matrix of whole measurement

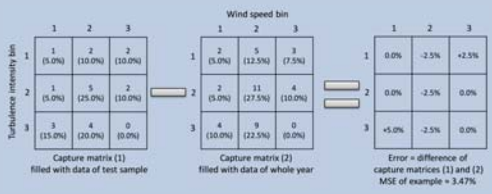

Fig. 3: Example scheme for calculation of MSE.

Results

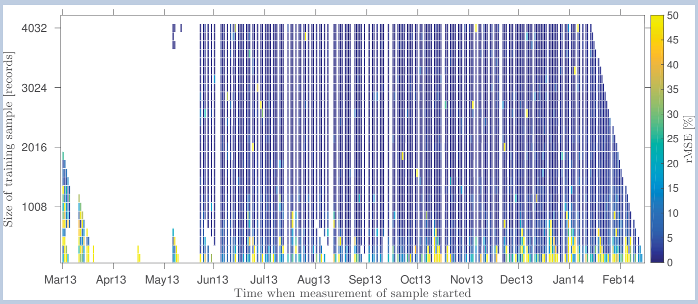

Fig. 3: Prediction error in relation to the time the training sample was measured for one blade B01. The gaps within the data are caused by the data availability and filtering of overly large time periods per training sample which were as caused by missing measurements.

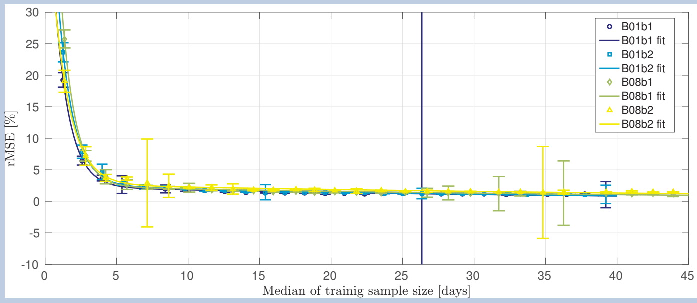

Fig. 5: Relation of prediction error (rMSE) and training sample size. For each training sample size, the median of the time periods needed to gather the number of records is plotted with its standard deviation. The sample size of about 26 days (2736 records) shows a standard deviation greater than 15% which occurred due to a falsified prediction of one out of 204 training samples.

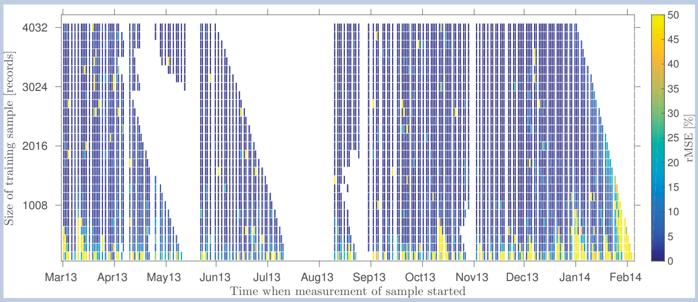

Fig. 4: Prediction error in relation to the time the training sample was measured for one blade B08. The gaps within the data are caused by the data availability and filtering of overly large time periods per training sample which were as caused by missing measurements.

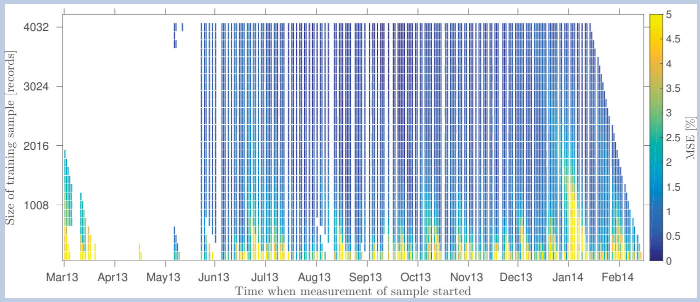

Fig. 6: Representativeness of training samples for one blade of B01 assessed with the MSE of the filling degree of their capture matrices according to the example scheme.

Conclusion

- Reliable fatigue load prediction is possible even for small sized training samples of 2016 records (about 20 days)
- Representativeness of small sized training samples (2016 records, about 20 days) is given
- Seasonal effects are neglectable low and do not affect the prediction accuracy
- To generalise these findings the evaluation has to be extended for other loads

Acknowledgements

This work was partly funded by the German Federal Ministry of Economic Affairs and Energy and the Ministry of Science and Culture of the State of Lower Saxony as part of the research projects “Baltic I” “OWEA Loads”, “DFWind” and “Ventus Efficiens” under grant number 0325215A, 0325577B, 0325936C and ZN2988 & ZN3024 respectively.

References

[1] Cosack N. Fatigue load monitoring with standard wind turbine signals. PhD thesis. University of Stuttgart; 2010.

[2] Obdam TS, Rademakers LWMM, Braam H. Flight Leader Concept for Wind Farm Load Counting and Performance Assessment. Energy Research Centre of the Netherlands. ECN-M-09-054, The Neatherlands, 2009.

[3] Smolka U, Cheng PW. On the Design of Measurement Campaigns for Fatigue Life Monitoring of Offshore Wind Turbines. In: Proceedings of the Twenty-third International Offshore and Polar Engineering. USA; 2013.

Recommended practices for wind farm data collection and reliability assessment for O&M optimization

SINTEF

Berthold Hahn[a], Thomas Welte[b], Stefan Faulstich[a], Pramod Bangalore[c], Cyril Boussion[d], Keith Harrison[e], Emilio Miguelanez-Martin[f], Frank O'Connor[g], Lasse Pettersson[h], Conaill Soraghan[e], Clym Stock-Williams[i], John Dalsgaard Sørensen[j], Gerard van Bussel[d], Jørn Vatn[k]

[a] Fraunhofer IWES, [b] SINTEF Energy Research, [c] Chalmers University of Technology, [d] Delft University of Technology, [e] Offshore Renewable Energy Catapult, [f] Atkins, [g] ServusNet Informatics, [h] Vattenfall Research and Development, [i] ECN Energy Research Centre of the Netherlands, [j] Technical University of Denmark/Aalborg University, [k] Norwegian University of Science and Technology

IEA Wind Task 33

re•li´•a•bil´•i•ty (ri, lī ə 'bil ə tē) n.

IEA Wind Task 33 commenced in 2012 with focus on data collection and reliability assessment for O&M optimization of wind turbines. The task 33 group finalized the work in September 2016 and the results will be published in 2017 by IEA Wind in the recommended practices (expert group report) for "Wind farm data collection and reliability assessment for O&M optimization"

IEA Wind Task 33 has strived at finding answers to the following questions:

- *Which information do operators and other stakeholders need?*
- *What analyses can provide the requested information?*
- *Which data has to get recorded to feed these analyses?*

Task 33 Approach

1. *Role and purposes (use cases)*
   Identify your individual circumstances and reliability objectives
2. *Analyses*
   Identify analyses that support your purposes and objectives
3. *Data groups and data entries*
   Identify data groups and data entries required for the intended analyses
4. *Standards and taxonomies*
   Identify useful standards, guidelines and taxonomies

Levels of complexity:

Level	Possible application	Possible analyses	Needed data groups	Requirement on organizational foundation of reliability
A	Performance, Availability	Simple statistical calculations (average values, histograms, ...)	Equipment data, Operational data Measurement values	Assessment of assets is recognized as important.
B	Plus: Root cause analysis	Fault-Tree-Analysis, Pareto-analysis, Basic physical models (e.g. Miner's rule)	Plus: Failure data	Reliability is recognized as important, some processes around reliability exist.
C	Plus: Design optimization, Maintenance optimization, Degradation monitoring	Degradation models, Advanced physical models (e.g. modelling fluid-structure interaction), Maintenance and logistics optimization, Data mining, Vibration analysis, Optimization (renewal, stock keeping, etc.)	Plus: Maintenance and inspection data (Costs)	A clear and formal reliability process is defined and regularly reviewed with stakeholders.

Data groups and examples of sub-groups:

Data groups	Sub-groups
Equipment data (ED)	Identification, time data, technical information
Operating data / Measurement values (OP)	Time stamp, measurement values (SCADA, etc.), operational states
Failure data (FD)	Identification, time data Failure description, failure effect, failure detection, fault properties
Maintenance & inspection data (MD)	Identification, time data, task/measure/activity, resources, maintenance results

Data groups and related taxonomies:

Taxonomies	ED	OP	FD	MD
RDS-PP®	o			
NERC GADS	o	-		-
Reliawind	o			
ISO 14224	(o)		(+)	(+)
FGW ZEUS		o	+	+
IEC 61400-25		+		
IEC 61400-26		o		

+ wind-specific entries with a high level of detail
o wind-specific entries with a high level of detail, but not complete
- wind-specific entries on a more general level
(+) entries with a high level of detail, not wind-specific
(o) entries with a high level of detail, not wind-specific, but not complete
(-) entries on a more general level, not wind-specific

Conclusions and further work

- There is a strong demand for making better use of operational experience to improve O&M as well as other applications.
- The recommended practices of IEA Wind Task 33 mean an important step towards making use of operational experience for reliability improvement.
- The IEA Wind Task 33 results have been developed and reviewed by experts from research and industry in the field of reliability.
- The results may be adopted in part or in total by other standards developing organizations and one of the IEC working groups dealing with availability and reliability has already announced to base their future work on these results.

Task 33 Recommendations

Developers / owners / operators	**1. Make sure you get access to all relevant data** Consider reliability data to be of high value from the early stages of wind asset development and a key operational factor throughout the life of the wind asset. Ensure access to reliability data and required data are factored into negotiations with developers / OEMs / suppliers / service providers.
	2. Identify your use-case and be aware of the resulting data needs Identify use cases linked to your organizational reliability ambitions and use these to define data collection requirements.
	3. Map all WT components to one taxonomy / designation system Map all wind asset components and maintenance activities to one of the taxonomies / designation systems identified in the Task 33 recommended practices. This will allow for improvements in both the consistency and integrity of reliability data throughout an organization and at the interfaces with the supply chain.
	4. Align operating states to IEC 61400-26 Align operating states with those specified in IEC 61400-26, the standard for a time- and production-based availability assessment for wind turbines.
	5. Train your staff understanding, what data collection is helpful for All staff engaged directly, or indirectly, in the production, collation and analysis of reliability metrics should be educated on the strategic significance of reliability data and empowered to improve related business processes and practices.
	6. Support data quality by making use of computerized means Whenever practical, seek to automate the data collection / collation process as a means of reducing the risk of human error and improving data quality.
	7. Share reliability data to achieve a broad statistical basis Wind farm owners / operators should engage in the external, industry-wide sharing of reliability and performance data. This will align data collection methodologies, drive organizational improvements and achieve statistically significant populations of data for reliability analyses.
Development of standards for the wider wind industry	**8. Develop comprehensive wind-specific standard based on existing guidelines/standards** Develop a comprehensive wind specific standard based on ISO 14224, FGW ZEUS, and other existing guidelines/standard. This would provide a core standard for the language and scope of reliability and maintenance data for the wind industry (based on accepted reliability data best practice in oil and gas industry), while minimizing the time and cost associated with the development of the standard.
	9. Develop component- / material-specific definition of faults, location, and severity As a longer-term recommendation, there is a need to develop standard definitions for damage classification and severity for structural integrity issues.

Countries represented in IEA Wind Task 33:

iea wind

Task 33 Operating Agent:

Fraunhofer IWES

Integration of Degradation Processes
in a Strategic Offshore Wind Farm O&M Simulation Model

Thomas M. Welte, Espen Høegh Sørum, Iver Bakken Sperstad, Magne L. Kolstad

SINTEF Energy Research (Contact: thomas.welte@sintef.no)

Full integration of degradation process:

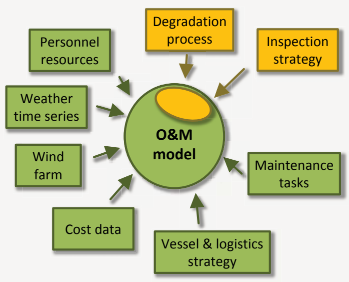

Loose integration of degradation process:

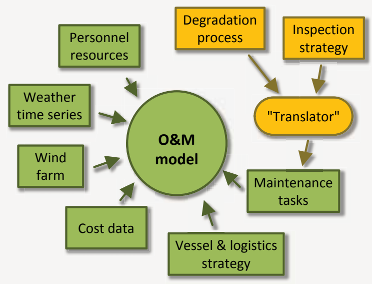

Abstract

Strategic decision support tools for offshore wind O&M need to represent the failure behaviour of components. This work discusses two different alternatives for integrating component degradation processes in a strategic offshore wind farm O&M simulation model:

- *Full integration* of a degradation process in the O&M simulation model
- *Loose integration* of a degradation process, using a simpler representation

Although loose integration models some effects less accurately than full integration, the accuracy is for most purposes sufficient for such O&M models.

Background

- Typical application of offshore wind farm O&M simulation models: Strategic decision support, e.g. for wind farm investment decisions, selection of vessel and logistics strategy, etc.
- Most such models use only a high-level representation of the failure behaviour, such as failure rates, but using more detailed models representing components' failure behaviour may improve the models and the results.
- Evaluating the value of more detailed modelling and discussing alternatives for integration of degradation processes is the aim of this work.

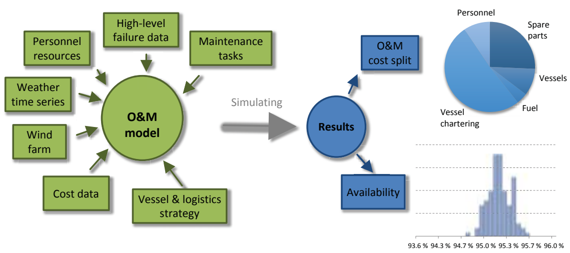

Figure: Typical inputs and outputs of a strategic O&M simulation model.

Full integration of degradation model

- The NOWIcob O&M simulation tool is used for this work.
- Full integration means that existing NOWIcob tool must be extended.
  → Additional computational work.
  → Each type of model that can be applied for modelling degradation (Markov process, Gamma process, Paris law, ...) requires the full implementation of the model in NOWIcob with corresponding changes to the user interface.
- Case study:
  As a simple but practical example, a Markov chain model for blade degradation with discrete condition states as presented by Florian and Sørensen (2017), has been considered in our case study.

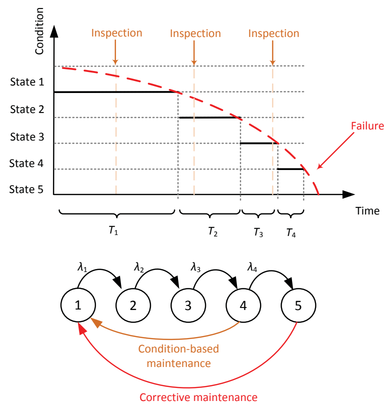

Figure: Simple example of Markov process for degradation (below) and conceptual illustration of underlying degradation pattern (above).

Methodology for loose integration

- The link between the degradation model and NOWIcob is established by means of an integration tool ("translator") that "translates" the inputs of the degradation process and the inspection strategy to the high-level inputs required by NOWIcob's existing condition-based maintenance module:
  - p_{det} : The overall probability that a potential failure is detected and a warning is given (given a specific inspection strategy)
  - T_{det} : The number of days between the warning and when the failure would have occurred if the warning had not been given
- That is, the degradation and inspection processes are simulated outside NOWIcob, neglecting effects such as weather and logistics.

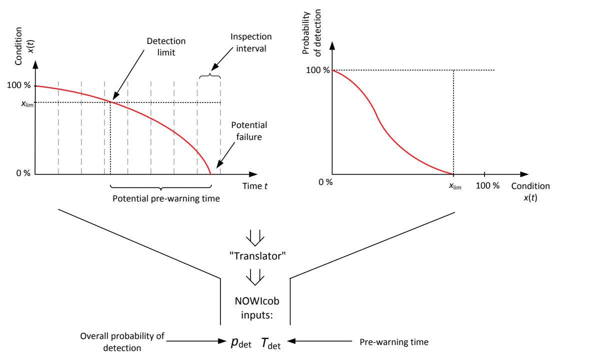

Figure: Conceptual illustration of the "translation" from a degradation process and inspection strategy to a simplified representation in a strategic O&M simulation model.

Results and conclusions

The difference between full and loose integration in aggregated result parameters such as availability and O&M cost are very small in the case study.

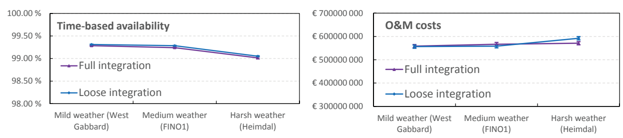

Advantages of full integration	Advantages of loose integration
Higher accuracy (given detailed and accurate input data) for more detailed result parameters	**Easier to implement** (not necessary to implement and integrate one model for each component and failure mode)
Detailed representation of inspection strategy (allows for better optimization of strategies)	**More flexible** (generic model can represent different degradation patterns)

References

Hofmann, M.; Sperstad, I. B. (2013). "NOWIcob – A tool for reducing the maintenance costs of offshore wind farms". *Energy Procedia*, vol. 35, 2013, pp. 177–186.
Florian, M.; Sørensen, J. D. (2017). "Case study for impact of D-strings on levelised cost of energy for offshore wind turbine blades". *International Journal of Offshore and Polar Engineering* (accepted).

Acknowledgements

This project has received funding from the European Union's 7th Framework Programme for Research and Technological Development under grant agreement No. 614020 (LEANWIND) and was co-funded by the Research Council of Norway through the Norwegian Research Centre for Offshore Wind Technology (NOWITECH).

A Preliminary Study of Reliability-based Controller Scheduling in Offshore Wind Turbines

Jan-Tore H. Horn[a,b], Bernt J. Leira[b], Jørgen Amdahl[a,b]
[a]Centre for Autonomous Marine Operations and Systems (NTNU AMOS),
[b]Department of Marine Technology, NTNU, Trondheim, Norway.
Email: jan-tore.horn@ntnu.no

NTNU AMOS
Centre for Autonomous Marine Operations and Systems

Introduction

In this work, a study of the long-term fatigue reduction effects in offshore wind turbines due to an active controller is conducted. Several approaches are tested, including possible life extension of a monopile foundation, compensation for reduced material consumption and the uncertainty of the long-term stress amplitude distribution. The physical model and environmental loads are represented with a Weibull stress distribution, and the controller is assumed to be modifying the distribution by scaling the distribution scale parameter. This first approach to fatigue reduction control is simple, but will give an indication of how well an advanced controller should be working to get financial benefits or increased lifetime reliability.

Basic Concepts

It is assumed that the long-term stress range at a specific location in the foundation can be expressed by a two-parameter Weibull distribution:

$$f_S(s) = \frac{b}{a}\left(\frac{s}{a}\right)^{b-1} e^{-\left(\frac{s}{a}\right)^b} \tag{1}$$

where the mean and variance of the stress amplitudes are given as:

$$\mu = a\Gamma(1+1/b) \tag{2a}$$

$$\sigma^2 = a^2\left[\Gamma(1+2/b) - \big(\Gamma(1+1/b)\big)^2\right] \tag{2b}$$

Further, the controller action r_c is taken as the fraction of reduced mean and standard deviation of the distribution, yielding a modification of the scale parameter, from a:

$$r_c = \frac{a_c}{a} = \frac{\mu_c}{\mu} = \frac{\sigma_c}{\sigma} \tag{3}$$

The above-mentioned load effect representation and controller model will form the basis of this study.

Models

The expected fatigue damage during N cycles can be found by integrating the stress amplitude distribution using the Palmgren-Miner summation and bi-linear SN-curves. A similar expression can be found in [1] and [2] for single-slope SN-curves.

$$\begin{aligned} D_N &= \sum_{i=1}^{N} \frac{s_i^{m_1}}{K_1}\mathcal{H}(s_i - s_0) \\ &\quad + \frac{s_i^{m_2}}{K_2}[1-\mathcal{H}(s_i - s_0)] \\ &= N\left\{\frac{a^{m_1}}{K_1}\Gamma\left[1+\frac{m_1}{b}, \left(\frac{s_0}{a}\right)^b\right]\right. \\ &\quad \left. + \frac{a^{m_2}}{K_2}\gamma\left[1+\frac{m_2}{b}, \left(\frac{s_0}{a}\right)^b\right]\right\} \\ &= N\Big\{D_1(a,b) + D_2(a,b)\Big\} \end{aligned} \tag{4}$$

Here, $\Gamma[\cdot,\cdot]$, $\gamma[\cdot,\cdot]$ and $\mathcal{H}(\cdot)$ are the upper incomplete, incomplete gamma and Heaviside step functions, respectively. The remaining parameters are given in Table 1. As deduced, the fatigue damage is a closed-form, linear summation of contributions from the upper and lower part of the SN-curves. To evaluate the time-dependent reliability, the limit state equation for N load periods are given as:

$$g_N = \Delta - D_N \tag{5}$$

where Δ is log-normally distributed with a mean value of 1 and standard deviation of 0.3. The probability of failure

$$P_{f,N} = P[g_N \leq 0] \tag{6}$$

and corresponding reliability index

$$\beta_N = -\Phi^{-1}(P_{f,N}) \tag{7}$$

are then found by Monte Carlo Simulation or the first order reliability method (FORM).

Fatigue lifetime and Reliability

First, an overview of relevant stress distributions are obtained and plotted in Figure 1. By this figure, we can find the Weibull parameters giving an expected fatigue lifetime of 20 years by evaluating the time until the reliability limit is reached. The minimum reliability index is 3.1, which means a probability of failure of 10^{-3}. The remaining parameters are given in the table below, which is similar to what is presented in [3]. Figure 1 also shows the contributions from the two slopes in the SN-curve, meaning that the lighter area contains a larger contribution from the low-cycle slope. Next, a Monte Carlo simulation is performed to obtain a time-dependent reliability, where a controller action of $r_c = 0.95$ is introduced when the reliability is below 3.7, corresponding to a probability of failure of 10^{-4}. In Figure 2, an increase of the foundation lifetime of 2 years can be observed.

Table 1: Simulation parameters

Parameter	Distribution	Mean	Std.dev.
Δ	Log-normal	1	0.3
$\log K_1$	Normal	12.164	0.25
$\log K_2$	Normal	16.106	0.25
m_1	Fixed	3	-
m_2	Fixed	5	-
s_0	Fixed	52.63	-
N_y	Fixed	8e6	-
P [MW]	Fixed	10	-
D [m]	Fixed	9	-
t [m]	Fixed	0.11	-
H [m]	Fixed	80	-

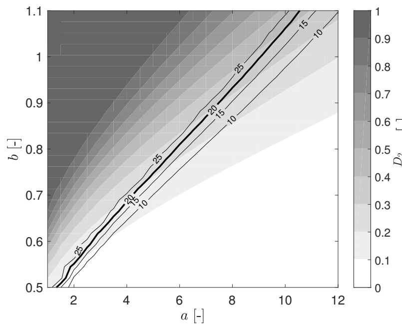

Figure 1: Structural lifetime and SN-curve contributions as a function of Weibull parameters

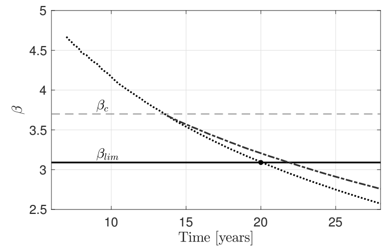

Figure 2: Time-varying reliability index

Results

Using the same simulation parameters as above, a test is performed on how much controller-induced fatigue reduction is required to compensate for some variance introduced to the Weibull parameters.

Figure 3 shows the required r_c for several COV values introduced to the parameters a and b, which are now considered to be normally distributed. Note that only a is given, since there is a one-to-one relationship between a and b in Figure 1 on the 20 year contour line. Also, the controller is assumed to be active during the whole lifetime.

Finally, an estimate of cost reductions and increased revenue due to lifetime extension is made, using the rated power, monopile diameter, thickness and height given in Table 1. The capacity factor is taken as 0.5, and the energy price is assumed to be constant at 0.1[€/kWh]. All incomes related to extended lifetime production are discounted with a rate of return of 9% and the combined steel and production price is 2€/kg. However, the load mitigating controller is not active until a reliability index of 3.7 is expected, which is approximately after 12 years. The vertical axis in Figure 4 shows the production loss factor, where 0.98 indicates a 2% power production loss when the controller is active. ΔC_E is the relative foundation cost change due to increased energy production, while ΔC_S is the capital saved on reducing the steel thickness while maintaining reliability and assuming only quasi-statically added load effects. To conclude, there is a potential in indirectly reducing the cost of energy with a different controller algorithm, but focus should be on extended production or reduced damage uncertainty.

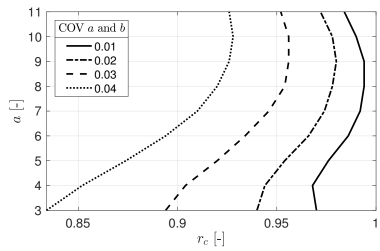

Figure 3: Control action to compensate for stress parameter variance

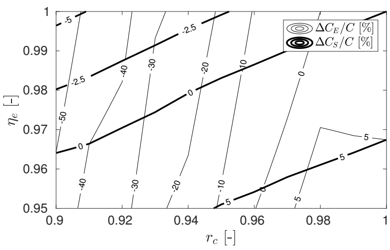

Figure 4: Foundation cost change in %

References

[1] Efren Ayala-Uraga and Torgeir Moan. Fatigue reliability-based assessment of welded joints applying consistent fracture mechanics formulations. *International Journal of Fatigue*, 29(3):444–456, mar 2007.

[2] Kenneth G Nolte and John E Hansford. Closed-Form Expressions for Determining the Fatigue Damage of Structures Due to Ocean Waves. In *Offshore Technology Conference*, 1976.

[3] Sergio Marquez-Dominguez and John D Sorensen. Fatigue Reliability and Calibration of Fatigue Design Factors for Offshore Wind Turbines. *Energies*, 5(6):1816–1834, 2012.

Acknowledgements

This work has been carried out at the Centre for Autonomous Marine Operations and Systems (NTNU AMOS). The Norwegian Research Council is acknowledged as the main sponsor of NTNU AMOS. This work was supported by the Research Council of Norway through the Centres of Excellence funding scheme, Project number 223254 - NTNU AMOS.

Key Performance Indicators for Wind Farm Operation and Maintenance

Elena Gonzalez[a,*], Emmanouil M. Nanos[b,*], Helene Seyr[c,*], Laura Valldecabres[d,*], Nurseda Y. Yürüsen[a,*] Ursula Smolka[e], Michael Muskulus[c], Julio J. Melero[a]

[a] CIRCE – Universidad de Zaragoza, C/Mariano Esquillor Gómez 15, 50018 Zaragoza, Spain
[b] Wind Energy Institute, Technische Universität München, 85748 Garching bei München, Germany
[c] Department of Civil and Environmental Engineering, Norwegian University of Science and Technology, NTNU, 7491 Trondheim, Norway
[d] ForWind - University of Oldenburg, Institute of Physics, Ammerländer Heerstraße 136, 26129 Oldenburg, Germany
[e] Ramboll Wind, Stadtdeich 7, 20097 Hamburg, Germany

These authors contributed to the work equally

AWESOME
PhD'S IN WIND POWER O&M

http://awesome-h2020.eu/

Introduction

- The wind industry is now facing a challenging scenario with more offshore presence and without incentives for both development and operations. The current growing interest in optimising operations makes **wind farm (WF) operation and maintenance (O&M)** a new challenging field of study.
- The use of **key performance indicators (KPIs)** is one of the most widespread tools to get a comprehensive overview of a business and to measure the progress towards its stated goals. WF O&M would benefit from having a **suitable, well defined and standard set of KPIs** as many other industries and sectors. KPIs should inform about the general status of an operating asset, influence the decision-making process and reflect changes in the O&M strategy.
- During a joint industry workshop (JIW) organised by the **Advanced Wind Energy System Operation and Maintenance Expertise (AWESOME) project**, the definition of KPIs arose as one of the main needs for WF O&M.
- We present a **review** of the major existing indicators used in the O&M of WFs, not available in the literature so far. A final list of KPIs is suggested and verified against necessary properties, together with an analysis of the stakeholders involved in O&M and their interests.

Methodology & Results

Stakeholders involved in WF O&M activities

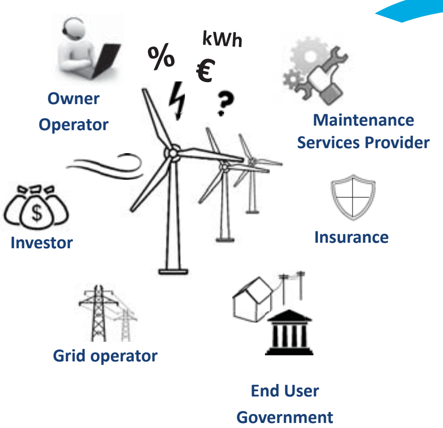

Clustering of main concepts of interest

Necessary properties for KPIs

Relevant	• Valuable information
Specific	• Clear and easy to understand
Measurable	• Quantitative/Qualitative
Comparable	• Allows benchmarking
Traceable in time	• Tracks changes
Standard	• Unique definition

Review of the main used indicators per category

Discussion

- We suggest a list of KPIs verified against the necessary properties.
- A check-mark (✓) indicates it fulfils it; a cross-mark (✗) it does not fulfil it; an asterisk (✓*) indicates that with some modifications it would fulfil the property.

	Relevant	Specific	Measurable	Comparable	Traceable in time	Standard
Performance						
Time-based availabilty (%)	✓	✓	✓	✓	✓	✗
Energy-based availability (%)	✓	✓	-	✓	✓	✗
Maintenance						
Interventions per WT	✓	✓	✓	✓	✓	✓*
Reactive maintenance (%)	✓	✓	✓	✓	✓	✓*
Schedule compliance (%)	✓	✓	✓	✓	✓	✓*
Overtime jobs (%)	✓	✓	✓	✓	✓	✓*
Labour costs vs. TMC (%)	✓	✓	✓	✓	✓	✓*
TMC vs. AMB (%)	✓	✓	✓	✓	✓	✓*

	Relevant	Specific	Measurable	Comparable	Traceable in time	Standard
Reliability						
MTBF & Failure rate (%)	✓	✓	✓	✓	✓	✓*
MTTR & Repair rate (%)	✓	✓	✓	✓	✓	✓*
MTTF	✓	✓	✓	✓	✓	✓*
Finance						
OPEX (€/MW)	✓	✓	✓	✓	✓	✓
EBITDA margin (%)	✓	✓	✓	✓	✓	✓
LLCR (%)	✓	✓	✓	✓	✓	✓
DSCR (%)	✓	✓	✓	✓	✓	✓
LCOE (€/MW)	✓	✓	✓	✓	✓	✓

Conclusion & Outlook

- This paper constitutes a good first contact to WF O&M aspects for those wind professionals and researchers that have not yet approached the field.
- After analysing the stakeholders involved, defining the properties for KPIs and a thorough review of the existing ones, we propose and discuss a suitable list.
- Further numerical validation is highly recommended to make quantitative evaluation for both onshore and offshore cases.

Selected References

[6.] SETIS European Commission, Key performance indicators for the European wind industrial initiative
[10.] H. Kerzner, Project management metrics, KPIs, and dashboards
[24.] /[25.] IEC TS 61400-26-1: Wind turbines - Part 26-1 and IEC TS 61400-26-2: Wind turbines - Part 26-2
[26.] H. J. Krokoszinski, Efficiency and effectiveness of wind farms-keys to cost optimized operation and maintenance
[30.] IEA Wind, Task33 - Reliability Data: Standardization of data collection for wind turbine reliability and maintenance analyses
[33.] T. Wireman, Developing performance indicators for managing maintenance
[41.] J. D. Stowe, T. R. Robinson, J. E. Pinto, D. W. McLeavy, Equity asset valuation

Acknowledgements

This project has received funding from the European Union's Horizon 2020 research and innovation programme under the Marie Skłodowska-Curie grant agreement No 642108.

circe RESEARCH CENTRE FOR ENERGY RESOURCES AND CONSUMPTION
TUM
NTNU Norwegian University of Science and Technology
ForWind Zentrum für Windenergieforschung
RAMBØLL

EERA DEEPWIND'2017, 14TH DEEP SEA OFFSHORE WIND R&D CONFERENCE, 18 - 20 JANUARY 2017

Optimisation of Data Acquisition in Wind Turbines with Data-Driven Conversion Functions for Sensor Measurements

L. Colone*[,a], M. Reder*[,b], J. Tautz-Weinert*[,c], J.J. Melero[b], A. Natarajan[a], S.J. Watson[c]
[a] Technical University of Denmark, Frederiksborgvej 4000, Roskilde, Denmark
[b] CIRCE - Universidad de Zaragoza, C/ Mariano Esquillor 15, 50018, Zaragoza, Spain
[c] CREST - Loughborough University, Holywell Park, Loughborough, LE113TU, UK
Shared first authorship - authors contributed equally to the publication but are presented in alphabetical order.

AWESOME
PhD'S IN WIND POWER O&M

Introduction

- **Operation and Maintenance (O&M)** is an important cost driver of modern wind turbines [1]. Condition monitoring (CM) allows the implementation of predictive O&M strategies helping to reduce costs [2].
- A novel approach for wind turbine condition monitoring is proposed focusing on **synergistic effects of coexisting sensing technologies** based on the *1st Joint Industrial Workshop* within the AWESOME project [3].
- The approach uses a multi-step procedure to pre-process data from signals, train a set of **conversion functions** and evaluate their performance.
- A subsequent sensitivity analysis measuring the impact of the input variables on the predicted response reveals hidden relationships and synergistic effects.
- The concept feasibility is tested in a **case study** using Supervisory Control And Data Acquisition (SCADA) data from an offshore turbine.

Objectives

- To understand the predictability of signals using information from other measurements recorded at different locations of the machine.
- Enable better understanding of measurement data and eventually exclude irrelevant input variables.

General framework

1. **Pre-processing and feature extraction**
   e.g. averaging, interpolation, normalising, FFT
2. **Build conversion functions for *n* signals**
   $x_i = f_i(x \in X \setminus x_i)$
   with $X = \{x_1, x_2, x_3, \ldots, x_n\}$
3. **Evaluate conversion functions**
   e.g. Mean Absolute Error (MAE), Root Mean Square Error (RMSE) and R^2

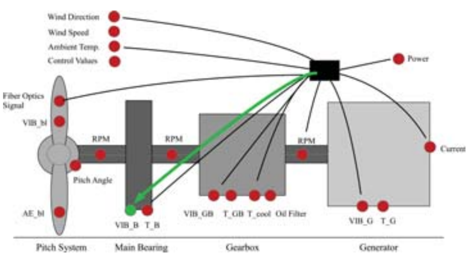

Fig. 1: Exemplary scheme for modelling the main bearing vibrations (VIB_B, green dot) with the conversion function (black box) and all possible inputs (red dots).

Case study

SCADA data from a 2 MW offshore wind turbine with six signals:

- Rotor speed
- Pitch angle
- Yaw angle
- Tower-top acceleration in x-direction (fore-aft)
- Tower-top acceleration in y-direction (side-side)
- Active power

Comparison of modelling techniques:

- Generalised Linear Model (GLM) [4]
- Random Forests (RF) [5]
- Gradient Boosting Machine (GBM) [6]
- Artificial Neural Networks (ANNs) [7]

Sensitivity study on variable importance:

- Training and testing of conversion functions for all possible combinations of inputs (31 each)

Results – Performance of modelling techniques

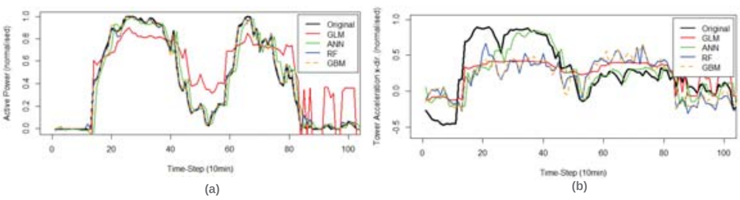

Fig. 2: Original and predicted (a) power production and (b) tower vibration in x-direction for each modelling technique.

Table 1: Testing performance for predicting the tower acceleration in *x*-direction (normalised to maximum value)

	48 days training			108 days training			156 days training		
Technique	MAE	RMSE	R^2	MAE	RMSE	R^2	MAE	RMSE	R^2
GLM	0.194	0.230	0.301	0.210	0.251	0.245	0.207	0.247	0.273
RF	0.103	0.142	0.740	0.091	0.130	0.809	0.091	0.127	0.811
GBM	0.084	0.132	0.790	0.070	0.115	0.851	0.073	0.115	0.850
ANNs	0.050	0.094	0.884	0.039	0.075	0.933	0.054	0.093	0.899

Results – Sensitivity study on variable importance

ANN were chosen for this analysis as they performed best in predicting active power and tower acceleration in *x*-direction. The results of the sensitivity study are presented for each parameter included in the presented case study.

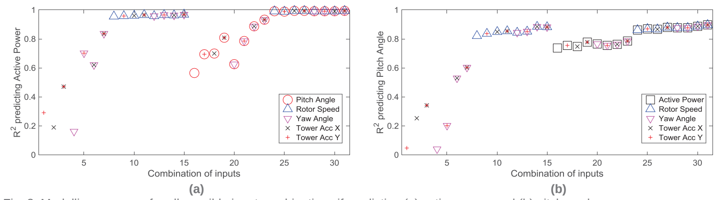

Fig. 3: Modelling accuracy for all possible input combinations if predicting (a) active power and (b) pitch angle.

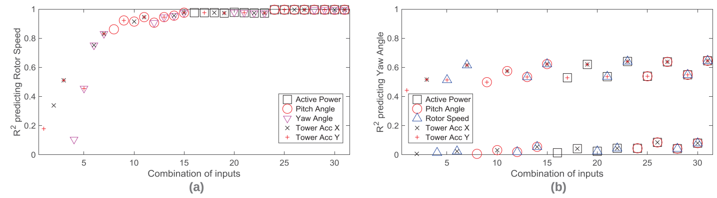

Fig. 4: Modelling accuracy for all possible input combinations if predicting (a) rotor speed and (b) yaw angle.

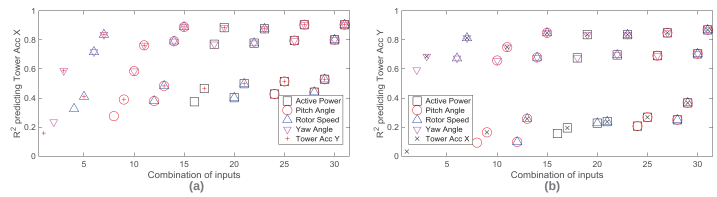

Fig. 5: Modelling accuracy for all possible input combinations if predicting (a) tower x-acceleration and (b) tower y-acceleration.

Active power, pitch angle and rotor speed showed a very strong relationship. The strongest synergistic effects are seen in combining yaw angle with the tower vibrations.

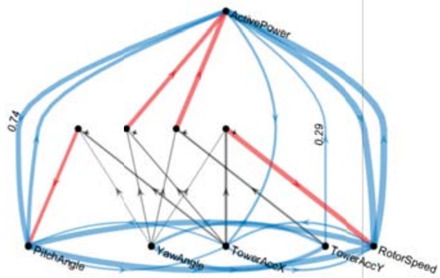

Fig. 6: Diagram of the relationship between investigated SCADA signals in terms of correlation measure R^2. Blue arrows depict single-input predictions (with $R^2 > 0.25$), grey arrows contributions to a combination of two inputs in a node marked with '+' and red arrows combined predictions significantly better than individual modelling.

Conclusions

GBM, RF and ANN showed very good for prediction active power and tower vibrations. Nonetheless, **ANN showed slightly better results**, especially for predicting the tower vibrations, and were used to carry out a sensitivity study demonstrating the variable importance of the predictors and the predicted parameters. The **sensitivity study** suggests how **to interpret the synergistic effects of combined measurements** to predict a specific response and helps to select a suitable set of sensors for the predictions of others.

References

[1] Rademakers, L., Braam, H., Obdam, T., Pieterman, R.. Operation and maintenance cost estimator (OMCE) to estimate the future O&M costs of offshore wind farms. European Offshore Wind 2009 Conference 2009;(1):p.14–16.
[2] Besnard, F., Nilsson, J., Bertling, L. On the economic benefits of using Condition Monitoring Systems for maintenance management of wind power systems. In: 2010 IEEE 11th International Conference on Probabilistic Methods Applied to Power Systems. IEEE; 2010, p.160–165.
[3] Artigao, E., Colone, L., Pandit, R., Reder, M., Weinert, J., Ziegler, L.. Optimisation of data acquisition in wind turbines with data-driven conversion functions for measurements. Tech. Rep.; 2016. Melero, J.J., Muskulus, M., Smolka, U., editors. In: 1st Joint Industry Workshop Scientific report; Zaragoza, Spain; URL: http://awesome-h2020.eu/1st-joint-industry-workshop-scientific-report/. Last Accessed: 12/01/2017.
[4] Nelder, J., Wedderbu, R. Generalized Linear Models. Journal of the Royal Statistical Society, Series A-General 1972;135(3):p.370-384.
[5] Breiman, L.. Random Forests. Tech. Rep.; Statistics Department - University of California; Berkeley, CA; 2001. URL: http://link.springer.com/10.1023/A:1010933404324. Last Accessed: 12/01/2017.
[6] Friedman, J.H. Greedy Function Approximation : A Gradient Boosting Machine. The Annals of Statistics 2001;29(5):p.1189–1232.
[7] Bangalore, P., Tjernberg, L.B. An Artificial Neural Network Approach for Early Fault Detection of Gearbox Bearings. IEEE Transactions on Smart Grid 2015;6(2): p.980–987.

DTU
circe
RESEARCH CENTRE FOR ENERGY RESOURCES AND CONSUMPTION
Loughborough University

The authors thank the participants of the *1st Joint Industrial Workshop (JIW)* within the AWESOME project, in particular Estefania Artigao, Ravi Pandit, Lisa Ziegler, Michael Muskulus and Ursula Smolka, who contributed to the development of the idea.
This project has received funding from the European Union's Horizon 2020 research and innovation programme under the Marie Skłodowska-Curie grant agreement No 642108.

Design and fatigue analysis of monopile foundations to support the DTU 10 MW offshore wind turbine

Joey Velarde*, Erin E. Bachynski

Department of Marine Technology, Norwegian University of Science and Technology, NO-7491 Trondheim, Norway

INTRODUCTION

This study focuses on FLS analysis of large monopile foundations. Preliminary monopile designs for four water depths are established to support the DTU 10 MW reference wind turbine [1]. Pile-soil interaction is accounted for by deriving nonlinear P-Y curves using a finite element (FE) method. A method for predicting fatigue damage using fewer sea states is introduced and shown to be promising for the given designs and location.

MODELING AND SIMULATION

Pile-soil interaction for large-diameter piles is modeled in Plaxis 3D [2] using the methodology proposed by Hanssen [3]. For a 30,000 kN applied load, the resulting interface stresses and pile displacement are illustrated in **Fig. 1**. Nonlinear P-Y curves representing the lateral stiffness of the soil were extracted and used as main input in the aero-hydro-servo-elastic tool, RIFLEX [4].

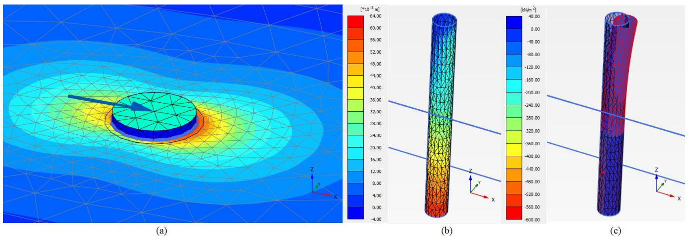

Figure 1: Graphical stress and displacement calculation showing (a) Load application, (b) Stress at the interface and (c) pile defection

RIFLEX is a modeling tool capable of static, dynamic and eigenvalue analysis based on FE analysis with beam (or bar) elements. The DTU 10 MW RWT model is shown in **Fig. 2**. Unidirectional loads due to wind, wave and current are applied for all simulations. Preliminary pile dimensions (see **Table 1**) were designed to achieve an overall natural frequency within the soft-stiff region (0.25 Hz) while satisfying ULS and stability requirements [5,6].

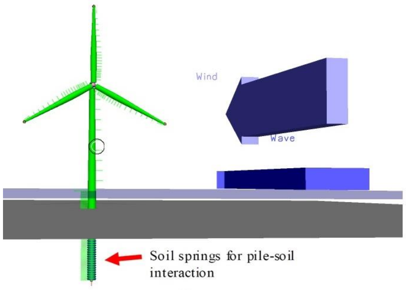

Figure 2: DTU 10 MW model in RIFLEX

Hydrodynamic loads on the monopile are modelled using Morison's equation and linear wave kinematics (with constant potential up to the instantaneous free surface), while aerodynamic loads are computed using the blade element/momentum theory.Fatigue damage is calculated for a reduced set of 29 operational conditions from the long-term wind and wave distribution (Site 15) of the MARINA platform project [7].

Table 1: Preliminary monopile design

Water depth [m]	Pile diameter [m]	Pile thickness [mm]	Tower D scale [-]	Tower thickness scale [-]	Penetration Depth [-]	Natural Frequency [Hz]
20	9	110	1.125	1.25	35	0.251
30	9	110	1.125	1.75	45	0.251
40	10	125	1.25	1	35	0.249
50	10	125	1.25	1.5	45	0.251

FATIGUE DAMAGE PARAMETER (FDP)

FDP is established to correlate fatigue damage with the parameters thrust, H_s, and T_p. The formulation assumes that wind and wave interaction is insignificant and fatigue damage is not directly correlated with mean thrust. **Fig.3** outlines the procedure for estimating fatigue damage.

Calculate FDP for all environmental conditions of the scatter diagram → Select N representative conditions with the highest FDP value → Conduct simulations and calculate fatigue damage from N selected conditions → Calculate total fatigue damage by applying a scale factor based on normalized FDP

Figure 3: FDP procedure for calculating fatigue damage

The formulations for the FDP and the scale factor (S_F) are given below. M is the total number of environmental conditions, while N is the number of conditions for which simulations are carried out.

$$FDP = H_s^5 \, T_p^{-11} P \qquad (1)$$

$$(FDP_{norm})_i = \frac{FDP_i}{\sum_{i=1}^{M}(FDP_i)} \qquad (2)$$

$$S_F = \frac{\sum_{i=1}^{M}(FDP_{norm})_i}{\sum_{i=1}^{N}(FDP_{norm})_i}, \text{ where } \sum_{i=1}^{M}(FDP_{norm})_i = 1 \qquad (3)$$

RESULTS

The calculated 20-year fatigue damage is shown in the outer envelope of **Fig. 4**. The relative contribution of each sea state (arranged in increasing H_s) implies that hydrodynamic loads become more significant with higher depths.

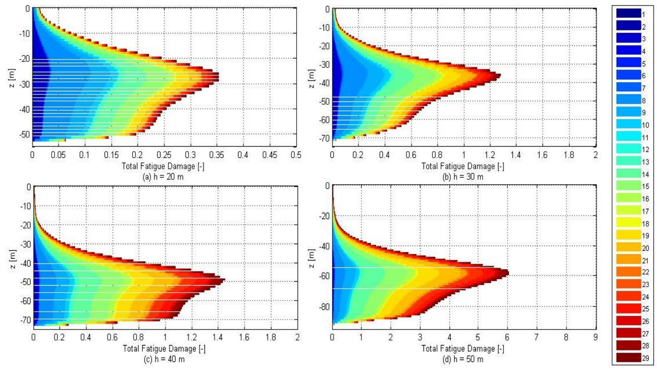

Figure 4: Total fatigue damage, showing contributions from each environmental condition.

The calculated fatigue damage for different numbers of representative conditions (N = 3, 9, 15, 20, 26) out of 29 sea states is shown in **Fig. 5**. The accuracy of damage prediction at the section where maximum fatigue damage occurs is shown in **Fig. 6**.

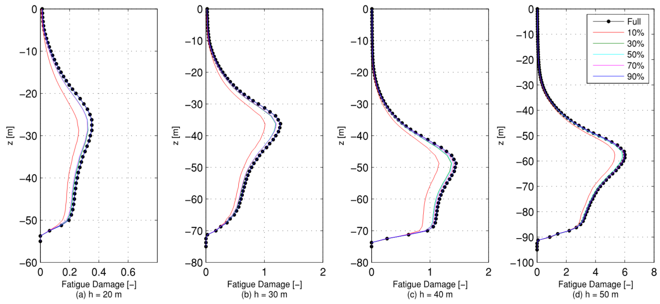

Figure 5: Fatigue damage prediction (along the monopile, where 0 is the mean still water level) for different values of N

Using a larger number of sea states generally increased the accuracy of prediction. The method is also observed to be more accurate for higher water depths. Using at least 30% of the total number of conditions resulted in at least 90% accuracy.

Further work includes accounting for wave diffraction, investigation of the applicability of the FDP procedure with other types of support structures and other (more extensive) site-specific environmental conditions, including misalignment.

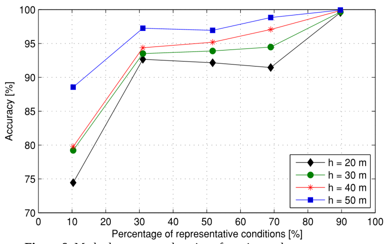

Figure 6: Method accuracy at location of maximum damage

ACKNOWLEDGEMENT

The author acknowledges the support from the European Commission through the Erasmus Mundus European Wind Energy Master (EWEM) Program. The authors also wish to acknowledge the financial support from Research Council of Norway through Center for Ships and Ocean Structures (CeSOS) and Centre for Autonomous Marine Operations and Systems (AMOS, RCN project number 223254). Thanks are extended to Dr. Stian Baardsgaard Hanssen, Prof. Gudmund Reidar Eiksund, Asst. Prof. Eliz-Mari Lourens and Prof. Andrei Metrikine for stimulating discussions.

REFERENCES

[1] Bak C, Zahle F, Bitsche R, Kim T, Yde A, Henriksen LC, Andersen PB, Natarajan A, Hansen MH. Design and performance of a 10 MW wind turbine. DTU Wind Energy Report; 2013.
[2] PLAXIS. PLAXIS 2015, The Netherlands; 2015.
[3] Hanssen SB. Response of laterally loaded monopiles, PhD Thesis. Norwegian University of Science and Technology, Trondheim, Norway. 2016:226, ISBN 978-82-326-1791-3.
[4] Ormberg, Harald, and Erin E. Bachynski. Global analysis of floating wind turbines: Code development, model sensitivity and benchmark study. The Twenty-second International Offshore and Polar Engineering Conference. International Society of Offshore and Polar Engineers, 2012.
[5] Det Norske Veritas. Design of Offshore Wind Turbine Structures. Technical Report, DNV; 2014. DNV-OS-J101.
[6] Krolis VD, van der Zwaag GL, de Vries W. Determining the Embedded Pile Length for Large-Diameter Monopiles. Marine Technology Society Journal; 2010.p. 24-31.
[7] Li L, Gao Z, Moan T. Joint Environmental Data at Five European Offshore Sites for Design of Combined Wind and Wave Energy Concepts. ASME 2013 32nd International Conference on Ocean, Offshore and Arctic Engineering; Nantes, France, 2013.

EERA DEEPWIND'2017 14TH DEEP SEA OFFSHORE WIND R&D CONFERENCE
18 - 20 JANUARY 2017
TRONDHEIM, NORWAY

*Contact: jovl@cowi.com

DTU Wind Energy
Department of Wind Energy

DTU

Response analysis of a 10MW floating wind turbine: flexible substructure modelling in HAWC2 & WAMIT

Michael Borg, Anders M Hansen and Henrik Bredmose

Motivation

Until recently, substructure flexibility was not considered during integrated dynamic simulations of floating wind turbines due to the relative placement of substructure natural frequencies. As floater dimensions increase to support larger turbines, substructural flexibility may increase to the extent where substructure natural frequencies approach the range of wave and wind turbine excitations. Therefore it becomes relevant to include substructure flexibility within integrated dynamic calculations to capture the relevant physical and load effects on the wind turbine.

Previous work by Borg et al. [1] described a method to achieve this, implemented in HAWC2 and WAMIT, and illustrated the method for a 10MW wind turbine on a simplified spar platform. The present work applies the method to the Triple Spar concept [2], and illustrates the influence of substructure flexible modes on the response of the wind turbine and platform.

Flexibility in HAWC2 & WAMIT

The process of setting up such a dynamic model first involves a number of pre-processing steps that establish the relevant flexible modes of the substructure, the associated hydroelastic effects and a reduced model representing the substructure, illustrated below.

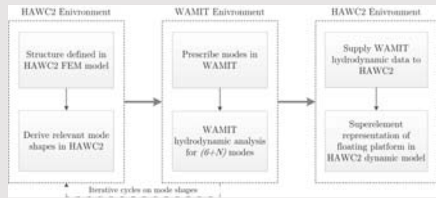

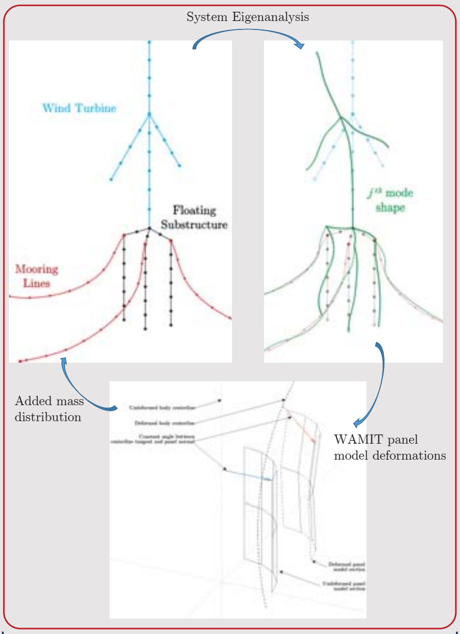

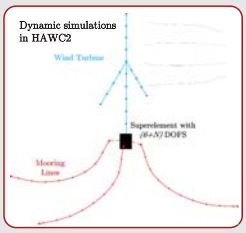

Floating Wind Turbine

Draft [m]	54.46
Water depth [m]	180.0
System mass [t]	29278.4
Displacement [m³]	29311.1
Rated power [MW]	10.0
Rated wind speed [m/s]	11.4
Rated RPM [-]	9.6
Hub height [m]	119.0
Tower length [m]	90.63
Column diameter [m]	15.0
Column distance to centreline [m]	26.3
Heave plate diameter [m]	22.5
Catenary line length [m]	610.0
Fairlead/Anchor radius [m]	54.58/600
Fairlead height above MSL [m]	8.7
Dry/Wet mass per unit length [kg/m]	594/517

The Triple Spar concept [2], depicted above, was considered as a case study. The platform consists of 3 vertical reinforced concrete, partially ballasted cylinders connected to the tower base through a steel tripod structure. A catenary mooring system is used consisting of three lines, where each one is connected to each cylinder. The platform is oriented such that in aligned wind and wave conditions, two cylinders are located upwind of the turbine and one cylinder is located directly downwind of the turbine.

Using the HAWC2 implementation described in [3], an eigenanalysis of the system was carried out and 6 substructure flexible modes were identified to be relevant to the wave and wind turbine excitation frequency ranges. They were included in the reduced order hydroelastic model that forms the superelement within the HAWC2 dynamic calculations. The flexible modes and relative placement in the frequency spectrum are illustrated below.

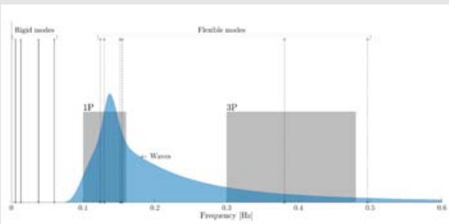

Two load cases were considered, representing rated stochastic operating conditions and an extreme event represented by a focused wave. For each load case, dynamic calculations were carried out with and without the substructure flexibility included in the model, labelled 'flexible' and 'rigid', respectively, within the following figures.

	U_{hub} [m/s]	H [m]	T_p [s]	Duration [s]
LC1	11.4	4.16	7.30	3600.0
LC2	11.4	18.84	-	700.0

Transient Response

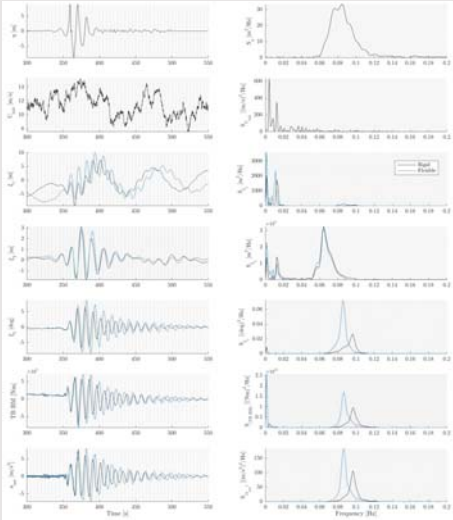

Flexible modes significantly affect pitch, tower bending moment and nacelle accelerations. This is due to resonance of a flexible mode induced by the focused wave.

Stochastic Response

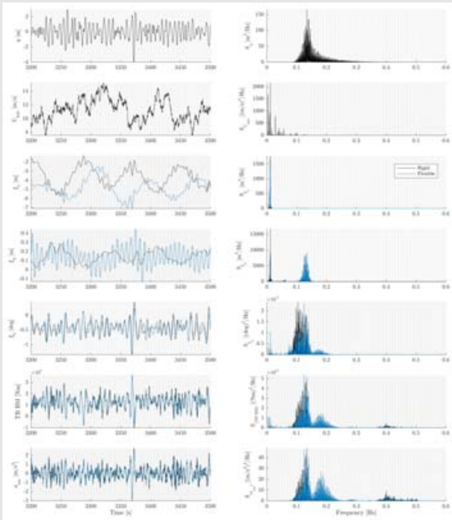

In stochastic wind and wave conditions, the substructure flexible modes augment the response around the peak wave frequency, as well as close to the tower bending mode (0.4Hz). In heave there is a significant increase in response around the peak wave frequency, but it should be noted that hydrodynamic viscous forcing was not included for flexible modes and as such these results are only qualitatively indicative of the increased motion in heave.

References

[1] Borg M, Hansen AM, Bredmose H (2016) Floating substructure flexibility of large-volume 10MW offshore wind turbine platforms in dynamic calculations. *J. Phys.: Conf. Ser.*, **753**, p. 082024.
[2] Lemmer F, Amann F, Raach S, Schlipf D (2016) Definition of the SWE-TripleSpar floating platform for the DTU 10MW reference wind turbine. *University of Stuttgart*
[3] Borg M (2016) Generic floating substructure configuration and numerical models for wind turbine controller tuning in LIFES50+. *DTU WE Report-I-0449.*

Acknowledgements

The authors acknowledge that this project has received funding from the European Union's Horizon 2020 research and innovation programme under grant agreement No 640741 (LIFES50+)

A New Foundation Model for Integrated Analyses of Monopile-based Offshore Wind Turbines

NTNU Norwegian University of Science and Technology

Ana M. Page[1,2], Kristoffer S. Skau[1,2], Hans Petter Jostad[1,2], Gudmund R. Eiksund[1]

[1] *Norwegian University of Science and Technology (NTNU), Trondheim, Norway*

[2] *Norwegian Geotechnical Institute (NGI), Oslo, Norway*

NGI

Introduction

For monopiles supporting offshore wind turbines (OWT), the current design practice is to model the foundation response by API *p-y* curves [1].

Discrepancies between the API *p-y* curves and the actual pile behaviour have been identified:

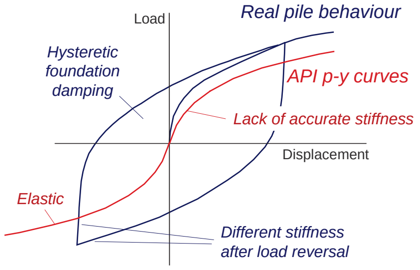

Their applicability to predict pile behaviour in integrated analyses of OWT has been questioned, and new foundation models are needed.

Findings from Finite Element Analyses

3D Finite Element Analyses (FEA) of the soil volume and the foundation have been performed for different soil profiles with the software PLAXIS 3D. A 6 m diameter steel pile, with a wall thickness of 0.06 m, embedded 36 m in an overconsolidated clay is considered. The soil response is reproduced with the NGI-ADP [2], a constitutive model which mimics the behaviour of cohesive soils.

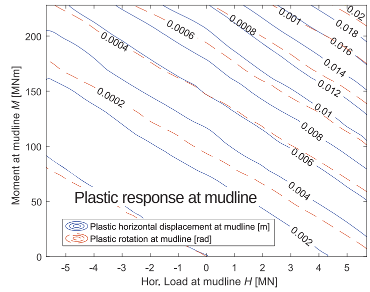

Changing the reference point

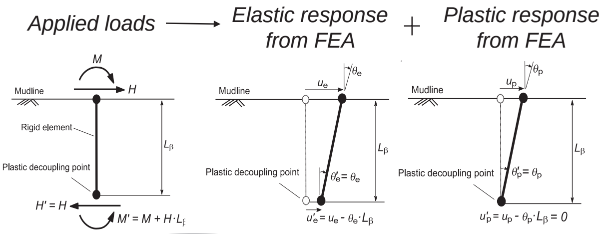

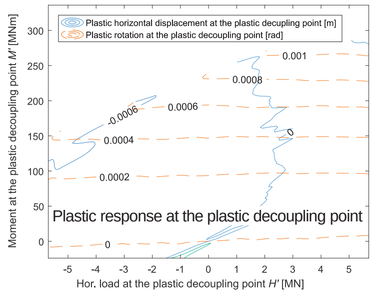

A new foundation model

The model follows the macro-element concept, where the response of the foundation and the surrounding soil is reduced to a force - displacement relation at mudline.

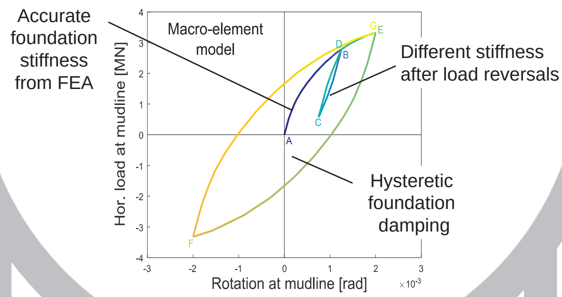

Comparison with API *p-y* model response

In contrast to the API *p-y* curves, the new model can reproduce different foundation stiffness for unloading and reloading and foundation damping depending on the loading history, which is observed in real pile behaviour.

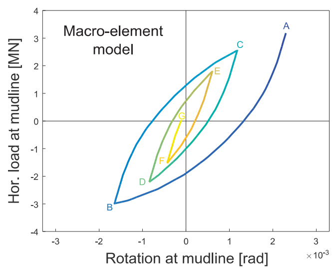

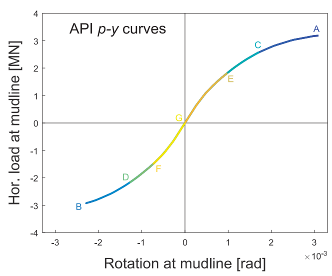

Model formulation

The relation between displacements and forces at the plastic decoupling point:

$$u' = u'_e + u'_p = u'_e(H') + u'_e(M') + \underbrace{u'_p(H') + u'_p(M')}_{0}$$

$$\theta' = \theta'_e + \theta'_p = \theta'_e(H') + \underbrace{\theta'_e(M') + \theta'_p(M')}_{\theta'_{M'}(M')} + \underbrace{\theta'_p(H')}_{0}$$

Where:

- $u'_e(H'), u'_e(M')$ and $\theta'_e(H')$ can be calculated with an elastic stiffness matrix.
- The relation between $\theta'_{M'}(M')$ and M' is elasto-plastic, and can be reproduced by a 1D kinematic hardening model [3]:

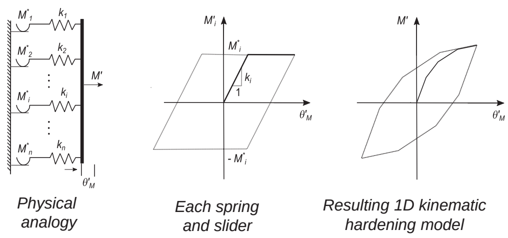

The model is composed of a rigid element connecting mudline with the plastic decoupling point, an elastic stiffness matrix and a 1D kinematic hardening model

Calibration and implementation

The calibration of the foundation model requires two types of input:

- Elastic stiffness matrix.
- A table containing the moment, horizontal displacement and rotation at mudline from non-linear FEA with $H = 0$.

The macro-element model is being implemented in the OWT load simulation code *3DFloat* [4] via a *dll* interface.

Discussion and conclusions

A simple macro-element foundation model for piles with an intuitive physical analogue has been developed. The formulation is based on trends observed in FEA of the soil and the foundation.

A fixed plastic decoupling point is assumed in the formulation. This assumption seems to be acceptable for fatigue load levels, but needs to be checked for higher load levels.

Acknowledgements

The financial support by the Norwegian Research Council and industrial partners through REDWIN is gratefully acknowledged.

[1] American Petroleum Institute, Recommended Practice for Planning, Designing and Constructing Fixed Offshore Platforms, 2011.

[2] G. Grimstad, L. Andresen, H.P. Jostad, NGI-ADP: Anisotropic shear strength model for clay, International Journal for Numerical and Analytical Methods in Geomechanics, 36 (2012) 483-497.

[3] W.D. Iwan, On a class of models for the yielding behavior of continuous and composite systems, Journal of Applied Mechanics, 34 (1967) 612-617.

[4] T.A. Nygaard, J. De Vaal, F. Pierella, L. Oggiano, R. Stenbro, Development, Verification and Validation of 3DFloat; Aero-servo-hydro-elastic Computations of Offshore Structures, Energy Procedia, 94 (2016) 425-433.

University of Stuttgart

Damage Assessment of Floating Offshore Wind Turbines Using Response Surface Modeling

Kolja Müller[a], Martin Dazer[b], Po Wen Cheng[a]
[a]Stuttgart Wind Energy (SWE), University of Stuttgart
[b]Institute of Machine Components (IMA), University of Stuttgart

Problem Description

Fatigue assessment for floating wind turbines is commonly established by comprehensive simulation studies of integrated time-domain simulations. Procedures which incorporate simplifications of the environment in order to limit the number of simulations typically lead to more conservative designs. An alternative approach is proposed here based on response surface modeling using Latin hypercube sampling and artificial neural networks (ANN). The presented method takes into account the statistical characteristics of environmental parameters during the systems life time (resulting in more realistic and accurate damage calculations) while keeping the numerical effort to a minimum.

Considered System and Environment

The considered system is the **DTU10MW** reference turbine positioned on the **SWE TripleSpar**. The turbine's characteristic wind speeds are:
$v_{cut-in} = 4\ \frac{m}{s}, v_{rated} = 11.4\ \frac{m}{s}, v_{cut-out} = 25\ \frac{m}{s}$
Simulations are carried out in time domain using **FAST8**, using BEM for aerodynamics, first-order potential-flow theory for hydrodynamics and a quasi-static model with dynamic relaxation for mooring line forces (MoorDyn).

Figure 1: considered system

The environment is set up based on **LIFES50+ site A** (mild environmental conditions) design load case (DLC) 1.2 [1]. Measurement data based on the ANEMOC and CANDHIS buoy network is used as well as FINO1data for turbulence intensity.

The variations of **wind speed, turbulence intensity, wave height and wave period** are considered in this study. Three **load ranges** are defined for differentiating between fundamentally different system behavior based on the controller mode: partial load range below rated wind speed (PLR), transitional load range around rated wind speed (TLR) and full load range above rated wind speed (FLR)

A reference case was established for comparison based on conservative assumptions of environmental conditions.

Response Surface Modeling (RSM)

The overall procedure used in this study is as follows:

1) Define simulation points using **Latin hypercube sampling (LHS).** We considered 3 different sample sizes for each load range: 50, 100 and 150

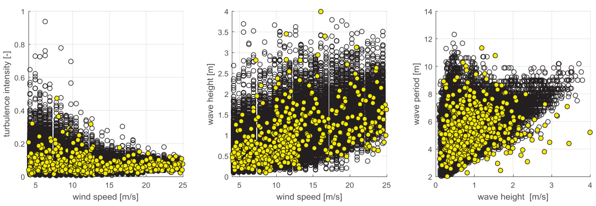

Figure 2: Environmental conditions. Original data from measurements (black) and determined from LHS-algorithm (shown here are the version with 150 samples per load range resulting in a total of 450 data points to be evaluated for the complete power production load case).

2) Carry out simulations, calculate damage equivalent loads (**DEL**)

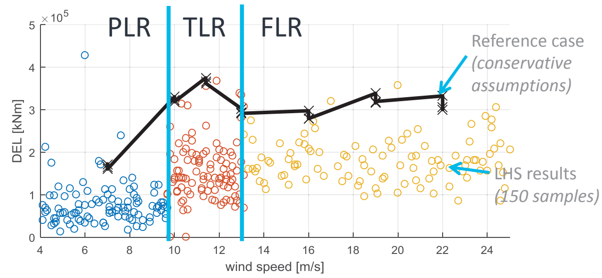

Figure 3: Tower base fore-aft DEL results for all load ranges (PLR: blue, TLR: red, FLR: yellow) from LHS simulations based on 150 samples.

3) Based on the simulation results, determine a **response surface using artificial neural network (ANN) regression.** Then, evaluate the regression model at defined bin centers of the environmental model. As the regression results change with each run, 20 regression evaluations were performed and the statistics of the results are analyzed.

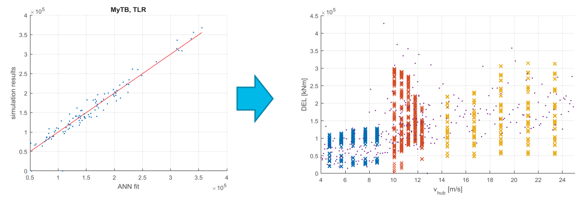

Figure 4: Performance of ANN describing damage equivalent load of tower base fore-aft bending moment. Simulation results vs. ANN fit- results (left plot) and
Exemplary comparison of LHS simulation results (dots) and RSM evaluation at grid center points (150 samples, all load ranges. PLR: blue x, TLR: red x, FLR: yellow x). (right plot)

4) Weight all bin-center DELs according to the related bin occurrence probability. Then calculate the **resulting DELs over lifetime.**

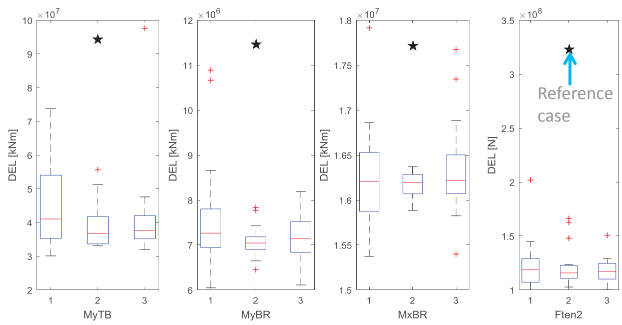

Figure 5: Box plots of predicted overall DELs from RSM evaluations for different positions (tower base, blade root, fairlead mooring line) based on different numbers of samples (1:50, 2:100, 3:150). Plot indicating median, 25th and 75th percentiles (boxes) and 0.35th and 99.65th percentiles (whisker). DELs from reference calculation indicated by ★.

Conclusions and Outlook

The first results of this initial, hypothetical study promise that a fully stochastic approach for fatigue assessment is possible and indicate the potential for a significant reduction of the fatigue load estimate. Future studies will focus on more accurate regression models and include more environmental conditions (e.g. wind direction, wind-wave misalignment, etc.).

Acknowledgements and References

The research leading to these results has received partial funding from the European Union's Horizon 2020 research and innovation programme under grant agreement No. 640741 (LIFES50+).

[1] Antonia Krieger, Gireesh K. V. Ramachandran, Luca Vita, Pablo Gómez Alonso, Joannès Berque and Goren Aguirre, "LIFES50+ D7.2 Design Basis" DNVGL, Tech. rep. 2015.

SWE Stuttgart Wind Energy @ Institute of Aircraft Design

www.ifb.uni-stuttgart.de/windenergie

Development and validation of an engineering model for floating wind turbines

Antonio Pegalajar-Jurado (ampj@dtu.dk), Michael Borg and Henrik Bredmose
DTU Wind Energy, Nils Koppels Allé, Building 403, DK-2800 Kgs. Lyngby, Denmark

Introduction

The initial phase in the design of a floating platform for offshore wind deployment involves simulations of several configurations under different environmental conditions. Time-domain numerical tools, although accurate, can be computationally expensive if one needs to evaluate several floater designs. A quick, frequency-domain model (QuLA, Quick Load Analysis) for bottom-fixed offshore wind turbines has been recently developed at DTU Wind Energy [1]. Now, we have extended the QuLA model to a floating foundation: QuLAF. The tool is here benchmarked against a FAST [4] model of the same floating wind turbine, which has been validated against test data. The FAST model is also used for cascading, i.e. enhancement of the engineering model by using the state-of-the-art model. Once fully validated, QuLAF can become a reliable tool to be employed in the first stages of floater design, while more advanced, state-of-the-art codes can be used once the conceptual floater design is established.

Results

Response to regular waves

The response is dominated by the wave frequency.

There is a very good match in the response to regular waves for all degrees of freedom.

Response to irregular waves and wind

The response shows energy at the wave and wind frequency ranges, which are able to excite some of the system natural frequencies – marked for each DoF with a black line in the PSD plot.

The match is good, and it can be further improved by a better calibration of the hydrodynamic damping, which is part of the planned future work.

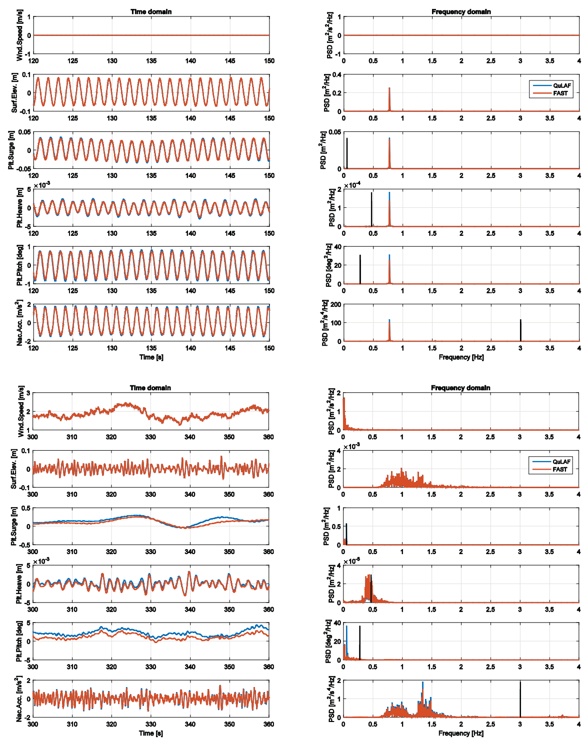

QuLAF model in a nutshell

- Linear, frequency-domain model
- Quick: ratio simulation time/CPU time up to 1000
- DTU10MW wind turbine on SWE-TripleSpar [2] floater, 1:60 scale
- 4 DoF: floater surge, heave, pitch and tower modal deflection
- EoM in frequency domain: $\left(-\omega^2\left(\boldsymbol{M}+\boldsymbol{A}(\omega)\right)+i\omega\boldsymbol{B}(\omega)+\boldsymbol{C}\right)\boldsymbol{x}(\omega)=\boldsymbol{F}(\omega)$
- Hydrodynamic loads extracted from diffraction-radiation solver WAMIT [3]
- Hydrodynamic viscous effects included through Morison drag term
- Aerodynamic loads precomputed with FAST for a fixed hub
- Aerodynamic damping extracted from free decay simulations in wind
- Mooring system linearized around equilibrium position

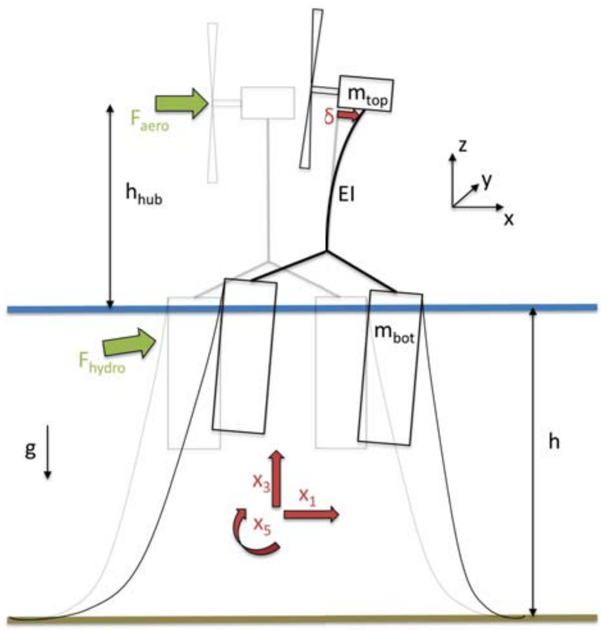

Literature cited

[1] Schløer S, Castillo LG, Fejerskov M, Stroescu E, Bredmose H, 2016. A model for Quick Load Analysis, QuLA, for bottom fixed offshore wind turbine substructures. *Journal of Physics: Conference series*, vol.753, 092008.

[2] Lemmer F, Amann F, Raach S, Schlipf D, 2016. Definition of the SWE-TripleSpar floating platform for the DTU 10MW reference wind turbine. Tech. rep., University of Stuttgart.

[3] Lee C, Newman J, 2006. *WAMIT ® User Manual, Versions 6.3, 6.3PC, 6.3S, 6.3S-PC*. Chestnut Hill, MA.

[4] Jonkman J, Jonkman B. NWTC Information Portal (FAST v8). https://nwtc.nrel.gov/FAST8

Acknowledgments

This work is part of the project LIFES50+. The research leading to these results has received funding from the European Union Horizon2020 programme under the agreement H2020-LCE-2014-1-640741.

DTU Wind Energy
Department of Wind Energy

LIFES50+

Prediction of the shape of extreme inline force and free surface elevation using First Order Reliability Method (FORM)

Amin Ghadirian (amgh@dtu.dk), Henrik Bredmose and Signe Schløer
DTU Wind Energy, Nils Koppels Allé, Building 403, DK-2800 Kgs. Lyngby, Denmark

1. Introduction

The extreme wave loads which are of interest in these cases are estimated by choosing extreme events from linear random sea states and replacing them by either non-linear regular waves (stream function wave theory) or the New Wave theory combined with a stretching method as suggested in the design requirements.

Both of these theories are associated with imitations the most important of which is the symmetry of these waves. FORM, was used in the present work systematically to estimate the extreme wave shapes.

Two parameters of maximum crest height and maximum inline force were used as definers of extreme events.

The results of this process were then compared to the designer wave (wave averaged measurements) of the same criteria (same maximum crest height or maximum inline force).

2. Experiments

The experiments were conducted in the shallow water basin at DHI Denmark at a scale of 1:50.

The full scale diameter of the monopile was 7~m and the water depth was 33~m and 20~m. The monopile was mounted on two force transducers to measure the in-line force and the bending moment.

25 distinct random sea states were tested for a length of between 6 to 70 hours (in lab scale) from which four were selected to investigate in the current paper.

The four sea states were tested both with and without 3D spreading.

3. First Order Reliability Method

Reliability is defined as the probability of failure function, X, being larger than zero where **X** is a vector of stochastic input variables.

First Order Reliability Method (FORM) uses first order Taylor expansion to find the shortest distance between the failure function and center of combined probability distribution of the input variables.

In other words, FORM provides one with the most probable combination of the stochastic inputs that lead to failure and the probability of its occurrence.

This method can be used for structural reliability analysis and for extreme value prediction.

$$\begin{aligned}
\eta^{(1)} &= \textstyle\sum_{j=1}^{N_{freq}} \sum_{i=1}^{N_{dir}} (a_{ij}\cos(\omega_{ij}t) + b_{ij}\sin(\omega_{ij}t)) \\
g &= |\eta_{expected} - \eta^{(1)}| \\
\textit{Represented by} &: FORM(\eta_1)
\end{aligned}$$

$$\begin{aligned}
\eta^{(2)} &= \tfrac{1}{4}\textstyle\sum_{i=1}^{N_{freq}} \sum_{j=1}^{N_{freq}} \cdots \\
&\quad \textstyle\sum_{k=1}^{N_{dir}} \sum_{l=1}^{N_{dir}} \cdots \\
&\quad (a_{ik} + ib_{ik})(a_{jl} + ib_{jl})[\{C^-_{ijkl}\}\cos(\omega_{ik}t - \omega_{jl}t) + \{C^+_{ijkl}\}\cos(\omega_{ik}t + \omega_{jl}t)] \\
g &= |\eta_{expected} - (\eta^{(1)} + \eta^{(2)})| \\
\textit{Represented by} &: FORM(\eta_1 + \eta_2)
\end{aligned}$$

$$\begin{aligned}
F^{(1)} &= \rho A C_M \textstyle\int_{-h}^{0} u_t^{(1)} dz \\
g &= |F_{expected} - F^{(1)}| \\
\textit{Represented by} &: FORM(F_1)
\end{aligned}$$

$$\begin{aligned}
F^{(2)} &= \rho A C_M \textstyle\int_{-h}^{0} u_t^{(2)} + u^{(1)}u_x^{(1)} + w^{t} \\
&\quad \rho A C_m \textstyle\int_{-h}^{0} u^{(1)} w_z^{(1)} dz + \\
&\quad 0.5\rho D C_D \textstyle\int_{-h}^{0} u^{(1)}|u^{(1)}| dz + \\
&\quad \rho A C_M \eta u_t^{(1)}(z = 0) \\
g &= |F_{expected} - (F^{(1)} + F^{(2)})| \\
\textit{Represented by} &: FORM(F_1 + F_2)
\end{aligned}$$

where:

$(a_{i,j}, b_{i,j}) \in N(0, \sqrt{S_{\omega\theta}\partial f \partial\theta})$

4. New Wave and New Force theories

New Wave:

$$\eta_{\text{New Wave}}(\mathbf{X}, \tau) = \frac{\alpha_\eta}{\sigma_\eta^2} \sum_n \sum_m \mathrm{Re}\{d_{n,m} \exp(i(\mathbf{k}_{n,m} \cdot \mathbf{X} - \omega_n \tau))\}$$

where

$$d_{n,m} = S_\eta(\omega_n)\Delta\omega_n\Delta\theta_m$$

And $k_{n,m}$ is the linear wave number vector. Further:

$$\mathbf{X} = \mathbf{x} - \mathbf{x}_1$$

$$\sigma_\eta^2 = \overline{\eta^2} = \int_{\theta=0}^{2\pi} \int_{\omega=0}^{\infty} S_\eta(\omega_n, \theta_m) d\omega\, d\theta$$

The force transfer function is defined as

$$\Gamma(\omega, \theta) = i\rho\pi R^2 C_M \cos(\theta)\omega^2 / k$$

So the inline force time series of New Wave is

$$F_{\text{New Wave}}(\mathbf{X}, \tau) = \frac{\alpha_\eta}{\sigma_\eta^2} \sum_n \sum_m \mathrm{Re}\{d_{n,m}\Gamma(\omega_n, \theta_m) \exp(i(\mathbf{k}_{n,m} \cdot \mathbf{X} - \omega_{n,m}\tau))\}$$

New Force:

$$S_F(\omega, \theta) = |\Gamma(\omega_n, \theta_m)|^2 S_\eta$$

$$F_{\text{New Force}}(\mathbf{X}, \tau) = \frac{\alpha_F}{\sigma_F^2} \sum_m \sum_n \mathrm{Re}\{S_F \Delta\omega\Delta\theta \exp(i(\mathbf{k}_{n,m} \cdot \mathbf{X} - \omega_n \tau))\}$$

Free surface elevation time series of the New Force is

$$\eta_{\text{New Force}}(\mathbf{X}, \tau) = \frac{\alpha_F}{\sigma_F^2} \sum_m \sum_n \mathrm{Re}\{\Gamma^*(\omega_n, \theta_m) S_\eta \Delta\omega\Delta\theta \exp(i(\mathbf{k}_{n,m} \cdot \mathbf{X} - \omega_n \tau))\}$$

5. Results

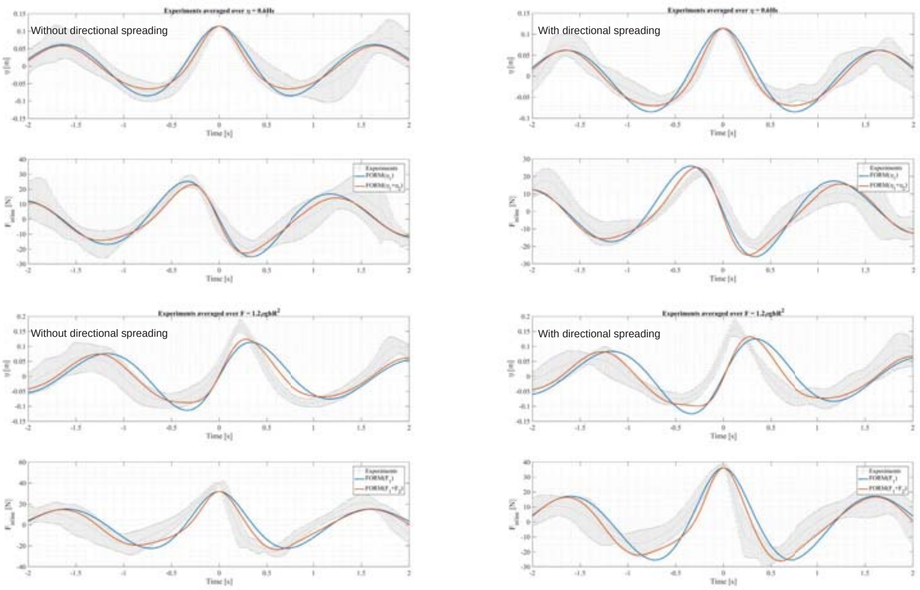

6. Conclusions

In summary, a relatively good agreement between the First Order Reliability Method results of free surface elevation including the second order effects, and the wave averaged measurements was observed. It can be concluded that with a more nonlinear model a better agreement between the numerical results and the measurements is expected.

The inline force time series reproduced using the numerical method were not as consistent with the measurements as the free surface elevation time series. This was explained with the negligence of the drag terms above still water level. Hence a more nonlinear model, can reduce this discrepancy too.

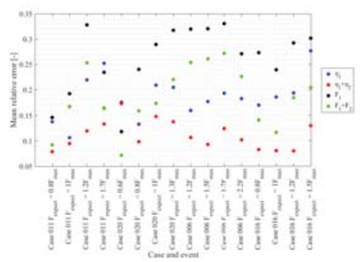

Literature cited

[1] Grice, J.R., Taylor, P.H., Taylor, R.E.. Second-order statistics and designer ' waves for violent free-surface motion around multi-column structures Subject Areas : 2014.

[2] Jensen, J.J.. Extreme value predictions and critical wave episodes for marine structures by FORM. Ships and O shore Structures 2008;3(4):325–333.

[3] Schløer, S., Bredmose, H.. Analysis of experimental data: The average shape of extreme wave forces on monopile foundations. In: DeepWind. 2017,.

[4] Ghadirian, A., Bredmose, H., Dixen, M.. Breaking phase focused wave group loads on oshore wind turbine monopiles. Journal of Physics: Conference Series 2016;753:092004.

Acknowledgments

The present research was partly funded by the DeRisk project of Innovation Fund Denmark, grant number 4106-00038B. Further funding was provided by Statoil, DHI and DTU. All funding is gratefully acknowledged.

A 3D FEM model for wind turbines support structures

Alexis Campos; **Climent Molins**; Pau Trubat; Daniel Alarcón
Universitat Politècnica de Catalunya. Escola de Camins
UPC BARCELONATECH

Dynamic co-rotational FE analysis for FOWT's

With the aim of improving the tools for the analysis of floating spar type structures for offshore wind turbines, a model which includes the nonlinear FEA for large displacements based on a co-rotational formulation is under development at the UPCBarcelonaTech.

The model is able to take into account the wind loads over the structure, the hydrodynamic loads from the wind turbine, hydrodynamic loads, the elasticity of the full structure and the mooring response in both, in quasi static or accounting for its dynamics. All forces integrated in the time domain. The model assumes one-dimensional beam elements, extended to the 3D domain.

FEM discretization

The FE numerical model is based in the Euler beam theory, which in combination with elasticity and one-dimensional finite elements may be used to analyze the most common types of onshore and offshore wind turbines support structures. Also special elements like rigid links are implemented to deal with some limitations of the one-dimensional elements as shown in an example below.

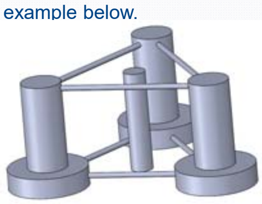

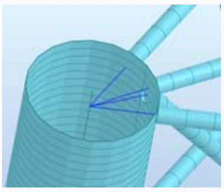

Co-rotational approach

To analyze floating structures with large rigid body motions but small strains, a consistent co-rotational formulation for dynamic analysis proposed by Crisfield [1] is implemented. This formulation allows the computation of the equivalent local angles with respect a co-rotational frame, which is moving attached to the element as shown.

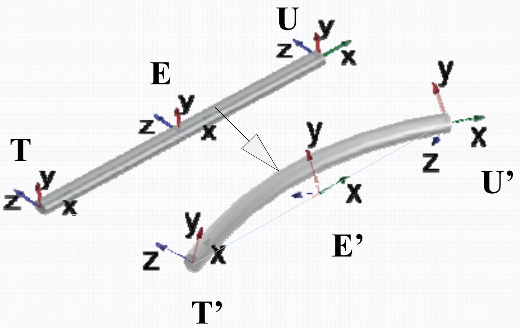

Dynamic Analysis

The dynamic analysis is performed in the time domain by solving the equations of motion of the system, based on the Newton's 2nd law. For the time integration a Hilber-Huges-Taylor [2] scheme is adopted in combination of an iterative Newton-Raphson method to deal with the nonlinearity.

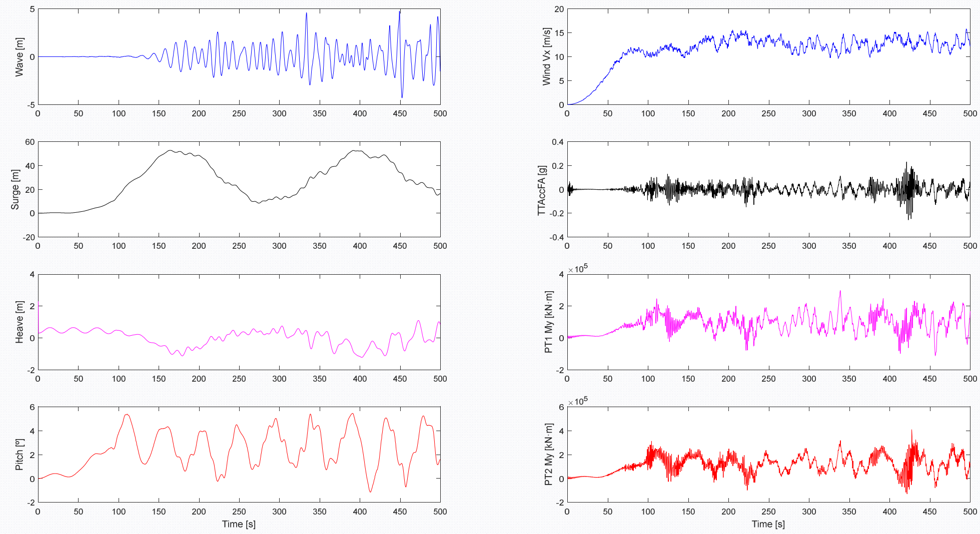

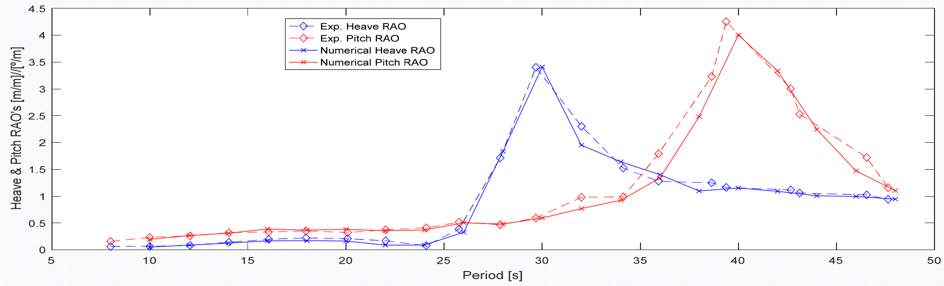

External loads

The external forces considered in the model include the effects of the environmental loads (buoyancy and waves), the mooring system, the wind turbine, the self-weight as well as user defined input forces.

The equivalent buoyancy forces acting over the structure are computed by the 3D integration of the pressures over the structure at each time step from the global position of the mesh elements centroids to finally compute the hydrostatic pressures to compute the resultant force at each element.

The drag forces and the wave loads are computed with the Morison's equation, from where the water particle kinematics can be computed with regular or irregular Airy waves theory or the Stokes 5th order non-linear wave theory. For the irregular waves the kinematics can be computed from a defined sea spectrum or from a wave data record.

For the mooring system loads, the model allows to compute in a quasi static way or considering the full mooring dynamics, based in the Garret [3] and Kim [4] works.

Validation and Numerical Results

The results obtained during the Windcrete concept experimental campaign [5] have been used to validate the numerical results of the model. The results from a simulation under normal operation conditions in combination with the NREL 5MW WT and the adjusted numerical model of Windcrete are shown in the upper part while a RAO comparison between simulations and experimental results is shown below.

Acknowledgements

We would like to express our gratitude for the financial support obtained from the Catalan government, Generalitat de Catalunya, through its AGAUR agency and from the KIC InnoEnergy.

References

[1] Crisfield,M. A., Non-linear finite element analysis of solids and structures, vol. 2. John Wiley & Sons Inc, 1991.

[2] H. M. Hilber, T. J. R. Hughes, and R. L. Taylor, "Improved numerical dissipation for time integration algorithms in structural dynamics," Earthq. Eng. Struct. Dyn., no. 5, pp. 283–292, 1977.

[3] D. L. Garrett, "Dynamic Analysis of Slender Rods," J. Energy Resour. Technol., vol. 104, no. 4, pp. 302–306, 1982.

[4] Y.-B. Kim, "Dynamic Analysis of multiple-body floating platforms coupled with mooring lines and risers," Texas A&M University, 2003.

[5] Campos,A.;Molins,C.;Gironella,X.;Trubat,P.;and A Alarcón,D., "Experimental RAO's analysis of a monolithic concrete spar structure for offshore floating wind turbines," in Proceedings of the 34th International Conference on Ocean, Offshore and Arctic Engineering OMAE2015, 2015.

Fully integrated load analysis included in the structural reliability assessment of a monopile supported offshore wind turbine

ECN

www.ecn.nl
P.O. Box 1
1755 ZG Petten
The Netherlands

Authors

J.M. Peeringa
G. Bedon

Corresponding author: peeringa@ecn.nl

Objective

To investigate where cost reduction are possible in the support structure while keeping a sound and safe design:

- Probabilistic design methods are used.
- For time efficient load computations TURBU, a fast fully integrated wind turbine design and analysis tool in the frequency domain, is integrated in the probabilistic approach.

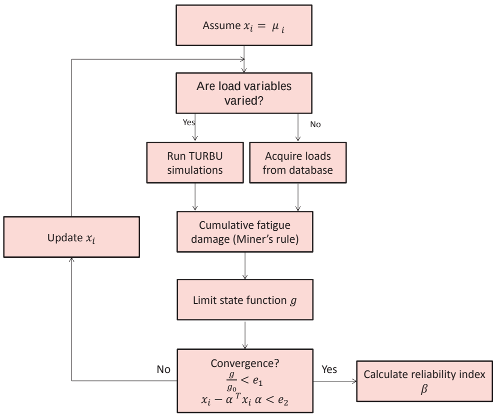

TURBU

- Full non-linear steady state model (multi-body average deformation)
- Time-invariant linear dynamic model (multi-body, Newton, Coleman)
- Linear frequency and time domain analysis of 3-bladed Horizontal Axis Wind turbines

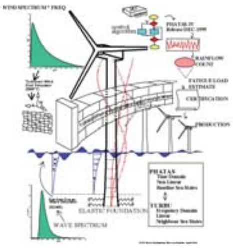

Fatigue limit state:

$$g = \Delta - D = 0$$

Nmax = f(logC1,logC2) of SN- curve (DNV RP-C203)

$$D = \sum_i \frac{n_i}{N_{max,i}}$$

FERUM

- Open source structural reliability code in MATLAB.
- First Order Reliability Method (FORM) selected.
- Advantage FORM is information on contribution of selected stochastic variables to the variance of the limit state function g.

Variable	Distribution	Mean	Standard deviation
logC1	Normal	12.164	0.20
logC2	Normal	16.106	0.25
Δ (Miner)	Lognormal	1.00	0.30
Young modulus	Lognormal	210e9	42e9
CD	Normal	0.70	0.10
CM	Normal	2.00	0.10
Soil stiffness	Lognormal	6.603e10	1.321e10

Case study

- Modern 4MW wind turbine with monopile support structure, rotor diameter 130m, in 30m water depth.
- Twelve wind bins with for every wind bin six time series of one hour.
- Windspeed Weibull distribution k = 2.15 and u = 9.36m/s.

Bin	Wind velocity [m/s]	Significant wave height [m]	Spectra Peak Period [s]	peak shape parameter (gamma)
1	3	0.375	4.5	1.00
2	5	0.625	4.5	1.00
3	7	0.875	4.5	1.24
4	9	1.125	5.5	1.00
5	11	1.375	5.5	1.43
6	13	1.875	6.5	1.34
7	15	2.375	7.5	1.17
8	17	3.125	7.5	2.39
9	19	3.875	8.5	2.19
10	21	4.375	9.5	1.69
11	23	5.125	9.5	2.52
12	25	6.375	10.5	2.63

Results

- Rainflow count of fore-aft bending moment at mudline only.
- Design reliability index β > 3.7 (DNV OS-J101)
- Reliability index β = 6.35 (Failure probability = 1E-10) in case study.

Variable	Design point	Contribution to variance limit state function
logC1	12.164	0%
logC2	14.72	75%
Δ (Miner)	0.42	20%
Young modulus	210e9	0%
C_D	0.81	4%
C_M	2.13	1%
Soil stiffness	5.956e10	0%

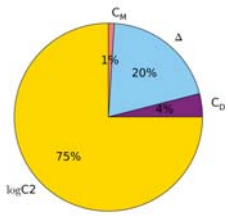

Contribution to variance

Conclusions and recommendations

- Integration of full load calculations in probabilistic design method (FORM) is successful for fatigue limit state at mudline.
- The contribution of the Miner rule (Delta) and SN-curve (logC2) variables to the variance of the limit state function is largest.
- Calculated reliability index β = 6.35 shows there is room for design optimisation.
- Ultimate limit state and additional locations still need to be included.

Acknowledgements

The Design for Reliable Power Performance (D4REL) project is partially sponsored by TKI Wind op Zee TKIWO2007. Partners are TU-Delft, Siemens, Van Oord, IHC Hydrohammer and Eneco.

Parametric Study of Mesh for Fatigue Assessment of Tubular K-joints using Numerical Methods

Jorge Mendoza Espinosa [a,b], Sebastian Schafhirt [a], Michael Muskulus [a]
[a] Department of Civil and Environmental Engineering, Norwegian University of Science and Technology. Trondheim 7491, Norway
[b] Ramboll Wind. Hamburg 20097, Germany

Abstract

Wind turbine jacket structures are complex structures, whose **joints** design is generally driven by **fatigue**. These joints, along with their complex **welds**, are of special interest in terms of cost reduction. Therefore, a thorough analysis and understanding of the background behind the assessment proposed in guidelines is motivated. The paper presents a study of the **influence of meshing** for the assessment of tubular **K-joints** following the **hot-spot approach** using **numerical methods**. The accuracy of the results is discussed for several mesh layouts. Influence of the **mesh density, element shape** and **element type** are investigated. Furthermore, a parametric study is performed in order to see the variation in the results for different conventional geometry situations. The hot-spot method is proved to be robust regarding mesh regularity. However, the efficiency of irregular mesh models is very low and an asymptotic behavior that tends to a constant solution for increasing number of elements is sometimes found for very high number of nodes. Conclusions can be drawn for which cases it is worth to invest time in semi-automatic meshing. A discussion is done regarding which element size and type is better regarding accuracy and computational time.

Method

K-joint is modelled parametrically using FEM simulations in Ansys©. Hot-spot stress (HSS) is computed as the linear extrapolation to the weld toe as recommended in DNV-GL [1]. Stress Concentration Factor (SCF) is computed at the brace weld toe position. Standard steel and elastic behavior is used in all models.

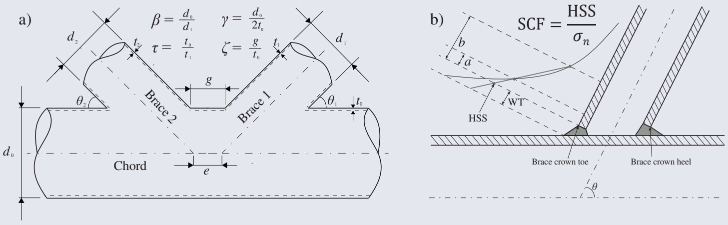

Influence of Element Regularity

Two mesh layouts are compared, i.e. **Automatic** meshing and **Semi-automatic** meshing.

Automatic meshing

Mesh is generated using ANSYS© built in subroutines. Element regularity is quite random at the chord-brace intersection and irregular elements are present

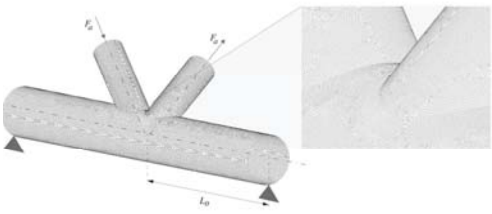

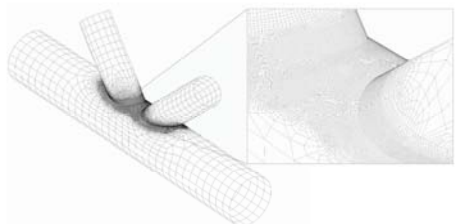

Semi-automatic meshing

Regular elements are present at the joint influenced area.
Mesh refinement in this area can be modified parametrically.

44 FEM simulations are run to compare both kind of meshing. SCF is computed at the brace toe position.

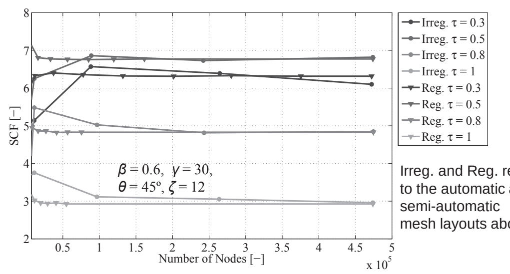

Irreg. and Reg. refer to the automatic and semi-automatic mesh layouts above.

Convergence of the solution to a constant value for increasing number of nodes is clear for the semi-automatic mesh models. An asymptotic tendency is not obtained for the automatic mesh models for all cases until a great refinement is set.
Solutions between both kind of models match for increasing mesh density. This grants the irregular mesh model reliability for a dense enough mesh.

Influence of Element Type

Two element types are compared: 4-node SHELL43 and 8-node SHELL93. **60 FEM simulations** are used for this investigation.

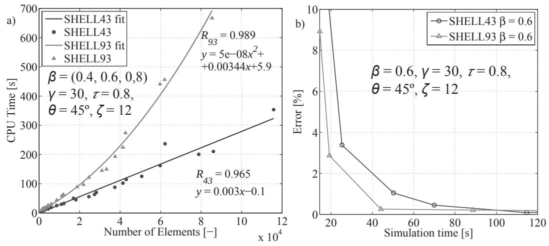

An error of less than 1% for SHELL93 is found for an element size of t_1 x t_1 and t_{CPU} = 35 s. Same precision requires around 55 s for SHELL43.

Elem. size	Element Type	# Elements	# Nodes	t_{CPU} [s]	SCF [-]	Error [%]
$2t_1$ x $2t_1$	SHELL43	3376	3398	13	5.38	16.13
$2t_1$ x $2t_1$	SHELL93	3348	10088	19	4.67	2.87
t_1 x t_1	SHELL43	8654	8672	25	4.79	3.38
t_1 x t_1	SHELL93	8711	26177	44	4.55	0.26
$1/2t_1$ x $1/2t_1$	SHELL43	28249	28264	70	4.65	0.45
$1/2t_1$ x $1/2t_1$	SHELL93	31055	93191	145	4.55	0.16
$1/3t_1$ x $1/3t_1$	SHELL43	59776	59766	162	4.64	0.22
$1/3t_1$ x $1/3t_1$	SHELL93	59693	179055	441	4.54	0.00
$2/7t_1$ x $2/7t_1$	SHELL43	78836	78811	201	4.63	0.00
$2/7t_1$ x $2/7t_1$	SHELL93	87484	262416	688	4.54	0.00

Results for both element type do not match, i.e. a difference of 2% exist. Therefore, it would be unrealistic to ask for an accuracy higher than that. Error in the computation of SCF is done with respect to $2/7t_1$ x $2/7t_1$ results.

Influence of Mesh Density

147 FEM simulations are run varying the refinement factor R_f. Semi-automatic model using SHELL43 is used.

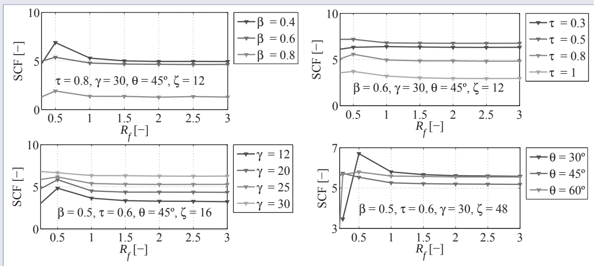

Element size:
$$A_{El} = \frac{t_1}{R_f} \times \frac{t_1}{R_f}$$

Guidelines recommend the use of an element size from $R_f = 1$ up to $R_f = ½$. For some cases, this may lead to underconservative solutions, e.g. the top-right plot for $\tau = 0.3$

Conclusions

A parametric study to investigate the influence of meshing for the computation of SCF for the hot-spot method was carried out. Several local FEM models are built to investigate the effect of **mesh density, regularity of the elements and element type**.

Generally speaking, **automatically generated meshes** do not provide a good balance between accuracy and computational time. **Great refinement is needed** in order to provide a trustworthy solution. Solutions between the regular mesh model and the automatically generated mesh models match when the number of nodes is increased sufficiently. Thus, their use can be justified for certain cases. They can be a better solution in certain situations since they do not require time to be spent in the manual definition of patterns to create a regular mesh.

8-node elements are more efficient than **4-node elements** for the accuracy required in the hot-spot method. SCF obtained by using both element types do not match, i.e. a difference of around **2%** exist.

Influence of the refinement of the joint influenced area was investigated. For most of the tested geometry situations, the **most efficient element size is t_1 x t_1** However, this is not a general rule. Using a smaller element size could yield underconservative solutions. It is recommended to always perform a mesh density parametric study to ensure that the solution is accurate enough.

Acknowledgements

The present study has been done at the Department of Civil and Environmental Engineering of the Norwegian University of Science and Technology. The authors would like to thank Dr.-Ing. Marc Voβbeck from Ramboll for the original idea here developed.

References

1. Fatigue Design of Oshore Steel Structures. DNVGL-RP-C203; Oslo, Norway: DNV GL AS; 2016.
2. S. A. Karamanos A. Romeijn, J.W.. Stress Concentrations in Tubular Gap K-joints: Mechanics and Fatigue Design. Engineering Structures 2000;22(7):4–14.
3. Romeijn, A.. Stress and Strain Concentration Factors of Welded Multiplanar Tubular Joints. PhD dissertation; Delft University of Technology; Civil Engineering Department; 1994.
4. O. Doerk W. Fricke, C.W.. Comparison of Dierent Calculation Methods for Structural Stresses at Welded Joints. International Journal of Fatigue 2003;25:359–69.

Contact: Jorge Mendoza Espinosa (jorgemendozaesp@gmail.com)

Lifetime extension for large offshore wind farms: Is it enough to reassess fatigue for selected design positions?

Corantin Bouty[1,2], Lisa Ziegler[2,3], Sebastian Schafhirt[2], Michael Muskulus[2]
[1] Institut Supérieur de Mécanique de Paris (Supméca), France
[2] Norwegian University of Science and Technology (NTNU), Norway
[3] Ramboll Wind, Germany

Introduction

Lifetime extension becomes soon important as the first larger offshore wind farms reach a mature age. For lifetime extension, a reassessment of structural integrity of the support structure is needed. Environmental conditions vary within **large wind farms** and lead to location-specific loading. This study addresses if reassessment must be performed for each turbine when **hydrodynamic parameters** change uniformly in the wind farm – or if trends can be derived from **design positions**? In this study, **time-domain simulations** were performed to reassess fatigue loads for monopile support structures located at five positions within a fictive wind farm. Results are presented for **turbine operation;** idling was not addressed at this stage of the project.

Numerical Model

OFFSHORE WIND TURBINE

- Monopile with NREL 5MW reference turbine atop (used in Phase II of the OC3 project)
- Soil-pile interaction is modelled with lateral springs distributed along the pile
- Implemented in the flexible multibody simulation tool Fedem WindPower (Version R7.2)

GENERIC OFFSHORE WIND FARM

- Reference values from UpWind Design Basis[1] with variations in water depth and soil conditions
- Length of monopile adjusted to water depth (no changes in dimensions of monopile)
- Unidirectional wind and waves
- Wake effects are taken into account using Frandsen wake model[2]

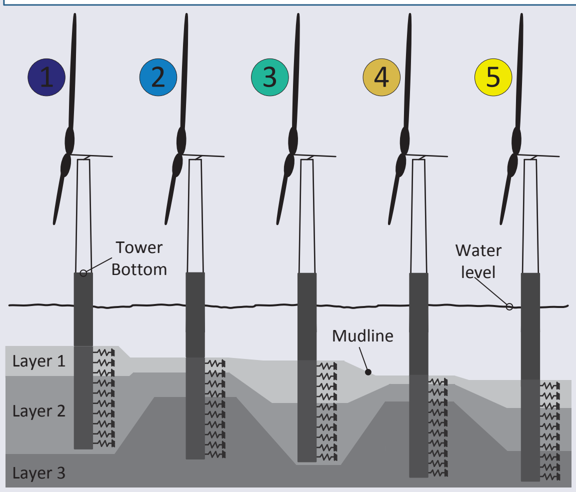

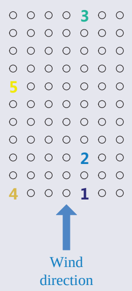

Pos	water depth [m]	f_{nat} [Hz]
1	15	0.246
2	20	0.237
3	22	0.232
4	26	0.226
5	30	0.217

Load Simulations and Equivalent Fatigue Load Calculation

Load analyses were carried out under combined aero- and hydrodynamic loading in time-domain. In total 11 operational load cases with wind speed in the range between 4m/s and 24m/s were performed. Each load case with a duration of 3600 seconds (excluding transients). Wind turbines located at five different positions with variations in terms of soil conditions, water depth and neighboring wind turbines (wake effect) are selected. Load simulations were performed for each position individually. Bending moments at tower bottom are extracted and used to calculate an Equivalent Fatigue Load (EFL):

$$EFL = \left(\sum_{i=1}^{N} \frac{S_i^m}{N} \right)^{\frac{1}{m}}$$

Fatigue Assessment for Design

Results are shown for EFLs per load case and position and the accumulated EFL per position.

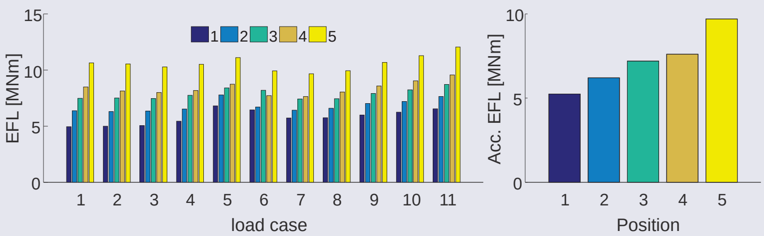

Equivalent Fatigue Loads per load case and accumulated fatigue damage

- Load cases are weighted with the probability of occurrence
- Increase of total EFL with increasing water depth

Fatigue Reassessment

In order to account for discrepancies between environmental data used for the design and the actual environmental conditions that the offshore wind turbine was exposed to during operational life, the significant wave height (H_s) and peak period (T_P) were changed in a range of 5% around their original value. Structural loads were recalculated using the same numerical models, but updated environmental data. The fatigue assessment is performed in the same manner as it was done for the design phase, allowing a comparison between design and reassessment phases.

Single Parameter Variations

H_s and T_P are varied individually, while keeping the remaining parameters constant.

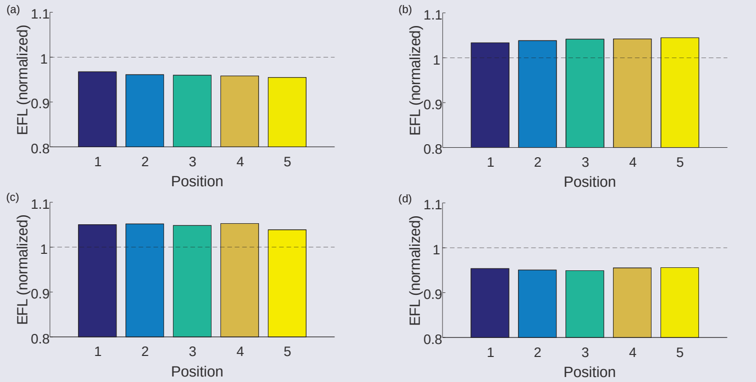

Accumulated EFL for (a) H_s -5%, (b) H_s +5%, (c) T_p -5%, and (d) T_p +5%. Results are normalized to the design case.

Peak period:

- A decrease of T_P moves the wave excitation frequencies closer to the fundamental frequency of the models, thereby increasing the fatigue loads on the structure
- Nearly linear behavior: a 5% change in T_P value leads to changes in accumulated EFL in the range between 4.4% and 5.2%

Significant wave height

- Similar to T_P, the accumulated EFL shows a nearly linear behavior for the changes within the range of +/- 5% for H_s

Combined Parameter Variations

For the case shown the parameters were simultaneously varied as follows: H_s+5% and T_p-5%.

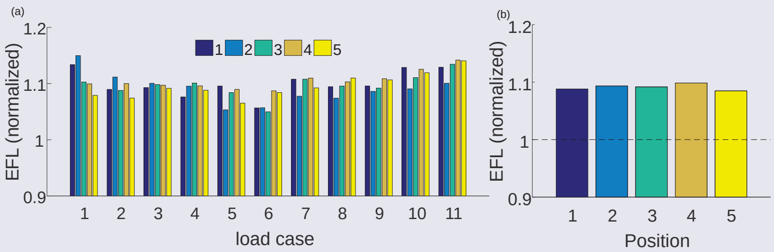

(a) EFLs for the full set of load cases and all positions and (b) accumulated EFL. Results are normalized to the design case

- The combined variation shown in the figure above leads to higher EFLs for each load case in comparison to the initial design
- The accumulated EFL increases for all five positions in a similar range (8.5% - 9.5%)

Conclusions

- **Design:** Fatigue loads increase for deeper water and lower support structure natural frequency. This is in line with previous studies[3]
- **Reassessment:** Preliminary results indicate that an extrapolation from one position to others might be feasible. Results should be treated carefully as several limitations apply.
- **Limitations:** Idling load cases are missing (count up to 20% of fatigue life); other environmental and operational parameters apart from hydrodynamics must be assessed (wind speed, turbulence intensity, corrosion, turbine downtime, etc.)
- **Future work:** Include turbine idling and extend the study for other load-driving parameters

References

1. Fischer T., De Vries W., Schmidt B. (2010). UpWind Design Basis (WP4 : Offshore Foundations and Support Structures).
2. Frandsen S.T., Barthelmie R., Pryor S., Rathmann O., Larsen S., Højstrup J., Thøgersen M. (2006). Analytical Modelling of Wind Speed Deficit in Large Offshore Wind Farms. Wind Energy, 9(1-2), 39-53.
3. Ziegler, et al. (2015). Sensitivity of wave fatigue loads on offshore wind turbines under varying site conditions. Energy Procedia, 80, 193-200.

Contact: corantin.bouty@edu.supmeca.fr

EERA DeepWind'2017
14th Deep Sea Offshore Wind R&D Conference
Trondheim, 18 – 21 January 2017

Optimization of offshore wind farm installations

Stian Backe
University of Bergen
stian.backe@student.uib.no

Harvesting offshore wind is an expensive way of producing electricity. Cost reductions can be made by optimizing through the supply chain. This work focus on optimizing logistics when installing the turbines.

An illustration of the installation process as it is modelled.

As wind farms offshore grow in size, the need for decision support in planning installation becomes evident when seeking cost reduction. This model will be a decision support system (DSS) that may be used to optimize the logistics of installing an offshore wind park. Using mixed integer linear programming (MILP), the problem is described mathematically. Through implementation in AMPL, an optimal solution is sought.

Problem description

Given an amount of turbines, where each turbine consist of components that need to be installed in a certain order, the goal is to find an optimal composition of installation vessels and inventory ports such that the costs of installing all components is minimized.

Assumptions

All installations must be finished within a time window. Each vessel can carry its own capacity in components during one circuit. When performing a circuit, a vessel installs all components on board. Each vessel can perform several circuits, always returning to a port in between. A vessel is not restricted to only operate from one inventory port. All components are assumed to be available at any inventory port when it is needed for loading.

Input

The model needs certain data in order to calculate an optimal solution:

- **Vessels:**
  - Costs of mobilization
  - Time charter costs
  - Capacity
  - Task costs (transportation, installation etc.)
  - Efficiency (time consumption)
  - Ability to perform task
- **Ports:**
  - Costs of using port
  - Location
- **Turbines:**
  - Park size
  - Location
  - Components
- **Time horizon**
  - Total time available
  - Vessel circuits possible

Output

Upon minimizing the total costs of performing the installation, the solution will provide:

- **Optimal vessels:**
  - Choice of vessels to use
  - How to load a vessel
  - Cooperation with other vessels
  - What components to install
- **Optimal ports:**
  - Choice of ports to operate from
  - What components must be available at what time
- **Optimal schedule:**
  - When to perform loading
  - When to perform installation
  - When to time charter vessels

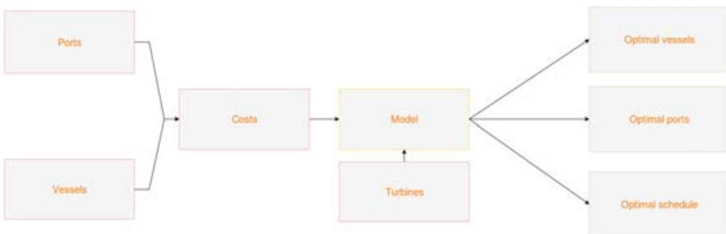

Challenges

When formulating such a model, taking into account uncertainties can be a challenge. A great challenge includes weather restrictions, making certain tasks not possible to perform. This project will seek to consider this uncertainty on a later stage.

Application

The tool can be applied for several purposes including:

- Strategic wind farm installation planning
- Development of wind farm installation vessels
- Investigation of potential wind farm location

ACKNOWLEDGEMENTS
The project is supervised by professor Dag Haugland, and it is pursued in association with MARINTEK AS through the participation in the European project LEANWIND.

UNIVERSITY OF BERGEN

Modelling of Marine Operations in the Installation of Offshore Wind Farms

ECN

www.ecn.nl
P.O. Box 1
1755 ZG Petten
The Netherlands

Authors

A. Dewan
G. Katsouris
C.F.W. Stock-Williams
M. Alvarez Fernandez

Corresponding author: dewan@ecn.nl

Introduction

Installation is critical to the profitability of offshore wind farms, due to the complexity of offshore works and the dependency on weather uncertainties. Thorough planning, quantification of uncertainties and minimization of project risks are required.

ECN's tool *ECN Install* models the complete installation process of an offshore wind farm in the time-domain. The benefits of the installation modelling include:

- Quantification of project delays, risks and associated costs
- Optimization of resource management and strategy selection
- Testing of innovative installation concepts and vessels
- Dissemination of knowledge between all relevant actors.

ECN Install

Inputs

- Wind turbine specifications
- Weather data
- Operation bases
- Vessels
- Equipment
- Working shift patterns
- Components
- Cost parameters

Planning

- Installation steps breakdown
- Starting dates and inter-dependencies
- Location of activities
- Required resources
- Operations duration
- Weather operating limits
- Learning curve

Simulator

- Time-domain simulation of installation activities
- Scenario modelling based on stochastic weather time-series
- Constraints include resource availability, working shift patterns, permit constraints and weather limits

Outputs

- Installation planning including delays
- Resources utilization and costs per scenario
- Detailed breakdown of delays and costs
- Excel summary of results
- Gantt charts of the installation scenarios
- Time, cost and resources graphs of various KPIs

Objective

This study aims to understand the most cost-effective installation strategies in context of the trend towards ever larger wind farms and wind turbines.

The following case studies are simulated for different numbers of 8MW turbines, using weather data from the Borssele site:

I. One medium-sized jack-up vessel

II. Two medium-sized jack-up vessels

III. One large jack-up vessel

The jack-up used in Case Studies I & II carries 3 foundations, or 4 turbines. The jack-up in Case Study III carries twice as many units.

Results

Fig. 1 shows the raw results from the three case studies, where the medium and large jack-ups are both assumed to cost €150k/day. The total production of the wind farm and the total installation costs are next used as the basis to compare the case studies.

Fig. 2 demonstrates, from a comparison of Case Studies I and II, that when the total farm size exceeds 50 turbines, using two medium-size jack-up vessels is a preferable strategy.

Finally, Fig. 3 examines the vessel day rate which would make use of one large jack-up (Case Study III) preferable to use of one smaller jack-up (Case Study I). As the farm size increases, the ratio of vessel day rate at which the wind farm breaks even increases.

Figure 1: Case Study Raw Results (top: Installation Cost; bottom: Income)

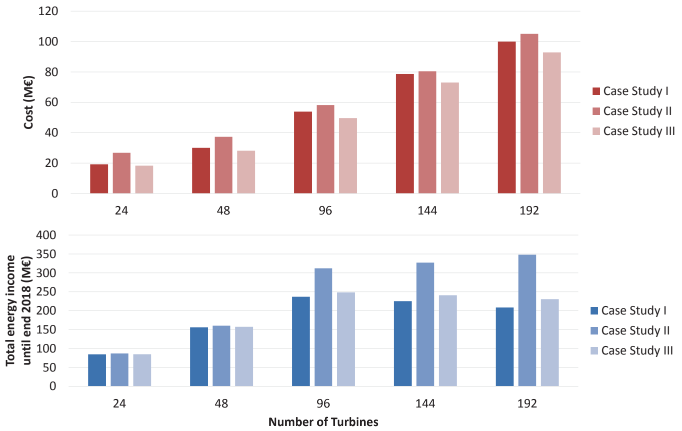

Figure 2: Comparison of Case Studies I and II (one vs. two medium jack-up vessels)

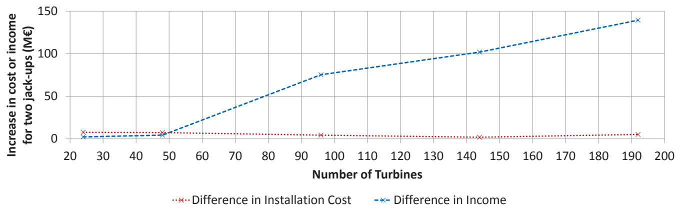

Figure 3: Comparison of Case Studies I and III (acceptable large jack-up day rate)

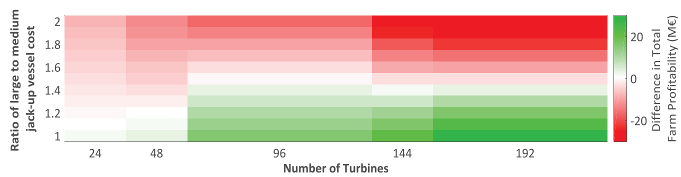

Conclusions

1. *ECN Install* assists wind farm developers, contractors and investors in planning and installation scheduling of their large and upcoming offshore wind farms.

2. *ECN Install* supports the vessel manufacturers to plan their capacity and operational design parameters based on wind turbine market development.

3. Parallel installation of wind turbines by multiple vessels is a cost-effective solution especially with the gain in income due to early production.

4. Use of larger jack-up vessels with more capability are profitable depending on the logistic characteristics of the wind farm to be installed.

A Review of Slamming Load Application to Offshore Wind Turbines from an Integrated Perspective

Ying Tu[a], Zhengshun Cheng[b], Michael Muskulus[a]

a. Department of Civil and Environmental Engineering, NTNU b. Department of Marine Technology, AMOS, NTNU

Contact: ying.tu@ntnu.no

Abstract

In harsh sea conditions, it is possible for offshore wind turbines (OWTs) to be exposed to slamming loads due to breaking waves, especially plunging breaking waves. These slamming loads lead to significant structural responses and can affect the ultimate limit state (ULS) design and the fatigue limit state (FLS) design of OWTs. However, detailed consideration of slamming loads is not a common practice in the design of primary structures in offshore wind industry. Studies on integrated dynamic analysis of OWTs with consideration of slamming loads are very limited. When applying slamming loads on OWTs, several aspects should be considered, such as the detection of breaking waves, the calculation of slamming loads, and the approaches to integrate the slamming loads in fully coupled analysis, etc. This paper provides an extensive review of key issues concerning these aspects, which can benefit the application of slamming loads on OWTs.

Plunging Breaking Wave and Slamming Load

Plunging breaking wave

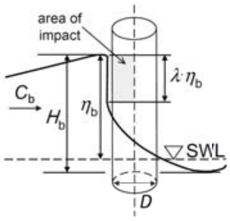

Sketch of a breaker interacting with a cylinder [5]

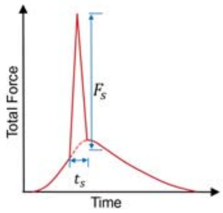

Typical wave slamming force

In engineering practice, the total force from a plunging breaking wave on a cylinder is usually calculated by: $F = \underbrace{F_D + F_M}_{\text{Morison's force}} + \underbrace{F_S}_{\text{Slamming force}}$

A general expression of slamming force: $F_S = \int_l C_s(z)\frac{1}{2}\rho U(z)^2 W(z)dz$

C_s slamming coefficient; ρ water density; U water particle velocity; W project width of the structure; l height range of the impact

Depending on used slamming model, it can be simplified for example as:

$F_S = C_s\frac{1}{2}\rho C_b^2 D\lambda\eta_b$ Wienke and Oumeraci's model [5]

C_b celerity of the breaking wave; D diameter of the cylinder; λ curling factor; η_b elevation of the breaking wave

Slamming Load Application for Offshore Wind Turbines

Detection of slamming events

Four types of breaking criteria [3]

- The McCowan type: $\frac{H_b}{h_b} = \gamma(s, \lambda_0)$
- The Miche type: $\frac{H_b}{L_b} = \alpha(s, \lambda_0)\tanh\left[\xi(s, \lambda_0)\frac{2\pi h_b}{L_0}\right]$
- The Goda type: $\frac{H_b}{L_0} = \alpha'(s, \lambda_0)\left\{1 - \exp\left[-1.5\xi'(s, \lambda_0)\frac{2\pi h_b}{L_0}\right]\right\}$
- The Munk type: $\frac{H_b}{H_0} = \beta(s)\left(\frac{H_0}{L_0}\right)^m$

Two types of plunging criteria

- Through surf similarity parameters:

  $\xi_o = \frac{\tan\alpha}{\sqrt{H_o/L_o}}$ and $\xi_b = \frac{\tan\alpha}{\sqrt{H_b/L_o}}$

  According to IEC 61400-3, if $0.45 < \xi_o < 3.3$ or $0.4 < \xi_b < 2.0$, plunging breaker occurs
- Through breaker depth to offshore wave height ratio:

  Plunging breaker occurs, if the ratio $\frac{h_b}{H_o} < 1.8$

Detection approach

- Apply zero-crossing analysis to irregular wave field to determine the wave parameters
- Apply suitable breaking and plunging criteria selected based on bathmetry, water depth, etc
- If necessary, conduct CFD simulations for better parameter estimation, and use additional indicators for the detection

Calculation of slamming loads

Slamming load calculation method

- Numerical approach (e.g. CFD), which is more time consuming.
- Engineering approach by using slamming load models, which is suitable for the design practice.
  - o Estimate characteristic wave parameters by e.g. zero-crossing analysis
  - o Select a slamming load model according to the structure type

Different slamming load models for cylindrical structure and jacket structure

	Author	Theory	Maximum C_s	Slam duration, t_s	Time history, $C_s(t)$
Cylindrical structure	Goda et al.	von Karman	π	$\frac{D}{2C_b}$	$\pi\left(1 - \frac{2C_b}{D}t\right)$
	Campbell and Weynberg	Experimental study	5.5	$\frac{D}{C_b}$	$5.15\left(\frac{D}{D+19C_b t} + \frac{0.107C_b t}{D}\right)$
	Cointe and Armand	Wagner and matched asymptotic expansions	2π	$\frac{3D}{2C_b}$	$2\pi - \left(4.72 - \ln\left(\frac{2C_b}{D}t\right)\right)\sqrt{\frac{2C_b}{D}t}$
	Wienke and Oumeraci	Wagner	2π	$\frac{13D}{64C_b}$	$2\pi - 2\sqrt{\frac{2C_b}{D}t}\left(\tanh^{-1}\sqrt{1 - \frac{C_b}{2D}t}\right)$
Jacket structure	Tu et al.	Experimental study	2.05	-	Triangular
	Tu et al.	Experimental study	2.05	-	Exponential

Integration of slamming loads to analysis

Current simulation tools for integrated analyses, such as FAST, do not have the option to directly include the wave slamming loads.

Solution 1: Modify the codes to include the slamming loads

Solution 2: Do not modify the codes, but include the slamming loads as an additional term in the Morison force, usually as an additional inertia term.

$$a_x^{new} = a_x + a'_x$$

$$a'_x = 2\frac{C_s}{C_m}\frac{C_b^2}{D\pi}$$

Key Points on Slamming Load Application

For detecting the slamming events

- The effect of the structure on the waves is not considered, when zero-crossing analysis is used.
- Criteria should be carefully selected according to the individual local conditions

For calculating the slamming loads

- Characteristic wave parameters required in the slamming load models can only be estimated approximately by using zero-crossing analysis
- A reliable slamming load models should be carefully selected

References

1. Robertson, B., Hall, K., Zytner, R., Nistor, I., 2013. Breaking waves: Review of characteristic relationships. Coastal Engineering Journal 55 (01), 1350002.
2. Hallowell, S., Myers, A., Arwade, S., 2016. Variability of breaking wave characteristics and impact loads on offshore wind turbines supported by monopiles. Wind Energy 19 (2), 301–312.
3. Liu, Y., Niu, X., Yu, X., 2011. A new predictive formula for inception of regular wave breaking. Coastal Engineering 58 (9), 877–889.
4. Marino, E., 2011. An integrated nonlinear wind-waves model for offshore wind turbines. Ph.D. thesis, University of Florence, Firenze, Italy.
5. Wienke, J., Oumeraci, H., 2005. Breaking Wave Impact Force on a Vertical and Inclined Slender Pile - Theoretical and Large-Scale Model Investigation. Coastal Engineering 52, 435–462.
6. Tu, Y., Cheng, Z., Muskulus, M., 2017. Global slamming forces of jacket structures for offshore wind applications. Marine Structures (under review).

14th Deep Sea Offshore Wind R&D Conference, EERA DeepWind'2017

Trondheim, Norway 18-20 January 2017

NOWITECH Norwegian Research Centre for Offshore Wind Technology

Offshore Turbine Wake Power Losses: Is Turbine Separation Significant?

Peter Argyle, Simon Watson
CREST, Loughborough University, UK

Introduction

The UK offshore regions currently being developed into wind farms are much larger than those developed previously, leading to turbines being built further apart. It has long been known that longer distances between turbines enable greater wake recoveries and thus higher farm output power productivity when the wind blows parallel to turbine rows. However the offshore wind rose is not unidirectional, meaning it is important to consider the wake recovery for all directions, especially as turbines spaced further apart are directly affected by wake conditions for fewer flow directions. This work uses Computational Fluid Dynamics (CFD) to simulate a 40 turbine offshore wind farm with 30 turbine separation options and 2 configurations. By weighting the results from 4 wind speeds and 10 degree bins, wind power production in the UK offshore climate is linked to turbine separation.

Analysis

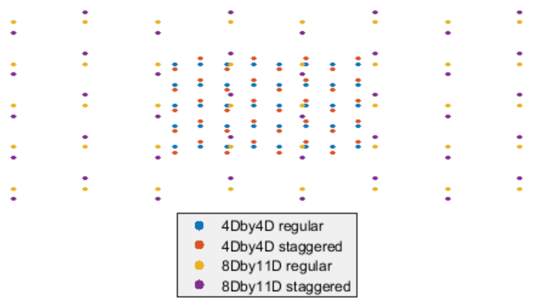

Figure 1. Extreme variation of turbine separation for both layout configurations

Results are presented for 60 farm layouts (30 regular and 30 staggered arrays, examples in Figure 1) conducted with 4 wind speeds at 10° directional intervals using CFD software package Ansys Windmodeller [1]. Expected power production is shown in Figure 2, assuming a uniform wind rose. The most significant differences in power output in relation to turbine layout occur at $10ms^{-1}$ and $8ms^{-1}$ whilst variation is less significant at $5ms^{-1}$ and $15ms^{-1}$ due to the thrust curve of the Siemens 3.6MW simulated turbine.

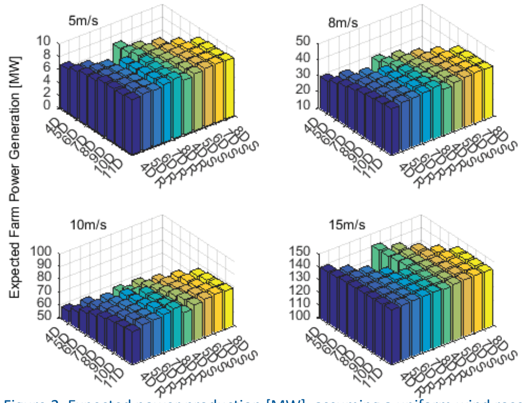

Figure 2. Expected power production [MW], assuming a uniform wind rose

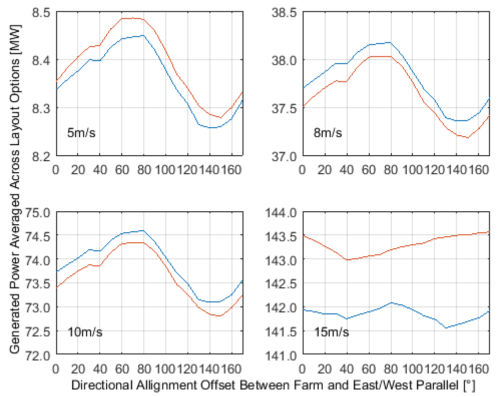

Figure 3. Variation in average power from regular (blue) and staggered (red) arrays caused by rotating the farm layout with respect to the wind rose.

As the uniform wind rose may be contributing to the limited variation in productivity, simulations were weighted according to the UK offshore wind rose [2] with the farm orientation changed to observe any effect of prevailing wind direction (Figure 3). Using the optimal farm alignment, Figure 4 displays the expected farm power output for each turbine layout. Increasing turbine separation in either direction leads to greater productivity most significantly below rated wind speeds and for distances less than 8D, though staggering the array may have a greater effect above rated power.

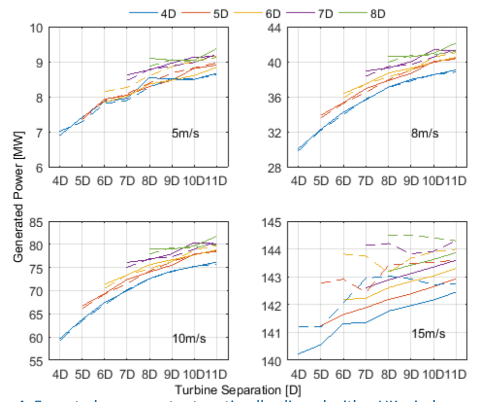

Figure 4. Expected power output, optimally aligned with a UK wind rose for both regular (solid lines) and staggered (dashed lines) array options.

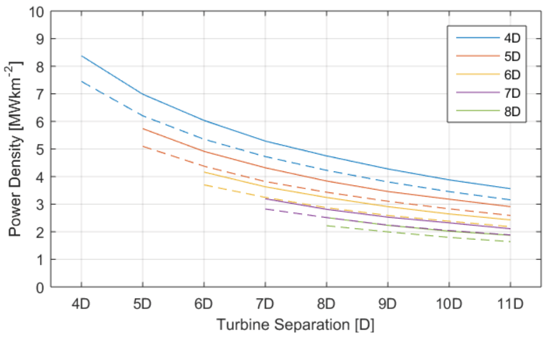

Figure 5. Power densities for each turbine layout option

Figure 5 shows that despite producing more power, greater turbine separation distances reduce the efficiency of sea area developed. For a given development area, increasing turbine numbers may be more beneficial than increasing spacing. Increased spacing is also shown (Figure 6) shown to significantly reduce both max and mean values of expected turbulence intensity values simulated at any turbine. Though this is less noticeable beyond 8D.

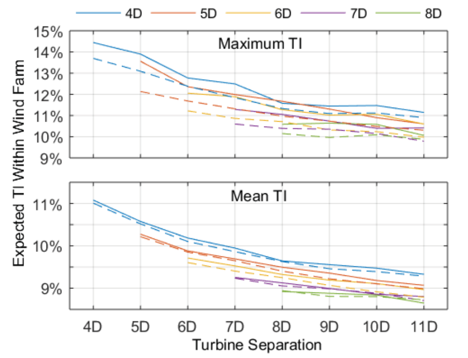

Figure 6. Expected turbulence intensity at any given wind turbine

Conclusions

This work presented production and turbulence results for 60 different turbine layouts from 4 wind speeds at 10° intervals. The farm was found to have an optimal orientation parallel to the 350-170° axis in terms of total power production. Difference in productivity due to farm alignment, was smaller than the increases with turbine separation distances. Results from both regular and staggered arrays showed additional power production was less significant beyond 8D turbine separation. Turbulence intensity was shown to decrease as turbines are located further apart, most significantly for separation distances less than 8D, though improvements are still observable for the furthest separation, 11D by 8D.

References

1. Montavon C, Jones I, Staples C, Strachan C, Gutierrez I. Practical Issues in the use of CFD for Modelling Wind Farms," *Proceedings EWEA Conference and Exhibition*, Marseille, 2009
2. Argyle P. & Watson S.J.: "A Comparison of the UK Offshore Wind Resource from the Marine Data Exchange", *Proceedings: Wind Energy,* Hamburg 2016

Experimental study on power curtailment of three in-line wind turbines

Jan Bartl[a] , Yaşar Ostovan[b], Lars Sætran[a], Oguz Uzol[b]

email: *jan.bartl@ntnu.no*

[a] Department of Energy and Process Engineering., Norwegian University of Science and Technology, Trondheim, Norway

[b] METU Center for Wind Energy, Department of Aerospace Engineering, Middle East Technical University, Ankara, Turkey

Background

- Show up the potential of wind farm power optimization through tip speed ratio control
- Provide a well-defined experimental dataset for verification of computational models

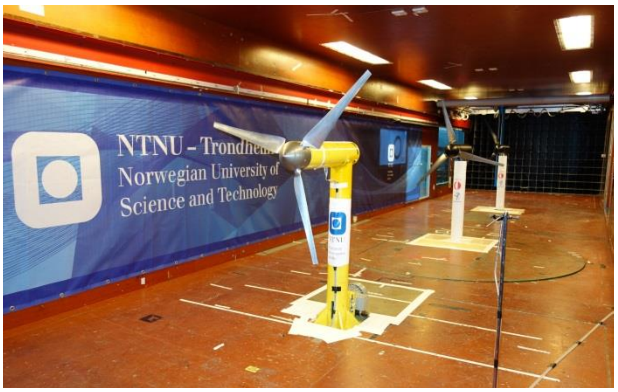

Figure 1 Experimental setup of three model wind turbines in the large wind tunnel at NTNU

Experimental setup

- Wind tunnel at NTNU, test section of 1.9 x 2.7 x 12.0 m
- Three model turbines with a rotor diameter of D_{rotor} = 0.944 m
- Rotor based on NREL S826 airfoil
- Rated tip speed ratio $\lambda_{T1} = \lambda_{T2} = \lambda_{T3} = 6.0$
- Inter-turbine spacing of x/D=3
- Uniform inflow at u_{ref} = 11.5 m/s
- Inflow of low turbulence intensity at TI_{T1}=0.23% (at first turbine pos.)

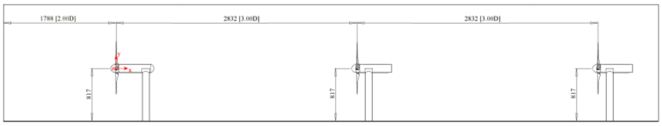

Figure 2 Experimental setup of three model wind turbines in the large wind tunnel at NTNU

- In-nacelle torque- and RPM-sensors
- Wake flow measurements by Laser-Doppler-Anemometer (LDA)
- Scanning turbine power in steps of $\Delta\lambda_{T1}$= 0.5 and $\Delta\lambda_{T2}=\Delta\lambda_{T3}$=0.2

Reference case

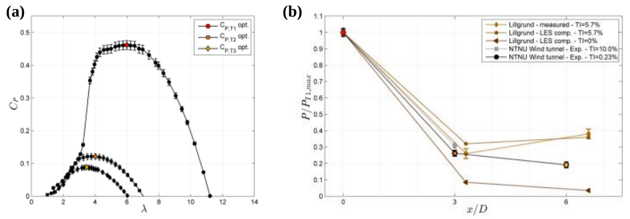

Figure 3 (a) C_P-λ-curves of the three aligned turbines, all referred to u_{ref}=11.5m/s
(b) relative power of test cases compared to full-scale data from Lillgrund windfarm
[Nilsson et al. Large-eddy simulations of the Lillgrund wind farm. *Wind Energy 2015*;18:449–467]

1st turbine curtailment

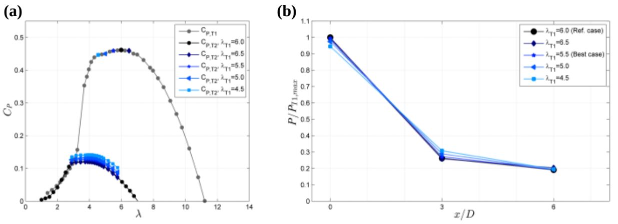

Figure 4 (a) C_P-λ-curves of the second turbine T2 depending on different tip speed ratios of T1
(b) relative power for T1, T2 and T3 for a curtailed first row turbine T1

2nd turbine curtailment

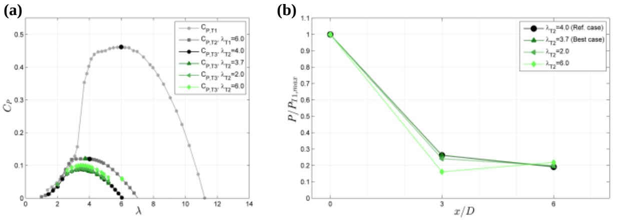

Figure 5 (a) C_P-λ-curves of the third turbine T3 depending on different tip speed ratios of T2
(b) relative power for T1, T2 and T3 for a curtailed second row turbine T2

Wake flow analysis

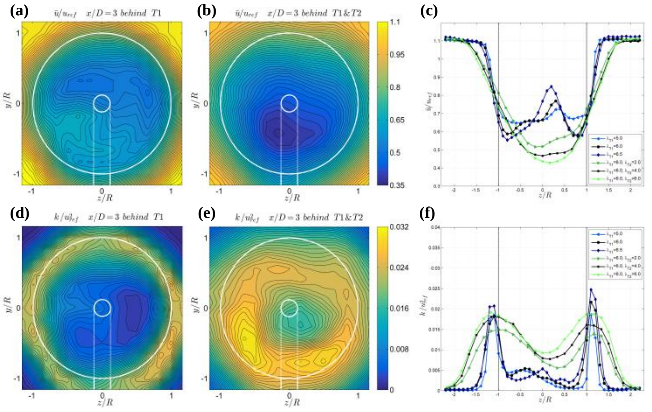

Figure 6 **(a,b,c)** Normalized mean velocity and **(d,e,f)** Normalized turbulent kinetic energy
(a,d) behind T1 operated at λ_{T1}=6; **(b,e)** behind T1 operated at λ_{T1}=6 and T2 operated at λ_{T2}=4 (reference case);
(c,f) behind T1 operated at λ_{T1}=5,6,7 (blue) resp. T1 and T2 operated at λ_{T2}=2,4,6 (green) (curtailed cases)

Conclusions

- Power measurements show good agreement with full-scale data from Lillgrund
- Considerably bigger power drop from T1 to T2 (74%) than from T2 to T3 (27%)
- Higher mean velocity loss in the wake behind T2 than in the wake behind T1
- More spread out distribution of turbulent kinetic energy behind T2 than behind T1
- Only insignificant total power gains ($P_{T1}+P_{T2}+P_{T3}$) of less than 1% achieved by T1 curtailment; (T1 curtailment more effective than T2 curtailment)
- Best combined efficiencies achieved for slightly lower than rated tip speed ratios
- Small potential of curtailment for wind farm power optimization, but effective method for load distribution between turbine rows at constant power?

METU
Center for Wind Energy

NTNU
Energi- og Prosessteknikk

A step towards reduced order modelling of flow characterized by wakes using Proper Orthgonal Decomposition

Eivind Fonn, Mandar Tabib, Adil Rasheed, Trond Kvamsdal
SINTEF Digital
eivind.fonn@sintef.no — +47 41 44 98 89

Introduction

Problem: High fidelity simulations of flow can be quite demanding, involving up to 10^6–10^9 degrees of freedom and several hours (or days) of computational time, even on powerful and parallel hardware architectures. These techniques can be prohibitive in dealing quickly and efficiently with repetitive solution of PDEs.

Answer: To address the issues, the field of reduced order modelling (ROM) is evolving quickly. We investigate proper orthogonal decomposition (POD) as a potential method for constructing reduced bases for use in ROMs. In the case of flows around cylindrical bodies we found that only a few modes were sufficient to represent the dominant flow structures and their associated energies.

Method

High fidelity simulations were performed of flow around a cylinder, at three different Reynold's numbers ($\mathrm{Re} = 265, 2580, 40000$). Simulations were performed with uniform and pulsating inflow boundary conditions,

$$u_{\text{uniform}} = u_\infty = 1\,\mathrm{m/s},$$
$$u_{\text{pulsating}}(t) = u_\infty + \Delta u \sin(2\pi f t)$$

chosen so that $\Delta u = 0.2 \cdot 2\pi f D$, where D is the diameter of the cylinder.

Two-dimensional snapshots were generated from these simulations, representing in each case at least one principal period, sampled at $20\,\mathrm{Hz}$. All snapshots were interpolated on a common, uniform grid and reduced using proper orthogonal decomposition (POD) to an "optimal" ensemble.

Partial Orthgonal Decomposition

Given an ensemble of solutions $\{\varphi_i\}_{i=1}^p$, we seek a set of orthogonal modes $\{\zeta_j\}_{j=1}^p$ such that the reconstructed ensemble truncated at some order N,

$$\varphi_i^{(N)} = \sum_{j=1}^N a_i^j \zeta_j$$

represents the original ensemble "closely", as measured by some norm $\|\cdot\|_a = \sqrt{\langle\cdot,\cdot\rangle_a}$. This gives the covariance matrix $C_{ij} = \langle\varphi_i, \varphi_j\rangle_a$. Its eigenpairs $(\boldsymbol{q}_i, \lambda_i)$ yield the desired modes as

$$\zeta_i = \frac{1}{\sqrt{\lambda_i}} \sum_j q_i^j \varphi_j,$$

The sum of eigenvalues is equal to the trace of $\boldsymbol{C}$, and is interpreted as the average variance in the ensemble. Each eigenvalue λ_i is equal to the average variance captured by its corresponding mode ζ_i throughout the ensemble. Therefore, a condition on N should be

$$\textstyle\sum_{i=N+1}^p \lambda_i / \sum_{i=1}^p \lambda_i \leq \epsilon.$$

We choose to focus on the representation of velocity, so that the covariance function can be written

$$\langle(\overline{\boldsymbol{u}}_i, p_i), (\overline{\boldsymbol{u}}_j, p_j)\rangle_a = \int_\Omega \overline{\boldsymbol{u}}_i \cdot \overline{\boldsymbol{u}}_j.$$

Acknowledgements

We acknowledge financial support from the Norwegian Research Council and the partners of FSI-WT (grant no: 216465/E20; fsi-wt.no).

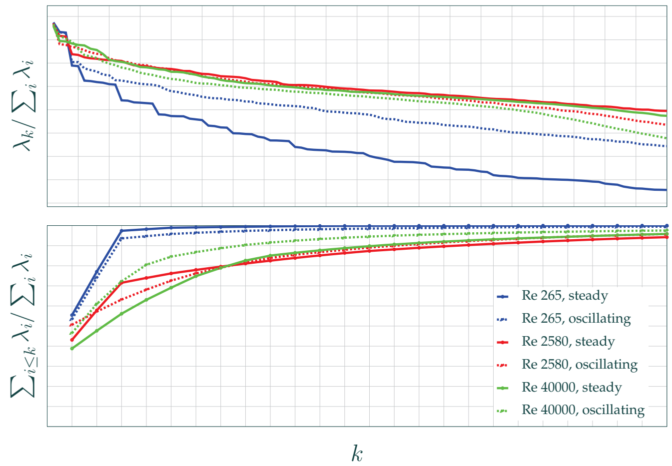

Energy spectrum and cumulative energy spectrum for the six different cases.

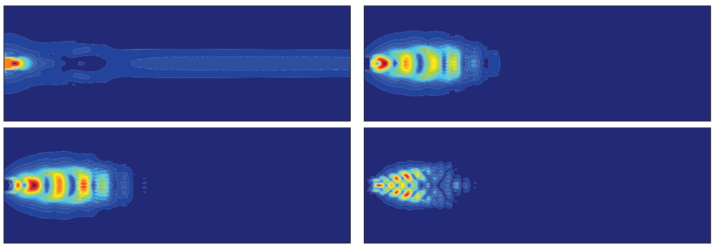

First modes for $\mathrm{Re} = 265$.

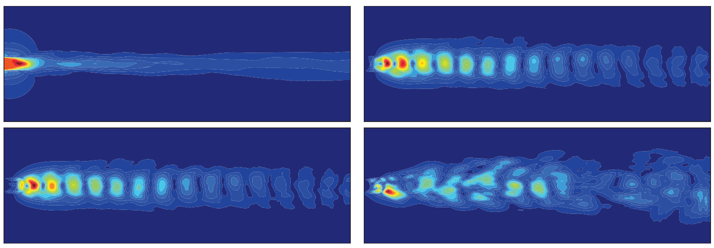

First modes for $\mathrm{Re} = 2580$.

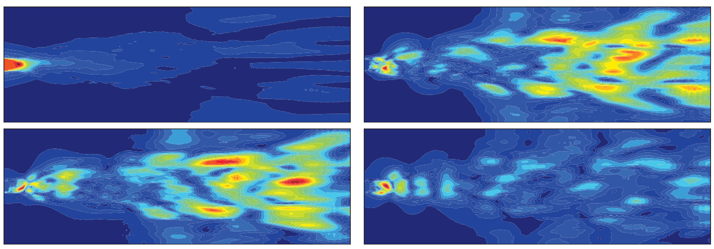

First modes for $\mathrm{Re} = 40000$.

Discussion

In all cases, about 30 modes suffice to cover 90% of the energy content. For low Reynold's number cases, the number of considerably smaller. For the other cases, the energy decay is consistent, suggesting this decay rate may be representative for a wider range of parameters. The first mode is always "laminar" and the following two modes appear to be phase-shifted principal oscillations. Higher modes provide turbulent content.

For the kinds of flows considered here, POD appears an attractive method for constructing the reduced bases required by ROMs.

Explaining the Torque vs TSR curve in a Fully Resolved Setting on a Mega Watt Size Wind Turbine.

M. Salman Siddiqui[1], Adil Rasheed[2], Mandar Tabib[2], Trond Kvamsdal[1,2]
[1]NTNU, Dept. of Mathematical Sciences, NO 7491 Trondheim. [2]SINTEF ICT, Dept. of Applied Mathematics, NO 7465 Trondheim.

INTRODUCTION

A fully resolved Sliding Mesh Interface(SMI) and Multiple Reference Frame (MRF) techniques are implemented to predict the aerodynamic performance and wake distribution of a complete wind machine. The present study identify the predictive capabilities of both numerical techniques against the experimental results to study the performance of wind turbine under various Tip Speed Ratio's(TSR). NREL 5MW reference wind turbine design is employed as the baseline model. Performance predictions are studied in terms of overall torque produce by the turbine. We also analysed the velocity deficit behind the turbine, along with the estimate of the profiles of turbulent fluctuations in the wake behind the wind turbine.

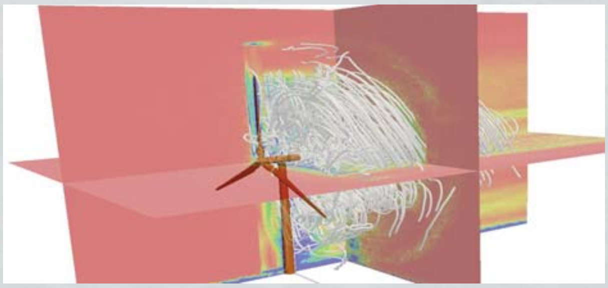

METHODOLOGY

The computational model employed to simulate the flow behaviour is shown in Figure 3 with the corresponding boundary conditions. Complete wind turbine is modeled including the support structure. A hybrid finite element mesh with structured hexahedral elements close to the rotor and structure surface and tetrahedral mesh elsewhere is used.

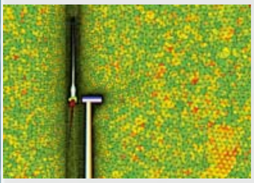

Figure 1: Mesh domain

Figure 2: Mesh rotor

Two different approaches are implemented to model the rotating turbine: a)computationally expensive but supposedly more accurate Sliding Mesh Interface (SMI), b)faster but less reliable Multiple Reference Frame (MRF). Eventually, MRF, is used to evaluate the performance of a full scale turbine under different TSR.

Figure 3: Computational setup

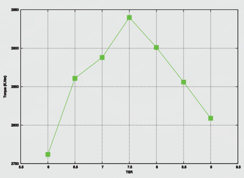

Figure 4: Torque vs. TSR

RESULTS AND DISCUSSION

Impact of TSR on torque generated

AT low TSR values (6.5 or 6), wind starts impinging on the top of the blade section instead of the leading edge, resulting in massive flow separation. This is true for all the cross sectional profiles along the blade(Figure6). The arrival of stall at lower TSR values than the optimal TSR is the cause of under performance of a wind turbine at low TSR values. An opposite trend is observed when one approaches a TSR of 9. The flow becomes more symmetric relative to the blade and hence the lift generated diminishes resulting in a lower torque generation. . It also suggest that the cross sectional geometry tends to get more aerodynamically shaped away from the hub and towards the blade edge and since a big contribution of torque comes from the outer section of the blade

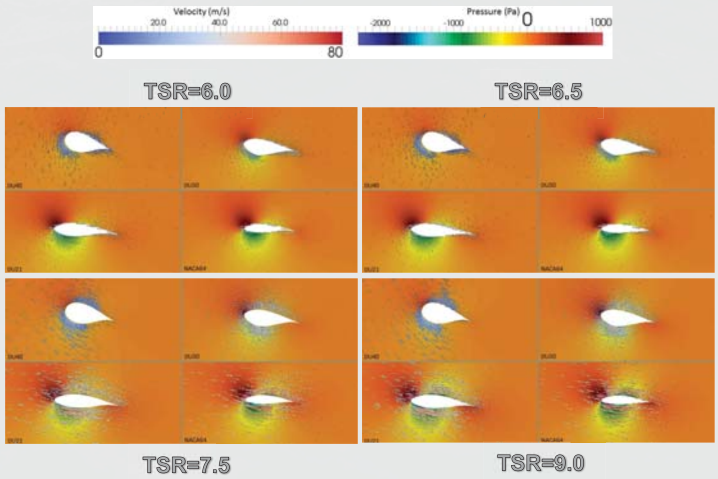

Fig 5: Velocity and pressure contour along the blade

The contours of velocity deficit behind the wind turbine is plotted to highlight the characteristics of wake distribution at certain distances in downstream direction at optimal TSR=7.5

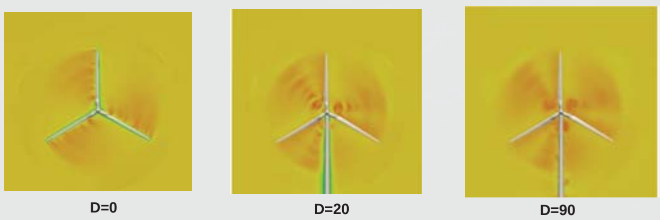

Fig 6 : Wake distribution pattern in the downstream direction

Effect on wake

Rotation of wind turbine leads to distortion of field variables in the downstream direction. In order to parametrize the behavior we have plotted the wake distribution in terms of turbulent kinetic enegry behind the wind turbine in the vertical and lateral directions.

The support structure is found to disrupt the flow field, especially, the presence of tower cause a significant increase in the turbulent levels in the vertical direction. Oscillatory behavior of profiles are observed adjacent to the tower, however, the eddies emanating gets adverted and loses their energy due to turbulent mixing and wake diffusion.

Where as, in the lateral direction, sharp gradients of turbulent kinetic energy are observed on one side, which is attributed to the deflection of wake behind the trailing edge of turbine blade.

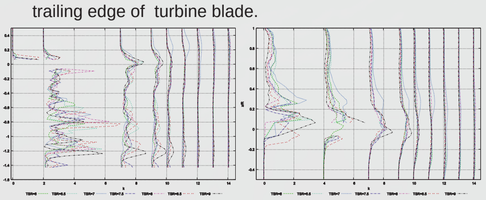

Turbulent kinetic energy in vertical direction TSR=7.5

Turbulent kinetic energy in lateral direction TSR=7.5

Fig 7 : Wake structure

CONCLUSION

- Flow simulation around a full scale 5MW NREL reference turbine is conducted with SMI and MRF approach using turbulence models. The performance of turbine operating at different TSR are evaluated using MRF.
- The variation of torque at various tip speed is qualitatively explained using the contours of pressure magnitude imposed with velocity vector field at various cross sections in the spanwise direction, which identified the flow distribution which alter the torque characteristics.
- TSR 7.5 corresponds to the maximum torque. Below this TSR, the performance degrades due to stall experienced by the outer sections of the blade. Above the optimal value of TSR, the incoming flow becomes symmetric relative to the blade section and this results in smaller magnitude of generated lift and hence the torque.

The authors acknowledge the financial support from the Norwegian Research Council and the industrial partners of the FSI-WT-project (216465/E20) and NOWITECH-project (Grant No.:193823/S60)
Contact: muhammad. siddiqui@math.ntnu.no

SINTEF · NTNU Norwegian University of Science and Technology · FFI Forsvarets forskningsinstitutt · Meteorologisk institutt · TrønderEnergi · windsim · Statoil · KJELLER · Forskningsrådet

A 3D Vs Q3D Vs 2D CFD analysis of 5MW NREL reference wind-turbine

Mandar Tabib, Adil Rasheed, M. Salman Siddiqui Trond Kvamsdal
[1]Mathematics and Cybernetics, SINTEF Digital, Strindveien 4, 7035, Trondheim, Norway.

INTRODUCTION AND OBJECTIVES

Turbine-blade manufactured for a real wind-farm operation generally comprises of multiple-airfoil segments. These segments impart a complex 3D geometry to the whole blade involving span-wise variations of the chord length, blade thickness ratio and blade twist . Hence, there is a need to understand the influence of 3D bluff body effects. The current study focusses on stand-still aerodynamics, which has relevance in wind turbine operation. Generally, wind-turbine blades are designed for rotating conditions with tapering of blade thickness from root to tip and varied span-wise blade twist (which helps to maintain an optimum power coefficient and similar angle of attack throughout blade-span). This geometric optimization works well in the rotating operational environment for which it is meant. However, in non-rotating environment (i.e. the stand-still aerodynamics condition), the blade twist optimized for rotation will make the flow artificially 3D compared to the actual rotor flow itself. Such conditions of stand-still aerodynamics may arise when both yaw and pitch regulations are off-line, say during the turbine-erection phase before the wind turbines are connected to the electrical grid. In absence of a wind turbine control situation during off-line, the angles of attack of the flow on the blades are determined by the free wind direction, and the wind-turbine may operate outside the narrow normal operational range. In such stand-still situations, complex 3D effects may exist owing to both the operating circumstances and the 3D complex turbine geometry. Hence, the **main objectives of this work are : (a) To identify the impact of bluffness of turbine-geometry and impact of changing cross-section of NREL 5MW under a stand-still aerodynamics condition on the flow-physics, and, (b) Comparing the flow physics obtained from 2D Vs Q3D (2.5D) vs 3D simulations.**

METHODOLOGY- VALIDATION AND SIMULATION

The NREL 5 MW turbine is a popular reference industrial scale wind turbine and hence has been chosen for this study. Four airfoil segments of the NREL 5 MW blade which are located at varied span wise radial distance from hub (as shown in Table 1) are considered for comparing the 3D effects due to bluff shape and to compare the flow physics predicted by 2D Vs Q3D Vs 3D simulation. The 3D simulation refers to a full scale 3D blade simulations with computational domain (shown in Figure 1) and near blade mesh and segment location (shown in Figure 2) respectively. The Q3D (or 2.5D segments) are created by clipping the specific 3D airfoil section from the full scale 3D model so as to include the tapering effects along the radial direction Modeling this intermediate QSD (2.5D) behaviour enhances the intuition of the characteristic change in flow behaviour from simple two dimension to complete three dimension. 2D simulations involve four individual airfoil simulation along planes in Fig 2.

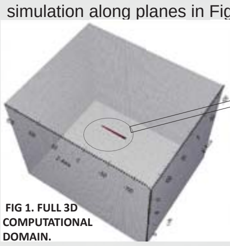

FIG 1. FULL 3D COMPUTATIONAL DOMAIN.

FIG 2. ZOOMED - LOCATION OF AIRFOIL SEGMENTS AND MESH NEAR BLADE.

Segment	location of segment from hub, m	Angle of attack,°	Chord length, m
NACA-64	at z=44.55 m	α=3.12°	c=3.01 m
DU-21	at z=36.35 m	α=-5.36°	c= 3.50 m
DU-35	at z=15.85 m	α=-11.48°	c=4.65 m
DU-40	at z=11.75 m	α=-13.30°	c=4.55 m

TABLE 1. LOCATION OF AIRFOIL SEGMENTS AND PROPERTIES.

The validation of results from 2D model is given below

RESULTS – VALIDATION OF 2D MODEL AND COMPARISON OF 2D VS 2.5D AND 3D ON DRAG AND LIFT COEFFICIENTS.

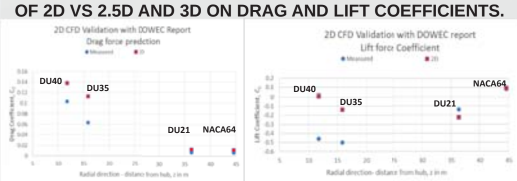

Figure 3 **above** – In regions away from hub (at NACA64), the 2D simulated lift and drag coefficient results are in close agreement with the measured results (DOWEC* report). This is because the flow is mostly 2D away from hub. As we move in the near hub region at DU40, the 2D results deviates a lot from measurements as influence of 3D effect dominates. **Figure 5** shows the increase in flow complexity as we move away from hub.

*Kooijman et. al.. 2003. DOWEC 6 MW Pre-Design. Public report - DOWEC 10046-009.

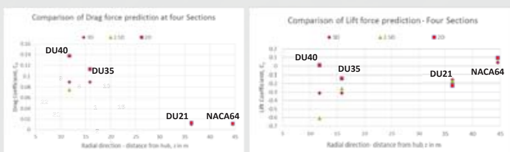

Figure 4 **above**[1]: Comparison of 2D Vs 2.5D Vs 3D predictions of drag and lift coefficient. 3D and 2.5D results cannot be compared with measured values reported in DOWEC because the turbine blade geometry has more tapering than the individual airfoil geometry studied in DOWEC.

RESULTS– 2D VS Q3D VS 3D PREDICTED FLOW AT FOUR AIRFOIL SEGMENTS.

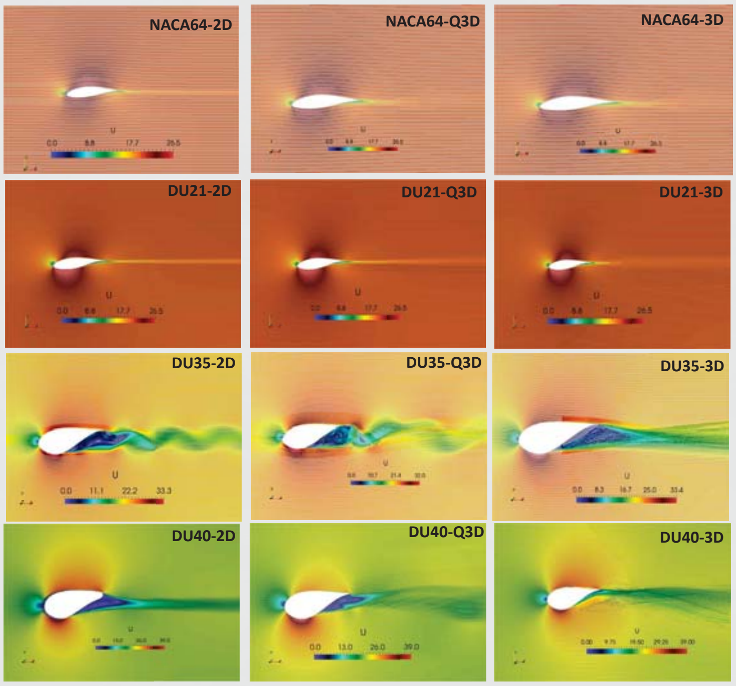

Figure 5: Flow profiles obtained by 3D Vs 2.5D Vs 2D simulation at four airfoil segments of the turbine blade.

NACA64 airfoil profile is located farthest from the hub (at z=44.5m) with an angle of attack of 3.12^0. It experience a streamlined flow and there is negligible difference between the three simulations (2D, 2.5D, 3D) and the predicted drag and lift coefficient, implying, a lack of three dimensionality and associated unsteadiness in the flow behavior.

The DU40 airfoil is the closest section to the hub that has been studied (at z=11.75m) with highest angle of attack of 13.3^0. Here, the reported drag and lift coefficient values (Figure 4) are higher in magnitude than the simulated values for DU35, DU21 and NACA64. Similar to DU35, the DU40 case also have shown a **high variations** in the predicted drag and lift coefficient values from the three approaches which can be attributed to difference in flow physics captured by 3 approaches (Figure 5).

CONCLUSION

This work has been able to identify the impact of bluffness of turbine-geometry. The results indicate that even for a non-rotating blade (in stand-still aerodynamic condition), the blade-segments nearer to the hub, the flow is dominated by complex 3D structures and as one moves away towards blade segments located towards the tip, the flow begins to loose its 3D characteristics and can be reasonably well represented by efficient 2D simulations. Since the outer part of the blade makes a significant contribution to the total torque generated, a 2D approach might be sufficient to predict torque and associated power reasonably well. However, a 3D approach will still be required to predict structural failure and for efficient blade design.

The authors acknowledge the financial support from the Norwegian Research Council and the industrial partners of the FSI-WT-project (216465/E20) and NOWITECH-project (Grant No.:193823/S60)
Contact: Mandar.Tabib@sintef.no

Simulating single turbine and associated wake development - comparison of computational methods (Actuator Line Vs Sliding Mesh Interface Vs Multiple Reference Frame) for an industrial scale wind turbine

Mandar Tabib[1], Adil Rasheed[1], M. Salman Siddiqui, Trond Kvamsdal
[1]Mathematics and Cybernetics, SINTEF Digital, Strindveien 4, 7035, Trondheim, Norway.

INTRODUCTION AND OBJECTIVES

Accurate modelling of turbine behaviour will lead to an accurate assessment of loading and wake behaviour, which helps in obtaining better assessment of power generation capability and better designing of turbines. Wakes generated from turbines can influence power production in multi-turbine wind farm set-up. Amongst various computational models, a wind farm performance can be simulated in a computationally efficient way using Actuator line model (ALM) and is popularly used to do so. An improved understanding of accuracy of ALM through comparison with more accurate but computationally exhaustive methods (like sliding mesh interface (SMI)) will be helpful in quantifying uncertainties associated with ALM. The objective of this work is to evaluate and compare predictive capability of various computational methods: ALM, SMI and Multiple Reference Frame (MRF) for a single industrial scale turbine.

METHODOLOGY

The methodology involves simulating behaviour of a popular three bladed industrial scale wind-turbine, the NREL 5 MW industrial scale turbine, using three different computational techniques (ALC, SMI, MRF). The 5MW NREL turbine consists of three 63m long blades, with each blade comprising of 8 airfoils at different locations away from the hub (see Table 1).

Airfoil profile	Thickness (t/c)	Distance from the center (m)	Chord (m)	Twist angle(°)
Cylinder1	100%	2.00	3.542	0.000
Cylinder2	100%	5.60	3.854	0.000
DU40-A17	40.50%	11.75	4.557	13.308
DU35-A17	35.09%	15.85	4.652	11.480
DU30-A17	30.00%	24.05	4.249	9.011
DU25-A17	25.00%	28.15	4.007	7.795
DU21-A17	21.00%	36.35	3.502	5.361
NACA64-A17	18.00%	44.55	3.010	3.125

Regarding the three approaches used in this work : the Sliding Mesh Interface (SMI) (Geometry and mesh in figure 1) captures the unsteady flow by explicitly modelling the blades and its rotation using a dynamic mesh, while Multiple Reference Frame (MRF) (in Figure 2) captures a steady state flow as it employs a frozen rotor hypothesis (i.e. static blade) and involves use of Coriolis and centrifugal forces in momentum equation to account for rotation. A 120^0 sector geometry is used with rotational periodicity employed across two boundary. On other hand, the Actuator Line Model (Figure 3) is a transient model where the blades are not modelled explicitly but each blade is resolved as a rotating line (made of N actuator segments), over which the forces are computed. The ALM model relies on input blade aerofoil data to compute lift and drag coefficient at each segment. This non-explicit way of resolving blade in ALM leads to use of coarser mesh and efficient computation, as there is no need to resolve boundary layers and no rotating mesh.

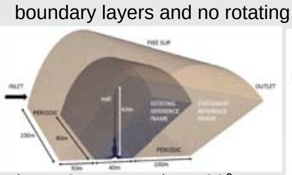

Figure 2 . MRF using 120^0 sector with rotational periodicity.

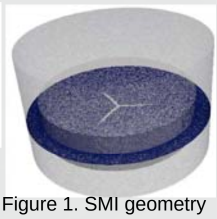

Figure 1. SMI geometry and mesh used.

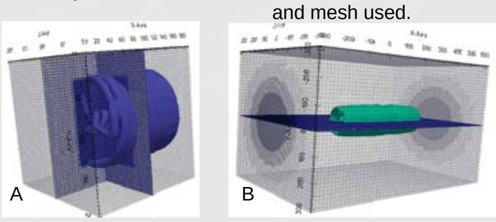

Figure 3 Actuator line model. (A) Finer mesh near turbine and (B) Coarser mesh with wider geometry.

RESULTS– COMPARISON OF THREE METHODS

Figure 4 shows predictions of Wake deficit (*X-axis*) by 3 models at TSR of 7.5 along a vertical line perpendicular to the axis of the turbine (z/*R*, on *Y axis*) for six locations located downstream of turbines i.e. 0.15R downstream, 0.30R 0.45R, 0.60R, 0.90R, 1.30R). R is the radius of turbine diameter (=63 m).

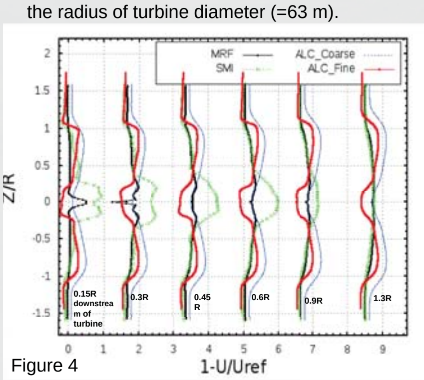

Figure 4

The ALC models is seen to differ from MRF and SMI models in 2 major ways,

A. In all downstream regions near the hub axis (0.25>z/R>-0.25), ALC models suggest no wake deficit as the hub is not modelled.
B. At all downstream locations in range (1>z/R>0.3), the ALC models predict higher wake deficit than MRF and SMI. In other words, the MRF and SMI models show faster wake recovery.

Figure 5A below shows influence of tip speed ratios (as predicted by the 3 models) on wake deficit for six locations located downstream of turbines i.e. 0.15R downstream, 0.30R 0.45R, 0.60R, 0.90R, 1.30R). R is the radius of turbine diameter (=63 m).

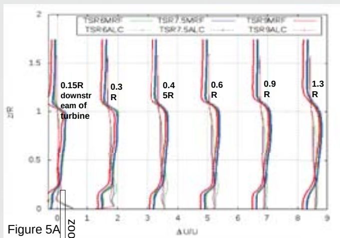

Figure 5A

zoomed

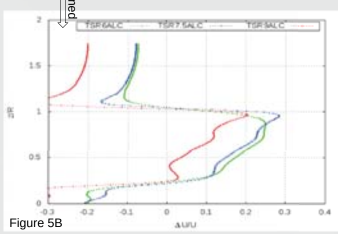

Figure 5B

As observed earlier in Figure 4, the ALC for all three TSR's in Figure 5 too show higher wake deficit between range (1>z/R>0.3) as compared to the corresponding TSRs from MRF method.

Like MRF (Figure 5A), The ALC (Fig 5A and zoomed figure in Figure 5B), shows that at TSR=6, the wake deficit is largest while at TSR=9, the wake deficit is the lowest wake. The reason for this is attributed to the change in angle of attack of flow with TSR. As TSR reduces below 7.5, the flow becomes separated leading to enhanced wake effects and lower coefficient of power, while as TSR increases to 9, the flow becomes more symmetric relative to the blade and hence the lift generated diminishes resulting in a lower power coefficient. As reported by Jonkman, the optimal TSR of 7.55 has highest Cp.

CONCLUSION

The three models have been compared at three different tip speed ratio (at optimum TSR of 7.55, at below the optimum TSR, TSR=6 and at higher than optimum TSR, TSR = 9). The comparison reveals the regions in which the models differ in their predictions and some similarities in qualitative estimation of trends. The differences in quantitative values predicted by the three models can be attributed to the inherent limitations of the ALC model. Despite these limitations, the ALC model is popularly used in wind farms involving multiple turbines due to its computational efficiency. Future work involves comparison of turbulence quantities and flow-pattern analysis as predicted by the 3 models.

The authors acknowledge the financial support from the Norwegian Research Council and the industrial partners of the FSI-WT-project (216465/E20) and NOWITECH-project (Grant No.:193823/S60)
Contact: Mandar.Tabib@sintef.no

2D VAR single Doppler LIDAR vector retrieval and its application in offshore wind energy

Nihanth W. Cherukuru[1], Ronald Calhoun[1], Raghavendra Krishnamurthy[1], Savardal Benny[2], Joachim Reuderb[3]

1 Arizona State University

2 Christian Michelsen Research

3

Introduction

- Doppler lidars can map the winds with high spatial and temporal resolutions
- One of the potential applications of lidars is in adaptive wind turbine control techniques to maximize the power output of a wind farm
- One limitation of a Doppler lidar is its ability to measure only the line of sight (LOS) component of velocity (radial velocity)
- Hence, a reliable wind vector retrieval technique with real-time running capability is a necessary first step in this process
- Existing vector retrievals either rely on the homogeneous wind field assumption (which does not preserve small scale structure) or on computationally expensive 4D-VAR methods (which are impractical for real-time applications)
- A new 2D-VAR method for low elevation PPI scans was devised to address this issue

Formulation

- The 2D-VAR retrieval is based on a parameter identification technique in which the vector field (u,v) is determined such that the cost function (J) composed of a set of constraint equations is minimized
- Apart from the radial velocity, background and the radial velocity advection equations, a new constraint corresponding to the tangential velocity at low elevation angles is formulated by differentiating the radial velocity equation
- The weights were chosen based on the relative importance of the respective terms
- A quasi-Newton method was implemented for minimization

$$J(u,v,P) = \frac{1}{2\Omega}\int (W_a A^2 + W_b B^2 + W_c C^2 + W_d D_a^2 + W_d D_b^2 +)\, d\Omega$$

$$(\Omega = retrieval\ domain)$$

Term	Expression	Description
A	$\left(\frac{ux}{r}+\frac{vy}{r}\right) - V_r^{obs}$	Radial velocity
B	$\left(-\frac{uy}{r}+\frac{vx}{r}\right) - \frac{\partial V_r^{obs}}{\partial\theta} + P$	Tangential velocity
C	$\frac{\partial\tilde{V}_r}{\partial t} + u\,\frac{\partial\tilde{V}_r}{\partial x} + v\,\frac{\partial\tilde{V}_r}{\partial y}$	Radial velocity advection
D_a	$u - u_b$	Background from VVP
D_b	$v - v_b$	

Test Case

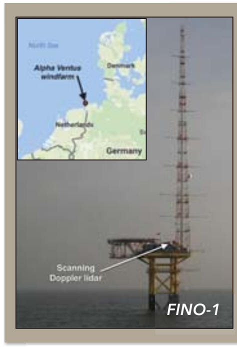

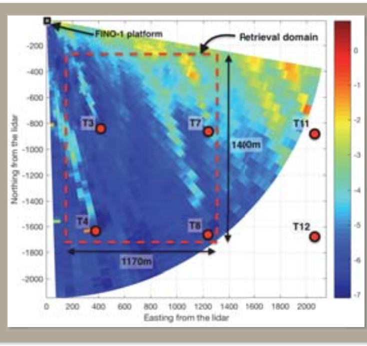

- FINO-1 (Forschungsplattformen in Nord- und Ostsee Nr.1) is a German offshore wind energy research platform located close to the Alpha Ventus wind farm in the North Sea
- A scanning Doppler wind lidar (Leosphere's windcube 100s) was configured to perform repeated low elevation angle (0.5°) PPI scans (90° sector) in the direction of the wind farm
- The 2D-VAR and Volume Velocity Processing (VVP) algorithms were applied in a 1170m x 1400m domain and the results were corroborated with a cup and vane anemometer (CVA) measurements

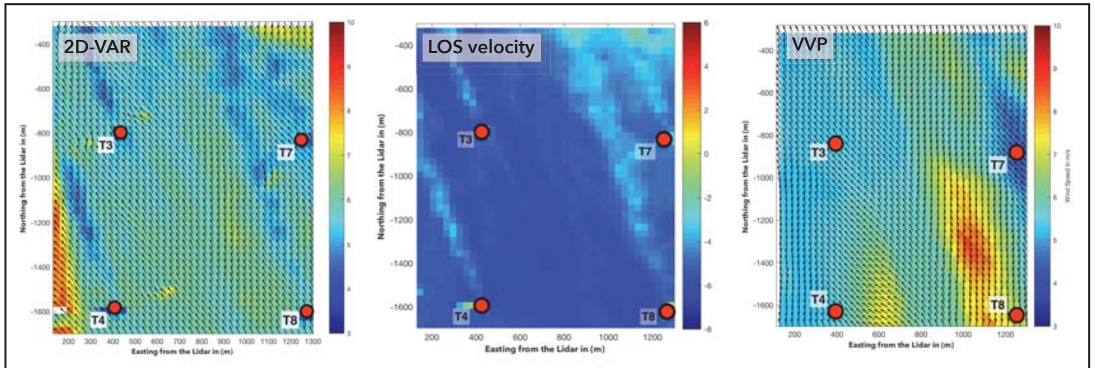

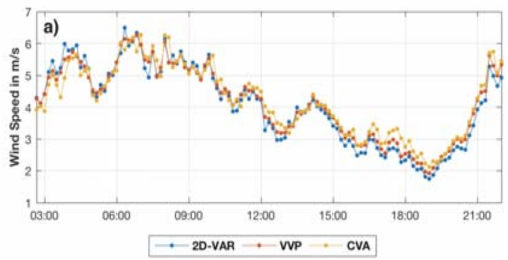

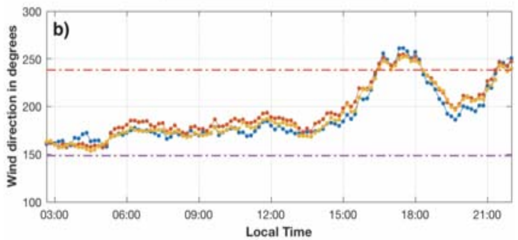

ABOVE: Comparison of the 2D-VAR and VVP retrievals against radial velocity (Line of sight- LOS velocity) as measured by the lidar

LEFT: Comparisons of (a) wind speed and (b) wind direction, retrievals from 2D-VAR, VVP and cup and vane anemometer. These are 10-minute averaged values corresponding to the mean flow

BELOW: Error statistics corresponding to the 10-minute averaged quantities from 2D-VAR and VVP, with the cup and vane anemometer measurements.

Algorithm /Variable	Wind speed error	Wind speed correlation	Wind direction error	Wind direction correlation
2D-VAR	0.383 m/s (5.04%)	0.96	-1.4°	0.98
VVP	0.290 m/s (2.01%)	0.98	4.3°	0.99

Discussion

- The 10-minute averaged wind data from the cup and vane anemometer (CVA) situated at 33m LAT on the meteorological mast was used for corroborating and validating the wind retrieval from both 2D-VAR and VVP algorithms
- Since the lidar and the met mast were both located on the FINO-1 platform, retrieved wind vector from the grid point closest to the platform was considered to construct the 10-minute averaged time series
- It is evident that both VVP and the new 2D-VAR methods estimate the mean flow with good accuracy
- VVP performs slightly better that 2D-VAR in capturing the mean flow primarily due to its underlying formulation which is designed to obtain the mean quantities under the homogeneous wind field assumption
- It is evident from this figure that the wind vectors estimated by the 2D-VAR algorithm corroborate well with the radial velocity measurements, especially in capturing small scale flow structures, including what appear to be wakes behind the wind turbines

Future work

- From this study, it is evident that the true merit of the new 2D-VAR algorithm lies in its ability to preserve small scale flow features, while capturing the mean flow as good as VVP
- However, spatial errors could not be estimated from this dataset primarily due to the lack of instrumentation in the lidar scan region. Data from a lidar simulator running on a background LES windfield could be used to study these errors
- The assignment of weights in the cost function was fixed for all time steps. This could be improved by assigning weights dynamically based on the underlying flow- E.g. the residuals from the VVP stage could be used to increase (or decrease) the weightage of the background term in the cost function

Acknowledgements

- This work was funded by the US Navy Neptune Project
- The authors would like to thank BMWi (Bundesministerium fuer Wirtschaft und Energie), Federal Ministry for Economic Affairs and Energy and the PTJ (Projekttraeger Juelich, project executing organisation) for the FINO1 met- mast data, the NORCOWE consortium for the access to the Lidar data and the related assistance.

DTU Wind Energy
Department of Wind Energy

IRPWIND ScanFlow project

Charlotte Hasager (cbha@dtu.dk), Torben Mikkelsen, Nikolas Angelou, Alfredo Peña, Gregor Giebel, DTU Wind Energy, Denmark, Steen Andreasen, Andreasen Engineering, Denmark

Jan Willem Wagenaar, Gerard Schepers, Erwin Werkhoven, ECN, the Netherlands,

WindScanners from windscanner.eu

ScanFlow

The ScanFlow project is short for the full project title:
“High-resolution full-scale wind field measurements of the ECN’s 2.5 MW aerodynamic research wind turbine using DTU’s 3D WindScanner and SpinnerLidar for IRPWind’s and EERA’s benchmark”.

Objective

The objective of ScanFlow is to establish a unique turbine power performance and induction zone benchmark experiment.

Methodology

The methodology is to operate a DTU developed high-resolution nacelle 2D SpinnerLidar installed at a research wind turbine at ECN and, concurrently, operate three DTU ground-based short-range WindScanner lidars to perform 3D wind velocity field observations.

The scientific progress beyond previous experiments will be to achieve data from three vertical planes 10-minute averages of all three wind components. Furthermore we will also observe turbulence along one horizontal transect from 1Hz data. The baseline inflow i.e. when the turbine is not in operation and the induction zone from the operating row of turbines will be observed and quantified by a novel solution.

Furthermore the rotor plane equivalent wind speed can be reverse- calculated to wind speed from wind power production at 1 Hz fast production data and compared to WindScanner turbulence observations as well at turbulence data from the meteorological mast.

Test site

The ECN Wind turbine Test site allows for full scale wind turbine and wind farm related research, development and technology. The test site consists of flat, agricultural terrain with single farm houses and occasionally rows of trees. The average wind speed at 80m is 7.5 m/s and the main wind direction is South-West. The site comprises 5 modern, full scale research turbines (Nordex) with a hub height and rotor diameter of 80m and rated power of 2.5MW. The area is shown below.

Please see Poster G62 for further information!

ECN Test Site with 5 research turbines in flat agricultural terrain.

Measurements

The observations with the SpinnerLidar started early December 2016 and will end late January 2017. During January 2017 the three short-range lidars will measure.

Data access

www.irpwind-scanflow.eu
Please see Poster G62 for further information!

Preparing to drive from DTU to ECN with the SpinnerLidar

Preparation at ECN with the SpinnerLidar

Hoisting the the SpinnerLidar to the Nordex wind turbine at ECN

Acknowledgement: “The work described here has received support from IRPWind 609795, a project that has received funding from the European Union’s Seventh Programme for Research, Technological development and Demonstration”

Comparison of numerical response predictions for a bottom fixed offshore wind turbine

Stian Høegh Sørum[a,b], Jan-Tore H. Horn[a,b], Jørgen Amdahl[a,b]
[a]Centre for Autonomous Marine Operations and Systems (NTNU AMOS),
[b]Department of Marine Technology, NTNU, Trondheim, Norway.
Email: stian.h.sorum@ntnu.no

NTNU AMOS
Centre for Autonomous Marine Operations and Systems

Introduction

A large number of software codes are available for the analysis of offshore wind turbines. Due to the limited availability of full-scale measurements, verification of the codes are often done by code-to-code comparisons. Here, the codes SIMA from MARINTEK, vpOne/USFOS from Virtual Prototyping and FAST v8 from NREL are compared. The response to a selection of load cases are calculated, before a fatigue analysis is performed.

Models

The modelled turbine is based on the DTU 10 [MW] reference turbine [1, 2]. To reduce the frequencies of the 1st tower modes, the tower wall thickness is increased with 20 %, and the blades are modified as given in [3]. The foundation is of the monopile type, with a diameter of 9 [m] and wall thickness of 0.11 [m].
While the structure is modelled using FEM in both SIMA and vpOne, a modal model is used in FAST. The two first tower modes in fore-aft and side-side direction are modelled, as well as the two first flapwise modes and first edgewise mode of the blades. The natural frequencies of the models are given below:

Mode	Frequency range
1st tower side-to-side	0.226-0.227 [Hz]
1st tower fore-aft	0.228 [Hz]
1st blade asym. flap (yaw)	0.563-0.564 [Hz]
1st blade asym. flap (pitch)	0.592-0.594 [Hz]
1st blade collective flap	0.624 [Hz]
1st blade asym. edge 1	0.946-0.951 [Hz]
1st blade asym. edge 2	0.950-0.957 [Hz]
2nd tower side-to-side	1.241-1.303 [Hz]
2nd tower fore-aft	1.183-1.189 [Hz]
2nd blade asym. flap (yaw)	1.460-1.466 [Hz]
2nd blade asym. flap (tilt)	1.682-1.715 [Hz]

Analysis Parameters

A number of analysis types have been run to investigate the predicted responses. Here, two analyses are presented. The first is the steady state response of the turbine as a function of wind speed. For steps of 0.5 [m/s] the turbine response with all degrees of freedom enabled has been calculated, to give an overview of the basic aerodynamic properties and structural response.
The fatigue analysis was performed in operational conditions using bin sizes of 2 [m/s] for wind speed and the most probable significant wind speed and wave height for each wind speed. Metocean data were provided for the Dogger Bank area[4]. Wind turbulence is assumed to be of class B, while all waves are assumed to be long crested and travelling in the same direction as the wind. The analysis parameters are shown below.

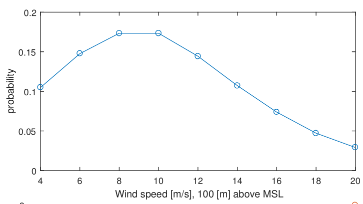

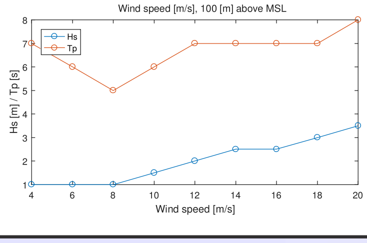

Program capabilities

The programs used have different capabilities for calculating loads and response. All codes calculate the hydrodynamic loads using Morrison's equation, while the differences in utilized mode capabilities are given below. In addition, there are differences in the engineering corrections applied to the BEM calculations.

	SIMA	vpOne	FAST
Aerodynamic loads	Steady BEM	Steady BEM	Unsteady BEM
Hydrodynamic stretching	Wheeler	Wheeler	None
Soil model	Non-linear springs	Non-linear springs	Equivalent beam
Strucutral model	Finite element model	Finite element model	Modal model

Results

The steady state analysis yielded similar results for all codes, with a few exceptions. For wind speeds above rated, both vpOne and FAST predicts a higher thrust force than SIMA, with a decreasing difference as the wind speed increases. This is partially caused by the controller in SIMA pitching the blades more than the other codes.
Furthermore, the equivalent beam in FAST is tuned to give the correct natural frequency, without regard to the displacement and rotation at mudline. This may again influence the aerodynamic damping due to reduced motions of the tower top.
The fatigue analysis shows a significant difference in the predicted utilization of the structure, evaluated at mudline. Especially for high aerodynamic thrust, the difference is clearly visible. Here, FAST predicts clearly larger damage than the two other codes. An explanation can be provided by investigating the thrust and mudline moment spectra for these environmental conditions. In the thrust spectrum, FAST can be seen to have a larger response amplitude at the low frequency end of the spectrum, as well as larger response at the 1st natural frequency of the tower and at the peak frequency of the wave spectrum. This indicates that the provided aerodynamic damping is to low in FAST, and that this is cause for the increased predicted fatigue utilization. Similarly, the reduced utilization in vpOne is believed caused by an increased aerodynamic damping, both of the first and second tower modes.

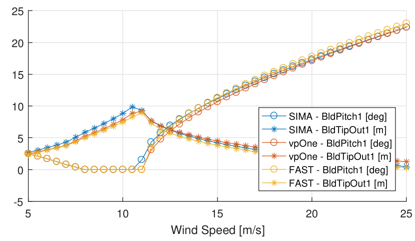

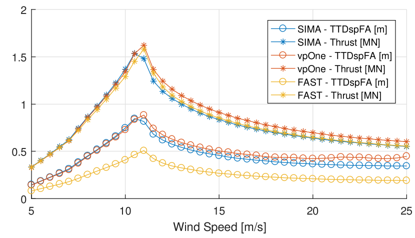

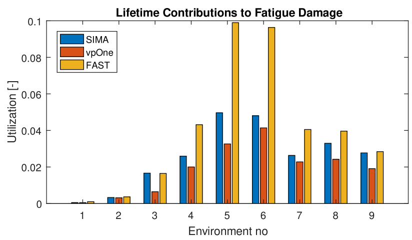

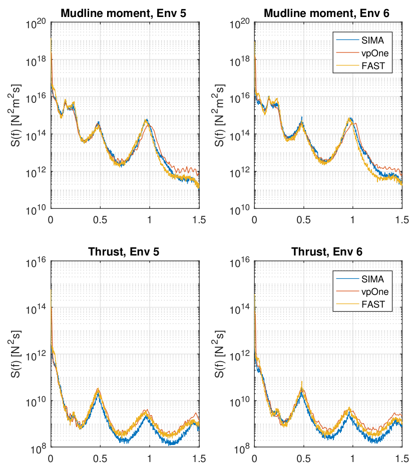

With the larger utilization predicted by FAST, the importance of correct representation of the soil data is demonstrated. However, there is also a large difference between SIMA and vpOne. These programs are quite similar in capabilities and steady-state responses, and show that there can be a large difference in the response predicted by the codes.

References

[1] C. Bak, F. Zahle, R. Bitsche, T. Kim, A. Yde, L. C. Henriksen, P. B. Andersen, A. Natarajan, and M.H. Hansen. Design and performance of a 10 MW wind turbine. *Wind Energy*, To be accepted.

[2] M. H. Hansen and L. C. Henriksen. Basic DTU wind energy controller. Report, DTU Wind Energy, 2013.

[3] E. E. Bachynski and H. Ormberg. Hydrodynamic modeling of large-diameter bottom-fixed offshore wind turbines. In *ASME 2015 34th International Conference on Ocean, Offshore and Arctic Engineering*. American Society of Mechanical Engineers, 2015.

[4] M. Reistad, Ø. Breivik, H. Haakenstad, O. J. Aarnes, B. R. Furevik, and J.R. Bidlot. A highresolution hindcast of wind and waves for the North Sea, the Norwegian Sea, and the Barents Sea. *Journal of Geophysical Research: Oceans*, 116, 2011.

Acknowledgements

This work has been carried out at the Centre for Autonomous Marine Operations and Systems (NTNU AMOS). The Norwegian Research Council is acknowledged as the main sponsor of NTNU AMOS. This work was supported by the Research Council of Norway through the Centres of Excellence funding scheme, Project number 223254 - NTNU AMOS.

ForWind Center for Wind Energy Research

CARL VON OSSIETZKY universität OLDENBURG

Effect of intermittency on a model wind turbine's wake recovery

I. Neunaber[1], J. Schottler[1], J. Peinke[1] and M. Hölling[1]

[1]ForWind - Center for Wind Energy Research, University of Oldenburg, Germany

Motivation & Methods

We present an experimental examination of the influence of different inflow turbulences on the wake of a model wind turbine.

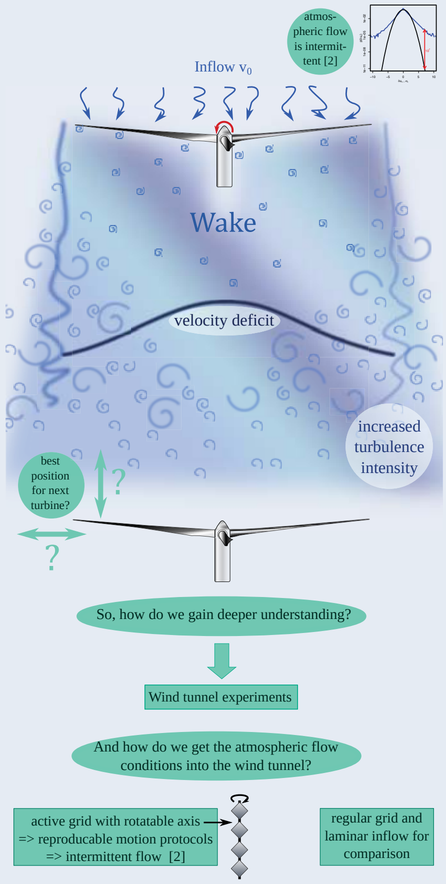

wind tunnel setup

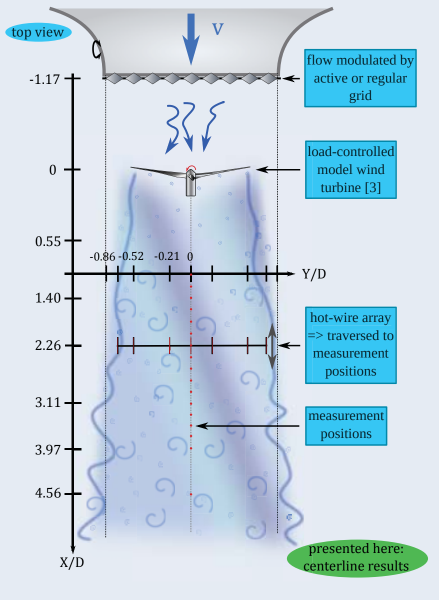

Mean velocity $\bar{v}_0$ and turbulence intensity TI_0 of the different inflow conditions at rotor position (no turbine installed)

	laminar	regular grid	active grid
$\bar{v}_0$ / m/s	7.56	7.28	8.07
TI_0 / %	1.36	6.72	12.81

Results

Probability density functions (PDFs) $p(\delta v(\tau))$ of velocity increments $\delta v(\tau) = v(t+\tau) - v(t)$ for different time lags τ and different turbulent inflow conditions

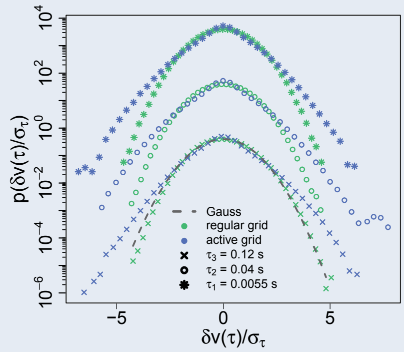

- Regular grid-generated inflow: Gaussian distributed increment PDFs
- Active grid-generated inflow: intermittent distribution

Development of the normalized mean velocity (plot a)) and the TI (plot b)) plotted logarithmically over X/D

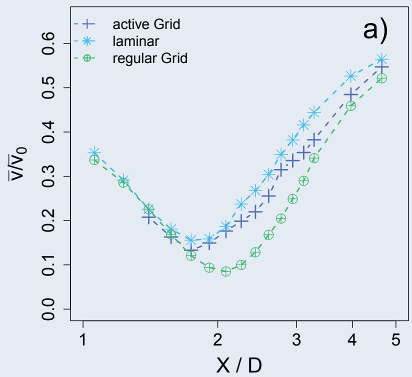

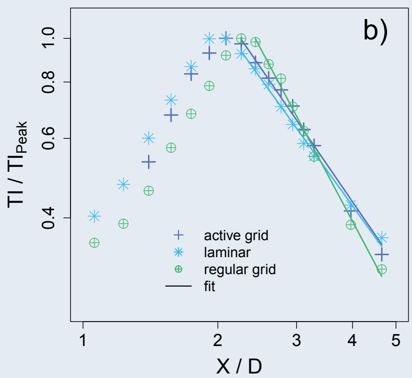

- Decreased recovery of mean velocity in case of intermittent inflow compared to Gaussian inflow - despite a higher inflow TI that is usually associated to be beneficial for the wake recovery [4][5]
- Decreased turbulence decay in case of intermittent inflow compared to Gaussian inflow
- Power-law decay of the turbulence intensity for $X/D > 2$
- An effect of the intermittency on the turbulence intensity is also shown. The normalized turbulence intensity decreases slower

Results

Power spectral density at $X/D = 2$ and $X/D = 4$ for both turbulent inflow conditions

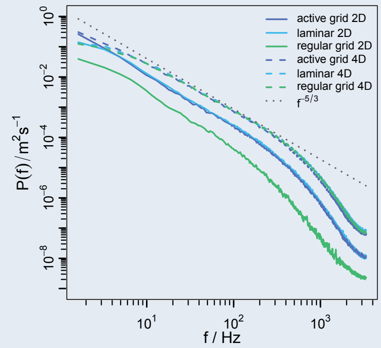

- Dependence on the intermittency in the inflow is visible in the turbulence decay at $X/D = 2$ where the curves (—) for laminar and intermittent inflow collapse but deviate from the curve for regular grid-generated inflow turbulence
- Statistical characteristics of the inflow do not influence the turbulence decay in the far wake at $X/D = 4$ where all three curves (- -) collapse
- A wind tunnel study of Singh et al (cf. [1]) indicates that the intermittency is reduced by the turbine. Our study suggests, that this reduced intermittency might be beneficial for the wake recovery behind the second turbine. This has to be examined in the future.

Summary and conclusion

- Examination of the influence of inflow conditions with different statistical characteristics on the wake of a model wind turbine
- Evidence of effect of the intermittency in the inflow on the evolution of mean velocity and turbulence intensity in the wake
- Turbulence decay in far wake not influenced by statistical characteristics of inflow

In conclusion, different statistical characteristics do have an influence on the wake. Therefore, the statistics of the inflow have to be taken into account when studying the wake of a turbine. A description with mean velocity and turbulence intensity is not sufficient, as the intermittency is neglected in this description.

References

[1] Singh et al. 2014, doi:10.1063/1.4863983
[2] Wächter et al. 2012, doi:10.1080/14685248.2012.696118
[3] Schottler et al. 2016, doi:10.1088/1742-6596/753/7/072030
[4] Chamorro et al. 2009, doi:10.1007/s10546-009-9380-8
[5] Jin et al. 2016, doi:10.3390/en9100830

Acknowledgements

This work is funded by the Federal Environmental Foundation (DBU), Germany.

Contact

Contact: ingrid.neunaber@uni-oldenburg.de

G62

IRPWind ScanFlow Public database

J.W. Wagenaar[1], C. Hasager[2], G. Bergman[1], T. Mikkelsen[2], I. Alting[1],
N. Angelou[2], C.B.M. Pedersen[2]
1. ECN, Unit Wind Energy, P.O. Box 1, NL 1755 ZG Petten, Netherlands
2. DTU Wind Energy, Risø campus Frederiksborgvej 399, DK-4000, Roskilde, Denmark

ECN

ScanFlow project

ECN and DTU have set-up an extensive measurement campaign at the ECN test site to characterize the wind turbine inflow wind field. The campaign comprises nacelle LiDAR, short range scanning LiDAR, meteorological mast, ground based LiDAR and turbine measurements. It is put up in the framework of **IRPWind** 1st call for joint projects.

ScanFlow project: "High-resolution full-scale wind field measurements of the ECN's 2.5 MW aerodynamic research wind turbine using DTU's 3D WindScanner and SpinnerLidar for IRPWind's and EERA's benchmark".

Aim: The aim is to establish a unique turbine power performance and induction zone measurement dataset for benchmark purposes.

Key Performance Indicators
- 2 weeks of short-range windscanners (3x)
- 6 weeks of nacelle LiDAR measurements
- 6 weeks of ground based LiDAR, meteorological mast and turbine data
- Public database

Experimental set-up

Layout of the test site with turbine, mast and LiDARs indicated.

ECN Test Site
- 50km North of Amsterdam
- Flat terrain
- 5 research turbines
- West to East line configuration

Turbine (N9):
- 1st from East
- Nordex 2.5MW
- H=D=80m

WindCube V2:
- 2.5D from turbine
- East

Nacelle LiDAR:
- Cooler mounted
- Scanpattern
- ~0.8D in front rotor

IEC mast (MM3):
- 1km from turbine
- West
- Ws, wd, T, P, TI, etc.

Short range windscanners:
- R2D1, R2D2, R2D3
- Scanpattern
- ~0.8D in front of rotor

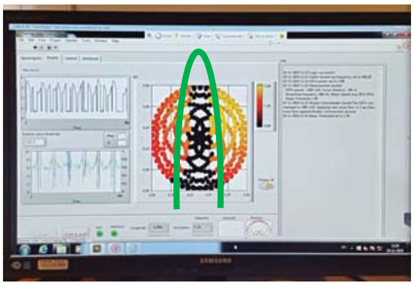

Nacelle LiDAR measurement with blade passage

Nacelle LiDAR installation

Instrumented research turbine

Short range windscanner

Public Database

Data Download Scheme:

1. Registration
- ➢ Go to www.irpwind-scanflow.eu website and click on 'DATA'
- ➢ Register as new user
- • An email is send to the new user
- ➢ Confirm the registration

2. Data selection
- ➢ Go to www.irpwind-scanflow.eu website and click on 'DATA'
- ➢ Fill out form and click 'Agree and request data' (the NDA/DISCLAIMER is accepted)
- • Data request is being considered

3. Data request evaluation
- • The request is being evaluated by the project data maintainer/owner
  - • Deny. User receives email with denial motivation
  - • Accept. User receives email with a download link, which is temporarily valid
- ➢ Download the data

Available data

MM3	Wind speed 52m, 80m, 108m	**Turbine**	PLC Yaw
	Wind direction 52m, 80m, 108m		PLC Power
	RHT 80m		PLC Rotational speed
	Pressure 80m		PLC Status (binary)
	TI		
WindCube V2	Horizontal wind speed	**Short range scanner R2D1**	Time
	Vertical wind speed	**Short range scanner R2D2**	X coordinate of a right-handed Cartesian coordinate system.
	Wind direction	**Short range scanner R2D3**	Y coordinate of a right-handed Cartesian coordinate system.
	Data availability		Z coordinate of a right-handed Cartesian coordinate system.
	40m, 50m, 60m, 70m, 80m, 90m, 100m, 110m, 120m, 130m		Radial wind speed
Nacelle LiDAR	Time		U-component wind vector
	Index: sample number in scan pattern		V-component wind vector
	LOS velocity		W-component wind vector
	Quality		Scan pattern index
	Power in spectrum		Quality index velocity estimation
	Azimuth		Max power
	x-component unit vector		Total power Doppler spectrum
	y-component unit vector		# measurements per point
	Focus distance		Status
	Inclination		
	ScalingFactor		

Acknowledgements

The work described here has received support from IRPWind, a project that has received funding from the European Union's Seventh Programme for Research, Technological development and Demonstration.

Final Statement

In the ScanFlow project various measurements are being performed to characterize the inflow wind field. These data will publically become available at the end of the project (February 2017) via the website www.irpwind-scanflow.eu. Related websites and important links are www.irpwind.eu, www.windbench.eu and www.windscanner.net.

EERA DeepWind 2017 – Trondheim – 18-20 January 2017

Wind Tunnel Hybrid/HIL Tests of the OC5/Phase II Floating System

I. Bayati, M. Belloli, A. Facchinetti
ilmasandrea.bayati@polimi.it, marco.belloli@polimi.it, alan.facchinetti@polimi.it
Politecnico di Milano - Department of Mechanical Engineering, Via La Masa 1, 20156, Milan (Italy)

SUMMARY

- Numerical and experimental implementation of a 2 degrees-of-freedom (DoF) setup for simulating Surge and Pitch motion of the OC5 semi submersible floating offshore wind turbine, through the "hardware-in-the-loop" (HIL) approach in wind tunnel tests.
- Real-time combination of computations and measurements are carried out during the experiments: separatation of model testing of floating wind turbines into wave/ocean basin and wind tunnel tests (e.g. Marintek Ocean Basin & PoliMi Wind Tunnel - H2020/LIFES50+ project)
- Hybrid/HIL approach: exploiting the advantages of each facility and overcoming the scaling issues and conflicts of model tests of FOWTs
- In this work the modelling approach and experimental implementation are presented, with focus on the management of signals and data in the real-time HIL control system, aimed at minimizing the negative effect of model/full scale discrepancies, and the effective implementation.
- Results are shown for free decays, regular and irregular sea states in still air, showing promising results for the next 6-DoF system generation.

APPROACH

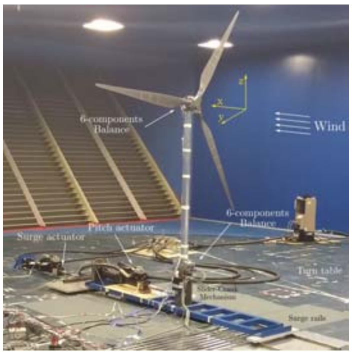

- Lifes50+ Polimi scale model: 1/53 (NREL 5MW)
- 1/3 velocity scale factor
- Hydraulic actuators for Surge and Pitch motion
- Aerodynamic forces measured by means of 6-components dynamometric balances
- dSPACE real-time controller

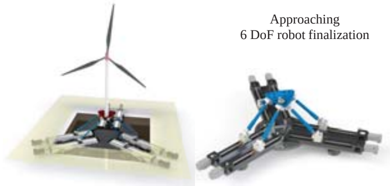

METHODOLOGY

$$\boxed{[[M_s]+[A_\infty]]\ddot{\underline{x}}+[R_s]\dot{\underline{x}}+[K_s]\underline{x}} = \boxed{\underline{F}_{rad}+\underline{F}_{visc}+\underline{F}_{moor}+\underline{F}^{(1)}_{diff}+\underline{F}^{(2)}_{diff}} + \boxed{\underline{F}_{aero}}$$
$$=\underline{F}_{hydro}+\underline{F}_{aero}$$

OC5 Semi-Submersible Floating System (IEA Task/Phase II): **SURGE** & **PITCH**

Hydrodynamic Forces: **COMPUTED**

Aerodynamic Forces: **MEASURED**

REAL-TIME IMPLEMENTATION

Hydrodynamic Forces (Computed)

RADIATION
State Space approach

$$\underline{F}_{rad}=\underline{\mu}(t)=\int_0^t[K(t-\tau)]\dot{\underline{x}}(\tau)d\tau \approx \begin{cases}\dot{\underline{q}}_r=[A_r]\underline{q}_r-[B_r]\dot{\underline{x}}\\ \hat{\underline{\mu}}=[C_r]\underline{q}_r\end{cases}$$

VISCOUS
Morrison

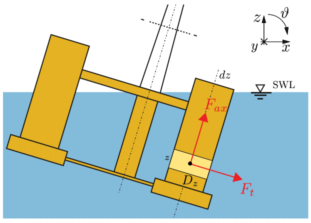

$$F_t(t)=\int_z \frac{1}{2}C_d D_z|v_{rel,t}|v_{rel,t}dz$$

$$F_{ax}(t)=\int_z \frac{1}{2}C_{ax}\pi\frac{D_z^2}{4L_z}|v_{rel,ax}|v_{rel,ax}dz$$

DIFFRACTION 1ST ORDER
WAMIT

$$F^{(1)}_{diff}=\Re\left\{\sum_{k=1}^{N}A_kX_i(\omega_k)e^{j\omega_k t}\right\}$$

MOORING LINES
Look-up tables from FAST/MoorDyn

DIFFRACTION 2nd ORDER
(Difference frequency only)
WAMIT

$$F^{(2)}_{diff}=\Re\left\{\sum_{k=1}^{N}\sum_{l=1}^{N}A_kA_l^*X_i^-(\omega_k,\omega_l)e^{j(\omega_k-\omega_l)t}\right\}$$

Validation of the hydrodynamic model within OC5 Phase II project

General Control Scheme

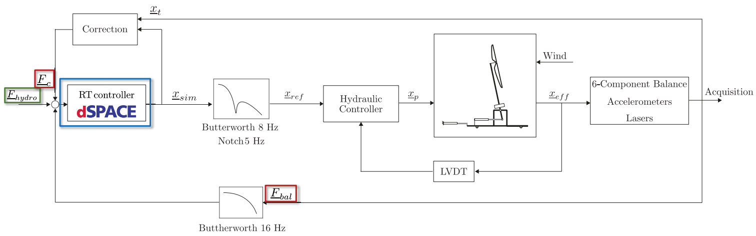

Aerodynamic Forces (Measured)

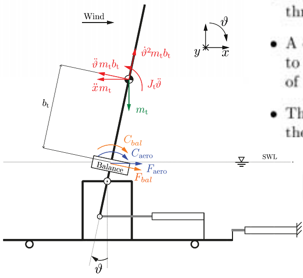

- Aerodynamic forces $\underline{F}_{aero}$ measured through the 6-components balance $\underline{F}_{bal}$
- A correction force $\underline{F}_c$ is needed to take into account the inertial and gravitational contribution of the scale model
- This correction force $\underline{F}_c$ is under the assumption $\underline{x}_{sim}\approx\underline{x}_t$: the simulated and real turbine states are the same

$$\boxed{\underline{F}_{aero}}=\underline{F}_{bal}+\underline{F}_c=$$
$$=\underline{F}_{bal}+\begin{bmatrix}m_t & b_tm_t\\ b_tm_t & b_t^2m_t+J_t\end{bmatrix}\ddot{\underline{x}}_{sim}+\begin{bmatrix}0 & -m_tg\\ 0 & -m_tb_tg\end{bmatrix}\underline{x}_{sim}$$

Important issues to minimize the residual forces due to the methodology

- Identification of the model's parameters (m_t,b_t,J_t)
- Identification of the control's transfer functions
- Effective management of numerical filters
- Identification of the measurement chain (phase shifts)

Still air tests to check the methodology (i.e. minimizing the residual forces)

$$\underline{F}_{bal}+\underline{F}_c=\underline{F}_{aero}\neq 0 = \underline{F}_{res}$$

RESULTS

Free Decays

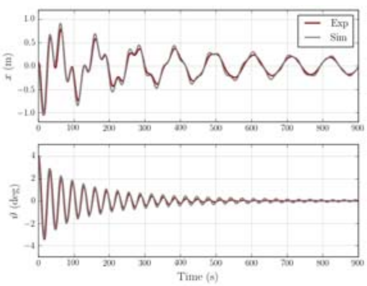

Initial displacement on Pitch ϑ

Regular Sea

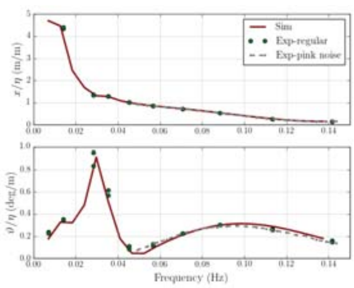

Response Amplitude Operators (RAO) with respect to the incident wave η, for two different experimental conditions
- Regular waves
- Irregular pink noise in the wave frequency range

Irregular Sea

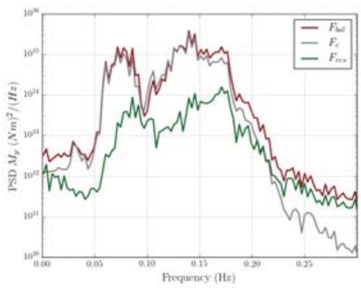

Irregular sea in OC5 operational condition, pitch moments My: the measured forces (*bal*) and the correction forces (*c*) are overlapped almost everywhere: the residual forces (*res*) are at least 1 order of magnitude lower

Initial Calibration of a FAST model of the MARINTEK Hybrid Semisubmersible Experiment

Gordon Stewart, Michael Muskulus
Norwegian University of Science and Technology (NTNU)

Abstract

Small-scale experiments of floating offshore wind turbines are invaluable for validation of design codes used in research and the industry. However, there are difficulties in scaling the aerodynamic and hydrodynamic forces of small-scale tests. The experiment from MARINTEK conducted in October 2015 uses a novel aerodynamic actuation system to eliminate the scaling effects by applying simulated aerodynamic forces using a system of wires and motors attached to the top of the tower of the experimental platform. This system allows for correctly scaled forces that can be measured directly during the experiment. Simulating this experiment presents some challenges, as modeling this aerodynamic system requires some additions to most design codes. In this poster, a FAST model of the MARINTEK semisubmersible platform is developed and compared to data from the experiments, with special consideration to the aerodynamic simulation.

Motivation

How to best model the aerodynamics of the hybrid system in a simulation?

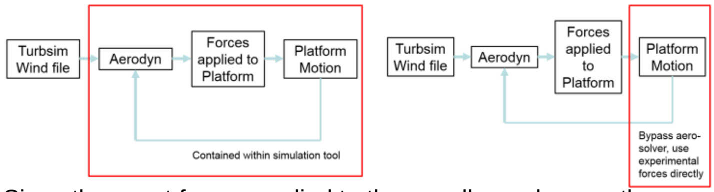

Since the exact forces applied to the nacelle are known, these could be applied directly to the simulation, bypassing the aerodynamic solver, but any inaccuracies in the hydrodynamic modeling would mean that the aerodynamic damping forces caused by motion of the rotor would be incorrect.

Initial Work

- A change to the source code of FASTv7 was written to enable an external file of aerodynamic force to be applied to the rotor, bypassing AeroDyn.
- A series of simulations were run using this modified version of FAST and the OC3 spar buoy model.
- An artificial experiment was created by running a set of baseline simulations
- The rotor forces of the baseline simulation were recorded and used in place of the aerodynamic forces in a second set of simulations.

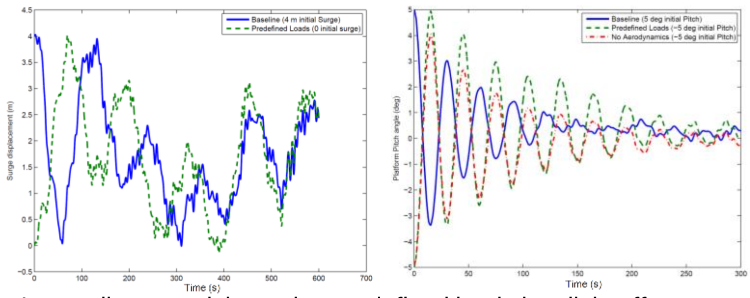

- It was discovered that using predefined loads has little effect on the results if the platform model is similar to the platform that the aerodynamic loads are from.
- However, as the above figures show, if the phase of the platform motion is different, the out-of-phase aerodynamic damping forces have a large impact on the platform motion

Calibration of the Model

The MARINTEK experiment uses a braceless semisubmersible platform and a unique aerodynamic actuator consisting of tension-controlled wires attached to a rigid frame in place of a spinning rotor, as can be seen in the picture to the right.

The experiment included many combinations of wind and waves, including free-decay tests, free-decay with wind, regular waves, regular waves with wind, irregular waves, irregular waves with wind, and a variety of fault cases. This poster will focus on the decay tests with and without wind.

The intention of this work was to repeat the aerodynamic investigation performed on the OC3 spar buoy in previous work. However, the FAST model currently exhibits inaccuracies that will be discussed here instead.

Free Decay Tests:

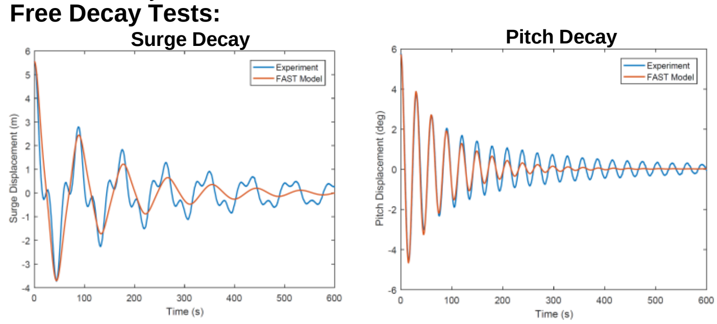

- Mass and inertia from report, drag coefficients tuned by hand
- Experimental surge decay exhibits coupling between the surge and pitch DOFs that the model did not show
- Both surge and pitch free decay's have large quadratic damping that isn't modeled correctly

Free Decay Tests with Constant Wind:

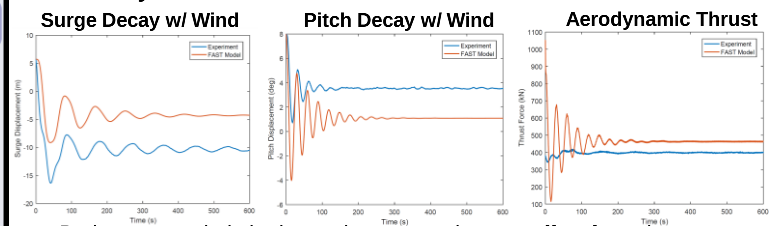

- Both surge and pitch show a larger steady state offset from the constant (8m/s) wind in the experiment than the simulation.
- This was thought to be due to more aerodynamic thrust in the experiment, but there is actually slightly higher thrust in the simulation
- Therefore, there must be a discrepancy in the mass/inertia of the simulation model (if the mass was correct but the stiffness wasn't, the frequencies would be incorrect). Future investigation is needed to determine where this discrepancy is.
- In addition, there is more influence from the platform motion on the aerodynamic thrust in the simulation, further motivating this work, but the geometric model needs to be corrected before proceeding

References

1. Sauder, T., Chabaud, V., Thys, M., Bachynski, E., and Saether, L. *Real-time Hybrid Model Testing of a Braceless Semi-submersible Wind Turbine. Part I: The Hybrid Approach.* Proceedings of the 35th International Conference on Ocean, Offshore, and Arctic Engineering. June 2016.
2. Bachynski, E., Thys, M., Sauder, T., Chabaud, V., and Saether, L. *Real-time Hybrid Model Testing of a Braceless Semi-submersible Wind Turbine. Part I: Experimental Results* Proceedings of the 35th International Conference on Ocean, Offshore, and Arctic Engineering. June 2016.
3. Berthelsen, P., Bachynski, E., Karimirad, M., and Thys, M. *Real-time Hybrid Model Testing of a Braceless Semi-submersible Wind Turbine. Part I: Calibration of the Numerical Model.* Proceedings of the 35th International Conference on Ocean, Offshore, and Arctic Engineering. June 2016.

University of Stuttgart
Germany

The TripleSpar Campaign: Implementation and Test of a Blade Pitch Controller on a Scaled Floating Wind Turbine Model

W. Yu[a], F. Lemmer[a], H. Bredmose[b], M. Borg[b], A. PegalajarJurado[b], R. F. Mikkelsen[b], T. Stoklund Larsen[b], T. Fjelstrup[b], A. K. Lomholt[b], L. Boehm[b], D. Schlipf[a], J. Azcona Armendariz[c]

[a]Stuttgart Wind Energy (SWE), University of Stuttgart, Germany
[b]DTU Wind Energy, Denmark; [c]CENER, Spain

www.uni-stuttgart.de/windenergie

Introduction

Experimental tests of floating wind turbines are usually done with Froude-scaling, which implies re-designing the blades for low Reynolds numbers. However, in the past tests as for full-scale turbines, blade-pitch control has not been included. Instead the rotor speed was kept constant through a servo motor. This poster presents a real-time blade pitch control system, with which the pitch control of the rotational speed for a low-Reynolds rotor at Froude-scaled frequencies was demonstrated.

Controller design

Figure 1 shows the principle concept of the gain-scheduled proportional-integral PI controller which is based on the NREL 5MW baseline controller.

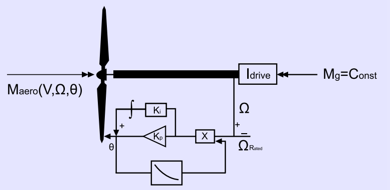

Figure 1: Blade-pitch control block diagram.

Very early the stability problem of floating wind turbines with a conventional on-shore pitch controller has been shown, which is caused by the aerodynamic damping $\frac{\delta F_a}{\delta V}$ in the 1DOF equation of pitch mode

$$\left(\frac{M_{55}+A_{55}}{L_T^2}\right)\ddot{x}_T+\left(\frac{B_{55}}{L_T^2}+\frac{\delta F_a}{\delta V}\right)\dot{x}_T+\frac{C_{55}}{L_T^2}x_T=F_{a,0}. \quad (1)$$

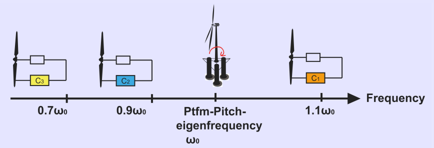

Figure 2: Controller with detuned gains.

One recommended solution is to keep the closed-loop (including control feedback) eigenfrequency of the drivetrain below the platform pitch mode to ensure stability. According to this theory, 3 different gain scheduling methodologies are implemented as Figure 2. here, C1 should show the most unstable behavior, whereas C3 should be stable.

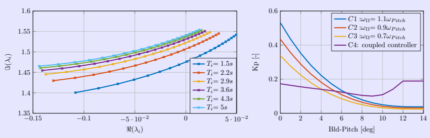

Figure 3: (a) Poles of pitch mode with K_p = 0.1...0.4 at wind speed 1.6[m/s]; (b) Gains of different controllers.

Another solution is discussed in [1], in which the closed-loop is considered with 5-DOFs. The simplified model is linearized at different wind speed so that the poles and zeros of the transfer function of the whole dynamic system can be plotted as Figure 3 (a) shows. By limiting the real part of the pole, the gains for each wind speed can be found (see Figure 3 (b)).

Simulation model

Figure 4 presents the test model, a 1:60 scaled DTU 10MW wind turbine, which is mounted on the INNWIND.EU TripleSpar. A simplified low-order simulation model is set up with only 3 rigid bodies: platform, tower, nacelle and a total of 5 DOFs: surge, heave, pitch, tower top displacement in downwind direction and the azimuth of the rotor. The 3 joints are marked with red color in the sketch. A fixed coordinate system with its origin on the sea water level and at the initial center of flotation is used to describe the platform's position and orientation.

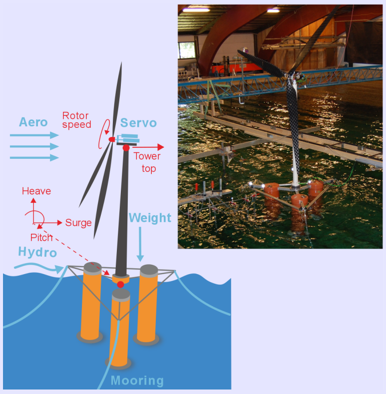

Figure 4: Configuration and coordinate system of the floating wind turbine.

BEM theory is used to create the aerodynamic model. First order hydrodynamic radiation and diffraction forces of the full-scale Triple-Spar are calculated with Ansys AQWA and then scaled into the model size according to the Froude similarity. The mooring dynamics are solved by using the quasi-static model.

Hardware implementation

Figure 5 shows the final hardware setup of the control loop, including two JVL MAC050 integrated servomotors as actuator, an Arduino DUE board, an Arduino R3 ethernet shield, a router, a power supply and supporting cables. LabView is used to log test data both from Arduino and analog-signal data acquisition system in DHI. Control algorithm code is in C associated with a real-time clock and executed in Arduino.

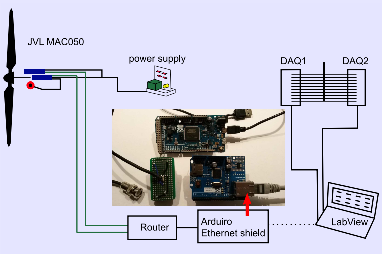

Figure 5: Hardware setup of the control loop.

Wave tank test

According to the time response in irregular wave (Figure 6), the rotor speed is well controlled. C1 has the greatest pitch response as expected.

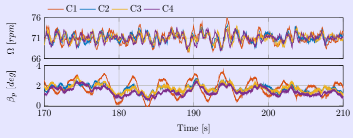

Figure 6: Time responses in irregular wave(sea-state 7).

The power spectral density of measured signals including thrust, rotor speed, blade-pitch, surge and pitch is shown in Figure 7. The identified resonance peaks which correspond to the eigenfrequencies of surge, pitch, wave and rotor speed 3P are marked.

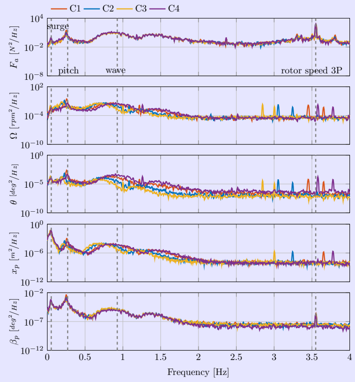

Figure 7: Frequency responses in irregular wave(sea-state 7).

The controller with detuned gains changes the system dynamic properties according to the different resonance frequencies of the rotor speed, blade-pitch and surge from the rotor speed 3P excitation. C4 has greater blade-pitch response but smaller platform-pitch movement.

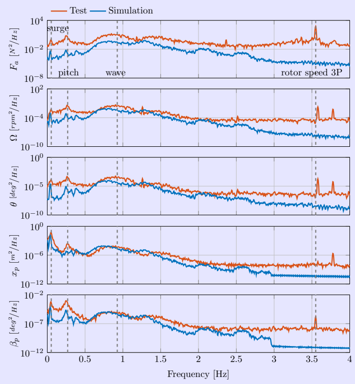

Figure 8: Frequency responses of simulation model and test model in irregular wave(sea-state 7).

Figure 8 shows the comparison of the reduced simulation model and test results in a severe sea-state. The resonance frequencies including surge, pitch and the rang of wave frequencies agree well. The rotor speed 3P excitation isn't replicated since the rotor is modeled as an actuator disk.

Conclusion

A reduced-order simulation model of the scaled floating wind turbine was set up to design the blade pitch controller, which is based on the NREL 5MW baseline controller but with five different gain scheduling methodologies. The controller is later implemented on an Arduino-board to be tested under wind&wave combined environmental loading. The rotor speed is well controlled in different load cases, which shows a good reliability of the simulation model for early controller design.

[1] Sandner, F. (2014) Integrated optimization of floating wind turbine systems. *Proceedings of the 33rd International Conference on Ocean, Offshore and Arctic Engineering OMAE;*.

SWE Stuttgart Wind Energy @ Institute of Aircraft Design

NTNU

A computational fluid dynamics investigation of the performance of tip winglets for horizontal axis wind turbine blades

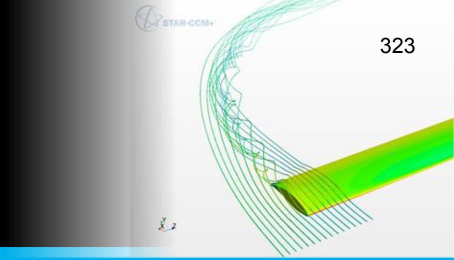

Kristian F. Sagmo* | Jan Bartl** | Lars Sætran**

* Department of Physics, NTNU, Trondheim, Norway. E-mail: krissag@stud.ntnu.no. ** Department of Energy and Process Engineering, NTNU

Introduction

- Both in offshore and onshore wind turbine installations limitations may arise for wind turbine blade radii due to for example either structural loading or noise issues. In such a case, in order to achieve a higher maximum power output from a single wind turbine it becomes a natural goal to increase its maximum power coefficient. This study aims to shed some light on the aerodynamic effects induced by the addition of turbine blade tip winglets by use of both steady state and transient computational fluid dynamics (CFD) approaches.
- A substantial amount of work exists on the topic of winglets, with respect to the development of wings on airplanes and race-cars, but the research is less extensive with respect to use in wind turbine blades. Many studies however, seem to agree that the addition of winglets may substantially improve the efficiency of the turbine, though more so in cases with high aspect ratio blades and relatively low Reynolds numbers (1).
- A recent study, by Y. Ostavan (2) further suggested that the addition of winglets on blades on a up-stream turbine may be beneficial for the total power output of two in-line HAWT's, such as could be the case in wind turbine farms.

Methods

- The first part of the study concerns the effects of simple tip vanes/end-plates, similar to MIE-vanes (1) on isolated blades and utilizes steady state RANS simulations, with turbulence modelled with the Realizable k-epsilon formulation.
- Two types of situations are investigated; straight flow and planar rotational flow implemented by introducing a rotating reference frame.
- The isolated wing is rectangular, with a span to chord ratio of ~15, similar to the blades of the test turbines used in experimental studies at NTNU (5). The profile of the wing is the NREL S826.
- The wing is split into several segments for analyzing lift and drag distribution, analogous to analyzing techniques used in blade element momentum (BEM) codes.

Curved and straight domains. Z axis is aligned with the span of the blades, X along the streamwise velocity for the straight tunnel.

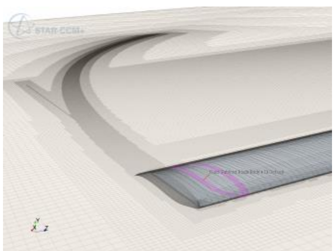

Mesh of the curved domain, with one element highlighted. Each connected blade element is 1 mm wide or ~1/25 Chord legths.

Results

- In presented order; lift coefficients and glide ratio span wise distributions for an isolated wing, pressure distribution for cases A and B (without and with end plates (EP), respectively), and finally a path line illustration of the pair of vortexes generated in the cases with EP's. Note that only glide ratio distribution is calculated for the blade experiencing rotational flow.

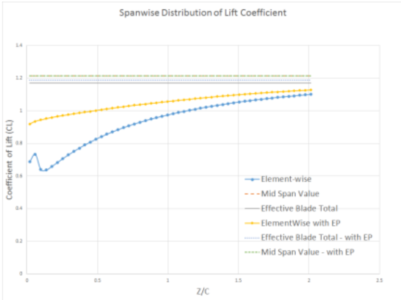

Span-wise lift coefficients for blade with and witout end-plates. The end-plate is one chordlength high, and extends slighty beyond the wing tip dimensions in the streamwise direction. For the case without an end-plate it's interesting to note the small local peak in lift at the tip, where the vortex roll-up creates a local low pressure zone on the suction side, at the cost of large values of drag. Wing tip is located at Z=0.

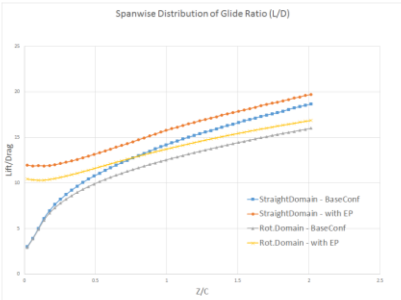

Glide ratio distributions along blade falling off toward tips; Z=0. Note the excellent agreement between the rotational and straight flow cases without end plates attached towards the tip of the blades where Reynolds numbers are matched.

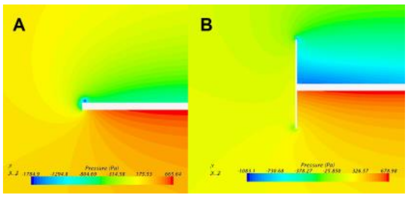

Side by side comparison of static pressure distributions for cases with A; no tip-vane, and B; with rectangular tip vane. Plane is perpendicular to flow direction, looking downstream at position 0.64 chordlengths downstream of leading egde. Note that full formation of the vortex core is delayed in the winglet case.

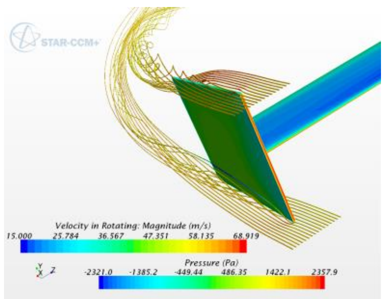

Blade with rectangular tip-vane. Surfaces are colored according to static pressure distribution. Pathlines colored according to velocity. On the suction side of the wing (top here) air is sucked (pushed) toward the inside of the vane, while the opposite happens on the pressure side causing vortex cores to align on opposite sides of the plate, as can also be seen in B.

Observations

- In the case of a wing or turbine blade of limited length, with rectangular shaped tips, the addition of simple end-plate structures can greatly improve the span-wise distribution of glide-ratio several chord-lengths into the blade.
- The study suggest that the addition of a winglet type add-on for a wing works much in the same way for a rotating blade as for a blade gliding along a straight path.
- By creating a physical barrier for the circulation of air at the tip, circulation is shifted and lift is increased along the span of the blade. This is along the same observation made by Gaunaa and Johansen (5).

Ongoing and Future Work

- Simulations using URANS and DES numerical schemes are currently under way investigating a winglet's effect on velocity deficits and turbulent kinetic energy in the wake of a turbine, as well as blade loads. Two in-line turbine geometries are modelled to help understand how the combined power-output can be optimized.
- Investigate the feasibility of developing an empirical model of the effect of simple winglet-type add-ons to turbine blades for use in BEM-theory design codes.

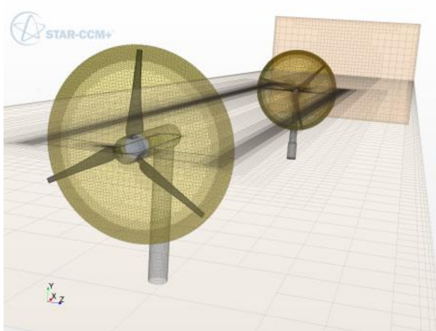

Computational domain modelling two interacting turbines to assess the effects of winglets mounted on an upstream HAWT turbine on it's wake and the performance of a downstream turbine. The blind-test experiment performed at NTNU presented in (5) serves as the reference case for validation of the simulations.

Acknowledgements

- This work is supported with an academic license from CD-Adapco, as well as computational resources at NTNU provided by NOTUR.

References

1) Y. Shimizu et. al., Power Augmentation of a HAWT by Mie-type Tip Vanes, considering Wind Tunnel Flow Visualisation, Blade-Aspect Ratios and Reynolds Number, *Wind Engineering,* 27, No. 3, 2003, pp 183–194
2) Y. Ostavan and O. Uzol, Experimental Study on the Effects of Winglets on the Performance of Two Interacting Horizontal Axis Model Wind Turbines, *Journal of Physics: Conference Series*, 753, September 2016
3) K. F. Sagmo, L. Sætran, and J. Bartl, Numerical simulations of the NREL S826 airfoil. *Journal of Physics: Conference Series*, 735, September 2016
4) M. Gaunaa, J. Johansen; Determination of the Maximum Aerodynamic Efficiency of Wind Turbine Rotors with Winglets. *Journal of Physics: Conference Series*, 75, 2007
5) J. Bartl and L. Sætran: Blind test comparison of the performance and wake flow between two in-line wind turbines exposed to different atmospheric inflow conditions, *Wind Energy. Sci. Discuss.*, doi:10.5194/wes-2016-31, in review, 2016

Numerical study of irregular breaking wave forces on a monopile for offshore wind turbines

Ankit Aggarwal[1], Mayilvahanan Alagan Chella[1], Hans Bihs[1], Øivind Asgeir Arnsten[1]
[1]Department of Civil and Environmental Engineering
Norwegian University of Science and Technology
Trondheim 7491, Norway

Introduction

- Wave spectrum is used to define irregular breaking waves.
- Irregular breaking waves and breaking wave forces: an important parameter in designing substructures of offshore wind turbines.
- REEF3D to study the regular and irregular wave forces

Numerical Model

- Reynolds Averaged Navier-Stokes (RANS) equations are the governing equations of computational fluid dynamics (CFD).
- Explicit TVD third-order Runge-kutta scheme and fifth-order finite difference WENO scheme in multi-space dimensions are used.
- k-w model is used to model the turbulence.
- Level set method (LSM) is used for modelling the free surface
- The relaxation method is used in the present numerical model to generate the waves.
- Bretschneider spectrum is used for the wave generation.

Grid Convergence Study for Wave Surface Elevation

Three different grid sizes are tested and compared with experimental results.
Case 1: Hs = 0.457m, Tp=2.9s.
For grid refinement study, different grid sizes dx = 0.05m,0.025m and 0.01m are tested.

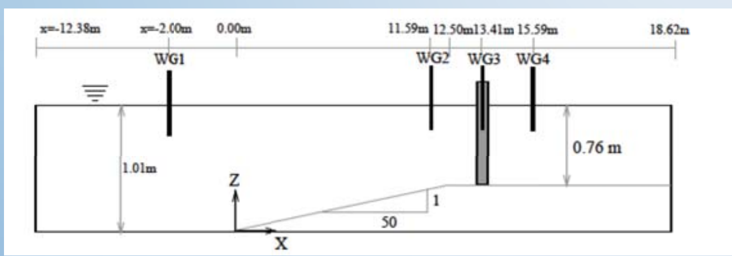

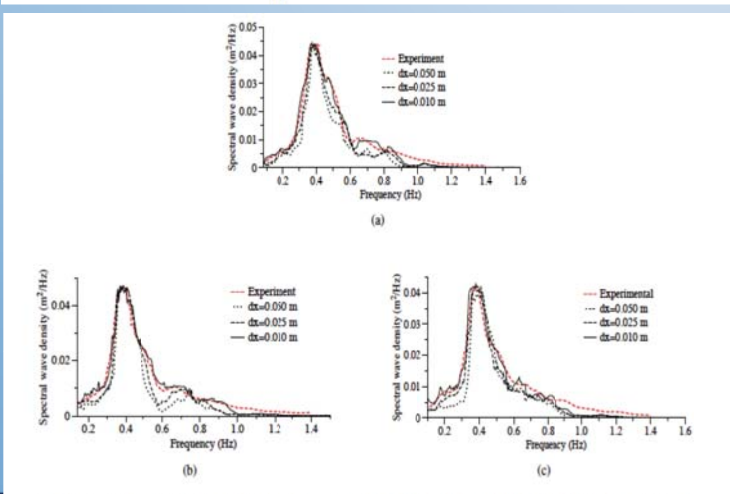

Fig. 2: Comparison of numerical and experimental spectral wave density (m^2/Hz) over frequency (Hz) for three different grid sizes for case 1 at a) WG2 b) WG3 c) WG4

Grid Convergence Study for Irregular Breaking Wave Force

Three different grid sizes are tested and compared with experimental results.
Case 2: Hs = 0.330m, Tp=2.9s.
For grid refinement study, different grid sizes dx = 0.05m,0.025m and 0.01m are tested.

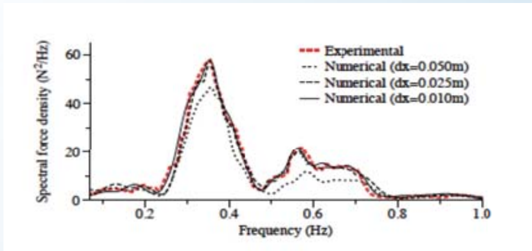

A good match between experimental and numerical results.

Study With Different Wave Steepnesses

Case No.	Significant wave height, H_s (m)	Peak Period, T_p (s)	Grid size, dx (m)	Significant force, F_s (N)
Case 3	0.400 m	2.9 s	0.010 m	18.87
Case 4	0.500 m	2.9 s	0.010 m	22.88
Case 5	0.330 m	2.0 s	0.010 m	17.23
Case 6	0.330 m	3.8 s	0.010 m	19.36

Spectral wave density

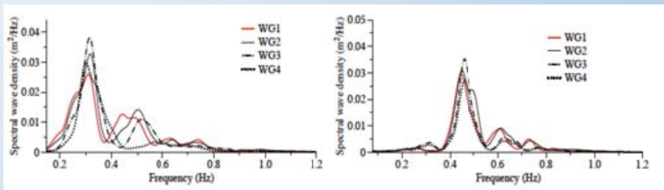

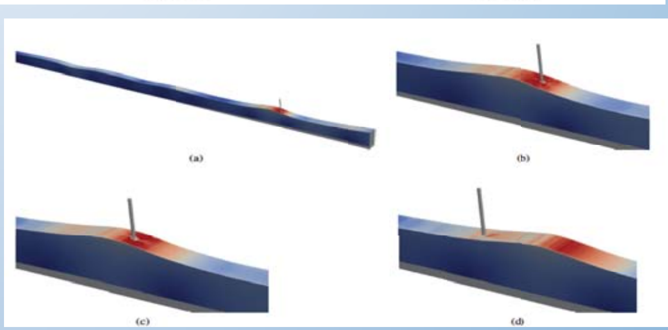

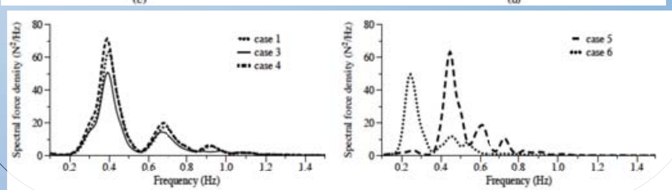

Conclusions

- Contribution of secondary peak towards higher harmonics.
- The numerical model REEF3D can be used as a good tool to study irregular breaking wave forces.
- Longer periods lead to more than one secondary peaks in force spectrum.

Modelling of the Viscous Loads on a Semi-Submersible Floating Support Structure Using a Viscous-Flow Solver and Morison Formulation Combined with a Potential-Flow Solver

Simon Burmester[*1], Sebastien Gueydon[*1], Yannick Debruyne[*2] and Jordan Curt[*3]
[*1] Maritime Research Institute Netherlands (MARIN), Wageningen, The Netherlands
[*2] WavEC – Offshore Renewables, Lisbon, Portugal
[*3] Student from Ecole Centrale de Nantes at MARIN, Wageningen, The Netherlands

What is the problem?

Introduction

Potential-flow (PF) codes are suitable for computing the motions and loads on the floating support structure of floating wind turbines.
However, there are limits of PF codes e.g. for severe sea-states or when the structure is equipped with damping plates. A common practice to overcome this problem is to include viscous loads by a Morison-like approach that uses a constant drag coefficient (C_D) on each structural element. Comparison of the results using standard C_D with model tests of the OC5 DeepCwind semi-submersible showed significant differences of the motion responses when excited at lower frequencies. Wrong viscous loads are suspected to cause this discrepancy. Reynolds-Averaged Navier-Stokes (RANS) based codes are expected to provide a better estimation of the drag coefficients and viscous loads.
The **objective** of this study: A better comparison of the numerical results using a combined "potential-flow and Morison drag" solver with model test data of the OC5 semi-submersible.

Investigated model

Decay tests of the DeepCwind model at 1/50th scale

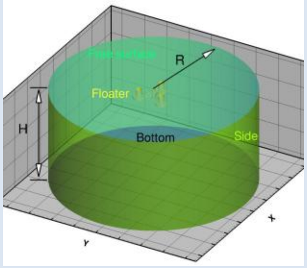

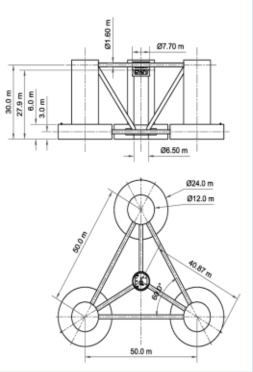

What is the idea and what are the tools?

Numerical tools

- Viscous flow simulations
  - ReFRESCO (uRANS CFD code): http://www.refresco.org/
  - Structural equation of motion to solve: $\mathbf{M}\ddot{\mathbf{x}}(t)+\mathbf{C}\dot{\mathbf{x}}+\mathbf{K}\mathbf{x}=\mathbf{F}_H$, ***M***-mass matrix, **C**-damping matrix, **K**-stiffness matrix
- Combined Morison equation and potential flow simulations (PF+M):
  - WavEC's FF2W [1]
  - Combines potential flow theory and the use of Morison-like drag members
  - Rigid body motion for 6dof as follows:

$$\mathbf{M}\ddot{\mathbf{x}}(t)+\mathbf{F}_{rad}(t)+\mathbf{F}_{hs}(t)=\mathbf{F}_{exc}(t)-\mathbf{F}_{drag}(t)+\mathbf{F}_{ext}(t)$$

  - Morison-like drag force to each virtual member:

$$\mathbf{f}_{drag}=\frac{1}{2}\rho C_{d,n}DL\left(\left(\mathbf{V}_{elmt,n}-\mathbf{V}_{fluid,n}\right)\cdot\mathbf{n}\left|\left(\left(\mathbf{V}_{elmt,n}-\mathbf{V}_{fluid,n}\right)\cdot\mathbf{n}\right)\right|\right)\mathbf{n}$$
$$+\frac{1}{2}\rho C_{d,t}DL\left(\left(\mathbf{V}_{elmt,t}-\mathbf{V}_{fluid,t}\right)\cdot\mathbf{t}\left|\left(\left(\mathbf{V}_{elmt,t}-\mathbf{V}_{fluid,t}\right)\cdot\mathbf{t}\right)\right|\right)\mathbf{t}$$

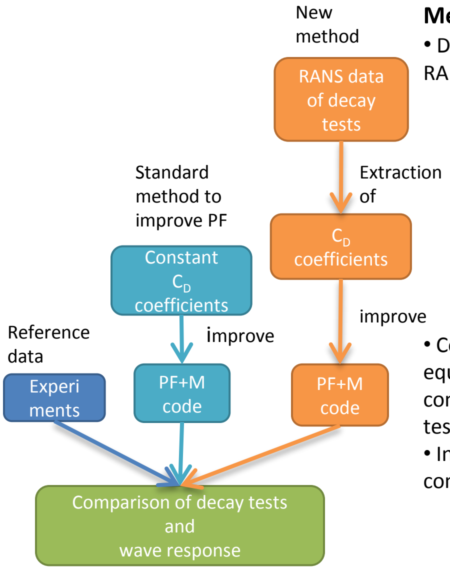

Methodology

- Determine the drag coefficients from RANS:
  - Minimize ε^2 between measured and predicted forces [2]:

$$\varepsilon^2=\frac{1}{I}\sum_{i=1}^{I}\left(F_{mi}-F_{pi}\right)^2$$

  - F_m from CFD, F_p from Morison
  - Data groups of similar velocity to account for Reynolds dependency
- Comparison with combined Morison equation and potential flow solver using constant drag coefficients and with model tests
- Investigation of the abilities of RANS compared to potential flow, i.e.:

$$F_{\mathrm{CFDw/o}}=F_{ref,vis}$$
$$F_{\mathrm{CFDw/}}=F_{ref,vis}+F_{ref,rad}$$
$$F_{pot,rad}=F_{\mathrm{CFDw/}}-F_{\mathrm{CFDw/o}}=?$$

What is done and what needs to be done?

Numerical sensitivity

9 RANS computations to estimate the descretization uncertainty: 3 grids with 3 time steps
Using Eca's approach [3] leads to a discrepancy of < 10%

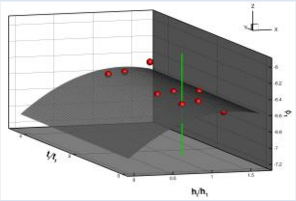

Preliminary CFD results

- Surge decay tests

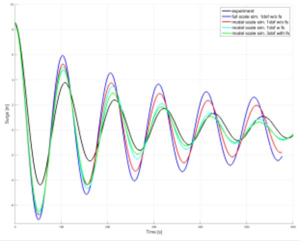

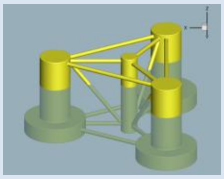

- CFD simulations with and without free surface
- CFD simulations at full and at model scale
- CFD simulations with 1dof and 3dof

Ongoing investigations

- Determination of CD coefficients
- Abilities of RANS compared to PF
- Comparison of decay tests

References:

[1] Alves, M. 2012. *Numerical simulation of dynamics of point absorber wave energy converters using frequency and time domain approaches.* PhD thesis at Universidade Tecnica de Lisboa
[2] Dean, R.G., Aagaard, P.M. 1970. *Wave Forces, Data Analysis and Engineering Calculation Method.* Journal of Petrol. Technol.
[3] Eca, L., Hoekstra, M. 2014. *A procedure for the estimation of the numerical uncertainty of CFD calculations based on grid refinement studies.* Journal of Computational Physics, 262:104-130

Acknowledgements

The research leading to these results is part of the OceaNET project, which has received funding from the European Union's Seventh Framework Programme for research, technological development and demonstration under grant agreement no 607656. We would like to acknowledge Guilherme Vaz, from MARIN for his advice and assistance.

Technology for a better society

www.sintef.no